

**SWAT Model Application to Estimate Runoff for
Ungauged Arid Catchments Experiencing Rapid
Urbanisation: Riyadh case study**

Abdulaziz M. Alsaleh

Thesis submitted to the University of Nottingham for the degree of
Doctor of Philosophy

November 2022

School of Geography
The University of Nottingham

Abstract:

The built-up area of Riyadh city increased from approximately 4.5 km² in 1950 to reach approximately 1,600 km² by 2022 spreading over vast areas of the Wadi Hanifah and Wadi As Silayy catchments. The rapid growth of the city has led to repeated urban flooding. There is an urgent need to study surface runoff and how it is affected by land-use/land-cover (LULC) change in the ungauged catchments of the city. This study addressed that knowledge gap and was the first attempt to calibrate, validate, and run a semi-distributed model to simulate runoff depths and discharge rates for Riyadh's main catchments and sub-basins using five historical and five future scenarios. The Soil Water Assessment Tool (SWAT) was used for the modelling.

TerraClimate evapotranspiration (ET) data was used to calibrate the SWAT model owing to a dearth of observed runoff data across Riyadh city. The literature review revealed that the use of Terraclimate ET to calibrate SWAT models is still very limited so far. The only previous study found is Herman et al. (2020). Therefore, this study is fairly unique in that it uses Terraclimate ET to successfully calibrate and validate a SWAT model. A one-by-one sensitivity analysis was performed to evaluate the impact of changing parameter values on the runoff simulations. The results indicated that simulated runoff sensitivity to selected parameter values in the calibrated SWAT models was minimal in the study area, where the relationships between simulated annual runoff and max and min runoff resulted in a very strong R² (0.9998).

The calibrated and validated SWAT models were run monthly and daily to simulate runoff and to assess the impact of several LULC change scenarios on surface runoff for both historical and future periods. The results of SWAT models of the main catchments and

sub-basins located within the built-up areas demonstrated the positive effect of Riyadh's development on runoff and discharge values for historical LULC scenarios and LULC 2030 probabilities scenarios. But the increasing rates of simulated runoff were not the same for all sub-basins due to the different proportions of urbanisation in each sub-basin. On the contrary, simulation results showed that runoff depths and discharge rates in sub-basins outside the boundaries of the built-up areas of Riyadh did not have significant changes when using historical LULC scenarios or LULC 2030 probabilities scenarios. The increase in runoff depths and discharge rates in the sub-basins reflected the direct influence of the urbanisation process on surface runoff. The increase in simulated surface runoff and discharge can be attributed mainly to the potential decrease of relatively permeable barren lands and the increase of impervious urban surfaces.

Limitations faced during the SWAT model development suggest further research should aim to get detailed and accurate runoff estimates in Riyadh city to sufficiently assist decision-makers and city officials to adopt runoff and flood hazard management schemes in the city.

Acknowledgments:

I would like to thank and express my deep sense of gratitude to my supervisors Professor Simon Gosling and Dr. Matthew Johnson (Associate Professor) for their guidance, constructive feedback, patience, encouragement, and outstanding academic support throughout the development of this thesis. My supervisors were always ready to help to find solutions for the problems faced during the stage of the development of the SWAT models. They were so cooperative to answer my questions and help me at any time. I was lucky, and at the same time, I feel honoured and privileged that I was able to advance my knowledge under the supervision of these two distinguished scholars. Thanks also to Dr. Steve Dugdale for being my internal assessor through three years of annual reviews. He was fair and provided constructive suggestions. I would also like to thank all staff at the School of Geography for providing an appropriate scientific environment to complete my degree.

My appreciation and thanks are also extended to my colleagues at the Geography Department, King Saud University. Particular thanks to Dr. Mofareh Qoradi, the chairman of the department, and Mr. Sulaman Alharbi. Thanks are due to King Saud University for offering me the scholarship. Many thanks to the Royal Commission for Riyadh City, the Ministry of Environment, Water and Agriculture, and the General Authority for Survey and Geospatial Information for providing some of the needed raw data. Special thanks to Dr. Muhamad Alrajhi, Deputy Minister for Land and Surveying, Dr. Abdalla Alobeid, Ministry of Municipality and Rural Affairs and Mr. Abdullah AlNasser, Royal Commission for Riyadh City.

Special thanks go to my parents, brothers, and sisters for their great support and encouragement throughout my Ph.D. journey. Also, I would like to thank my wife for her patience, great support, and wishes for me to complete my research successfully. Thanks go to my daughter Maria.

Table of Contents:

Chapter 1: Introduction.....	1
1.1. Overview	1
1.2. Statement of the problem.....	2
1.3. Aim and objectives	7
1.4. Study area.....	8
1.5. Outline of thesis	10
Chapter 2: Literature Review	13
2.1. Overview	13
2.2. Rainfall in Saudi Arabia	14
2.2.1. Quantity of rainfall and gauge network	14
2.2.2. Spatial variability in rainfall across Saudi Arabia.....	17
2.2.3. Rainfall frequency in Saudi Arabia	19
2.2.4. Remote sensed rainfall data	20
2.2.5. Changes in rainfall through time	22
2.3. Runoff and floods in Saudi Arabia	24
2.3.1. Background.....	24
2.3.2. Urban flooding in Saudi Arabia.....	24
2.3.3. Urban flooding in Riyadh	26
2.3.4. Statistical models of runoff in Saudi Arabia.....	32
2.3.5. SWAT modelling in Saudi Arabia	37
2.3.6. Discharge estimation	39
2.4. Application of the SWAT model in arid regions.....	41
2.4.1. Runoff and discharge simulation	42
2.4.2. Assessment of water resources	48
2.4.3. Evaluation of the impact of LULC changes on runoff and discharge processes.....	48

2.5. Evapotranspiration for calibration and validation of the SWAT model	49
2.5.1. Model calibration and validation by streamflow and ET	53
2.5.2. Model calibration by streamflow and ET	56
2.5.3. Model calibration and validation by ET	57
2.5.4. Model calibration by ET	58
2.6. Summary	59
Chapter 3: Geological and Geographical Background of the Riyadh City Region	61
3.1. Overview	61
3.2. Geology.....	62
3.3. Synoptic patterns associated with precipitation in Saudi Arabia	67
3.4. Vegetation cover	75
3.5. Water supply and consumption.....	77
3.6. Summary	81
Chapter 4: SWAT Model Inputs	82
4.1. Overview	82
4.2. SWAT Model Description	83
4.3. Digital Elevation Models (DEMs)	87
4.3.1. Background to DEMs	87
4.3.2. DEMs applied in this study.....	89
4.4. Land use/Land cover (LULC) Maps	90
4.4.1. Background of LULC maps.....	90
4.4.2. Historical LULC	90
4.4.3. Projections of LULC	97
4.5. Soil Data	104

4.5.1. Background of soils data	104
4.5.2. Soil categories in Riyadh	105
4.5.3. SWAT soil database	110
4.6. Slope Map.....	113
4.6.1. Background on slope data	113
4.6.2. Deriving slopes in Riyadh	114
4.7. Climate data	116
4.7.1. Background of available climate data	116
4.7.2. Selection of climate data for SWAT	118
4.8. Observed data for model calibration and validation	124
4.9. Summary	132
Chapter 5: SWAT Model Initial Setup and Pilot Study	133
5.1. Overview	133
5.2. SWAT Model Setup	136
5.3. SWAT-CUP (calibration and uncertainty procedures)	144
5.4. SWAT model performance indices	146
5.5. Wadi Namar sub-basin as a pilot study	148
5.6. Additional calibration attempts on other sub-basins	156
5.7. Initial sensitivity analysis, calibration, and validation.....	164
5.7.1. Initial SWAT model calibration and sensitivity analysis	164
5.7.2. Attempts to validate SWAT model	168
5.8. Summary	175
Chapter 6: Final SWAT Model Setup.....	177
6.1. Overview	177
6.2. SWAT model calibration and sensitivity analysis	177

6.3. SWAT model validation	185
6.4. Impact of changing model parameter values on simulated runoff	188
6.5. Accuracy of simulated runoff	195
6.6. Summary	198
Chapter 7: Impacts of historical LULC on runoff and discharge	
201	
7.1. Overview	201
7.2. LULC change in Riyadh’s catchments.....	201
7.3. Methodology of runoff simulation and analysis under LULC scenarios	204
7.4. Modelling annual runoff	206
7.4.1. Modelling annual runoff on catchments level.....	206
7.4.2. Modelling annual runoff on sub-basins level.....	211
7.5. Modelling the seasonal cycle of runoff	218
7.5.1. Modelling the seasonal cycle at catchments level	218
7.5.2. Modelling seasonal cycle of runoff on sub-basins level	228
7.6. Modelling annual maximum daily runoff.....	237
7.6.1. Modelling annual maximum daily runoff on catchments level	237
7.6.2. Modelling annual maximum daily runoff on sub-basins level	246
7.7. Summary	266
Chapter 8: Projections of runoff and discharge for Riyadh under future LULC scenario	269
8.1. Overview	269

8.2. Modelling annual runoff	270
8.3. Modelling monthly runoff	279
8.4. Modelling daily extreme runoff	290
8.5. Summary	296
Chapter 9: Discussion	299
9.1. Overview	299
9.2. The challenges in setting-up SWAT models for Riyadh	301
9.2.1. Initial calibration and validation of the SWAT model .	303
9.2.2. Performance of the SWAT model in the study area ...	305
9.2.3. Rainfall characteristics in arid areas.....	308
9.3. Impact of LULC change on surface runoff.....	310
9.3.1. Time steps for model calibration and validation	311
9.3.2. LULC scenarios	313
9.4. Research limitations.....	317
9.5. Impact of the rapid and not properly planned expansion of Riyadh	320
9.6. Impact of shortage of public green spaces in Riyadh	322
9.7. Impact of Riyadh development on flood occurrence potential	326
9.8. Summary	329
Chapter 10: Conclusion	331
10.1. Overview	331
10.2. Calibrated SWAT models and runoff sensitivity to LULC change	331
10.3. Recommendations	334
References	336
Appendix A	383

Appendix B 388
Appendix C 403
Appendix D 423

List of Figures:

Figure 1.1: Urban expansion of Riyadh city from 1950 to 2022. 3

Figure 1.2: Riyadh city the capital of Saudi Arabia. 4

Figure 1.3: Flood that occurred on the 3rd of May 2010 covering an area in the An Nazim neighbourhood, Riyadh city. 5

Figure 2.1: Locations of reviewed rainfall, runoff, and flood studies in Saudi Arabia..... 14

Figure 3.1: Geological map of Riyadh city catchment. 64

Figure 3.2: Air masses affecting the climate of Saudi Arabia..... 68

Figure 3.3: Successive hourly radar images for 24-hours captured 28-29 Nov. 2020. 71

Figure 3.4: Radar images captured from King Khalid International Airport Radar Station, Riyadh..... 74

Figure 3.5: The NDVI image superimposed on the false-colour image showing vegetation cover within the built-up area of Riyadh, 2022. 75

Figure 3.6: Location map of water supply sources for Riyadh city.79

Figure 4.1: A hypothetical map to show dividing a catchment into hydrologic response units by the SWAT model..... 84

Figure 4.2: LULC in the catchments of Riyadh city for the year 1996..... 92

Figure 4.3: LULC in the catchments of Riyadh city for the year 2004..... 93

Figure 4.4: LULC in the catchments of Riyadh city for the year 2009.....	94
Figure 4.5: LULC in the catchments of Riyadh city for the year 2012.....	95
Figure 4.6: LULC in the catchments of Riyadh city for the year 2016.....	96
Figure 4.7: LULC 2019 for the main catchments of Riyadh city obtained from the Global Land Cover Map.....	97
Figure 4.8: 3% Probability of Riyadh city expansion to 2030. ...	100
Figure 4.9: 49% Probability of Riyadh city expansion to 2030...	101
Figure 4.10: 75% Probability of Riyadh city expansion to 2030.	102
Figure 4.11: 77% Probability of Riyadh city expansion to 2030.	103
Figure 4.12: 100% Probability of Riyadh city expansion to 2030.	104
Figure 4.13: Distribution of the soils in the Riyadh city region based on USDA Soil Taxonomy.....	106
Figure 4.14: Distribution of the soils in the Riyadh city region Base on the classification system of the Soil Map of the World.....	108
Figure 4.15: Slope angle map of the catchments in Riyadh city generated from the 5 m spatial resolution DEM.	115
Figure 4.16: Locations of weather stations, rain gauges, and CFSR coverage points in the catchments of Riyadh city....	117

Figure 4.17: Missing values of daily temperature in the record of Riyadh weather station.....	118
Figure 4.18: Average monthly rainfall in Riyadh weather station-R001 for the period 1964-2017.	121
Figure 4.19: Average monthly temperatures in Riyadh weather station-R001 for the period 1964-2017.	123
Figure 4.20: Average monthly relative humidity in Riyadh weather station-R001 for the period 1964-2017.	123
Figure 4.21: Average monthly solar radiation in Riyadh weather station-R001 for the period 1964-2017.	124
Figure 4.22: Average monthly pan evaporation in Riyadh weather station-R001 for the period 1964-2017.	124
Figure 4.23: Comparison between monthly TerraClimate PET and adjusted evaporation pan ($\text{pan} * 0.7$) data from Riyadh weather station.	129
Figure 4.24: Comparison between monthly temperature data from the TerraClimate and Riyadh weather station.	129
Figure 4.25: Correlation between TerraClimate PET and adjusted (0.7) evaporation pan for the period 1991-2010.....	130
Figure 4.26: Correlation between TerraClimate PET and adjusted (0.7) evaporation pan for the period 1991-2000.....	130
Figure 4.27: Correlation between monthly maximum temperature data from TerraClimate and maximum temperature	

data from Riyadh weather station for the period 1991-2010.....	131
Figure 4.28: Correlation between monthly minimum temperature data from TerraClimate and minimum temperature data from Riyadh weather station for the period 1991-2010.	131
Figure 5.1: Stages of SWAT model calibrations and validations and LULC modelling in the study area.	135
Figure 5.2: Distribution of sub-basins in the Wadi Hanifah and the Wadi As Silayy catchments.	143
Figure 5.3: Uncalibrated outputs of the hydrological cycle components in the pilot sub-basin using data for the period 1991-2000.....	151
Figure 5.4: The correlation between the R ² values of individual year calibrations and annual rainfall values at the Riyadh weather station.	156
Figure 5.5: Location map of the 7 sub-basins used for preliminary calibrations to improve the SWAT model performance. Wadi Namar is the original pilot sub-basin.	157
Figure 5.6: Multi-temporal remote sensing images, Landsat OLI images acquired Mach/April 2021 and Spot images acquired April 1986, showing destruction and filling of some natural valleys in Riyadh city.	162

Figure 5.7: The boundaries of Ubarah sub-basin delineated using different DEMs superimposed on 1976 aerial photo and 2021 Landsat OLI image.	163
Figure 5.8: A comparison of simulated evapotranspiration values with TerraClimate derived data for initial calibration.	167
Figure 5.9: A comparison of simulated evapotranspiration values with TerraClimate derived data for initial validation (2001-2010).	169
Figure 5.10: Relationships between monthly rainfall in Riyadh station and rainfall from other sources for the period 1991-2000.	172
Figure 5.11: Relationships between monthly rainfall in Riyadh station and rainfall from other sources for the period 2001-2010.	173
Figure 5.12: Relationships between monthly rainfall from King Khalid International Airport (KKIA) station and rainfall from other sources for the period 2001-2010.	174
Figure 5.13: Annual rainfall at the catchments of Riyadh city....	174
Figure 6.1: A comparison of simulated monthly evapotranspiration values with TerraClimate derived data for the models validation period (1996-2000).	186
Figure 6.2: Spatial distribution of the NSE, R^2 , RSR, and PBIAS values for validation in Riyadh's catchments.	187

Figure 6.3: A comparison of simulated monthly ET values with TerraClimate during the period 1965-2000.	188
Figure 6.4: Annual simulated surface runoff curve and error bar curves of max and min runoff given by one-by-one sensitivity analyses using the highest and lowest parameter range values.	194
Figure 6.5: Relationships between simulated annual runoff and max and min runoff for the period 1991-2000.....	194
Figure 6.6: A comparison of historically measured annual runoff data for the Wadi Hanifah catchment with runoff values simulated by the developed SWAT model.	197
Figure 7.1: Areas of LULC categories in Riyadh catchments for the period 1996-2016.....	202
Figure 7.2: Proportions of LULC categories in Riyadh catchments for the period 1996-2016.	203
Figure 7.3: Effect of LULC change on average annual simulated runoff, runoff coefficient, and runoff change (%) from 1996.....	209
Figure 7.4: Correlation between simulated annual runoff values and areas of LULC classes in Riyadh catchments for the years 1996, 2004, 2009, 2012, and 2016.....	211
Figure 7.5: Spatial distributions of average annual surface runoff using different LULC scenarios at Riyadh's catchments.	216

Figure 7.6: Spatial distributions of average annual runoff coefficient using different LULC scenarios at Riyadh's catchments.	217
Figure 7.7: Spatial distributions of average annual discharge using different LULC scenarios at Riyadh's catchments.....	218
Figure 7.8: Number of occurrences of monthly runoff in Riyadh's catchments for the period 1991-2000.	221
Figure 7.9: Effect of LULC change on average simulated monthly runoff.	223
Figure 7.10: Effect of LULC change on average simulated seasonal runoff.	224
Figure 7.11: Relationships between monthly rainfall and simulated monthly runoff based on five different LULC scenarios in the Wadi Hanifah catchment.	226
Figure 7.12: Relationships between monthly rainfall and simulated monthly runoff based on five different LULC scenarios in the Wadi As Silayy catchment.	227
Figure 7.13: Average simulated monthly runoff using different LULC scenarios for sub-basins of the Wadi Hanifah catchment.	231
Figure 7.14: Average simulated monthly runoff using different LULC scenarios for sub-basins of the Wadi As Silayy catchment.	232

Figure 7.15: Average simulated monthly discharge using different LULC scenarios for sub-basins of the Wadi Hanifah catchment.	233
Figure 7.16: Average simulated monthly discharge using different LULC scenarios for sub-basins of the Wadi As Silayy catchment.	234
Figure 7.17: Spatial distributions of average simulated runoff for January using different LULC scenarios at Riyadh's catchments.....	235
Figure 7.18: Spatial distributions of average discharge for January using different LULC scenarios at Riyadh's catchments.	236
Figure 7.19: Comparison of simulated annual maximum daily runoff depths in Riyadh's catchments under LULC change for a period of 20 years using climate data 1965-2000. ..	240
Figure 7.20: Change (%) of simulated annual maximum daily runoff values using the LULC 2016 scenario compared to their counterpart using the LULC 1996 scenario..	241
Figure 7.21: Annual maximum daily runoff depth in various return periods under five different historical LULC scenarios for Riyadh's catchments.	242
Figure 7.22: Simulated impact on runoff of LULC change between 1996 and 2016 for various return periods for Riyadh's catchments.....	243

Figure 7.23: Percent exceedance of simulated annual maximum daily runoff in Riyadh’s catchments under five different historical LULC scenarios.	244
Figure 7.24: Impact of LULC change for 20 years period on percent exceedance of simulated annual maximum daily runoff in Riyadh’s catchments.....	245
Figure 7.25: Impact of LULC change between 1996 and 2016 on simulated annual maximum daily runoff for the 30-year return period for the sub-basins of Riyadh’s catchments.....	256
Figure 7.26: Impact of LULC change between 1996 and 2016 on simulated annual maximum daily discharge for the 30-year return period for the sub-basins of Riyadh’s catchments.....	257
Figure 7.27: Spatial distribution of simulated annual maximum daily runoff for the 2-year and 30-year return periods under historical LULC change.	258
Figure 7.28: Spatial distribution comparison of simulated annual maximum daily runoff for percent exceedances of Q1 and Q99 under historical LULC change.	259
Figure 7.29: Spatial distribution comparison of simulated annual maximum daily discharge in the 2-year and 30-year return periods under historical LULC change.	260

Figure 7.30: Spatial distribution comparison of simulated annual maximum daily discharge for percent exceedances of Q1 and Q99 under historical LULC change.	261
Figure 7.31: Percent exceedances of the simulated daily runoff for sub-basins of the Wadi Hanifah catchment under five different historical LULC maps.	263
Figure 7.32: Percent exceedances of the simulated daily runoff for sub-basins of the Wadi As Silayy catchment under five different historical LULC maps.	264
Figure 7.33: Percent exceedances of the simulated daily discharge for sub-basins of the Wadi Hanifah catchment under five different historical LULC maps.	265
Figure 7.34: Percent exceedances of the simulated daily discharge for sub-basins of the Wadi As Silayy catchment under five different historical LULC maps.	266
Figure 8.1: Probabilities of Riyadh Urban Expansion in 2030.....	270
Figure 8.2: Proportions of urban area in Riyadh catchments for probabilities of urban expansion in 2030.....	270
Figure 8.3: Projected annual runoff for 2030 for five LULC change probabilities in Riyadh’s catchments (percentages indicate to the comparison of runoff depth with the results of the 2016 LULC scenario).	272

Figure 8.4: Spatial distribution of projected average annual runoff in 2030 for five LULC change probabilities in Riyadh’s catchments.....	277
Figure 8.5: Spatial distribution of projected average annual runoff coefficients in 2030 for five LULC change probabilities in Riyadh’s catchments.	278
Figure 8.6: Spatial distribution of projected average annual discharge rates in 2030 for five LULC change probabilities in Riyadh’s catchments.....	279
Figure 8.7: Projections of the impact of LULC changes on the average simulated monthly runoff for Riyadh’s catchments using different LULC 2030 scenarios. ...	281
Figure 8.8: Average simulated monthly runoff using different LULC 2030 scenarios for sub-basins of the Wadi Hanifah catchment.	284
Figure 8.9: Average simulated monthly runoff using different LULC 2030 scenarios for sub-basins of the As Silayy catchment.	285
Figure 8.10: Average simulated monthly discharge using different LULC 2030 scenarios for sub-basins of the Wadi Hanifah catchment.	286
Figure 8.11: Average simulated monthly discharge using different LULC 2030 scenarios for sub-basins of the As Silayy catchment.	287

Figure 8.12: Spatial distributions of projected average simulated runoff for January in Riyadh's catchments using five probabilities of LULC 2030.	288
Figure 8.13: Spatial distributions of projected average discharge for January in Riyadh's catchments using five probabilities of LULC 2030.	289
Figure 8.14: A comparison between simulated annual maximum daily runoff values using LULC 2016 and 100% probability LULC 2030 scenarios.	292
Figure 8.15: Impact of LULC changes on computed annual maximum daily runoff for various return periods using different historical and future scenarios.	293
Figure 8.16: Impact of LULC changes on computed annual maximum daily discharge for various return periods using different historical and future scenarios.	294
Figure 8.17: Spatial distributions of computed maximum daily runoff for the 2-year (top panels) and 30-year (bottom) return period using 100% (left panels) and 49% (right) probabilities of LULC 2030.	295
Figure 8.18: Spatial distributions of computed maximum daily discharge for the 2-year (top panels) and 30-year (bottom) return period using 100% (left panels) and 49% (right) probabilities of LULC 2030.	296

Figure 9.1: Problem of groundwater level rise in some neighbourhoods of the Riyadh city.	300
Figure 9.2: Peak discharge in an urban stream and rural stream having the same area and total volume of water. ...	311
Figure 9.3: Green area per capita in Riyadh city compared to WHO standard and selected cities.	324
Figure 9.4: Accumulation of runoff water in the Western Ring Road in Riyadh near Exit 33 after the 25 November 2015 storm.	328
Figure 9.5: Accumulation of runoff water in the Al Aziziyah and Al Fayha neighbourhoods in Riyadh after the rain storm on 31st July 2022.	329

Table of Contents:

Table 2.1: Recommended minimum densities of precipitation stations (area in km ² per station).	19
Table 2.2: Curve number (CN) and potential direct runoff for urban watersheds of the Riyadh metropolitan area.	32
Table 2.3: Average recorded volume of annual runoff and average measured runoff coefficient (C_{Rm}) in Saudi Arabia.	35
Table 2.4: Geomorphological and runoff characteristics for 12 drainage basin in the vicinity of Jeddah city.	36
Table 2.5: Flood Peak and Total Volume Runoff for the catchment area above the Mushwab dam, Jeddah.	40
Table 2.6: SWAT models performance indices in previous studies simulating runoff in arid and semi-arid environments.	44
Table 2.7: Performance indices of SWAT models in previous studies that used ET for calibration and validation.	51
Table 3.1: Geological formations in the Riyadh city region.	63
Table 3.2: Population growth of Riyadh City.	77
Table 3.3: Water supply sources for Riyadh city.	78
Table 3.4: Water consumption volume in Riyadh city.	80
Table 4.1: Data used for the development of SWAT models for Riyadh's catchments, for the pilot study (one sub-basin) and the final SWAT models that were for the two main catchments of Riyadh city and its sub-basins. ..	87

Table 4.2: The grouped LULC categories of Riyadh’s catchments for use as inputs for the SWAT model.	91
Table 4.3: Probabilities of Riyadh Urban Expansion to 2030.....	99
Table 4.4: Soil units in Riyadh’s catchments of the General Soil Map of Saudi Arabia.	107
Table 4.5: Soil units in Riyadh’s catchments of the FAO Digital Soil Map.....	109
Table 4.6: Soil properties required to build a database for the SWAT model.	110
Table 4.7: FAO soil properties in the catchments of Riyadh city.	111
Table 4.8: Soil properties in the catchments of Riyadh city.....	112
Table 4.9: The IGU slope classification system.....	114
Table 4.10: Slope classes in the catchments of Riyadh city.....	115
Table 4.11: Climate data used to develop the SWAT model for Riyadh’s catchments.	117
Table 4.12: Annual rainfall (mm) in Riyadh’s catchments.	120
Table 4.13: Annual maximum daily rainfall in Hanifah rain gauge.	121
Table 4.14: Average monthly climate data in Riyadh weather station-R001 for the period 1964-2017.	122
Table 4.15: The recorded annual runoff in Wadi Hanifah station (24° 39' 28"N 46° 36' 32"E).	126
Table 5.1: Selected parameters to develop the SWAT model for the catchments of Riyadh city.....	138

Table 5.2: Model performance ratings for monthly simulations of streamflow.....	147
Table 5.3: Statistical results for 40 calibration attempts for the pilot sub-basin (Wadi Namar) using NSE (20 simulations) and R ² (20 simulations) as the objective functions..	153
Table 5.4: The LULC 1996 of some sub-basins of the main catchments of Riyadh city.....	157
Table 5.5: Statistical results of attempts applied on six sub-basins in the two main catchments to calibrate the SWAT model using NSE and R ² as the objective functions.	159
Table 5.6: Statistical results of initial four calibrations using 38 parameters.	165
Table 5.7: Statistical results of model performance indices for initial models' validation in in the study are catchments. ..	168
Table 5.8: Statistical results of model performance indices of the additional attempts to improve calibrations using 1991-2010 data.....	170
Table 6.1: Monthly statistical results of the SWAT models calibrations using 38 parameters.	178
Table 6.2: Sensitivity analyses of the Wadi Hanifah catchment.	180
Table 6.3: Sensitivity analyses of the Wadi As Silayy catchment.	182

Table 6.4: Statistical results of the SWAT model performance indices for the sensitivity analyses of the Wadi Hanifah catchment.	184
Table 6.5: Statistical results of the SWAT model performance indices for the sensitivity analyses of the Wadi As Silayy catchment.	185
Table 6.6: Statistical results of model performance indices for the final models' calibrations and validations for the study area catchments.....	186
Table 6.7: Statistical results of the indices to verify the closeness of the simulated and observed ET values for the period 1965-2000.	188
Table 6.8: The SWAT model parameters having p-values of 0.05 or smaller for the Wadi Hanifah catchment.	190
Table 6.9: The SWAT model parameters having p-values of 0.05 or smaller for the Wadi As Silayy catchment.	191
Table 6.10: Results of annual surface runoff estimations (mm) for the Wadi Hanifah catchment.	192
Table 6.11: Results of annual surface runoff (mm) estimations for the Wadi As Silayy catchment.	193
Table 6.12: Measured annual runoff data and runoff values simulated by the calibrated SWAT model for the Wadi Hanifah catchment.....	196

Table 6.13: Degree of agreement between the simulated annual runoff values and historical annual measured data for the Wadi Hanifah catchment.	198
Table 7.1: LULC in the Riyadh city region.	202
Table 7.2: Trend of LULC changes from 1996 to 2016 in Riyadh’s catchments.	203
Table 7.3: Effect of LULC change on simulated annual surface runoff in Riyadh’s catchments.	208
Table 7.4: Average annual surface runoff (mm) for the sub-basins in the Wadi Hanifah catchment under different LULC conditions.	212
Table 7.5: Average annual surface runoff (mm) for the sub-basins in the Wadi As Silayy catchment under different LULC scenarios.	213
Table 7.6: Average annual runoff coefficients for the sub-basins in the Wadi Hanifah catchment under different LULC scenarios.	213
Table 7.7: Average annual runoff coefficients for the sub-basins in the Wadi As Silayy catchment under different LULC scenarios.	214
Table 7.8: Average annual discharge (m ³ /s) for the sub-basins in the Wadi Hanifah catchment under different LULC scenarios.	214

Table 7.9: Average annual discharge (m ³ /s) for the sub-basins in the Wadi As Silayy catchment under different LULC scenarios.	215
Table 7.10: Monthly simulated runoff (mm) for the Wadi Hanifah catchment using LULC 1996 scenario.	219
Table 7.11: Monthly simulated runoff (mm) for the Wadi As Silayy catchment using LULC 1996 scenario.	220
Table 7.12: Number of occurrences of monthly runoff in Riyadh’s catchments for the period 1991-2000.	220
Table 7.13: Impact of LULC change in 20 years period (1996 – 2016) on the highest values of simulated monthly runoff (mm) in Riyadh’s catchments.	222
Table 7.14: Coefficient of determination (R ²) of relationships between average monthly rainfall and average simulated monthly runoff using five different LULC scenarios.	225
Table 7.15: SWAT model simulations of annual maximum daily surface runoff using different LULC scenarios for Riyadh’s catchments.	239
Table 7.16: Computed annual maximum daily runoff depth (mm) for various return periods using simulated data for the period 1965-2000 under five different historical LULC scenarios for Riyadh’s catchments.	242

Table 7.17: Percent exceedance of simulated annual maximum daily runoff (mm) using data for the period 1965-2000 for five different historical LULC scenarios for Riyadh's catchments.....	244
Table 7.18: EVI distribution estimates and the percent exceedances of annual maximum daily runoff (mm) using LULC 1996 scenario for sub-basins of the Wadi Hanifah catchment.	247
Table 7.19: EVI distribution estimates and percent exceedances of annual maximum daily runoff (mm) using LULC 2004 scenario for sub-basins of the Wadi Hanifah catchment.	248
Table 7.20: EVI distribution estimates and percent exceedances of annual maximum daily runoff (mm) using LULC 2009 scenario for sub-basins of the Wadi Hanifah catchment.	248
Table 7.21: EVI distribution estimates and percent exceedances of annual maximum daily runoff (mm) using LULC 2012 scenario for sub-basins of the Wadi Hanifah catchment.	249
Table 7.22: EVI distribution estimates and percent exceedances of annual maximum daily runoff (mm) using LULC 2016 scenario for sub-basins of the Wadi Hanifah catchment.	249

Table 7.23: EVI distribution estimates and percent exceedances of annual maximum daily runoff (mm) using LULC 1996 scenario for sub-basins of the Wadi As Silayy catchment.	250
Table 7.24: EVI distribution estimates and percent exceedances of annual maximum daily runoff (mm) using LULC 2004 scenario for sub-basins of the Wadi As Silayy catchment.	250
Table 7.25: EVI distribution estimates and percent exceedances of annual maximum daily runoff (mm) using LULC 2009 scenario for sub-basins of the Wadi As Silayy catchment.	250
Table 7.26: EVI distribution estimates and percent exceedances of annual maximum daily runoff (mm) using LULC 2012 scenario for sub-basins of the Wadi As Silayy catchment.	251
Table 7.27: EVI distribution estimates and percent exceedances of annual maximum daily runoff (mm) using LULC 2016 scenario for sub-basins of the Wadi As Silayy catchment.	251
Table 7.28: EVI distribution estimates and percent exceedances of annual maximum daily discharge (m ³ /s) using LULC 1996 scenario for sub-basins of the Wadi Hanifah catchment.	252

Table 7.29: EVI distribution estimates and percent exceedances of annual maximum daily discharge (m ³ /s) using LULC 2004 scenario for sub-basins of the Wadi Hanifah catchment.	252
Table 7.30: EVI distribution estimates and percent exceedances of annual maximum daily discharge (m ³ /s) using LULC 2009 scenario for sub-basins of the Wadi Hanifah catchment.	253
Table 7.31: EVI distribution estimates and percent exceedances of annual maximum daily discharge (m ³ /s) using LULC 2012 scenario for sub-basins of the Wadi Hanifah catchment.	253
Table 7.32: EVI distribution estimates and percent exceedances of annual maximum daily discharge (m ³ /s) using LULC 2016 scenario for sub-basins of the Wadi Hanifah catchment.	254
Table 7.33: EVI distribution estimates and percent exceedances of annual maximum daily discharge (m ³ /s) using LULC 1996 scenario for sub-basins of the Wadi As Silayy catchment.	254
Table 7.34: EVI distribution estimates and percent exceedances of annual maximum daily discharge (m ³ /s) using LULC 2004 scenario for sub-basins of the Wadi As Silayy catchment.	255

Table 7.35: EVI distribution estimates and percent exceedances of annual maximum daily discharge (m ³ /s) using LULC 2009 scenario for sub-basins of the Wadi As Silayy catchment.	255
Table 7.36: EVI distribution estimates and percent exceedances of annual maximum daily discharge (m ³ /s) using LULC 2012 scenario for sub-basins of the Wadi As Silayy catchment.	255
Table 7.37: EVI distribution estimates and percent exceedances of annual maximum daily discharge (m ³ /s) using LULC 2016 scenario for sub-basins of the Wadi As Silayy catchment.	256
Table 8.1: The projected effect of LULC change on annual surface runoff (mm) in the Wadi Hanifah catchment under five probabilities of LULC 2030 change.	271
Table 8.2: The projected effect of LULC change on annual surface runoff (mm) in the Wadi As Silayy catchment under five probabilities of LULC 2030 change.	272
Table 8.3: Average simulated annual surface runoff (mm) for the sub-basins in the Wadi Hanifah catchment under five probabilities of LULC 2030 change.	273
Table 8.4: Simulated average annual surface runoff (mm) for the sub-basins in the Wadi As Silayy catchment under five probabilities of LULC 2030 change.	274

Table 8.5: Simulated average annual runoff coefficients for the sub-basins in the Wadi Hanifah catchment under five probabilities of LULC 2030 change.	274
Table 8.6: Simulated average annual runoff coefficients for sub-basins in the Wadi As Silayy catchment under five probabilities of LULC 2030 change.	275
Table 8.7: Simulated average annual discharge (m ³ /s) for the sub-basins in the Wadi Hanifah catchment under five probabilities of LULC 2030 change.	275
Table 8.8: Simulated average annual discharge (m ³ /s) for the sub-basins in the Wadi As Silayy catchment under five probabilities of LULC 2030 change.	276
Table 8.9: The projected average monthly surface runoff depths (mm) in the Wadi Hanifah catchment under five probabilities of LULC 2030 change.	280
Table 8.10: The projected average monthly surface runoff depths (mm) in the Wadi As Silayy catchment under five probabilities of LULC 2030 change.	281
Table 8.11: SWAT model simulations of annual maximum daily surface runoff using different probabilities of LULC 2030 scenarios for Riyadh's catchments.	291
Table 8.12: Computed annual maximum daily runoff depth (mm) in various return periods using simulated data for the	

period 1965-2000 under five different probabilities of LULC in 2030 of Riyadh's catchments. 292

Table 8.13: Computed annual maximum daily discharge rate (m³/s) in various return periods using simulated data for the period 1965-2000 under five different probabilities of LULC in 2030 of Riyadh's catchments. 293

List of Abbreviations:

Abbreviation	Definition
ALOS	Advanced Land Observing Satellite
AMSR-E	Advanced Microwave Scanning Radiometer-EOS
AO	Arctic Oscillation
APL	Arabian Peninsula Low
ASTER	Thermal Emission and Reflection Radiometer
CFSR	Climate Forecast System Reanalysis
CFVI	Composite Flash Flood Vulnerability Index
DEM	Digital Elevation Model
DSM	Digital Surface Model
DTM	Digital Terrain Model
ENSO	El Niño Southern Oscillation
ET	Actual Evapotranspiration
EVI	Gumball Probability Distribution
GAMEP	General Authority for Meteorology And Environmental Protection
GIS	Geographic Information System
GLEAM	Global Land Evaporation Amsterdam Model
GPCC	Global Precipitation Climatology Centre
HEC-HMS	Hydrologic Engineering Center-Hydrologic Modeling System
HRUs	Hydrologic Response Units
HYDGRP	Including Soil Hydrologic Group
IGU	International Geographic Union
KGE	Kling–Gupta Efficiencies
KKIA	King Khalid International Airport

LPS	Vertically-Tilted Lows At Lower Levels Associated With Deep Troughs At the 500 Hpa Level
LULC	Land Use/Land Cover
MC	Mediterranean Cyclogenesis
MCM	Million Cubic Meters
MODIS	Moderate Resolution Imaging Spectroradiometer
MTM	Modified Talbot Method
NAO	North Atlantic Oscillation
NDVI	Normalized Difference Vegetation Index
NRCS	National Resources Conservation Service
NSE	Nash–Sutcliffe Efficiency
PBIAS	Percentage Bias
PET	Potential Evapotranspiration
PRM	Probabilistic Rational Method
PT	Persian Trough
R ²	Coefficient Of Determination
RFFA	Regional Flood Frequency Analysis
RMSD	Root Mean Square Deviation
RSL	Red Sea Low
RST	Red Sea Trough
SCS-CN	Soil Conservation Service Curve Number
SOL ALB	Moist Soil Albedo
SOL AWC	The Available Water Capacity Of The Soil Layer
SOL BD	Moist Bulk Density
SOL CBN	Organic Carbon Content
SOL CLAY	Clay Content
SOL K	Saturated Hydraulic Conductivity

SOL ROCK	Rock Fragment Content
SOL SAND	Sand Content
SOL SILT	Silt Content
SOL Z	Depth From the Soil Surface to Bottom of Layer
SOL ZMX	Maximum Rooting Depth of Soil Profile
SRTM	Shuttle Radar Topography Mission
SUFI-2	Sequential Uncertainty Fitting Version 2
SWAT	Soil and Water Assessment Tool
SWAT-CUP	SWAT Calibration and Uncertainty Procedures
TRMM	Tropical Rainfall Measuring Mission
USDA	United States Department of Agriculture
USLE K	USLE Equation Soil Erodibility Factor

Chapter 1: Introduction

1.1. Overview

Urbanisation is increasing worldwide. It has been reported that approximately 64% of developing countries and 86% of developed countries will be urbanised by 2050 (Hu et al. 2020). Although urbanisation can provide social and economic benefits to the communities, there are also potentially detrimental consequences to urban residents, especially in developing countries and rapidly urbanising cities. The process of urbanisation leads to the transformation of large amounts of agricultural and other non-urban land into land types with impervious surfaces, changing hydrological processes. Urban impervious surfaces decrease infiltration, reduce runoff response time, and increase the total volume and peak discharge of the streamflow, resulting in more frequent flooding incidents (Zhu and Li 2014; Hu et al. 2020). *Land-use/land-cover* (LULC) changes are one of the most important factors in driving future environmental change, and urbanisation is one of the major forces that drive LULC changes (Sun et al. 2011).

There are several models developed to simulate surface runoff in catchments. Based on spatial representation, the developed models are classified as lumped, semi-distributed, or distributed. Unlike lumped models, semi-distributed and distributed models consider the spatial variability of hydrological processes, inputs, and catchment properties. The Soil and Water Assessment Tool (SWAT) model is among the most widely used semi-distributed models. Approximately 4,700 studies have applied the SWAT model in the last 35 years (SWAT Literature Database, n.d.). The primary reasons for its wide applicability and acceptability lie in the fact that it is readily applicable through geographic information system (GIS) based interfaces, freely available, easy to link to sensitivity,

calibration, and uncertainty analysis tools, and is a powerful scientific environmental tool tested across a wide variety of global locations (Arnold et al. 2012b; Zhu and Li 2014; Kiros et al. 2015; Singh et al. 2015).

Calibration and validation of hydrological models are a prerequisite for accurate hydrological simulations in any catchment. Measured runoff data are, traditionally, used to calibrate hydrological models, but streamflow records are usually sparse and scarce in developing countries. Recently, hydrological simulations using distributed and semi-distributed models in ungauged and poorly gauged catchments have increased due to the availability of powerful software for models' calibration, the increased availability of earth observation data, and the introduction of tested alternative data sources for calibration and validation such as evapotranspiration (Immerzeel and Droogers 2008; Sirisena et al. 2020).

1.2. Statement of the problem

Saudi Arabia has experienced changes in spatial, social and economic patterns since the oil boom in the mid-1970s (Barth and Quiel 1987). Huge oil revenues influenced urban development in the country resulting in rapidly growing cities. Riyadh city is an example, with its built-up area increasing from approximately 4.5 km² in 1950 to 18 km² in 1968 (Al-Gabbani, 1991) before rapidly expanding to approximately 1,600 km² by 2022 (Figure 1.1). The city population grew from 106,000 in 1954 to 5,200,000 in 2010 and it may reach 15,000,000 by 2030 (Riyadh Municipality n.d.; Ministry of Municipal and Rural Affairs 2018; Kane 2021). Currently, the city spreads over vast areas of two main catchments; the Wadi Hanifah and the Wadi As Silayy (Figure 1.2).

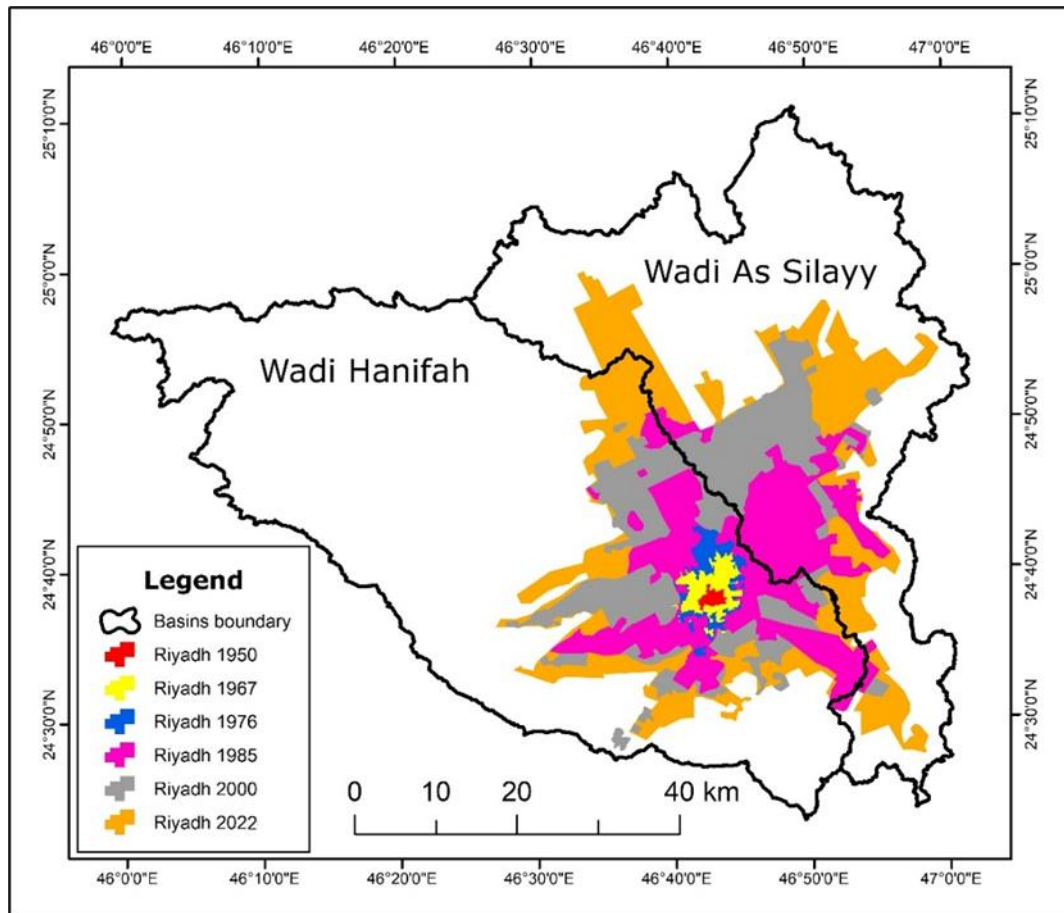


Figure 1.1: Urban expansion of Riyadh city from 1950 to 2022.

Source: Prepared by the author using aerial photograph 1950, aerial photographs 1967, aerial photographs 1976, Landsat TM image 1985, Landsat ETM+ image 2000, and Landsat OLI image 2022.

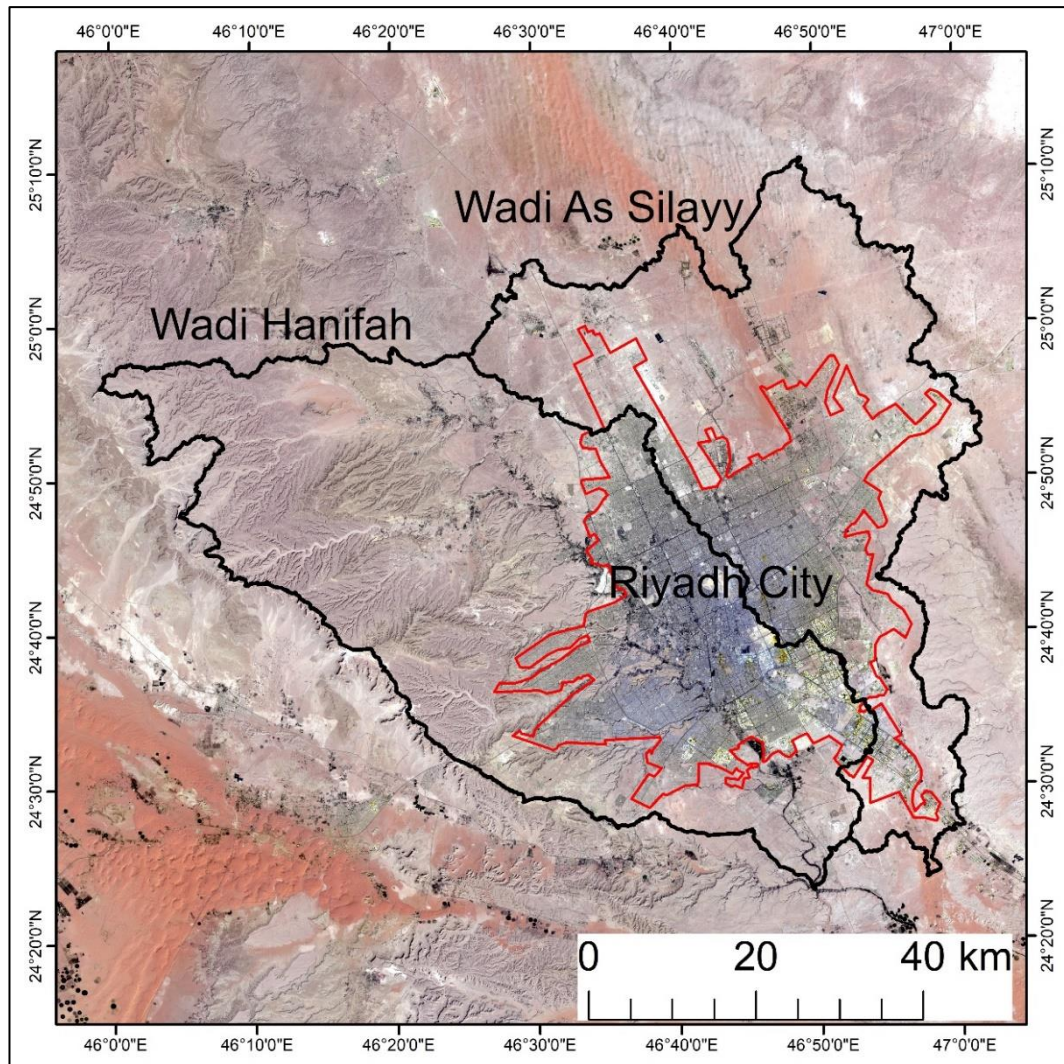


Figure 1.2: Riyadh city the capital of Saudi Arabia.

Source: This photomap produced by author using Landsat-8 OLI images acquired February 2022.

The rapid growth of the city has led to serious environmental problems such as repeated urban flooding. Urban flooding in Riyadh occurred in 1995, 1997, 2005, 2010, 2011, 2012, 2013, 2014, 2015, 2016, 2019 and 2022 (Al Saud, 2010; Alamri, 2011; Abosuliman et al., 2013; Almazroui, 2013; Al-Momani and Shawaqfah, 2013; Qari et al., 2014; Al Saud, 2015; Hijji et al., 2015; Rahman et al., 2016; Akhbaar24, 2019; Abu Hamad, 2022; Al-Wsabi 2022). Flash floods may occur in some parts of Riyadh city due to extreme rainfall events. However, the more frequent flood problem in the city tends to be water accumulation rather than flash flooding (Figure 1.3). The vulnerability of Riyadh city to flood hazards can be linked to the

development of the city. For example, Riyadh's mayor told a press conference following the flood on 3rd May 2010, that 70% of Riyadh city has no stormwater drainage networks. Riyadh's mayor emphasised that no flooding occurred in neighbourhoods with efficient stormwater drainage networks (Alhaddan, 2010).



Figure 1.3: Flood that occurred on the 3rd of May 2010 covering an area in the An Nazim neighbourhood, Riyadh city.

Source: Abo Zuhair, (2010).

Birkinshaw et al. (2021) stressed that urban expansion within catchments has the potential to increase flooding. The authors

emphasised that hydrological modelling is an important tool to analyse and manage the increasing flood hazard in such catchments. They highlighted this task is difficult in many catchments owing to the unavailability of adequate data. The rapid urban expansion of Riyadh city has had a profound influence on runoff and results in larger and more frequent incidents of flooding in the city. Therefore, runoff estimation is of great importance for solving urban environmental problems, urban planning, and policymakers. Drainage basins in Riyadh city are ungauged and there is no available runoff data, which presents a major challenge for developing hydrological models for the city.

By undertaking a literature review of previous studies, only four published research papers have estimated runoff and/or studied flash floods in the city of Riyadh (Tahir Hussein et al. 2009; Rahman et al. 2016; Sharif et al. 2016; Radwan et al. 2018). Critical reviews of these studies have revealed limitations and deficiencies. Thus, there is still an urgent need to study surface runoff and how it is affected by LULC change in the main catchments of Riyadh city, which can help policymakers to take necessary actions to mitigate and prevent environmental problems. This study addresses that knowledge gap, and it is the first to calibrate, validate and run a semi-distributed hydrological model that accounts for physical hydrological processes, for Riyadh city.

The use of SWAT to estimate runoff in Saudi Arabia is limited. Sultan et al. (2015) and Fallatah et al. (2019) are the only studies known to the author to use the SWAT model to estimate runoff in Saudi Arabia. Sultan et al. (2015) applied the SWAT model to estimate streamflow in 19 major eastern Red Sea catchments (total area of 176,683 km²) originating in high mountains and discharging downstream into the Red Sea and Gulf of Aqaba. Fallatah et al.

(2019) applied the SWAT model to the assessment of modern recharge of the Saq aquifer in Saudi Arabia, covering an area of 377,080 km². Both studies applied regionalisation techniques for the SWAT model calibration by extrapolating catchment-specific parameters from the Wadi Girafi catchment (3,350 km²) in the Sinai Peninsula, Egypt (Milewski et al. 2009) based on the assumption that the Wadi Girafi catchment exhibits similar climatic and topographic characteristics, areal extent, and soil types compared to catchments in their study area covering very large areas. Certainly, every catchment is distinct, and ideally, model parameters should be calibrated on a catchment-by-catchment basis. Moreover, the SWAT models used to simulate surface runoff in these two previous studies were not validated.

1.3. Aim and objectives

The main aim of this Ph.D. research is to setup SWAT models for the two ungauged main catchments of Riyadh city to simulate surface runoff and to explore runoff sensitivity to LULC change. This aim is accomplished via the following objectives:

- 1) Use derived evapotranspiration from TerraClimate datasets to calibrate and validate a SWAT hydrological model to get an estimate of runoff in the ungauged catchments of Riyadh city.
- 2) Examine the influences of the coefficient of determination (R^2) and Nash–Sutcliffe efficiency (NSE) objective functions on the calibration results in the catchments of the study area.
- 3) Assess surface runoff sensitivity to model parameter values of the SWAT model using a one-by-one sensitivity analysis method.
- 4) Apply the developed SWAT models to investigate the impact of LULC change on runoff under rapid urbanisation scenarios.

- 5) Evaluate the historical and future impact of LULC change on runoff and discharge by performing yearly, monthly, and daily analyses on both the main catchments and sub-basin levels.

1.4. Study area

Riyadh, the capital and largest city in Saudi Arabia, is located near the geographical centre of the country. Currently, the city spreads on vast areas of two main catchments which are the Wadi Hanifah - sometimes spelled as Hanifa- and the Wadi As Silayy - sometimes spelled as As Sulayy, As-Sulay, As Suly, As-Sulaiy, Al Sulay, Al Silay, Sulay, or Sulaiy. Due to different spellings for places names in the available maps and previous studies of the study area, names used in the governmental 1:50,000 topographic maps were adopted in this thesis. Riyadh is located between 24°30'N and 25°00'N and between 46°30'E and 47°00'E, situating on average about 600m above sea level.

As a capital of Saudi Arabia, Riyadh city is the seat of government and main private administrations. It houses all ministries and principal offices of various departments and organisations of the nation. By 1955, all ministries and government offices were moved to Riyadh city or later established in it. Additionally, all embassies and diplomatic missions were moved to Riyadh. Riyadh also functions as an important centre for most of the country in terms of commercial, industrial, financial, cultural, educational and health services. Riyadh is now home to one of the biggest airports in the world, six government-owned/public universities, five privately owned universities, many middle-level colleges, specialised institutes, large public, private, and specialised hospitals, high-level sports facilities, and stadiums, huge hotels, and public libraries (Ministry of Municipal and Rural Affairs 2018). Based on Riyadh city functions and location, major Saudi highways radiate from Riyadh to

east, west, north and south of the country (Al-Gabbani 1991). The concentration of governmental and private activities in the Riyadh city is a major factor of its dramatic growth rates. The expansion of Riyadh is still a main target of the Saudi government. The Saudi capital city is aiming to double its population and become one of the 10 richest cities in the world under ambitious plans unveiled by the Saudi Crown Prince at the Future Investment Initiative gathering held in Riyadh on 27-28 January 2021 (Kane 2021).

Riyadh was one of the small agricultural villages that spread throughout the Wadi Hanifah catchment. The old Riyadh was established within the sub-basin of Wadi Al Battha which is a small tributary of Wadi Hanifah. The centre of the old Riyadh is located on the geographic coordinates of 24°37'52'' North latitude and 46°42'36'' East longitude. The main channel of the Wadi Hanifah runs from north to south with many western tributaries draining the back slope of the Tuwayq mountain cuesta. The main western tributaries of Wadi Hanifah are Wadi al Harigah, Wadi Safar, Wadi Mahdiya, Wadi Ubayr, Wadi Laban, and Wadi Namar. There are two main eastern tributaries of the Wadi Hanifah which are the Wadi Al Aysin sub-basin and the Wadi Al Battha sub-basin.

Due to the continued rapid expansion of Riyadh in the past four decades, the city has spread to cover a large area of another major catchment; the Wadi As Silayy. Contrary to the Wadi Hanifah, the Wadi As Silayy basin is characterised by terrain with low slopes. The main tributaries of the Wadi As Silayy catchment are Wadi Banban, Sa'ib An Nazim, Ghadīr Al Husan, Sa'ib Abu Shajarah, Sa'ib Aba Al Jirfan, Sa'ib Al Birsha'ah, Qiri Abu Tulayhah, and Sa'ib Abu Sidayrah.

1.5. Outline of thesis

- Chapter 2 is a literature review on the topic and region of the thesis which focuses on the development of SWAT models for catchments of Riyadh city and the impact of rapid urban development on runoff in the city. This chapter summarises, synthesises, and integrates previous studies to highlight any deficiency or gap in the existing literature on the research topic and region. It presents thematically the reviewed studies under four main titles, which are rainfall in Saudi Arabia, runoff and floods in Saudi Arabia, application of the SWAT model in arid and semi-arid environments, and ET for calibration and validation of the SWAT model.
- Chapter 3 provides a general description of geological and geographical aspects that influence surface runoff in the study area. It includes information on geology, synoptic patterns including precipitation in Saudi Arabia, vegetation cover, and water resources and consumption.
- Chapter 4 describes the SWAT model. In addition, this chapter characterises the essential inputs of the SWAT model to simulate surface runoff including topographic data (DEMs), LULC data, soil data, and climate data.
- Chapter 5 documents the processes conducted in the initial setup of the SWAT models to simulate surface runoff in the catchments of Riyadh. The chapter provides details of model performance in both pilot sub-basins and entire catchments. Moreover, it presents the initial sensitivity analysis of model parameters and the calibration and validation of the model.
- Chapter 6 provides the final setup of the SWAT models in the study area. The chapter presents the final sensitivity analysis of model parameters and the calibration and validation of the model. It includes one-by-one sensitivity to assess the impact

of parameter values' change on runoff simulations. This chapter also contains the results of the accuracy test of simulated runoff in the Wadi Hanifah catchment.

- Chapter 7 focuses on the effects of historical LULC change on runoff in catchments of Riyadh city. The chapter also includes an interpretation and explanation of SWAT model results for annual, monthly, and daily extreme runoff using five historical LULC scenarios for 20 years extending from 1996 to 2016. The chapter presents information on runoff modelling on two scales: the two main catchments and sub-basins.
- Chapter 8 is on the effects of future LULC change on runoff in catchments of the study area. The chapter includes an interpretation and explanation of SWAT model results for annual, monthly, and daily extreme runoff using five future urbanisation scenarios for the year 2030. The chapter presents information on runoff modelling on two scales: the main catchments and sub-basins.
- Chapter 9 provides a discussion of the challenges in modelling surface runoff in ungauged arid catchments where there is a scarcity of climate data and uneven distribution of weather stations. Also, it presents a discussion of the evaluation of LULC change's impact on surface runoff. The chapter also contains a discussion of the impact of the rapid and not properly planned expansion of Riyadh, and the impact of public green spaces in Riyadh.
- Chapter 10 concludes the thesis by presenting the core of the research findings. It emphasises the need for reliable and well-distributed hydrological measurements to improve the assessment of runoff and to get accurate simulations to inform effective management of urban hydrology in the city. The chapter gives recommendations to apply the developed SWAT models for only approximate estimates of surface runoff in the

catchments of Riyadh due to the limitations faced during the SWAT model development. It suggests further research should aim to get detailed and accurate runoff estimates in Riyadh city to assist decision-makers and city officials to adopt runoff and flood hazards management schemes in the city.

Chapter 2: Literature Review

2.1. Overview

Reviewing past studies is an essential and preliminary task when carrying out scientific research (Kumar 2011). In this study, the literature review process was used to bring clarity and understanding to the research problem, to justify its originality and importance, and to broaden and deepen knowledge of the fields associated with the research topic. Relevant studies to the research area were scattered through time and output type, with many in specialised or regional journals, and government reports. Several search engines were used to obtain previous academic studies (e.g. Web of Science, Google Scholar, Microsoft Academic, WorldWideScience, etc).

The theme of this research focuses on the development of SWAT models for catchments of Riyadh city, Saudi Arabia, and so focus was given to reviewing modelling in arid regions, and hydrological conditions in Saudi Arabia. The intention is to present a clear picture of the development and applications of the SWAT model in arid environments, and the availability of rainfall and surface runoff information in Saudi Arabia. Thus, previous studies were summarised, synthesised, and integrated to reveal the current conditions, and to highlight deficiencies and/or gaps in existing knowledge (Figure 2.1). The studies were thematically reviewed under four main titles, which are: 1) rainfall in Saudi Arabia, 2) runoff and floods in Saudi Arabia, 3) application of the SWAT model in arid and semi-arid environments, and 4) ET for calibration and validation of the SWAT model.

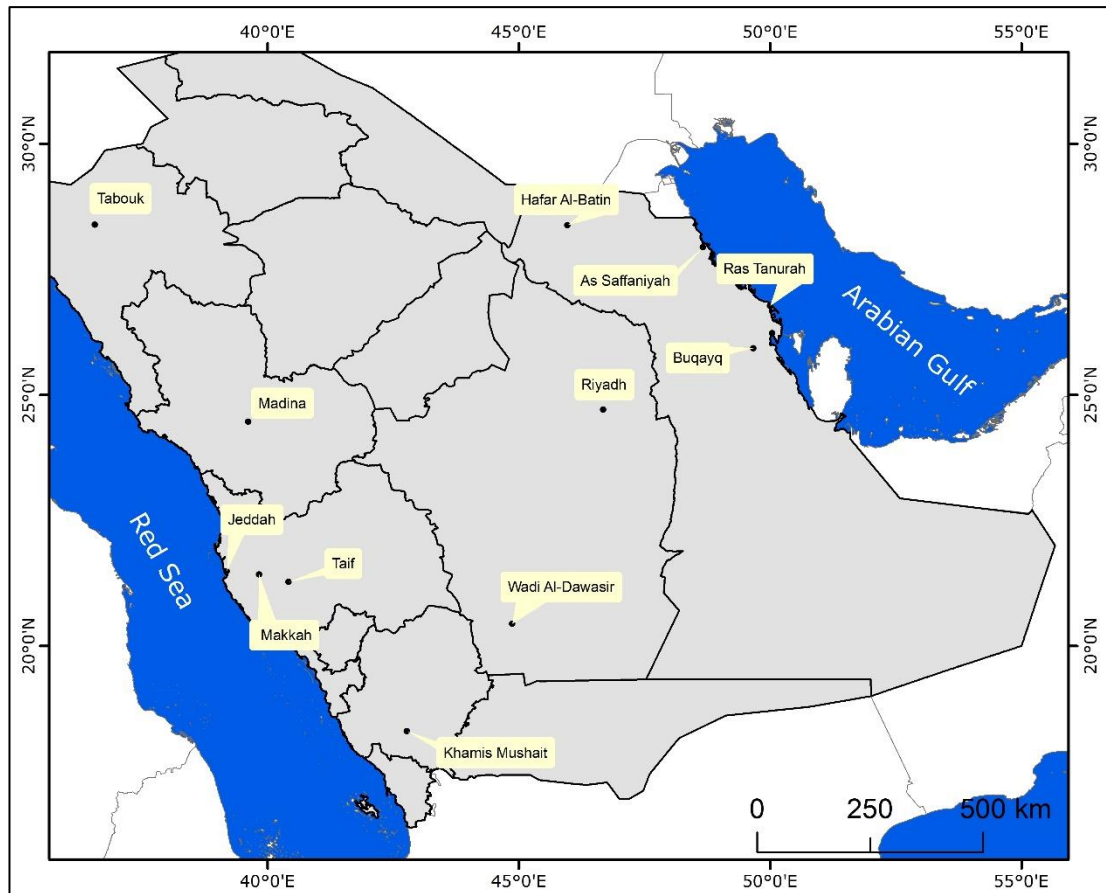


Figure 2.1: Locations of reviewed rainfall, runoff, and flood studies in Saudi Arabia.

2.2. Rainfall in Saudi Arabia

2.2.1. Quantity of rainfall and gauge network

There are no rivers or permanent streams in Saudi Arabia. Therefore, the occurrence of runoff is mainly associated with local intense rainfall. With the exception of the mountain ranges parallel to the coast of the Red Sea in the west and southwest of Saudi Arabia, the country is extremely hot and dry and is classified as an arid climate (Almazroui 2012a). Goudie and Wilkinson (1977, p. 7) indicated "precipitation in arid zones, in addition to showing temporal variability, also shows considerable spatial variability. Indeed, desert rainfall is often described as being spotty". The spottiness characteristic is associated with convective precipitation in arid environments (Maliva and Missimer 2012). Among the important

features of precipitation in Saudi Arabia are: its irregularity, low annual quantities (e.g. 16mm in 2000 recorded at Hanifah Rain Gauge), the significance of 24 hour contributions to annual totals (e.g. 24 hours can contribute 53% of annual totals such as recorded in 2000 for the Hanifah rain gauge), relatively high spatial and temporal variability, limited overall areal extent, and the small number of rainy days each year (e.g. two days for 2000 in Hanifah rain gauge) (Schyfsma 1978; Jones et al. 1981; Abouammoh 1991; Wheeler et al. 1991; Alyamani and Sen 1993; Al-Saleh 1997; Subyani 2004; Mashat and Abdel Basset 2011 ; El Kenawy et al. 2014; Hasanean and Almazroui 2015; Subyani and Hajjar 2016). Rainfall studies of Saudi Arabia were categorised and reviewed thematically based on rainfall distribution and variability, frequency, estimation of rainfall from remotely sensed data, and climate change.

Prior to reviewing previous studies of rainfall in Saudi Arabia, it is appropriate to give a brief background on rainfall stations in the country. Saudi Aramco in the mid-1930s established the first four weather stations in Saudi Arabia, namely Dhahran, Ras Tannurah, Abqaiq, As Safaniyah (Schyfsma 1978). Since the 1960s, the Ministry of Environment, Water and Agriculture (the heir of the former Ministry of Agriculture and Water, and the former Ministry of Electricity and Water) founded and operated 46 weather stations and more than 150 rain gauges (Ministry of Agriculture and Water 1984). The General Authority for Meteorology and Environmental Protection (GAMEP), another official establishment, runs a further 29 meteorological stations to serve Saudi Airports, having uneven records. GAMEP was administratively affiliated to the Ministry of Defence and Aviation, but since 2016 it has been affiliated to the Ministry of Environment, Water and Agriculture. By the mid of 2018, the Minister of Environment, Water and Agriculture has given an

authoritative direction to the deputy Minister for water affairs to transfer tasks of operating 85 solar-powered meteorological stations from the Division of Hydrology in the ministry to the GAMEP (Alawi 2018). However, the metrological stations and rain gauges are not well distributed in Saudi Arabia and the length of records in these stations are not homogenous (Mashat and Abdel Basset 2011).

The limitations in meteorological data in Saudi Arabia influence the results of rainfall analysis. For example, some previous studies investigating rainfall characteristics only used data from serving airports (29 stations or less) to represent rainfall over approximately 2,000,000 km² (Alyamani and Sen 1993; Almazroui 2011; Mashat and Abdel Basset 2011). The spatial variability of rainfall in an area will also partially dictate the implications of low rainfall sampling sites. The general spatial and temporal characteristics of rainfall in Saudi Arabia and some of its regions were studied by Abouammoh (1991) using monthly precipitation totals at seven weather stations operated by the GAMEP (Dhahran, Jeddah, Khamis Mushait, Madina, Riyadh, Tabouk, and Taif). Monthly statistics such as the number of dry months per year were reported for the period from 1966 to 1986 (21 years). For example, dry months were from June to September in Dhahran; in Jeddah were June and August; and in Tabouk were June, July, and September. Abouammoh (1991) states that the months with rainfall <5 mm were May in Dhahran; March, July, September and October in Jeddah; August in Madina; and in August in Tabouk. Alyamani and Sen (1993, p. 131) also carried out a statistical analysis to assess monthly rainfall patterns over Saudi Arabia using monthly data at 29 stations with records more than 15 years from the Ministry of Environment, Water and Agriculture. They concluded that:

- (i) "four distinctive reasons of rainfall can be depicted within the Kingdom due to the movement of various air masses.
- (ii) monthly rainfall amounts are almost log-normally distributed in the Kingdom.
- (iii) as expected invariably the maximum rainfall concentrations are located in the mountainous heights in the southwestern corner. Additionally, in February and October there exists another concentration area of rainfall in the central provinces.
- (iv) standard deviation variations in all the months are rather wide which implies that the change in rainfall intensity might occur unexpectedly sudden throughout the Kingdom of Saudi Arabia."

2.2.2. Spatial variability in rainfall across Saudi Arabia

Spatial and temporal variations of rainfall in Riyadh city were evaluated by Al-Saleh (1997) using rainfall data (1964-1993) from three weather stations (Riyadh-R001, Riyadh Old Airport, and King Khalid Airport). The results showed high spatial and temporal variability in Riyadh city. Subyani (2004) applied geo-statistical methods in the southwest mountainous region of Saudi Arabia using data from 63 stations for a 21 year period. The results revealed high regional variations in rainfall across all seasons, while the variance decreased in rain shadow areas. Mashat and Abdel Basset (2011, p. 59) analysed monthly and annual rainfall using monthly precipitation data from 28 stations operated by the GAMEP. The highest amounts of rainfall occurred in spring and winter, respectively, because "the most significant synoptic feature appears in spring when the cold air associated with secondary Mediterranean depressions meets the moist hot southerly air associated with Red Sea trough over KSA". Al-Ahmadi and Al-Ahmadi (2014) examined relationships between

annual and seasonal rainfall from 75 stations with 35 year records, and five topographic factors derived from 30m ASTER DEMs (physiographic features, altitude, slope, proximity to a ridge or crest of mountains, and proximity to the Red Sea) in southwest Saudi Arabia using Kruskal–Wallis one-way analysis of variance. All local topographic factors were statistically significant in producing annual and seasonal rainfall and rainfall was higher at higher altitudes and in more mountainous areas, with steeper slopes and areas closer to ridges (Al-Ahmadi and Al-Ahmadi 2014).

At finer scales, rainfall is similarly patchy. Wheeler et al. (1991) provided the results of an extensive hydrological investigation of five wadis in the mountainous area of southwest Saudi Arabia, utilising hourly data from a network of 100 autographic rain gauges. Rainfall occurrences were highly localised, and the spatial distribution of rainfall was generally sparse, but some storms (once or twice per year) showed more widespread occurrence. In terms of the temporal distribution, they indicated that rainfall was mainly initiated in the late afternoon and lasted 1 hour or less (Wheeler et al. 1991). Wheeler (2008) explained this spatial variability in an intensive five-year study of the Wadi Yiba (2,869 km²) catchment in southwestern Saudi Arabia, instrumented with a dense network of rain gauges, with 8-10 km's between sites. About 51% of rainy days were only recorded at one or two of the 20 rain gauges and sub-daily rainfall showed an even more patchy picture. Some wadi flows were associated with this patchy rainfall, and where zero rainfall was observed locally. Therefore, the high spatial variability in rainfall Saudi Arabia requires an adequate density of rainfall stations to avoid serious deficiencies in analysing rainfall data. WMO (2008) has recommended minimum densities of stations (Table 2.1). Schyfsma (1978, p. 32) highlighted the inadequacy of climate data in the Arabian Peninsula stating, "the number and distribution of weather

observation stations in the area and the compiled data over the last few years are far from adequate for the accurate analysis of regional climatic data".

Table 2.1: Recommended minimum densities of precipitation stations (area in km² per station).

Physiographic unit	Non-recording	Recording
Coastal	900	9,000
Mountains	250	2,500
Interior plains	575	5,750
Hilly/undulating	575	5,750
Small islands	25	250
Urban areas	-	10-20
Polar/arid	10,000	100,000

Source: WMO (2008).

2.2.3. Rainfall frequency in Saudi Arabia

Several studies have performed frequency analyses of rainfall in Saudi Arabia (Sendil and Salih 1987; Al-Saleh 1997; AlHassoun 2011; Elsebaie 2012; Subyani and Al-Amri 2015; Abd Rahman et al. 2016; Alahmadi 2017; Ewea et al. 2017; Abdeen et al. 2020). Most of these studies demonstrated that Gumbel probability distribution (EVI) is the best model to describe the distribution of rainfall in Saudi Arabia. For Riyadh city, Sendil and Salih (1987) quantified frequencies of maximum rainfall with durations of 10, 60 and 720-minutes in Central Saudi Arabia by fitting EVI probability distribution. For example, the estimated 1-hour annual maximum rainfall return periods (2, 5, 10, 25, and 50 years) for Riyadh city are 9mm, 14mm, 17mm, 21mm, and 24mm, respectively. Al-Saleh (1997), using rainfall data (1964-1993) from three weather stations in Riyadh city, developed frequencies of 24-hour annual maximum rainfall for point rainfall and regional rainfall by fitting EVI probability distribution, indicating that the derived models can be used for prediction purposes.

AlHassoun (2011) developed an empirical formula to estimate rainfall intensity for Riyadh city, based on intensity–duration–frequency (IDF) curves generated from a 32-year (1963-1994) rainfall record at Riyadh Station. The highest value of annual extreme 30-minutes duration rainfall was 22.2mm, recorded in 1972. Moreover, the study concluded that there is little difference between Gumbel and Log Pearson Type III distribution (LPTIII) methods in results of rainfall analysis of IDF curves in Riyadh. The derived predicting model to obtain rainfall intensity I_T (mm/h) for any design storm of specified duration t_d (min) and return period T_r (years) for Riyadh city was as follows:

$$I_T = 153 * T_r^{0.35} / t_d^{0.82} \quad (2.1)$$

2.2.4. Remote sensed rainfall data

Globally, remotely sensed rainfall data and derived rainfall data can be used as a supporting or alternative data source to gauges, including datasets from the Tropical Rainfall Measuring Mission (TRMM), Climate Forecast System Reanalysis (CFSR), and TerraClimate. Almazroui (2011) used recorded daily rainfall data at 29 weather stations operated by the GAMEP to calibrate remotely sensed data from the TRMM for the period 1998–2009. Almazroui (2011) stated that daily precipitation comparisons show that TRMM precipitation trends are very similar to observed data. The TRMM precipitation data also closely follow the observed annual cycle on a monthly scale. The correlation coefficient of TRMM precipitation and rain gauge data was around 0.90, with a level of significance of 99% on the monthly scale. The TRMM average annual rainfall for the country is 89.42 mm, while the observed data is 82.29 mm. He suggested that the rainfall in Saudi Arabia is the value of TRMM

multiplied by 0.93 plus 0.04. After this calibration, the TRMM precipitation is almost 100% of the observed data.

Kheimi and Gutub (2014) evaluated the performance of satellite precipitation products of TRMM 3B42, CMORPH, GSMaP_MVK and PERSIANN in Saudi Arabia using daily rainfall from 29 rain gauges for the period 2003-2010. The authors concluded that TRMM 3B42 data offers the best possibility for accurate estimation of precipitation and that, overall, all products can predict rainfall in the study area reasonably well but with overestimation in some regions of Saudi Arabia.

Tekeli and Fouli (2016) used the TRMM 3B42 real time (RT) to forecast flash flooding in Riyadh city. The authors used the 3 hourly TRMM 3B42RT images for the 2000–2013 period to develop three flash flood indices which are Constant Threshold (CT), Cumulative Distribution Functions (CDF) and Riyadh Flood Precipitation Index (RFPI). They concluded that only indices of RFPI and CDF with 90% threshold detected all the three major flooding events that occurred in February 2005, May 2010 and November 2013 in the Riyadh city.

Sultana and Nasrollahi (2018) evaluated daily and monthly remotely sensed precipitation data in Saudi Arabia, obtained from five satellites with a $0.25^\circ \times 0.25^\circ$ spatial resolution (PERSIANN, PERISANN-CDR, TRMM-RT, TRMM-3B42, and CMORPH) for the period from January 2003 to December 2011. The authors concluded that most of the satellite data provide better estimates of rainfall in the west and east regions during the wet season (November through April), but poor performance in the eastern region during the dry season (June to September). Overall, PERSIANN-CDR, TRMM-3B42 and CMORPH performed the best over Saudi Arabia.

Mahmoud et al. (2018) attempted to validate the IMERG satellite rainfall products of early, late and final runs throughout Saudi Arabia for the period from October 2015 to April 2016. The authors concluded that the IMERG early run and late run products only work well in some regions and that the final run product performed significantly better than these other products over most of Saudi Arabia. They state that the IMERG final run product could complement or substitute the measured ground data for poorly gauged or ungauged regions.

2.2.5. Changes in rainfall through time

It has been reported that rainfall generally decreased throughout the first decade of the 21st century in Saudi Arabia. The Presidency of Meteorology and Environment (2011) indicated that the period 2004-2008, showed that of 26 weather stations across Saudi Arabia, 6 had a positive trend, 13 had a negative trend, and 7 showed a steady trend. These varying trends of rainfall do not clearly indicate the impact of climate change on the amounts of rainfall in the country. Perhaps the variations in rainfall trends, in the country, are related to the rainfall variability in time and space. Hasanean and Almazroui (2015) used observed rainfall data from 26 stations (GAMEP) in Saudi Arabia and found a decreasing linear trend of 6.2 mm per decade during the period 1978–2009, with the period 1994-2009 having a statistically significant decreasing trend of 47.8 mm per decade.

Using the interpolated monthly rainfall dataset of the Global Precipitation Climatology Centre (GPCC) for the period 1981–2019, Alsaaran and Alghamdi (2022) explored spatial features and temporal trends of precipitation over the Arabian Peninsula. The results of their study showed that the average annual areal

precipitation over Arabia is 88.61 mm, receiving about 40%, 29%, 18%, and 13% during the boreal spring, winter, fall, and summer seasons respectively. The authors reported that boreal winter and spring rainfall over Arabia had statistically significant decreasing trends at rates of -3.65 mm (14.3%) and -5.66 mm (15.8%) mm per decade, respectively, pointing out that the decreasing trend of rainfall in this wet season over the whole of Arabia has not been reported in any previous work.

In contrast, some studies of climate change in Saudi Arabia have found an increase in the frequency and intensity of rainfall events. Based on rainfall data for the period from 1971 to 2012, Subyani and Hajjar (2016) analysed rainfall in the Jeddah region and concluded that rainy months had more intense rainfall and drier months less rainfall due to the impact of climate change. Abu Abdullah et al. (2019) reported that Saudi Arabia has been facing significant changes in rainstorm intensities, frequencies, and distributions leading to flash flood events over the last decade. Almazroui (2020) emphasised that the frequency of intense rainfall events was increasing, and the frequency of weak events was decreasing for most meteorological stations in Saudi Arabia. Luong et al. (2020) investigated changes in large-scale weather patterns associated with extreme precipitation events over Jeddah and concluded that extreme precipitation events are becoming less frequent but more intense.

The above-reviewed studies have revealed that rainfall in Saudi Arabia is characterised by low quantities, irregularity, variability in space and time, and long-term changes in intensity and quantities.

2.3. Runoff and floods in Saudi Arabia

2.3.1. Background

Despite the aridity of Saudi Arabia, rainfall can be intense enough to generate local runoff. Some storms with low frequencies can be very intense and can lead to flash flooding. For example, Alamri (2011) reported that at about 6:30 am on Wednesday 25th November 2009, heavy rainfall began in Jeddah, and lasted about 12 hours. The rainfall amount was about 90 mm which was double the average annual rainfall in Jeddah. With no proper infrastructure and no proper sewage system, this event of rainfall turned out to be the worst disaster Jeddah has seen in 27 years or so.

Therefore, the following five subsections represent summaries of previous studies on runoff and flood hazards in Saudi Arabia. It should be noted clearly that three of the following studies on runoff (Rahman et al. 2016; Sharif et al. 2016; Radwan et al. 2018) are closely related to the topic and area of this current study and, therefore, special emphasis has been given to these (subsection 2.3.3). Previous studies on runoff, discharge, and flood were thematically grouped and then sequentially reviewed for each group based on the year of publication.

2.3.2. Urban flooding in Saudi Arabia

Although central Saudi Arabia is a dry environment, severe runoff may occur causing flooding. For example, Naval Intelligence Division (2005) described floods and torrents in some areas of Saudi Arabia stating that in the centre of the Najd region, the ancient city of Al-Yamamah, southeast of Riyadh, is believed to have been destroyed by a flood in Wadi Hanifa. Farther south in the same area extensive damage, with loss of life among humans and stock, occurred in the

upper part of Wadi Al-Dawasir and one of its tributaries in the summer of 1917; it was not known that the valley flowed in living memory, but a violent flood, descending from the mountains, caused destruction and loss of life in the channel of Wadi Tathlith; it even reached the villages in the Wadi Al-Dawasir oasis, where a small village was destroyed and many wells at the bottom of the valley were destroyed.

Al Saud (2010, p. 847) assessed flood hazard risk in Jeddah region concluding that the chaotic urban expansion along watercourses has significantly increased the risk of flooding. This is supported by Daoudi and Niang (2019) who highlight that in the 1970s, Jeddah City received large amounts of rainfall (e.g. 1972, 1973, 1978, and 1979) but no floods occurred due to the absence of urban expansion in this period in risk areas. Similarly, 1996 had exceptional rainfall but no major floods occurred. Daoudi and Niang (2019) hypothesis that more recent flooding is associated with unplanned major urban expansion.

Alamri (2011) highlighted the flood damage over a 30-year period in Saudi Arabia and the lack of preparations for such hazards. The author mentioned that several lessons can be derived from the Jeddah 2009 and the Riyadh 2010 floods. He stressed that history repeats itself: first as tragedy, second as farce' which has been true in the history of disasters in Saudi Arabia. Floods hit the country several times in 2000, 2001, 2003, 2005, 2009 and 2010. But the lessons from these events go unnoticed. The preparations for such disasters are still lacking and people are returning to their normal lives as if nothing had happened. It may be because of the widely accepted position that what God has ordained will happen, and there is nothing we can do about that.

Al-Momani and Shawaqfah (2013) analysed remotely sensing images and DEMs in a GIS to provide basic information for preliminary flood risk assessments and mapping for the city of Tabuk. Youssef et al. (2015) used remote sensed images and GIS to examine causative factors of 2009 and 2011 flash flooding in Jeddah city, finding that geomorphological features, anthropogenic activities (urban changes), network and catchment factors, and rainfall and climatic changes factors, were all important. In particular, increased rainfall intensity coupled with steep and narrow wadi tributaries can generate flash flooding in the area. Anthropogenic activities such as the proliferation of slums and construction in valleys without suitable water management increase flood risk.

Al-Zahrani et al. (2016) used the Curve Number method to estimate runoff in the city of Hafr Al-Batin, Saudi Arabia, reporting that the method proves to be applicable in different environments, is reliable and gives appropriate results despite its simplicity and similar results obtained compared to very complex models. The authors estimated the inundated area of Hafr Al-Batin city to be 9.21, 10.11, 10.72, 11.3, 12.51 and 13.41 km² for the 2-, 5-, 10-, 25-, 50- and 100-year return periods, respectively, which represent 7.5%, 8.3%, 8.8%, 9.3%, 10.3% and 11.0% of the total area (122 km²). They stressed that the city is expected to experience flooding even for events with small return periods because of its location and topography.

2.3.3. Urban flooding in Riyadh

Three published papers have examined flash floods in Riyadh city (Rahman et al. 2016; Sharif et al. 2016; Radwan et al. 2018). All three studies do not included any information about the calibration

and validation of the models applied to estimate flash floods in Riyadh. These studies are critically reviewed.

Rahman et al. (2016) aimed to calculate a composite flash flood vulnerability index (CFVI) for Riyadh. To get the composite flood vulnerability index (CFVI) they multiplied the physical vulnerability index by the social vulnerability index ($CFVI = PVI \times SVI$). The PVI was computed by dividing the square root of the product of ranked physical variables by the total number of variables. The physical variables included in their study were land elevation, soil, vegetation, and urban land use and simulated rainfall using the Gridded Surface Subsurface Hydrologic Analysis (GSSHA) of Watershed Modelling Systems (WMS v. 9.1). To construct the social vulnerability index (SVI), the authors transformed social variables into a standardized score for the study area which includes neighbourhood census data on population density, percentage of population <7 years and >65 years of age, percentage of population non-Saudi Arab, percentage of population Asian, percentage of the population unemployed and/or not in the labour force, and percentage of land under urban residential and road transport network use. The results of their study emphasised that the CFVI map revealed that the low-lying central and southern half of the city was highly vulnerable; northern and north-eastern peripheral neighbourhoods were moderately to highly vulnerable; and western neighbourhoods were the least vulnerable to flash flooding. Low-income and unemployed expatriate families living in densely populated central, south, and south-eastern neighbourhoods were more vulnerable to flooding than rich Saudi families living in the sparsely populated northern half of the central city, western, north-western, and southwestern neighbourhoods.

The results of Rahman et al. (2016) appear to conflict with reality. By looking at rainfall amounts during the occurrences of floods in Riyadh between 1985 and 2016 as shown in the Table 1 of their study, the highest amount of 24-hours rainfall was 41.5mm in 2011. Besides, the highest annual rainfall in Riyadh weather station records for the period 1964-2017 was 234 mm in 1995. Therefore, simulating 60 mm per hour for 6 continual hours (360 mm/6h) was highly exaggerated to compute PVI. Moreover, the simulation results that flash floods attain a maximum height of 5.8 m will inundate large sections of central and southern neighbourhoods of Riyadh city doesn't coincide with the actual neighbourhoods frequently flooded. This is because most of central and southern neighbourhoods are relatively old urban areas and have storm water drainage. In fact, neighbourhoods frequently flooded are in the east and northeast in areas with low slope which do not have an efficient storm water system. Actually, Riyadh's mayor pointed out, in a press conference following floods on 3rd May 2010, that no floods occurred at the Riyadh neighbourhoods with efficient storm water drainage networks such as Al Malaz and Al Maather residential neighbourhoods. Furthermore, the hydrological modelling in this paper was limited to the built-up areas of the Riyadh city which only occupy the lower and middle reaches of two main catchments. This means that major areas contributing to flooding water were excluded.

Sharif et al. (2016, p. 716) examined flash flooding and estimated peak discharge for 5, 25 and 100 years return periods in the Wadi Al-Aysen catchment (with a drainage area of 191 km²) located in north-west Riyadh using the Hydrologic Engineering Center - hydrologic modelling system (HEC-HMS). The authors reported that the 2015 level of urbanisation of the Wadi Al-Aysen basin "increased the pre-development peak discharge by 525%, 150%, and 80% for the 5-year, 25-year, and 100-year storms, respectively". They have

produced a map showing the areas with runoff depth ranging between 100 mm and 400 mm for the 100-year storm and have defined them as the hazard areas within the basin. Although not mentioned by the authors, it should be emphasised that storm water drainage was constructed for the lower and middle reaches of the basin in 1999/2000 (Al-Fuhaid, 2013), which means that urban areas within this basin would be less hazardous than other built-up areas of Riyadh without stormwater drainage. As stated frankly by the mayor of Riyadh in a press conference following flood on the 3rd of May 2010, that there were no floods occurred at the Riyadh neighbourhoods having efficient storm water drainage networks (Alhaddan, 2010). In addition, the produced flood hazard map has demonstrated that some of the hazardous areas in the basin were located in the upper reaches and near the basin boundary, but the study did not include any explanation for this. Moreover, the most hazardous areas in the map were mainly road tunnels, which are designed with their own stormwater drainage.

Radwan et al. (2018) used a 30 m resolution DEM, geologic map, soil map, and precipitation data downloaded from the Climate Forecast System Reanalysis (CFSR) to apply the CN method to estimate runoff volume for 40 urban watersheds in Riyadh with a total area of 8,500 km². They provided some geomorphological and hydrological characteristics of the delineated 40 basins as shown in

Table 2.2. However, it should be emphasised that some minor and major limitations have been found in the paper. The map of the delineated 40 basins in their study area does not show any names or numbers of the basins. Therefore, it is difficult to locate the basins numbered in their study area. Moreover, with the exception of the Wadi Hanifa and the Wadi As Silayy basins, the other 38 are outside the boundary of greater Riyadh as determined officially by Riyadh Development Authority (Qhtani and AlFassam 2011; Minister of Municipal and Rural Affairs 2019). In addition, the study only used the CFSR maximum daily rainfall data despite the availability of measured climate data from three climate stations and three rain gauges. As such, the authors report that the annual rainfall in Riyadh is about 62 mm, but this is an underestimate based on observed data from the climate and rain gauge stations (presented in Chapter 4). Likewise, it can be noticed that the SCS runoff equation reported in their study is not the same as the original formula reported by USDA (1986) and used in recent studies (Al-Zahrani et al. 2016; Khalil 2017). In the original SCS runoff equation the initial abstraction (I_a) = $0.2S$, where S = potential maximum retention after runoff begins ($S = 25400/CN - 254$). Whereas the authors of the paper have reported that $I_a = 0.05S$. According to the authors' results presented in

Table 2.2, basin no.1 was estimated runoff of 22.72 mm, but if using the original equation, the estimate would be 15.57 mm, giving a difference of 31.5%.

Table 2.2: Curve number (CN) and potential direct runoff for urban watersheds of the Riyadh metropolitan area.

HSG	Watershed no.	Area (km ²)	Average slope (%)	Watershed CN	Precipitation (mm)	S (mm)	I _a (mm)	Q (mm)
A	1	22	6.8	77	58.2	75.87	3.79	22.72
	2	18	5.8	77	58.2	75.87	3.79	22.72
	3	12	9.9	77	52.7	75.87	3.79	19.17
	4	30	7.1	78	51.6	71.64	3.58	19.27
	5	10	8.2	80	50.9	63.50	3.18	20.48
B	6	141	2.9	86	45.7	41.35	2.07	22.40
	7	44	3.6	86	45.7	41.35	2.07	22.40
	8	132	2.8	88	45.7	34.64	1.73	24.59
C	9	515	2.8	90	47.9	28.22	1.41	28.93
D	10	45	4.6	91	58.2	25.12	1.26	39.51
	11	20	5.5	91	45.6	25.12	1.26	28.31
	12	2,389	3.8	91	47.7	25.12	1.26	30.14
	13	6	5.9	91	50.9	25.12	1.26	32.96
	14	1,013	3.4	92	47.6	22.09	1.10	31.52
	15	447	12.9	93	53.8	19.12	0.96	38.80
	16	6	4.9	93	45.6	19.12	0.96	31.26
	17	2,945	8.8	94	47.8	16.21	0.81	34.94
	18	98	2.7	94	53.0	16.21	0.81	39.82
	19	33	2.5	94	53.0	16.21	0.81	39.82
	20	97	3.0	94	53.0	16.21	0.81	39.82
	21	22	2.6	94	53.0	16.21	0.81	39.82
	22	58	2.8	94	53.0	16.21	0.81	39.82
	23	49	3.6	94	45.6	16.21	0.81	32.89
	24	46	5.3	94	58.2	16.21	0.81	44.75
	25	28	13.2	94	52.0	16.21	0.81	38.88
	26	21	5.7	94	53.2	16.21	0.81	40.01
	27	16	6.2	94	45.6	16.21	0.81	32.89
	28	16	4.8	94	50.9	16.21	0.81	37.84
	29	12	6.4	94	58.2	16.21	0.81	44.75
	30	24	9.3	94	52.0	16.21	0.81	38.88
	31	12	17.3	94	56.0	16.21	0.81	42.66
	32	14	9.3	94	56.0	16.21	0.81	42.66
	33	27	16.5	94	56.0	16.21	0.81	42.66
	34	13	16.2	94	56.0	16.21	0.81	42.66
	35	3	11.4	94	56.0	16.21	0.81	42.66
	36	7	5.0	94	51.0	16.21	0.81	37.94
	37	1	7.9	94	45.6	16.21	0.81	32.89
	38	2	6.9	94	45.6	16.21	0.81	32.89
	39	7	4.2	94	45.6	16.21	0.81	32.89
	40	6	4.5	94	45.6	16.21	0.81	32.89

Source: Radwan et al. (2018).

2.3.4. Statistical models of runoff in Saudi Arabia

Runoff is variable in space and challenging to measure. As such, runoff across catchments is typically modelled from precipitation data and information about catchment land use and slope. Three statistical models have been provided to estimate runoff coefficients in ungauged wadis in Saudi Arabia using relationships between runoff and drainage basin morphometric variables (Sen and Al-Subai 2002, Al-Hasan and Mattar 2014). It should be noted that the models

provided by Sen and Al-Subai (2002) and Al-Hasan and Mattar (2014) were generated by using measured annual runoff data with limited record length from large drainage basins. In addition, the statistical models provided were not validated.

Sen and Al-Subai (2002) used observed annual surface runoff for the period 1970-1986 in the Tihamat region (Wadi Baysh, 4,652 km²; Wadi Damad, 1,108 km²; Wadi Jizan, 1,430 km²; Wadi Khulab, 900 km²) estimating runoff coefficients between 0.048 to 0.078. They suggest an equation based on an exponential relationship with the basin area to estimate runoff coefficients for ungauged wadis as follows:

$$C_R = A^{-0.359} \quad (2.2)$$

Where

C_R = runoff coefficient

A = basin area in square kilometres

Al-Hasan and Mattar (2014, p. 2028) used data from 16 runoff gauges with different recording years (Table 2.3) and geomorphic parameters in an attempt to develop linear regression models to estimate mean runoff coefficient for ungauged streams in Saudi Arabia. Based on the values of main stream slope (S_m), the authors divided the studied basins into two groups. Group A included basins with main stream slope (S_m) < 0.01, whereas group B included basins with main stream slopes (S_m) ≥ 0.01. They found positive correlations between measured runoff coefficients and main stream slopes in both groups of catchments, although it was much stronger in group A. The authors suggested two regression equations as follows:

1) the equation for ungauged wadis with stream slopes <0.01 is:

$$C_{Re}=0.498 \times S_b \quad (2.3)$$

where

C_{Re} = estimated runoff coefficient of the ungauged wadi

S_b = the basin slope

2) the equation for ungauged wadis with stream slopes equal to or greater than 0.01 is:

$$C_{Re}=2.841 \times S_m \quad (2.4)$$

where:

S_m = the main-stream slope

Abdel-Lattif and Al-Shamrani (2013, p. 15) have aimed "to create a simplified method to estimate the runoff coefficient of ungauged streams to calculate annual runoff volume" in south-western Saudi Arabia. They used runoff coefficients for 16 catchments calculated by Al-Hasan and Mattar (2014) to correlate log runoff coefficients with log areas. The generated model in their study was:

$$\text{Runoff Coefficient } R_c = -0.01 \ln (A) + 0.12 \quad (2.5)$$

where A represents the basin area in km^2 .

Table 2.3: Average recorded volume of annual runoff and average measured runoff coefficient (C_{Rm}) in Saudi Arabia.

Station name	Geographic Coordinates		Recording years	Basin area (km ²)	Basin slope (S_b) m/m	Stream slope (S_m) m/m	Average annual rainfall (mm)	Average annual runoff ($\times 10^6 m^3$)	Average Runoff Coefficient (C_{Rm})
	Lat. North	Long. East							
Yiba	19.042°	41.458°	1972–1978	2,861	0.221	0.016	254	25.62	0.0353
Tabalah	20.028°	42.270°	1969–1983	1,186	0.128	0.010	267	14.24	0.0450
Tathlith	19.535°	43.515°	1967–1979	12,816	0.052	0.006	85	6.42	0.0059
Bissel	21.194°	40.714°	1968–1985	235	0.112	0.015	168	2.62	0.0663
Hali	18.768°	41.574°	1968–1985	4,898	0.244	0.015	354	95.61	0.0551
Khulis	22.194°	39.456°	1966–2000	2,855	0.135	0.009	94	20.13	0.0750
Ranyah	21.188°	42.763°	1973–1992	10,216	0.063	0.004	160	53.04	0.0324
Khulab	16.716°	43.018°	1972–1984	783	0.238	0.033	450	31.52	0.0895
Jazan	17.046°	42.954°	1970–1986	1,410	0.249	0.028	528	56.99	0.0766
Damad	17.149°	42.904°	1970–1986	994	0.297	0.032	515	40.40	0.0789
Baysh	17.573°	42.612°	1970–1986	4,808	0.326	0.013	373	76.07	0.0425
Hanifah	24.658°	46.609°	1965–1983	1,637	0.065	0.003	86	4.88	0.0347
Al Khanaq	24.424°	39.944°	1969–1980	35,659	0.025	0.003	61	11.95	0.0055
Al Hinakiyah	24.867°	40.505°	1969–1980	3,105	0.030	0.005	71	3.50	0.0159
Uqlat As Suqur	25.834°	42.219°	1969–1982	3,1850	0.024	0.002	63	25.25	0.0126
Ar Rass	25.750°	43.167°	1969–1980	78,989	0.014	0.002	67	12.31	0.0023

Source: Al-Hasan and Mattar (2014).

El Maghraby et al. (2014, p. 287) provided a general framework for assessing runoff in the basin (covering an area about 104,679 km²) in the city of Al Madinah through the integration between Geographic Information System (GIS), morphometric parameters and very scarce data measurements. The authors concluded that the runoff volumes of the Wadi Al Hamd sub-basin were estimated for four different storms (23.5 mm, 14 mm, 20 mm, and 30 mm) whose return periods ranged from 1.5 to 2 years with a probability of 63% to 44%.

Khalil (2017) used the CN method to estimate runoff for 12 drainage basins in the vicinity of Jeddah city, ranging in area 6.98 to 555.5 km². The author used estimated daily rainfall of the 100-year return period (106.3 mm) to calculate runoff depth and volume for each basin (Table 2.4). However, the runoff coefficients differ greatly from the average measured runoff coefficient (C_{Rm}) reported by Al-Hasan and Mattar (2014), mentioned above. For example, based on the estimated daily rainfall of the 100-year return period and the values presented in Table 2.4, the runoff coefficients for the basin B1 is 0.71.

Table 2.4: Geomorphological and runoff characteristics for 12 drainage basin in the vicinity of Jeddah city.

Basin No.	Basin area (km ²)	Longest flow path (m)	CN	Slope %	Runoff depth (mm)	Runoff volume (million m ³)
B1	555.47	77,410.48	88.8	5.63	75.8	42.553
B2	143.28	32,825.69	91.4	5.25	82.5	11.452
B3	192.27	42,556.96	90.3	4.60	80.3	14.382
B4	448.60	62,297.97	90.7	5.83	80.8	36.001
B5	59.04	12,715.07	88.7	1.37	75.5	4.501
B6	201.10	35,140.56	90.5	7.62	80.4	16.458
B7	84.79	19,882.92	87.5	3.22	72.7	6.224
B8	14.61	10,231.69	93.6	2.11	88.1	1.287
B9	9.40	7,486.95	93.6	2.14	88.0	0.827
B10	6.98	9,332.22	93.5	2.12	87.8	0.613
B11	15.47	9,040.97	91.2	1.64	81.8	1.265
B12	11.21	8,113.69	91.5	1.43	82.3	0.923

Source: Khalil (2017).

Al-Ghobari et al. (2020) integrated remote sensing with the GIS-based soil conservation service curve number (SCS-CN) method to estimate the surface runoff in the Wadi Uranah catchment in the western region of Saudi Arabia. Different thematic maps including slope, hydrologic soil group (HSG), LULC, and daily rainfall were created in the GIS environment and processed to generate the CN and surface runoff maps. The authors reported that a linear regression between rainfall and runoff showed a very strong correlation of 0.98. Peak flows in the wadi for 10-year, 50-year, and 100-year return periods were 828, 1,353, and 1,603 m³/s, respectively.

Alhumimidi (2020) applied the SCS-CN method to estimate the potential runoff in the mountain catchment of the Wadi ḍamâd (1,084 km²), Southwest Saudi Arabia. The study used maximum daily rainfall at six stations (ḍamâd, Ayban, Wadi ḍamâd, Jabal Fayfa, Malaki, and Al Aridhah) for the period 1970 to 2016. The average of the maximum daily rainfall varies from 37.4 mm at the Malaki station and 51.6 mm at the Ayban station. The author used the land resources map scale 1:500,000 to obtain CN stating that the CN is 62 at ḍamâd, 66 at Ayban and Jabal Fayfa, and 70 at Wadi ḍamâd, Malaki, and Al Aridhah. The results indicated that the runoff coefficient of the wadi did not exceed 17.6% giving average yearly runoff of 16.1 mm at ḍamâd, 71.0 mm at Ayban, 53.0 mm at Wadi ḍamâd, 49.7 mm at Jabal Fayfa, 19.8 mm at Malaki, and 30.5 mm at Al Aridhah.

2.3.5. SWAT modelling in Saudi Arabia

The SWAT is a spatially semi-distributed physically-based hydrological model developed mainly for humid environments, and also it has been successfully applied to arid environments (as

described in section 4.2.). To the best of the author's knowledge, the use of the SWAT model to estimate runoff in Saudi Arabia is very limited. Sultan et al. (2015) and Fallatah et al. (2019) are the only two studies that used the SWAT model for hydrological modelling in Saudi Arabia. The SWAT models applied in these two studies were not validated.

Sultan et al. (2015) applied the SWAT model to estimate streamflow in 19 major eastern Red Sea catchments originating in high mountains and discharging downstream into the Red Sea and Gulf of Aqaba. Estimated streamflow ranged from 0.09 mm in Wadi Ifal to 33.8 mm in Wadi Haly. It is worth mentioning that Sultan et al. (2015) used parameters values of the calibrated SWAT model for the Wadi Girafi catchment in Sinai (Milewski et al. 2009) to simulate the eastern Red Sea catchments assuming that the basins in the two areas have similar characteristics. Thus, they applied regionalisation to extrapolate catchment-specific parameters from the Wadi Girafi catchment in Sinai Peninsula, Egypt. Of course, every catchment is distinct, and ideally model parameters should be calibrated on a catchment-by-catchment basis, rather than being spatially generalised.

Fallatah et al. (2019) applied the SWAT model for the assessment of modern recharge of the Saq aquifer in Saudi Arabia. The authors obtained the essential inputs of the SWAT model from: 1) climatic data extracted from the Global Weather Data (GWD); 2) a Digital Elevation Model (DEM) from the Shuttle Radar Topography Mission (SRTM) with spatial resolution 90 m; 3) soil data from Saudi Arabia geological mapping, and; 4) land use data from Global Land Cover with 30 m resolution. Like Sultan et al. (2015), the authors used 12 SWAT model parameters calibrated for the Wadi Girafi catchment in Sinai, Egypt (Milewski et al. 2009) based on the assumption that the

Wadi Girafi catchment (3,350 km²) exhibits similar climatic and topographic characteristics, areal extent, and soil types compared to catchments in their study area (about 377,080 km²). The simulated runoff results in modelled catchments ranged from 2.18 mm in the Al Baten catchment (area 27,496 km² and precipitation 55.77 mm) to 11.71 mm in the Al Rumah catchment (area 215,521 km² and precipitation 59.79 mm). These results mean that the runoff coefficients were 0.0391 and 0.1958 in the Al Baten catchment and the Al Rumah catchment, respectively.

2.3.6. Discharge estimation

In addition to modelling surface runoff, some studies have estimated catchment discharge in Saudi Arabia.

The Institute of Hydrology (1984) studied the design flood of the catchment area of the Wadi Mushwab above the dam to use its flat land for future urban development in Jeddah city. The Institute of Hydrology used formulas that consider the stream length and slope to estimate flood peak discharge and total volume runoff for each return period (years) in the undeveloped catchment area (37.9 km²) with 10% runoff and predicted the future in a developed urban case with 20% runoff as shown in Table 2.5. For example, the 5-year return period runoff had volumes of 237,300 m³ and 495,907 m³ in the non-urbanised catchment and urbanised catchment respectively.

Tahir Hussein et al. (2009) used daily rainfall at King Khalid Airport station for the period 1985-2005 to estimated peak discharge in a small basin (11.26 km²) located within an urban centre in the northwest of Riyadh city between longitudes 46°37'26"E - 46°39'20"E and latitudes 24°45'00"N- 24°46'45"N. The authors applied the rational formula using 0.75 runoff coefficient and

reported that the maximum annual daily rainfall was 47.8 mm with peak runoff 4.67 m³/s and the minimum annual daily rainfall was 25.4 mm with peak flow 2.48 m³/s. They also assumed higher values of rainfall storms at 2.5 mm/h and 5 mm/h resulting into peak flows 5.86 m³/s and 11.73 m³/s respectively.

Table 2.5: Flood Peak and Total Volume Runoff for the catchment area above the Mushwab dam, Jeddah.

Return Period (Years)	Design Flood (m ³ /s)		Total Volume Peak of Flood Runoff (m ³)	
	Present Undeveloped Case	Future urbanised case	Present Undeveloped Case	Future urbanised case
5	10.50	35.98	237,300	495,907
10	13.32	44.44	296,440	609,570
20	14.83	49.45	329,000	680,410
50	19.34	67.43	433,359	919,389
100	22.09	75.79	500,408	1,047,900

Source: Institute of Hydrology (1984).

Dawod and Koshak (2011) used the National Resources Conservation Service (NRCS) method to estimate peak discharges for six drainage basins (drainage areas between 360.6 km² to 74.3 km²) within the holy Makkah metropolitan area, west Saudi Arabia. Time to peak discharge of the basins varied from 1.15 hours to 4.47 hours, and the peak discharges range from 10.14 m³/s to 16.74 m³/s. The authors concluded that the smallest basin had the shortest time to peak discharge, making it the most hazardous catchment. A similar study was carried out by Al-Ghamdi et al. (2012) also used the NRCS method to estimate peak discharge and flood volume in Makkah city for the 1990 and 2010 floods, and to assess urbanisation impacts on flood hazard. The authors concluded that the built-up areas of Makkah city had increased by 197% from 1990 to 2010 and the total flood volumes enlarged by 248%.

Al-Shareef et al. (2013) used peak discharge measurements for the Wadi Marwani basin in Jeddah, Saudi Arabia (catchment area of

2,875 km²) to estimate the return periods of peak discharge by applying EVI distribution. The main objective of their study was to compare four estimating peak discharges methods with measured peak discharge to recommend the most accurate model for peak discharge estimation. The applied models were the Hydrologic Engineering Center-Hydrologic Modeling System (HEC-HMS), the probabilistic rational method (PRM), the modified Talbot method (MTM) and regional flood frequency analysis (RFFA) regression equations. They concluded that the PRM was an accurate model, the HEC-HMS was the second most accurate model and the MTM and RFFA equations had much higher errors.

2.4. Application of the SWAT model in arid regions

Although an appreciable number of studies use SWAT in semi-arid regions, the application of SWAT models in arid environments is rare, especially compared to its application in other climates. The SWAT Literature Database documents approximately 4,700 studies for the period 1984 to March 2022 and 280 of these studies were conducted in arid or semi-arid environments. A total of 125 of these studies applied the SWAT model in arid and semi-arid regions. Three articles have reviewed SWAT modelling in arid and semi-arid lands, revealing good performance (Kiros et al. 2015; Samimi et al. 2020; Akoko et al. 2021). Five of the reviewed SWAT studies were uncalibrated (Chaponniere et al. 2003; Al-Dousari et al. 2010; Zende and Nagarajan 2015; Khan et al. 2020; Toosi et al. 2020). Instead of using conventional statistical tests that compare simulated streamflow or ET with measured or generated data, Perrin et al. (2012) and Milewski et al. (2014) calibrated SWAT models using field-based observations and remote sensing data. Both studies did not include any information about the SWAT parameters used, nor their values before and after model calibration. Four SWAT studies adapted the regionalisation approach to apply SWAT models using

parameters derived from other areas with similar characteristics (Sultan et al. 2015; Fallatah et al. 2019; Mengistu et al. 2019; Mengistu et al. 2020). The remaining 111 studies applied conventional statistical tests (e.g., NSE and R^2) for calibrating and validating models using streamflow data.

Studies using conventional statistical methods (e.g., NSE and R^2) to calibrate and validate the SWAT model in arid and semi-arid regions were derived from China (39 studies), Iran (22 studies), the USA (15 studies), India (11 studies), Morocco (7 studies), Tunisia (5 studies), South Africa (4 studies), Turkey (3 studies), Italy, Jordan, Kuwait, Saudi Arabia (all 2 studies), Algeria, Australia, Egypt, Mexico, Nepal, Palestine, Peru, and Portugal (all 1 study). These SWAT model applications in arid and semi-arid regions covered several topics.

For reviewing purposes, studies that applied the SWAT model in arid and semi-arid environments were grouped based on their objectives into three types which are runoff and discharge simulation, assessment of water resources, and evaluation of the impact of LULC changes on runoff and discharge processes. From each group, one paper in the areas close to the current study area was selected and summarised.

2.4.1. Runoff and discharge simulation

A considerable number of studies applied the SWAT model to simulate runoff and discharge in different arid and semi-arid environments (Menking et al. 2003; Chaponnière et al. 2008; Xu et al. 2009; Li et al. 2010; Fadil et al. 2011; Luo et al. 2012; Niraula et al. 2012; Mosbahi et al. 2015; Jajarmizadeh et al. 2014; Yuan et al. 2014; Jajarmizadeh et al. 2015; Matin and Bourque 2015; Mosbahi et al. 2015; Singh et al. 2015; Suliman et al. 2015; Jajarmizadeh et

al. 2016a; Jajarmizadeh et al. 2016b; Liu et al. 2016; Srinivas et al. 2016; Tian et al. 2016; Zhang et al. 2016a; Zou et al. 2016; Brouziyne et al. 2017; Khelifa et al. 2017; Li et al. 2017; Licciardello et al. 2017; Makwana and Tiwari 2017; Qi et al. 2017; Zhang et al. 2017; Gao et al. 2018; Paul and Negahban 2018; Ahmadi et al. 2019; Aqnouy et al. 2019; Bouslihim et al. 2019; Eini et al. 2019; Koycegiz and Buyukyildiz 2019; Markhi et al. 2019; Zhang et al. 2019; Gu et al. 2020; Meng et al. 2020; Mosbahi and Benabdallah 2020; Nasiri 2020; Pradhan et al. 2020; Pulighe et al. 2020; Abu-Zreig and Hani 2021; Esmali et al. 2021; Koycegiz et al. 2021; Carlos Mendoza et al. 2021; Peng et al. 2021). For example, a recent study assessed a SWAT model to simulate runoff in the arid environment of the Yarmouk River catchment, Jordan (Abu-Zreig and Hani 2021). The monthly statistical results indicated very good performance for calibration and satisfactory for validation, with indices for calibration and validation of $R^2 = 0.95$ and $NSE = 0.96$ and $R^2 = 0.91$ and $NSE = 0.63$, respectively.

The simulated runoff depths and/or discharge rates agree with observed data in the majority of these studies. Most of the reviewed studies were calibrated and validated using conventional statistical tests (e.g., NSE and R^2) and have proved the good performance of the SWAT model in arid areas. Table 2.6 shows the performance indices of models in 46 previous studies that applied the SWAT model to simulate runoff in arid and semi-arid environments. The NSE for calibration in these studies ranged between -0.12 and 0.96. Based on the NSE results, in 52% of studies, the model was with very good performance; in 9% of studies, the model was with good performance; in 26% of studies, the model was with satisfactory performance; in 9% of studies, the model was with acceptable performance; in 4% of studies, the model was with unsatisfactory performance.

Table 2.6: SWAT models performance indices in previous studies simulating runoff in arid and semi-arid environments.

Studies	Number of parameters used	Time step	Calibration		Validation	
			Period Length	Performance Indices	Period Length	Performance Indices
Chaponnière et al. 2008	unavailable	daily	10 months	NSE 0.83	six separate hydrological years	NSE ranged between 0.11 and -0.53
Xu et al. 2009	20	daily	3 years	NSE 0.60 and 0.90, R ² 0.75 and 0.90	3 years	NSE 0.60 and 0.85, R ² 0.60 and 0.90
Li et al. 2010	32	daily	4 years	NSE 0.77	3 years	NSE 0.46
Fadil et al. 2011	14	monthly	9 years	R ² 0.81, NSE 0.80, PBIAS -1.01, RSR 0.44	8 years	R ² 0.89, NSE 0.85, PBIAS 8.69, RSR 0.38
Luo et al. 2012	unavailable	daily	20 years	NSE 0.68 and 0.76, PBIAS -4.0 and -2.6	20 years	NSE 0.62 and 0.69, PBIAS -3.5 and -3.6
Niraula et al. 2012	26	monthly	11 years	NSE 0.75, R ² 0.77, PBIAS -18	10 years	NSE 0.54, R ² 0.81, PBIAS 26
Jajarmizadeh et al. 2014	15	daily	7 years	NSE 0.40 and 0.66	5 years	NSE 0.51 and 0.71
Yuan et al. 2014	11	monthly & annual	10 years	NSE 0.45 to 0.82, R ² 0.55 to 0.66, PBIAS -1.29 to 25.46	10 years	NSE 0.55 to 0.94, R ² 0.70 to 0.84, PBIAS -16.27 to 1.38
Jajarmizadeh et al. 2015	7	monthly	13 years	NSE 0.92	6 years	NSE 0.83
Mosbahi et al. 2015	8	monthly	2 years	NSE 0.78, R ² 0.85, PBIAS -13.22	5 years	NSE 0.75, R ² 0.90, PBIAS -16.5
Matin and Bourque 2015	2	monthly	4 years	NSE 0.56 to 0.94, R ² 0.76 to 0.83, PBIAS -3.88 to 21.48, RSR 0.25 to 0.66	Not available	Not available

Table 2.6: SWAT models performance indices in previous studies simulating runoff in arid and semi-arid environments. (Continued)

Studies	Number of parameters used	Time step	Calibration		Validation	
			Period Length	Performance Indices	Period Length	Performance Indices
Singh et al. 2015	15	daily & monthly	4 years	NSE 0.62 and 0.74, R ² 0.69 and 0.80, PBIAS 20.99 and 21.14	3 years	NSE 0.53 and 0.84, R ² 0.55 and 0.88, PBIAS 13.97 and 14.26
Suliman et al. 2015	12	daily	13 years	NSE 0.75, R ² 0.75	6 years	NSE 0.68, R ² 0.68
Jajarmizadeh et al. 2016a	12	daily	14 years	NSE 0.75, PBIAS 1.50	6 years	NSE 0.64, PBIAS 21
Jajarmizadeh et al. 2016b	unavailable	daily	14 years	NSE 0.54 and 0.75	5 years	NSE 0.45 and 0.64
Liu et al. 2016	unavailable	daily	5 years	NSE 0.76, R ² 0.78, PBAIS 0.22 %	2 years	Not available
Srinivas et al. 2016	unavailable	sub-hourly	no statistical results are available for the model performance			
Tian et al. 2016	unavailable	monthly	9 years	NSE 0.88, R ² 0.93	15 years	NSE 0.93, R ² 0.96
Zhang et al. 2016a	6	daily	15 years	NSE 0.68, R ² 0.81, RSR 0.57	5 years	NSE 0.64, R ² 0.81, RSR 0.57
Zou et al. 2016	10	monthly	7 years	NSE 0.66 to 0.69, R ² 0.73 to 0.80, PBIAS -4.32 to -7.24, RSR 0.49 to 0.57	6 years	NSE 0.69 to 0.82, R ² 0.76 to 0.83, PBIAS 6.74 to 18.34, RSR 0.44 to 0.46
Brouziyne et al. 2017	12	monthly	2 years	NSE 0.58 and 0.68, R ² 0.79 and 0.85, PBIAS 19 and 17	2 years	NSE 0.65 and 0.88, R ² 0.73 and 0.91, PBIAS 20 and 13
Khelifa et al. 2017	10	daily	4 years	NSE 0.64 to 0.89, R ² 0.70 to 0.90	3 years	NSE 0.60 to 0.68, R ² 0.68 to 0.91
Li et al. 2017	20	monthly	5 years	NSE 0.43 to 0.83	4 years	Not available
Licciardello et al. 2017	22	daily	11 years	NSE 0.82 and 0.85, R ² 0.82 and 0.86	8 years	NSE 0.57 and 0.47, R ² 0.56 and 0.67
Makwana and Tiwari 2017	14	daily	2 years	NSE 0.60, R ² 0.66	2 years	NSE 0.61, R ² 0.68

Table 2.6: SWAT models performance indices in previous studies simulating runoff in arid and semi-arid environments. (Continued)

Studies	Number of parameters used	Time step	Calibration		Validation	
			Period Length	Performance Indices	Period Length	Performance Indices
Qi et al. 2017	11	monthly	6 years	NSE 0.94 and 0.78, R ² 0.95 and 0.78, PBIAS -9.69 and 5.31, RSR 0.24 and 0.47	3 years	NSE 0.96 and 0.77, R ² 0.96 and 0.87, PBIAS 1.17 and 8.98, RSR 0.21 and 0.47
Zhang et al. 2017	22	daily	10 years	NSE 0.86, R ² 0.92	10 years	NSE 0.88, R ² 0.86
Gao et al. 2018	11	monthly	15 years	NSE 0.86, R ² 0.90	15 years	NSE 0.71, R ² 0.78
Paul and Negahban 2018	18	monthly	8 years	NSE 0.84, R ² 0.91, PBIAS -40.45	6 years	NSE 0.84, R ² 0.88, PBIAS -7.33
Ahmadi et al. 2019	8	daily	5 years	NSE 0.79, R ² 0.77	4 years	NSE 0.65, R ² 0.68
Aqnouy et al. 2019	6	daily	5 years	NSE 0.76, R ² 0.74, and PBIS 12.24, RSR 0.52	3 years	NSE 0.84, R ² 0.82, and PBIS 8.93, RSR 0.41
Bouslihim et al. 2019	8	monthly	3 years	NSE 0.64, R ² 0.65	2 years	NSE 0.76, R ² 0.57
Eini et al. 2019	13	monthly	28 years	NSE 0.42 to 0.72, R ² 0.51 to 0.74	4 years	NSE 0.45 to 0.78, R ² 0.51 to 0.81
Koycegiz and Buyukyildiz 2019	20	monthly	6 years	NSE 0.78, R ² 0.79, PBIAS -7.562	4 years	NSE 0.50, R ² 0.51, PBIAS -8.163
Markhi et al. 2019	23	monthly	21 years	NSE 0.61 and 50, R ² 0.62 and 0.51	No validation step was performed	
Zhang et al. 2019	unavailable	monthly	Runoff reconstruction during the mid-Holocene		10 years	NSE 0.62, R ² 0.74
Gu et al. 2020	15	monthly	4 years	NSE 0.75 and 0.64, R ² 0.75 and 0.69, PBIAS -1.5 and -2.89	3 years	NSE 0.66 and 0.82, R ² 0.67 and 0.83, PBIAS -12.60 and -7.89
Meng et al. 2020	27	daily	Not available	NSE 0.27 to 0.69, R ² 0.55 to 0.85	Not available	NSE 0.36 to 0.69, R ² 0.65 to 0.85
Mosbahi and Benabdallah 2020	8	monthly	2 years	NSE 0.80, R ² 0.78, PBIAS -13.22	5 years	NSE 0.75, R ² 0.90, PBIAS -16.5
Nasiri 2020	25	monthly	8 years	NSE 0.75 to 0.85, R ² 0.82 to 0.92, PBIAS 2.5 to 3.8	3 years	NSE 0.72 to 0.80, R ² 0.76 to 0.85, PBIAS 1.5 to -2.8

Table 2.6: SWAT models performance indices in previous studies simulating runoff in arid and semi-arid environments. (Continued)

Studies	Number of parameters used	Time step	Calibration		Validation	
			Period Length	Performance Indices	Period Length	Performance Indices
Pradhan et al. 2020	24	daily	3 years	NSE 0.59, R ² 0.62, PBIAS -9.16, RSR 0.64	3 years	NSE 0.52, R ² 0.53, PBIAS -5.39, RSR 0.70
Pulighe et al. 2020	27	monthly	6 years	NSE 0.50, PBIAS 2.2, RSR 0.71	8 years	NSE 0.70, PBIAS 18.7, RSR 0.55
Abu-Zreig and Hani 2021	12	monthly	8 years	NSE 0.96, R ² 0.95	2 years	NSE 0.63, R ² 0.91
Esmali et al. 2021	12	monthly	11 years	NSE 0.64, R ² 0.71, PBIAS 4.13	6 years	NSE 0.69, R ² 0.74, PBIAS 5.29
Koycegiz et al. 2021	20	daily	6 years	NSE 0.78, R ² 0.79, PBIAS -7.56	4 years	NSE 0.50, R ² 0.51, PBIAS -8.16
Carlos Mendoza et al. 2021	15	daily	5 years	NSE 0.69 and 0.86, R ² 0.70 and 0.87, PBIAS 14.7 and 14.4, RSR 0.55 and 0.38	5 years	NSE 0.52 and 0.70, R ² 0.67 and 0.87, PBIAS 5.89 and 5.87, RSR 0.69 and 0.55
Peng et al. 2021	28	daily	9 years	NSE -0.12 to 0.80, R ² 0.12 to 0.81	9 years	NSE -0.12 to 0.76, R ² 0.12 to 0.80

2.4.2. Assessment of water resources

A significant number of the SWAT model studies were conducted to assess the availability, abstraction, and management of water resources in arid and semi-arid regions (Muttiah and Wurbs 2002; Afinowicz et al. 2005; Milewski et al. 2009; Ouessar et al. 2009; Garg and Wani 2013; Welderufael et al. 2013; Li et al. 2015; Zettam et al. 2017; Aghakhani Afshar et al. 2018; Fang et al. 2018; Jin et al. 2018; Deb et al. 2019; Talebi et al. 2019; López-Lambraño et al. 2020; Mahmoodi et al. 2020; Naderi 2020; Desai et al. 2021; Luo and Li 2021). In particular, Milewski et al. (2009) calibrated SWAT model parameters in the Wadi Girafi catchment, extrapolated from two studies conducted in Saudi Arabia. The authors used the SWAT model to estimate average annual runoff and average annual recharge through transmission losses for 14 catchments in the Sinai Peninsula and the Eastern Desert of Egypt covering an area of about 281,000 km². The authors calibrated the SWAT model for the Wadi Girafi catchment (3,656 km²). The R² of observed and simulated streamflow was 0.86 indicating the good performance of the model. SWAT parameters values were then extrapolated to other ungauged catchments in the study area. For the investigated watersheds in the Sinai Peninsula, they found the simulated average annual runoff to be about 508x10⁶ m³ (17.1% of precipitation), and the simulated average annual recharge through transmission losses to be about 463x10⁶ m³ (15.7% of precipitation).

2.4.3. Evaluation of the impact of LULC changes on runoff and discharge processes

Calibrated SWAT models were applied to evaluate the impact of LULC changes on runoff and discharge processes in various arid and semi-arid catchments (Masih et al. 2011; Li et al. 2013; Dong et al. 2014;

Zhang et al. 2015b; Chen et al. 2016; Eshtawi et al. 2016; Gyamfi et al. 2016; Zhang et al. 2016b; Yin et al. 2017; Ahn et al. 2018; Shukla and Gedam 2018; Andaryani et al. 2019; Jin et al. 2019; Shukla and Gedam 2019; Azgin and Celik 2020; Yan et al. 2020; Tanksali and Soraganvi 2021). Shukla and Gedam (2019), one of the most recent studies looking at the impacts of urbanisation, found evaluated hydrological responses to the urbanisation processes of the Upper Bhima River catchment located in a semi-arid climatic zone of Maharashtra state, India. The statistical results of observed and simulated discharge rates indicated a good performance of the SWAT model in simulating the hydrological parameters. The urban area in the Upper Bhima River catchment increased from about 161 km² in 1992 to reach 706 km² in 2014 (338.5%). Due to the increase in urbanisation, the SWAT model outputs revealed that the average annual surface runoff increased to 10.4 mm, percolation decreased to 14.5 mm, and base flow decreased to 11.7 mm.

2.5. Evapotranspiration for calibration and validation of the SWAT model

Calibration of SWAT parameters is fundamental for accurate hydrological modelling (Shivhare et al. 2018). Conventionally, measured streamflow data are used to calibrate hydrological models, but streamflow records are usually sparse and, in developing countries, scarce. Hydrological simulations for ungauged or poorly gauged catchments have increased recently because of innovative scientific approaches to calibration using earth observation data (Immerzeel and Droogers 2008; Sirisena et al. 2020). Auto-calibration and parameter optimisation methods have been developed that deploy a systematic approach for parameter estimation to overcome cumbersome methods in distributed hydrological models with numerous parameters that have high spatial and temporal heterogeneity (Immerzeel and Droogers 2008;

Li and Lu 2012). The developments in remote sensing instruments of earth observation satellites have improved the availability of data for hydrological modelling, which include DEMs, LULC, and hydro-meteorological products with different (high and coarse) spatial and temporal resolutions. The use of remotely sensed ET data is a relatively new approach for SWAT model calibration and validation in ungauged catchments (Cheema et al. 2014; Zou et al. 2017).

Immerzeel and Droogers (2008) introduced a successfully innovative calibration procedure of the SWAT model based on remotely sensed ET as an alternative option to overcome the lack of streamflow data in data-scarce areas. Then, the use of evapotranspiration has grown gradually to calibrate and validate the SWAT model in ungauged catchments. 19 studies have successfully used ET to calibrate and validate hydrological models (Table 2.7). Most of these studies applied the SWAT model. These studies are grouped and reviewed under subtitles which are model calibration and validation by streamflow and ET, model calibration by streamflow and ET, model calibration and validation by ET, and model calibration by ET. Approximately 79% of these studies were published in the last five years. Most previous studies used the ET data generated from Moderate Resolution Imaging Spectroradiometer (MODIS) product and the Global Land Evaporation Amsterdam Model (GLEAM) datasets.

Table 2.7: Performance indices of SWAT models in previous studies that used ET for calibration and validation.

Studies	Number of parameters used	Calibration			Validation		
		Period Length	Data source	Performance Indices	Period Length	Data source	Performance Indices
Immerzeel and Droogers (2008)	unavailable	2004/2005	MODIS ET	R ² 0.81	1970-1996	Flow data	No statistical indices available
Githui et al. (2012)	8	2002/2003	Flow data	NSE 0.80, R ² 0.82	2003-2004	Flow data	No statistical indices available
			MODIS ET	R ² 0.87			
Kunnath-Poovakka et al. (2013)	11	2003-2007	MODIS ET	R ² 0.72	2008-2010	MODIS ET	R ² 0.65
Cheema et al. (2014)	unavailable	2007	MODIS ET	NSE 0.93, R ² 0.86	Not validated model		
Park et al. (2014)	12	2007-2008	Flow data	NSE 0.67, R ² 0.81	2003-2006&2009	Flow data	NSE 0.77, R ² 0.78
		2007-2008	Derived ET	R ² 0.58	2009	Derived ET	R ² 0.66
Kunnath-Poovakka et al. (2016)	5	2003-2007	Flow data MODIS ET	No statistical indices available	No validation available		
Verma (2016)	13	2004-2006	MODIS ET	NSE 0.53-0.76, R ² 0.74-	2007-2008	MODIS ET	NSE 0.70-0.91, R ²
Emam et al. (2017)	22	2006-2008	Flow data	NSE 0.74, R ² 0.71	2009-2010	Flow data	NSE 0.51, R ² 0.88
		2006-2010	MODIS ET	NSE 0.80, R ² 0.86	2011-2013	MODIS ET	NSE 0.79, R ² 0.82
Franco and Bonumá 2017	11	2007-2009	Flow data	NSE 0.78, R ² 0.78	2006	Flow data	NSE 0.66, R ² 0.75
			MODIS ET	R ² 0.63		MODIS ET	R ² 0.39
Zou et al. (2017)	10	2000-2009	Derived ET	NSE 0.71	2010-2013	Derived ET	NSE 0.70
Ha et al. (2018)	15	2003-2007	MODIS ET	NSE 0.61, R ² 0.65	2008-2011	MODIS ET	NSE and R ² 0.71
Parajuli et al. (2018)	14	2002-2005	Flow data	NSE 0.72-0.78, R ² 0.78-0.84	2006-2009	Flow data	NSE 0.80-0.81, R ² 0.86
			MODIS ET	NSE 0.78-0.80, R ² 0.79-		MODIS ET	NSE 0.71-0.75, R ²
Oduşanya et al. (2019)	11	1989-2000	GLEAM ET	NSE 0.34-0.61, R ² 0.59-0.7	2001-2012	GLEAM ET	NSE 0.2-0.45, R ² 0.54-0.62
		2000-2006	MODIS ET	NSE -0.37-0.1, R ² 0.53-0.64	2007-2012	MODIS ET	NSE -1.25- -0.83, R ² 0.51-0.55

Table 2.7: Performance indices of SWAT models in previous studies that used ET for calibration and validation.
(Continued)

Studies	Number of parameters used	Calibration			Validation		
		Period Length	Data source	Performance Indices	Period Length	Data source	Performance Indices
Jin and Jin (2020)	10	2006-2015	Flow data	NSE 0.73-0.98, R ² 0.74	No validation available		
			GLEAM ET	NSE >0.84, R ² >0.90			
Herman et al. 2020	18	2003-2014	Flow data	NSE 0.57	2003-2014	Flow data	No statistical indices available
			ET of multi remote sensing dataset	NSE 0.75-0.79		ET of multi remote sensing dataset	
Sirisena et al. (2020)	22	2003-2010	Flow data	NSE 0.93-0.98, R ² 0.95-0.98	No validation available		
			GLEAM ET	NSE 0.09-0.80, R ² 0.44-0.86			
Tapia-Arenas et al. (2020)	6	2010-2013	MODIS ET	R ² 0.45-0.47	2006-2009	MODIS ET	R ² 0.38-0.43
Shah et al. (2021)	15	2003-2010	Flow data	NSE 0.87-0.93, R ² 0.87-0.94	2011-2014	Flow data	NSE 0.68-0.87, R ² 0.83-0.89
			Flow data & MODIS ET	NSE 0.86-0.93, R ² 0.86-0.93		Flow data & MODIS ET	NSE 0.69-0.88, R ² 0.86-0.91
Odusanya et al. (2021)	13	1980-1992	Flow data	NSE 0.55-0.84, R ² 0.68-0.87	1993-2005	Flow data	NSE 0.51-0.85, R ² 0.77-0.86
			GLEAM ET	NSE -0.87-0.17, R ² 0.25-0.33		GLEAM ET	NSE -1.4-0.09, R ² 0.24-0.34

2.5.1. Model calibration and validation by streamflow and ET

Immerzeel and Droogers (2008) calibrated a SWAT model using remotely sensed ET on the Upper Bhima catchment (45,678 km²), southern India. A time series of MODIS images containing ET was used to calibrate the SWAT model, with the R² of monthly simulated and measured ET of 0.81. The model was validated using historical streamflow data with modelled discharges well within one standard deviation of the observed data.

Githui et al. (2012) estimated groundwater recharge rates for a semi-arid, irrigated catchment using a SWAT model calibrated under dry climatic conditions (August 2002 to July 2003) using monthly flow from two gauging stations and monthly remotely sensed ET data from MODIS. The statistical results for calibration showed good agreement between the monthly observed and simulated flow at the catchment with Nash Sutcliffe efficiency (NSE) of 0.80. The results also revealed a high correlation between simulated monthly ET and the MODIS ET with an R² of 0.87. The authors indicated that the model was validated using flow data for 2003/2004 but the paper has not included statistical indices for the validation of the model. The authors pointed out that the estimated annual catchment recharge tended to be higher for irrigated land cover than for non-irrigated land.

A SWAT model was evaluated using multiple ET variables and soil moisture, in addition to streamflow data, for a heavily forested catchment in South Korea (8.54 km²) (Park et al. 2014). The statistical results for calibration indicated satisfactory/good performance of the SWAT model. The results for calibration of the SWAT model performance were the NSE 0.67 and R² 0.81 using streamflow data. When using derived ET, the R² result was 0.58 and

0.66 for calibration and validation respectively. The authors stated that the use of ET and soil moisture in addition to streamflow for the calibration of the SWAT model provided a more reliable interpretation of model parameters by inducing the reduction of parameter uncertainty and understanding the behaviour of the watershed water balance.

Emam et al. (2017) applied the SWAT model to evaluate the water resources availability and water management in Song Sia River catchment in Vietnam. The authors calibrated the SWAT model on daily, monthly, and yearly time steps using discharge, MODIS ET, and crop yield, respectively. ET calibration of the SWAT model for the catchment yielded NSE and coefficient of determination (R^2) values higher than 0.79, indicating good performance. Validation of the SWAT model using MODIS ET yielded NSE 0.79 and R^2 0.82.

MODIS ET was used for SWAT model calibration in the upper Negro River catchment, situated in Santa Catarina and Paraná, Brazil (Franco and Bonumá 2017). A multi-variable calibration using measured streamflow and MODIS ET produced better streamflow performance than conventional calibration using streamflow only; however, the authors stated that only using ET required more research.

The use of ET data for the calibration of the SWAT model has been used in the USA. Parajuli et al. (2018) evaluated the use of MODIS ET data in the SWAT model by utilising monthly streamflow data from two stations within the Big Sunflower River catchment, north-western Mississippi. Three scenarios were tested to calibrate and validate the SWAT models including the calibration using monthly streamflow data only, the calibration using MODIS ET data only, and multi-variable calibration using both. The statistical results found

that single-variable approaches both showed equally good model performances with R^2 and NSE values from 0.71 to 0.86. In contrast to other studies, the multi-variable calibration led to lower R^2 and NSE values, ranging from 0.66 to 0.83. The authors stated that the SWAT model over-simulated ET when using MODIS ET.

Calibration of a SWAT model of Honeyoey Creek-Pine Creek catchment in Michigan, USA, used measured streamflow, monthly datasets of seven remotely sensed actual ET, calculated ET, and average values of ET from all products (ensemble) (Herman et al. 2020). ET datasets included: (1) the Operational Simplified Surface Energy Balance (SSEBop), (2) the Atmosphere-Land Exchange Inverse (ALEXI), (3) MODIS - Global ET Project (MOD16A2) 500 m, (4) the MOD16A2 1 km, (5) the North American Land Data Assimilation Systems phase 2 (NLDAS-2) Mosaic product, (6) the NLDAS-2 Noah product, (7) the NLDAS-2 Variable Infiltration Capacity (VIC), and (8) the TerraClimate dataset. Nine calibration scenarios of the SWAT model were performed using a multi-objective approach with two variables, one being measured streamflow and the other being actual ET. Calibration with streamflow and ensemble ET had the best overall performance, with NSE values of 0.79 and 0.95, respectively.

Shah et al. (2021) stated that the conventional practice of calibrating hydrological models using streamflow can lead to parameter uncertainty, causing significant uncertainties in the representation and simulation of sub-processes. The authors tested a multi-variable calibration approach by combining streamflow and remotely sensed MODIS ET in the Meichuan catchment. They pointed out that the multi-variable approach reduced uncertainty for calibrated parameters and model outputs compared to results of single-variable when using only streamflow data and demonstrated the

added value of using ET data for improving the hydrological model calibration.

Odusanya et al. (2021) used measured streamflow from four gauges and GLEAM actual ET separately for the calibration and validation of a SWAT model in the Oueme River catchment (48,292 km²) in West Africa. The authors stressed that the streamflow simulations from the GLEAM actual ET were not as good as those using measured streamflow. For the calibration using GLEAM actual ET, the acceptable NSE values were 0.45 and 0.66, obtained in two catchments only, while NSE values were 0.55 and 0.72 for these same two catchments.

2.5.2. Model calibration by streamflow and ET

Kunnath-Poovakka et al. (2016) examined the efficacy of calibrating AWRA-L with MODIS ET and AMSR-E soil moisture for 11 catchments in eastern Australia to improve streamflow predictions. The authors used 15 objective functions considering the root mean square deviation (RMSD) and correlation of ET and soil moisture, to calibrate the model. The performance of most objective functions was found to be good in catchments with medium to high average runoff, while calibration based on the normalized RMSD between observed and simulated ET provided the best streamflow predictions in high flow catchments, which was as good as the prediction from model calibrated with streamflow.

Sirisena et al. (2020) compared three calibration approaches of a SWAT model of Chindwin catchment, Myanmar, using measured streamflow and remotely sensed ET from GLEAM, separately and in combination. The authors indicated that single-variable calibrations led to good performance in the calibration variable but reduced

performance in the other variable. In contrast, the multi-variable calibration resulted in a good performance for both variables, with NSE values of 0.97 and 0.64 for streamflow and ET, respectively.

2.5.3. Model calibration and validation by ET

Kunnath-Poovakka et al. (2013) used microwave soil moisture retrievals from the Advanced Microwave Scanning Radiometer-EOS (AMSR-E) and daily estimates of ET from MODIS to calibrate a selection of the Australian Water Resources Assessment Landscape model (AWRA-L) parameters. The simulated ET showed a good agreement with MODIS ET with linear correlation coefficient of 0.85 (R^2 0.72) for calibration period and R^2 0.65 for validation period.

Daily and monthly MODIS actual ET data were used to calibrate and validate the SWAT model for twelve ungauged sub-basins of the Sirsa River catchment in Western Himalayas, India (Verma 2016). The author used data for the period 2004–2006 to calibrate the SWAT model and the period 2007–2008 for validation and stated that daily and monthly validation results of the simulations were better than calibration results. The performance of developed SWAT models was good for daily (8-day composite) simulations and very good for monthly simulations. For the calibration and validation, the NSE indices of daily simulations ranged from 0.53 to 0.72 and monthly values ranged from 0.71 to 0.91. The R^2 values varied from 0.74 to 0.77 for daily and 0.81 to 0.91 for monthly simulations.

A SWAT model was calibrated and validated using remotely-sensed ET to simulate the spatiotemporal distribution of actual ET in 31 sub-basins of the Heihe agricultural region in northwest China during 1984–2014 (Zou et al. 2017). The NSE was >0.6 in 78.6% of the calibrated sub-basins and 58.8% of the validated sub-basins.

To improve the performance for the Day catchment in Vietnam, Ha et al. (2018) used MODIS ET and leaf area index to calibrate the SWAT model. The NSE results for model calibration and validation were 0.61 to 0.65, respectively. Whereas the R^2 result was 0.71 for calibration and validation.

Odusanya et al. (2019) used monthly ET data from GLEAM and MODIS to calibrate and validate a SWAT model of the Ogun River catchment (20,292 km²), Nigeria. The available Hargreaves, Priestley–Taylor, and Penman-Monteith equations in the SWAT model were used to simulate actual ET and thereby obtain six calibration–validations. The authors indicated that the best SWAT model performance was obtained when using the Hargreaves equation and GLEAM data. The statistical results of calibration showed the SWAT model performance of $NSE > 0.50$, $KGE > 0.50$, and $R^2 > 0.6$ in more than half of the 53 sub-basins and a $PBIAS < \pm 15\%$ in all 53 sub-basins.

Tapia-Arenas et al. (2020) assessed the hydrological impacts of land-use change in the Reventado River catchment, Costa Rica, using MODIS ET to calibrate a SWAT model. The authors stated that, overall, using MODIS actual ET provided satisfactory calibration.

2.5.4. Model calibration by ET

A SWAT model was applied to derive the total annual irrigation applied in the Indus catchment in 2007, using MODIS ET data (Cheema et al. 2014). The authors indicated that the calibration increased NSE values from 0.52 to 0.93, the PBIAS values improved from -17.3% to -0.4% , and the Pearson correlation coefficient values improved from 0.78 to 0.93. It should be noticed that this model was not validated. In 2007, estimated abstracted

groundwater in the Indus catchment was 68 km³ (262 mm) and depletion of water was 31 km³ (121 mm).

Jin and Jin (2020) used monthly ET data from GLEAM to calibrate a SWAT model for the Bayinhe River, concluding that the performance of the SWAT model to simulate streamflow and water balance was reliable when calibrated with streamflow only, and the combination of the streamflow and GLEAM ET further improved the model performance.

2.6. Summary

This chapter reviewed and summarised pertinent previous studies working on rainfall in Saudi Arabia, runoff and flooding in Saudi Arabia, the application of the SWAT models in arid environments, and using ET for calibration and validation of SWAT models.

The review of previous studies revealed that there is a significant knowledge gap in scientific knowledge of the hydrology of arid environments. The literature relating to rainfall and runoff in Saudi Arabia is limited in number, geographically scattered, and limited by sparse data. In addition, some studies suffer from limitations related to their methodology. For example, most of the few published runoff studies in Saudi Arabia used generalised statistical models for very large drainage basins. Although the study areas covered a wide region, often of thousands of km², the two studies that applied semi-distributed SWAT models used parameter values from SWAT models calibrated for catchments in Egypt.

Conventionally, measured streamflow data are used to calibrate hydrological models, but reliable hydrological records are scarce in developing countries. However, an appreciable number of studies have successfully applied the SWAT model in arid and semi-arid

environments. Recently, hydrological simulations for ungauged or poorly gauged catchments have successfully utilised ET data for both calibration and validation, offering promise for future studies where streamflow, rainfall and runoff data are lacking.

Chapter 3: Geological and Geographical Background of the Riyadh City Region

3.1. Overview

Saudi Arabia is situated in southwest Asia between the Red Sea in the west and the Arabian Gulf in the east occupying an area of around 2,000,000 km² (Saudi Geological Survey 2012). Geologically, the country consists of two major parts: the Arabian Shield in the west and Arabian Shelf in the east. The shield area is mainly composed of ancient igneous and metamorphic rocks, while the eastern part is sedimentary strata dipping east and northeast. Saudi Arabia has a diverse topography which includes the coastal plains of the Red Sea and Arabian Gulf, high western mountains, volcanic harrats, inland plateaus and plains, and sand dune fields (Chapman 1978). Saudi Arabia is one of the hottest, sunniest, and driest countries in the world. Rainfall is low and irregular with averages range from 29.3 mm in Tabuk to 230.3 mm in Abha (Hasanean and Almazroui 2015).

Administratively, Saudi Arabia consists of 13 provinces; one of them is Riyadh province. The Riyadh province includes most of the central part of the country covering an area of about 380,000 km² (Saudi Geological Survey 2012). This province includes Riyadh city, the capital of Saudi Arabia.

Understanding geographical features of study areas is important when predicting runoff and flooding. Therefore, this chapter provides a general description of geological and geographical variables that influence surface runoff in Riyadh city, including geology, synoptic patterns inducing precipitation, vegetation cover, and water resources and consumption.

3.2. Geology

Geologically, Riyadh city sits on outcrops of sedimentary formations. In fact, central Saudi Arabia is composed of sequential sedimentary formations, dipping gently and uniformly to the east (Powers et al. 1966). Riyadh city lies mainly on nine geological formations which, from younger to older, are the Kharj, Biyadh, Buwaib, Yamama, Sulaiy, Arab, Jubaila, Hanifa, and Tuwaiq Mountain formations (Table 3.1). These formations belong to the Jurassic and Cretaceous ages except for the Kharj formation which belongs to the Miocene and Pliocene ages. Generally speaking, the geological formations in the west of Riyadh city are composed of compact limestone, such as the Jubaila, and the Tuwaiq Mountain formations. In contrast, some formations in the middle and east of the city, such as the Sulaiy and Arab formations, are characterised by diverse and disturbed lithology including limestone, calcarenite, and dolomite. Quaternary deposits (alluvial and Aeolian) bury considerable areas of these formations, especially the Sulaiy formation (Bramkamp and Ramirez, 1958). The geological map of the study area (Figure 3.1) shows that the Wadi Hanifah catchment occupies mainly outcrops of Arab, the Jubaila, Hanifa, and the Tuwaiq rock types. On the other hand, the Wadi As Silayy extends on relatively younger outcrops of the Kharj, Biyadh, Buwaib, Yamama, Sulaiy and Arab formations. A brief description of each geological formation is given below, depending on the geological map at scale 1:500,000 and information provided by Bramkamp and Ramirez (1958) and Powers et al. (1966).

The Kharj formation is a distinctive patches of lake deposits plastered on the Sulaiy outcrop belt. The thickness of this formation is about 28 m. The Kharj formation is composed of limestone, lacustrine limestone, gypsum, and gravel. In the study area, it covers a small part of the lower reach of the Wadi As Silayy catchment about 35 km², but a relatively large part (374 km²) of

the Wadi As Silayy catchment is covered by limestone pebbles and cobbles locally cemented by dark slightly ferruginous caliche equivalent to the Kharj formation (Bramkamp and Ramirez 1958; and Powers et al. 1966).

Table 3.1: Geological formations in the Riyadh city region.

Age (Period)	Formation	Generalised lithologic description	Thickness (m)	Coverage in the study area (Km ²)
Miocene and Pliocene	Kharj	Limestone, lacustrine limestone, gypsum, and gravel	28	409
Cretaceous	Aurma	Limestone, subordinate dolomite and shale	142	11
	Biyadh	Sandstone; subordinate shale	425	223
	Buwaib	Biogenic calcarenite and calcarenitic limestone interbedded with fine sandstone in upper part	18	39
	Yamama	Biogenic-pellet calcarenite; subordinate aphanitic limestone and biogenic calcarenitic limestone	46	85
	Sulayy	Chalky aphanitic limestone; rare biogenic calcarenite and calcarenite limestone	170	694
Jurassic	Arab	Calcarenite, calcarenitic and aphanitic limestone, dolomite and some anhydrite. Solution-collapse carbonate breccia on outcrop due to loss of interbedded anhydrite	124	625
	Jubaila	Aphanitic limestone and dolomite; subordinate calcarenite and calcarenitic limestone	118	1,188
	Hanifa	Aphanitic limestone, calcarenitic limestone, and calcarenite	113	339
	Tuwaiq Mountain	Aphanitic limestone; subordinate calcarenitic limestone and calcarenite. Abundant corals and stromatoporoids in upper part	203	704

Source: Powers et al. (1966).

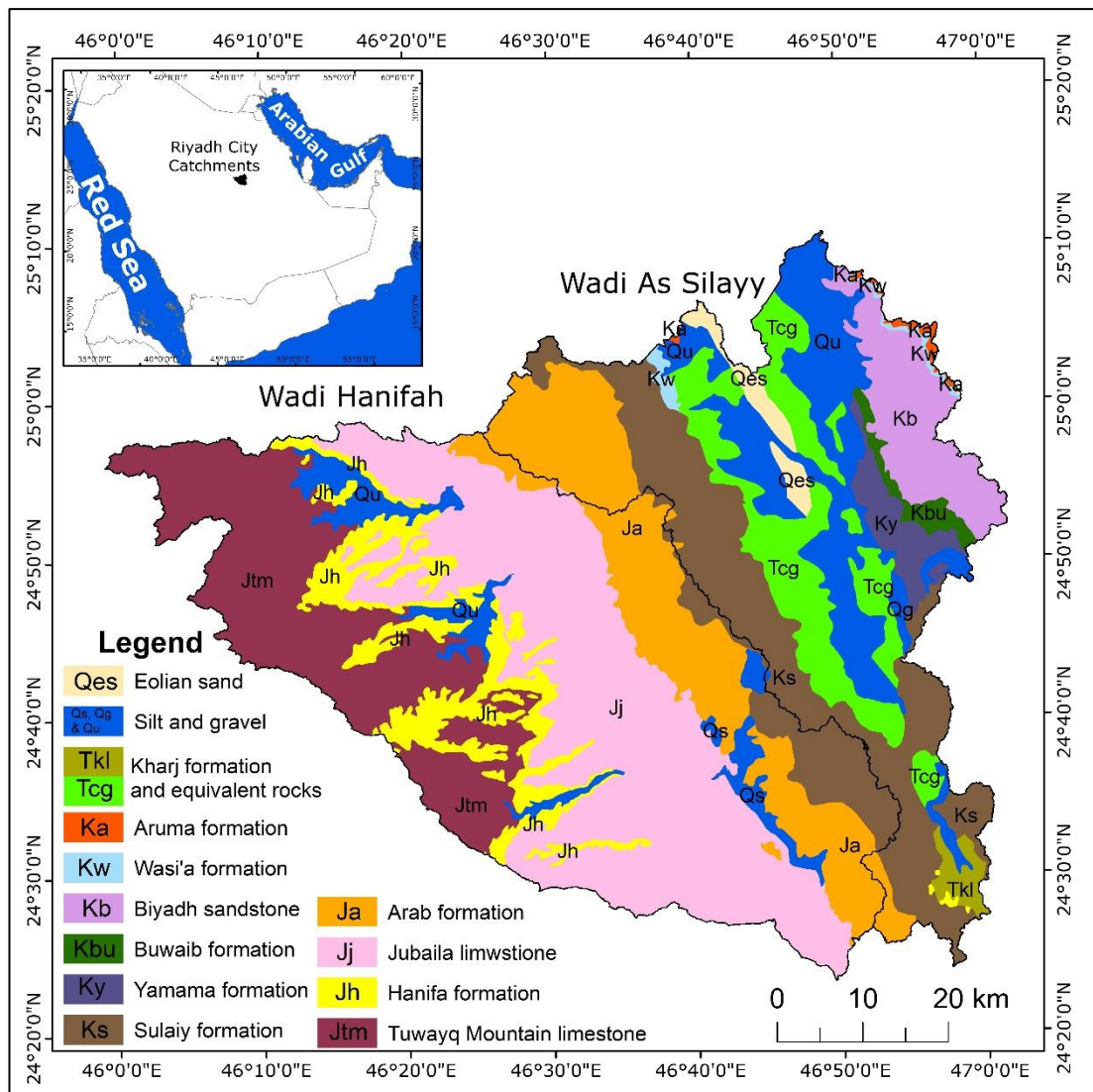


Figure 3.1: Geological map of Riyadh city catchment.
Source: Bramkamp and Ramirez, (1958).

The Biyadh formation is exposed in the northeast of Riyadh and belongs to the middle Cretaceous. The thickness of this formation reaches 425 m and is composed of sandstone and subordinate shale. It covers about 223 km² of the Wadi As Silayy catchment, representing 11% of the whole area of the Wadi As Silayy catchment (Bramkamp and Ramirez 1958; and Powers et al. 1966).

The Buwaib formation is exposed on the surface as a narrow and relatively long strip in the east of Riyadh and belongs to the middle Cretaceous. This formation overlies the Yamama formation and underlies the Biyadh formation. The thickness of this formation is

about 18 m. This formation consists of calcarenitic limestone and fine sandstone. It covers about 39 km² of the Wadi As Silayy catchment representing 2% of the whole area of the basin (Bramkamp and Ramirez 1958; and Powers et al. 1966).

The Yamama formation is exposed on the surface in the eastern part of Riyadh. It belongs to Lower Cretaceous. The thickness of this formation reaches 46 m. It is mainly composed of calcarenitic, aphanitic limestone and calcarenite. It overlies the Sulaiy formation and underlies the Buwaib formation. It covers about 85 km² of the Wadi As Silayy catchment representing about 4% of the whole area of the basin (Bramkamp and Ramirez 1958; and Powers et al. 1966).

The Sulaiy formation overlies the Arab Formation and underlies the Yamama formation. It occupies a major portion of the surface in the Riyadh, mainly in the Wadi As Silayy catchment. It belongs to the lower Cretaceous age and reaches a thickness of 170 m. This formation is composed of limestone, chalky aphanitic, and calcareous limestone. It covers about 694 km² of the Riyadh city region, including 547 km² of the Wadi As Silayy catchment and 147 km² of the Wadi Hanifah catchment. It represents 27% of the area of the Wadi As Silayy basin and 5% of the area of the Wadi Hanifah basin (Bramkamp and Ramirez 1958; and Powers et al. 1966).

The outcrop of the Arab formation extends from south to north to the east of the main channel of the Wadi Hanifah in the middle part of Riyadh and continues to cover the northwest part of the Wadi As Silayy. This formation is of Late Jurassic age and is overlying the Jubaila formation and underlying the Sulaiy formation. The thickness of the Arab formation reaches 124 m. It is composed of calcarenite, calcarenitic and aphanitic limestone, and dolomite with anhydrite interbeds. It covers about 625 km² in the Riyadh city region, where

402 km² covers the Wadi Hanifah catchment and 223 km² covers the Wadi As Silayy catchment. It represents 14% of the area of the Wadi Hanifah basin and 11% of the area of the Wadi As Silayy basin (Bramkamp and Ramirez 1958; and Powers et al. 1966).

The Jubaila formation exists in the Wadi Hanifah catchment only, extending from northwest to southeast in the central part of the catchment, and west of the main channel. It covers 1,188 km² of the catchment, representing about 40% of the area. The formation rests on the Hanifa formation and is overlain by the Arab formation. The thickness reaches 118 m. The Jubaila formation belongs to the upper Jurassic age. It is composed of aphanitic limestone, dolomite, calcarenite and calcarenitic limestone (Bramkamp and Ramirez 1958; and Powers et al. 1966).

The Hanifa formation is exposed on the surface as sinuous narrow strips in Riyadh city. It belongs to the Late Jurassic age. The thickness of this formation reaches 113 m. It overlies the Tuwaiq Mountain formation and underlies the Jubaila formation. The formation is mainly composed of aphanitic limestone, calcarenitic limestone, and calcarenite. The Hanifa formation covers only about 335 km² of the Wadi Hanifah catchment representing about 11% of the whole area of the basin (Bramkamp and Ramirez 1958; and Powers et al. 1966).

An outcrop of the Tuwaiq Mountain formation covers a wide area of west and northwest of the Wadi Hanifah catchment. It consists of 704 km² of the Wadi Hanifah catchment, representing 24% of the whole basin area. It overlies the Dhurma formation and underlies the Hanifah formation, belonging to the middle Jurassic. The thickness of the Tuwaiq Mountain formation is about 203 m. It is composed of limestone, aphanitic limestone, calcarenitic limestone

and calcarenite (Bramkamp and Ramirez 1958; and Powers et al. 1966).

3.3. Synoptic patterns associated with precipitation in Saudi Arabia

Synoptic patterns are weather systems that produce disturbances such as frontal depressions, tropical cyclones, and anticyclones with a horizontal scale of many hundreds to a few thousand kilometres and a lifetime counted in days (Reynolds 2015). The large-scale atmospheric circulations and surface features are major factors that influence regional and local climates over Saudi Arabia (Marcella and Eltahir 2008; Nicholson 2011; Alharbi 2018). Almazroui (2012a) found that high variability in temperature was closely associated with large-scale forcings, including the North Atlantic Oscillation (NAO), the Arctic Oscillation (AO), and El Niño Southern Oscillation (ENSO) events. Hasanean and Almazroui (2015) pointed out that regional and local variations or changes in rainfall characteristics are influenced by atmospheric circulation patterns determined by the NAO, ENSO, and other patterns. Almazroui (2020) indicated that the ENSO significantly impacted the variability of rainfall over Saudi Arabia through large changes in moisture availability, as well as variability in the westerly jet passing over the region.

The climate of Saudi Arabia, as well as the Riyadh region, is affected by the movement of four air masses: continental polar, continental tropical, maritime polar, and maritime tropical (Figure 3.2) (Fisher and Membery 1998). The most dominant are the continental polar and continental tropical masses. During the winter, the country is influenced by the continental polar air mass, which originates over central Asia. The characteristics of this air mass are relatively low temperatures and dry weather, with clear skies. In the summer, the country is dominated by the continental tropical air mass, which

originates in the late spring over the hot and dry land surfaces of North Africa and extends from June-September to the interior of the Arabian Peninsula. It is characterised by very high temperatures, low humidity, and cloudless skies. The intense heating of surfaces results in vigorous dry convection leading to the transportation of dust particles into the mid-troposphere, creating hazy conditions (Fisher and Membery 1998).

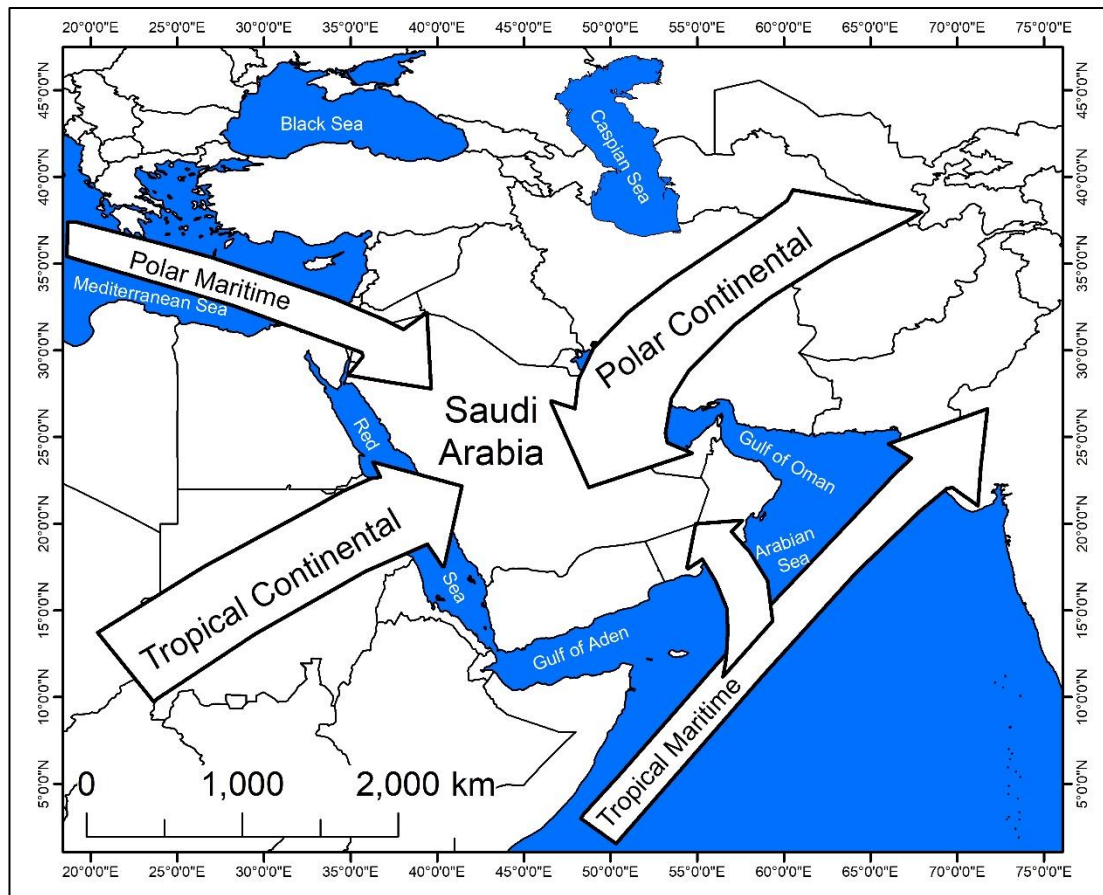


Figure 3.2: Air masses affecting the climate of Saudi Arabia.
Source: Fisher and Membery (1998).

Occasionally, Saudi Arabia is affected by polar and tropical maritime air masses. The maritime polar air mass originates from the eastern Mediterranean Sea and the maritime tropical air mass (monsoon type) originates from the Indian Ocean and the Arabian Sea (Alyamani and Sen 1993; Abdullah and Al-Mazroui 1998; Alyamani 2001; Gosling et al. 2011; Nicholson 2011; Al-Ahmadi and Al-

Ahmadi 2013; Alahmadi 2017; Abu Abdullah et al. 2019). Samman and Gallus (2018) reported that storms occurring over Saudi Arabia derived moisture from the Mediterranean Sea, the Arabian Sea, the Red Sea, and tropical African areas; however, they also found that some of the events that occurred in the eastern and central regions were influenced by moisture transport from the Arabian Gulf.

Mediterranean cyclones are responsible for a high proportion of rainfall in Saudi Arabia (Almazroui et al. 2016). Another important synoptic phenomenon that contributes to precipitation in Saudi Arabia is the Red Sea Trough (Fett et al. 1983; Nicholson 2011; Almazroui et al. 2016). The interaction of the Red Sea Trough with the westerly jet stream boosts the baroclinicity and thus the rainfall in Saudi Arabia (Almazroui 2020). The Red Sea Trough is a low-pressure at lower atmospheric levels extending northward from eastern Africa along the Red Sea toward the eastern Mediterranean. It is generally accompanied by an upper-level cyclonic storm. The origin of the Red Sea Trough is the Sudan Monsoon Low centred over eastern Africa or Arabia. It occurs frequently in autumn, winter, and spring but disappears entirely in summer (Tsvieli and Zangvil 2005; Nicholson 2011; De Vries et al. 2016). It results in unstable conditions over the region when it is accompanied by an upper-tropospheric trough extending from the north over the eastern Mediterranean, which could give intense rainfall in the eastern Mediterranean and Middle East countries (Almazroui et al. 2016).

Samman and Gallus (2018) used gridded meteorological data from the National Center for Environmental Prediction-National Center for Atmospheric Research (NCEP/NCAR) reanalysis for the period 2000-2014 to investigate the synoptic patterns associated with the development of heavy rainfall in five different regions of Saudi Arabia. From 186 cases, they found six major synoptic features

which are: (1) the Red Sea Trough (RST), (2) the Arabian Peninsula Low (APL), (3) the Persian trough (PT), (4) the Red Sea Low (RSL), (5) vertically-tilted lows at lower levels associated with deep troughs at the 500 hPa level (LPS), and (6) the Mediterranean cyclogenesis (MC). The authors indicated that the Red Sea Trough feature is much more common than the other features except in the eastern region of Saudi Arabia where the APL and PT are more common. They stressed that the RSL affects only the western and southern regions of the country, whereas the features of the vertically-tilted lows at lower levels associated with deep troughs at the LPS and MC affect only the northern parts of Saudi Arabia. Out of 186 cases in their study, 5 cases occurred in the central region of the country where Riyadh city situated, with 1 case in Autumn and the 4 cases in Spring. The authors stated that precipitation in the central region is influenced by the RST (60%) and the PT (40%).

The westerly jet stream passes over Saudi Arabia during the rainy season that extends from October to May (Almazroui 2020). Due to the reversal of heating over the Himalayan plateau in June, a dramatic shift occurs from the dominance of the westerly subtropical jet stream to the tropical easterly jet in the summer season (Nicholson 2011). Thus, storms in central Saudi Arabia move generally eastwards along their tracks in the autumn, winter and spring seasons, whereas the very rare summer storms move westward. Figure 3.3 is composed of successive hourly radar images for 24-hours during 28-29 Nov 2020 (Yanbuweather n.d.). The figure shows multiple storm cells moving from west to east across Saudi Arabia. Also, it shows that within one hour some storm cells decayed, and new cells developed. In addition, the spatial extension of cells and their intense-rain cores changed as well.

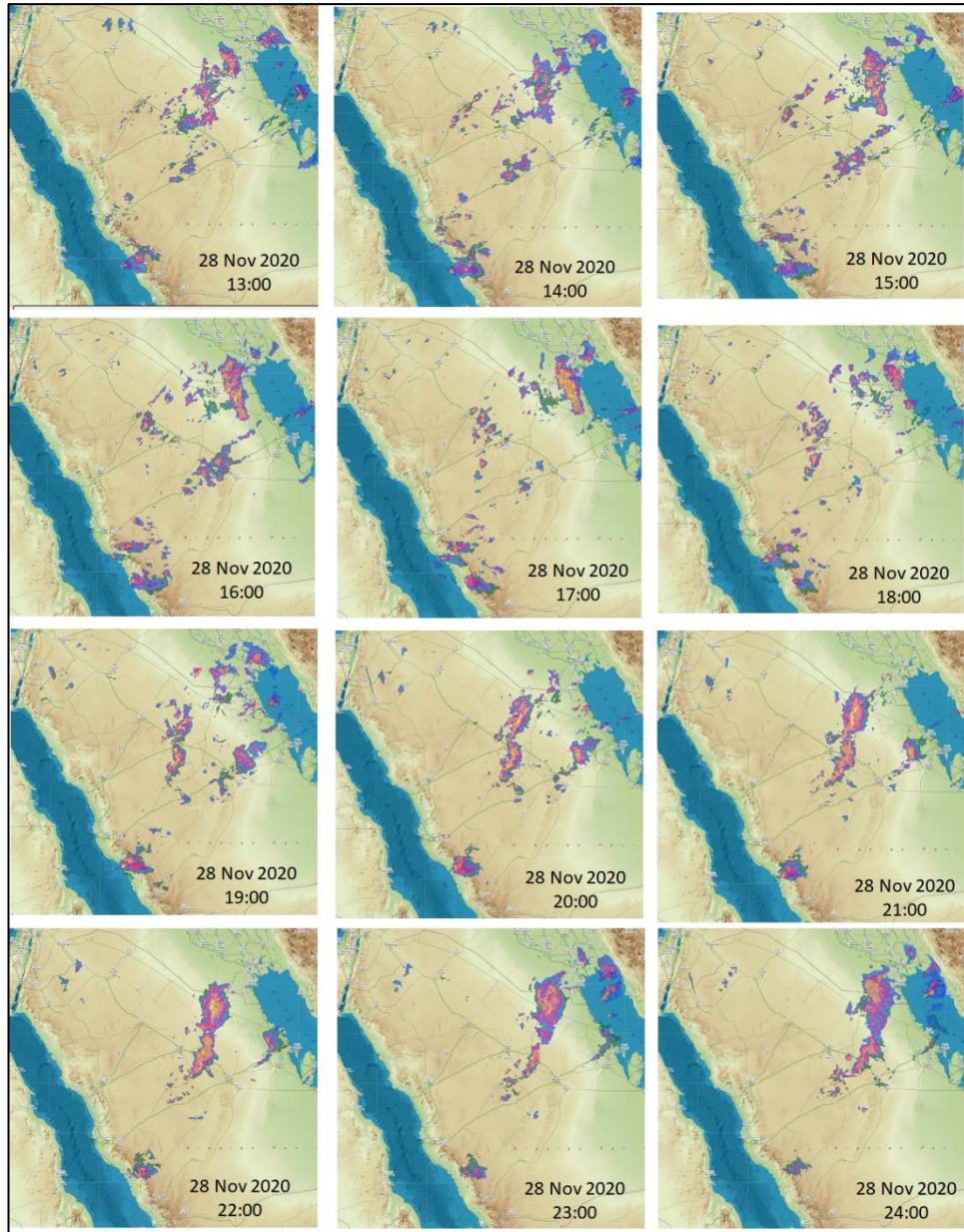


Figure 3.3: Successive hourly radar images for 24-hours captured 28-29 Nov. 2020.

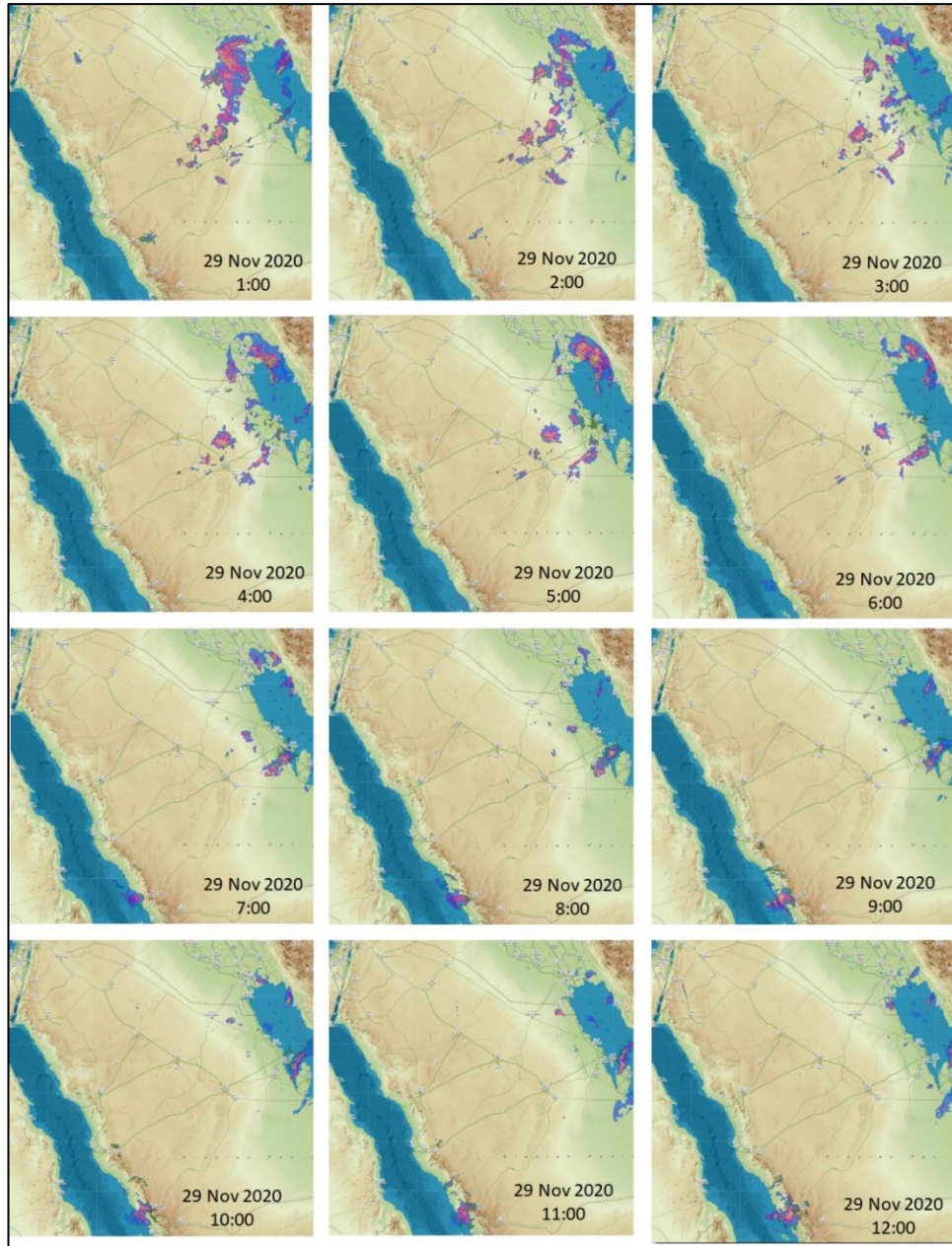


Figure 3.3: Successive hourly radar images for 24-hours captured 28-29 Nov. 2020. (continued)
 Source: This figure was produced by the researcher using Radar images obtained from Yanbuweather (n.d.).

Figure 3.4 illustrates a storm cell in the region of Riyadh city captured from King Khalid International Airport Radar Station, Riyadh ($24^{\circ}55'31.89''N$, $46^{\circ}43'18.32''E$) at 16:44 and 17:24 of the 18 Nov 2018. Multiple storm cells are moving from southwest to northeast with rainfall of about 47 mm/h (US National Weather Service n.d.). The images illustrate the spottiness and spatial

variability of rainfall in the vicinity of Riyadh city, and that within 40 minutes storm cells decay and new cells develop.

The life cycle of rainfall systems from their formation to dissipation over Saudi Arabia varies, ranging from sub-daily to multiple days. Almazroui (2012b) described a rainfall system of multiple cells that occurred from 13th to 20th November 1996. The system formed over eastern Sudan near the western coast of the Red Sea on 13th November 1996, moving eastward and crossing the Red Sea into western Saudi Arabia, where it reached its mature stage on 16th November. By the 20th November 1996 the storm had decayed.

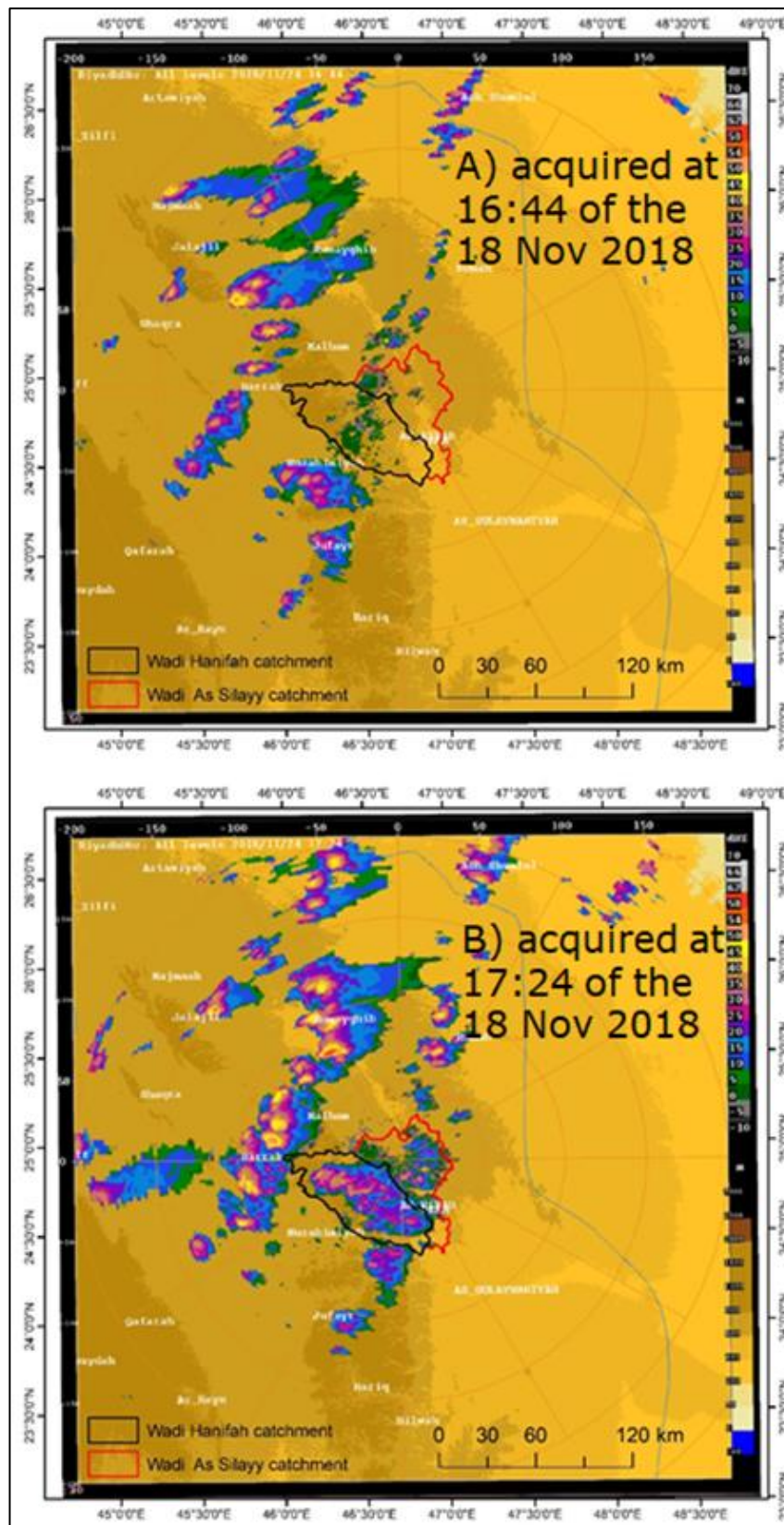


Figure 3.4: Radar images captured from King Khalid International Airport Radar Station, Riyadh.
 Source: This figure was produced by the researcher using Radar images obtained from Saudi National Center for Meteorology (n.d.).

3.4. Vegetation cover

Vegetation cover can be mapped from remotely sensed images using the Normalized Difference Vegetation Index (NDVI). The NDVI describes the reflectance difference between vegetation cover in the near-infrared (NIR) image and the red (R) image. The NDVI image from Landsat OLI acquired in February 2022 indicated that vegetation cover represented 3% of the built-up area of Riyadh city (Figure 3.5). To increase total green space in Riyadh city, an ambitious urban forestation project called “Riyadh Green” was launched in March 2019 with the aim to plant 7.5 million trees by 2030 using recycled water. It is to be planted across Riyadh city in gardens, parks, mosques, schools, universities, public facilities, King Khalid International Airport, roads, streets, car parking spaces, and valleys (Riyadh Green n.d.).

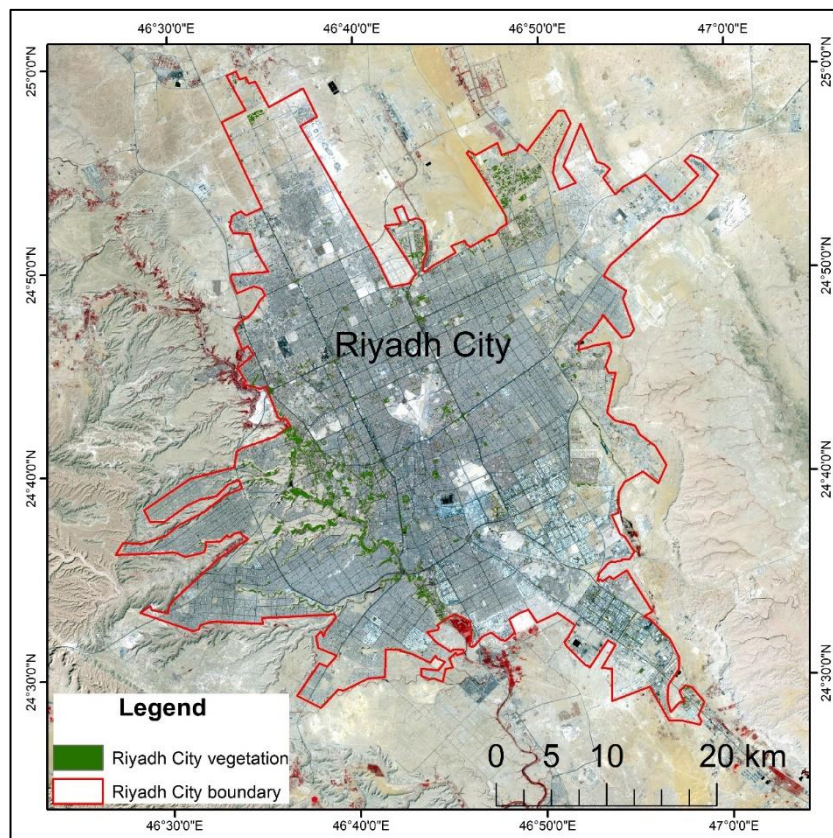


Figure 3.5: The NDVI image superimposed on the false-colour image showing vegetation cover within the built-up area of Riyadh, 2022.

Current vegetation cover in Riyadh city includes both natural vegetation and planted vegetation. Natural vegetation is sparse due to the areas aridity and includes both perennial and ephemeral plants. These plants are resistant to aridity including xerophytes (perennial trees and shrubs) and phreatophytes (e.g. succulents) (Goudie and Wilkinson 1977). Wetlands in the Wadi Hanifah and Wadi As Silayy have developed since the late 1970s, with aquatic plants (Thomas 2011). For example, phragmites is well known in the Wadi Hanifah wetlands (Riyadh High Commission for the development of Arriyadh 2014). Currently, the middle and lower parts of the main channel in Wadi Hanifah and the lower main channel of the Wadi As Silayy are permanently flowing streams due to the release of water from the wastewater treatment plants and groundwater level rise in the city.

Perennial plants are mostly scattered across the wadi floor, consisting of alluvial deposits. The most dominant perennial plants are *Acacia ehrenbergiana*, *Acacia gerrardii*, *Acacia tortilis*, *Tamarix aphylla*, *Tamarix senegalensis*, and *Ziziphus spina-christi* (Thomas 2011). Ephemeral plants are marked by short life cycles, which sprout after rainfall and grow for a few weeks before completing its life cycle. Ephemeral vegetation grows densely in shallow depressions and wadi floors, and relatively sparsely in valley talus slopes. These plants include *Rumex vesicarius*, *Malva parviflora*, *Trigonella anguina*, *Horwoodia dicksoniae*, *Calendula tripterocarpa*, *Anthemis deserti*, and *Moltkiopsis ciliate* (Thomas 2011, Riyadh High Commission for the development of Arriyadh 2014).

Planted vegetation is present in formal parks, gardens and green spaces, as well as trees and green spaces in houses. Public parks are located across the city of Riyadh, including Salam park, King Abdulaziz historical centre park, King Abdullah Park in Malaz, King

Salman Park in Banban. Open green spaces also extends along the banks of the rehabilitated channel of the Wadi Hanifah (Riyadh High Commission for the development of Arriyadh 2014). Considerable vegetation cover has also been planted along streets and roads within the city. There are also traditional palm groves present along the wadi floors of Wadi Hanifah, with a positive effect on the local climate and improving the aesthetic environment for residents.

3.5. Water supply and consumption

Riyadh is one of the fastest-growing cities in the world. In 1902, the population of Riyadh was estimated to be 8,000 habitants and reached 6.5 million habitants in 2016 (Table 3.2). The population growth of the city has been accompanied by an increase in water demand. Access to safe drinking water has been a serious challenge facing Saudi Arabia due to the water scarcity and high population growth rates in the country. Water supply in Riyadh city comes from two sources: groundwater and desalinated water (Table 3.3).

Table 3.2: Population growth of Riyadh City.

Year	Population	Average annual growth rate (%)	Year	Population	Average annual growth rate (%)
1902	8,000*		1978	760,000*	5.1
1930	27,000*	8.5	1987	1,389,000*	9.2
1945	80,000*	13.1	1990	2,100,000*	17.1
1954	106,000*	3.6	1992	2,776,096*	16.1
1960	160,000*	8.5	1997	3,100,000*	2.3
1962	185,000*	7.8	2001	3,829,000*	5.9
1965	231,000*	8.3	2004	4,260,000*	3.7
1972	420,000*	11.7	2006	4,600,000*	4.0
1974	662,000*	28.8	2010	5,200,000**	3.3
1977	690,000*	1.4	2016	6,500,000**	4.2

Sources: *Riyadh Municipality (n.d.). **Ministry of Municipal and Rural Affairs (2019).

Table 3.3: Water supply sources for Riyadh city.

Water Source	Aquifer	Daily Supply m ³
Al Hair wells	Alluvial and Minjur aquifers	51,000
Nisah wells	Alluvial and the Mesozoic Minjur and Dhurma aquifers	54,000
Shemessy well	Minjur aquifer	32,000
AL-Malaz wells	Minjur aquifer	16,000
Manfouha wells	Minjur aquifer	45,000
Riyadh Water Wells Project	Minjur aquifer	68,000
Salboukh wells	Minjur aquifer	10,900
Buwyb wells	Minjur aquifer	95,000
Saad	Wasia and Biyadh aquifer	500,000
Alheni wells	Umm er Radhuma aquifer	450,000
Yabreen wells	Umm er Radhuma aquifer	800,000
Jubail Desalination Plant	Desalinated water	300,000
Ras Al-Khair Desalination Plant	Desalinated water	800,000

Source: Saudi Press Agency (2014); DMS Projects (n.d.); Royal Commission for Riyadh City (2002); Royal Commission for Riyadh City (2006); Harrigan (2017); Al-Juaidi and Attiah (2020).

Both renewable and non-renewable groundwater sources have been developed to supply water for Riyadh city. In the 1950s, the city received its water supply from 18 wells dug in shallow alluvial aquifers in Nisah, Namar and Al Hair areas (El-Sharif 1985; Al-Mutaz 1987). Production of fossil groundwater to supply water for Riyadh city started in 1957 when the Shemessy deep well (> 1,300 m deep) was dug into the Minjur aquifer (Alhawas 2011). More deep wells were dug as population grew, and the expansion of the city water demand increased into other areas, such as the Hair and Manfouha areas. In 1964, 22 wells were dug in the Biyadh-Wasia aquifer. In 1978, 16 wells were dug in Minjur aquifer in the Salboukh area. In 1981, 63 wells were dug in Wasia and Biyadh aquifer at Saad area and in 2005, 65 wells were dug in Umm er Radhuma aquifer in the Alheni area. In 2014, a further 43 wells were dug in the Minjur aquifer in the vicinity of the city, called the Riyadh Water Wells Project (Figure 3.6) (Alhawas 2011; Al-Juaidi and Attiah 2020).

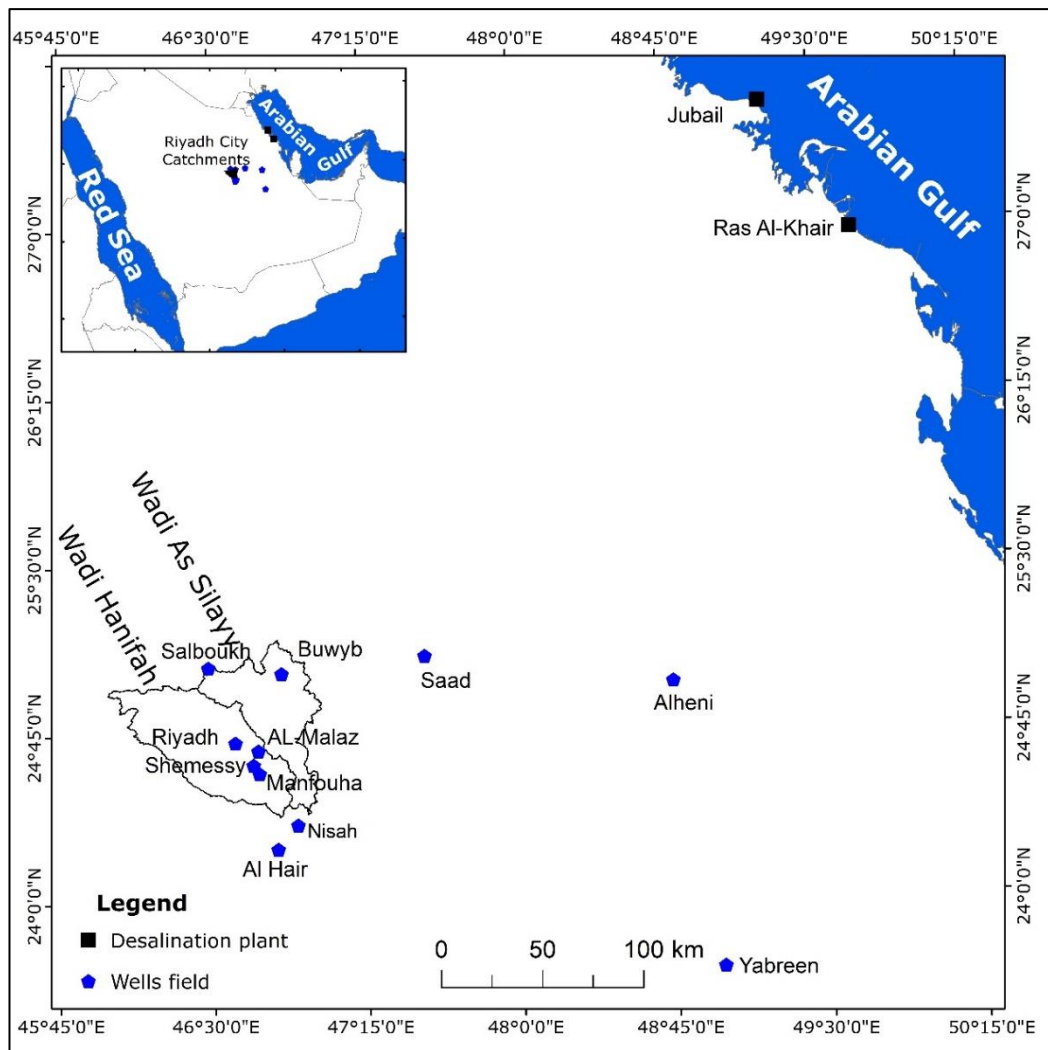


Figure 3.6: Location map of water supply sources for Riyadh city.

To satisfy the rapidly increasing demand for water in the city, desalinated water has been used since 1983 from desalination plants (Jubail Desalination Plant and Ras Al-Khair Desalination Plant) located about 500 km to the east of Riyadh on the western coast of the Gulf. In 2017, about 591.84 million cubic meters desalinated water was supplied to the city, where about 33% and 67% received from the Jubail Desalination Plant and the Ras Al-Khair Desalination Plant, respectively. In 2017, desalination water and groundwater represent about 62% and 38% of the total water supply to the city, respectively (Al-Juaidi and Attiah 2020).

Demand for water by households in Saudi Arabia is growing by 7.5%, annually. The high levels of water consumption for municipal purposes in Saudi Arabia are referred to fast population growth and improved living standards. Between 1987 and 2014, annual water consumption in Riyadh city increased 2.5 times, equating to average annual growth of 6% (Table 3.4). Based on the estimations in Table 3.4, water consumption per day per capita was 105 litres, 286 litres, and 327 litres in 2001, 2006 and 2010, respectively. The Safe Drinking Water Foundation (n.d.) believes that 235 litres per person per day is an adequate amount of water to use. Thus, the per-capita water consumption in Riyadh in 2010 was higher than the value recommended by the Safe Drinking Water Foundation. To optimise water consumption, Saudi Arabia officially announced a national program called 'Qatrah' (which means 'droplet' in Arabic) for water conservation in the country. It aimed to reduce daily per capita water consumption to 200 litres in 2020, and to 150 litres in 2030 (Royal Commission for Riyadh City 2020).

Table 3.4: Water consumption volume in Riyadh city.

Year	Consumption MCM	Year	Consumption MCM
1986	241.990	2001	403.449
1987	275.037	2002	406.162
1988	319.614	2003	438.421
1989	339.910	2004	454.732
1990	364.645	2005	471.192
1991	394.848	2006	481.033
1992	418.373	2007	493.115
1993	403.534	2008	513.655
1994	418.077	2009	516.067
1995	414.039	2010	621.321
1996	395.325	2011	639.455
1997	424.768	2012	649.184
1998	409.770	2013	700.000
1999	415.487	2014	748.250
2000	413.929		

Sources: General Authority for Statistics (n.d.). Ministry of Water and Electricity (2014).

3.6. Summary

This chapter provided an overview of the geological and geographical context of Saudi Arabia and, specifically, the Riyadh city region that will be the focus of this PhD. In summary, Riyadh city lies on eight geological formations from the Jurassic and Cretaceous ages, dipping gently and uniformly to the east. The climate of the Riyadh region is affected by the movement of four air masses, which create variable and seasonal rainfall which can be intense in magnitude. Riyadh is one of the fastest-growing cities in the world, with an annual growth rate of about 3.6%. The population growth of the city has been accompanied by an increase in water demand, which is met through groundwater (38%) and desalinated water (62%).

Chapter 4: SWAT Model Inputs

4.1. Overview

The movement of water over or below the land surface is called runoff and there are two main types: surface runoff (i.e., overland flow) and subsurface runoff (i.e., interflow, throughflow) (Holden 2005). Typically after precipitation, water will infiltrate into the soil subsurface and either contribute to groundwater or move slowly through soils downslope before reaching either the river channel network of a standing water body. Surface flow occurs when the surface precipitation is falling on is impermeable or already saturated, preventing infiltration, or when rainfall is so intense infiltration capacity is reached. Surface runoff is quicker than subsurface runoff and can contribute to surface erosion, the extension of the channel network (e.g., gullying) and to flooding. In temperate environments, many rivers are perennial with flow year-round associated with interactions between groundwater and the channel network (e.g., baseflow), with precipitation events increasing river discharge above baseflow temporarily as the water volume associated with the precipitation moves through the catchment. In arid environments such as the catchments of Riyadh city, streams are ephemeral and dry for most of the year, only flowing for relatively short time periods (days) during and after infrequent, heavy rainfall events.

This chapter provides a description of the SWAT model and its main data inputs. Since SWAT is a comprehensive model, it requires many variables to run, although many are only required to simulate certain features that are not common for all watersheds (Arnold et al. 2012a). Focus is given to the data inputs required for the hydrological modelling performed as part of this thesis, and to data sources available in Saudi Arabia. Most of the following sections

characterise the essential inputs of the SWAT model to simulate surface runoff including topographic data (DEMs), land use/cover data, soil data, and climate data.

4.2. SWAT Model Description

SWAT is a hydrological model developed by the United States Department of Agriculture (USDA) and Texas A&M University (USDA ARS 2018). The SWAT model is a free, comprehensive environmental modelling software which can be applied to both small and large catchments (Gao et al. 2018). The SWAT model is one of the widely used tools for runoff estimation and is readily applicable through GIS-based interfaces and links to sensitivity, calibration and uncertainty analysis tools (Kiros et al. 2015). The first version of the SWAT model was developed and released in the early 1990s (Arnold et al. 2012b). The latest revised version of the model is SWAT 2012 (SWAT n.d.b). SWAT is a continuous-time model developed to operate initially on a daily time step. It is a process-based model, computationally efficient, and capable of continuous simulation over long time periods (Arnold et al. 2012b; Iskender and Sajikumar 2016). The model is designed to simulate surface water and groundwater qualities and quantities, and to predict the environmental impact of land use and land management practices at a catchment scale (USDA ARS 2018). The major components of a SWAT model can include weather, hydrology, soil properties, erosion/sedimentation, plant growth, nutrients, pesticides, bacteria and pathogens, and land management (Arnold et al. 2012b).

SWAT divides a catchment into multiple sub-basins, and then each sub-basin is subdivided into hydrologic response units (HRUs). Each HRU has a lumped land area within the sub-basin which comprises of homogeneous land use, management, slope, and soil characteristics. The homogenous HRU within the sub-basin are

represented as a percentage of its area and may not be contiguous (Rostamian et al. 2008; Arnold et al. 2012b; Zettam et al. 2017) (Figure 4.1).

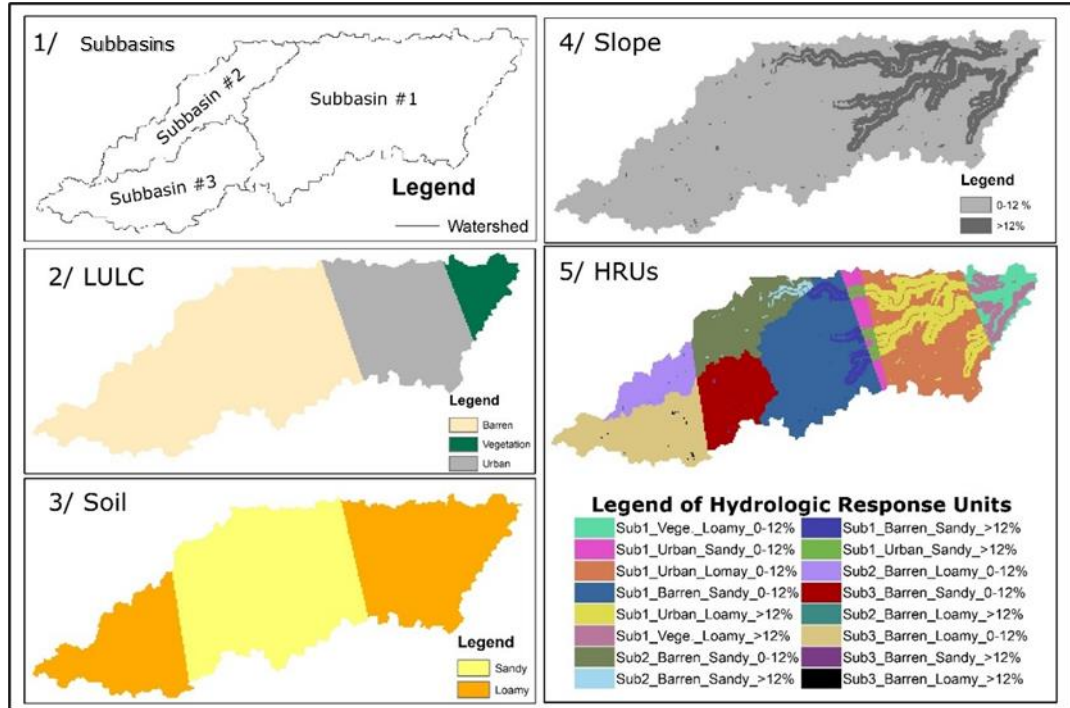


Figure 4.1: A hypothetical map to show dividing a catchment into hydrologic response units by the SWAT model.

The SWAT model simulates components of the hydrological cycle based on the water balance equation (Menking et al. 2003):

$$SW_t = SW + \sum_{i=1}^t (R - Q - ET - P - QR) \quad (4.1)$$

Where SW_t is the daily final soil water content (mm of water), SW is the initial soil water content on day i (mm of water), t is the time (days), R is the amount of precipitation on day i (mm of water), Q is the amount of surface runoff on day i (mm of water), ET is the amount of evapotranspiration on day i (mm of water), P is the amount of percolating water on day i (mm of water) and QR is the amount of return flow on day i (mm of water).

Climate drives the hydrological cycle and controls the water balance because it provides moisture and energy inputs, such as precipitation, temperature, solar radiation, wind speed, and relative humidity. The SWAT model reads the observed data directly from files or generates simulated data at runtime from observed monthly statistics. The driving force behind all the processes in the SWAT model is the water balance because it influences plant growth and the movement of sediments, nutrients, pesticides, and pathogens (Arnold et al. 2012b).

The SWAT model calculates some of the hydrological cycle components including surface runoff and ET. The model provides three methods for estimating potential evapotranspiration (PET) and the corresponding ET which are Penman-Monteith (default), Hargreaves, and Priestley-Taylor (Rostamian et al. 2008). Potential evapotranspiration (PET) can be defined as the maximum water loss, if enough water were available, via soil evaporation and plant transpiration from the HRU during a time step in millimetres. The actual evapotranspiration (ET) can be defined as soil evaporation and plant transpiration from the HRU during a time step in millimetres (Arnold et al. 2012a). SWAT provides two methods to estimate surface runoff volume from HRUs, which are Soil Conservation Service curve number (SCS-CN) method and Green-Ampt Mein-Larson infiltration method (Menking et al. 2003; Kiros et al. 2015). Surface runoff from hourly rainfall data can be estimated using the Green-Ampt Infiltration method. The model also estimates the peak runoff rate by using the modified rational method. The SWAT model calculates lateral subsurface flow simultaneously with the percolation process. The model uses a kinematic storage routing based on the slope degree, slope length, and saturated hydraulic conductivity to predict lateral flow in each soil layer. Lateral subsurface flow occurs when the storage in any subsurface layer

exceeds its field capacity after the percolation process (Rostamian et al. 2008). Water flow can be routed through the channel network by one of the available methods in the SWAT model which are the variable storage routing method or the Muskingum method (Arnold et al. 2012a). The variable storage routing method is the default and has been used in this study.

Typically, the most important challenges when hydrological modelling with SWAT in a data-sparse, arid catchment are the availability and quality of input data. The required data to develop and apply the SWAT model for runoff estimation in Riyadh's catchments were collected from Saudi government sources and global open-source data (Table 4.1). Initially, as a pilot study, a SWAT model was setup for one sub-basin (192 km²) and calibrated, with data sources shown in Table 4.1. The purpose of the pilot sub-basin was to identify any issues with model performance, before setting-up and running the model over multiple sub-basins. After the satisfactory performance of the SWAT model in the sub-basin, a SWAT model for the whole of Riyadh's catchments was developed using 5 m resolution DEMs, the governmental LULC maps, the Global Grid of Probabilities of Urban Expansion to 2030, the General Soil Map of Saudi Arabia 1:250,000, and climate data from local weather stations and rain gauges. TerraClimate ET data were used to calibrate and validate the developed SWAT models. The processes of setting up SWAT models for the study area are explained in Chapters 5 and 6.

Table 4.1: Data used for the development of SWAT models for Riyadh’s catchments, for the pilot study (one sub-basin) and the final SWAT models that were for the two main catchments of Riyadh city and its sub-basins.

SWAT input data	Pilot study	Final SWAT models	Source
DEM 5 m resolution	✓	✓	Royal Commission for Riyadh City, Saudi Arabia
DEM 10 m resolution	✓		General Authority for Survey and Geospatial Information, Saudi Arabia
DEM 30 m, Shuttle Radar Topography Mission (SRTM)	✓		Earthexplorer n.d.
DEM 30 m, Advanced Spaceborne Thermal Emission and Reflection Radiometer (ASTER)	✓		Earthdata, n.d.
DEM 30m, Advanced Land Observing Satellite (ALOS)	✓		ALOS, n.d
LULC 1996 map	✓	✓	Royal Commission for Riyadh City, Saudi Arabia
LULC 2004 map		✓	Royal Commission for Riyadh City, Saudi Arabia
LULC 2009 map		✓	Royal Commission for Riyadh City, Saudi Arabia
LULC 2012 map		✓	Royal Commission for Riyadh City, Saudi Arabia
LULC 2016 map		✓	Royal Commission for Riyadh City, Saudi Arabia
LULC 2019 map 100 m	✓		Buchhorn et al. (2020)
Global Grid of Probabilities of Urban Expansion to 2030		✓	Seto et al. (2012)
General Soil Map of Saudi Arabia 1:250,000	✓	✓	Ministry of Agriculture and Water (1986)
FAO Digital Soil Map of the World 9 km resolution	✓		FAO (n.d.)
Daily climate data from Riyadh Weather Station R001	✓	✓	Ministry of Environment, Water and Agriculture, Saudi Arabia
Daily climate data from Riyadh Old Airport Weather Station (no solar radiation data)	✓	✓	Ministry of Environment, Water and Agriculture, Saudi Arabia
Daily climate data from KKIA Weather Station (no solar radiation data)	✓	✓	Ministry of Environment, Water and Agriculture, Saudi Arabia
Daily rainfall data from Wadi Hanifah rain gauge	✓	✓	Ministry of Environment, Water and Agriculture, Saudi Arabia
Daily rainfall data from AlJubailah rain gauge	✓	✓	Ministry of Environment, Water and Agriculture, Saudi Arabia
Daily rainfall data from Sudoos rain gauge	✓	✓	Ministry of Environment, Water and Agriculture, Saudi Arabia
Daily climate data from Climate Forecast System Reanalysis (CFSR)	✓		SWAT n.d.a
Monthly climate data from TerraClimate	✓	✓	Abatzoglou et al. (2018)
Monthly evapotranspiration from Moderate Resolution Imaging Spectroradiometer (MODIS) 50 km resolution	✓		Abbaspour et al. (2019)

4.3. Digital Elevation Models (DEMs)

4.3.1. Background to DEMs

A DEM is a raster dataset with a regular grid of elevations arranged by column and row related to a particular datum such as Mean Sea Level (MSL), and free of trees, buildings and other constructed objects. In the literature, two more terms similar to DEM are used

to represent the digital elevation in areas, namely, digital surface model (DSM) and digital terrain model (DTM). There is some overlap between definitions but, generally a DSM is defined as an elevation model that represents the top of all surface features including buildings and treetops. In contrast, a DTM is a more generic term that refers to a DEM with one or more types of terrain information, such as, terrain morphological features, drainage patterns, and other geographical characteristics (Zhou et al. 2008; Zhou 2017).

Local and national DEMs are produced by official and/or government institutions or specialised companies. There are also many DEMs that are freely available, open source products for any part of the world (Mukherjee et al. 2013). Among the most commonly used global DEMs are the Shuttle Radar Topography Mission (SRTM), Advanced Spaceborne Thermal Emission and Reflection Radiometer (ASTER), and Advanced Land Observing Satellite (ALOS). The SRTM data was acquired in 2000 and previously sampled for public release at 3 arc-seconds for areas outside of the United States. In 2015, topographic data were released globally with a full spatial resolution of 1 arc-second (30 m). The ASTER data has been provided since 2011 at 1 arc-second (30 m) spatial resolution. The Japanese ALOS Global Digital Surface Model at 1 arc-second (30 m) spatial resolution was generated from stereo mapping equipment images aboard the Advanced Land Observing Satellite (ALOS) from 2006 to 2011.

The derived geomorphological information from a DEM such as slope, aspect, drainage area and network are important parameters for many applications including modelling water flow. Thus, the accuracy of DEMs used will affect the results of hydrological models (Mukherjee et al. 2013). Many studies have compared the DEM values of SRTM and ASTER DEMs with accurate GPS measurements or reference DEMs to assess their vertical accuracy. Hassan (2018),

in an area located at the southeast of Iraq, compared SRTM DEM and ASTER DEM with observed data obtained by the differential global positioning system (DGPS). The overall vertical accuracy showed RMS error of 2.276 m and 6.241 m for ASTER and SRTM DEM respectively. Over the south-central Chinese province of Hunan, Liu et al. (2020) used the high precision ICESat-2 altimetry points to evaluate the accuracy of SRTM and ASTER DEMs. The results of their study revealed that the SRTM DEM offers the best quality with a RMSE of 8.0 m, and ASTER DEM has the worst quality with the RMSE of 10.1 m. Using local high-precision elevation models as reference models, Uuema et al. (2020) examined the accuracy of SRTM, ASTER DEMs in four geographical regions (Estonia, Norway, New Zealand, and China) having different topographic and land use conditions. They found SRTM performed well, and ASTER was the least accurate and had the highest uncertainty across all study areas. The results of their study demonstrated that slope was the most important factor affecting DEM accuracy, where the smallest bias in the elevation values was detected on flat areas and increased with increasing slope.

4.3.2. DEMs applied in this study

Five DEMs were trialled when constructing the SWAT model for estimating runoff in the study area:

- A DEM with 5 m spatial resolution obtained from the Royal Commission for Riyadh City, Saudi Arabia.
- Another high-resolution DEM of 10 m obtained from the General Authority for Survey and Geospatial Information, Saudi Arabia. The DEM was generated using areal imagery acquired in 2011.
- Three DEMs from open sources with a medium spatial resolution of around 30m were tested, including the SRTM DEM

(EarthExplorer n.d.), the ASTER DEM (EarthExplorer n.d.), and ALSO (ALOS n.d.).

The decision on which DEM to use involved preliminary SWAT modelling, described in Chapter 5 in sections 5.5. and 5.6.

4.4. Land use/Land cover (LULC) Maps

4.4.1. Background of LULC maps

Land cover represents the natural and semi-natural features that overlay the surface of the earth including landforms, vegetation, and water bodies. Land use refers to human activities that modify the natural environment such as settlements, agricultural fields, and roads. Originally, Riyadh city was an agricultural settlement established on the bank of the Wadi Al Battha; a tributary of the Wadi Hanifah. Traditionally, agricultural fields were located along the banks of the Wadi Hanifah and its tributaries (Harrigan 2017). In contrast, the Wadi As Silayy basin in the past had no agricultural activities. Agriculture in the Wadi Hanifah now mainly consists of palm groves and crop and feed fields (Al-Sobaihi 1976; ICOMOS Consultant 2010). The cultivated lands in the wadi are irrigated by pumped shallow groundwater and by treated sewage water. Groundwater for irrigation in the area is pumped from traditional hand-dug wells and borehole wells (Alhamid et al. 2007).

4.4.2. Historical LULC

Shapefiles of five land use/land cover maps corresponding to the years 1996, 2004, 2009, 2012, and 2016 respectively, were obtained from the Royal Commission for Riyadh City, Saudi Arabia. These maps have 16 categories of land use/land cover. For this

present study, LULC types were grouped into four major classes to reproduce the maps (Table 4.2).

The derived LULC maps of the study area are shown in Figure 4.2 to Figure 4.6. The LULC categories of these maps are barren land, vegetation, urban, and roads. The barren land is natural land consisting mainly of geomorphological features including sand fields, cuesta back slopes, pediplains, hills, pediments, alluvial deposits, and sand fields. The vegetation class includes both natural vegetation and planted vegetation, but is mainly composed of planted areas including parks and farms. The urban class consists of construction lands including residential, commercial, and industrial areas. The road class is composed of highways, roads, streets, and paved car parks.

Table 4.2: The grouped LULC categories of Riyadh’s catchments for use as inputs for the SWAT model.

Barren land	Undeveloped lands and cemeteries
Urban	Industrial, warehouse and storage, transfer services, communications and public facilities, commercial, professional and business services, government services, health services, educational services, mosques, cultural, residential, and unknown
Vegetation	Agricultural and resources extraction, and Recreational gardens
Roads	Streets and Roads

Open-source, global LULC maps with 100 m spatial resolution are also available for 2019 from the Copernicus Global Land Service (Buchhorn et al. 2020) and were used in one attempt to calibrate the SWAT model. Figure 4.7 illustrates the LULC 2019 distribution in the catchments of Riyadh city. This map includes only three categories which are urban, vegetation, and barren land. The barren land class covered an area about 4,150 km² representing 83% of the study area in 2019. The second dominant LULC was the urban class covering an area about 752 km² which represented 15% of the

study area in 2019. The vegetation class came third covering an area about 90 km² and representing only 2% of the study area in 2019. It should be noted that the barren land area in this map was higher in the LULC 2019 map than it was in the LULC 2016 map.

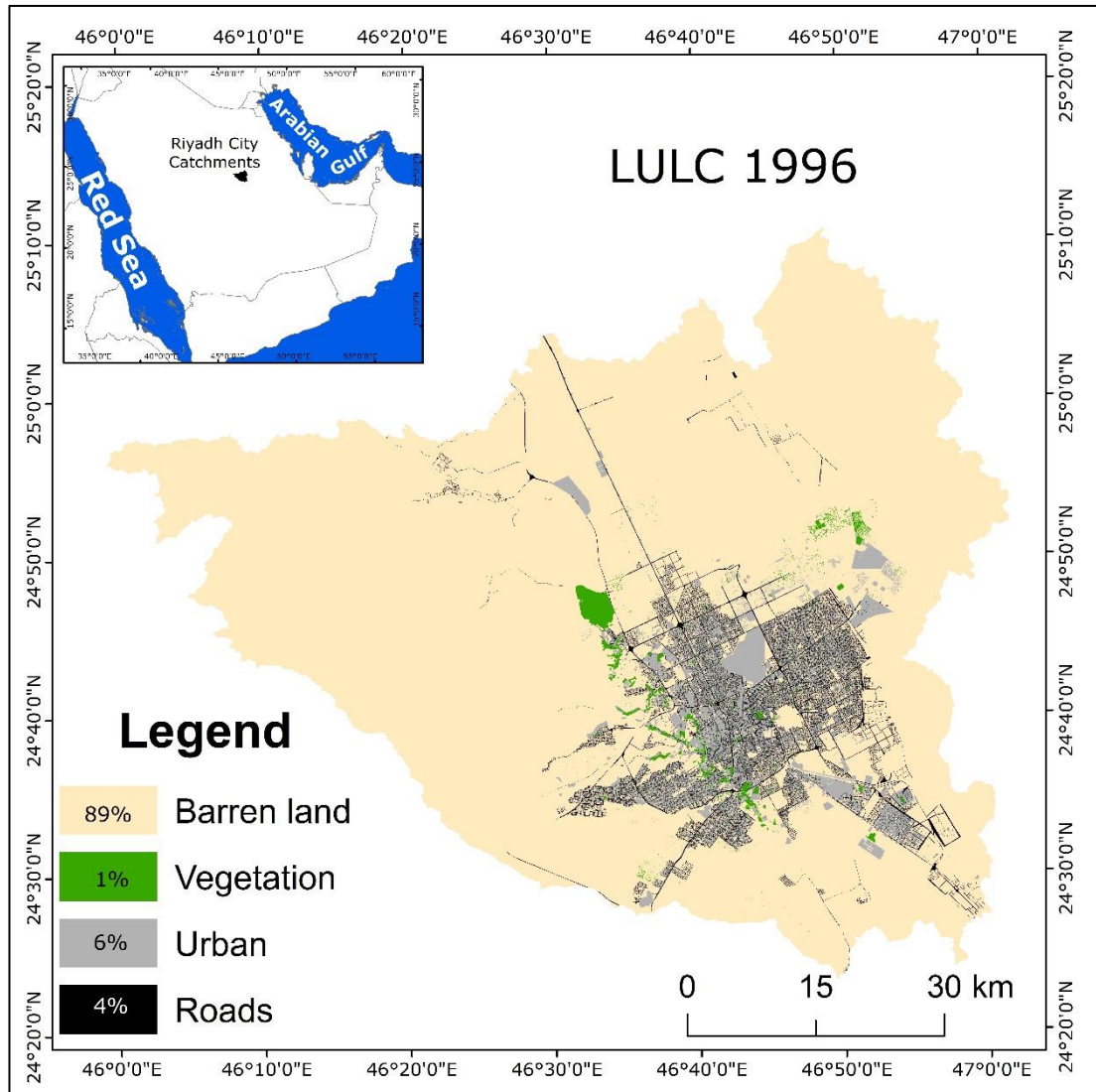


Figure 4.2: LULC in the catchments of Riyadh city for the year 1996.

Source: Royal Commission for Riyadh City, Saudi Arabia.

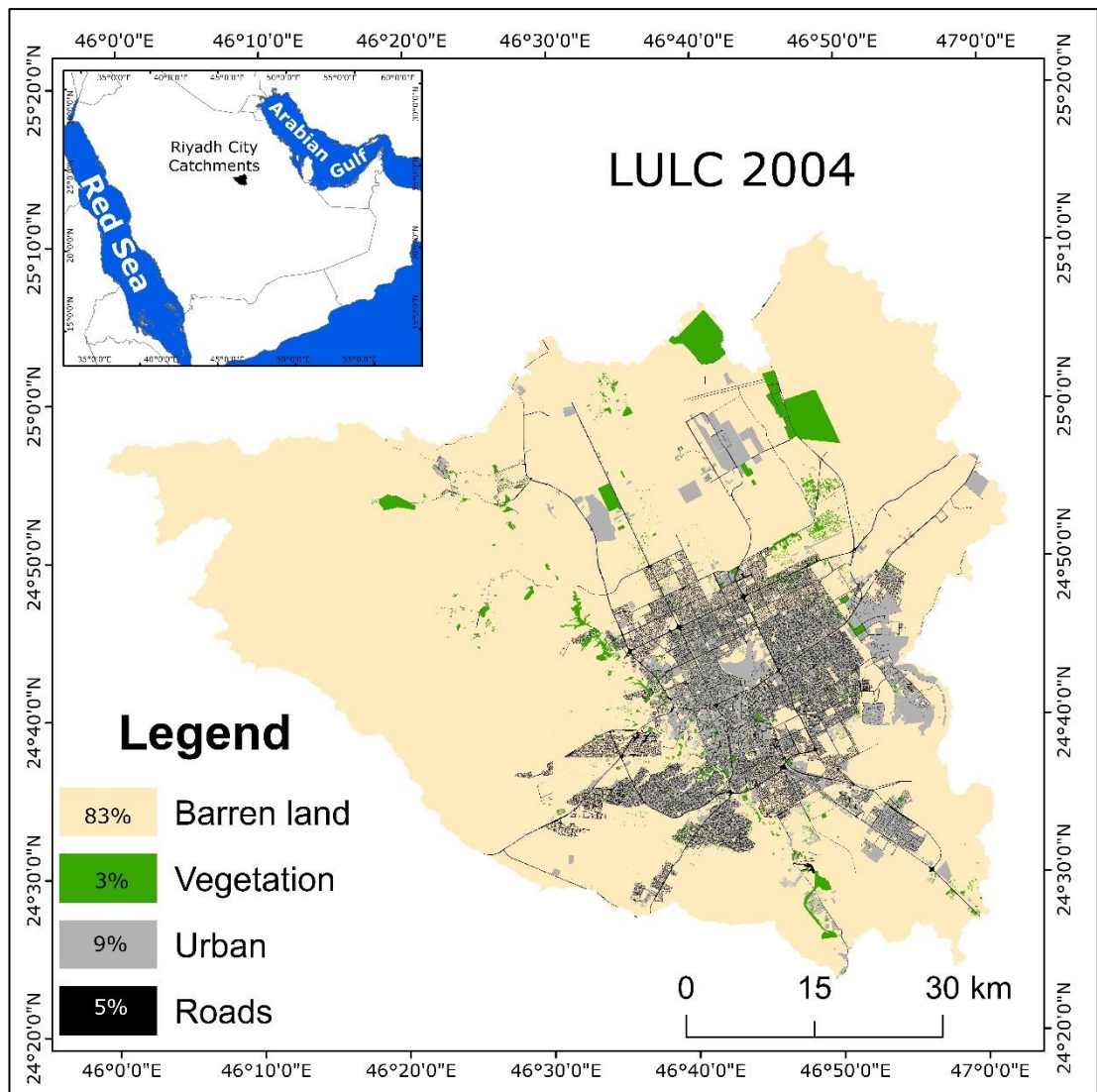


Figure 4.3: LULC in the catchments of Riyadh city for the year 2004.

Source: Royal Commission for Riyadh City, Saudi Arabia.

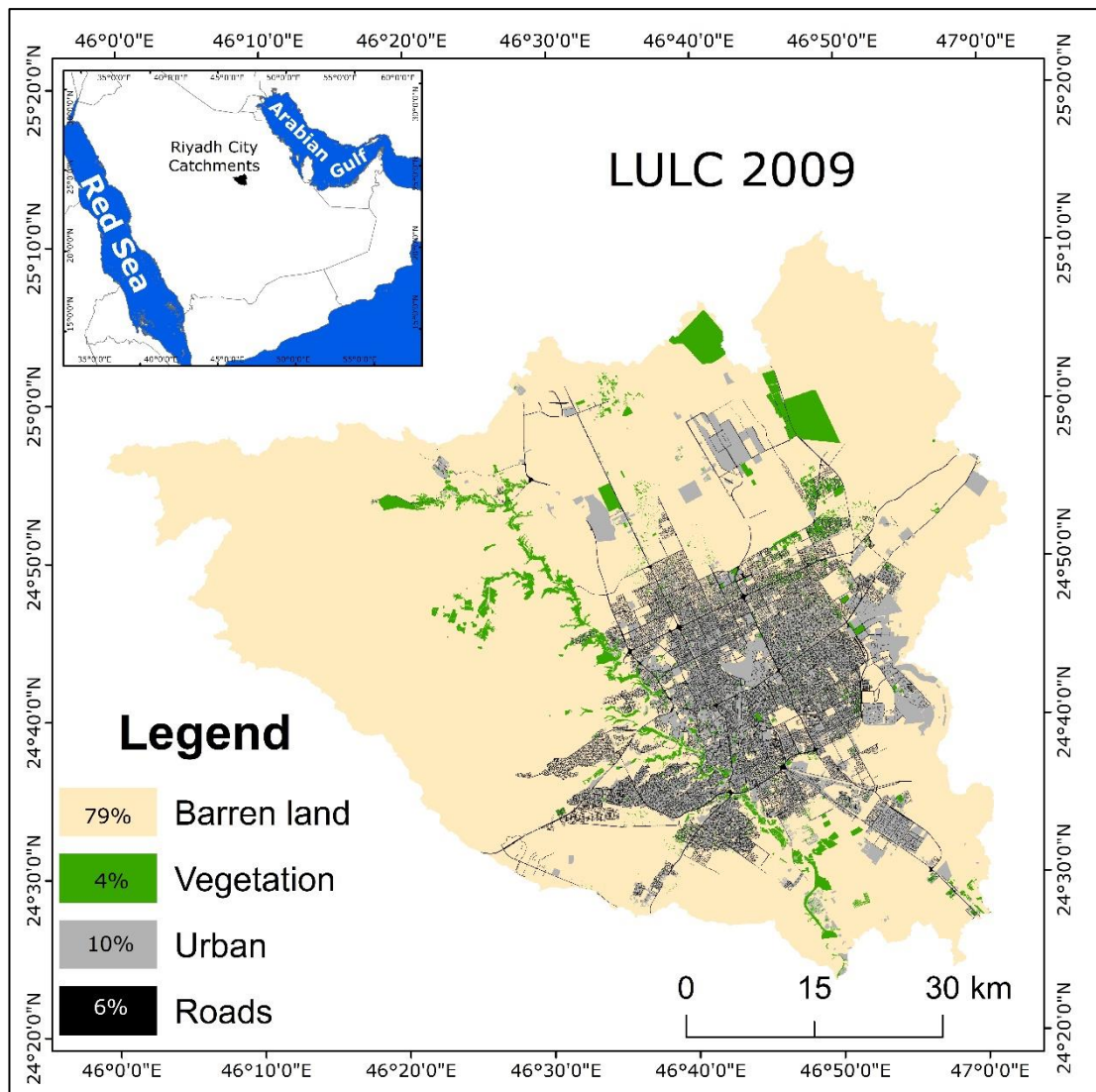


Figure 4.4: LULC in the catchments of Riyadh city for the year 2009.

Source: Royal Commission for Riyadh City, Saudi Arabia.

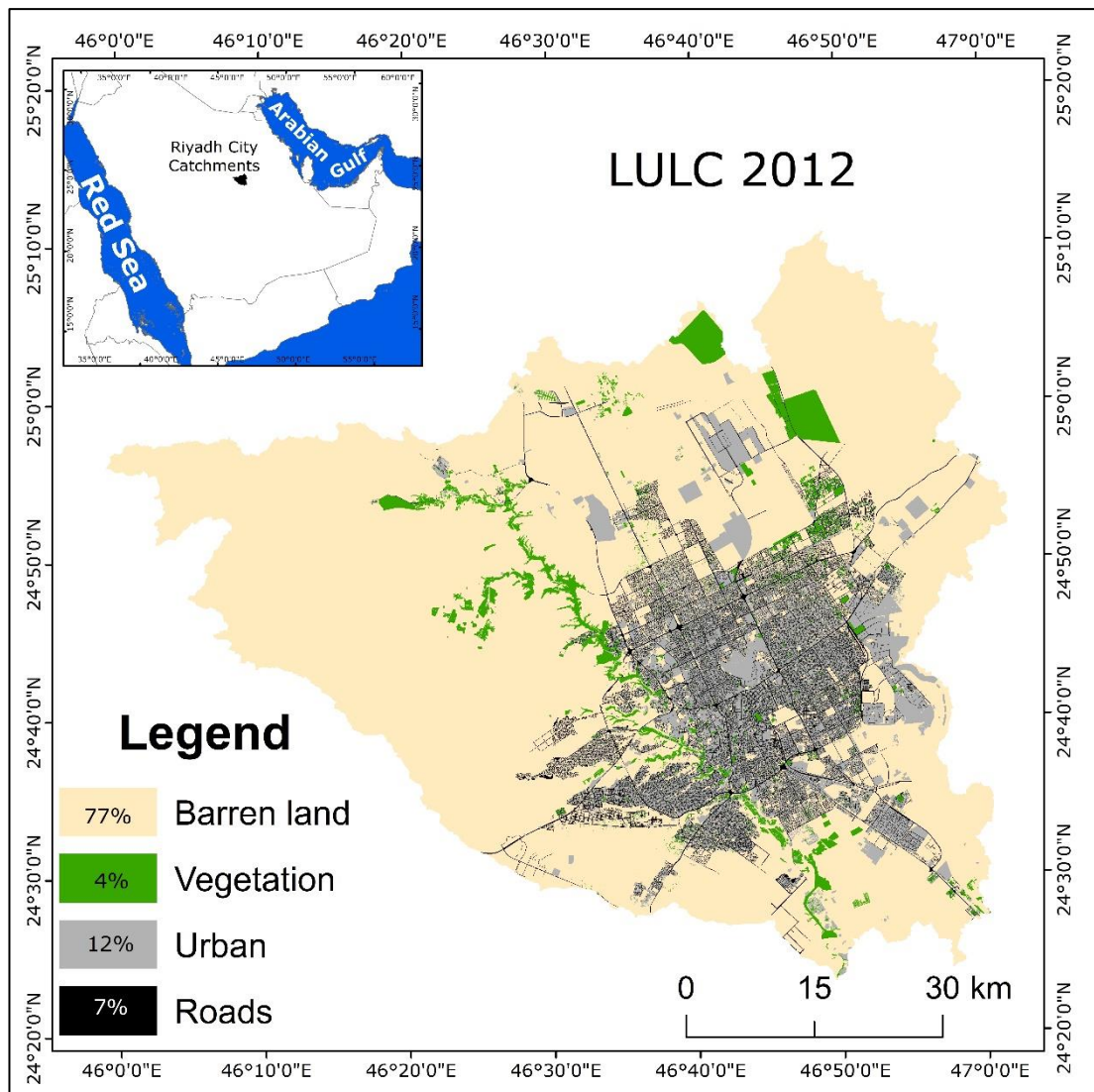


Figure 4.5: LULC in the catchments of Riyadh city for the year 2012.

Source: Royal Commission for Riyadh City, Saudi Arabia.

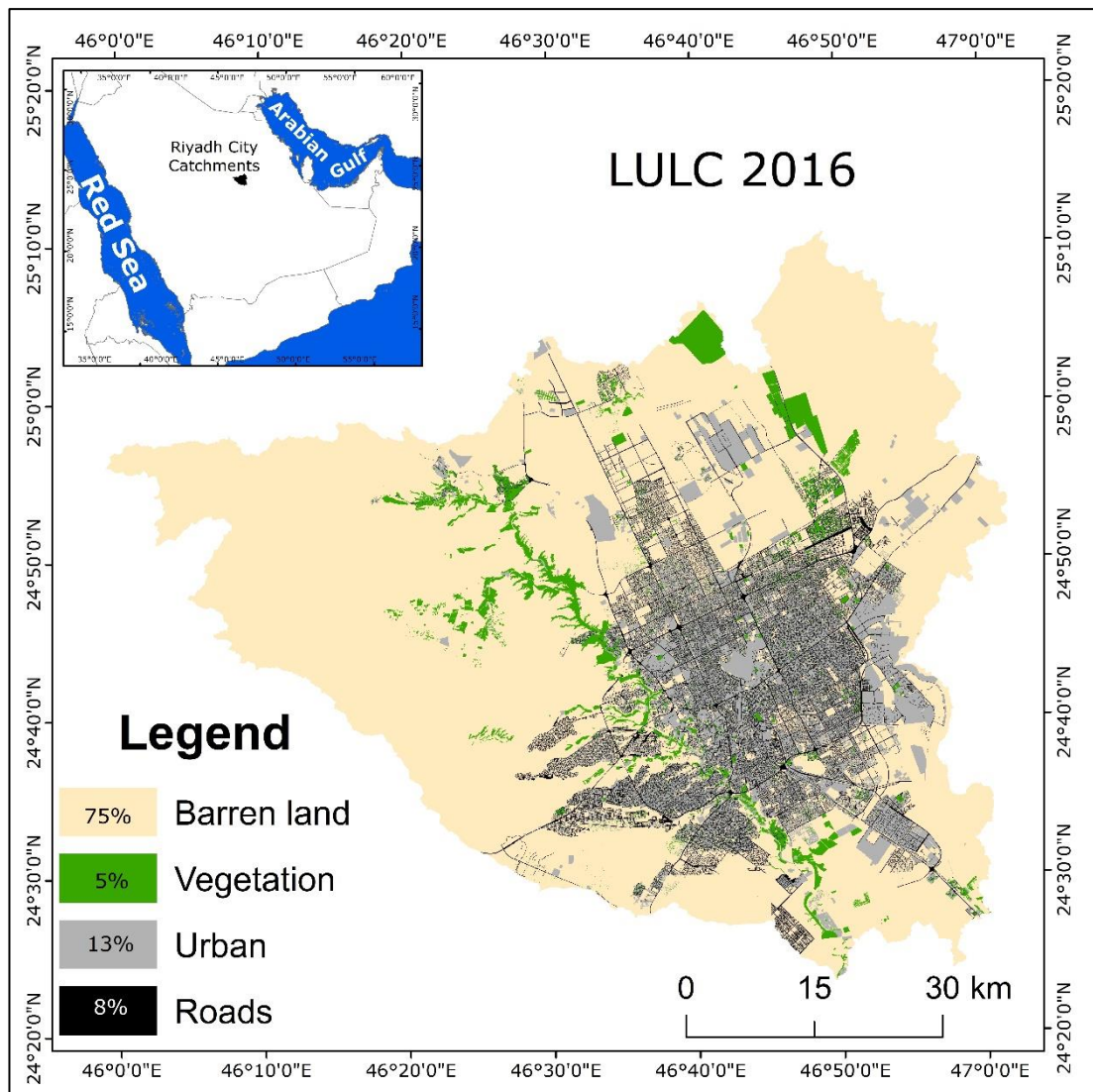


Figure 4.6: LULC in the catchments of Riyadh city for the year 2016.

Source: Royal Commission for Riyadh City, Saudi Arabia.

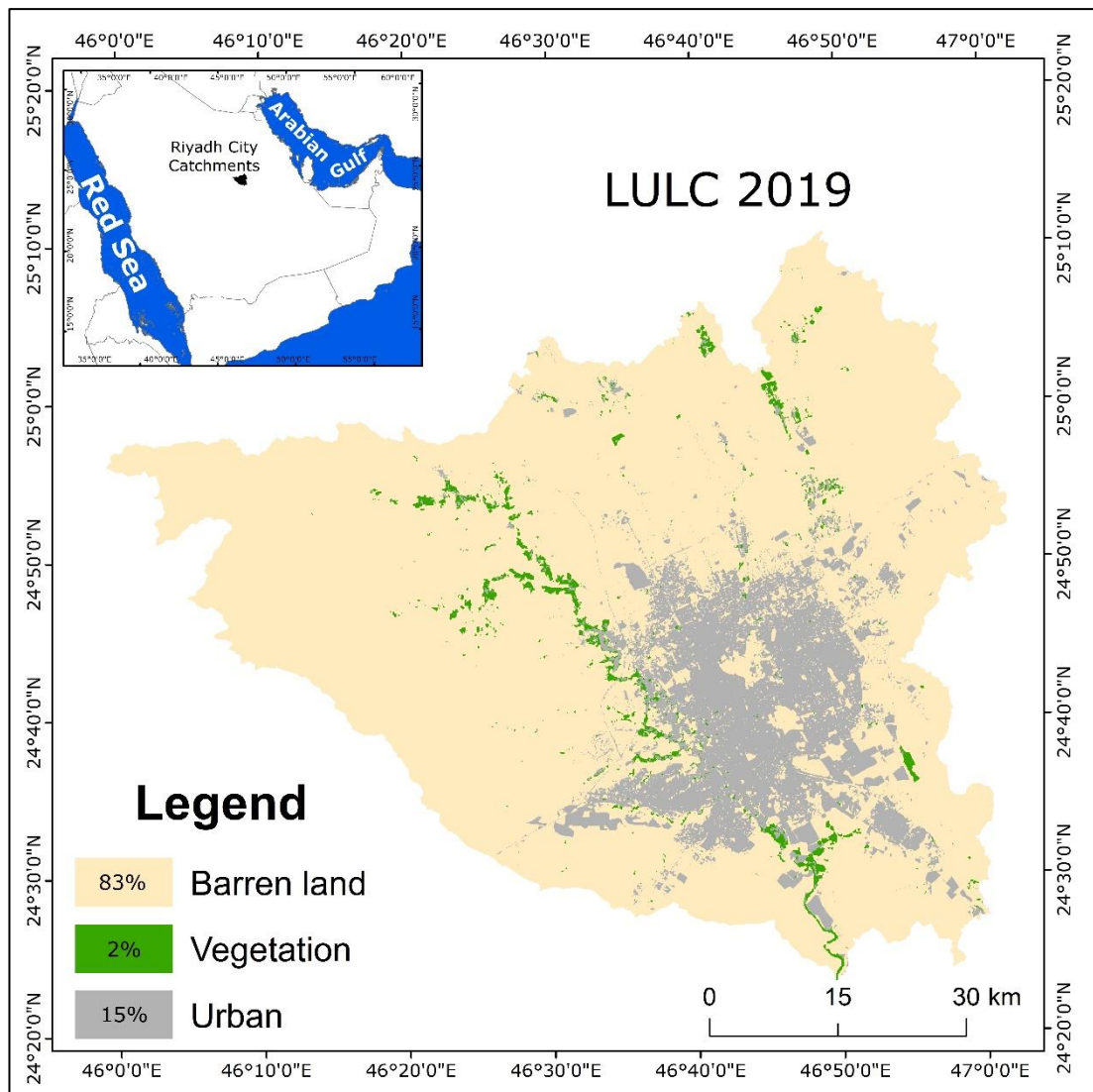


Figure 4.7: LULC 2019 for the main catchments of Riyadh city obtained from the Global Land Cover Map.
Source: Buchhorn et al. 2020.

4.4.3. Projections of LULC

Seto et al. (2012) provided a Global Grid of Probabilities of Urban Expansion to 2030. The maps of probabilities consist only of two categories which are barren land and urban. To forecast global urban expansion to 2030 they developed models for 16 geographical regions using five sources of data, including global urban extent circa 2000, urban population projections to 2030, population projection uncertainty ranges, population density estimates, and country-level gross domestic product (GDP) projections. The authors estimated

urban expansion in each geographical region by 2030 in a Monte-Carlo fashion based on the present empirical distribution of regional urban population densities and probability density functions (PDFs) of projected regional population and gross domestic product growth values for 2030. For each geographical region, they generated 1,000 estimates of the aggregate amount of urban expansion by randomly drawing 1,000 values each from the corresponding PDFs of projected gross domestic product growth and urban population. The authors then simulated the spatial distribution of predicted urban expansion using a spatially-explicit grid-based land change model that used slope, distance to roads, population density, and land cover as the main drivers of land-use change.

Forecasts of probabilities of Riyadh urban expansion for 2030 show in total urbanised areas of 4,682 km², 3,683 km², 3,089 km², 2,885 km², 2,431 km² and 1,902 km² for probabilities of 1%, 3%, 49%, 75%, 77%, and 100% respectively (Table 4.3). These probabilities were chosen for Riyadh because these probabilities have had substantial differences in areas. The Riyadh city expansion maps according to these probabilities are shown in Figure 4.8 to Figure 4.12. These data were used with the SWAT model to develop projections of runoff for Riyadh city for 2030 (Chapter 8). Since it was hard to estimate future increments in vegetation cover and road coverage, missing from the predictions of Seto et al. (2012), and impossible to define their future locations, roads and vegetation cover from the LULC 2016 map was added to the 2030 probability maps to run the SWAT model.

Table 4.3: Probabilities of Riyadh Urban Expansion to 2030.

% Probabilities	Urban area km ²	Barren area km ²
Urban 2000	861	4,131
100	1,902	3,090
80	1,905	3,088
78	1,985	3,008
77	2,431	2,561
76	2,746	2,247
75	2,885	2,108
69	2,913	2,079
68	3,005	1,988
66	3,058	1,934
65	3,062	1,931
64	3,063	1,930
49	3,089	1,903
33	3,116	1,877
10	3,143	1,850
8	3,185	1,807
7	3,230	1,762
6	3,289	1,703
5	3,368	1,624
4	3,418	1,575
3	3,683	1,309
2	4,106	886
1	4,682	310

Source: Seto et al. (2012).

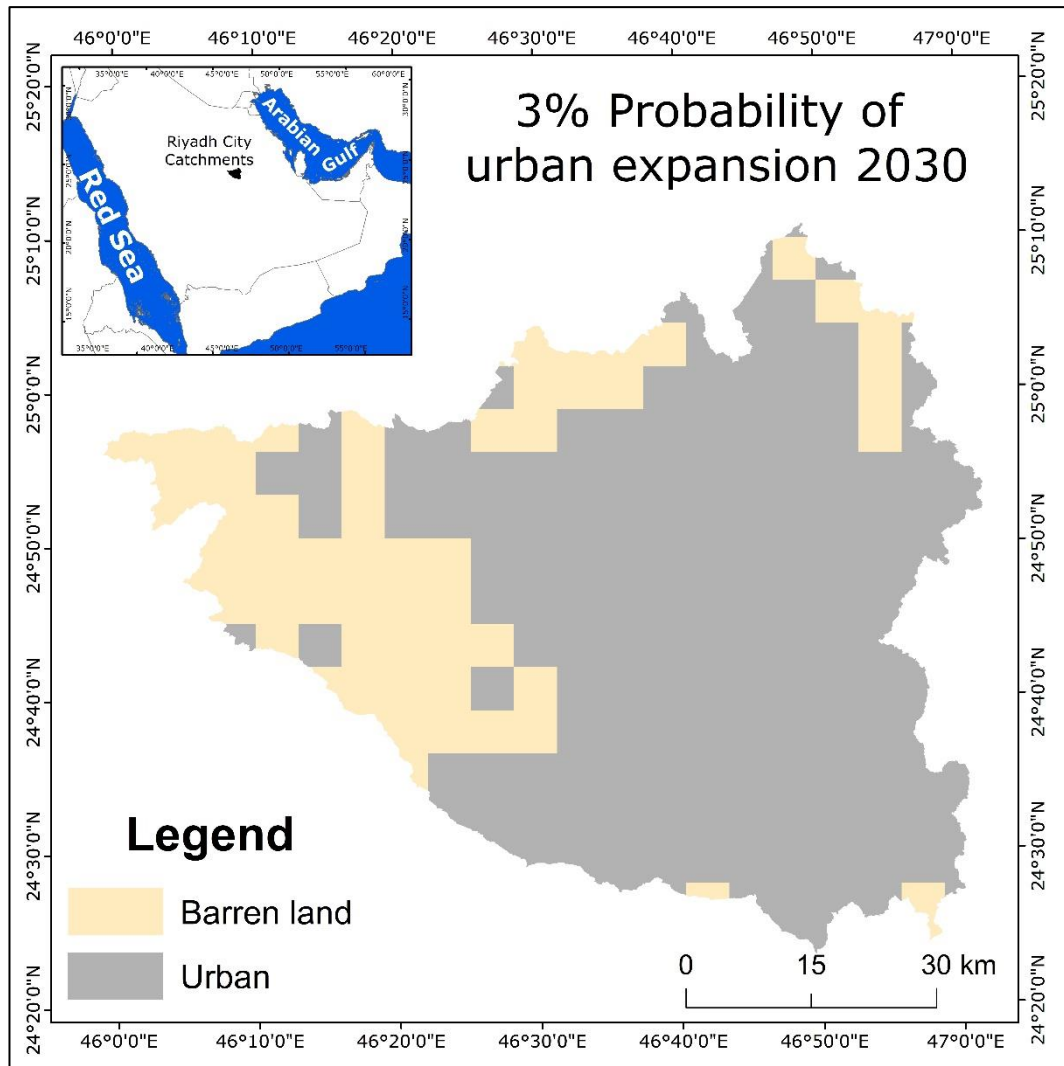


Figure 4.8: 3% Probability of Riyadh city expansion to 2030.
Source: Seto et al. (2012).

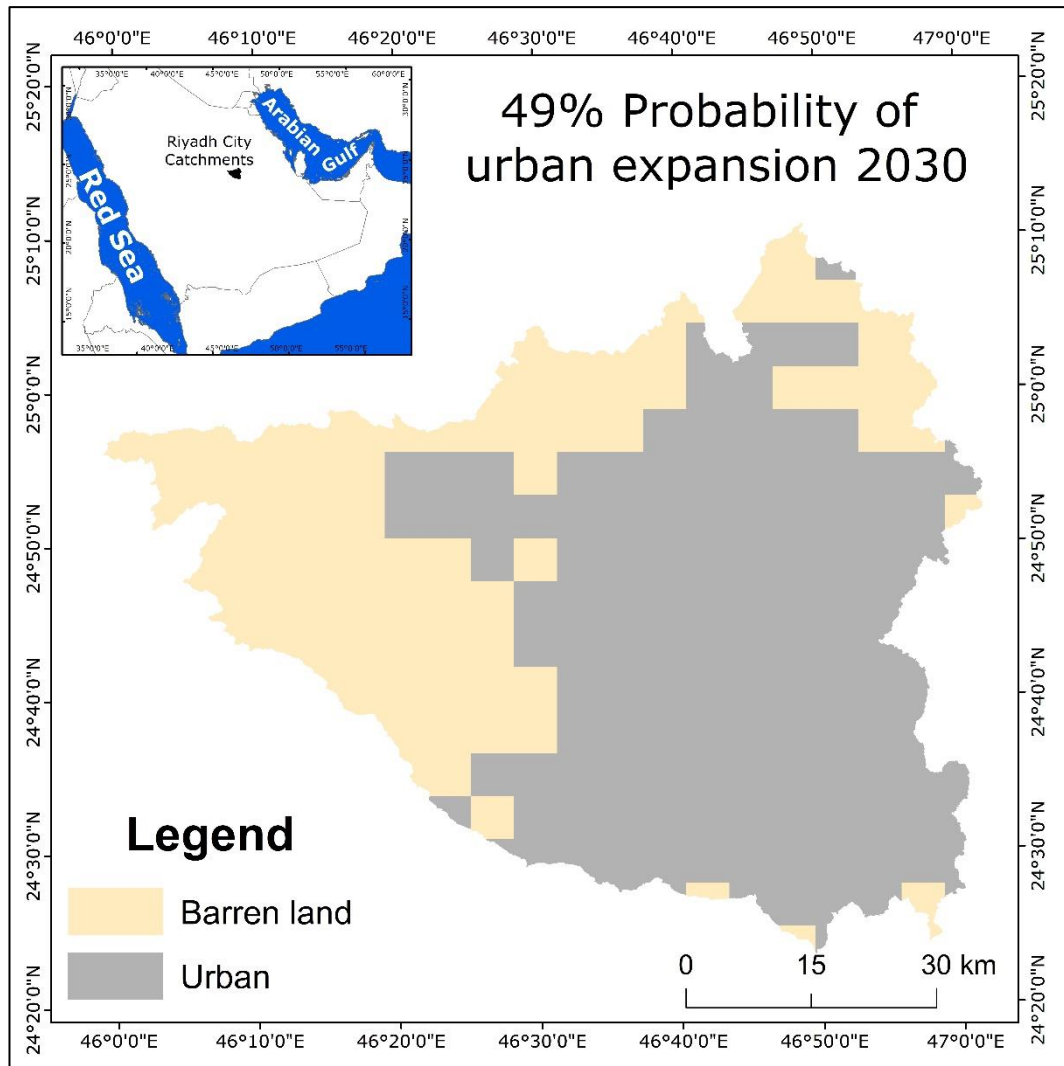


Figure 4.9: 49% Probability of Riyadh city expansion to 2030.
Source: Seto et al. (2012).

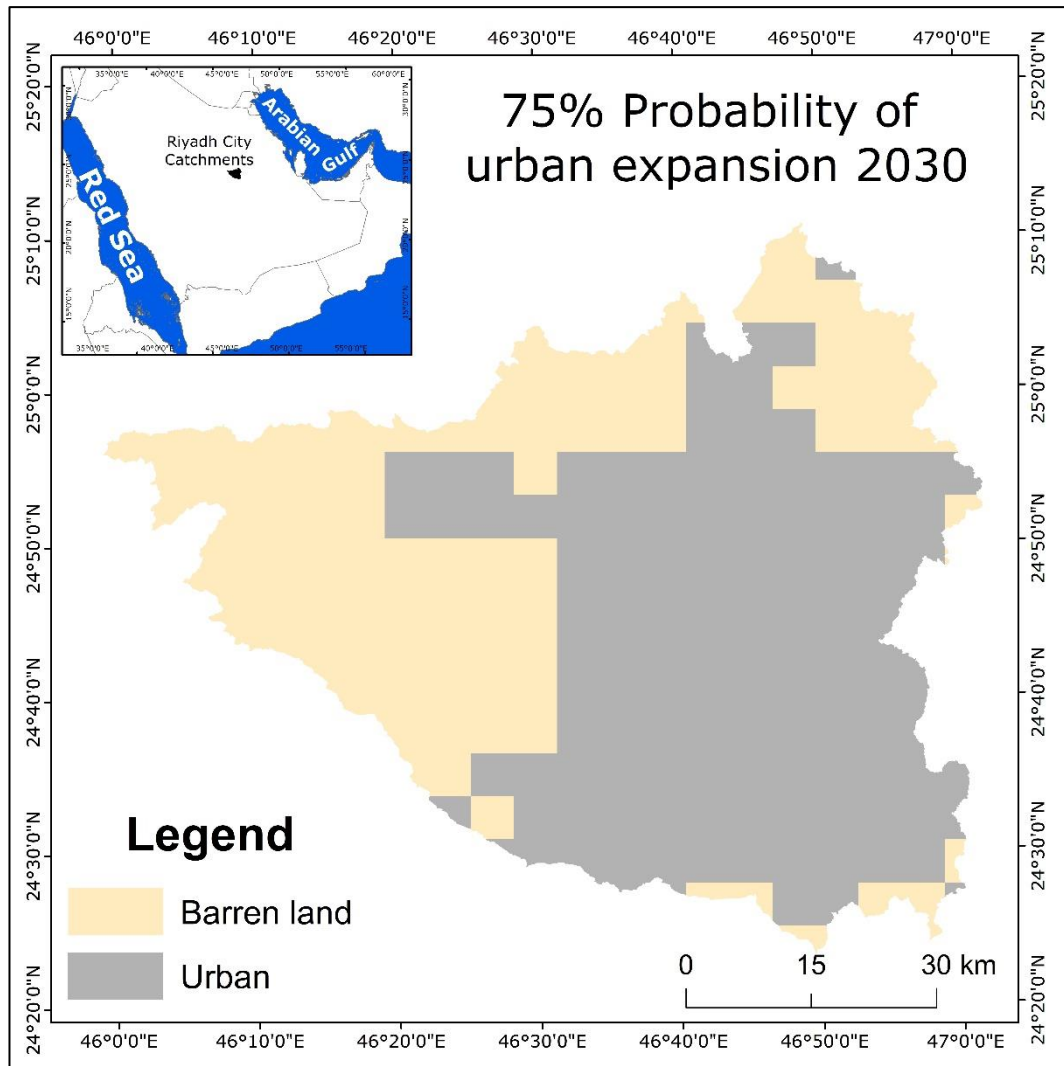


Figure 4.10: 75% Probability of Riyadh city expansion to 2030.
Source: Seto et al. (2012).

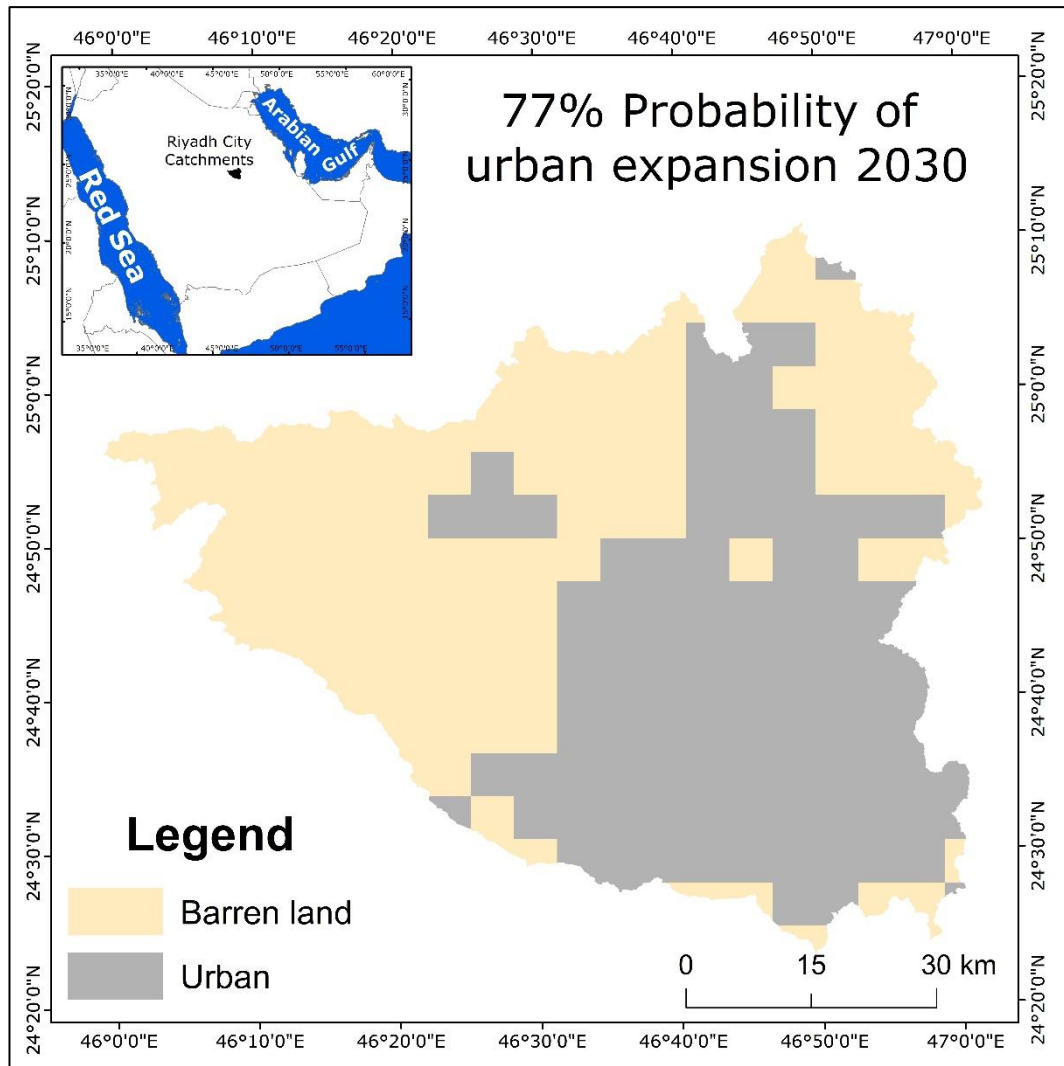


Figure 4.11: 77% Probability of Riyadh city expansion to 2030.
 Source: Seto et al. (2012).

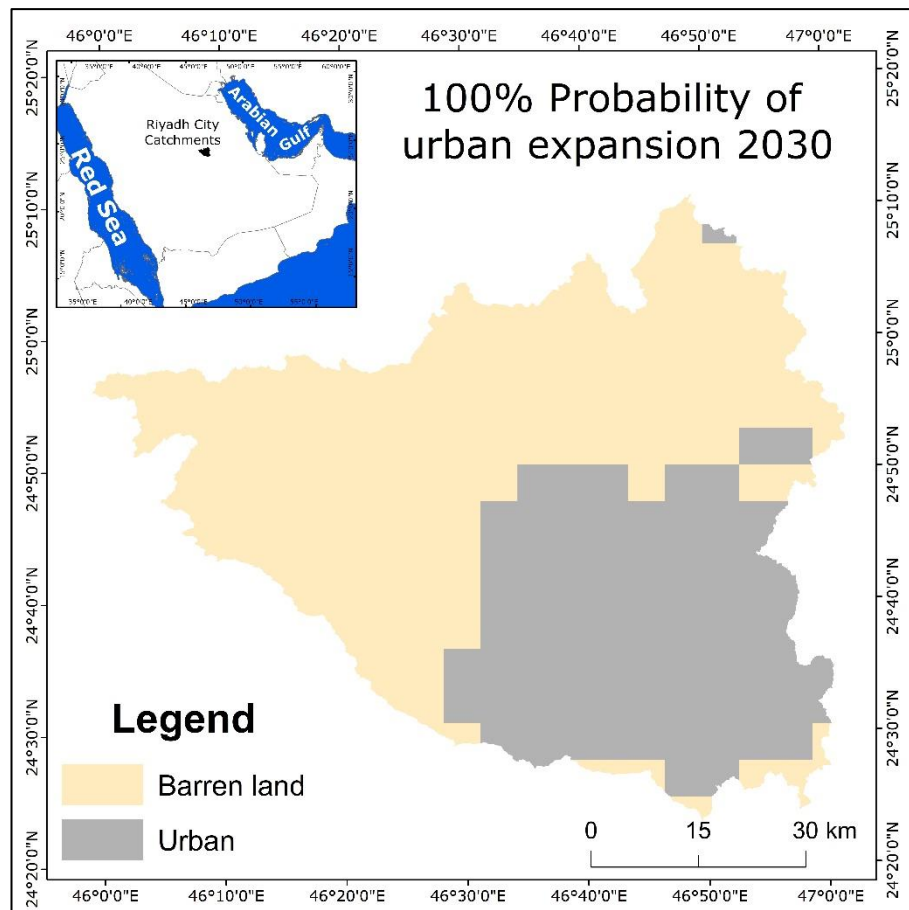


Figure 4.12: 100% Probability of Riyadh city expansion to 2030.
Source: Seto et al. (2012).

4.5. Soil Data

4.5.1. Background of soils data

The spatial distribution of soils in Saudi Arabia is available from the General Soil Map of Saudi Arabia scale 1:250,000 and the FAO Digital Soil Map of the World (spatial resolution 5 arc minutes or 9 km at the equator). At the first stage of the SWAT model development for the study area, many attempts were carried out to improve the model performance using different data sources. The General Soil Map of Saudi Arabia has been considered the main data source of soil for this current research, but in an attempt to improve SWAT model performance the FAO Digital Soil Map of the World was used and tested for the pilot study.

In 1995, the FAO Digital Soil Map of the World was digitised from the FAO-UNESCO Soil Map of the World published between 1974 and 1980 in 19 separate sheets at a mapping scale of 1:5,000,000 (Omuto et al. 2013). Originally, the legend of the Soil Map of the World was composed of 26 major soil groupings at the first level of generalisation which was subdivided at a second level into 106 soil units. In accordance with additional experience gained, the revised version of the soil classification system by the FAO resulted in the deletion of some major soil groupings and soil units and the addition of others. The revised system consists of 28 major soil groupings that subdivided at the second level into 153 soil units (FAO 1988). The soil units of the FAO-UNESCO system do not correspond to equivalent categories in different classification systems, but they are generally comparable to the Great Group level of USDA Soil Taxonomy (FAO 1974).

4.5.2. Soil categories in Riyadh

A generalised comprehensive mapping of soil has been carried out by the Ministry of Environment, Water and Agriculture (formerly Ministry of Agriculture and Water) in the 1980s. The Ministry of Agriculture and Water (1986) produced an atlas at a scale 1:250,000 entitled the General Soil Map of the Kingdom of Saudi Arabia to cover the whole country. The soils were identified and mapped at the level of great group according to the hierarchical system (Order - Suborder - Great Group) of the USDA Soil Taxonomy (USDA 1975). The Kingdom of Saudi Arabia has been covered by 49 soil units named and symbolled by numbers from 10 to 58. Each map unit represents an area that consists of one or more soil types and land types for which the unit is named. For example, the map unit with the symbol 10 is named Calciorthids: loamy, deep soils, 0 to 3 percent slopes (Ministry of Agriculture and Water 1986). A map of

soils for the catchments of Riyadh city is presented in Figure 4.13 and Table 4.4.

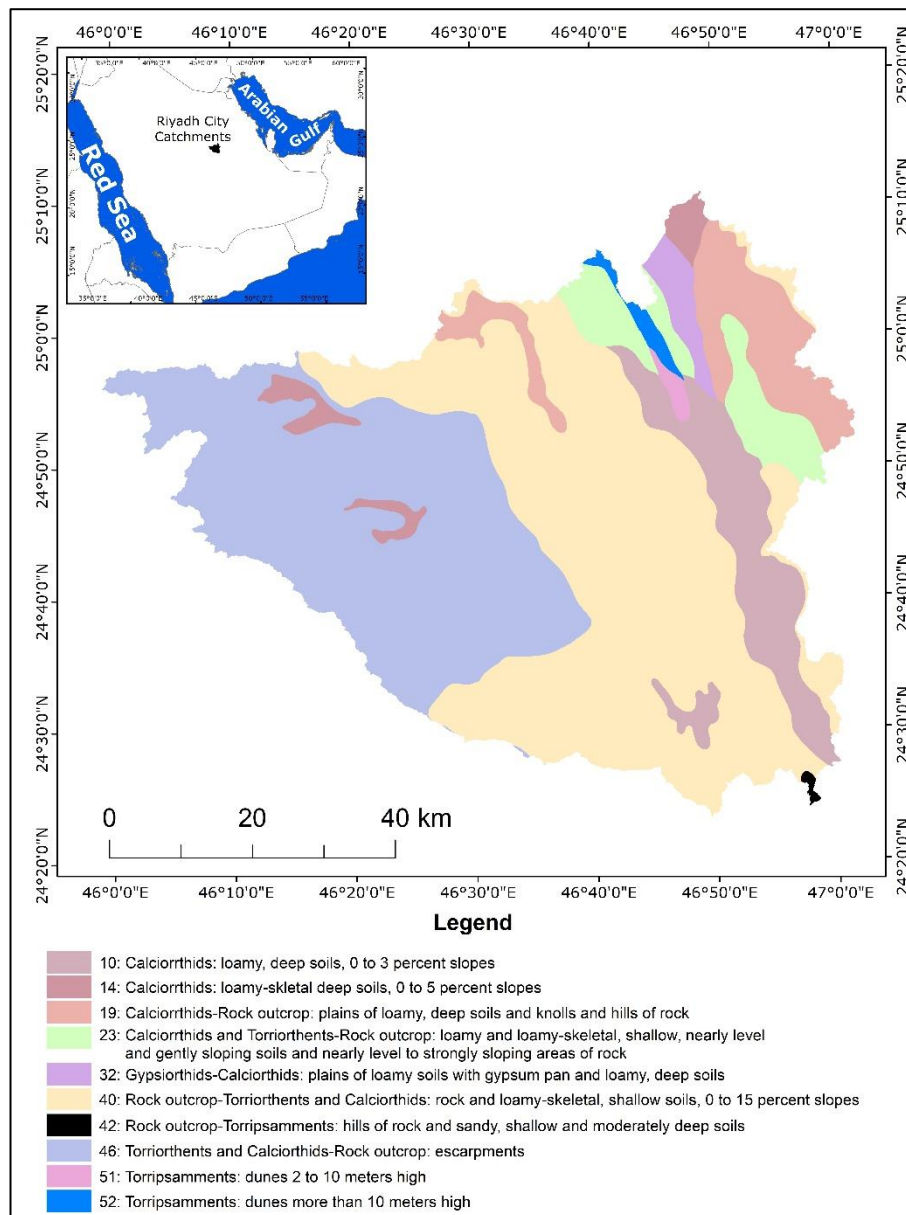


Figure 4.13: Distribution of the soils in the Riyadh city region based on USDA Soil Taxonomy.
Source: Ministry of Agriculture and Water (1986).

Table 4.4: Soil units in Riyadh's catchments of the General Soil Map of Saudi Arabia.

Soil unit symbol	Soil unit name
10	Calciorrthids: loamy, deep soils, 0 to 3 percent slopes
14	Calciorrthids: loamy-skeletal deep soils, 0 to 5 percent slopes
19	Calciorrthids-Rock outcrop: plains of loamy, deep soils and knolls and hills of rock
23	Calciorrthids and Torriorthents-Rock outcrop: loamy and loamy-skeletal, shallow, nearly level and gently sloping soils and nearly level to strongly sloping areas of rock
32	Gypsiorthids-Calciorrthids: plains of loamy soils with gypsum pan and loamy, deep soils
40	Rock outcrop-Torriorthents and Calciorrthids: rock and loamy-skeletal, shallow soils, 0 to 15 percent slopes
42	Rock outcrop-Torripsamments: hills of rock and sandy, shallow and moderately deep soils
46	Torriorthents and Calciorrthids-Rock outcrop: escarpments
51	Torripsamments: dunes 2 to 10 meters high
52	Torripsamments: dunes more than 10 meters high

The Wadi Hanifah catchment is covered by five map units of soil. But the soil map of the Riyadh city region demonstrates that 96% of the Wadi Hanifah catchment is covered by two map units composed mainly rock outcrops. The unit of Torriorthents and Calciorrthids-Rock outcrop: escarpment spreads in the northwest area of the Wadi Hanifah catchment representing about 1,607 km² (54% of the basin area). The unit Rock outcrop-Torriorthents and Calciorrthids: Rock and loamy-skeletal, shallow, up to 15 percent slopes, occupies the east and south the basin covering about 1,231 km² (42% of the basin area).

On the other hand, except for the map unit (Torriorthents and Calciorrthids-Rock outcrop: escarpment), the other nine soil map units are found in the Wadi As Silayy catchment. The unit (Rock outcrop-Torriorthents and Calciorrthids: Rock and loamy-skeletal, shallow, up to 15 percent slopes) is dominant in the western half of the Wadi As Silayy catchment, and it also exists in relatively small separate areas of the eastern half of the basin. This unit covers about 862.60km² representing approximately 42% of the basin area. The

relatively long strip extending from north to south in the central section of the Wadi As Silayy catchment consists mainly of sand dunes in the north and deep loamy soils in the middle and southern parts. The unit (Calciorthis: loamy, deep soils, 0 to 3 percent slopes) formed along the main channel of the Wadi As Silayy catchment covers about 394 km² representing approximately 19.23% of the basin area. Map units composed mainly of rock outcrops are dominant in the eastern half of the basin.

The FAO Digital Soil Map of the World illustrates four soil units in the catchments of Riyadh city which are Cambic Arenosols (Qc), Calcic Yermosols (Yk), Luvic Yermosols (Y1), and Orthic Solonchaks (Zo) (Figure 4.14). The descriptions of these soil units and their soil groupings are described in Table 4.5.

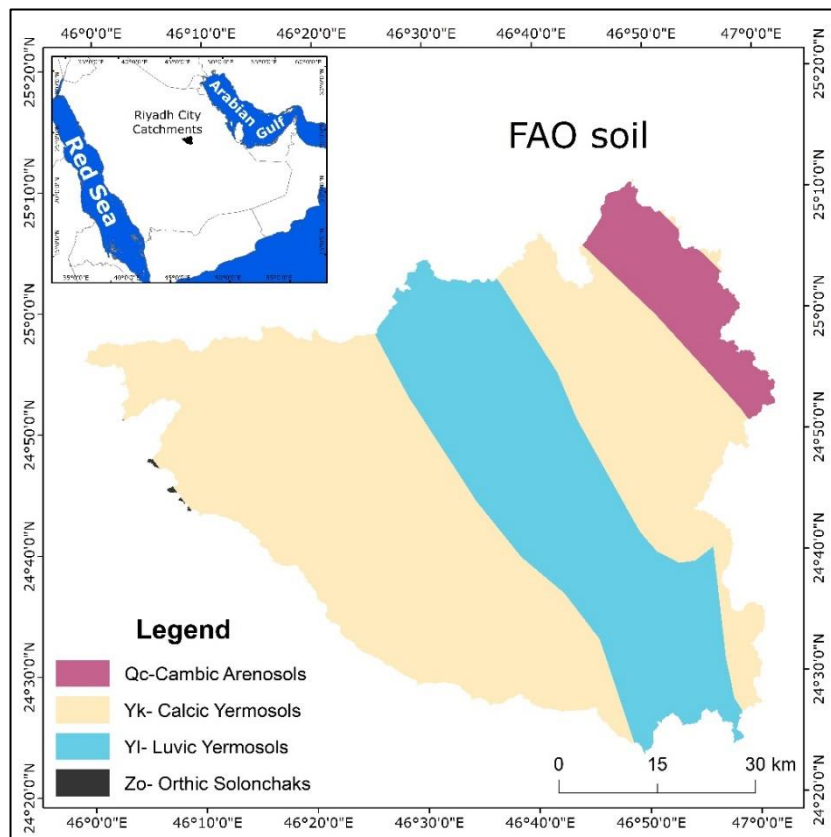


Figure 4.14: Distribution of the soils in the Riyadh city region Base on the classification system of the Soil Map of the World.

Source: Digital Soil Map of the World.

Table 4.5: Soil units in Riyadh's catchments of the FAO Digital Soil Map.

Soil Units	Description
ARENOSOLS (Q)	Soils from coarse-textured unconsolidated materials, exclusive of recent alluvial deposits, consisting of albic material occurring over a depth of at least 50 cm from the surface or showing characteristics of argillic, cambic or oxic B horizons which, however, do not qualify as diagnostic horizons because of textural requirements; having no diagnostic horizons (unless buried by 50 cm or more new material) other than an ochric A horizon; lacking hydromorphic properties within 50 cm of the surface; lacking high salinity.
Cambic Arenosols (Qc)	Arenosols showing colouring or alteration characteristic of a cambic B horizon immediately below the A horizon; lacking lamellae of clay accumulation; lacking ferrallic properties.
YERMOSOLS (Y)	Soils occurring under an aridic moisture regime; having a very weak oclucic A horizon and one or more of the following: a cambic B horizon, an argillic B horizon, a calcic horizon, a gypsic horizon; lacking other diagnostic horizons; lacking the characteristics which are diagnostic for Vertisols; lacking high salinity; lacking permafrost within 200 cm of the surface.
Calcic Yermosols (Yk)	Yermosols having a calcic horizon within 125 cm of the surface; lacking an argillic B horizon overlying the calcic horizon; lacking takyric features.
Luvic Yermosols (Y1)	Yermosols having an argillic B horizon; a calcic or a gypsic horizon may be present if underlying the B horizon; lacking takyric features.
SOLONCHAKS (Z)	Soils, exclusive of those formed from recent alluvial deposits, having a high salinity and having no diagnostic horizons other than (unless buried by 50 cm or more new material) an A horizon, a histic H horizon, a cambic B horizon, a calcic or a gypsic horizon.
Orthic Solonchaks (Zo)	Solonchaks having an ochric A horizon; lacking takyric features; lacking hydromorphic properties within 50 cm of the surface

Source (FAO 1974)

4.5.3. SWAT soil database

SWAT requires specific soil properties such as organic carbon content and moist soil albedo to be inputted to build a model (Table 4.6). Since the General Soil Map of Saudi Arabia and the FAO soil map do not include information on some of these variables, the values were derived from the literature (Donahue et al. 1983; Brouwer et al. 1985; Cronshey 1986; Foth 1990; Huang et al. 2012; Gregory and Nortcliff 2013; ICAR e-Course n.d.).

Soil types in Riyadh's catchment have been defined in both the General Soil Map of the Kingdom of Saudi Arabia and the FAO Soil Map. The FAO soil database prepared by Gungor (2014) was used only in one attempt for the pilot sub-basin. Table 4.7 shows the soil properties, used in the FAO soil database, for the SWAT model. On the other hand, the final SWAT model mainly has relied on the soil database prepared for the study area (Table 4.8).

Table 4.6: Soil properties required to build a database for the SWAT model.

Abbreviation	Description
HYDGRP	Including soil hydrologic group
SOL ZMX	Maximum rooting depth of soil profile
SOL Z	Depth from the soil surface to bottom of layer
SOL BD	Moist bulk density
SOL AWC	The available water capacity of the soil layer
SOL K	Saturated hydraulic conductivity
SOL CBN	Organic carbon content
SOL CLAY	Clay content
SOL SILT	Silt content
SOL SAND	The sand content
SOL ROCK	Rock fragment content
SOL ALB	Moist soil albedo
USLE K	USLE equation soil erodibility (K) factor

Table 4.7: FAO soil properties in the catchments of Riyadh city.

SNAM	Layer #	HYDGRP	SOL_ZMX	SOL_Z1	SOL_BD1	SOL_AWC1	SOL_K1	SOL_CBN1	CLAY1	SILT1	SAND1	ROCK1	SOL_ALB1	USLE_K1
Cambic Arenosols	1	C	810	300	1.4	0.11	20.33	0.8	15	20	65	0	0.1047	0.2989
	2			1,000	1.5	0.11	10.77	0.3	18	19	62	0	0.2747	0.2989
Luvic Yermosols	1	D	810	300	1.5	0.097	3.01	0.5	40	25	35	0	0.1867	0.2926
	2			1,000	1.5	0.097	3.22	0.3	41	23	35	0	0.2747	0.2926
Orthic Solonchaks	1	D	720	300	1.6	0.129	2.43	0.6	22	38	41	0	0.154	0.2926
	2			1,000	1.5	0.129	3.52	0.3	23	35	42	0	0.2747	0.2926
Calcic Yermosols	1	C	910	300	1.5	0.079	12.1	0.3	15	23	62	0	0.2747	0.3228
	2			1,000	1.4	0.079	16.66	0.3	17	20	62	0	0.2747	0.3228

Source: Gungor (2014).

Table 4.8: Soil properties in the catchments of Riyadh city.

Soil Type	HYDGRP	SOL ZMX (mm)	SOL Z (mm)	SOL BD (Mg/m ³ or g/cm ³)	SOL AWC1 (mm/300mm)	SOL K (mm/hr)	SOL CBN	SOL CLAY (%)	SOL SILT (%)	SOL SAND (%)	SOL ROCK (%)	SOL ALB	USLE K
Loamy	B (1)	>1,500 (3)	>1,500 (3)	1.65 (2) 1.28 (4) 1.4 (7)	0.16 (2) 0.13 (5)	15-51 (3) 6.12 (2)	0.03- 0.75 (9)	18	41	41		0.16 (8)	0.41 (2) 0.39 (6)
Loamy-skeletal	B (1)	250-500 (3)	250-500 (3)	1.28 (4) 1.4 (7)	0.16 (2) 0.13 (5)	15-51 (3) 6.12 (2)	0.03- 0.75 (9)	18	41	41		0.16 (8)	0.03 (2) 0.03 (6)
Loamy-skeletal	B (1)	<500 (3)	<500 (3)	1.28 (4) 1.4 (7)	0.16 (2) 0.13 (5)	15-51 (3) 6.12 (2)	0.03- 0.75 (9)	18	41	41		0.16 (8)	0.03 (2) 0.03 (6)
Loamy-skeletal	B (1)	250-1,000 (3)	250-1,000 (3)	1.28 (4) 1.4 (7)	0.16 (2) 0.13 (5)	15-51 (3) 6.12 (2)	0.03- 0.75 (9)	18	41	41		0.16 (8)	0.03 (2) 0.03 (6)
Sandy	A (1)	>1,500 (3)	>1,500 (3)	1.61 (4) 1.6 (7)	0.07 (2) 0.06 (5)	>150 (3) >150 (2)	0.03- 0.75 (9)	3	5	92		0.35 (8)	0.41
Rock outcrop	D (1) (9)	1,524 (9)	1,524 (9)	2.5 (9)	0.01 (9)	190 (9)	0(9)	5 (9)	25(9)	70(9)	98(9)	0.23 (9)	0.01(9)

- (1) USDA (1986).
- (2) Donahue et al. (1983).
- (3) Ministry of Agriculture and Water (1986).
- (4) Gregory and Nortcliff (2013).
- (5) Brouwer et al. (1985).
- (6) Foth (1990).
- (7) ICAR e-Course (n.d.)
- (8) Huang et al. (2012).
- (9) Arnold et al. (2012a).

4.6. Slope Map

4.6.1. Background on slope data

The term slope in this context refers to the gradient or angle that describes quantitatively the steepness of a ground surface. In geomorphology, two meanings of the term slope are commonly used; the first is the inclined surface of a landform, and the second refers to the inclination of the surface (Small and Clark 1982; Chorley et al. 1984). To avoid confusion, sometimes the inclined surface is called hillslope, and the inclination is referred to as slope gradient or slope angle (Chorley et al. 1984). Slopes are a basic element of landforms and affect geomorphological and hydrological processes. Additionally, it influences many human activities such as settlements, agriculture, road, land drainage, etc (Small and Clark 1982). Therefore, it has been the focus of geomorphological and other environmental studies for both academic and applied purposes (Chorley et al. 1984).

SWAT requires the definition of slope categories. Small and Clark (1982) indicated that several slope classification systems have been suggested over the years and one of the most widely acknowledged versions is that of the International Geographical Union's Commission on Geomorphological Survey and Mapping presented. The IGU slope classification system divides slopes into nine categories, which was used herein (Table 4.9).

Table 4.9: The IGU slope classification system.

Slope type	Slope angle	Slope gradient %
Plain	0° - 0.5°	0 - 0.01
Slightly sloping	>0.5° - 2°	0.01 - 3.49
Gently inclined	>2° - 5°	3.49 - 8.75
Strongly inclined	>5° - 15°	8.75 - 26.79
Steep	>15° - 25°	26.79 - 46.63
Very steep	>25° - 35°	46.63 - 70.02
Precipitous	>35° - 55°	70.02 - 143
Vertical	>55° - 90°	143 - ∞
Overhanging	>90	-

Source: Small and Clark (1982).

4.6.2. Deriving slopes in Riyadh

Since Arc-SWAT accepts a maximum of five slope classes from a DEM, a merging process was applied to the IGU slope categories to produce the slope map for the study area. Figure 4.15 is a slope angle map of the catchments of Riyadh city generated from a DEM with a 5 m spatial resolution. The map shows the distribution of slope types in both the Wadi Hanifah and the Wadi As Silayy catchments.

Generally speaking, most of the Wadi As Silayy basin and the middle and lower reaches of the Wadi Hanifah are characterised by plains. The plains (0° - 2°) cover about 1,243 km² of the Wadi Hanifah catchment, which represents about 42% of the total area (Table 4.10). This slope category prevails as well in the Wadi As Silayy catchment where it covers an area of about 1,251 km² of the basin (61% of total area). Gently inclined lands (>2° - 5°) represent about 17% of the study area, strongly inclined lands (>5° - 15°) occupy about 23% of the area and the remaining 10% of the study area has slopes greater than 15°.

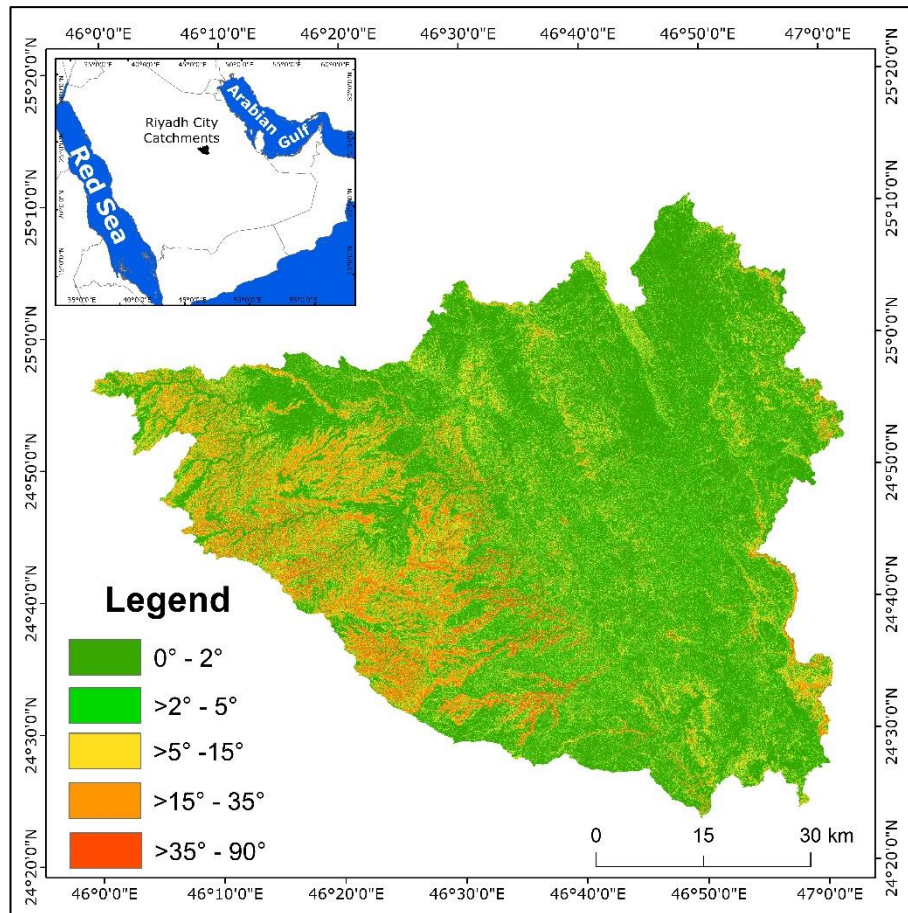


Figure 4.15: Slope angle map of the catchments in Riyadh city generated from the 5 m spatial resolution DEM.

Table 4.10: Slope classes in the catchments of Riyadh city.

Slope type	Slope angle	Slope gradient %	Hanifah Basin Km ²	As Silayy Basin Km ²	Riyadh City region	
					Km ²	%
Plain and slightly sloping	0° - 2°	0 - 3.49	1,243	1,251	2,493	50
Gently inclined	>2° - 5°	3.49 - 8.75	493	362	855	17
Strongly inclined	>5° - 15°	8.75 - 26.79	731	398	1,129	23
Steep and very steep	>15° - 35°	26.8 - 70.02	390	32	423	8
Precipitous and vertical	>35° - 90°	70 - ∞	88	4	92	2

4.7. Climate data

4.7.1. Background of available climate data

The daily climate data required for the SWAT model include the maximum and minimum temperatures, precipitation, relative humidity, wind speed, and solar radiation. Observed daily climate data for Riyadh city is available from three weather stations and three rain gauges (Figure 4.16).

Riyadh weather station (R001) has records of all climate elements required for the SWAT model with a relatively long time period starting from 1964 to date. Riyadh Old Airport weather station and King Khalid International Airport weather station also have records of the required climate data except for solar radiation. The records of the Riyadh Old Airport weather station cover the period from 1966 to 2010, whereas the recording period of the King Khalid International Airport weather station extends from 1985 to date.

Two rain gauges exist within the Wadi Hanifah catchment; the Wadi Hanifah rain gauge and the AlJubailah rain gauge. The Sudoos rain gauge is located outside of the Wadi Hanifah basin but very close to its upper reach border. The available daily rainfall record for the Wadi Hanifah rain gauge extends from 1965 to 2005. Whilst daily rainfall records from the AlJubailah rain gauge and the Sudoos rain gauge are available for the period from 1966 to the present.

In addition, daily datasets of Climate Forecast System Reanalysis (CFSR) were downloaded and used (Table 4.11).

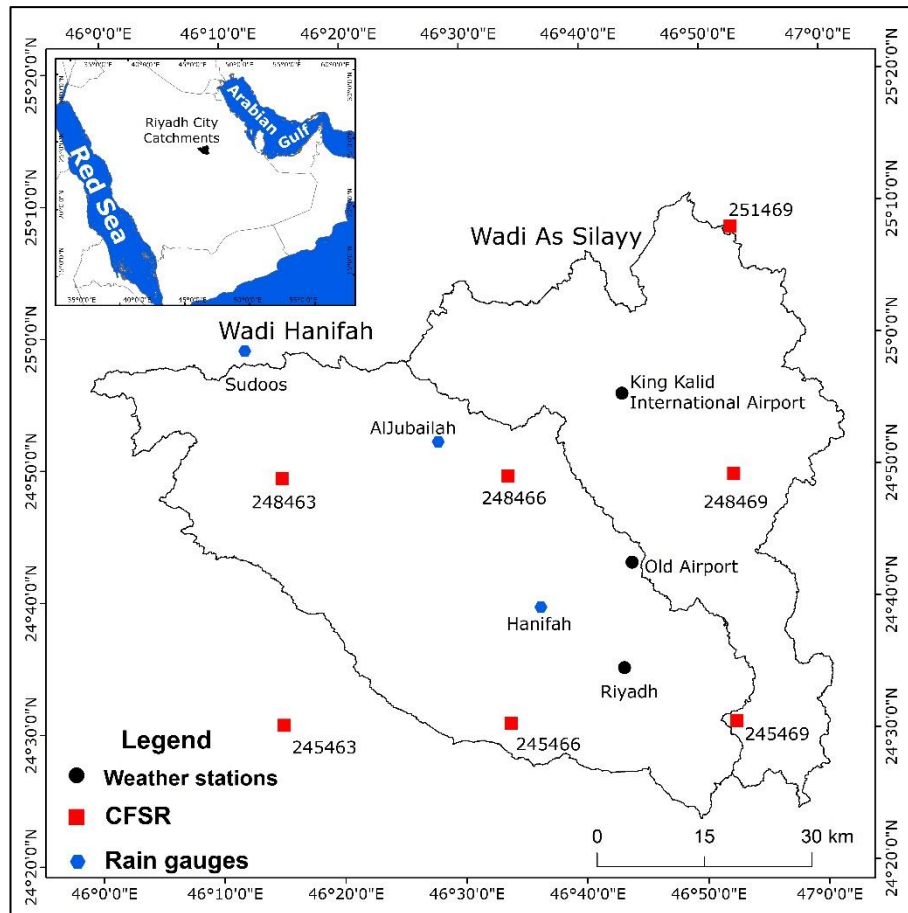


Figure 4.16: Locations of weather stations, rain gauges, and CFSR coverage points in the catchments of Riyadh city.

Table 4.11: Climate data used to develop the SWAT model for Riyadh's catchments.

Name	Data length	Spatial resolution	Temporal resolution	Elements used
Riyadh Weather Station	1964-2017	point	Daily	Rainfall, temperature, relative humidity, wind speed, and solar radiation.
Riyadh Old Airport Weather Station	1985-2010	point	Daily	Rainfall, temperature, relative humidity, and wind speed.
King Kalid International Airport Weather Station	1985-2017	point	Daily	Rainfall, temperature, relative humidity, and wind speed.
Hanifah Rain Gauge	1965-2005	point	Daily	Rainfall
AlJubailah Rain Gauge	1966-217	point	Daily	Rainfall
Sudoos Rain Gauge	1966-2017	point	Daily	Rainfall
TerraClimate	1958-2015	4km	Monthly	Rainfall, temperature, relative humidity, wind speed, solar radiation, actual evapotranspiration, and potential evapotranspiration.
Climate Forecast System Reanalysis (CFSR)	1979-2013	38 km	Daily	Rainfall, temperature, relative humidity, wind speed, and solar radiation.
Moderate Resolution Imaging Spectroradiometer (MODIS)	1982-2003	50km	Monthly	Actual evapotranspiration

4.7.2. Selection of climate data for SWAT

Almost all climate time series data have periods with missing data (Ropelewski and Arkin 2019) yet climate studies typically require complete time-series, meaning that imputation must be undertaken (Afrifa-Yamoah et al. 2020). The records of the Riyadh weather station (R001) had some missing values of daily temperature in most years (Figure 4.17). To get reliable results, missing values were estimated prior to the use of climate time series data in Riyadh.

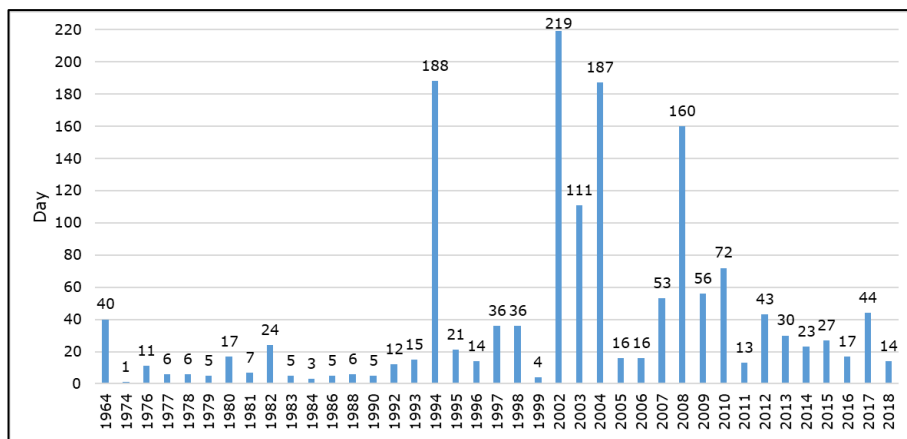


Figure 4.17: Missing values of daily temperature in the record of Riyadh weather station.

Several methods can be applied to estimate missing values. Arithmetic averaging is one of the simplest and most employed methods in climate studies (Sattari et al. 2017; Kanda et al. 2018). However, in the present study the SWAT model's built-in weather generator was initially used to estimate missing values of daily climate data. During the continued development of the SWAT model, two other supporting methods were trialled with the aim of enhancing the quality of climate data inputs. First, the daily average of all years in each station was used to fill missing daily data and, secondly, missing data in the Riyadh weather station was compensated from the King Khalid International Airport (KKIA)

weather station. Both methods did not improve model performance and so the in-built weather generator was used.

Like most parts of Saudi Arabia, the Riyadh region is characteristic of extremely hot and dry climatic conditions having irregular rainfall, very hot long summers, and relatively cold, short winters. The high temperatures of summer days tend to drop considerably at night. On the other hand, the low temperatures of winter nights tend to have an abrupt rise after sunrise (Almazroui 2011; Almazroui 2012b; Alghamdi and Moore 2014).

Table 4.12 shows the annual rainfall in Riyadh's catchments. The total annual rainfall varies greatly from year to year and from station to station. For example, in Riyadh weather station, the highest rainfall of 234 mm and lowest rainfall 15.9 mm occurred in 1995 and 2002, respectively. The average annual rainfall for 54-year period from 1964-2017 was about 83.3 mm. Average monthly rainfall reveals that March and April are the rainiest months in the study area (Figure 4.18). Since the rainfall record of the Hanifah rain gauge was used to model extreme runoff, the annual maximum daily rainfall is presented in Table 4.13. The highest annual maximum daily rainfall recorded on 23 March 1996 which was about 53 mm. This daily rainfall represented about 59% of the average annual rainfall.

Table 4.12: Annual rainfall (mm) in Riyadh's catchments.

Year	Riyadh station	Riyadh Old Airport Station	King Kalid International Airport Station	Hanifah Rain Gauge	AlJubailah Rain Gauge	Sudoos Rain Gauge
1964	151.6	-	-	-	-	-
1965	63.9	-	-	74.6	-	-
1966	26.1	-	-	19.9	2.5	18
1967	72.7	-	-	97.3	134	157.2
1968	113	-	-	108.4	116.5	96.7
1969	84	-	-	124.8	95.5	157.9
1970	17.1	-	-	17.9	19.5	3.1
1971	84.7	-	-	87.4	83.2	140.5
1972	111.7	-	-	179.4	127	175.5
1973	63.2	-	-	62.8	59	0
1974	66.3	-	-	97.2	103.1	167.5
1975	119.1	-	-	150.1	179.7	174
1976	162.3	-	-	182.2	147.5	207.8
1977	43.1	-	-	37.1	47.4	55
1978	27.4	-	-	68.4	30.5	49.2
1979	57.5	-	-	28.8	58.5	53.3
1980	67.2	-	-	56.9	51	33.4
1981	26.6	-	-	26	16.5	31.5
1982	149.5	-	-	148.1	171	130.5
1983	62	-	-	69.5	67	61.5
1984	66.7	-	-	93.1	77	81.5
1985	83.4	53.8	55.5	91.6	47	54
1986	146.5	176	168.7	155.3	213	135.5
1987	53	51.8	60.6	56.2	69	35
1988	76.4	69.3	102.3	74.3	141	78
1989	97.9	93	74.9	73.5	72.5	46.5
1990	39.6	26	40.8	33	32.5	30
1991	38.3	47.5	98.4	56.9	18	43.5
1992	96.6	96.3	192	104.1	43.5	61.5
1993	167.6	191.9	250.6	193.9	134	136
1994	39	66.9	54.5	51.2	22.5	6
1995	234	252.1	256.5	204	104	161
1996	196.6	193	203.2	200.6	157	134
1997	180.2	212.5	308.6	180.8	272	152
1998	77.5	73.8	72.3	82.3	16	30
1999	21.9	17.5	32.3	24.8	0	0
2000	51.3	54.7	75.9	16	56	46
2001	41.7	36.1	95.8	32.5	43	2
2002	15.9	69.2	93	77.3	25	34
2003	24	136	121.6	76.1	27	84
2004	-	111.2	111.9	82.7	0	84
2005	19.9	76.7	53.6	113.7	102	57
2006	67	106.2	98	-	64	85.5
2007	37.8	69.9	72.6	-	58	27
2008	29	16.3	32	-	9	113
2009	46.2	44.1	53.7	-	62	33
2010	54	38.3	86.2	-	0	35
2011	122	-	110.7	-	93	92
2012	118.1	-	82.4	-	31	92
2013	138.5	-	86.2	-	40	80
2014	135.5	-	83	-	103.4	61
2015	132.5	-	89.9	-	78	113
2016	110.5	-	119.9	-	219	80
2017	87	-	84.2	-	40	56
Average	83.3	91.5	106.7	90.5	76.5	78.3

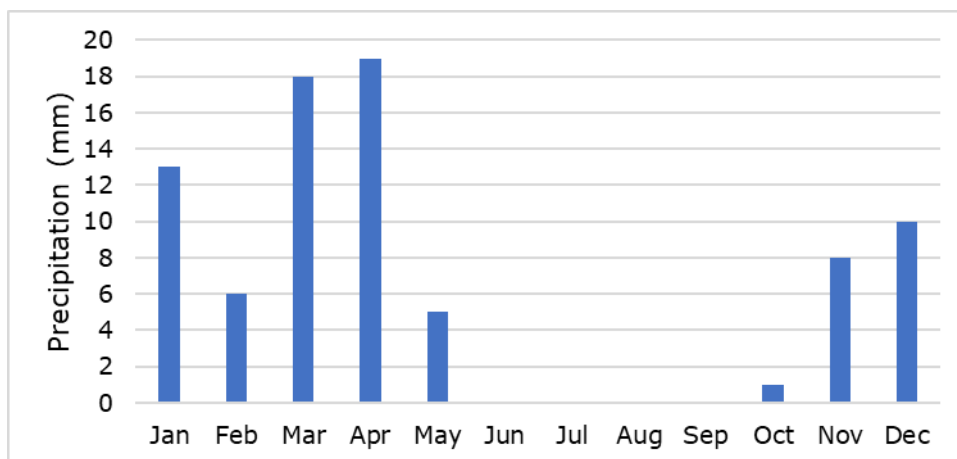


Figure 4.18: Average monthly rainfall in Riyadh weather station-R001 for the period 1964-2017.

Table 4.13: Annual maximum daily rainfall in Hanifah rain gauge.

Year	Occurrence date	Annual Max. Daily mm	Year	Occurrence date	Annual Max. Daily mm
1965	16 April	38.2	1986	5 March	18.2
1966	9 February	8.6	1987	26 March	28
1967	15 April	23.7	1988	14 April	14.2
1968	10 April	47.2	1989	14 April	21
1969	5 January	22.2	1990	14 January	9
1970	21 January	5.6	1991	26 February	11.6
1971	9 April	22	1992	16 December	12.6
1972	22 March	31	1993	11 May	30
1973	27 December	11.4	1994	11 March	17.2
1974	22 March	14	1995	20 March	33.7
1975	29 March	31	1996	23 March	53
1976	19 March	20	1997	11 November	20
1977	31 March	8.3	1998	6 March	17
1978	26 February	34.2	1999	15 January	12
1979	5 April	14.5	2000	9 November	8.5
1980	10 February	22.5	2001	21 March	13
1981	10 March	5	2002	4 November	18
1982	25 March	20.7	2003	12 February	25
1983	13 March	19.5	2004	17 January	29
1984	19 March	30	2005	27 February	32
1985	20 December	32			

Table 4.14 summarises the average monthly climate data in Riyadh weather station for the period 1964-2017. Daily temperatures in the city can exceed 45 °C in the summer, while during the winter season it may drop below 0 °C at night-time. The mean diurnal temperature range (DTR) in the city is 15.2 °C during the winter month of January and 19.2 °C in the summer month of July. The coldest month is January, and the hottest month is July having an average temperature of 13.9 and 35.1 °C, respectively (Figure 4.19). The average annual temperature of Riyadh city is about 25.4 °C. Strong

winds can occur in the months from December to May and calm winds from June to November. The average monthly relative humidity in the city varies between 21.8% in July and 48.6% in January, with an annual mean of approximately 34.5% (Figure 4.20). The daily solar radiation ranges from 302.3 Langley in December to 559.8 Langley in June (Figure 4.21). The dry and hot climate of Riyadh city leads to high pan evaporation rates. The average annual pan evaporation in the city is approximately 2,739.8 mm, and the monthly average ranges from 98 mm in December to 371.8 mm in July (Figure 4.22).

In addition to data of the local weather stations, other supporting open-source climate datasets have been developed at the global scale interpolated from surface observations, reanalysis, satellite data, and some combination thereof. These open-source data have been used in recent studies investigating rainfall over Saudi Arabia (Almazroui 2011; Miralles et al. 2016; Assiri 2017; Abatzoglou et al. 2018; Almazroui 2019; Komurcu et al. 2020; Luong et al. 2020).

Table 4.14: Average monthly climate data in Riyadh weather station-R001 for the period 1964-2017.

	Jan	Feb	Mar	Apr	May	Jun	Jul	Aug	Sep	Oct	Nov	Dec	Aver.
Precipitation (mm)	13.3	6.4	18.2	19.8	5.1	0.0	0.1	0.0	0.0	1.5	8.6	10.4	83.3
Max. Temp. (°C)	21	25	29	34	40	43	44	44	41	36	29	23	34
Min. Temp. (°C)	6	9	13	17	22	24	26	25	22	16	11	8	17
Mean Temp. (°C)	14	17	21	26	31	34	35	34	32	26	20	15	25
Max. R. Humidity %	73	65	60	57	45	33	31	33	35	47	65	72	51
Min. R. Humidity %	24	20	20	18	15	12	13	13	13	17	23	25	18
Mean R. Humidity %	49	42	40	38	30	23	22	23	24	32	44	48	35
Solar Radiation (Langley)	306	380	435	462	512	560	551	527	497	436	352	302	443
Pan Evaporation mm	103	133	185	216	292	355	372	359	282	218	127	98	2740

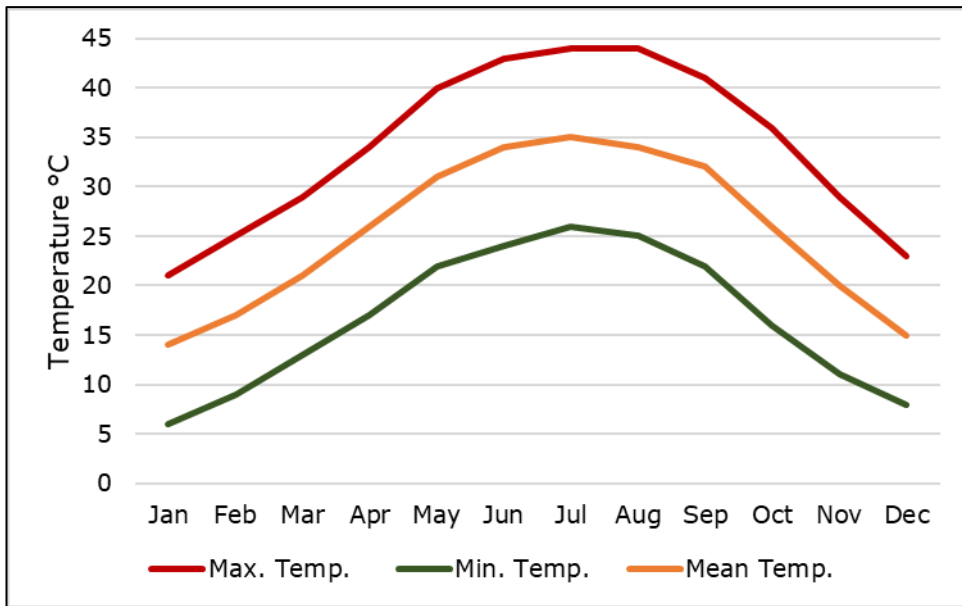


Figure 4.19: Average monthly temperatures in Riyadh weather station-R001 for the period 1964-2017.

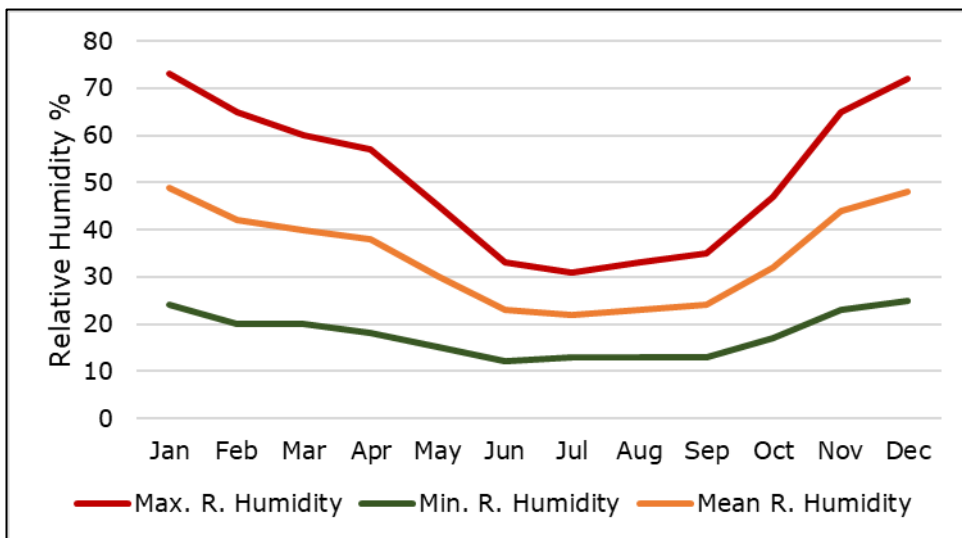


Figure 4.20: Average monthly relative humidity in Riyadh weather station-R001 for the period 1964-2017.

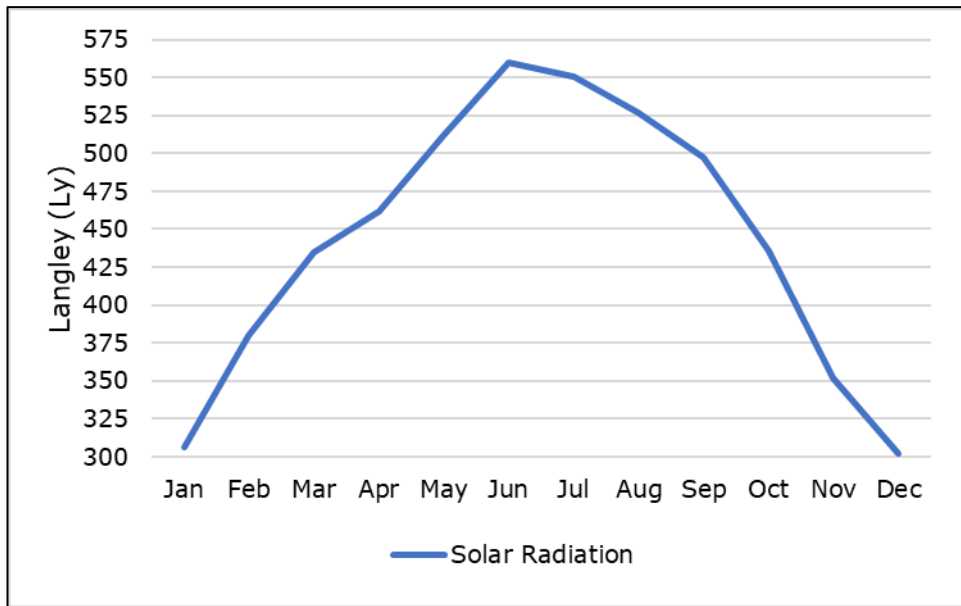


Figure 4.21: Average monthly solar radiation in Riyadh weather station-R001 for the period 1964-2017.

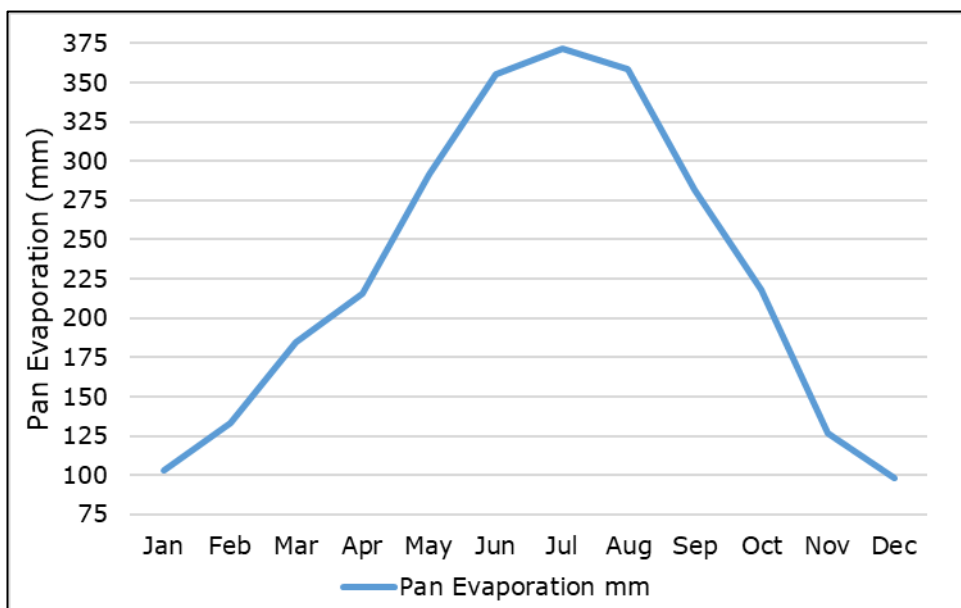


Figure 4.22: Average monthly pan evaporation in Riyadh weather station-R001 for the period 1964-2017.

4.8. Observed data for model calibration and validation

Good quality observed streamflow data is typically used for calibration and validation processes of SWAT models. The application of the SWAT model in arid and semi-arid regions is therefore challenging due to the unavailability of flow data for model calibration and validation procedures (Mengistu et al. 2019).

Runoff and streamflow data are very scarce for Saudi Arabia in general, and Riyadh in particular. The Ministry of Agriculture and Water (1984) reported that continuous runoff records were collected at 58 active runoff gauges and 19 inactive gauges in the early 1980s, but most of the collected records were short. The measured mean annual flow in the Wadi Hanifah gauge was 0.51 m³/s. From 1981 to the mid-1983, the Ministry installed and operated 200 crest-stage gauges throughout the country to determine peak flows. Al-Hasan and Mattar (2014) provided the recorded volumes of annual runoff at 16 stations in Saudi Arabia for the period 1965-2000 (Table 4.15). The runoff coefficient was reported to be 0.0324 in Wadi Hanifah. However, when the Ministry of Environment, Water, and Agriculture were approached in September 2019 with a request for runoff and discharge data, they responded that no runoff or discharge data was available.

Due to the lack of observed runoff or discharge data in the study area, ET was used as an alternative for calibration and validation. The term evapotranspiration combines the processes of evaporation and transpiration, both of which cause water loss. Using ET estimates to calibrate and validate hydrological models has been examined (Immerzeel and Droogers 2008; Cheema et al. 2014; Emam et al. 2017; Franco and Bonumá 2017; Roy et al., 2017; Herman et al. 2018; Ha et al. 2018; Mengistu et al. 2019; Odusanya et al. 2019; Jin and Jin 2020), and is reviewed in Chapter 2.

Table 4.15: The recorded annual runoff in Wadi Hanifah station (24° 39' 28"N 46° 36' 32"E).

Year	Measured runoff ($\times 10^6 \text{ m}^3$)	Measured runoff (mm)
1965	15.96	9.75
1966	0	0
1967	7.7	4.7
1968	18.06	11.03
1969	1.93	1.18
1970	0	0
1971	8.72	5.33
1972	9.77	5.97
1973	0	0
1974	10.64	6.5
1975	10.81	6.6
1976	4.407	2.7
1977	0	0
1978	0	0
1979	0.993	0.61
1980	0	0
1981	0	0
1982	0.772	0.47
1983	3.01	1.84
Average runoff	4.883	3
Basin area (km ²)	1,637	
Average annual rainfall (mm)	86	

Source: Al-Hasan and Mattar (2014).

GLEAM daily ET data is not available for the study area so a monthly AET gridded dataset from 1983-2006 derived from MODIS with a 50-km spatial resolution was initially used. The NSE and R^2 results were not adequate (documented in section 5.5. of Chapter 5) and thus monthly ET data from TerraClimate (4 km spatial resolution) were used instead. The TerraClimate provides a monthly gridded dataset of climate variables for global terrestrial surfaces from 1958–2015 (Abatzoglou et al. 2018). The TerraClimate also provides derived variables such as AET.

Uncertainty in monthly MODIS ET data was reported to be moderate to poor. Long et al. (2014) assessed uncertainty in monthly ET from four land surface models (Noah, Mosaic, VIC, and SAC in NLDAS-2), two remote sensing-based products (MODIS and AVHRR), and GRACE-inferred ET. The authors used data from three regions (humid-arid) in the South-Central United States as case studies and found uncertainties in ET are lowest in LSM ET (5 mm/mo), moderate in MODIS or AVHRR-based ET (10–15 mm/mo), and highest in GRACE-inferred ET (20–30 mm/month). Chen et al. (2020) reported that MOD16 models performed well in forests, but poorly in dryland biomes because MOD16 models were using atmospheric moisture conditions to reflect soil moisture constraints on ET rather than directly using the soil moisture to constrain the ET. The authors indicated that the results of their study were consistent with the results of previous studies. On the other hand, the only previous study found to evaluate Terraclimate ET is Herman et al. (2020). They reported that nine calibration scenarios of the SWAT model were performed using the multi-objective approach with two variables, one being measured streamflow and the other being actual evapotranspiration. By the comparison of the statistical results for the nine developed SWAT models, the authors found that the SWAT model calibrated with streamflow and Ensemble evapotranspiration had the best overall performance with a streamflow NSE of 0.79 and an actual evapotranspiration NSE of 0.95, and the model that calibrated with streamflow and TerraClimate had the worst model performance with a streamflow NSE of 0.75 and an actual evapotranspiration NSE of 0.76.

To check the accuracy of TerraClimate in the study area a comparison of TerraClimate PET with pan evaporation measured in Riyadh was performed. Pan evaporation data can be used to estimate ET rates. Huffman et al. (2013) determined adjustment

coefficients for comparing ET in different pan sitting environments and climate conditions, with coefficient ranges from 0.35 when the pan is placed in a dry fallow area, low humidity, and very strong wind to 0.85 when the pan is placed in a dry fallow area or short green cropped area, high humidity, and light wind speed. Pan evaporation when adjusted by the proper coefficient, approximates the evaporation from freshwater bodies which in turn are broadly equivalent to PET (Gruff and Thompson 1967). Similarly, Abteu and Melesse (2013) reported that pan coefficients are influenced by the local environment and coefficients around Lake Okeechobee, USA, ranged from 0.64 to 0.95.

An attempt to examine the accuracy of TerraClimate data was performed by comparing TerraClimate PET with adjusted evaporation pan (pan * 0.7, Gruff and Thompson 1967) measured in Riyadh weather station and by comparing temperature data between the two sources (Figure 4.23 and Figure 4.24). The R² values of the correlation between potential evapotranspiration against adjusted evaporation pan for the periods 1991-2010 and 1991-2000 are 0.72 and 0.88, respectively (Figure 4.25 and Figure 4.26). On the other hand, the R² values of the correlation between maximum and minimum temperature of the TerraClimate versus Riyadh Station temperature data for the periods 1991-2010 are 0.95 and 0.94 respectively (Figure 4.27 and Figure 4.28). These results suggest that the TerraClimate data can be used confidently for the study area.

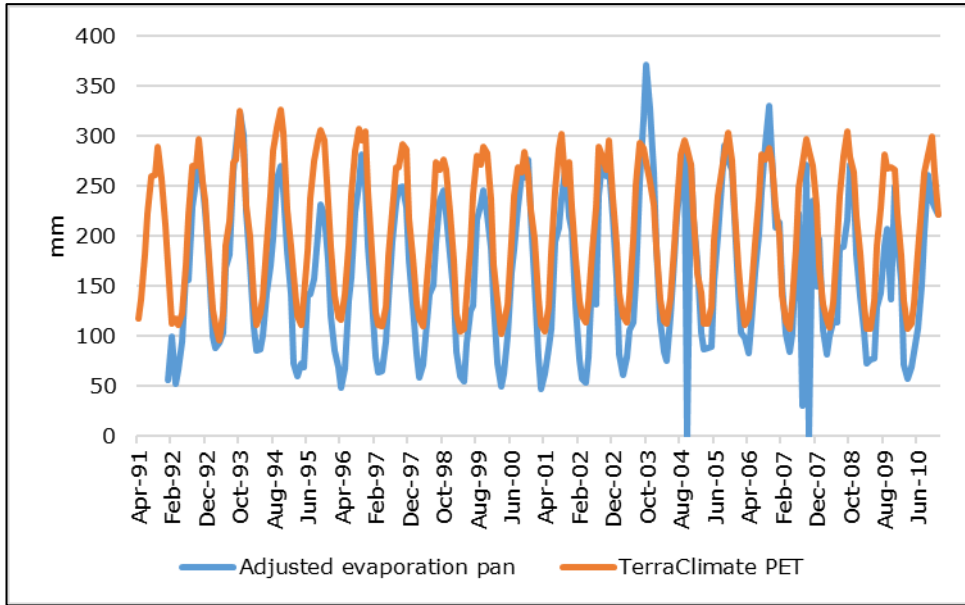


Figure 4.23: Comparison between monthly TerraClimate PET and adjusted evaporation pan (pan * 0.7) data from Riyadh weather station.

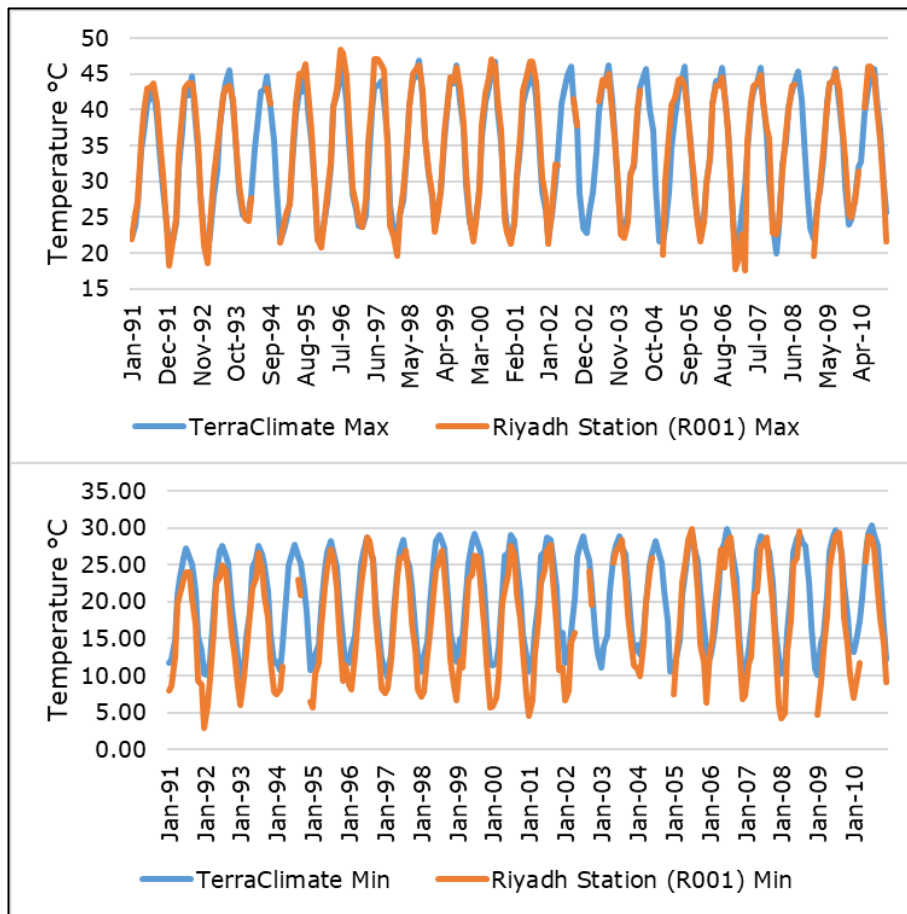


Figure 4.24: Comparison between monthly temperature data from the TerraClimate and Riyadh weather station.

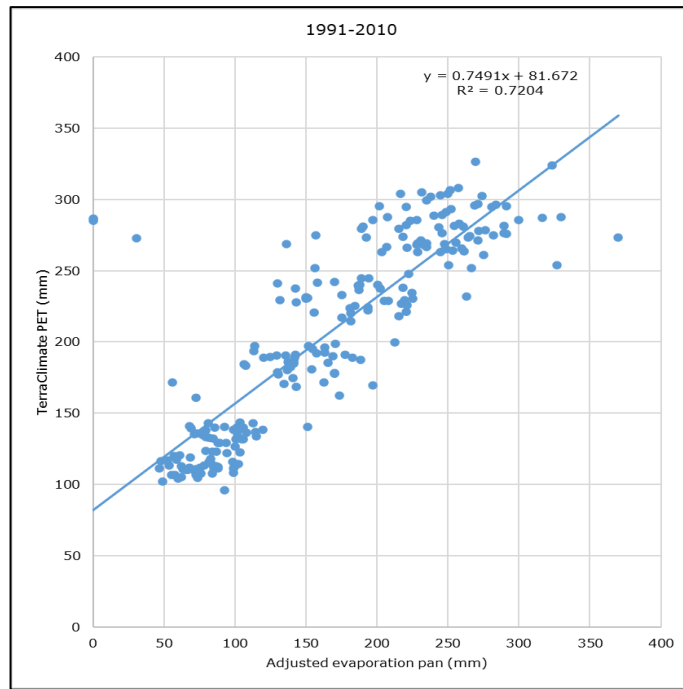


Figure 4.25: Correlation between TerraClimate PET and adjusted (0.7) evaporation pan for the period 1991-2010.

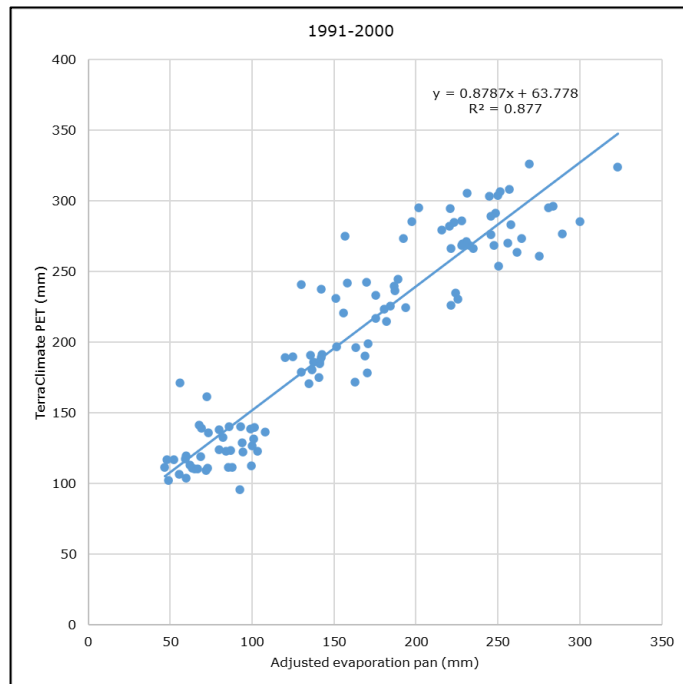


Figure 4.26: Correlation between TerraClimate PET and adjusted (0.7) evaporation pan for the period 1991-2000.

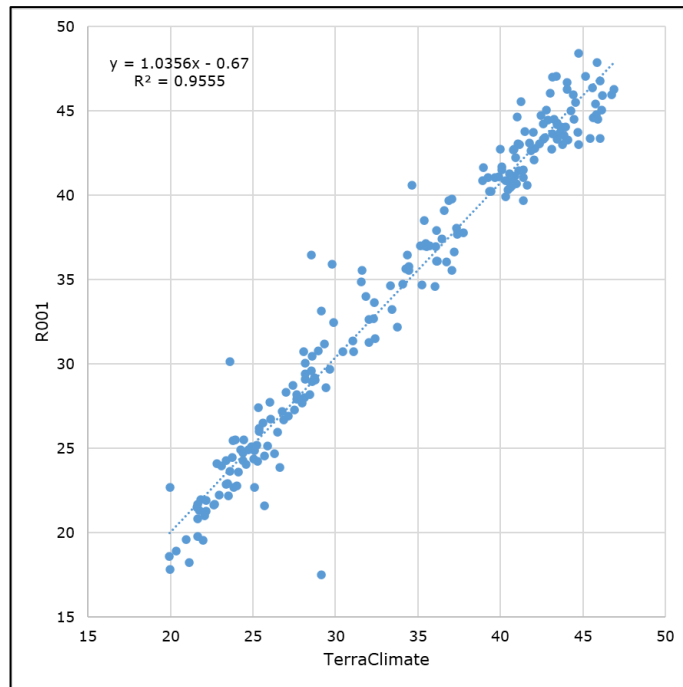


Figure 4.27: Correlation between monthly maximum temperature data from TerraClimate and maximum temperature data from Riyadh weather station for the period 1991-2010.

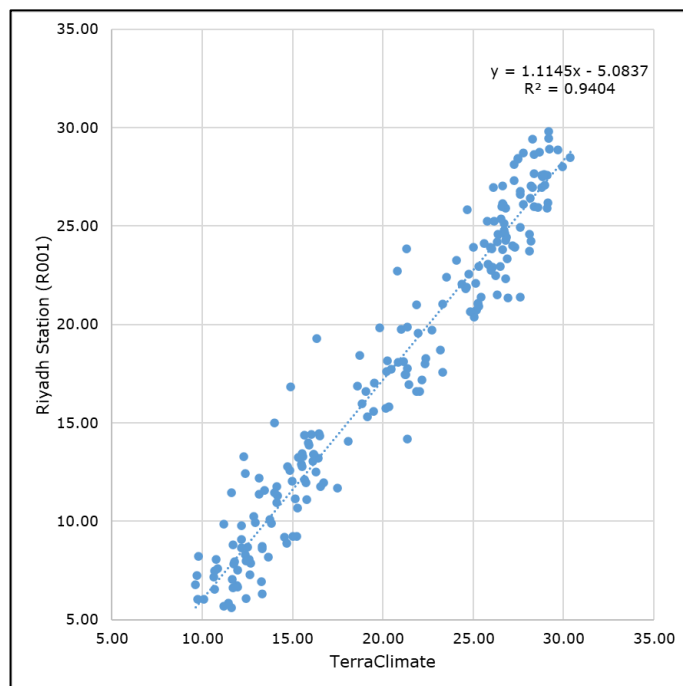


Figure 4.28: Correlation between monthly minimum temperature data from TerraClimate and minimum temperature data from Riyadh weather station for the period 1991-2010.

4.9. Summary

This chapter has provided a brief description of the SWAT model and the preparation process of its main inputs to develop models for Riyadh's catchments. The essential inputs of the SWAT model to simulate surface runoff include topographic data (DEMs), LULC data, soil data, and climate data. All data were available with the exception of suitable observed streamflow or runoff data for model calibration and validation. As such, ET data from TerraCLimate was used to calibrate and validate models, after it was found to approximate measured values well. Therefore, in the final development of the SWAT models for Riyadh's catchment, the inputs of the SWAT model were: DEM 5 m resolution, the governmental LULC maps, the Global Grid of Probabilities of Urban Expansion to 2030, the General Soil Map of Saudi Arabia 1:250,000, and climate data from local weather stations and rain gauges.

Chapter 5: SWAT Model Initial Setup and Pilot Study

5.1. Overview

Observed data of good quality are required to achieve effective calibration and validation of a SWAT model. Consequently, hydrological modelling in ungauged catchments is exposed to significant amounts of model uncertainty because of the unavailability of reliable data for calibration and validation processes (Mengistu et al. 2019). One major limitation in estimating runoff in Riyadh is the unavailability of some essential data, and the quality of the data that is available. Two key factors required for the accurate estimation of runoff present challenges in the case of Riyadh city. The first is the absence of runoff and discharge records in the catchments associated with Riyadh city, typically required for model calibration and validation. The second is meteorological data is collected at only a few locations in the Riyadh region and time-series are incomplete, with gaps in the timeseries.

This chapter documents the initial processes conducted to set up SWAT models for the simulation of surface runoff in the catchments of Riyadh. Initially, the calibration attempts of the SWAT model were applied to the Wadi Namar sub-basin (192 km²) as a pilot study using climate data for the period 1991-2000 and the LULC 1996 map. Then, six additional sub-basins (a subset of the 7 sub-basins across the two main catchments) were selected for more calibration attempts of the SWAT model to test the modelling approach across a larger number of sub-basins.

By achieving satisfactory model performance results for the 7 sub-basins, the SWAT model was applied to the two main catchments of the study area considering all sub-basins. For the two main catchments, the SWAT models performed satisfactorily when the

simulated ET was compared to observed ET for the model calibration period. However, model performance was not satisfactory when the model-observed comparison was made for the validation period. The poor performance was due to an issue with using 2001-2010 climate data, which was an unusually dry period characterised by very little precipitation, which hampered model calibration. The problem was solved by using pre-2000 data for the final calibration and validation of the model, as described in Chapter 6.

For the pilot study, the SWAT model calibrations were performed using satellite-based monthly ET data from MODIS, in the first instance. But when unsatisfactory model performance results were obtained, it was substituted by a higher spatial resolution monthly ET data from the TerraClimate, which yielded improved results (Figure 5.1).

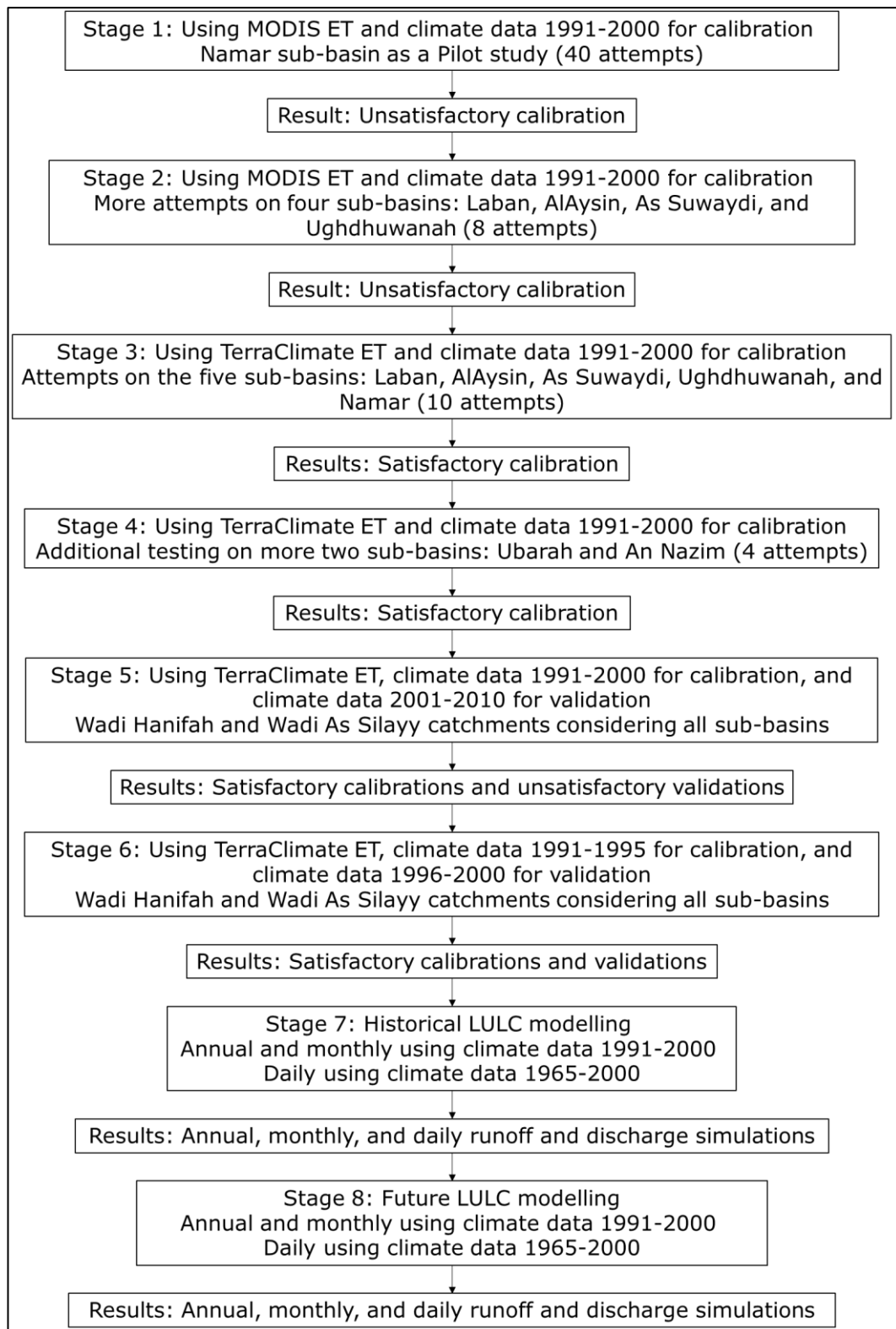


Figure 5.1: Stages of SWAT model calibrations and validations and LULC modelling in the study area.

5.2. SWAT Model Setup

The SWAT model is a Geographic Information System (GIS) software extension that can be used via ArcGIS or QGIS. ArcGIS-SWAT is a GIS interface and geodata model that uses a system of geodatabases to store and organise geographical, numerical, and text input data and results (Olivera et al. 2006). The SWAT model for the study area was set up using the GIS interface of SWAT, ArcGIS-SWAT. Several sequential steps were followed to apply the SWAT model including: 1) identifying which parameters in the SWAT are necessary to achieve project aims (i.e., for the simulation of the hydrological cycle), 2) building a GIS database for the required input data identified above, 3) performing sensitivity analysis on input data to determine which variables are disproportionately important to model outputs, and 4) calibration and validation of the SWAT model.

Since SWAT models can be used for a variety of purposes, there are numerous parameters, many of which are not relevant for the aims of this study. Therefore, the initial step was to identify and select the parameters that relate to hydrological processes for simulation in the study area. Normally, SWAT parameters selection is based on the user knowledge of the hydrologic processes in the study area and on the used parameters in similar previous studies (Mapes and Pricope 2020). Shivhare et al. (2018) indicated that 34 parameters have been distinguished for runoff that can be utilised for SWAT calibration. However, the authors used only 11 parameters to simulate runoff and sediment yield in their study area. In the present study, 38 parameters were selected for the estimation of runoff in the catchments of Riyadh city (Table 5.1).

The selection of the 38 parameters relied mainly upon previous studies, especially the SWAT input/output documentation prepared by Arnold et al. (2012a). The upper and lower limit values of these

parameters were obtained from the literature (Ministry of Agriculture and Water 1986; Arnold et al. 2012b; Boskidis et al. 2012; Ayele et al. 2017; Emam et al. 2017; Lin et al. 2017; Ha et al. 2018; Halefom et al. 2018; Herman et al. 2018; Odusanya et al. 2019). During the calibration process in the present study, the methods of change for these parameters are the replace method or the relative method, where replace change means that the existing parameter value is to be replaced by a given value within the parameter value range. Whereas the relative change means that the existing parameter value is multiplied by $1 +$ a given value (Abbaspour 2015).

Table 5.1: Selected parameters to develop the SWAT model for the catchments of Riyadh city.

ID	Parameters	Description	Method of change	Min	Max	Source
1	ALAI_MIN{17}.plant.dat	Minimum leaf area index for plant during dormant period (m ² /m ²)	Replace	0	0.99	Arnold et al. 2012a
2	ALPHA_BF. Gw	Baseflow alpha factor (1/days)	Replace	0	1	Odusanya et al. 2019, Halefom et al. 2018, Boskidis et al. 2012, Ayele et al. 2017, Herman et al. 2018, Ha et al. 2018
3	BLAI{17}.plant.dat	Maximum potential leaf area index	Replace	0.5	10	Arnold et al. 2012a
4	CANMX. Hru	Maximum canopy storage (mm H ₂ O)	Replace	0	100	Lin et al. 2017, Herman et al. 2018, Odusanya et al. 2019
5	CH_L1. Sub	Longest "tributary" channel length in sub-basin (km)	Relative	-0.2	0.2	Arnold et al. 2012a
6	CH_N1. Sub	Manning's "n" value for the tributary channels	Replace	0.01	30	Arnold et al. 2012a
7	CH_S1. Sub	Average slope of tributary channels (m/m)	Relative	-0.2	0.2	Arnold et al. 2012a
8	CN2. Mgt	Initial SCS runoff curve number for moisture condition II	Relative	-0.2	0.2	Halefom et al. 2018, Ayele et al. 2017
9	CNCOEF. Bsn	Plant ET curve number coefficient	Replace	0.5	2	Arnold et al. 2012a
10	CNOP{[,1].mgt	SCS runoff curve number for moisture condition II	Relative	-0.5	0.5	Arnold et al. 2012a
11	CNOP{[,5].mgt	SCS runoff curve number for moisture condition II	Relative	-0.5	0.5	Arnold et al. 2012a
12	CNOP{[,6].mgt	SCS runoff curve number for moisture condition II	Relative	-0.5	0.5	Arnold et al. 2012a
13	DEEPST. Gw	Initial depth of water in the deep aquifer (mm H ₂ O)	Replace	0	50,000	Arnold et al. 2012a

Table 5.1: Selected parameters to develop the SWAT model for the catchments of Riyadh city. (Continued)

ID	Parameters	Description	Method of change	Min	Max	Source
14	EPCO. Bsn	Plant uptake compensation factor	Replace	0	1	Odusanya et al. 2019, Boskidis et al. 2012, Herman et al. 2018, Ha et al. 2018, Emam et al. 2017
15	EPCO. Hru	Plant uptake compensation factor	Replace	0	1	Odusanya et al. 2019, Boskidis et al. 2012, Herman et al. 2018, Ha et al. 2018, Emam et al. 2017
16	ESCO. Bsn	Soil evaporation compensation factor	Replace	0	1	Odusanya et al. 2019, Herman et al. 2018, Ha et al. 2018, Emam et al. 2017, Boskidis et al. 2012, Lin et al. 2017
17	ESCO. Hru	Soil evaporation compensation factor	Replace	0	1	Odusanya et al. 2019, Herman et al. 2018, Ha et al. 2018, Emam et al. 2017, Boskidis et al. 2012, Lin et al. 2017
18	FFCB. Bsn	Initial soil water storage expressed as a fraction of field capacity water content	Replace	0	1	Odusanya et al. 2019
19	GSI{17}. plant.dat	Maximum stomatal conductance at high solar radiation and low vapor pressure deficit (m·s ⁻¹)	Relative	0	5	Odusanya et al. 2019
20	GW_DELAY. Gw	Groundwater delay time (days)	Replace	0	500	Herman et al. 2018
21	GW_REVAP. Gw	Groundwater "revap" coefficient	Replace	0	0.2	Ayele et al. 2017
22	GWQMN. Gw	Threshold depth of water in the shallow aquifer required for return flow to occur (mm H ₂ O)	Replace	0	5,000	Herman et al. 2018
23	ICN. Bsn	Daily curve number calculation method	Replace	0	1	Arnold et al. 2012a
24	OV_N. hru	Manning's "n" value for overland flow	Relative	-0.5	0.5	Arnold et al. 2012a

Table 5.1: Selected parameters to develop the SWAT model for the catchments of Riyadh city. (Continued)

ID	Parameters	Description	Method of change	Min	Max	Source
25	RCHRG_DP. Gw	Deep aquifer percolation fraction	Replace	0	1	Lin et al. 2017, Boskidis et al. 2012, Herman et al. 2018
26	REVAPMN. Gw	Threshold depth of water in the shallow aquifer for "revap" or percolation to the deep aquifer to occur (mm H2O).	Replace	0	1,000	Herman et al. 2018
27	SHALLST. Gw	Initial depth of water in the shallow aquifer (mm H2O)	Replace	0	50,000	Arnold et al. 2012a
28	SLSOIL. Hru	Slope length for lateral subsurface flow (m)	Replace	0	150	Arnold et al. 2012a
29	SLSUBBSN. Hru	Average slope length (m)	Relative	-0.5	0.5	Emam et al. 2017
30	SOL_ALB. Sol	Moist soil albedo	Replace	0	0.25	Arnold et al. 2012a
31	SOL_BD. Sol	Moist bulk density (Mg/m ³ or g/cm ³)	Relative	-0.5	0.5	Emam et al. 2017
32	SOL_CRK. Sol	Potential or maximum crack volume of the soil profile expressed as a fraction of the total soil volume	Replace	0	1	Arnold et al. 2012a
33	SOL_K. sol	Saturated hydraulic conductivity (mm/hr)	Relative	-0.8	0.8	Ayele et al. 2017
34	SOL_Z. sol	Depth from soil surface to bottom of layer (mm)	Replace	250	1,500	Ministry of Agriculture and Water 1986
35	SOL_AWC. Sol	Available water capacity of the soil layer (mm H ₂ O/mm soil).	Relative	-0.5	0.5	Emam et al. 2017
36	SURLAG. Bsn	Surface runoff lag coefficient	Relative	0.05	24	Herman et al. 2018
37	WUDEEP().wus	Average daily water removal from the deep aquifer for the month (10 ⁴ m ³ /day).	Replace	0	10,000	Arnold et al. 2012a
38	WUSHAL().wus	Average daily water removal from the shallow aquifer for the month (10 ⁴ m ³ /day).	Replace	0	10,000	Arnold et al. 2012a

Modelling using ArcGIS-SWAT requires data to be stored and accessible in folders and databases. For each catchment of the Riyadh city region (e.g., the Wadi Hanifah and Wadi As Silayy), data was sequentially added to these databases, starting with the DEM of the catchment; drainage basin delineation; the definition of land use, soil, and slope; Hydrologic Response Units (HRUs) creation; weather data integration; creation of input files; and, SWAT simulation. The datasets were formatted as required by the model. All the maps and DEMs were transformed into UTM projection zone 38N using the WGS_84 Datum to unify the coordinate system. Both the soil map and land use map were rasterised and resampled to unify the spatial resolution (5 meters). Initially, data for the period 1988-2010 were prepared to be used for warm-up, calibration, and validation. Data for the periods 1991-2000 and 2001-2010 were prepared to be used for initial model calibration and validation, respectively, also preceded by a three-year warm-up. A warm-up period is used to initialize and aid in the development of model variables (Ghadei et al. 2018) and is also sometimes called a spin-up period.

The automatic delineation tool in ArcGIS-SWAT was used to delineate the catchment and its sub-basins from the DEM. The catchment delineation process involved five sequential steps which are DEM setup, stream definition (flow direction and accumulation), stream network (outlet and inlet definition), basin outlet selection and calculation of sub-basin parameters. The outlets of the two main catchments were defined to be immediately downstream of the built-up area of the Riyadh city. The Wadi Hanifah outlet was defined to be at 24° 23' 17.6"N, 46° 49' 20.4"E, while the outlet of Wadi As Silayy was defined to be at 24° 27' 23.42"N, 47° 00' 11.23"E.

The inputs of land use, soil, and slope of the study area needed to be reclassified by SWAT into database codes. The LULC map was

reclassified into SWAT land cover/plant types database which contains the USGS LULC and NLCD (National Land Cover Database). The soil map was reclassified into categories according to soil types in Riyadh's catchments. The slopes in the basin were reclassified using the International Geographic Union (IGU) system (0%–3.5%, 3.5–8.7%, 8.7–26.8, 26.8–70 and >70) (Small and Clark 1982).

Next, the land use, soil, and slope layers were used to create HRUs in each sub-basin. The SWAT model divided the Wadi Hanifah catchment into 22 sub-basins and 371 HRUs. In comparison, the Wadi As Silayy was divided into 11 sub-basins and 223 HRUs (Figure 5.2). It should be noted that a 1% threshold of HRU was assigned for the SWAT model to create the HRUs in the study area catchments. Thresholds of LULC, soil, and slope in defining HRUs can be specified in the SWAT model to improve the computational efficiency of simulations (Her et al. 2015).

Finally, the files of climate data, weather station locations, and weather station elevations were assigned in the dialogue box of weather data definition. The database tables of the model were created and then the model was run to get uncalibrated and unvalidated results.

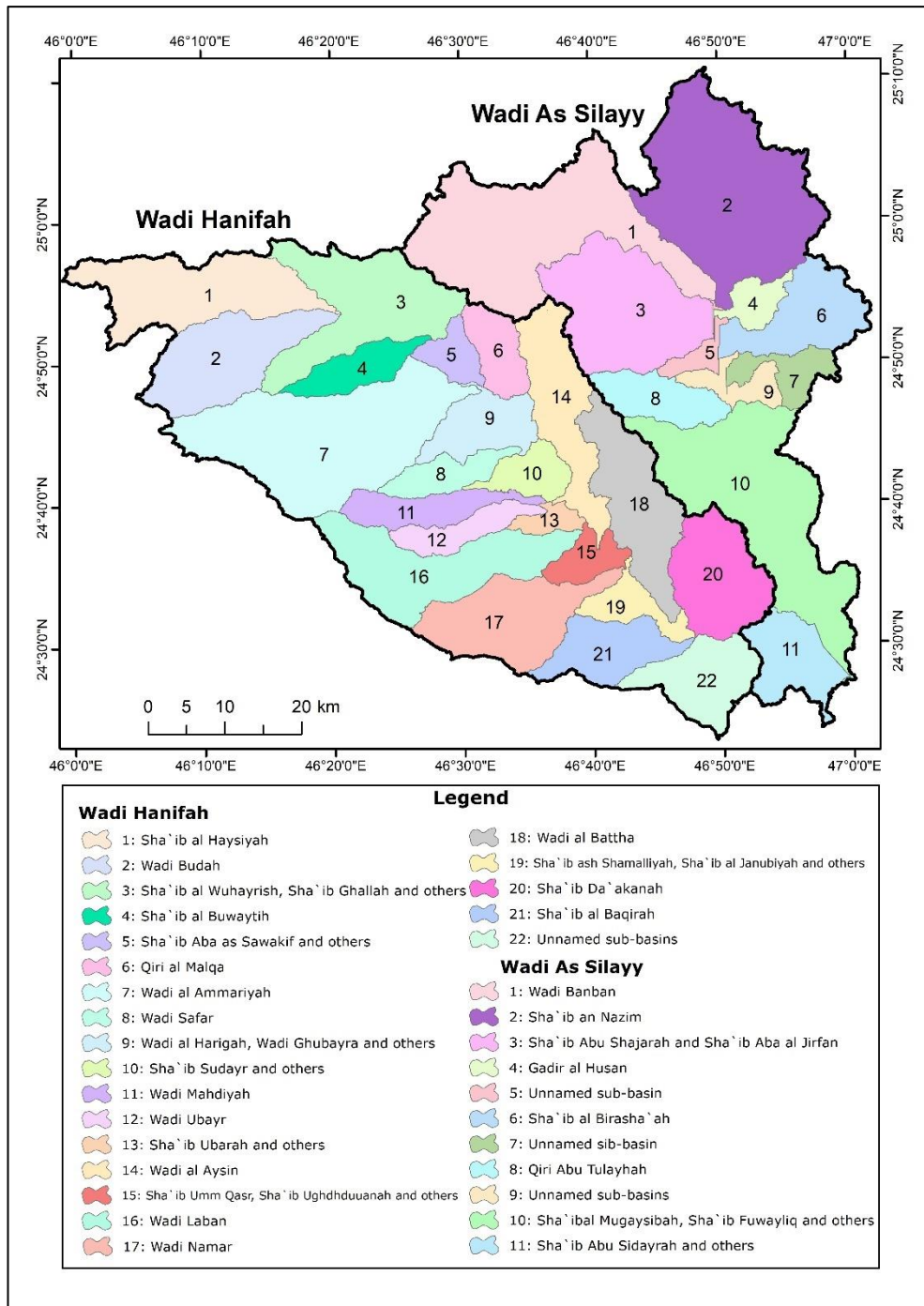


Figure 5.2: Distribution of sub-basins in the Wadi Hanifah and the Wadi As Silayy catchments.

5.3. SWAT-CUP (calibration and uncertainty procedures)

SWAT-CUP is a public domain software developed for calibration of the SWAT model. This computer program provides five algorithms to solve the statistical and mathematical problems needed for SWAT model calibration and validation, which are: Sequential Uncertainty Fitting version 2 (SUFI-2), Particle Swarm Optimisation (PSO), Generalised Likelihood Uncertainty Estimation (GLUE), Parameter Solution (ParaSol), and Markov Chain Monte Carlo (MCMC) (Abbaspour 2015).

Among algorithms of the SWAT-CUP, SUFI-2 is the most popular among users to conduct parameterisation, sensitivity analysis, calibration, validation, and uncertainty analysis of hydrological parameters (Shivhare et al. 2018; Sao et al. 2020). Taghvaye Salimi et al. (2016) reported that most researchers used the SUFI-2 algorithm for the SWAT model calibration and uncertainty analysis of parameters for the simulation of runoff. Thus, the SUFI-2 algorithm has been used in the present study.

The calibration methods require hundreds or thousands of iterative simulations to find the optimal solution. SUFI-2 calculates all uncertainties and tries to capture most data in the 95% prediction uncertainty (95PPU) of the model in each simulation (Arnold et al. 2012b). An objective function must be defined to apply SUFI-2 to calculate the sensitivity of parameters (Abbaspour et al. 2015). Objective functions can be defined as measures of mismatch between observed and simulated values and of mismatch between independent (prior) parameter information and calibrated parameter values (Foglia et al. 2009). SUFI-2 allows the usage of ten different objective functions such as the determination coefficient (R^2), Nash-Sutcliffe Efficiency (NSE), and mean square error (MSE). The most used objective functions are NSE and R^2 (Baddoo et al. 2020).

The SUFI-2 algorithm is a stochastic calibration approach that is most frequently used by scientists to evaluate uncertainty (Shivhare et al. 2018). This technique accounts for all sources of uncertainties including uncertainty in driving variables, conceptual model, parameters, and measured data. The uncertainties propagation in the parameters leads to uncertainties in the model output variables, expressed as the 95% probability distribution. It is calculated at the 2.5% and 97.5% levels of the cumulative distribution of an output variable which is generated by the propagation of the parameter uncertainties using Latin hypercube sampling. It is indicated as the 95% prediction uncertainty or 95PPU. The 95PPU is the model output in the stochastic calibration approach (Abbaspour 2015). Latin hypercube sampling is a method that generates a sample of plausible parameter values from a multidimensional distribution and ensures that the optimum solution is not a local minimum by ensuring that samples cover the entire parameter space (Me et al. 2015).

The SUFI-2 algorithm involves a process of fitting parameter values by comparing the predicted output and measured data until the best-fitted values for the objective function are achieved (Sao et al. 2020). SUFI-2 calculates parameter sensitivity by multiple regression, which regresses the Latin hypercube generated parameters against the objective function values (Abbaspour et al., 2007). The software calculates the values of t-statistics (t-stat) and p-values to evaluate parameter sensitivity. The more sensitive the parameter, the higher value of the t-stat and the smaller the value of the p-value. The t-stat is the regression coefficient of a parameter divided by its standard error (Abbaspour 2015). The t-stat is used to find the corresponding p-value and level at the t-Student distribution table (Moreira et al. 2018). The p-value for each independent parameter tests the null hypothesis that the regression coefficient is equal to zero and has no effect on the dependent variable. A p-value

less than 0.05 indicates that the null hypothesis should be rejected. In other words, a p-value of 0.05 indicates that there is a 95% probability that the change of the parameter will affect the dependent variable (Abbaspour 2015).

SUFI-2 calculates the values of the p-factor and R-factor to describe the uncertainty of the SWAT model simulation (Yuan and Forshay 2019). The P-factor is the percentage of measured data bracketed by 95% prediction uncertainty (95PPU), whereas the R-factor is the average thickness of the 95PPU band divided by the standard deviation of measured data. A simulation that exactly corresponds to measured data occurs with a P-factor value of 1 and an R-factor value of zero (Arnold et al. 2012b). The suggested values to be adequate for discharge are 0.7 or greater and 1.5 or less for p-factor and R-factor, respectively. Abbaspour (2015, p. 19) reported that “when acceptable values of R-factor and p-factor are reached, then the parameter uncertainties are the desired parameter ranges”. SUFI-2 algorithm has been used to run 1,000 simulations for each calibration in this study. Further goodness fit can be quantified between the observations and the final best simulation by other statistics described below.

5.4. SWAT model performance indices

The SWAT model performance is determined by several statistical tests including the coefficient of determination (R^2), the Nash-Sutcliffe efficiency coefficient (NSE), percentage bias (PBIAS), observation standard ratio (RSR), index of agreement (d), and Kling–Gupta efficiencies (KGE).

By far, R^2 and NSE are the most widely used statistics for SWAT calibration and validation (Gassman et al. 2007; Arnold et al. 2012b). Gassman et al. (2007) provided a list of R^2 and NSE

statistics results of 115 studies which calibrated and validated SWAT models for streamflow and surface runoff simulations. They mentioned that no absolute criteria have been defined to assertively judge the performance of model calibration and validation. However, ratings of R^2 , NSE, PBIAS, and RSR statistical tests results have been suggested to assess the performance of model calibration and validation as shown in Table 5.2 (Moriassi et al. 2007; Ayele et al. 2017). These performance classifications were used in this thesis.

Table 5.2: Model performance ratings for monthly simulations of streamflow.

Objective Function	Value range	Performance Classification
R^2	$0.7 < R^2 < 1$	Very good
	$0.6 < R^2 < 0.7$	Good
	$0.5 < R^2 < 0.6$	Satisfactory
	$R^2 < 0.5$	Unsatisfactory
NSE	$0.75 < ENS \leq 1.00$	Very good
	$0.65 < ENS \leq 0.75$	Good
	$0.50 < ENS \leq 0.65$	Satisfactory
	$0.4 < ENS \leq 0.50$	Acceptable
	$ENS \leq 0.4$	Unsatisfactory
PBIAS	$PBIAS < \pm 10$	Very good
	$\pm 10 \leq PBIAS < \pm 15$	Good
	$\pm 15 \leq PBIAS < \pm 25$	Satisfactory
	$PBIAS \geq \pm 25$	Unsatisfactory
RSR	$0.00 \leq RSR \leq 0.50$	Very good
	$0.50 < RSR \leq 0.60$	Good
	$0.60 < RSR \leq 0.70$	Satisfactory
	$RSR > 0.70$	Unsatisfactory

Source: Moriassi et al. (2007); Ayele et al. (2017).

Moriassi et al. (2015) reviewed the advantages and disadvantages of several model performance indices for streamflow. They recommend the use of R^2 , NSE, RSR, and PBIAS for model performance evaluation. Thus, for this research, the NSE, and R^2 were used as major objective functions in the SWAT calibration process. The PBIAS and RSR were also additional criteria used for the evaluation and are detailed below.

The R^2 determines the consistency between the observed and simulated values based on a best-fit line on a scatter plot. It can range from 0 to 1, where 0 indicates no correlation and 1 represents perfect correlation. R^2 Values greater than 0.5 have been considered acceptable (Moriasi et al. 2007).

NSE is a normalised statistical method used for the prediction of the relative amount of the residual variance (noise) compared with the measured data variance (information). NSE provides a measure of how well the plot of observed versus simulated data fits the 1:1 line. NSE values can range between $-\infty$ and 1 where an NSE value of 1 indicates a perfect fit between the simulated and observed data. Models have been considered acceptable when NSE values greater than 0.4 (Ayele et al. 2017).

PBIAS is a method that determines the average tendency of the simulated values to be larger or smaller than their observed counterparts. The ideal value of PBIAS is zero, with lower magnitude values indicating accurate model simulation. PBIAS values between -25 and +25 have been regarded acceptable (Moriasi et al. 2007).

RSR is the ratio of the root mean square error (RMSE) to standard deviation of measured data. The RSR values range from zero, its optimal value, to large positive values. RSR values less than 0.7 have been considered acceptable (Golmohammadi et al. 2014).

5.5. Wadi Namar sub-basin as a pilot study

In preparation for the development of the SWAT model of Riyadh catchments, a pilot study was performed on a sub-basin to test model performance quickly, without having to run the larger model for the entire area.

Initially, the SWAT model was applied to the Wadi Namar sub-basin (192 km²) as a pilot study. The Wadi Namar sub-basin is a tributary of the Wadi Hanifah. The reasons for choosing the Wadi Namar sub-basin as a pilot study were: 1) the area of the sub-basin has a reasonable size to minimize runtime for calibration, 2) the Wadi Namar sub-basin is partially urbanised and is representative of the larger study area, and 3) the sub-basin is close to the main weather station with the longest data records, which is the Riyadh Weather Station.

The SWAT-CUP software was used for the calibration. Due to the absence of streamflow observed data in the catchments of Riyadh city, satellite-based and derived ET data were considered as an alternative for model calibration to get an approximate estimate of runoff in the ungauged catchments. Since GLEAM (Global Land Evaporation Amsterdam Model) only partially covers Saudi Arabia and the ET data for the whole study area has been assigned as missing values, the SWAT model calibration was initially performed using satellite-based ET data from MODIS (Moderate Resolution Imaging Spectroradiometer). MODIS has been used successfully as an alternative for SWAT model calibration in several recent studies (Miralles et al. 2016; Parajuli et al. 2018; Abbaspour et al. 2019; Odusanya et al. 2019; Jin and Jin 2020).

It should be noted that the Penman-Monteith and SCS curve number methods are the default of the SWAT model to calculate ET and surface runoff, respectively. The initially used SWAT model inputs included climate records of Riyadh Weather Station for the period 1991-2000, a 5-meter resolution DEM, the general soil map of Saudi Arabia, and the LULC 1996 map. Additionally, missing values of daily climate data in the study area were estimated by the SWAT model's built-in weather generator. SWAT contains a weather generator

model called WXGEN (Lee et al. 2018). Then, the SWAT model was run in a monthly time step.

The first step was to run an uncalibrated SWAT model using the default SWAT parameter values to assure that the model would work. The obtained preliminary results of the simulated average annual AET and surface runoff by the uncalibrated model were 39.4 mm and 17.02 mm, respectively, for the Wadi Namar sub-basin (Figure 5.3). To conduct the calibration attempts of the SWAT model, firstly the NSE as an objective function was used and then the R^2 was used as an objective function. However, the focus in the following paragraphs was on R^2 values as an index for model performance in most attempts because the NSE values were poor.

The first attempt was to calibrate a monthly model for the Wadi Namar sub-basin using MODIS AET data. The calibration results of the model were -1.59 and 0.41 for NSE and R^2 respectively. It should be noted this model calculated the ET based on the Penman-Monteith equation. SWAT models can calculate the ET using two other methods; the Priestley-Taylor equation and the Hargreaves equation. Therefore, two more models were calibrated to calculate ET by applying the Priestley-Taylor equation and the Hargreaves equation respectively. The calibration results of these models slightly improved. By applying the Priestley-Taylor equation the models achieved -1.33 NSE and 0.44 R^2 . Whereas the models that applied the Hargreaves equation achieved -1.78 NSE and 0.44 R^2 (Table 5.3). Thus, the model still needed to be improved significantly.

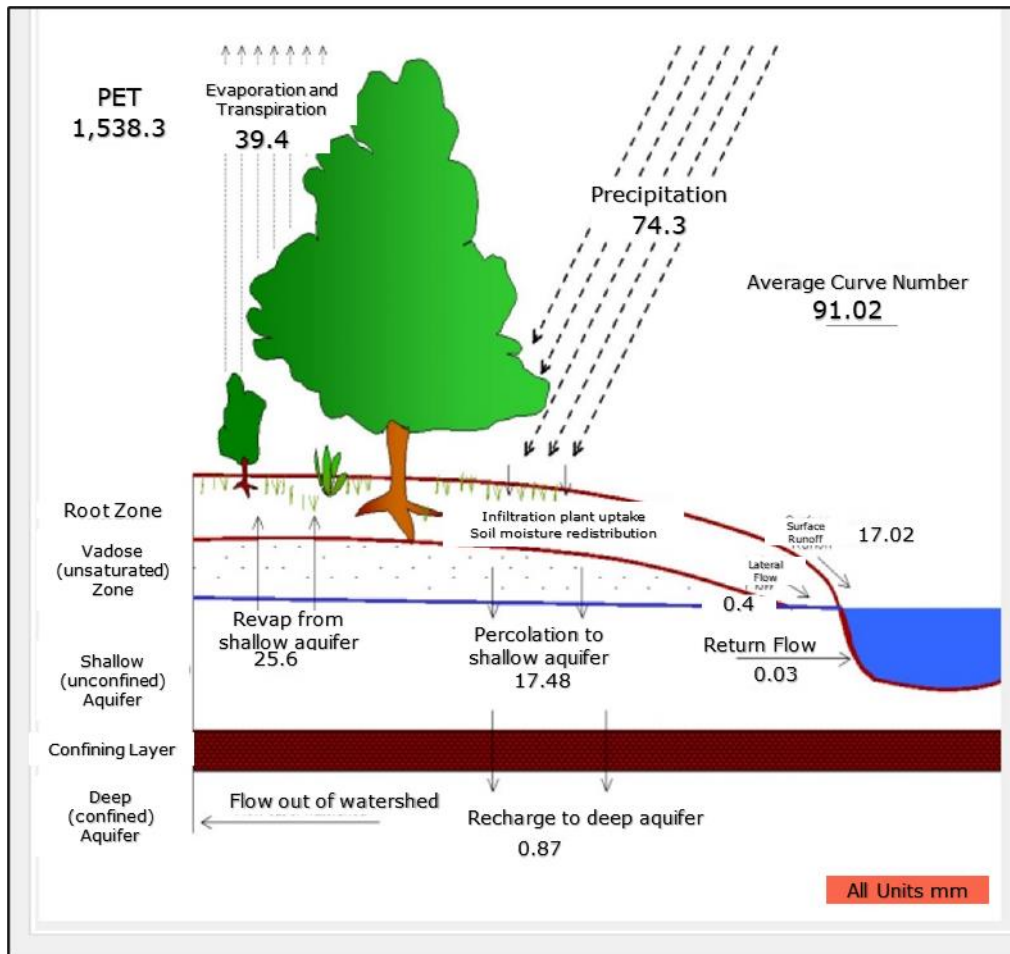


Figure 5.3: Uncalibrated outputs of the hydrological cycle components in the pilot sub-basin using data for the period 1991-2000.

To explore the calibration of models and factors that may limit calibration potential, another 37 attempts were made to improve the SWAT model performance by using different data sources for SWAT model inputs and different objective functions. Table 5.3 shows the statistical results of all 40 attempts at calibrating the SWAT model. The paragraphs below describe the factors considered in the 37 attempts.

Since climate data records of the Riyadh Weather Station have missing data, climate data of the Climate Forecast System Reanalysis (CFSR) was used to run three models. One of the models used the default Penman-Monteith equation to estimate ET, a second used the Priestley-Taylor equation, and a third used the Hargreaves

equation. However, the model performance was not much improved with poor NSE results and relatively better R^2 values which were equal to 0.51, 0.44, and 0.47 respectively.

Although the SWAT model's built-in weather generator has been widely used to estimate missing values of daily climate data, other supporting methods were attempted to enhance the quality of climate data inputs. Firstly, the daily average of all years in each station was used to fill the missing equivalent daily data in the record. Secondly, the missing data in the Riyadh Weather Station was replaced with data from the King Khalid International Airport (KKIA) Weather Station. The model performance was not greatly improved by using the two different weather statistics (R^2 0.41 and 0.50 respectively). Therefore, more attempts were carried out to seek better performance.

Different inputs of DEMs, soil data, and LULC data were used to improve the SWAT model performance for the pilot sub-basin. Several DEMs were used to calibrate the SWAT model including:

- 10 m spatial resolution DEM
- ASTER DEM 30 m spatial resolution
- SRTM DEM 30 m spatial resolution,
- ALOS DEM 30 m spatial resolution.

Moreover, the FAO soil map was used in the calibration of the SWAT model. Also, the Copernicus Global Land Service LULC was used as input to calibrate the SWAT model. The calibration statistical results of these calibrations indicated that no major improvement was achieved in the model performance, with R^2 values ranging between 0.40 and 0.48.

Table 5.3: Statistical results for 40 calibration attempts for the pilot sub-basin (Wadi Namar) using NSE (20 simulations) and R² (20 simulations) as the objective functions.

ID	Sub-basin	ET formula	Period	SWAT input data				ET source	p-factor	R-factor	NSE as the objective function				R ² as the objective function			
				Climate data	DEM	Soil	LULC				R ²	NSE	PBIAS	RSR	R ²	NSE	PBIAS	RSR
1	Namar	Penman-Monteith	1991 to 2000	Riyadh station	5-m DEM	GSMSA*	LULC 1996	MODIS	0.38	2.63	0.41	-1.6	-108	1.59	1	-2	-123	1.6
2	Namar	Priestley-Taylor	1991 to 2000	Riyadh station	5-m DEM	GSMSA*	LULC 1996	MODIS	0.29	2.75	0.44	-1.3	-113	1.52	1	-1	-118	1.6
3	Namar	Hargreaves	1991 to 2000	Riyadh station	5-m DEM	GSMSA*	LULC 1996	MODIS	0.33	2.6	0.44	-1.8	-122	1.65	1	-9	-257	3.2
4	Namar	Penman-Monteith	1991 to 2000	CFSR	5-m DEM	GSMSA*	LULC 1996	MODIS	0.4	1.86	0.51	-0.9	-91	1.36	1	-5	-178	2.5
5	Namar	Priestley-Taylor	1991 to 2000	CFSR	5-m DEM	GSMSA*	LULC 1996	MODIS	0.31	2.03	0.44	-0.7	-79	1.29	1	-4	-160	2.2
6	Namar	Hargreaves	1991 to 2000	CFSR	5-m DEM	GSMSA*	LULC 1996	MODIS	0.33	1.96	0.47	-0.7	-82	1.29	1	-5	-173	2.4
7	Namar	Penman-Monteith	1991 to 2000	Filling missing daily data of Riyadh station using equivalent daily data from its record	5-m DEM	GSMSA*	LULC 1996	MODIS	0.39	2.46	0.45	-1.7	-123	1.64	1	-2	-135	1.7
8	Namar	Penman-Monteith	1991 to 2000	Compensation of missing data in the Riyadh station from KKIA** station	5-m DEM	GSMSA*	LULC 1996	MODIS	0.41	2.59	0.5	-1.7	-126	1.63	1	-2	-126	1.6

GSMSA*: General Soil Map of Saudi Arabia

KKIA**: King Khalid International Airport

Table 5.3: Statistical results for 40 calibration attempts for the pilot sub-basin (Wadi Namar) using NSE (20 simulations) and R² (20 simulations) as the objective functions. (Continued)

ID	Sub-basin	ET formula	Period	SWAT input data				ET source	p-factor	R-factor	NSE as the objective function				R ² as the objective function			
				Climate data	DEM	Soil	LULC				R ²	NSE	PBIAS	RSR	R ²	NSE	PBIAS	RSR
9	Namar	Penman-Monteith	1991 to 2000	Riyadh station	ASTER 30-m	GSMSA*	LULC 1996	MODIS	0.38	2.61	0.4	-1.6	-110	1.6	1	-2	-124	1.6
10	Namar	Penman-Monteith	1991 to 2000	Riyadh station	SRTM 30-m	GSMSA*	LULC 1996	MODIS	0.38	2.69	0.41	-1.4	-105	1.55	1	-2	-121	1.6
11	Namar	Penman-Monteith	1991 to 2000	Riyadh station	ALOS 30-m	GSMSA*	LULC 1996	MODIS	0.38	2.59	0.4	-1.6	-110	1.61	1	-2	-123	1.6
12	Namar	Penman-Monteith	1991 to 2000	Riyadh station	10-m DEM	GSMSA*	LULC 1996	MODIS	0.38	2.67	0.41	-1.5	-106	1.55	0.5	-1.6	-121	1.6
13	Namar	Penman-Monteith	1991 to 2000	Riyadh station	5-m DEM	FAO	LULC 1996	MODIS	0.18	2.37	0.48	-0.8	-91	1.34	0.6	-6.8	-227	2.8
14	Namar	Penman-Monteith	1991 to 2000	Riyadh station	5-m DEM	GSMSA*	LULC 2019	MODIS	0.39	2.35	0.43	-1.8	-116	1.64	0.5	-1.7	-120	1.6
15	Namar	Penman-Monteith	1991 to 1995	Riyadh station	5-m DEM	GSMSA*	LULC 1996	MODIS	0.27	3.1	0.54	-4.0	-173	2.24	0.6	-17	-333	4.2
16	Namar	Penman-Monteith	1991	Riyadh station	5-m DEM	GSMSA*	LULC 1996	MODIS	0.45	1.33	0.35	-2.8	-169	1.95	0.4	-4.8	-215	2.4
17	Namar	Penman-Monteith	1992	Riyadh station	5-m DEM	GSMSA*	LULC 1996	MODIS	0.47	1.84	0.64	-1.4	-115	1.53	0.7	-1.5	-117	1.5
18	Namar	Penman-Monteith	1993	Riyadh station	5-m DEM	GSMSA*	LULC 1996	MODIS	0.05	6.16	0.54	-7.4	-236	2.88	0.7	-34	-496	5.9
19	Namar	Penman-Monteith	1994	Riyadh station	5-m DEM	GSMSA*	LULC 1996	MODIS	0.39	2	0.2	-19.7	-322	4.53	0.3	-40	-470	6.3
20	Namar	Penman-Monteith	1995	Riyadh station	5-m DEM	GSMSA*	LULC 1996	MODIS	0	3.72	0.71	-1.8	-117	1.63	0.9	-2.4	-142	1.8

GSMSA*: General Soil Map of Saudi Arabia
 KKIA**: King Khalid International Airport

Other tries, among the 37 attempts, were carried out by reducing the length of calibration years; namely, calibrating one year and five years rather than the longer record of ten years (1991-2000). The R^2 results of one-year calibration using climate data individually of 1991, 1992, 1993, 1994, and 1995 were 0.35, 0.64, 0.54, 0.20, and 0.71, respectively. It is clear that these results differ significantly. Since all input variables were nearly constant between years except precipitation, this suggests variations in model calibration are attributed to the temporal change in rainfall. Rainfall was 38.3 mm, 96.6 mm, 167.6 mm, 39 mm, and 234 mm in 1991, 1992, 1993, 1994, and 1995, respectively (see Table 4.12). The low R^2 values correspond to years with low rainfall (Figure 5.4). On the other hand, the R^2 result of calibration using climate data of five years (1991-1995) was 0.54. It appears that in the calibrations of some individual years and the 5 years' time periods, the model performs relatively better.

The objective function in the SWAT model was also changed to the R^2 (coefficient of determination) and all the above 20 calibration tries were repeated. The results of the R^2 in the last 20 calibrations generally improved and reached 0.62. However, the NSE results were worse in general. Thus, it was appropriate to try additional attempts to improve model performance, including checking whether the pilot sub-basin is representative of other sub-basins in the main catchment and trying to find another ET source of higher spatial resolution.

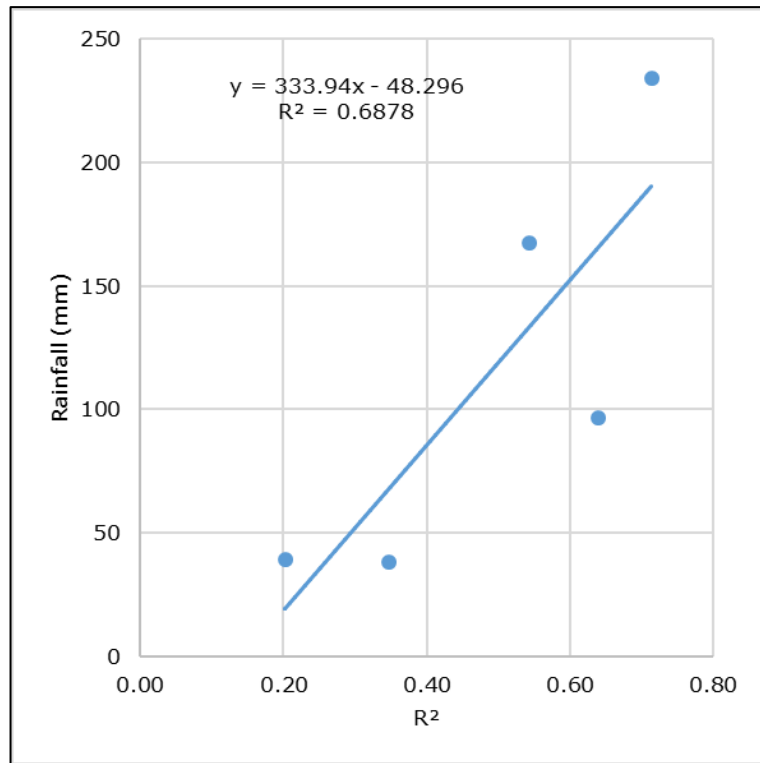


Figure 5.4: The correlation between the R² values of individual year calibrations and annual rainfall values at the Riyadh weather station.

5.6. Additional calibration attempts on other sub-basins

As it was proving illusive to achieve satisfactory model performance for the pilot sub-basin, four additional sub-basins were selected for model calibration, to explore whether the pilot sub-basin was anomalously difficult to calibrate. These sub-basins were chosen to be broadly representative of the study area whilst providing different characteristics to the pilot sub-basin to try and isolate the cause of poor calibration. The chosen basins had different sizes (larger and smaller than the pilot sub-basin), as well as lower and higher levels of urbanisation (Table 5.4). These sub-basins were the Wadi Laban (228 km²), the Wadi Alysin (158 km²), the Wadi Swaidi (8 km²), and the Wadi Ughdhuwanah (13 km²) (Figure 5.5).

Table 5.4: The LULC 1996 of some sub-basins of the main catchments of Riyadh city.

Sub-basin	Total area		Barren land class		Vegetation class		Urban class		Roads class	
	Km ²	Km ²	%	Km ²	%	Km ²	%	Km ²	%	
Wadi Namar	192.1	179.3	93.3	1.1	0.6	6.1	3.2	5.7	2.9	
Laban	228.0	212.7	93.3	1.1	0.5	7.9	3.4	6.4	2.8	
AlAysin	157.7	120.6	76.5	2.2	1.4	21.8	13.8	13.1	8.3	
As Suwaydi	8.1	1.9	23.1	0.5	5.8	4.0	49.4	1.8	21.7	
Ughdhuwanah	12.8	4.1	31.9	0.3	2.0	5.9	45.9	2.6	20.2	
Ubarah	11.3	10.4	92.0	0.2	1.8	0.1	0.9	0.6	5.3	
An Nazim	24.6	20.1	81.7	0.1	0.4	4.4	17.9	0	0	

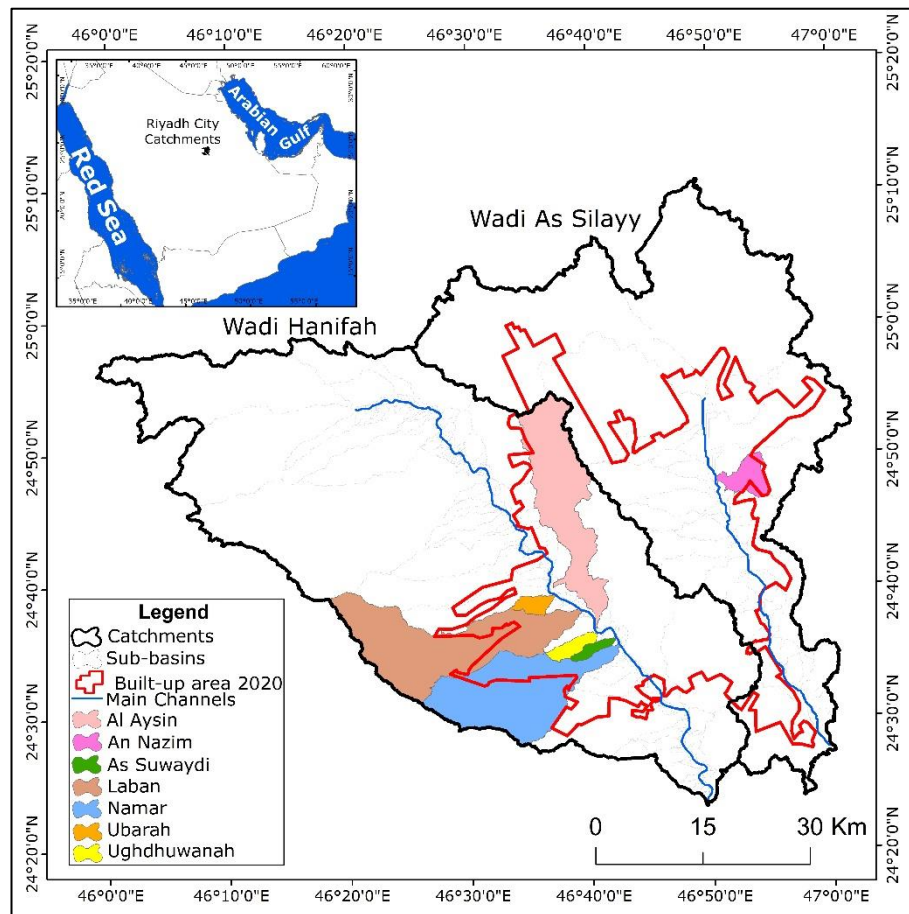


Figure 5.5: Location map of the 7 sub-basins used for preliminary calibrations to improve the SWAT model performance. Wadi Namar is the original pilot sub-basin.

The SWAT model calibration was performed for each one of these four sub-basins using firstly the NSE objective function, Penman-Monteith formula, observed weather data (1991-2000), 5-meter spatial resolution DEM, the general soil map of Saudi Arabia, and the LULC 1996 map. The NSE results were -0.66, -0.82, -4.28, and -

3.91 for Laban, AlAysin, AsSuwaydi, and Ughdhuwanah sub-basins, respectively. Equivalent R^2 values were 0.40, 0.46, 0.49, and 0.49. Subsequently, the objective function was changed to be R^2 and the SWAT model was calibrated for all four sub-basins. The NSE results were -4.08, -4.51, -4.28, and -3.91 for Laban, AlAysin, AsSuwaydi, and Ughdhuwanah sub-basins and R^2 results 0.52, 0.53, 0.49, and 0.49, respectively (Table 5.5). This means that the results of these 8 calibrations for the four sub-basins did not show any substantial improvement over the pilot sub-basin performance. Hence, the next endeavour in improving the SWAT model performance was to substitute MODIS ET with higher spatial resolution observed ET data of the TerraClimate.

The above 8 experiments for the four sub-basins were repeated using relatively high spatial resolution ET data extracted from monthly datasets of the TerraClimate (Abatzoglou et al. 2018). Since the TerraClimate datasets have a relatively high spatial resolution of 4 km, the calibrations of the SWAT model were performed on a sub-basin level using the average TerraClimate ET for each sub-basin. The NSE results were 0.57, 0.59, 0.54, and 0.55 for Laban, AlAysin, AsSuwaydi, and Ughdhuwanah sub-basins respectively, with R^2 results were 0.66, 0.62, 0.61, and 0.62, respectively. When the objective function was changed to be R^2 the NSE results were 0.56, 0.55, 0.50, and 0.50, and the R^2 values were 0.68, 0.64, 0.67, and 0.65, respectively (See Table 5.5). Additionally, the TerraClimate ET data were used to calibrate the Namar sub-basin. The NSE and R^2 results were 0.58 and 0.62, respectively. By changing the objective function to be R^2 , the results of NSE and R^2 were 0.63 and 0.51, respectively.

Table 5.5: Statistical results of attempts applied on six sub-basins in the two main catchments to calibrate the SWAT model using NSE and R² as the objective functions.

ID	Sub-basin	ET formula	Period	SWAT input data				ET source	p-factor	R-factor	NSE as the objective function				R ² as the objective function			
				Climate data	DEM	Soil	LULC				R ²	NSE	PBIAS	RSR	R ²	NSE	PBIAS	RSR
21	Laban	Penman-Monteith	1991 to 2000	Riyadh station	5-m DEM	GSMSA*	LULC 1996	MODIS	0.44	2.09	0.4	-0.66	-69	1.26	0.5	-4.1	-172	2.3
22	Al Aysin	Penman-Monteith	1991 to 2000	Riyadh station	5-m DEM	GSMSA*	LULC 1996	MODIS	0.37	2.11	0.46	-0.82	-82	1.33	0.5	-4.5	-177	2.3
23	As Suwaydi	Penman-Monteith	1991 to 2000	Riyadh station	5-m DEM	GSMSA*	LULC 1996	MODIS	0.36	1.44	0.49	-4.28	-180	2.3	0.5	-4.3	-180	2.3
24	Ughdhduuanah	Penman-Monteith	1991 to 2000	Riyadh station	5-m DEM	GSMSA*	LULC 1996	MODIS	0.36	1.58	0.49	-3.91	-167	2.22	0.5	-3.9	-167	2.2
25	Namar	Penman-Monteith	1991 to 2000	Riyadh station	5-m DEM	GSMSA*	LULC 1996	TerraClimate	0.36	0.39	0.62	0.58	26	0.65	0.6	0.51	40	0.7
26	Laban	Penman-Monteith	1991 to 2000	Riyadh station	5-m DEM	GSMSA*	LULC 1996	TerraClimate	0.52	0.32	0.66	0.57	35	0.66	0.7	0.56	38	0.7

GSMSA*: General Soil Map of Saudi Arabia

Table 5.5: Statistical results of attempts applied on six sub-basins in the two main catchments to calibrate the SWAT model using NSE and R² as the objective functions. (Continued)

ID	Sub-basin	ET formula	Period	SWAT input data				ET source	p-factor	R-factor	NSE as the objective function				R ² as the objective function			
				Climate data	DEM	Soil	LULC				R ²	NSE	PBIAS	RSR	R ²	NSE	PBIAS	RSR
27	Al Aysin	Penman-Monteith	1991 to 2000	Riyadh station	5-m DEM	GSMSA*	LULC 1996	TerraClimate	0.35	0.42	0.62	0.59	19	0.64	0.6	0.55	34	0.7
28	As Suwaydi	Penman-Monteith	1991 to 2000	Riyadh station	5-m DEM	GSMSA*	LULC 1996	TerraClimate	0.3	0.23	0.61	0.54	34	0.68	0.7	0.5	43	0.7
29	Ughdhduuanah	Penman-Monteith	1991 to 2000	Riyadh station	5-m DEM	GSMSA*	LULC 1996	TerraClimate	0.32	0.24	0.62	0.55	34	0.67	0.7	0.5	44	0.7
30	Ubarah	Penman-Monteith	1991 to 2000	Riyadh station	5-m DEM	GSMSA*	LULC 1996	TerraClimate	0.56	0.31	0.66	0.58	35	0.65	0.7	0.56	39	0.7
31	An Nazim	Penman-Monteith	1991 to 2000	Riyadh station	5-m DEM	GSMSA*	LULC 1996	TerraClimate	0.39	0.3	0.61	0.49	51	0.71	0.6	0.49	51	0.7

GSMSA*: General Soil Map of Saudi Arabia

The calibrations of these additional four sub-basins produced p-factor values ranging from 0.30 to 0.52 and R-factor values ranging from 0.23 to 0.42. It can be noted that the p-factor values were still below the recommended model performance of 0.7 (Abbaspour et al. 2015; Carlos Mendoza et al. 2021) for all tested sub-basins. However, all these four sub-basins had satisfactory results of the NSE, R^2 , and RSR performance indicators. In addition, all chosen performance indicators yielded satisfactory results for the Al Aysin sub-basin (0.62 for the R^2 , 0.59 for the NSE, 19 for the PBIAS, and 0.64 for the RSR). Apart from the relatively poor P-factor values, the results obtained using the TerraClimate ET data demonstrate acceptable SWAT model performance during calibrations of the tested sub-basins. Thus, the use of TerraClimate ET data represented a turning point in the SWAT model calibration process in this study area, producing a marked improvement in the SWAT model performance.

Based on these statistical findings, one may judge that the SWAT model can be applied to the whole study area. However, two more sub-basins that were affected by the rapid development of Riyadh city were used for additional testing of the model. The chosen sub-basins were Ubarah sub-basin (23 km²) and An Nazim sub-basin (25 km²) (See Figure 5.5). The Ubarah sub-basin has been subjected to major landform destruction and valley filling and blocking (Figure 5.6). The An Nazim sub-basin had serious flooding in May 2010 (see Figure 1.2). A problem of the delineation of the Ubarah sub-basin was faced using the 5 m spatial resolution DEM because only 11 km² were delineated, representing only 49% of its actual size. The omitted area of the Ubarah sub-basin was erroneously included in the neighboring Laban sub-basin. This issue was solved by using the SRTM 30 m spatial resolution DEM generated in 2000, overlaid onto an aerial photograph from 1976 (Figure 5.7). The SRTM 30 m

spatial resolution DEM was then used to calibrate the Ubarah sub-basin. The NSE results of the calibrations were 0.58 and 0.49 for the Ubarah and the An Nazim sub-basins respectively. Whilst the R^2 results were 0.66 and 0.61, respectively. When the objective function was changed to be R^2 the NSE results were 0.56 and 0.49 and R^2 values were 0.68 and 0.61, respectively.

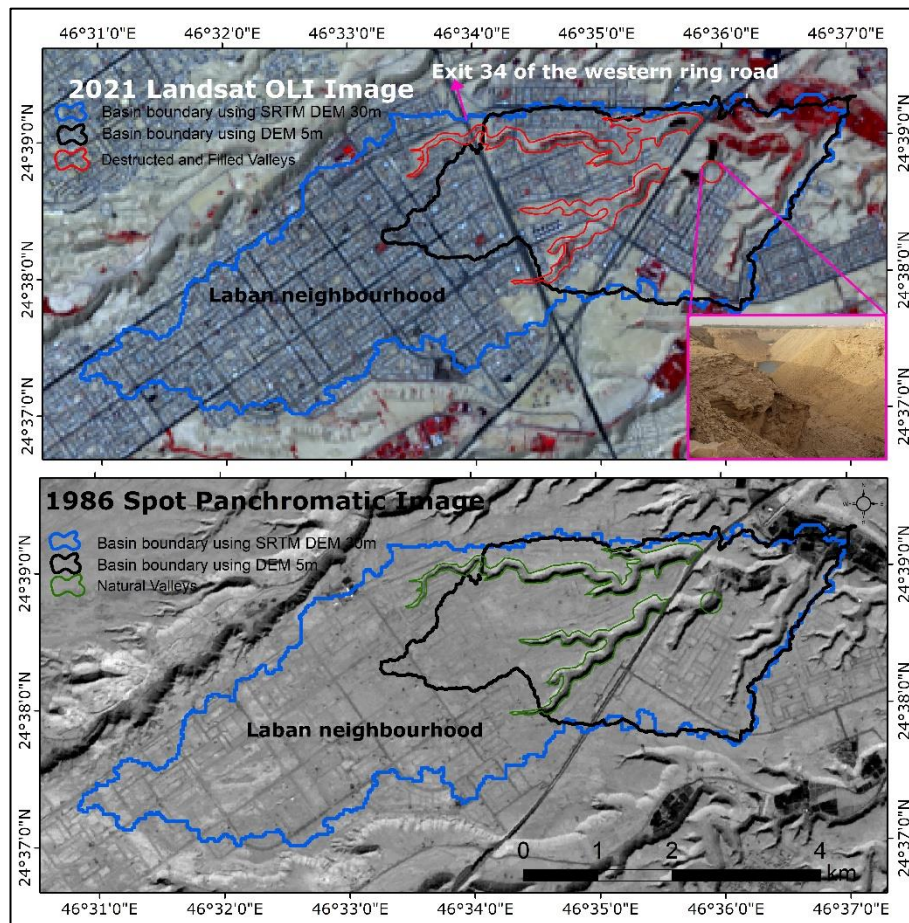


Figure 5.6: Multi-temporal remote sensing images, Landsat OLI images acquired Mach/April 2021 and Spot images acquired April 1986, showing destruction and filling of some natural valleys in Riyadh city.

Source: EarthExplorer n.d.

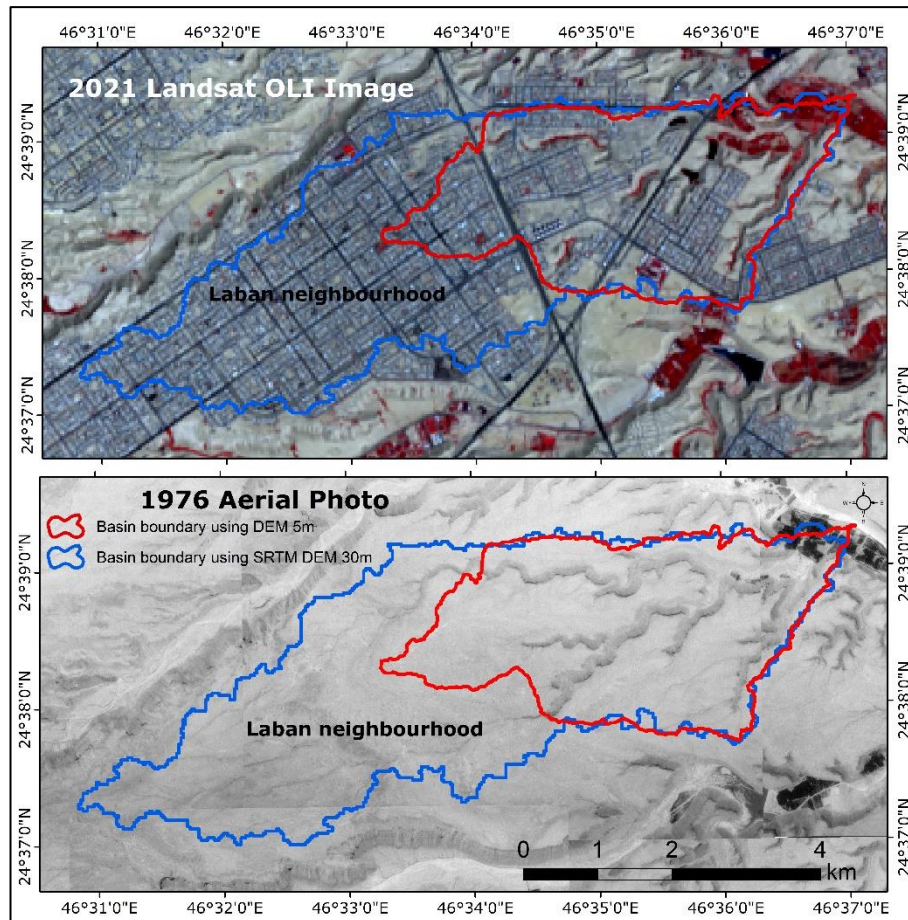


Figure 5.7: The boundaries of Ubarah sub-basin delineated using different DEMs superimposed on 1976 aerial photo and 2021 Landsat OLI image.

Source: EarthExplorer n.d.; General Commission for Survey, Riyadh.

TerraClimate and MODIS estimates of ET differ significantly during the calibration periods (1991-2000) for the Namar Sub-basin. The TerraClimate ET is much higher than the MODIS estimates. The simulated ET for the Wadi Namar sub-basin exists between that of TerraClimate and MODIS estimates. The simulated ET provides a reasonable match for the TerraClimate ET estimate most of the time. This result revealed that the SWAT hydrological model can be used to simulate the hydrological cycle components for the catchments in Riyadh city to a satisfactory level. Thus, the SWAT model was performed on the main catchments of the study area in the following sections.

5.7. Initial sensitivity analysis, calibration, and validation

After achieving an acceptable SWAT model for the seven tested sub-basins, the next step was to apply the processes of the parameters sensitivity analysis, followed by model calibration and validation on the main catchments in Riyadh city. Sensitivity analysis determines sensitive variables from the chosen 38 parameters that are adequate for the model to produce satisfactory predictions. Model calibration involved the processes of comparing the predicted output of ET and derived TerraClimate ET data to adjust the parameter values until the satisfactory standard for the NSE and R^2 objective functions are achieved.

Model validation is a process to evaluate whether the calibrated SWAT models can make adequate predictions of ET for the study area outside the period used for the calibration. The calibration and validation processes of the SWAT model were implemented using 23 years of data from 1988 to 2010 for the two main catchments. Data from the first 3 years was used as the warm-up period, the data from 1991 to 2000 for the calibration, and the data from 2001 to 2010 for the validation.

5.7.1. Initial SWAT model calibration and sensitivity analysis

Model calibration is an essential and critical step to achieving accurate model outputs. To evaluate the SWAT model performance for the Wadi Hanifah and the Wadi As Silayy catchments, the two catchments' calibrations were first conducted by using the 38 parameters listed in Table 5.1. The calibration of the Wadi Hanifah catchment was based on 22 sub-basins; whilst the calibration of the Wadi As Silayy catchment was based on 11 sub-basins. The SWAT model calibration of the two main catchments of Riyadh city, considering all sub-basins, resulted in p-factors of 0.40 (Wadi

Hanifah) and 0.33 (Wadi As Silayy) and R-factors of 0.28 and 0.43, respectively. For both catchments, the results of the p-factor were below the recommended model performance of 0.7 or greater. However, the results of the R-factor were within acceptable values (1.5 or less). Table 5.6 also shows that the two catchments had satisfactory results for the NSE, R², and RSR. Moreover, based on the criteria provided in Table 5.2, the SWAT model showed satisfactory and good performance for monthly ET prediction for the Wadi As Silayy catchment.

When the NSE objective function is used, three of the performance indicators yielded satisfactory results while the PBIAS yielded a good result. The results were 0.63 for the NSE, 14 for the PBIAS, and 0.61 for the RSR. Furthermore, the R² value (R² = 0.65) for annual TerraClimate ET versus the simulated ET give reasonable relationships. Aside from the relatively poor p-factor and PBIAS values, the result of the calibrations obtained by using the TerraClimate ET data demonstrates acceptable SWAT model performance for monthly predictions at the Wadi Hanifah and the Wadi As Silayy catchments.

Table 5.6: Statistical results of initial four calibrations using 38 parameters.

Catchment	P-factor	R-factor	NSE as the objective function				R ² as the objective function			
			NSE	R ²	PBIAS	RSR	NSE	R ²	PBIAS	RSR
Wadi Hanifah	0.4	0.28	0.51	0.63	42	0.7	0.51	0.63	41.89	0.7
Wadi As Silayy	0.33	0.43	0.63	0.65	13.65	0.61	0.57	0.68	31.72	0.66

When using the NSE objective function, all past calibrations showed insignificant changes in the values of the NSE and R² model performance indices for each calibration performed. Unlike the NSE objective function, the application of the R² objective function caused significant negative changes for the other indices used for

model performance, especially the PBIAS index. For example, Table 5.6 shows that the application of the NSE objective function yielded a 13.65 value for PBIAS in the calibration of the Wadi As Silayy catchment, but the application of the R^2 objective function yielded a 31.72 value for PBIAS. Based on the criteria of the PBIAS provided in Table 5.2, the SWAT model showed a good performance for monthly ET prediction for the Wadi As Silayy catchment using the NSE objective function and an unsatisfactory performance when using the R^2 objective function. Moreover, as illustrated in Figure 5.8, the simulated ET data was generally lower than the TerraClimate ET. It also reveals that the estimations of ET using the R^2 objective function were lower than the estimations when using the NSE objective function at the Wadi As Silayy catchment. It should be noted that the line of simulated evapotranspiration in the Wadi Hanifah catchment when using the R^2 objective function covers the line of simulated evapotranspiration when using the NSE objective function.

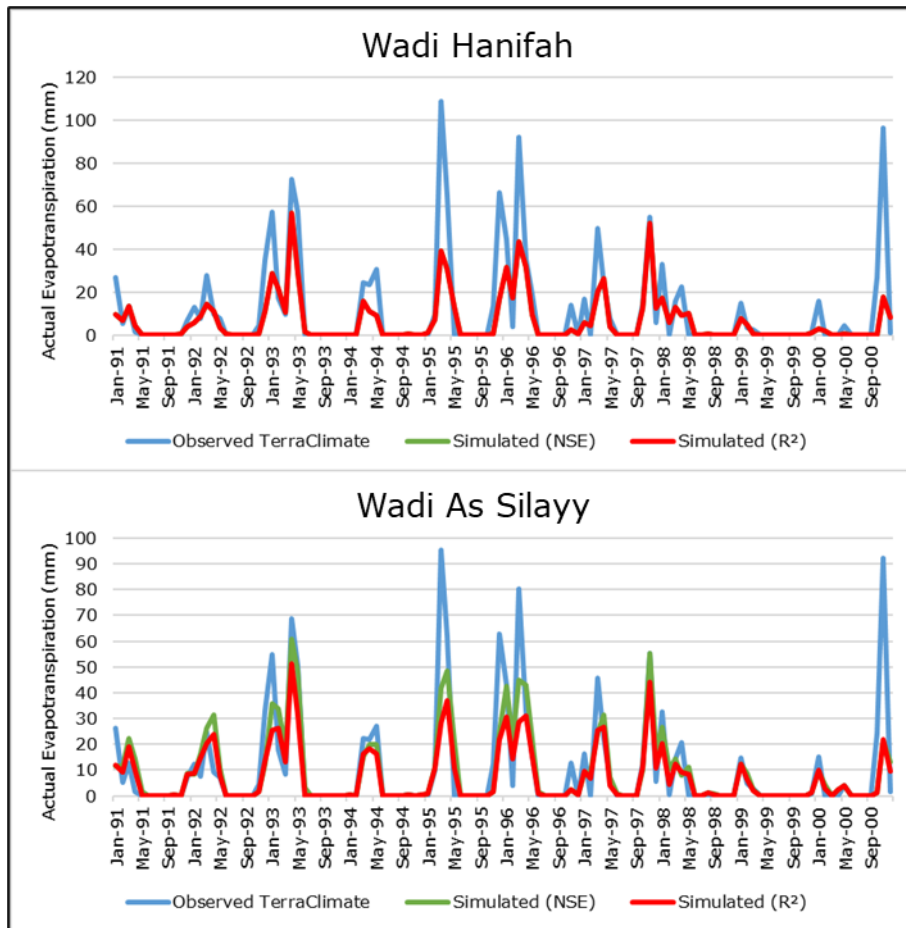


Figure 5.8: A comparison of simulated evapotranspiration values with TerraClimate derived data for initial calibration.

The formula for PBIAS measures the average tendency of the simulated to be larger or smaller than observation data. Accordingly, positive values of PBIAS indicate an underestimation by the model, and negative values suggest an overestimation by the model (Abbaspour, 2015). From Table 5.6, it is clear that the four calibrations for the two main catchments in the study area resulted in positive PBIAS values which means simulations of ET were underestimated. The underestimation was greater when using the R^2 objective function. The calibration results also reveal that Nash–Sutcliffe efficiency (NSE) objective function is more suitable for the study area than the R^2 objective function. Hence, the following analysis using the SWAT model depended on the NSE objective function.

To define the most influential SWAT parameters for predicting the hydrological cycle components in the study area, a global sensitivity analysis was implemented using the SUFI-2 algorithm. Nine sensitivity analysis runs were carried out for the Wadi Hanifah catchment, and eight sensitivity analyses were implemented for the Wadi As Silayy catchment (Appendix A). But the validation of the initial SWAT model (Section 5.7.2) showed unsatisfactory performance of the model.

5.7.2. Attempts to validate SWAT model

Validation compares the output results of calibrated SWAT models with the observed data at the study area. Data for the ten years (2001-2010) succeeding the calibration period were used to validate the SWAT models for the two main catchments at the study area. Table 5.7 summarises the statistical results of model performance indices for the SWAT models' validation in the Wadi Hanifah and the Wadi As Silayy catchments. The NSE values were 0.02 for the Wadi Hanifah catchment and 0.11 for the Wadi As Silayy catchment. These results indicated a poor agreement between the observed and simulated ET in the study catchments (Figure 5.9).

Table 5.7: Statistical results of model performance indices for initial models' validation in in the study are catchments.

Catchment	NSE	R ²	PBIAS	RSR
Wadi Hanifah	0.0	0.1	63.24	1
Wadi As Silayy	0.1	0.2	30.41	0.9

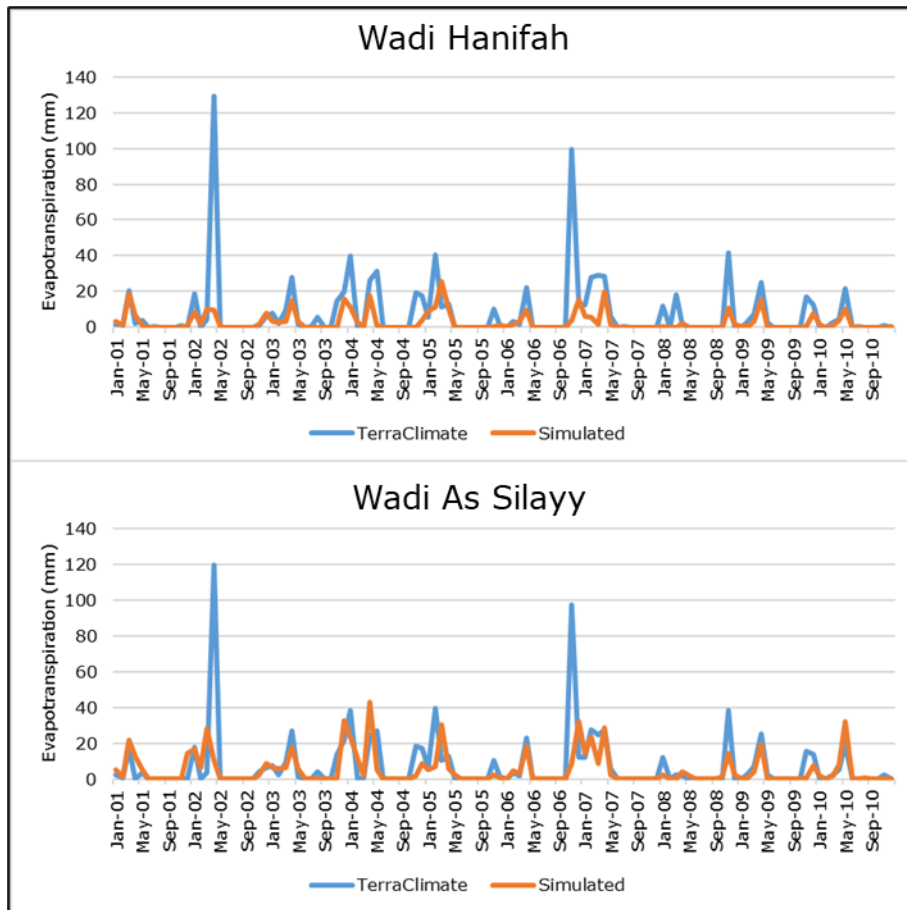


Figure 5.9: A comparison of simulated evapotranspiration values with TerraClimate derived data for initial validation (2001-2010).

The poor agreement between observed and simulated data means the SWAT model performance required improvement. Therefore, additional calibrations were performed for the Wadi Hanifah catchment using 15 years (1991-2005), 16 years (1991-2006), 17 years (1991-2007), 18 years (1991-2008), and 19 years (1991-2009) of data, but all attempts resulted in unsatisfactory calibrations (Table 5.8).

Table 5.8: Statistical results of model performance indices of the additional attempts to improve calibrations using 1991-2010 data.

Attempt	The Wadi Hanifah catchment				The Wadi As Silayy catchment			
	NSE	R ²	PBIAS	RSR	NSE	R ²	PBIAS	RSR
15 years	0.4	0.5	46.2	0.8	0.5	0.5	16.6	0.7
16 years	0.3	0.4	48.2	0.8	0.4	0.4	19.2	0.8
17 years	0.3	0.4	49.1	0.8	0.4	0.4	19.3	0.8
18 years	0.3	0.4	50.1	0.8	0.4	0.4	20.2	0.8
19 years	0.3	0.4	50.4	0.8	0.4	0.4	21.2	0.8
10 Odd years	0.5	0.6	40.9	0.7	0.7	0.7	12.8	0.6

Therefore, odd years in the period 1991-2010 were used for calibration and the even years for validation. The SWAT model calibrated using the ten-odd years had a satisfactory performance, yielding 0.49 NSE and the validation of this model using the ten even years was unsuccessful, which gave a performance index of 0.19 for NSE. These unsatisfactory models prompted the necessity to understand the factors leading to the poor model performance and to seek ways to improve the performance, if possible.

Given the good agreement during the calibration period (section 5.7.1), and when using odd numbered years, it appeared the issue was data in the period 2001-2010. Since precipitation is a key factor governing runoff regimes and the main driver of the hydrological cycle, comparisons of precipitation from different climate data sources were performed to examine rainfall data relationships. The comparison included global datasets (TerraClimate), measured data (Riyadh Weather Station and KKIA Weather Station), and reanalysis data (CFSR) (see Figure 4.16). The four products were compared using data for 20 years divided into two groups. The first group (calibration period) extends from 1991 to 2000 and the second group (validation period) extends from 2001 to 2010.

The comparison between data sources indicates that for the 10-year monthly precipitation records for 1991-2000 there are significant

relationships, with R^2 of 0.83, 0.78, and 0.57 for Riyadh Weather Station compared to TerraClimate, KKIA Weather Station, and reanalysis (CFSR) respectively (Figure 5.10). Conversely, the analysis results for the validation period (2001-2010) of monthly precipitation Riyadh station-R001 versus other sources showed that there was a very weak relationship, with R^2 ranging from 0.07 to 0.26 (Figure 5.11). Similar findings were found for King Khalid International Airport Weather Station (KKIA), with R^2 ranging between 0.22 and 0.42 (Figure 5.12).

In contrast, other climate variables such as temperature were found to have good relationships between different data sources (see Figure 4.27 and Figure 4.28). The key difference between the two periods is that 2000-2010 was a very dry decade (Figure 5.13), which may explain the discrepancy in measurement values and also why a model calibrated on 1991 – 2000 data is not able to accurately predict ET in this unusually dry decade. To overcome the problem of using climate data for the period 2001-2010 to validate the SWAT model, it was decided to use climate data measured before 2000 for both the calibration and validation of the final SWAT model. It should be noted that the period used for setting up the final SWAT model includes some dry years.

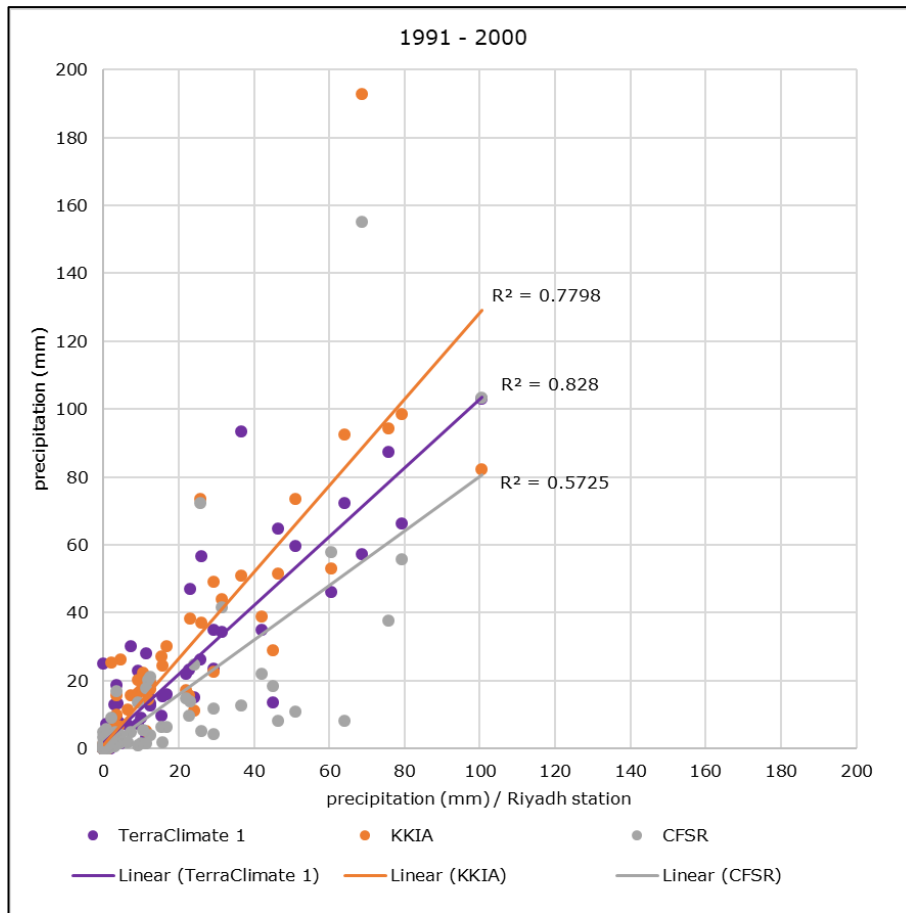


Figure 5.10: Relationships between monthly rainfall in Riyadh station and rainfall from other sources for the period 1991-2000.

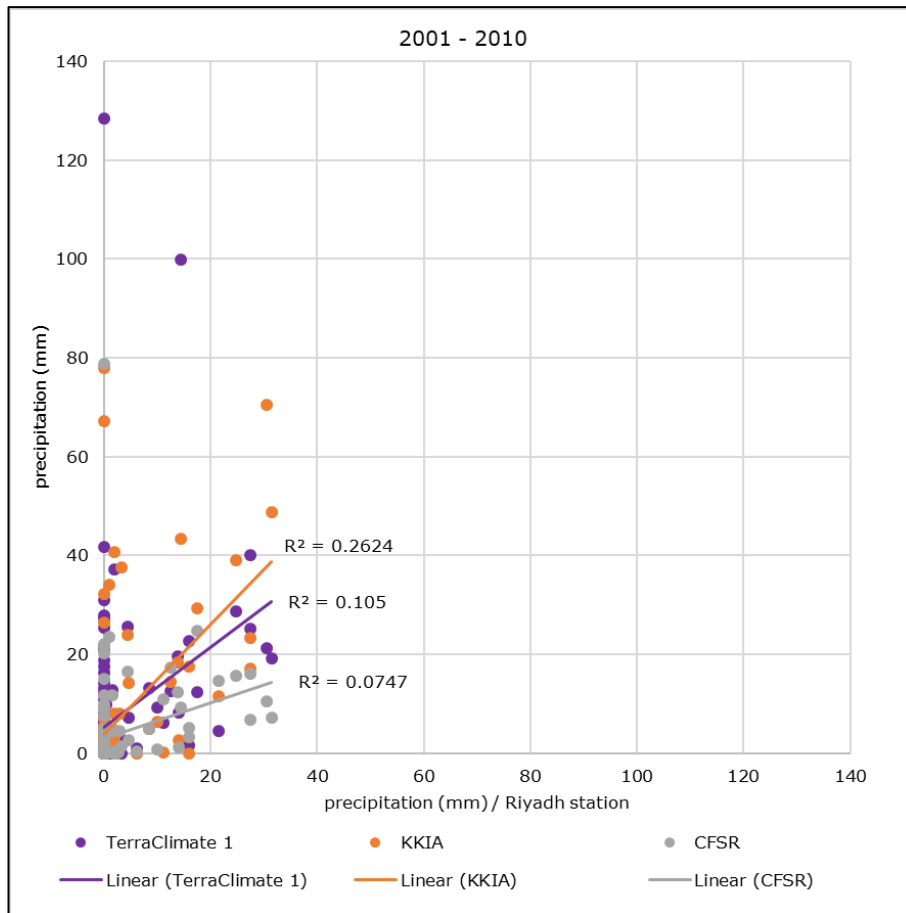


Figure 5.11: Relationships between monthly rainfall in Riyadh station and rainfall from other sources for the period 2001-2010.

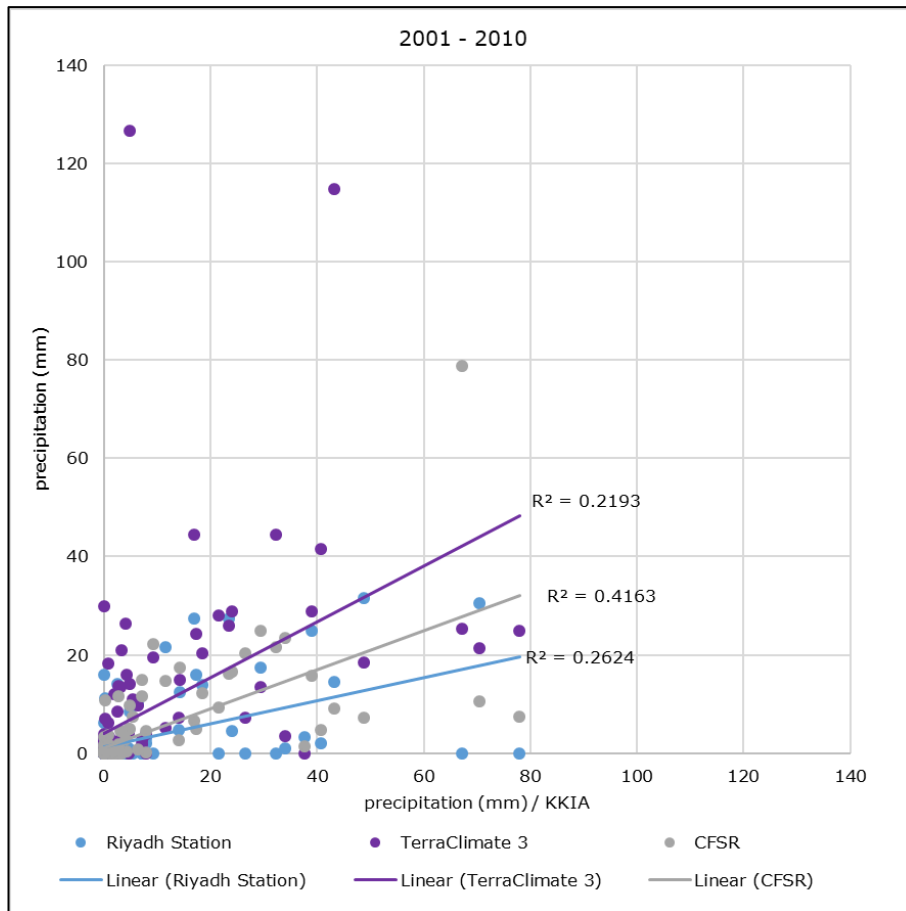


Figure 5.12: Relationships between monthly rainfall from King Khalid International Airport (KKIA) station and rainfall from other sources for the period 2001-2010.

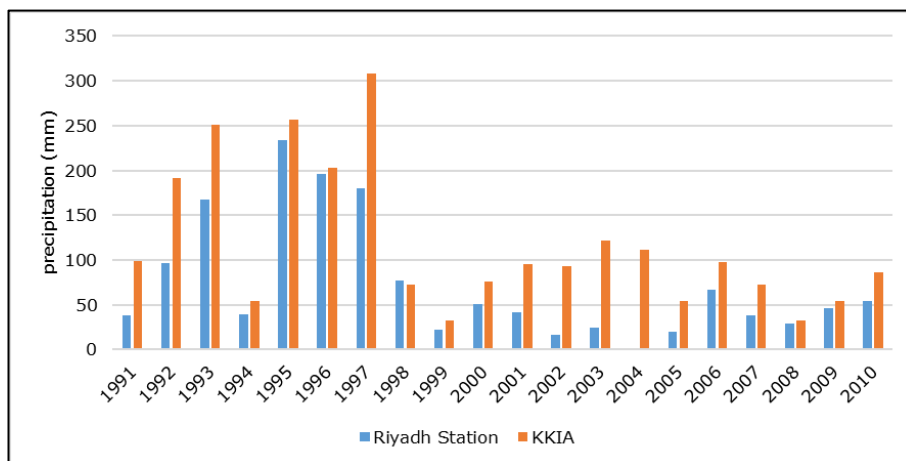


Figure 5.13: Annual rainfall at the catchments of Riyadh city.

5.8. Summary

The SWAT model was run in a monthly time step. Initially, 38 parameters were selected to develop SWAT models for runoff estimation in the catchments of Riyadh. SUFI-2 algorithm was used for the SWAT model calibration. The NSE, R^2 , PBIAS, and RSR indices were used to evaluate the SWAT model performance. Climate data for the periods 1991-2000 and 2001-2010 were intended for calibration and validation, respectively. In the beginning, the SWAT model calibrations were performed using satellite-based monthly evapotranspiration data from MODIS. But when unsatisfactory results were obtained using MODIS data, it was substituted by a higher spatial resolution monthly evapotranspiration data from the TerraClimate.

After 62 calibration attempts applied to 7 sub-basins, satisfactory statistical results were reached. Using the NSE and R^2 objective functions, 40 attempts were performed on the Wadi Namar sub-basin to improve the SWAT model performance. Most of the statistical results were poor. These unsatisfactory models prompted the necessity to try the model on other sub-basins. Thus, eight attempts on four sub-basins were implemented, but the statistical results did not improve. The next stage was to use the derived evapotranspiration of the TerraClimate to calibrate the SWAT model for the Wadi Namar sub-basin which led to two successful models. Then calibrations using TerraClimate evapotranspiration data of twelve more models for other sub-basins were successfully performed.

Hence, the next steps were to calibrate and validate SWAT models for the main catchments of Riyadh city. The calibrations using data for the period 1991-2000 succeeded but the validations using data for the period 2001-2010 failed. After several attempts to improve

the performance of the model, it was found that the first decade of this century was a dry period in Riyadh, which could be the reason for the failure of the verification of the model. Accordingly, the period during which the previous model calibration succeeded was divided to be used for both the final SWAT models calibrations and validations. As described in Chapter 6, five years from 1991 to 1995 were used to calibrate the SWAT model and five years from 1996 to 2000 were used for the model validation.

Chapter 6: Final SWAT Model Setup

6.1. Overview

Given the period 2001 to 2010 was an unusual weather period and, therefore, not ideal for calibration and validation of the model, data for the period 1991-2000 was used for both calibration and validation of the final SWAT models. The climate data of the first 5 years were used for model calibration and the remaining 5 years for model validation, preceded by the three-year warm-up (1988-1990). Inputs were otherwise the same as in section 5.7.

This chapter documents the processes conducted to set up the final SWAT models for the simulation of surface runoff in the catchments of Riyadh. The chapter includes the results of SWAT model calibration, sensitivity analysis and validation for the two main catchments of the study area. Besides, it presents the impact of parameter values' change on runoff simulation. Also, the chapter contains a comparison between historically measured annual runoff data for the Wadi Hanifah catchment, runoff values simulated by the calibrated and validated SWAT model, and annual runoff outputs of the uncalibrated SWAT model.

6.2. SWAT model calibration and sensitivity analysis

The global sensitivity analysis techniques were implemented using the SUFI-2 algorithm to identify the most influential SWAT parameters to predict the hydrological cycle components in the catchments of Riyadh city. Applying the NSE objective function, the sensitivity analyses and calibrations of the SWAT model for the two main catchments started using the selected 38 parameters (Table 6.1). The values in the table are the mean across the sub-basins in each catchment.

Table 6.1: Monthly statistical results of the SWAT models calibrations using 38 parameters.

Catchment	P-factor	R-factor	NSE objective function			
			NSE	R ²	PBIAS	RSR
Wadi Hanifah	0.38	0.25	0.53	0.68	45.3	0.68
Wadi As Silayy	0.27	0.42	0.67	0.69	12.7	0.57

The statistical results of the p-factor and R-factor for the Wadi Hanifah catchment were 0.38 and 0.25 respectively. For the Wadi As Silayy catchment, the statistical results of the p-factor and R-factor were 0.27 and 0.42 respectively. It can be noticed that the values of the R-factor were within acceptable values (1.5 or less). While values of the P-factor were still below the recommended model performance (0.7 or greater). However, the statistical results of model performance indices indicated the satisfactory performance of the SWAT model to predict monthly ET for both catchments and consequently other components of the hydrological cycle.

The NSE, R², and RSR performance indicators revealed satisfactory results while the PBIAS yielded a good result for the Wadi As Silayy catchment. The results for this catchment were 0.67 for the NSE and 13 for the PBIAS. The NSE, R², and RSR performance indicators yielded satisfactory results while the PBIAS index revealed an unsatisfactory result for the Wadi Hanifah catchment. The NSE result was 0.53 for the Wadi Hanifah catchment. Besides, the plots of lines for TerraClimate's ET and the simulated ET during the calibration period (1991-1995) indicated that the simulated ET acceptably matches with the TerraClimate's ET data. Additionally, the R² values for annual TerraClimate's ET versus the simulated ET suggest reasonable relationships. Apart from the unacceptable P-factor and PBIAS values, the results of the calibration obtained by using TerraClimate's ET data indicated acceptable SWAT model performance for monthly prediction at the Wadi Hanifah and the Wadi As Silayy catchments.

To decide how many parameters to use for the SWAT model calibration, five sensitivity analyses were performed for the Wadi Hanifah and Wadi As Silayy catchments respectively (Table 6.2 and Table 6.3). The p-value results of the 38 parameters ranged from 0 to 1 for the Wadi Hanifah catchment and from 0 to 0.98 for the Wadi As Silayy catchment. The parameters with a p-value of 0.05 or less were 12 parameters and 9 parameters at the Wadi Hanifah and the Wadi As Silayy catchments respectively. After that, another sensitivity analysis with fewer parameters was implemented by omitting all parameters with a p-value above 0.7. This final sensitivity analysis had 14 parameters for both Wadi Hanifah and Wadi As Silayy.

Table 6.2: Sensitivity analyses of the Wadi Hanifah catchment.

Parameter Name	38			28			23			18			14		
	Rank	t-Stat	P-Value												
CN2.mgt	1	-28.70	0.00	1	-28.45	0.00	1	-29.02	0.00	1	-27.76	0.00	1	-31.94	0.00
ESCO.hru	2	-22.32	0.00	2	-22.81	0.00	2	-22.34	0.00	2	-22.66	0.00	2	-23.51	0.00
ICN.bsn	3	14.45	0.00	3	16.91	0.00	3	15.91	0.00	3	16.08	0.00	3	17.51	0.00
SOL_Z(..).sol	4	-8.20	0.00	4	-10.55	0.00	4	-10.50	0.00	4	-9.73	0.00	4	-10.48	0.00
SOL_K(..).sol	5	-5.96	0.00	7	-4.60	0.00	8	-2.68	0.01	6	-4.58	0.00	6	-3.88	0.00
SOL_BD(..).sol	6	-5.80	0.00	5	-5.02	0.00	5	-5.87	0.00	5	-6.53	0.00	5	-4.25	0.00
EPCO.hru	7	4.14	0.00	8	2.93	0.00	6	3.24	0.00	8	3.20	0.00	7	3.29	0.00
CANMX.hru	8	2.67	0.01	6	4.70	0.00	7	2.80	0.01	7	3.72	0.00	9	2.16	0.03
SOL_CRK.sol	9	-2.47	0.01	12	1.34	0.18	21	-0.18	0.86						
SLSOIL.hru	10	2.43	0.02	24	0.33	0.74									
CNCOEF.bsn	11	-2.35	0.02	9	-1.81	0.07	11	-2.05	0.04	11	-1.56	0.12	11	-1.55	0.12
ESCO.bsn	12	2.24	0.03	13	1.27	0.20	16	-0.73	0.46	14	-0.43	0.67	14	-0.65	0.52
SOL_AWC(..).sol	13	-1.45	0.15	10	1.46	0.14	13	-1.20	0.23	16	-0.27	0.79			
SLSUBBSN.hru	14	1.38	0.17	28	0.00	1.00									
GW_REVAP.gw	15	1.20	0.23	27	-0.01	0.99									
GSI{..}.plant.dat	16	1.02	0.31	18	0.77	0.44	12	-1.87	0.06	12	-1.46	0.14	10	1.55	0.12
CH_L1.sub	17	-1.00	0.32	25	0.31	0.76									
SURLAG.bsn	18	0.77	0.44	26	0.25	0.81									
SOL_ALB(..).sol	19	-0.67	0.50	19	0.68	0.50	9	-2.44	0.01	9	-2.17	0.03	8	-2.44	0.01
CH_N1.sub	20	0.65	0.52	22	0.49	0.62	18	0.64	0.52	17	-0.23	0.82			
ALAI_MIN{..}.plant.dat	21	0.64	0.52	14	1.08	0.28	10	2.28	0.02	15	-0.29	0.77			

Table 6.2: Sensitivity analyses of the Wadi Hanifah catchment. (Continued)

Parameter Name	38			28			23			18			14		
	Rank	t-Stat	P-Value												
WUDEEP(..).wus	22	0.60	0.55	15	1.02	0.31	23	0.00	1.00						
SHALLST.gw	23	-0.59	0.55	21	0.65	0.52	14	-0.86	0.39	18	-0.10	0.92			
DEEPST.gw	24	-0.58	0.56	23	-0.42	0.67	19	-0.31	0.76						
BLAI{..}.plant.dat	25	-0.56	0.57	16	0.96	0.34	17	0.66	0.51	13	1.05	0.29	12	-1.26	0.21
CNOP{..}.mgt	26	-0.51	0.61	11	1.37	0.17	15	0.84	0.40	10	1.64	0.10	13	1.05	0.29
CNOP{..}.mgt	27	0.50	0.62	17	0.80	0.42	22	0.12	0.91						
OV_N.hru	28	-0.49	0.62	20	0.65	0.52	20	0.26	0.80						
GW_DELAY.gw	29	0.36	0.72												
RCHRG_DP.gw	30	0.33	0.74												
WUSHAL(..).wus	31	0.32	0.75												
CH_S1.sub	32	0.31	0.76												
EPCO.bsn	33	0.27	0.78												
GWQMN.gw	34	-0.21	0.83												
REVAPMN.gw	35	-0.20	0.84												
CNOP{..}.mgt	36	-0.08	0.93												
FFCB.bsn	37	0.04	0.97												
ALPHA_BF.gw	38	0.00	1.00												

Table 6.3: Sensitivity analyses of the Wadi As Silayy catchment.

Parameter Name	38			29			21			18			14		
	Rank	t-Stat	P-Value												
SOL_Z(..).sol	1	-62.68	0.00	1	-	0.00	1	-	0.00	1	-	0.00	1	-	0.00
ESCO.hru	2	-26.94	0.00	2	-	0.00	2	-	0.00	2	-	0.00	2	-	0.00
SOL_AWC(..).sol	3	-24.88	0.00	3	-	0.00	3	-	0.00	3	-	0.00	3	-	0.00
CN2.mgt	4	-12.92	0.00	4	-	0.00	4	-	0.00	4	-	0.00	4	-	0.00
ICN.bsn	5	8.28	0.00	5	-	0.00	5	-	0.00	5	-	0.00	5	-	0.00
SOL_K(..).sol	6	-3.21	0.00	24	-	0.85									
CANMX.hru	7	2.93	0.00	6	-	0.01	6	-	0.00	6	-	0.00	6	-	0.00
SLSOIL.hru	8	-1.99	0.05	28	-	0.98									
ESCO.bsn	9	1.97	0.05	14	-	0.48	14	-	0.28	10	-	0.16	10	-	0.15
GW_REVAP.gw	10	1.87	0.06	15	-	0.53	17	-	0.53	12	-	0.35	11	-	0.36
CNOP{..}.mgt	11	1.72	0.09	27	-	0.95									
SOL_ALB(..).sol	12	1.47	0.14	12	-	0.48	12	-	0.17	14	-	0.52	13	-	0.49
GWQMN.gw	13	1.31	0.19	26	-	0.93									
CNOP{..}.mgt	14	-1.25	0.21	19	-	0.62	9	-	0.03	13	-	0.38	12	-	0.40
CNOP{..}.mgt	15	1.22	0.22	13	-	0.48	16	-	0.46	9	-	0.06	9	-	0.06
SOL_BD(..).sol	16	-1.13	0.26	25	-	0.86									
SURLAG.bsn	17	1.11	0.27	29	-	0.99									
CH_N1.sub	18	-1.08	0.28	7	-	0.08	10	-	0.07	7	-	0.00	7	-	0.00

Table 6.3: Sensitivity analyses of the Wadi As Silayy catchment. (Continued)

Parameter Name	38			29			21			18			14		
	Rank	t-Stat	P-Value												
SHALLST.gw	19	-1.04	0.30	16	0.62	0.54	11	-1.48	0.14	15	-0.37	0.71			
ALPHA_BF.gw	20	-1.00	0.32	23	-0.22	0.83									
EPCO.hru	21	1.00	0.32	9	0.96	0.34	20	0.07	0.95						
SLSUBBSN.hru	22	0.99	0.32	20	0.48	0.63	18	-0.61	0.54	8	-2.20	0.03	8	-2.25	0.02
REVAPMN.gw	23	0.86	0.39	22	-0.27	0.79									
WUDEEP(..).wus	24	0.75	0.45	18	0.53	0.59	15	1.08	0.28	17	0.23	0.81			
FFCB.bsn	25	-0.72	0.47	10	0.81	0.42	7	-2.81	0.01	18	0.07	0.94			
RCHRG_DP.gw	26	-0.67	0.50	8	-1.26	0.21	13	1.30	0.19	16	0.31	0.76			
GSI{..}.plant.dat	27	0.61	0.54	11	0.72	0.47	8	2.57	0.01	11	0.96	0.34	14	-0.34	0.74
CH_L1.sub	28	-0.54	0.59	17	-0.57	0.57	21	-0.04	0.97						
SOL_CRK.sol	29	-0.44	0.66	21	-0.39	0.70	19	0.19	0.85						
OV_N.hru	30	-0.36	0.72												
EPCO.bsn	31	0.33	0.74												
GW_DELAY.gw	32	-0.33	0.74												
ALAI_MIN{..}.plant.dat	33	-0.26	0.79												
CNCOEF.bsn	34	0.22	0.82												
WUSHAL(..).wus	35	0.18	0.86												
BLAI{..}.plant.dat	36	-0.13	0.90												
CH_S1.sub	37	-0.05	0.96												
DEEPST.gw	38	0.03	0.98												

Table 6.4 and Table 6.5 present the statistical results of all the sensitivity analyses for the two main catchments, which indicates a small change in values between the five sensitivity analyses applied on the Wadi Hanifah. A larger change is observed for the PBIAS in the Wadi As Silayy catchment. The indices values for sensitivity analyses of the SWAT model ranged between 0.49-0.53 for the NSE for the Wadi Hanifah catchment. Whilst the indices values for model sensitivity analyses ranged between 0.61-0.67 for the NSE for the Wadi As Silayy catchment. All the SWAT model sensitivity analyses for the Wadi As Silayy catchment had satisfactory performance according to all indices used for the model evaluation, but the result of PBIAS revealed good performance for the sensitivity analysis of the 38 parameters.

The results of the sensitivity analyses showed that calibrating 38 parameters performs overall better than calibrating with fewer parameters (e.g., 18 or 14 parameters) for both catchments. Thus, the best fit values resulted from the 38 parameters sensitivity analysis, which were used to calibrate the SWAT models for the Wadi Hanifah and the Wadi As Silayy catchments.

Table 6.4: Statistical results of the SWAT model performance indices for the sensitivity analyses of the Wadi Hanifah catchment.

ID	Number of Parameters	P-factor	R-factor	NSE	R ²	PBIAS	RSR
1	38	0.38	0.25	0.53	0.68	45.3	0.68
2	28	0.4	0.26	0.49	0.64	45	0.71
3	23	0.38	0.26	0.51	0.67	45.9	0.69
4	18	0.38	0.26	0.49	0.64	46.2	0.71
5	14	0.41	0.24	0.49	0.61	42	0.72

Table 6.5: Statistical results of the SWAT model performance indices for the sensitivity analyses of the Wadi As Silayy catchment.

ID	Number of Parameters	p-factor	r-factor	NSE	R ²	PBIAS	RSR
1	38	0.27	0.42	0.67	0.69	12.71	0.57
2	29	0.29	0.43	0.64	0.69	19.06	0.6
3	21	0.29	0.44	0.62	0.65	14.62	0.61
4	18	0.3	0.44	0.61	0.67	21.75	0.62
5	14	0.3	0.44	0.61	0.67	21.75	0.62

6.3. SWAT model validation

Validation of the SWAT models for the Wadi Hanifah and the Wadi As Silayy catchments were performed using a five year period, succeeding directly the calibration period (Figure 6.1). Table 6.6 summarises the statistical results of model performance indices for the SWAT models' calibrations and validations in the Wadi Hanifah and the Wadi As Silayy catchments. These values are the mean across the sub-basins in each catchment. The statistical results of the model performance were much better than the previous attempt when using 2001-2010, with model indicators showing similar performance between the calibration and validation periods. Like the calibration statistical results, the NSE, R², and RSR model performance indicators, for the validation, yielded satisfactory results while the PBIAS index revealed an unsatisfactory result for the Wadi Hanifah catchment. In comparison, all statistical results of the calibration and validation yielded satisfactory or good model performance for the Wadi As Silayy catchment.

Figure 6.2 presents the spatial distribution of the NSE values in Riyadh's catchments for calibration and validation. Generally, it appears that the NSE values are higher in sub-basins of the Wadi As Silayy catchment than in sub-basins of the Wadi Hanifah catchment.

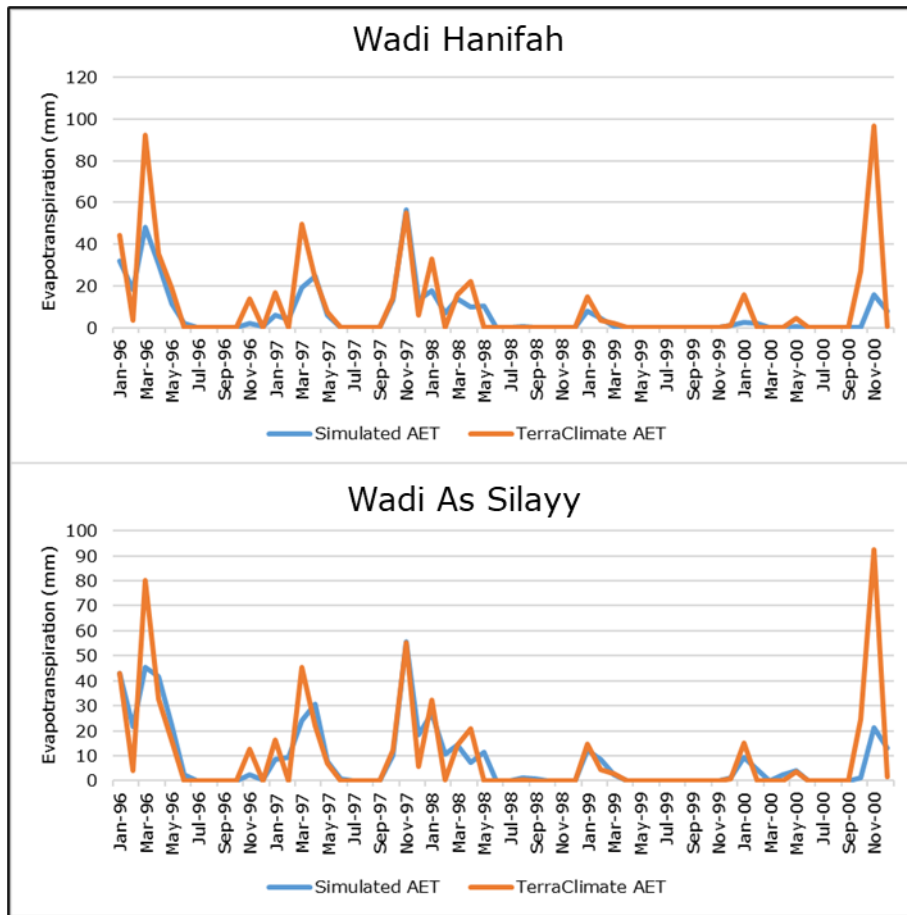


Figure 6.1: A comparison of simulated monthly evapotranspiration values with TerraClimate derived data for the models validation period (1996-2000).

Table 6.6: Statistical results of model performance indices for the final models' calibrations and validations for the study area catchments.

performance indices	Wadi Hanifah		Wadi As Silayy	
	Calibration 1991-1995	Validation 1996-2000	Calibration 1991-1995	Validation 1996-2000
NSE	0.53	0.49	0.67	0.58
R ²	0.68	0.58	0.7	0.6
PBIAS	45.75	37.83	12.86	14.32
RSR	0.68	0.72	0.58	0.65

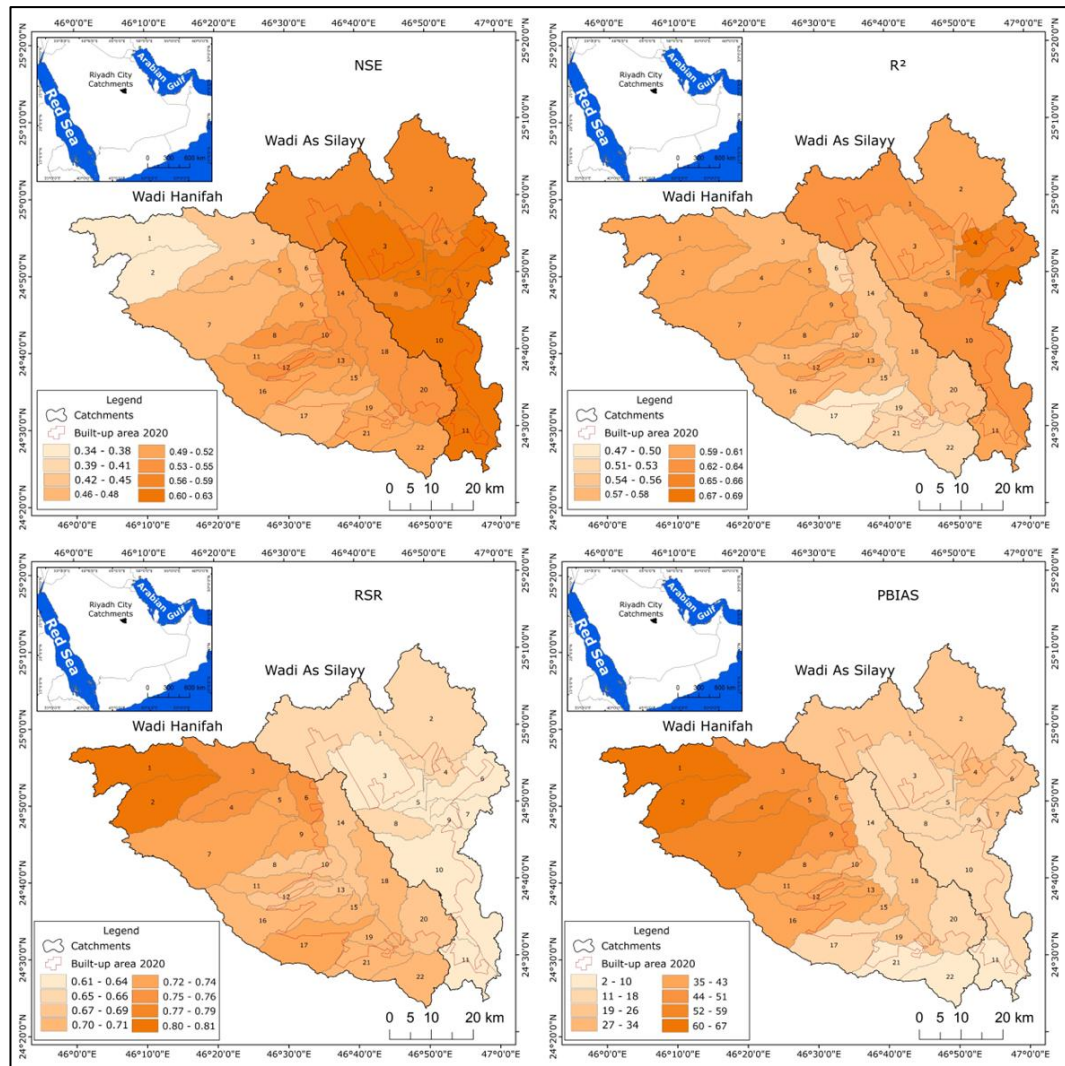


Figure 6.2: Spatial distribution of the NSE, R^2 , RSR, and PBIAS values for validation in Riyadh's catchments.

To test the ability of the model to simulate monthly ET in this area for the period before the year 2000, the model was run using the climate data for 36 years from 1965 to 2000. The plots of monthly simulated and TerraClimate ET values revealed an acceptable fit of data for this period (Figure 6.3). The TerraClimate ET values were larger than the SWAT model simulated ET values. Statistically, the degree of agreement between the simulated and the measured data for the two main catchments was evaluated by the NSE, R^2 , PBIAS, and RSR. Table 6.7 indicates acceptable results of the NSE and R^2 . The impact of parameter values' change on the developed SWAT models on runoff simulation was examined in the next section.

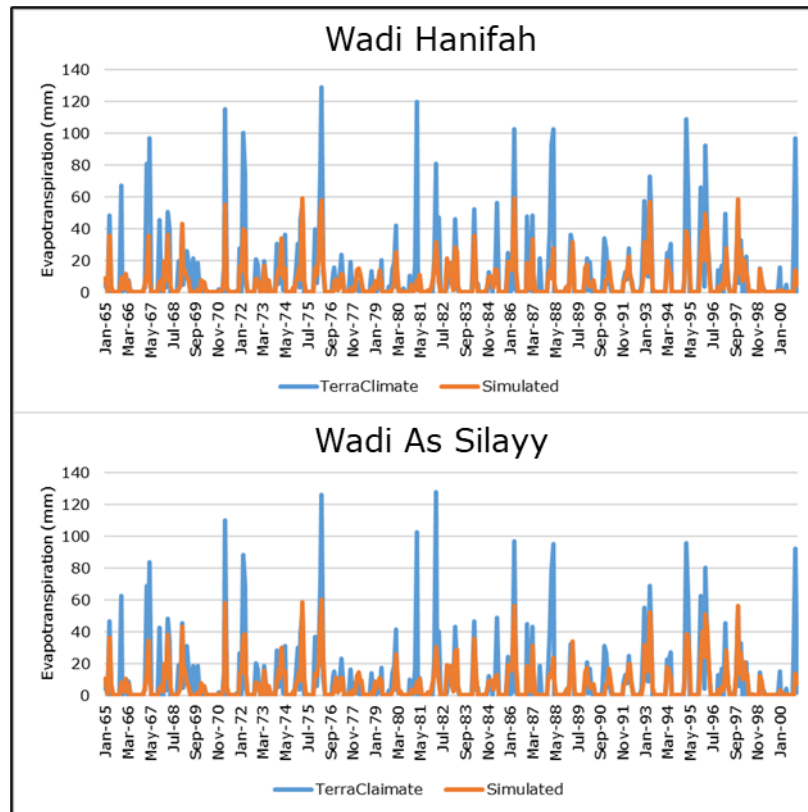


Figure 6.3: A comparison of simulated monthly ET values with TerraClimate during the period 1965-2000.

Table 6.7: Statistical results of the indices to verify the closeness of the simulated and observed ET values for the period 1965-2000.

65-90	NSE	R ²	PBIAS	RSR
Wadi Hanifah	0.44	0.53	41.08	0.75
Wadi As Silayy	0.46	0.54	35.63	0.73

6.4. Impact of changing model parameter values on simulated runoff

The SWAT models have been developed using ET data for the calibration and validation periods, but the key goal behind the development of the SWAT models for the study area has been to simulate surface runoff. Therefore, an attempt was made to assess surface runoff sensitivity to parameter values of the SWAT model using a one-by-one sensitivity analysis method. The first step was to identify model parameters having p-values of 0.05 or smaller (Table 6.8 and Table 6.9). This identified 9 parameters for the Wadi As Silayy catchment and 12 parameters for the Wadi Hanifah

catchment. The parameters were ranked according to p-values from smaller to larger. Plausible minimum and maximum values were determined for each based on a literature review for each parameter (see Table 5.1), and then a one-by-one sensitivity analysis conducted for the 12 and 9 parameters for each catchment, respectively.

Using the highest and lowest parameter range values for the one-by-one sensitivity analysis, led to the generation of 24 and 18 SWAT models for the two catchments. Table 6.10 and Table 6.11 present results of annual surface runoff estimations for the period 1991-2000. Figure 6.4 shows the error bar curves that result from plotting the maximum and minimum values of surface runoff obtained from the models of one-by-one sensitivity analyses. It can be noted that lines nearly match the simulated runoff curve and annual maximum and minimum surface runoff values from the 18 and 24 models of one-by-one sensitivity analysis. Besides, relationships between simulated annual runoff and max and min runoff for the period 1991-2000 resulted in very high R^2 (Figure 6.5). These relationships were strong with R^2 values of nearly 1. The results show that surface runoff sensitivity to the selected parameter values is minimal for the study area.

Table 6.8: The SWAT model parameters having p-values of 0.05 or smaller for the Wadi Hanifah catchment.

Parameter Name	Parameter Definition	Method of change	Value range*	Best value	t-Stat	P-Value	Ranking
CN2.mgt	Initial SCS runoff curve number for moisture condition II.	Relative	-0.2 to 0.2	-0.1686	-28.7	2.71E-131	1
ESCO.hru	Soil evaporation compensation factor	Replace	0 to 1	0.0475	-22.3	2.96E-89	2
ICN.bsn	Daily curve number calculation methods:	Replace	0 or 1	1	14.5	5.52E-43	3
SOL_Z(..).sol	Depth from soil surface to bottom of layer	Replace	250 to 1500	465.625	-8.2	7.80E-16	4
SOL_K(..).sol	Saturated hydraulic conductivity (mm/hr).	Relative	-0.8 to 0.8	-0.7688	-6.0	3.51E-09	5
SOL_BD(..).sol	Moist bulk density (Mg/m ³ or g/cm ³)	Relative	-0.5 to 0.5	-0.4585	-5.8	9.09E-09	6
EPCO.hru	Plant uptake compensation factor.	Replace	0 to 1	0.3635	4.1	3.78E-05	7
CANMX.hru	Maximum canopy storage (mm H ₂ O).	Replace	0 to 100	44.75	2.7	0.007676	8
SOL_CRK.sol	Potential or maximum crack volume of the soil profile expressed as a fraction of the total soil volume.	Replace	0 to 1	0.0265	-2.5	0.013633	9
SLSOIL.hru	Slope length for lateral subsurface flow (m).	Replace	0 to 150	109.275	2.4	0.015292	10
CNCOEF.bsn	Plant ET curve number coefficient.	Replace	0.5 to 2	1.52825	-2.3	0.019093	11
ESCO.bsn	Soil evaporation compensation factor	Replace	0 to 1	0.5005	2.2	0.025384	12

* For the references see Table 5.1

Table 6.9: The SWAT model parameters having p-values of 0.05 or smaller for the Wadi As Silayy catchment.

Parameter Name	Parameter Definition	Method of change	Value range*	Best value	t-Stat	P-Value	Ranking
SOL_Z(..).sol	Depth from soil surface to bottom of layer	Replace	250 to 1500	465.625	-62.7	0	1
ESCO.hru	Soil evaporation compensation factor	Replace	0 to 1	0.0475	-26.9	0	2
SOL_AWC(..).sol	Available water capacity of the soil layer (mm H ₂ O/mm soil).	Relative	-0.5 to 0.5	-0.3685	-24.9	0	3
CN2.mgt	Initial SCS runoff curve number for moisture condition II.	Relative	-0.2 to 0.2	-0.1686	-12.9	0	4
ICN.bsn	Daily curve number calculation methods:	Replace	0 or 1	1	8.3	0	5
SOL_K(..).sol	Saturated hydraulic conductivity (mm/hr).	Relative	-0.8 to 0.8	-0.768800	-3.2	0.0013545	6
CANMX.hru	Maximum canopy storage (mm H ₂ O).	Replace	0 to 100	44.75	2.9	0.0034795	7
SLSOIL.hru	Slope length for lateral subsurface flow (m).	Replace	0 to 150	109.275	-2.0	0.0465505	8
ESCO.bsn	Soil evaporation compensation factor	Replace	0 to 1	0.5005	2.0	0.0496884	9

* For the references see Table 5.1

Table 6.10: Results of annual surface runoff estimations (mm) for the Wadi Hanifah catchment.

Parameters	1991	1992	1993	1994	1995	1996	1997	1998	1999	2000
CANMX_0	1.04	2.98	7.59	1.71	11.06	8.84	7.65	2.88	0.44	1.44
CANMX_100	1.04	2.96	7.24	1.64	10.92	8.62	7.59	2.87	0.44	1.44
CN2_0.2	1.04	2.97	7.43	1.68	11	8.74	7.63	2.87	0.44	1.44
CN2_-0.2	1.04	2.97	7.43	1.68	11	8.74	7.63	2.87	0.44	1.44
CNCOEF_0.5	1.04	2.97	7.43	1.68	11	8.74	7.63	2.87	0.44	1.44
CNCOEF_2	1.04	2.97	7.43	1.68	11	8.74	7.63	2.87	0.44	1.44
EPCO.hru_0	1.04	2.97	7.42	1.68	10.99	8.72	7.62	2.87	0.44	1.44
EPCO.hru_1	1.04	2.97	7.4	1.67	10.98	8.73	7.62	2.87	0.44	1.44
ESCO.bsn_0	1.04	2.97	7.43	1.68	11	8.74	7.63	2.87	0.44	1.44
ESCO.bsn_1	1.04	2.97	7.43	1.68	11	8.74	7.63	2.87	0.44	1.44
ESCO.hru_0	1.04	2.97	7.39	1.67	10.99	8.7	7.62	2.87	0.44	1.44
ESCO.hru_1	1.03	2.96	7.33	1.66	10.98	8.67	7.61	2.86	0.44	1.44
ICN_0	1.04	2.97	7.43	1.68	11	8.74	7.63	2.87	0.44	1.44
ICN_2	1.04	2.97	7.43	1.68	11	8.74	7.63	2.87	0.44	1.44
SLSOIL_0	1.04	2.97	7.43	1.68	11	8.74	7.63	2.87	0.44	1.44
SLSOIL_150	1.04	2.97	7.43	1.68	11	8.74	7.63	2.87	0.44	1.44
SOL_BD_0.5	1.04	2.97	7.43	1.68	11	8.74	7.63	2.87	0.44	1.44
SOL_BD_-0.5	1.04	2.97	7.43	1.68	11	8.74	7.63	2.87	0.44	1.44
SOL_CRK_0	1.04	2.97	7.43	1.68	11	8.74	7.63	2.87	0.44	1.44
SOL_CRK_1	1.04	2.97	7.43	1.68	11	8.74	7.63	2.87	0.44	1.44
SOL_K_-0.8	1.04	2.97	7.45	1.68	11	8.75	7.63	2.87	0.44	1.44
SOL_K_0.8	1.04	2.97	7.44	1.68	11	8.74	7.63	2.87	0.44	1.44
SOL_Z_250	1.04	2.97	7.44	1.68	11.01	8.77	7.63	2.87	0.44	1.44
SOL_Z_1500	1.04	2.97	7.41	1.68	11.01	8.7	7.63	2.86	0.44	1.44
Max runoff	1.04	2.98	7.59	1.71	11.06	8.84	7.65	2.88	0.44	1.44
Min runoff	1.03	2.96	7.24	1.64	10.92	8.62	7.59	2.86	0.44	1.44

Table 6.11: Results of annual surface runoff (mm) estimations for the Wadi As Silayy catchment.

Parameters	1991	1992	1993	1994	1995	1996	1997	1998	1999	2000
CANMX_0	1.01	2.43	5.81	1.61	8.95	6.47	6.18	2.06	0.38	1.11
CANMX_100	1.01	2.42	5.52	1.55	8.82	6.28	6.12	2.06	0.38	1.11
CN2_0.2	1.01	2.43	5.68	1.58	8.88	6.38	6.16	2.06	0.38	1.11
CN2_-0.2	1.01	2.43	5.68	1.58	8.88	6.38	6.16	2.06	0.38	1.11
ESCO.bsn_0	1.01	2.43	5.68	1.58	8.88	6.38	6.16	2.06	0.38	1.11
ESCO.bsn_1	1.01	2.43	5.68	1.58	8.88	6.38	6.16	2.06	0.38	1.11
ESCO.hru_0	1.01	2.42	5.64	1.58	8.87	6.35	6.15	2.06	0.38	1.11
ESCO.hru_1	1.01	2.42	5.61	1.56	8.87	6.31	6.14	2.05	0.38	1.11
ICN_0	1.01	2.43	5.68	1.58	8.88	6.38	6.16	2.06	0.38	1.11
ICN_2	1.01	2.43	5.68	1.58	8.88	6.38	6.16	2.06	0.38	1.11
SLSOIL_0	1.01	2.43	5.68	1.58	8.88	6.38	6.16	2.06	0.38	1.11
SLSOIL_150	1.01	2.43	5.68	1.58	8.88	6.38	6.16	2.06	0.38	1.11
Sol_AWC_0.5	1.01	2.43	5.68	1.59	8.89	6.37	6.16	2.06	0.38	1.11
Sol_AWC_-0.5	1.01	2.43	5.67	1.58	8.89	6.4	6.16	2.06	0.38	1.11
SOL_K_0.8	1.01	2.43	5.68	1.58	8.88	6.38	6.16	2.06	0.38	1.11
SOL_K_-0.8	1.01	2.43	5.69	1.59	8.89	6.39	6.16	2.06	0.38	1.11
Sol_Z_250	1.01	2.43	5.68	1.58	8.9	6.4	6.16	2.06	0.38	1.11
Sol_Z_1500	1.01	2.43	5.66	1.59	8.9	6.35	6.16	2.05	0.38	1.11
Max runoff	1.01	2.43	5.81	1.61	8.95	6.47	6.18	2.06	0.38	1.11
Min runoff	1.01	2.42	5.52	1.55	8.82	6.28	6.12	2.05	0.38	1.11

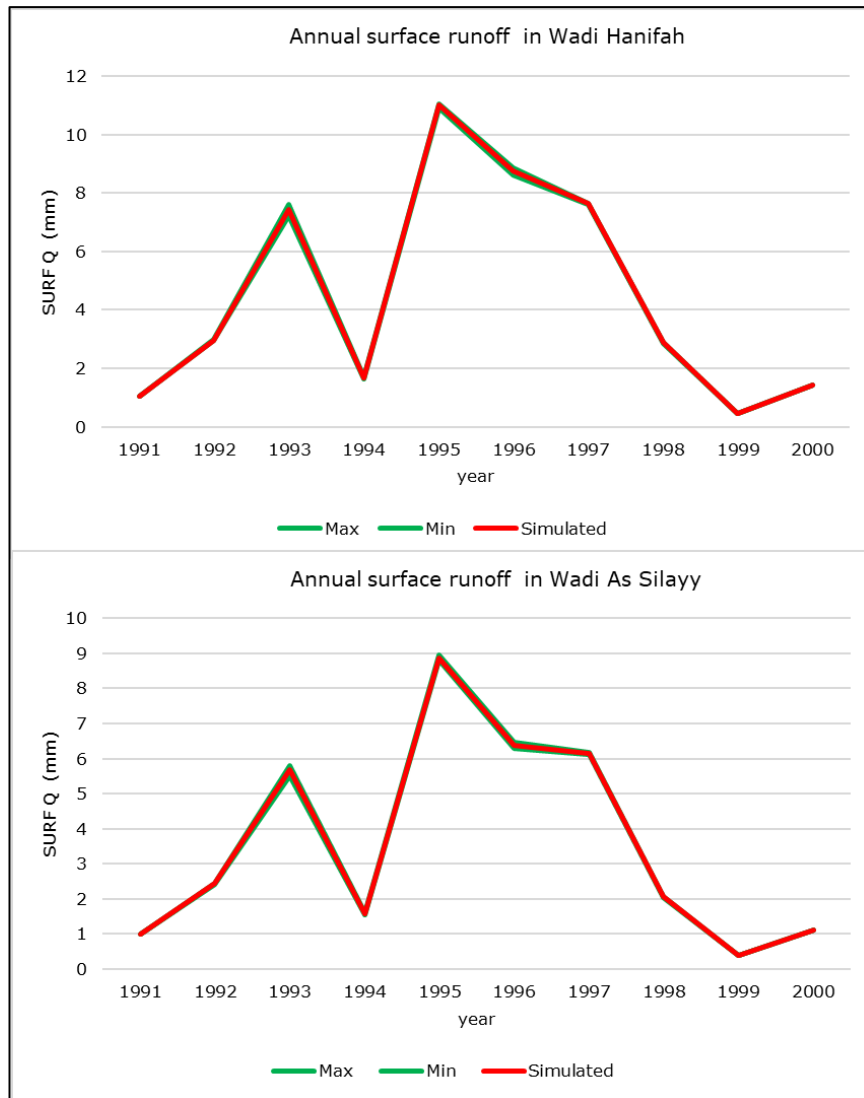


Figure 6.4: Annual simulated surface runoff curve and error bar curves of max and min runoff given by one-by-one sensitivity analyses using the highest and lowest parameter range values.

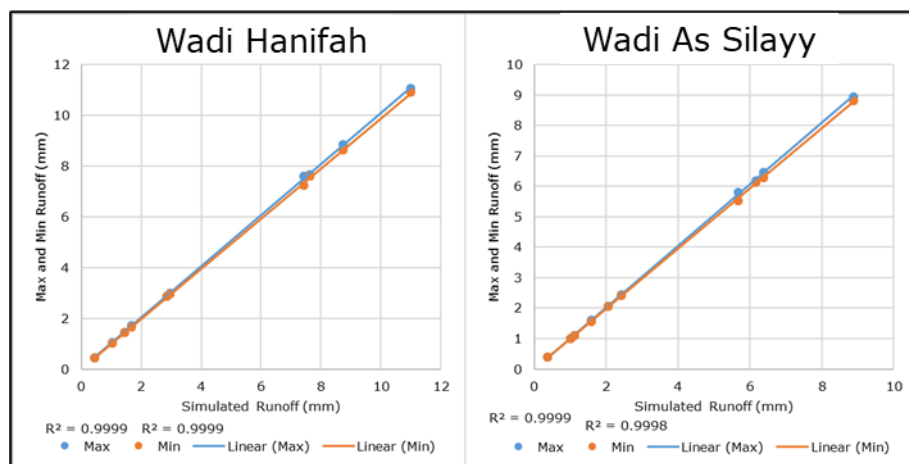


Figure 6.5: Relationships between simulated annual runoff and max and min runoff for the period 1991-2000.

6.5. Accuracy of simulated runoff

In an attempt to verify the accuracy of simulated surface runoff of the calibrated SWAT model for the Wadi Hanifah catchment, the model was run using data for the period 1965-2000. Then, the simulated annual surface runoff results were compared with their counterparts from measured historical data found in the literature (Al-Hasan and Mattar 2014), for the period 1965-1983, for the Wadi Hanifah catchment (Table 6.12). The annual surface runoff data for the Wadi Hanifah catchment were plotted and are shown in Figure 6.6. This figure reveals that the simulated annual surface runoff is broadly similar to the historical measured annual runoff data, except for the years 1965 and 1968. Before 1976, surface runoff data indicates that measured surface runoff values were generally higher than those simulated, whilst from the 1976 to 1983, the simulated surface runoff was greater than that measured. It is also clear from Figure 6.6 that the annual rainfall was more consistent with the simulated runoff than with the measured runoff.

To assess statistically the degree of agreement between the simulated surface runoff values and measured data, the NSE, R^2 , PBIAS, and RSR were calculated (Table 6.13). The statistical results were 0.28, 0.30, 12.53, and 0.85, respectively. This indicates a poor agreement, with the exception of the PBIAS which gave a good, positive agreement. The positive value of PBIAS may indicate surface runoff underestimations of the SWAT model for the Wadi Hanifah catchment.

Table 6.12: Measured annual runoff data and runoff values simulated by the calibrated SWAT model for the Wadi Hanifah catchment.

Year	Simulated Runoff (mm)	Measured runoff (mm)
1965	2.98	9.75
1966	0.55	0
1967	3.02	4.7
1968	4.44	11.03
1969	3.42	1.18
1970	0.29	0
1971	3.67	5.33
1972	4.45	5.97
1973	1.83	0
1974	1.65	6.5
1975	4.51	6.6
1976	5.44	2.7
1977	0.94	0
1978	1.67	0
1979	1.36	0.61
1980	2.03	0
1981	0.46	0
1982	4.69	0.47
1983	2.17	1.84
Average runoff	2.61	2.98
Average rainfall	83.44	86
Average runoff coefficient	0.0313	0.0347

Source of measured runoff: Al-Hasan and Mattar (2014).

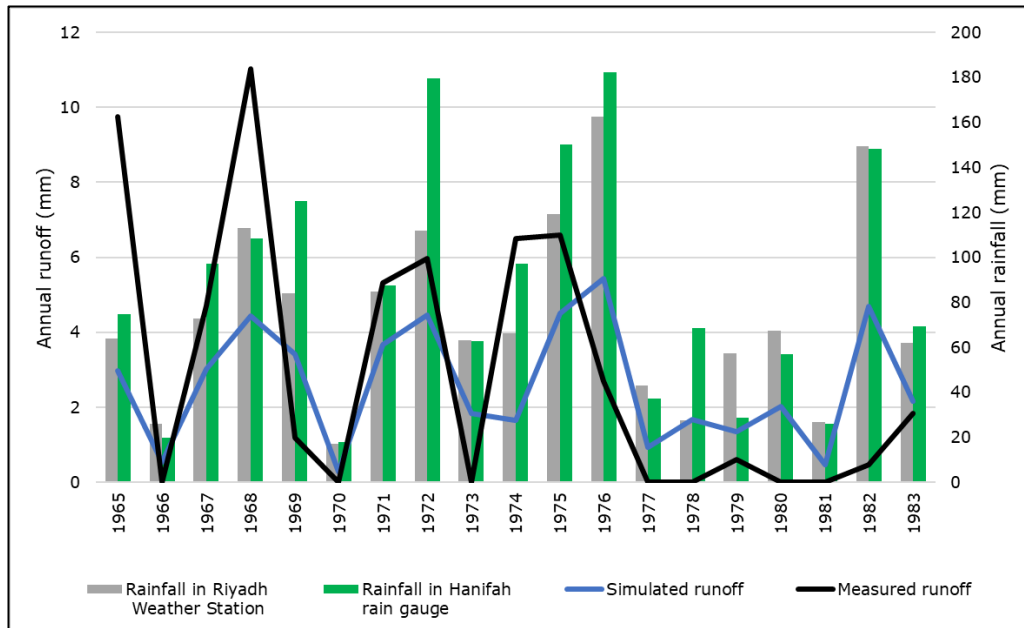


Figure 6.6: A comparison of historically measured annual runoff data for the Wadi Hanifah catchment with runoff values simulated by the developed SWAT model.

Source of measured runoff: Al-Hasan and Mattar (2014).

Table 6.13: Degree of agreement between the simulated annual runoff values and historical annual measured data for the Wadi Hanifah catchment.

NSE	R ²	PBIAS	RSR
0.28	0.30	12.53	0.85

Despite the clear limitations in the model, the results of model performance indices during calibration and validation justify the capability of the model to obtain approximate simulations of runoff in the study area. Also, the model is the best available given the data limitations.

6.6. Summary

38 parameters were selected to set up the final SWAT models for Riyadh's catchments. Applying the NSE objective function, the calibrations and sensitivity analyses of the final SWAT models started using all the selected parameters to evaluate the performance of the models and identify the most influential SWAT parameters to simulate the hydrological cycle components in the catchments of Riyadh city. The statistical results of model performance indices indicated the satisfactory performance of the SWAT model to simulate monthly ET for both catchments and consequently other components of the hydrological cycle. Additionally, plotted lines of the calibration period indicated that the simulated ET acceptably matches TerraClimate's ET data, and the R² values for annual TerraClimate's ET versus the simulated ET suggest acceptable relationships with R² values >0.74.

To decide how many parameters to use for the SWAT model calibration, five sensitivity analyses were performed for the Wadi Hanifah and Wadi As Silayy catchments. The first sensitivity analysis was conducted using all selected parameters. After that, another

sensitivity analysis with fewer parameters was implemented by omitting all parameters with a p-value above 0.7. This final sensitivity analysis had 14 parameters for both Wadi Hanifah and Wadi As Silayy. The results of sensitivity analyses showed that calibrating 38 parameters performs overall better than calibrating with fewer parameters for both catchments. Thus, the best fit values resulted from the 38 parameters sensitivity analysis, which was used to calibrate the SWAT models for the Wadi Hanifah and the Wadi As Silayy catchments.

The statistical results of the model performance indices showed similar performance between the calibration and validation periods. Like the calibration statistical results, the NSE, R^2 , and RSR model performance indicators, for the validation, yielded satisfactory results while the PBIAS index revealed an unsatisfactory result for the Wadi Hanifah catchment. In comparison, all statistical results of the calibration and validation yielded satisfactory or good model performance for the Wadi As Silayy catchment.

Since the key goal behind the setup of the SWAT models for the study area has been to simulate surface runoff, an attempt was made to assess surface runoff sensitivity to parameter values of the SWAT model using a one-by-one sensitivity analysis method. For this purpose, 9 parameters were identified for the Wadi As Silayy catchment and 12 parameters for the Wadi Hanifah catchment. Using the highest and lowest parameter range values for the one-by-one sensitivity analysis, led to the generation of 18 and 24 SWAT models for the two catchments. The results show that surface runoff sensitivity to the selected parameter values is minimal for the study area. The error bar curves that resulted from plotting the maximum and minimum values of surface runoff obtained from the 18 and 24 models of one-by-one sensitivity analyses show nearly match. The

relationships between the results were strong with R^2 values of nearly 1. The results show that surface runoff sensitivity to the selected parameter values is minimal for the study area.

Annual surface runoff was simulated with SWAT for the Wadi Hanifah catchment and compared to the annual measured runoff for the period 1965-1983 with approximate agreement. The plotted lines of simulated runoff and measured runoff reveal that the simulated annual surface runoff is broadly similar to the measured annual runoff data, except for the years 1965 and 1968. The lines indicate that measured surface runoff values were generally higher than those simulated before 1976 and were lower for the period from 1976 to 1983. However, the statistical assessment resulted in poor agreements for the NSE, R^2 , and RSR indices, but the PBIAS gave a good, positive agreement. Chapter 7 will apply the SWAT model developed in this chapter to predict the impacts of LULC on runoff in Riyadh.

Chapter 7: Impacts of historical LULC on runoff and discharge

7.1. Overview

This chapter focuses on the effects of historical LULC change on runoff in the catchments of Riyadh city. The chapter includes information on LULC change in Riyadh's catchments for 20 years extending from 1996 to 2016. The methods and techniques to simulate and analyse runoff and discharge are presented in this chapter for historical LULC scenarios and projected LULC scenarios (chapter 8). The chapter includes an interpretation and explanation of SWAT model results for annual, monthly, and annual maximum daily runoff using five historical LULC scenarios. The information on runoff modelling is presented on two scales: the two main catchments and sub-basins.

7.2. LULC change in Riyadh's catchments

LULC broadly represents the interaction between natural and human activities on the Earth's surface. *Land cover change* refers to a loss of natural areas due to human activities such as the loss of natural barren land to urban development, while *land-use change* is the substitution of a defined use in an area to another use such as the loss of an agricultural area to urban development. For decades, the two main catchments of Riyadh witnessed significant LULC change and experienced transition from a largely rural to a largely urbanised environment. This turned the originally barren land of the catchments into an expansive urban development consisting mainly of residential, commercial, educational, services, and industrial projects. As the capital city of Saudi Arabia, the direct driver of Riyadh's LULC change has been the urbanisation process, especially from 1950 onwards.

Five governmental LULC maps for Riyadh city for the years 1996, 2004, 2009, 2012, and 2016 have been used to assess the impact of historical LULC change on the simulated hydrological cycle components with the SWAT model described in Chapter 6 (Table 7.1, Figure 7.1 and Figure 7.2).

Table 7.1: LULC in the Riyadh city region.

LULC		Barren land	Vegetation	Urban	Roads	Total
Area in 1996	Km ²	4,418	49	302	223	4,992
	%	88%	1%	6%	4%	100%
Area in 2004	Km ²	4,147	133	442	270	4,992
	%	83%	3%	9%	5%	100%
Area in 2009	Km ²	3,959	211	519	304	4,992
	%	79%	4%	10%	6%	100%
Area in 2012	Km ²	3,869	212	575	337	4,992
	%	77%	4%	12%	7%	100%
Area in 2016	Km ²	3,736	226	643	387	4,992
	%	75%	5%	13%	8%	100%
1996-2016 changes	Change Km ²	-682	177	341	164	
	Growth %	-15%	361%	113%	74%	

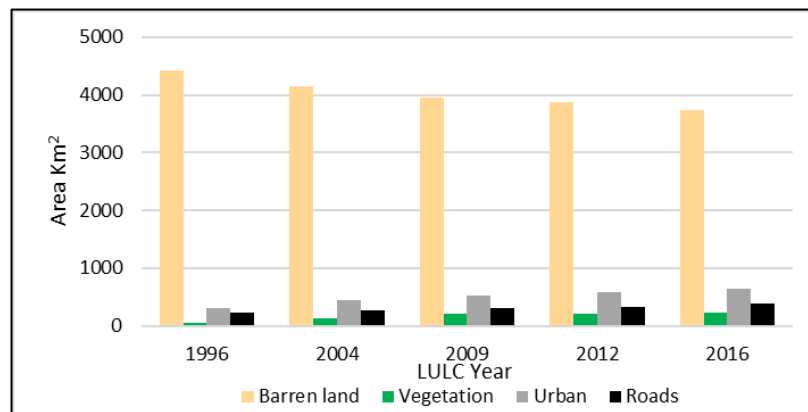


Figure 7.1: Areas of LULC categories in Riyadh catchments for the period 1996-2016.

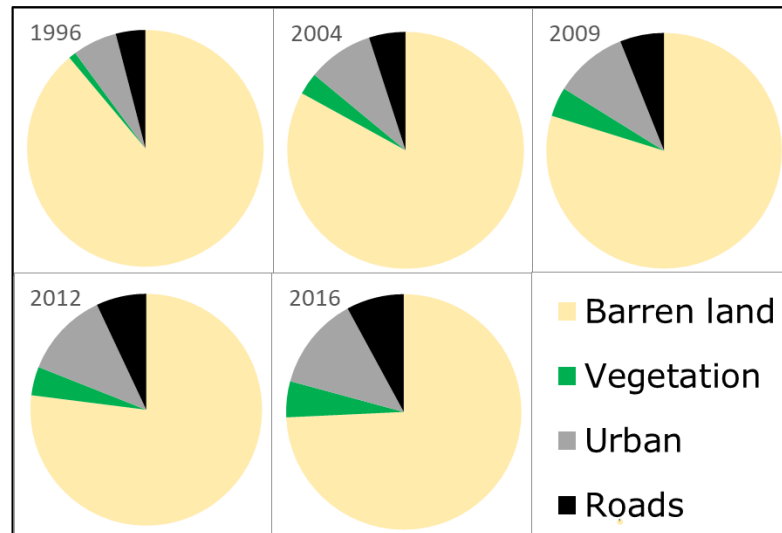


Figure 7.2: Proportions of LULC categories in Riyadh catchments for the period 1996-2016.

Table 7.2 shows the trend of LULC changes in Riyadh's catchments for the period 1996-2016. The investigation of the LULC change process for this period showed that the highest percentage of declining change was related to barren lands class with about -15%. On the other hand, the other three classes of LULC in Riyadh's catchments experienced incremental changes and the highest increase was observed for the urban and road classes (impervious layers) with 341 km² and 164 km² respectively.

Table 7.2: Trend of LULC changes from 1996 to 2016 in Riyadh's catchments.

LULC classes	Change type	Change rate (km ²)	Change percent
Barren land	Decrease	- 682	- 15
Urban	Increase	341	113
Roads	Increase	164	74
Vegetation	Increase	177	361

Most of the loss in the barren land class has been mainly transformed into urban and road classes and a small portion of it transformed to the vegetation class. Given the conversion of barren land to predominantly impervious surfaces (e.g., urban, roads), the changes in LULC are hypothesised to produce increased runoff which increases the need for runoff management based on existing land-

use practices. The low portion of vegetation in the catchments can be attributed to the low provision of public open space in Riyadh. Addas and Maghrabi (2020) reported that public open spaces in Riyadh were neglected in the past and were given low priority until the recently announced of Saudi Arabia's Vision 2030. The expansion of urban green spaces has been considered an effective approach to decrease urban surface runoff (Kim et al. 2016).

7.3. Methodology of runoff simulation and analysis under LULC scenarios

The SWAT model divides the Wadi Hanifah catchment into 22 sub-basins and the Wadi As Silayy catchment into 11 sub-basins. The sub-basins were numbered to define their locations within the main catchments of the study area (see Figure 5.2). The SWAT annual and monthly runoff simulations for the two catchments under the five different historical LULC scenarios were obtained by using the same climate data used for the calibration and validation periods (1991-2000).

Although the developed SWAT models, for the Wadi Hanifah and the Wadi As Silayy catchments, have been calibrated and validated at monthly time-step for the periods 1991-2000 using 3 weather stations and 3 rain gauges, the SWAT models were run daily to provide approximate simulations of the daily runoff using climate data for the period 1965-2000. To understand the effect of LULC on daily runoff in the study area, rainfall data from one station were used to run the SWAT models. The aim of doing this was to relate variations of daily surface runoff either to LULC type or to changes over time in LULC. To accomplish this purpose, the Hanifah rain gauge data were chosen because it has had a complete daily rainfall record for the period 1965-2000 and it is the closest station to the centre of the study area.

Analyses of the simulated runoff and discharge were carried out using the following techniques:

- 1) Calculation of return periods, exceedance probability and risk as follows (USDA 2007; ElQuliti et al. 2016):

$$T = n+1/m \quad (\text{Eq. 6.1})$$

$$P = m/n+1 \quad (\text{Eq. 6.2})$$

$$P (\%) = 100 (m/n+1) \quad (\text{Eq. 6.3})$$

where:

T = Return period in years.

n = number of years on record.

m = is the rank of simulated occurrences arranged in descending order.

P = exceedance probability.

P (%) = exceedance probability as a percent.

- 2) Fitting probability distributions of Extreme Value Type-1 (EV1) to simulated annual maximum daily runoff and discharge (Chow 1988) using CumFreq software (Oosterbaan, n.d.) as follows:

$$F(x_i) = \exp \left[- \exp \left(- \frac{x - u}{a} \right) \right] \quad (\text{Eq. 6.4})$$

$$a = 2.4495s/3.1416 \quad (\text{Eq. 6.5})$$

$$u = \bar{x} - 0.5772a \quad (\text{Eq. 6.6})$$

where:

s = the standard deviation.

x = the largest runoff/discharge value in each class interval.

\bar{x} = the mean of runoff/discharge.

$$x_T = \bar{x} + K_T s \quad (\text{Eq. 6.7})$$

Where:

x_T = runoff/discharge estimate for a desired return period (T).

\bar{x} = the mean of runoff/discharge.

s = the standard deviation.

K_T = the frequency factor expressed by the following equation:

$$K_T = -\frac{\sqrt{6}}{\pi} \left\{ 0.5772 + \ln \left[\ln \left(\frac{T}{T-1} \right) \right] \right\} \quad (\text{Eq. 6.8})$$

7.4. Modelling annual runoff

7.4.1. Modelling annual runoff on catchments level

Table 7.3 shows the annual surface runoff amounts for the Wadi Hanifah and the Wadi As Silayy catchments under the five different historical LULC scenarios. For the Wadi Hanifah catchment, the simulated annual runoff during this period when using LULC 1996 scenario ranged between 0.44 mm and 11 mm and between 0.73 mm and 17.94 mm when using the LULC 2016 scenario found in the years of 1999 and 1995 respectively. Whereas the annual surface runoff during this period when using LULC 1996 scenario ranged between 0.38 mm and 8.88 mm and between 1.35 mm and 22.27 mm when using the LULC 2016 scenario for the Wadi As Silayy catchment found in the years of 1999 and 1995, respectively. Under the five different historical LULC scenarios, the average surface runoff depth, for the period 1991-2000, varied from 4.5 to 7.6 mm and from 3.6 to 9.9 mm increasing about 67% and 179% for the Wadi Hanifah and the Wadi As Silayy catchments respectively.

Additionally, the average simulated runoff coefficient varied from 0.0461 to 0.0770 increasing about 67% at the Wadi Hanifah catchment and from 0.0251 to 0.0699 increasing about 180% at the Wadi As Silayy catchment (Figure 7.3). The increase of surface runoff rates in the two catchments of the study area is attributed to increasing impervious surfaces due to the urban expansion of the city.

Table 7.3: Effect of LULC change on simulated annual surface runoff in Riyadh's catchments.

Year	Wadi Hanifah SURQ (mm)						Wadi As Silayy SURQ (mm)					
	Rainfall	LULC 1996	LULC 2004	LULC 2009	LULC 2012	LULC 2016	Rainfall	LULC 1996	LULC 2004	LULC 2009	LULC 2012	LULC 2016
1991	38.1	1.0	1.2	1.4	1.6	1.8	80.3	1.0	2.2	2.7	3.2	3.9
1992	76.2	3.0	3.5	4.1	4.5	5.0	159.0	2.4	4.9	5.9	6.9	8.3
1993	161.4	7.4	8.9	10.4	11.2	12.5	229.0	5.7	10.2	12.0	13.7	16.1
1994	35.2	1.7	2.0	2.3	2.5	2.7	57.3	1.6	2.6	2.9	3.2	3.7
1995	176.4	11.0	12.8	14.8	16.2	17.9	254.0	8.9	15.0	17.3	19.4	22.3
1996	175.3	8.7	10.5	12.1	13.2	14.8	199.9	6.4	11.0	12.7	14.4	16.6
1997	209.7	7.6	9.3	10.5	11.4	12.9	273.7	6.2	11.5	13.5	15.6	18.5
1998	51.5	2.9	3.4	3.9	4.3	4.8	73.0	2.1	3.5	4.1	4.6	5.4
1999	12.8	0.4	0.5	0.6	0.7	0.7	27.4	0.4	0.8	0.9	1.1	1.4
2000	43.9	1.4	1.7	1.9	2.1	2.4	68.4	1.1	2.1	2.5	2.9	3.4
Average	98.1	4.5	5.4	6.2	6.8	7.6	142.2	3.6	6.4	7.5	8.5	9.9
Runoff Coefficient	-	0.0461	0.0550	0.0633	0.0689	0.0770	-	0.0251	0.0448	0.0524	0.0598	0.0699

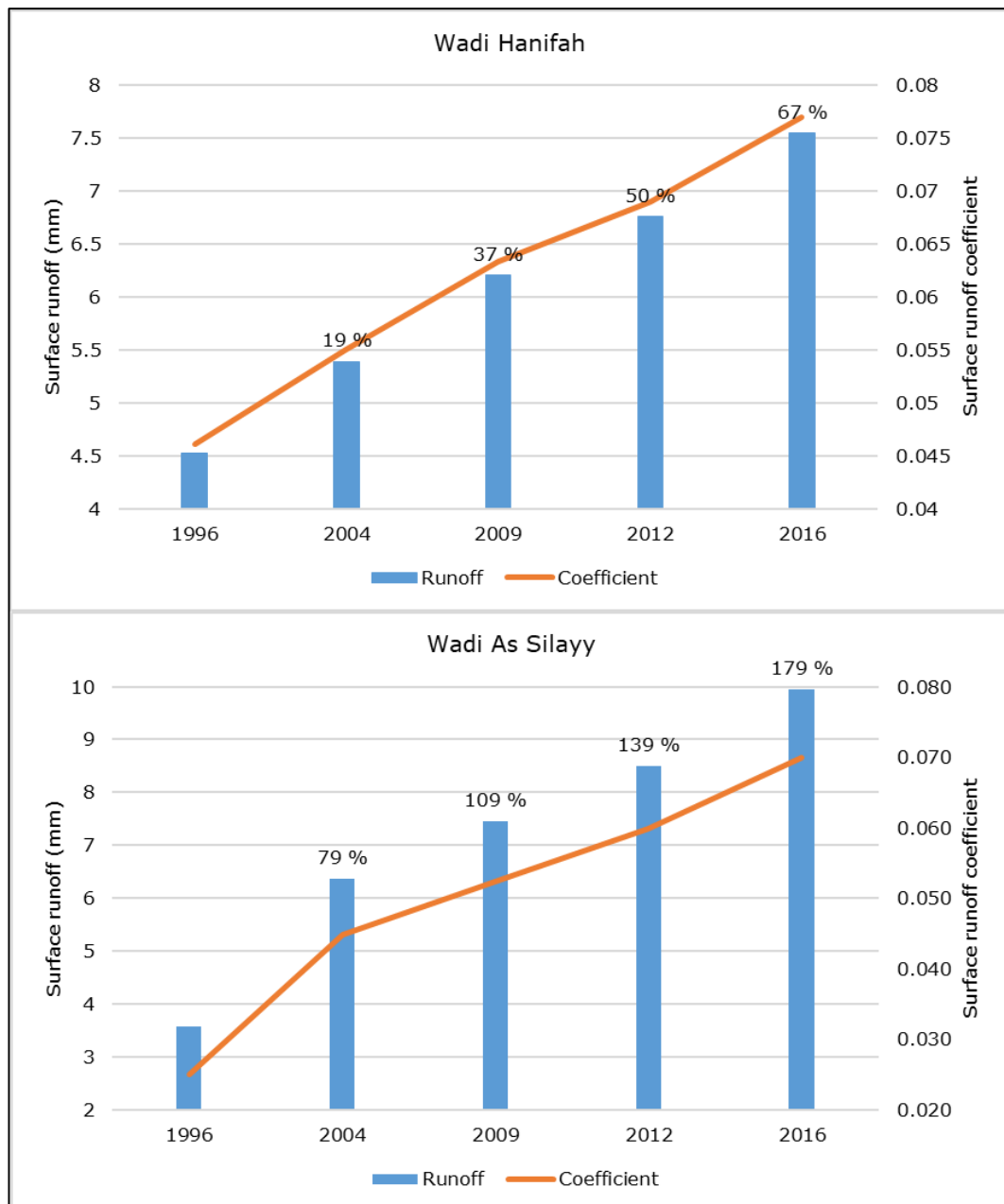


Figure 7.3: Effect of LULC change on average annual simulated runoff, runoff coefficient, and runoff change (%) from 1996.

The five historical LULC scenarios illustrated a decrease in the barren land class and an increase in the other three classes. The relationships between surface runoff and LULC class changes were evaluated in the two catchments of Riyadh city (Figure 7.4). The correlation of surface runoff and the barren land class resulted in a strong inverse relationship, this is probably due to the loss of soils and other permeable natural surfaces. The correlations of surface

runoff and urban and road classes were highly positive because these impervious surfaces increase urban surface runoff.

Somewhat unexpectedly, the correlation result of surface runoff versus vegetation class was positive in Riyadh's catchments. The result is not consistent with the expectation that increasing vegetation will lead to a decrease in surface runoff owing to increases in interception capacity and surface percolation. The explanation for this can be attributed to the small ratio of increments in the vegetation class compared to the ratio of impervious urban and roads classes. The total increments of vegetation class for the period 1996-2016 were about 117 km² while the total increments of urban and road classes were about 505 km². This means that although the areas of vegetation class increased during the development of the city, the direct driver of increasing surface runoff rates in the city (e.g. urban and road classes) increased more. Consequently, the relationship of annual runoff values and the vegetation class changes have been masked by the stronger influence of changes in urban and road classes.

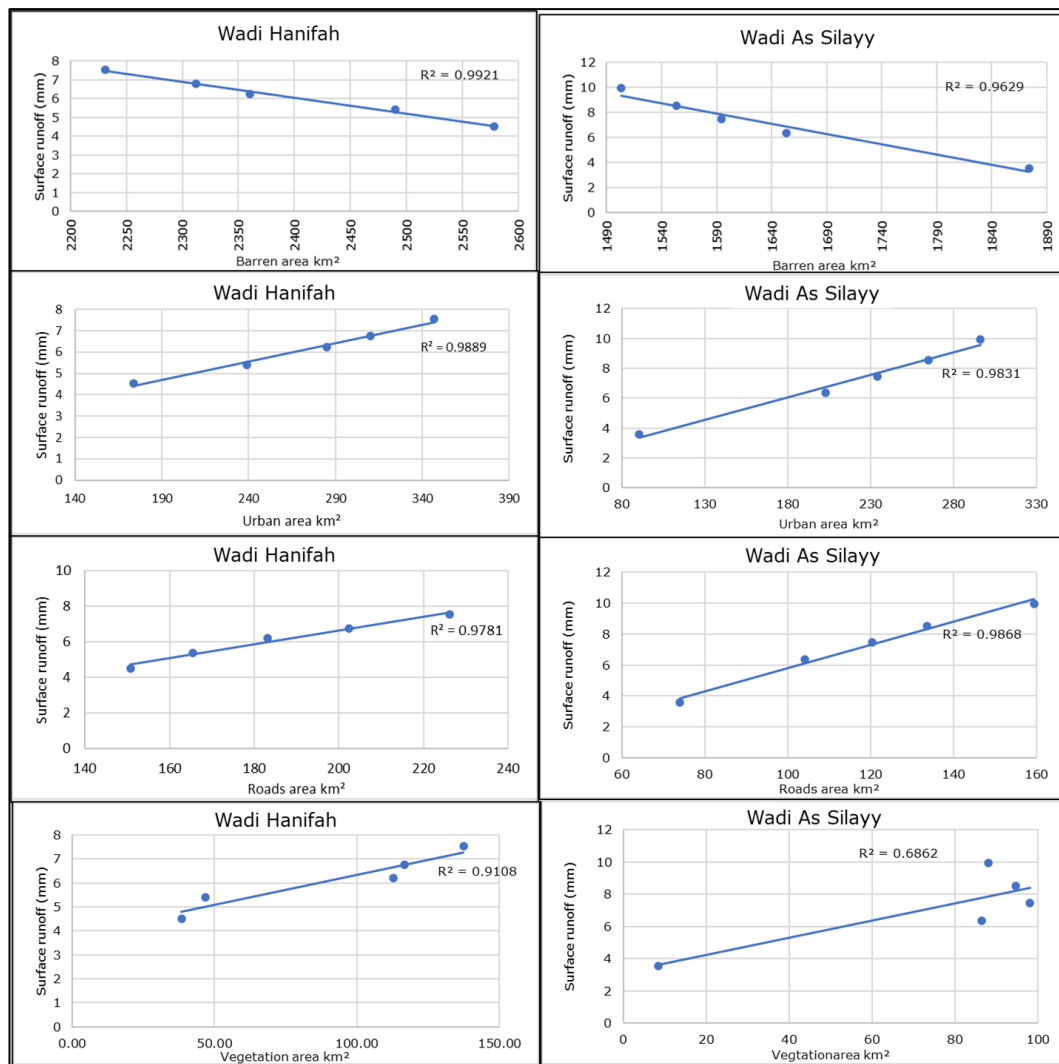


Figure 7.4: Correlation between simulated annual runoff values and areas of LULC classes in Riyadh catchments for the years 1996, 2004, 2009, 2012, and 2016.

7.4.2. Modelling annual runoff on sub-basins level

Under different LULC scenarios, the simulated results of annual runoff depths, runoff coefficients and discharge for sub-basins in the two catchments were calculated (Table 7.4, Table 7.5, Table 7.6, Table 7.7, Table 7.8, and Table 7.9). Results varied between sub-basins based on types and magnitudes of LULC. For example, surface runoff values in sub-basins No. 14 and No. 15 of the Wadi Hanifah catchment were 12.2 mm and 21.8 mm when using the LULC 1996 scenario and 24.5 mm and 25.6 mm when using the LULC 2016 scenario, respectively. The variation of runoff increments in these

sub-basins can be attributed to the different ratios of increased impervious surfaces. In sub-basin 14, there was 121% increase in impervious surfaces and a 101% increase in runoff. In contrast, sub-basin 15 had a 24% increase in impervious surface with a smaller increase in runoff (17%). Additionally, it can be noted from the tables that some sub-basins in the two catchments did not have runoff but had an outflow discharge. The discharge in such sub-basins occurred due to lateral flows and return flows.

Table 7.4: Average annual surface runoff (mm) for the sub-basins in the Wadi Hanifah catchment under different LULC conditions.

Sub-basin	Rainfall (mm)	LULC 1996	LULC 2004	LULC 2009	LULC 2012	LULC 2016
1	77.0	0.0	0.0	0.0	0.0	0.0
2	77.0	0.0	0.0	0.0	0.0	0.0
3	82.6	0.6	1.0	0.3	0.3	1.2
4	82.6	0.0	0.0	0.0	0.0	0.0
5	82.6	0.0	0.0	0.0	0.0	0.4
6	82.6	1.5	4.6	4.2	4.3	4.3
7	82.6	0.0	0.0	0.0	0.0	0.0
8	111.5	0.0	0.0	0.0	0.0	0.0
9	82.6	1.8	3.1	3.8	4.3	4.6
10	111.5	7.8	9.5	12.1	13.7	14.0
11	111.5	0.0	0.0	0.0	1.4	1.8
12	111.5	2.5	2.3	2.8	4.8	5.8
13	111.5	7.2	15.6	12.0	13.1	18.1
14	120.6	12.2	15.3	19.5	22.2	24.5
15	110.3	21.8	23.4	25.4	25.4	25.6
16	111.5	3.0	4.4	5.4	5.7	6.1
17	111.5	3.4	4.8	5.9	6.7	7.9
18	120.6	27.0	27.8	31.5	31.8	32.4
19	110.3	14.6	16.6	18.4	18.8	19.6
20	110.3	10.1	11.0	12.9	15.0	17.1
21	110.3	1.8	2.6	3.6	4.1	6.7
22	110.3	0.0	1.0	0.9	1.6	4.1

Table 7.5: Average annual surface runoff (mm) for the sub-basins in the Wadi As Silayy catchment under different LULC scenarios.

Sub-basin	Rainfall (mm)	LULC 1996	LULC 2004	LULC 2009	LULC 2012	LULC 2016
1	154.4	1.5	1.8	2.1	2.2	3.8
2	154.4	0.0	0.0	0.0	0.0	0.0
3	154.4	0.0	6.8	8.5	12.6	14.4
4	154.4	0.0	1.3	2.3	6.7	7.7
5	154.4	1.8	10.1	24.9	31.6	37.1
6	154.4	0.0	3.7	4.4	5.1	8.8
7	120.7	0.0	1.8	2.9	3.2	3.5
8	120.7	12.7	25.3	28.8	30.2	32.2
9	120.7	3.3	16.0	18.9	21.6	22.9
10	120.7	11.9	15.3	16.7	17.3	18.8
11	110.3	2.7	3.1	3.6	3.9	5.3

Table 7.6: Average annual runoff coefficients for the sub-basins in the Wadi Hanifah catchment under different LULC scenarios.

Sub-basin	Rainfall (mm)	LULC 1996	LULC 2004	LULC 2009	LULC 2012	LULC 2016
1	77.00	0	0	0	0	0
2	77.00	0	0	0	0	0
3	82.59	0.0071	0.0118	0.0037	0.0037	0.0146
4	82.61	0	0	0	0	0
5	82.61	0	0	0	0	0.0052
6	82.60	0.0180	0.0552	0.0508	0.0520	0.0526
7	82.60	0	0	0	0	0
8	111.47	0	0	0	0	0
9	82.61	0.0213	0.0376	0.0463	0.0519	0.0560
10	111.47	0.0699	0.0851	0.1089	0.1228	0.1260
11	111.47	0	0	0	0.0125	0.0158
12	111.47	0.0225	0.0202	0.0248	0.0431	0.0523
13	111.47	0.0649	0.1396	0.1076	0.1175	0.1627
14	120.64	0.1008	0.1272	0.1620	0.1838	0.2030
15	110.31	0.1974	0.2122	0.2306	0.2304	0.2318
16	111.46	0.0272	0.0391	0.0480	0.0514	0.0544
17	111.47	0.0302	0.0427	0.0533	0.0598	0.0711
18	120.62	0.2239	0.2306	0.2615	0.2640	0.2685
19	110.31	0.1325	0.1509	0.1668	0.1705	0.1781
20	110.31	0.0915	0.0999	0.1173	0.1359	0.1549
21	110.31	0.0164	0.0238	0.0324	0.0375	0.0605
22	110.29	0	0.0090	0.0086	0.0149	0.0371

Table 7.7: Average annual runoff coefficients for the sub-basins in the Wadi As Silayy catchment under different LULC scenarios.

Sub-basin	Rainfall (mm)	LULC 1996	LULC 2004	LULC 2009	LULC 2012	LULC 2016
1	154.43	0.0098	0.0115	0.0136	0.0143	0.0249
2	154.43	0	0	0	0	0
3	154.43	0.0000	0.0439	0.0551	0.0816	0.0934
4	154.43	0.0000	0.0085	0.0148	0.0436	0.0497
5	154.43	0.0119	0.0652	0.1611	0.2047	0.2400
6	154.43	0.0000	0.0237	0.0282	0.0328	0.0571
7	120.65	0.0000	0.0151	0.0238	0.0269	0.0292
8	120.65	0.1056	0.2097	0.2387	0.2500	0.2668
9	120.65	0.0270	0.1327	0.1568	0.1791	0.1896
10	120.65	0.0986	0.1272	0.1381	0.1432	0.1561
11	110.3	0.0244	0.0282	0.0326	0.0350	0.0481

Table 7.8: Average annual discharge (m³/s) for the sub-basins in the Wadi Hanifah catchment under different LULC scenarios.

Sub-basin	LULC 1996	LULC 2004	LULC 2009	LULC 2012	LULC 2016
1	0.17	0.17	0.17	0.17	0.17
2	0.34	0.34	0.34	0.34	0.34
3	0.71	0.80	0.84	0.84	0.97
4	0.10	0.10	0.10	0.10	0.11
5	0.65	0.73	0.75	0.75	0.90
6	0.11	0.18	0.17	0.17	0.18
7	1.63	1.63	1.80	1.80	1.84
8	0.14	0.15	0.16	0.16	0.16
9	2.07	2.26	2.46	2.48	2.69
10	2.15	2.39	2.65	2.70	2.90
11	0.11	0.11	0.13	0.16	0.20
12	0.19	0.19	0.21	0.26	0.29
13	2.34	2.65	2.90	3.05	3.36
14	0.69	0.88	1.12	1.27	1.45
15	3.74	4.37	5.01	5.34	5.86
16	0.62	0.73	0.85	0.88	0.91
17	0.26	0.36	0.45	0.50	0.59
18	1.88	1.93	2.19	2.21	2.27
19	5.71	6.52	7.52	7.93	8.65
20	0.75	0.81	0.94	1.06	1.18
21	0.13	0.16	0.20	0.22	0.33
22	6.06	7.01	8.15	8.73	9.80

Table 7.9: Average annual discharge (m³/s) for the sub-basins in the Wadi As Silayy catchment under different LULC scenarios.

Sub-basin	LULC 1996	LULC 2004	LULC 2009	LULC 2012	LULC 2016
1	3.66	3.90	3.95	3.93	4.16
2	4.04	4.19	4.18	4.18	4.16
3	0.79	1.59	1.76	2.21	2.38
4	0.16	0.18	0.21	0.27	0.28
5	8.21	9.49	9.87	10.42	10.85
6	0.44	0.60	0.67	0.75	0.95
7	0.03	0.07	0.09	0.10	0.10
8	0.43	0.84	0.96	1.00	1.07
9	8.45	10.14	10.66	11.34	12.00
10	12.11	14.73	15.56	16.40	17.51
11	0.12	0.14	0.16	0.17	0.22

Figure 7.5, Figure 7.6, and Figure 7.7 show the spatial distribution characteristics of the average annual amounts and coefficient of surface runoff and discharge at different periods. In general, the highest average annual runoff values are found in the sub-basins located within the boundary of the city. During 1996–2016, the sub-basins within the boundary of the city also showed an increasing trend of surface runoff. The increase of runoff depths in these sub-basins reflected the direct influence of the urbanisation process on surface runoff. For example, comparing runoff values when using the LULC 1996 scenario and the LULC 2016 scenario for the sub-basins of the Wadi As Silayy catchment showed that average annual runoff values in all sub-basins were 16 mm or less for the LULC 1996 scenario, but when using the LULC 2016 scenario some of the sub-basins had an average annual runoff within the 32.1-40 mm class. The increase in average annual runoff depths coincided with the increase in the average annual runoff coefficients. These increments could be driven by increasing impervious surfaces during the development of Riyadh city in this period. Discharge rates spatially varied and moderately increased through time in the sub-basins within the urbanised parts of the study area. The discharge rates in most of the sub-basins that experienced urbanisation increased from their discharge classes to a higher class.

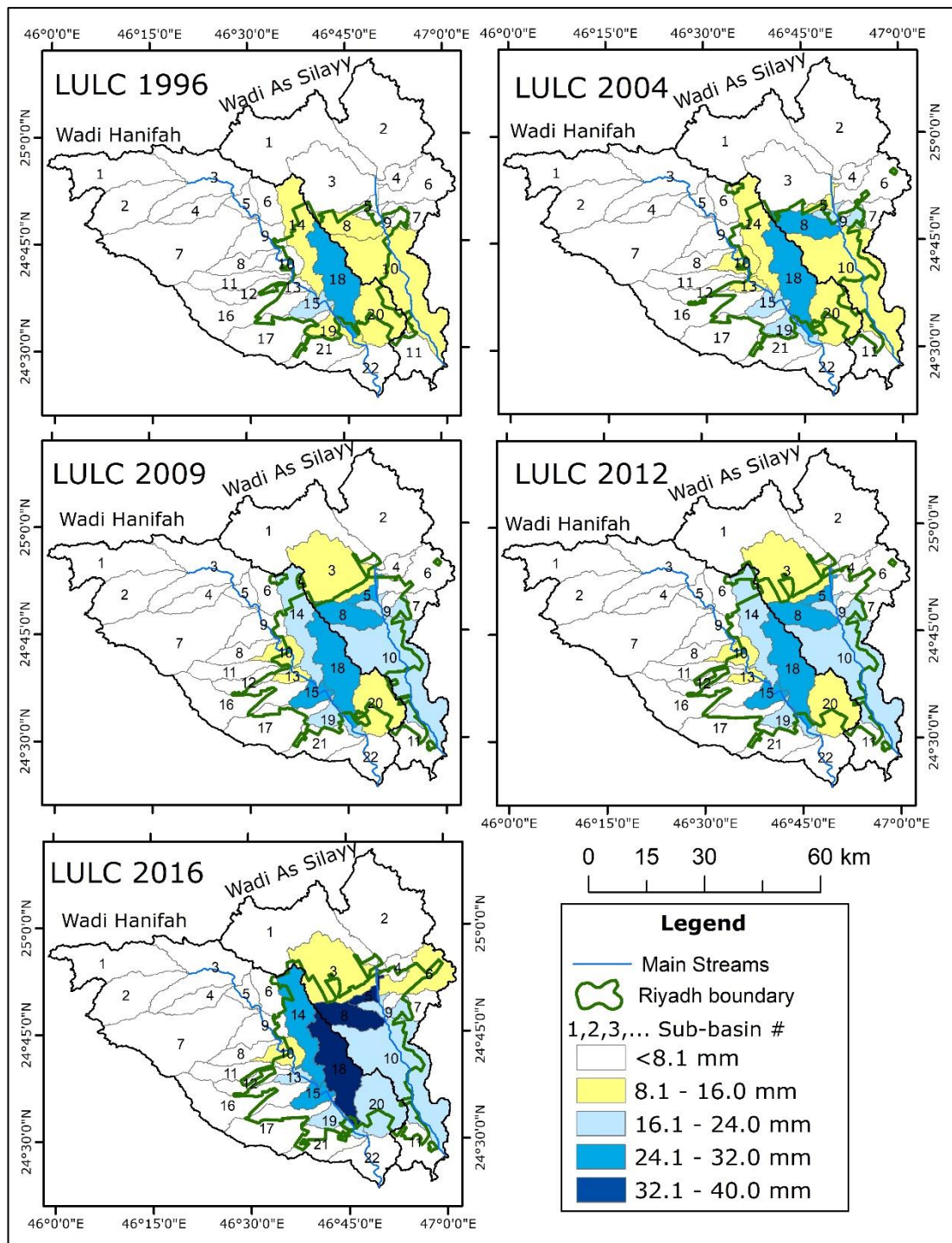


Figure 7.5: Spatial distributions of average annual surface runoff using different LULC scenarios at Riyadh's catchments.

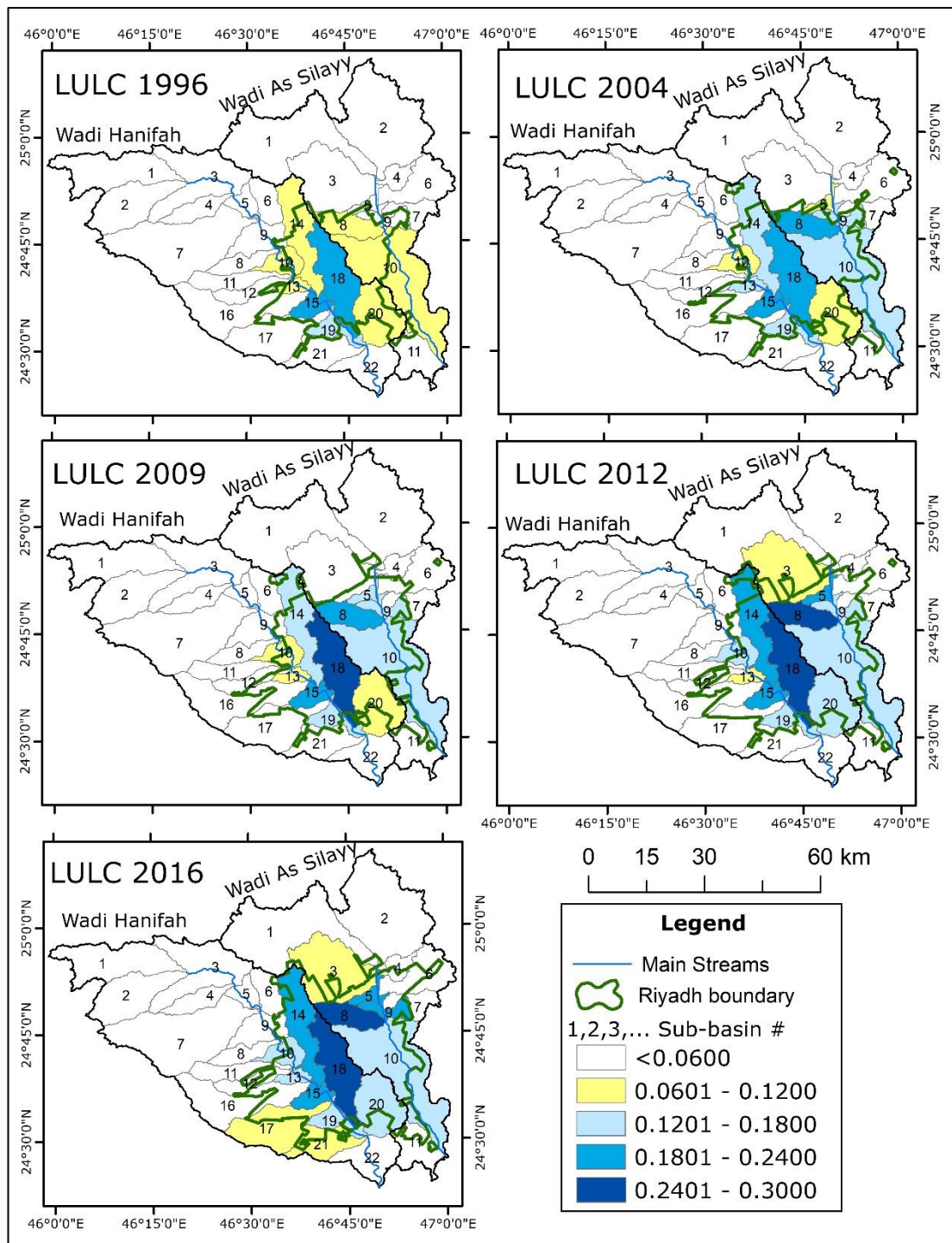


Figure 7.6: Spatial distributions of average annual runoff coefficient using different LULC scenarios at Riyadh's catchments.

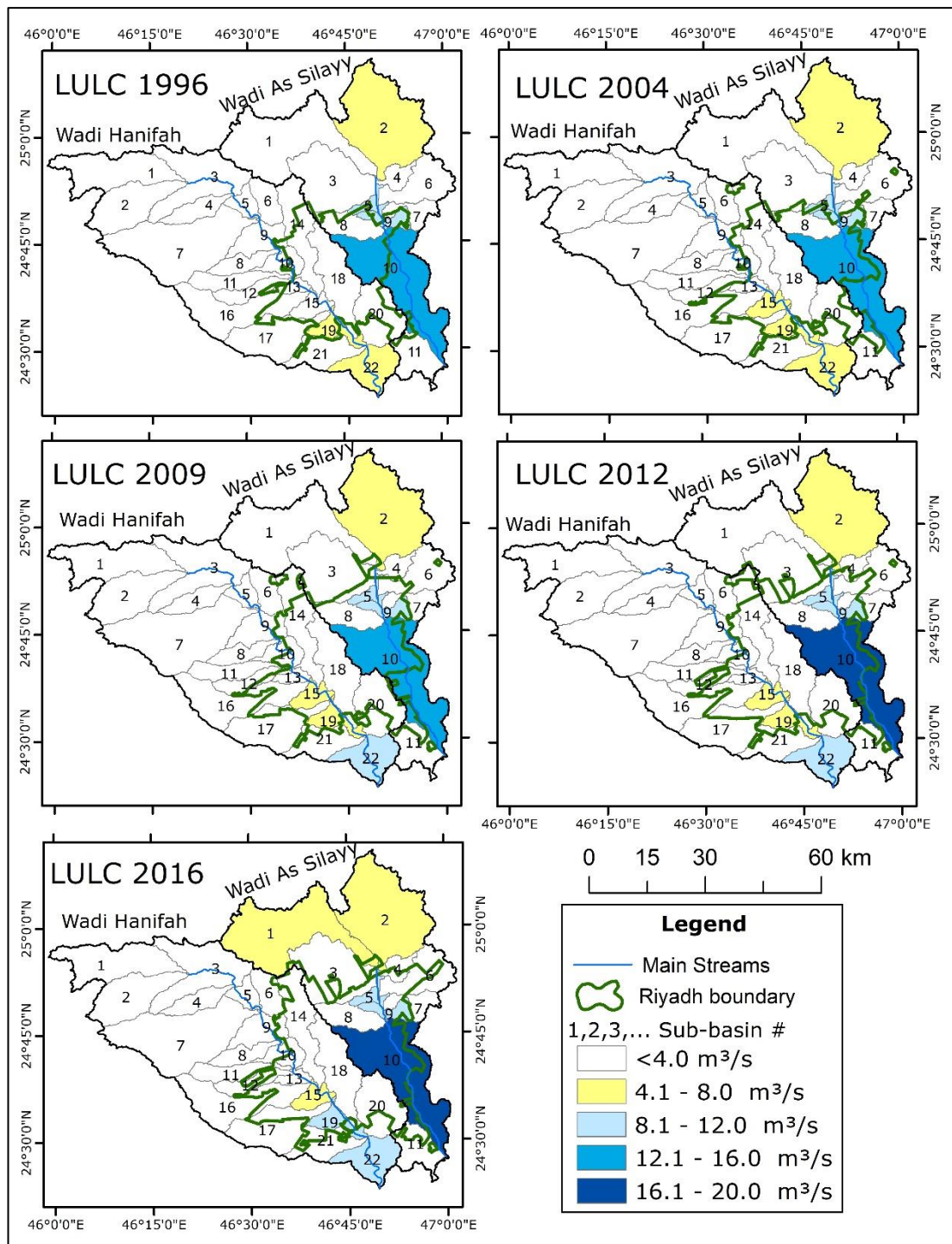


Figure 7.7: Spatial distributions of average annual discharge using different LULC scenarios at Riyadh's catchments.

7.5. Modelling the seasonal cycle of runoff

7.5.1. Modelling the seasonal cycle at catchments level

For both catchments in Riyadh, the simulated mean monthly surface runoff by the SWAT models for the period 1991-2000 using LULC

1996 scenario varied from month to month and from year to year (Table 7.10 and Table 7.11).

The highest monthly average of surface runoff values occurred in the month of March. On the contrary, the months of June, July, August, and September were dry with zero or very small amount of simulated runoff. During this period the number of occurrences of monthly runoff was 41 times in the Wadi Hanifah catchment and 55 times in the Wadi As Silayy catchment. Table 7.12 and Figure 7.8 present the temporal distribution of number of occurrences of simulated monthly runoff. The months of June, July, and September had no runoff occurrence and January, March and April had the highest number of occurrences (17%-20%) in the Wadi Hanifah and Wadi As Silayy. The percentages of the number of runoff occurrences for the Winter, Spring, Summer, and Autumn seasons were 42%, 47%, 2%, and 9% in the Wadi Hanifah, respectively. Equivalent values for Wadi As Silayy were 38% for the Winter, 49% for the Spring, 2% for the Summer, and 11% for the Autumn.

Table 7.10: Monthly simulated runoff (mm) for the Wadi Hanifah catchment using LULC 1996 scenario.

Year	Jan	Feb	Mar	Apr	May	Jun	Jul	Aug	Sep	Oct	Nov	Dec
1991	0.6	0.1	0.3	0.0	0.0	0.0	0.0	0.0	0.0	0.0	0.0	0.1
1992	0.4	0.3	0.9	0.2	0.1	0.0	0.0	0.0	0.0	0.0	0.0	1.2
1993	2.4	0.3	0.2	3.0	1.6	0.0	0.0	0.0	0.0	0.0	0.0	0.0
1994	0.0	0.0	0.7	0.5	0.5	0.0	0.0	0.0	0.0	0.0	0.0	0.0
1995	0.0	0.2	5.8	2.2	0.0	0.0	0.0	0.0	0.0	0.0	0.0	2.8
1996	2.2	0.1	4.8	1.5	0.2	0.0	0.0	0.0	0.0	0.0	0.1	0.0
1997	0.5	0.0	1.1	1.0	0.0	0.0	0.0	0.0	0.0	1.0	4.0	0.1
1998	1.2	0.0	0.8	0.8	0.0	0.0	0.0	0.1	0.0	0.0	0.0	0.0
1999	0.4	0.0	0.0	0.0	0.0	0.0	0.0	0.0	0.0	0.0	0.0	0.0
2000	0.4	0.0	0.0	0.0	0.0	0.0	0.0	0.0	0.0	0.0	1.0	0.0
Average	0.8	0.1	1.4	0.9	0.2	0.0	0.0	0.0	0.0	0.1	0.5	0.4

Table 7.11: Monthly simulated runoff (mm) for the Wadi As Silayy catchment using LULC 1996 scenario.

Year	Jan	Feb	Mar	Apr	May	Jun	Jul	Aug	Sep	Oct	Nov	Dec
1991	0.6	0.1	0.2	0.1	0.0	0.0	0.0	0.0	0.0	0.0	0.0	0.0
1992	0.3	0.2	0.7	0.2	0.1	0.0	0.0	0.0	0.0	0.0	0.0	0.9
1993	1.8	0.3	0.1	2.0	1.4	0.0	0.0	0.0	0.0	0.0	0.0	0.0
1994	0.0	0.0	0.4	0.5	0.6	0.0	0.0	0.0	0.0	0.0	0.0	0.0
1995	0.0	0.2	4.4	1.9	0.0	0.0	0.0	0.0	0.0	0.0	0.0	2.0
1996	1.2	0.0	3.6	1.1	0.3	0.0	0.0	0.0	0.0	0.0	0.1	0.0
1997	0.5	0.0	1.1	0.6	0.1	0.0	0.0	0.0	0.0	0.3	3.5	0.1
1998	0.9	0.0	0.4	0.6	0.0	0.0	0.0	0.1	0.0	0.0	0.0	0.0
1999	0.4	0.0	0.0	0.0	0.0	0.0	0.0	0.0	0.0	0.0	0.0	0.0
2000	0.4	0.0	0.0	0.0	0.0	0.0	0.0	0.0	0.0	0.0	0.6	0.0
Average	0.6	0.1	1.1	0.7	0.2	0.0	0.0	0.0	0.0	0.0	0.4	0.3

Table 7.12: Number of occurrences of monthly runoff in Riyadh's catchments for the period 1991-2000.

Months	Wadi Hanifah catchment		Wadi As Silayy catchment	
	Occurrences of non-zero runoff	Percentage of total cases	Occurrences of non-zero runoff	Percentage of total cases
Jan	8	20%	10	18%
Feb	5	12%	6	11%
Mar	8	20%	10	18%
Apr	7	17%	10	18%
May	4	10%	7	13%
Jun	0	0%	0	0%
Jul	0	0%	0	0%
Aug	1	2%	1	2%
Sep	0	0%	0	0%
Oct	1	2%	1	2%
Nov	3	7%	5	9%
Dec	4	10%	5	9%
Total	41	100%	55	100%

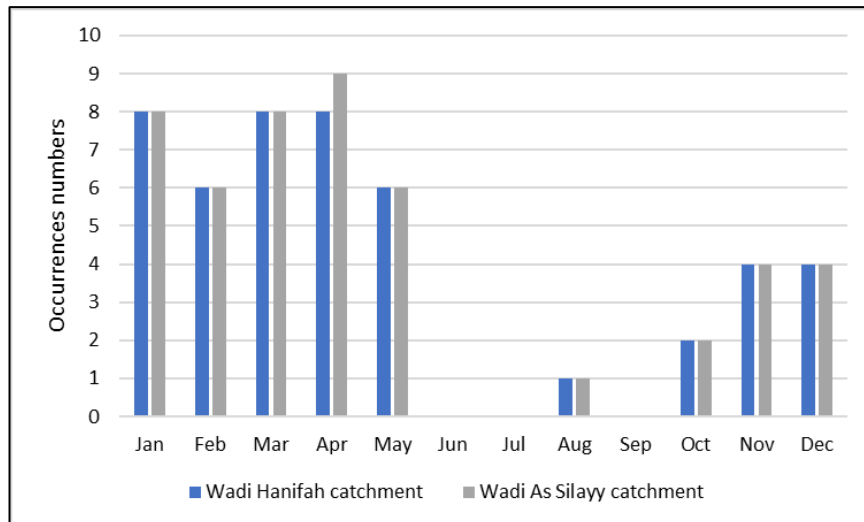


Figure 7.8: Number of occurrences of monthly runoff in Riyadh's catchments for the period 1991-2000.

The lowest simulated values of runoff were zero for all months during the period from 1990 to 2000 because of rainfall irregularity in the study area. When using LULC 1996 scenario, the highest monthly simulated runoff values during the rainy season months, extending from October to May in the study area, were ranging from 0.3 mm in February to 5.8 mm in March for the Wadi Hanifah catchment, and from 0.3 mm in February to 4.4 mm in March for the Wadi As Silayy catchment. Table 7.13 shows the impact of LULC changes on the highest values of simulated monthly runoff in Riyadh's catchments using climate data for the period 1991-2000. Modelling monthly runoff using five different historical LULC scenarios highlighted the positive effect of LULC changes on simulated runoff in Riyadh's catchments. The increase in impervious surfaces in Riyadh increased the runoff coefficient and consequently increased simulated runoff values. For example, over twenty years the highest simulated runoff depth in March increased from 5.8 mm to 9.5 mm in the Wadi Hanifah catchment, and from 4.4 mm to 10.8 mm in the Wadi As Silayy catchment. Generally speaking, the increase of the highest simulated runoff was about 67% and 200% in the Wadi Hanifah and the Wadi As Silayy catchments, respectively. Also, the increase of average simulated monthly runoff values was consistent with the

increase of impervious surfaces in the city due to LULC changes in the period from 1996 to 2016 (Figure 7.9).

Table 7.13: Impact of LULC change in 20 years period (1996 – 2016) on the highest values of simulated monthly runoff (mm) in Riyadh’s catchments.

Catchment	LULC scenarios	Months											
		Jan	Feb	Mar	Apr	May	Jun	Jul	Aug	Sep	Oct	Nov	Dec
Wadi Hanifah catchment	1996	2.4	0.3	5.8	3.0	1.6	0	0	0.1	0	1.0	4.0	2.8
	2004	2.8	0.4	6.8	3.6	1.9	0	0	0.1	0	1.3	4.9	3.2
	2009	3.3	0.4	7.8	4.2	2.3	0	0	0.1	0	1.4	5.5	3.8
	2012	3.6	0.5	8.6	4.5	2.4	0	0	0.1	0	1.6	6.0	4.1
	2016	4.0	0.5	9.5	5.1	2.6	0	0	0.1	0	1.8	6.7	4.6
	Change mm	1.6	0.2	3.7	2.1	1.0	0	0	0	0	0.8	2.7	1.8
	Change %	67	67	64	70	62	0	0	0	0	80	67	64
Wadi As Silayy catchment	1996	1.8	0.3	4.4	2.0	1.4	0	0	0.1	0	0.3	3.5	2.0
	2004	3.3	0.6	7.5	3.7	2.4	0	0	0.2	0	0.6	7.0	3.9
	2009	3.9	0.7	8.6	4.3	2.8	0	0	0.2	0	0.7	8.3	4.6
	2012	4.5	0.8	9.4	4.9	3.1	0	0	0.2	0	0.8	9.8	5.3
	2016	5.3	1.0	10.8	5.8	3.6	0	0	0.2	0	1.0	11.6	6.3
	Change mm	3.5	0.7	6.4	3.8	2.2	0	0	0.1	0	0.7	8.1	4.3
	Change %	194	233	145	190	157	0	0	100	0	233	231	215

Runoff in the study area corresponds highly to that of rainfall for the same period. Thus, runoff is expected to occur in the rainy season (October-May) which includes two months of Autumn and all Winter and Spring months. The highest average simulated runoff occurred during the Spring months, the Winter months came second and simulated runoff in Autumn months came third. For the Wadi Hanifah catchment, about 57% of average simulated runoff occurred in Spring months, 29% in Winter months, and 14% in Autumn months. The average simulated runoff percentages, for the Wadi As Silayy catchment, were about 54% in Spring months, 30% in Winter months, and 15% in Autumn months (Figure 7.10).

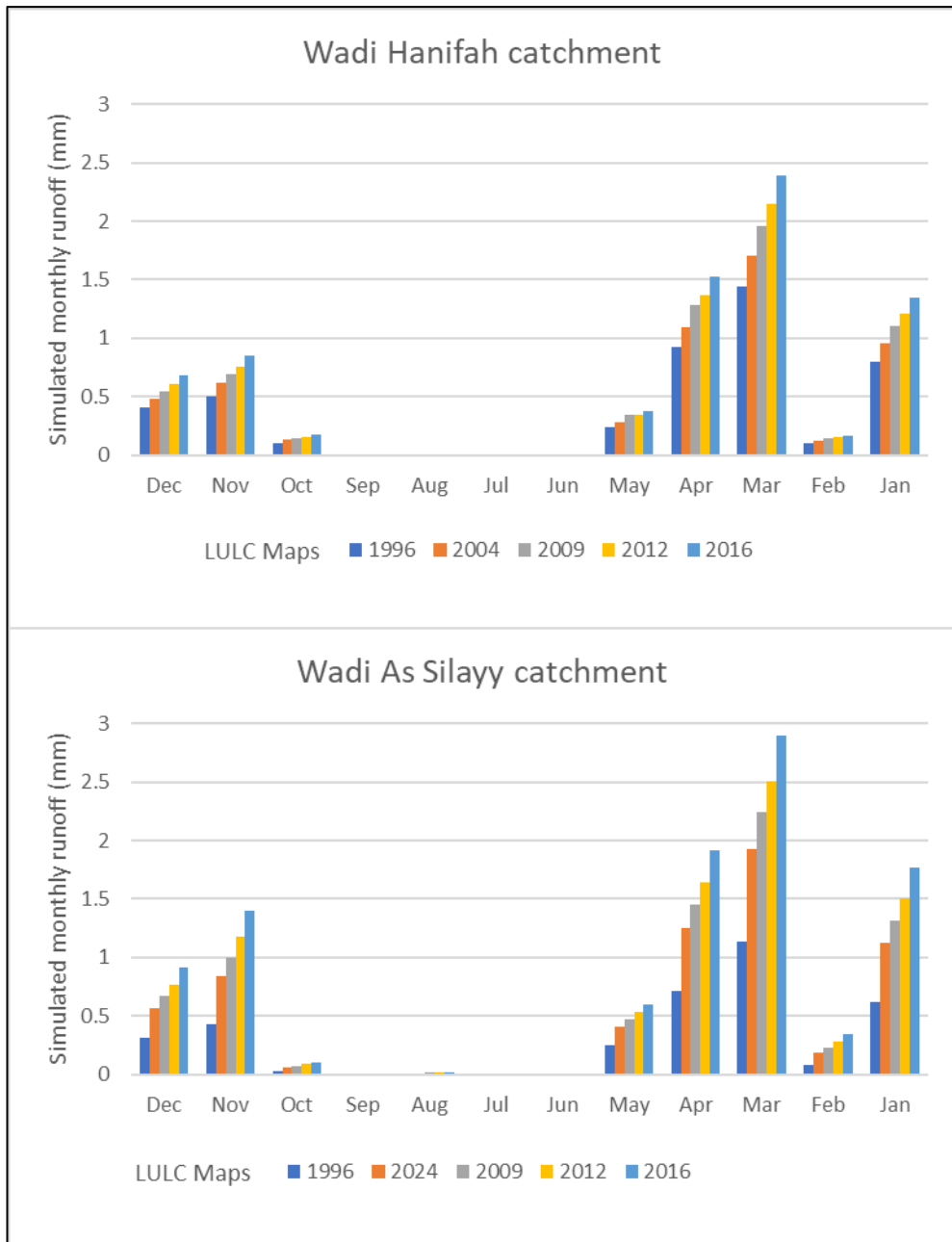


Figure 7.9: Effect of LULC change on average simulated monthly runoff.

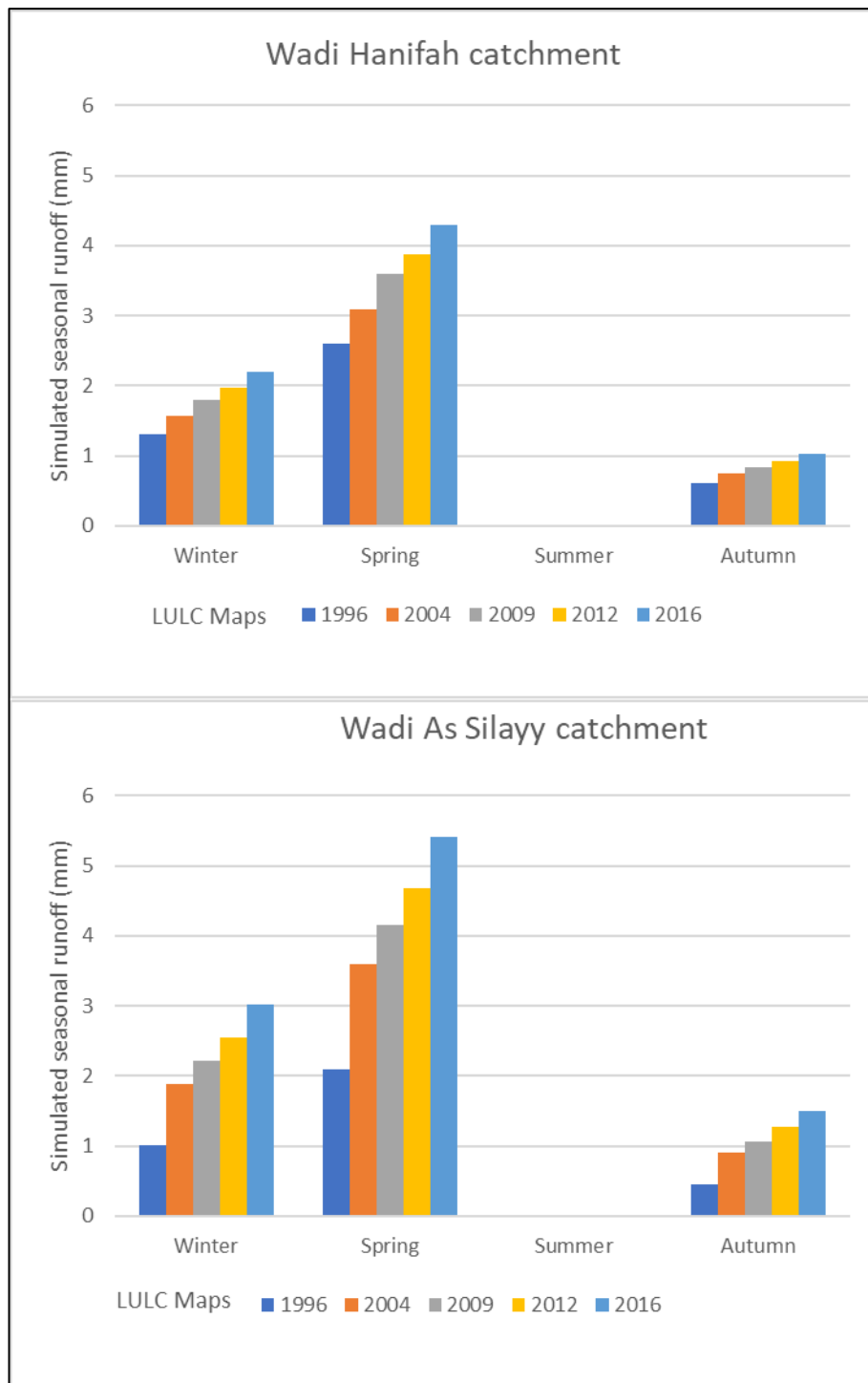


Figure 7.10: Effect of LULC change on average simulated seasonal runoff.

The rainfall-runoff relationship is well-established in hydrological studies and is influenced by several factors related to catchment characteristics, climate conditions, and land use types. Thus, some of the previous studies, especially performed in large catchments, have shown that the rainfall-runoff transformation is a nonlinear

process (Rodríguez-Blanco et al. 2012). Since all input data for the SWAT model are unchanged for runoff simulations except LULC data, it is assumed that the change of runoff is related to the change of LULC; and consequently, the change in coefficients of determination for the relationship between rainfall and runoff in the study area should not be high when using different LULC scenarios. The examination of the relationships between monthly rainfall and simulated monthly runoff, for the period 1991-2000, resulted in high correlations based on the five different LULC scenarios used for the SWAT modelling indicating the impact of LULC change on runoff (Table 7.14, Figure 7.11, and Figure 7.12).

Table 7.14: Coefficient of determination (R^2) of relationships between average monthly rainfall and average simulated monthly runoff using five different LULC scenarios.

	Wadi Hanifah					Wadi As Silayy				
	LULC 1996	LULC 2004	LULC 2009	LULC 2012	LULC 2016	LULC 1996	LULC 2004	LULC 2009	LULC 2012	LULC 2016
Jan	0.96	0.97	0.97	0.97	0.97	0.98	0.99	0.99	0.99	0.99
Feb	0.90	0.90	0.88	0.88	0.88	0.78	0.92	0.93	0.94	0.95
Mar	0.95	0.96	0.96	0.96	0.96	0.87	0.90	0.91	0.92	0.92
Apr	0.88	0.91	0.90	0.91	0.91	0.90	0.94	0.95	0.97	0.97
May	0.98	0.97	0.98	0.97	0.97	0.98	0.99	0.99	0.99	0.99
Jun										
Jul										
Aug	1	1	1	1	1	1	1	1	1	1
Sep										
Oct	0.99	0.99	0.99	0.99	0.99	0.99	0.99	0.99	0.99	0.99
Nov	0.99	0.99	0.99	0.99	0.99	0.99	0.99	0.99	0.99	0.99
Dec	0.97	0.97	0.97	0.97	0.97	0.99	0.99	0.99	0.99	0.99

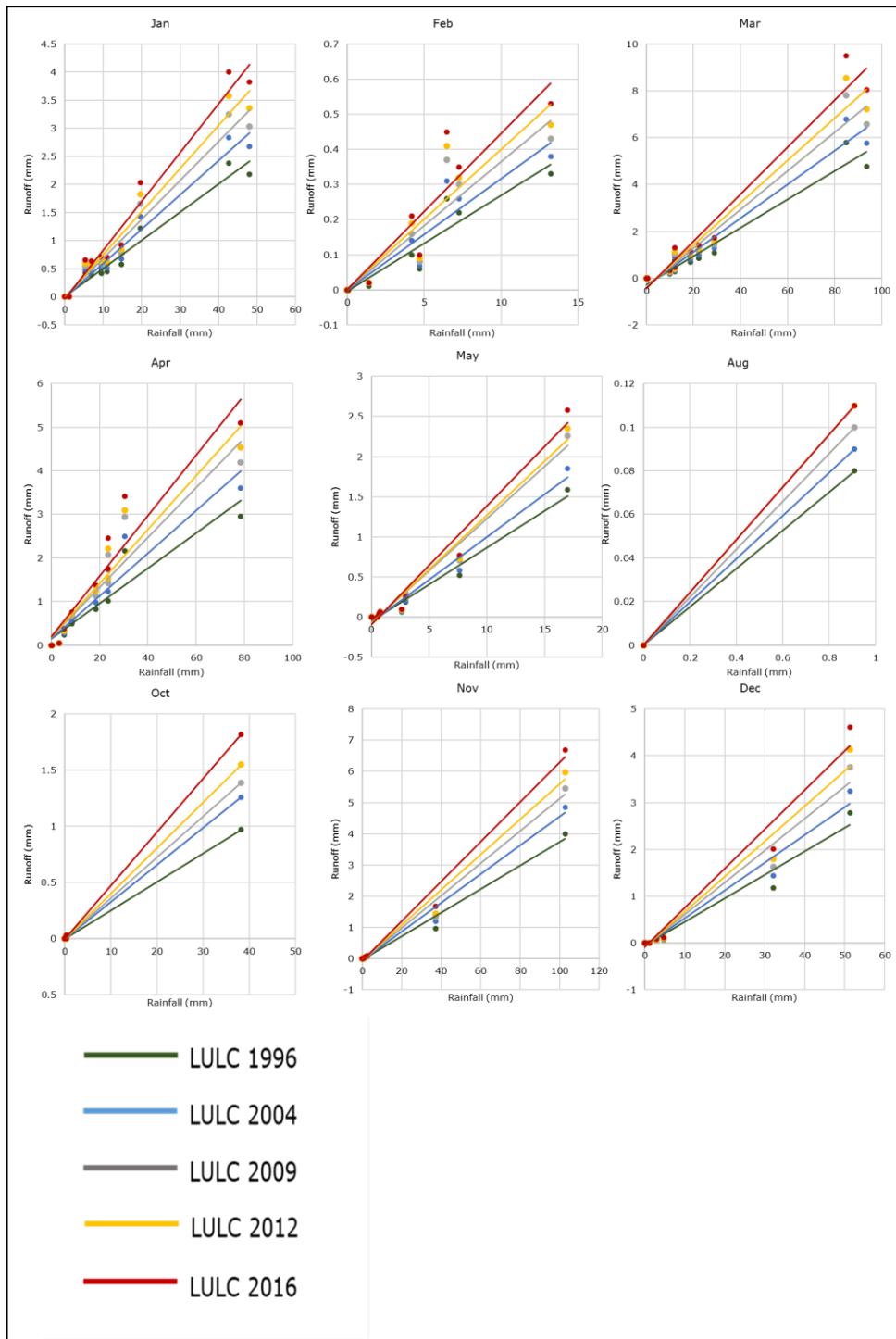


Figure 7.11: Relationships between monthly rainfall and simulated monthly runoff based on five different LULC scenarios in the Wadi Hanifah catchment.

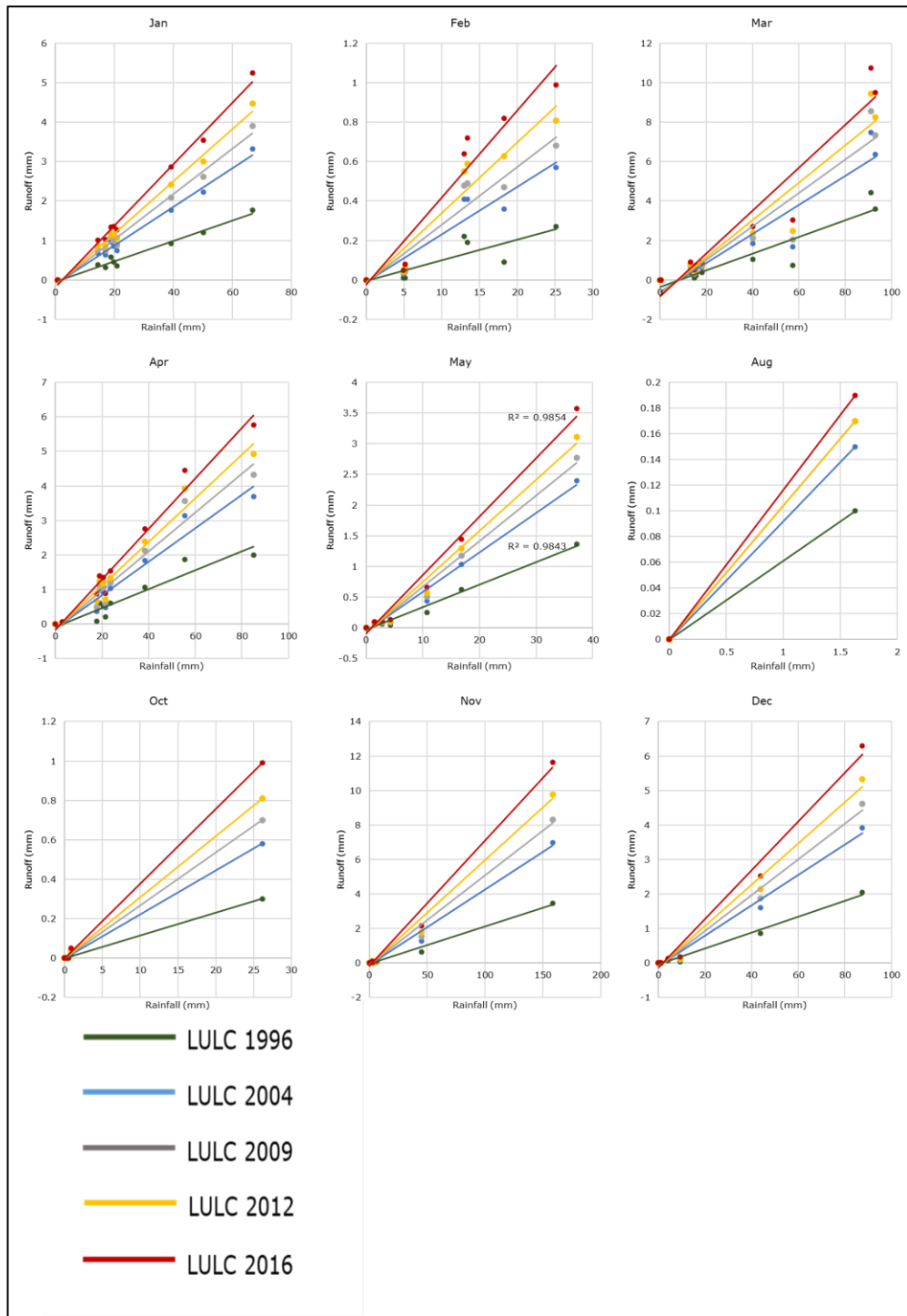


Figure 7.12: Relationships between monthly rainfall and simulated monthly runoff based on five different LULC scenarios in the Wadi As Silayy catchment.

7.5.2. Modelling seasonal cycle of runoff on sub-basins level

Using the calibrated SWAT models for the study area catchments, monthly runoff and discharge for the period 1991-2000 were simulated in the catchments of the study area, under five different historical LULC scenarios (Appendix B). Average simulated monthly runoff and discharge are plotted in Figure 7.13, Figure 7.14, Figure 7.15, and Figure 7.16 to assess the impact of LULC change on simulations of monthly runoff and discharge on the sub-basins level for the two main catchments. From these illustrations, it can be noticed that the average monthly runoff and discharge values varied from one sub-basin to another and from month to another in the study area. The graphs reveal an increasing trend of monthly simulated runoff depths and discharge rates that occurred in the sub-basins within the city's boundary. The gradual increases in runoff depths and discharge rates were due to the gradual change in LULC.

In Figure 7.13, it appears that the average monthly runoff in sub-basin 19 using LULC 2016 scenario was lower than the general trend. This may be attributed to vegetation in this sub-basin. Although the area of vegetation in 2016 was the same as in some previous years, the spatial distribution is different. Therefore, the main reason for the difference in 2016 is not just the area of LULC that is an important determinant of runoff, but also where the LULC occurs, and whether it occurs sporadically in a speckled pattern or large contiguous blocks as for the vegetation distribution in 2016. Moreover, Figure 7.15 shows that the average simulated monthly discharge in sub-basin 8 had a different response with the highest values in the summer. This might be attributed to the very low discharge rate (less than 0.014 m³/s) and came mainly from baseflow.

Changes in monthly runoff depth and discharge rate in the study area were positively influenced by the urbanisation process. Changes in runoff depth and discharge rate varied from one sub-basin to another depending on the rates of LULC change for each sub-basin. Based on the proportion of the impervious surface, simulated runoff in some sub-basins within the built-up area of the city increased by only less than 50%. For example, simulated runoff increased by 25% in sub-basin 18 in the Wadi Hanifah catchment for January, where the impermeable surfaces increased from 66% in 1996 to 81% in 2016 of the sub-basin total area. On the other hand, the increase of simulated runoff for January reached more than 1450% such as in the sub-basin 5 in the Wadi As Silayy catchment, where the impervious layers increased from less than 5% in 1996 to more than 53% in 2016 from the total area of the sub-basin.

The graphs of average monthly runoff and discharge show that some unaffected sub-basins by urbanisation had no significant runoff changes. Runoff depths in these sub-basins were confined to the lowest category in each graph when using the various five LULC scenarios for the period 1996-2016. For example, simulated runoff depths for sub-basin No. 1 in the Wadi Hanifah catchment for all months were zero mm when using either the LULC 1996 scenario or the LULC 2016 scenario. The unaffected sub-basins by urbanisation include 1, 2, 4, 7, and 8 in the Wadi Hanifah catchment, and sub-basin 2 in the Wadi As Silayy catchment. These unaffected sub-basins by the urbanisation process represent 33% of the Wadi Hanifah catchment area, 21% of the Wadi As Silayy catchment area, and 28% of the whole study area.

As an example, to show the effect of LULC change on the spatial distribution characteristics of the average simulated runoff and discharge in the study area, simulations of the calibrated SWAT

models using five different historical LULC scenarios for January were mapped (Figure 7.17 and Figure 7.18). The maps clearly illustrate the positive effect of the urbanisation process in Riyadh on runoff depths and discharge rates. Like the simulated runoff depths, discharge rates in the unaffected sub-basins by urbanisation in the north, northwest, northeast, west, and southwest of the study area had no significant changes when using the various five LULC scenarios for the period 1996-2016. For example, simulated discharge rates for sub-basin 1 in the Wadi Hanifah catchment in January were in the category of $<0.41 \text{ m}^3/\text{s}$ for all LULC scenarios. On the contrary, the maps show that runoff depths and discharge rates were increasing in the sub-basins that experienced urbanisation during the period from 1996 to 2016. For example, simulated discharge rates for sub-basin 10 in the Wadi As Silayy catchment for January increased from $1.40 \text{ m}^3/\text{s}$ to $2.31 \text{ m}^3/\text{s}$ when using the LULC 1996 and or the LULC 2016 scenarios, respectively.

The reason for the increasing trend of monthly runoff and discharge in some sub-basins of the Riyadh main catchments was the continuous expansion of the city within the catchments. The Riyadh city built-up area within the two catchments was 489 km^2 in 1996 and reached 1029 km^2 in 2016. The city expansion in 20 years represented 110%.

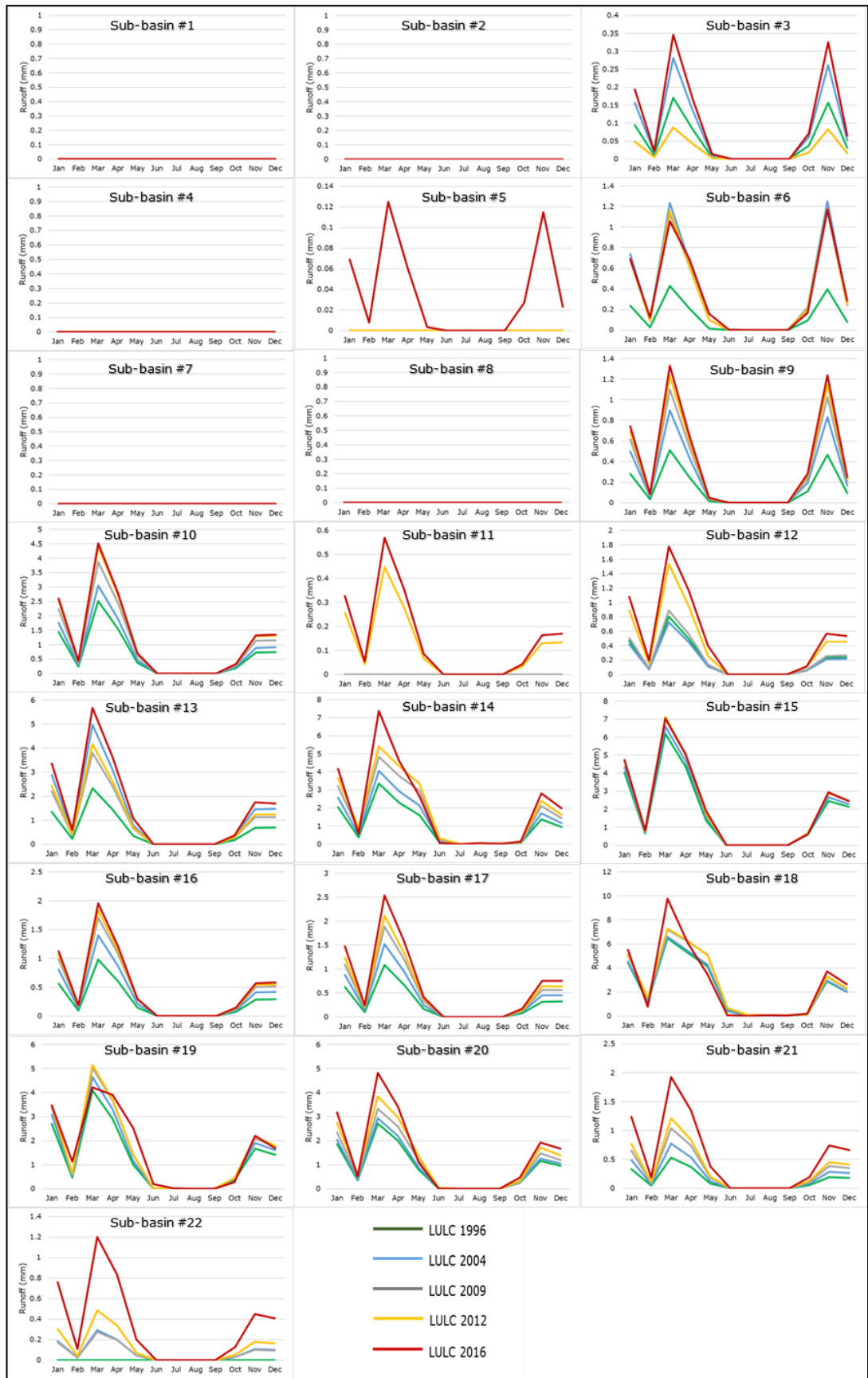


Figure 7.13: Average simulated monthly runoff using different LULC scenarios for sub-basins of the Wadi Hanifah catchment.

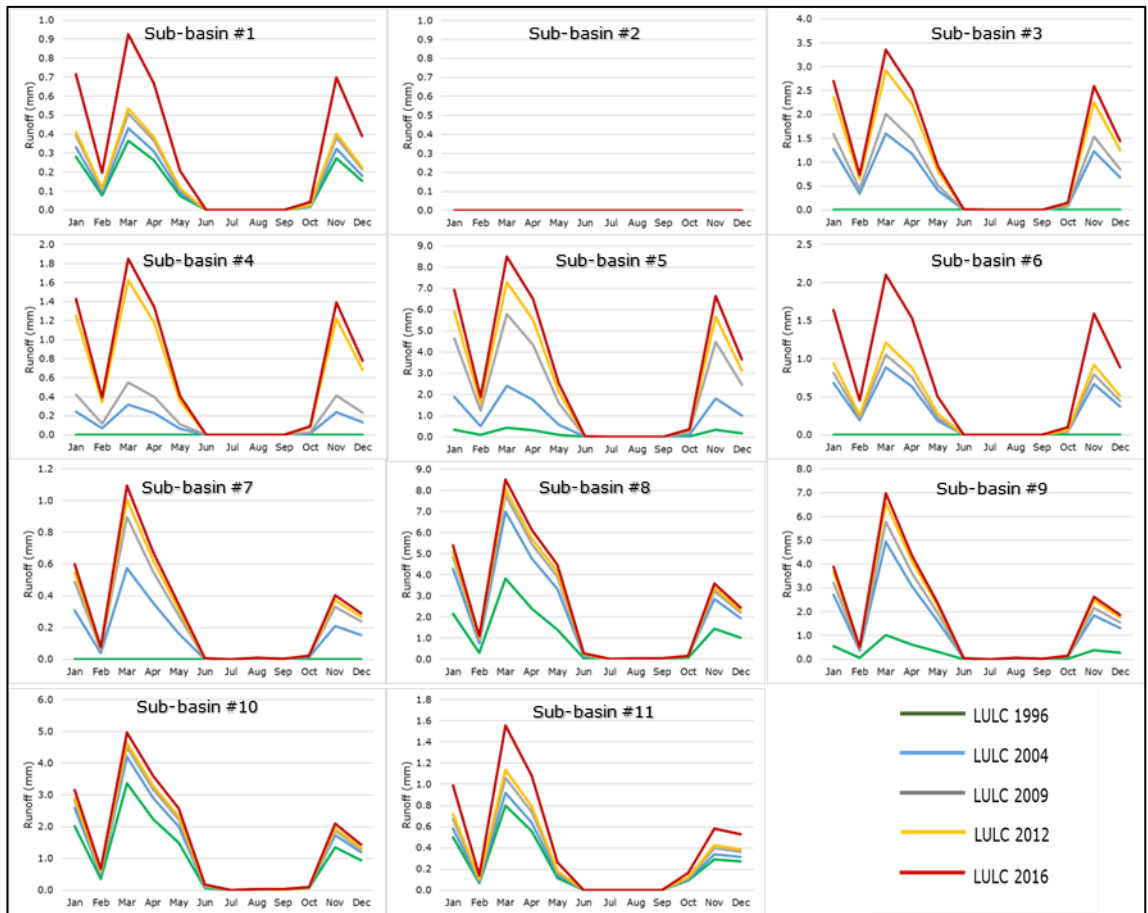


Figure 7.14: Average simulated monthly runoff using different LULC scenarios for sub-basins of the Wadi As Silayy catchment.

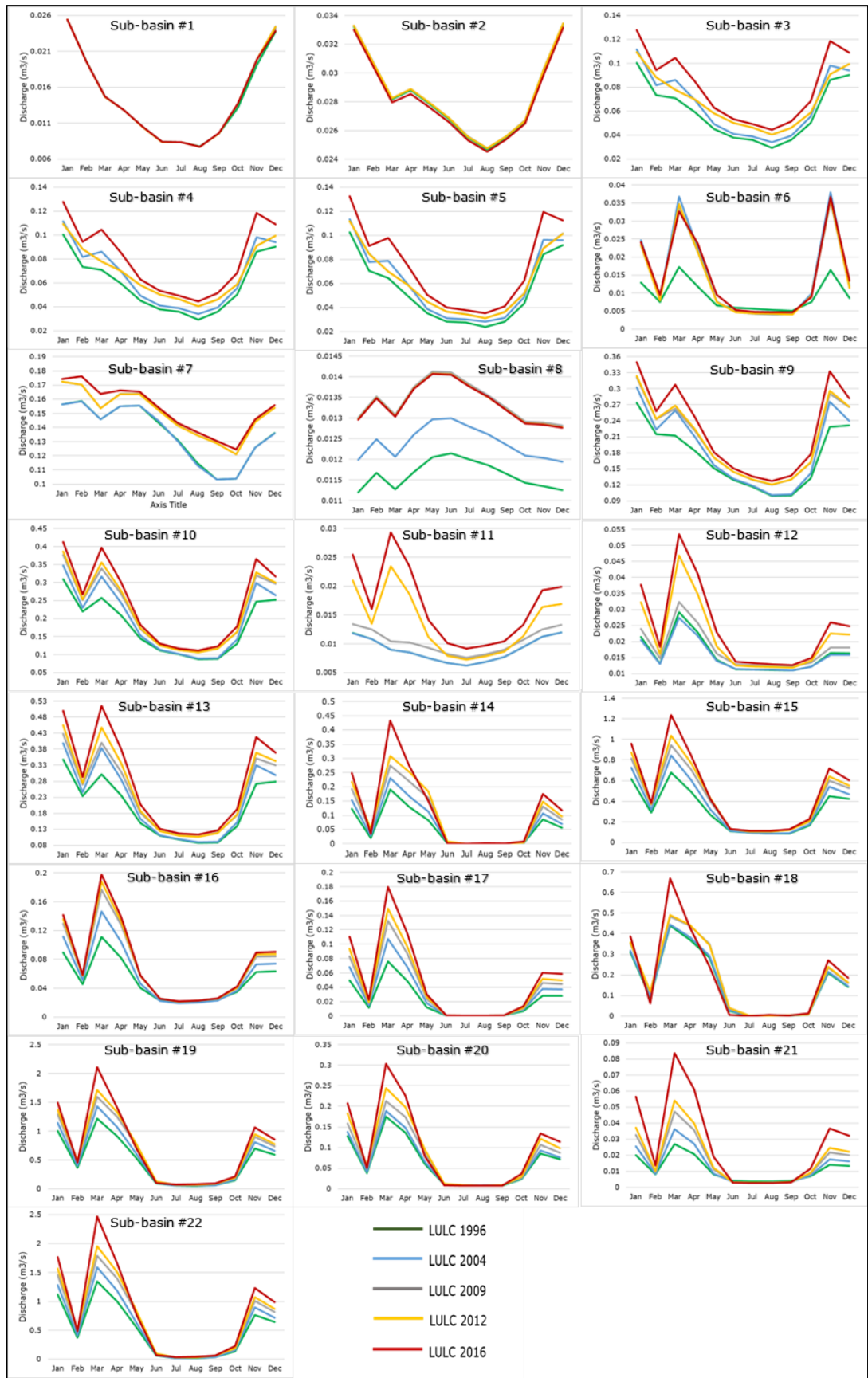


Figure 7.15: Average simulated monthly discharge using different LULC scenarios for sub-basins of the Wadi Hanifah catchment.

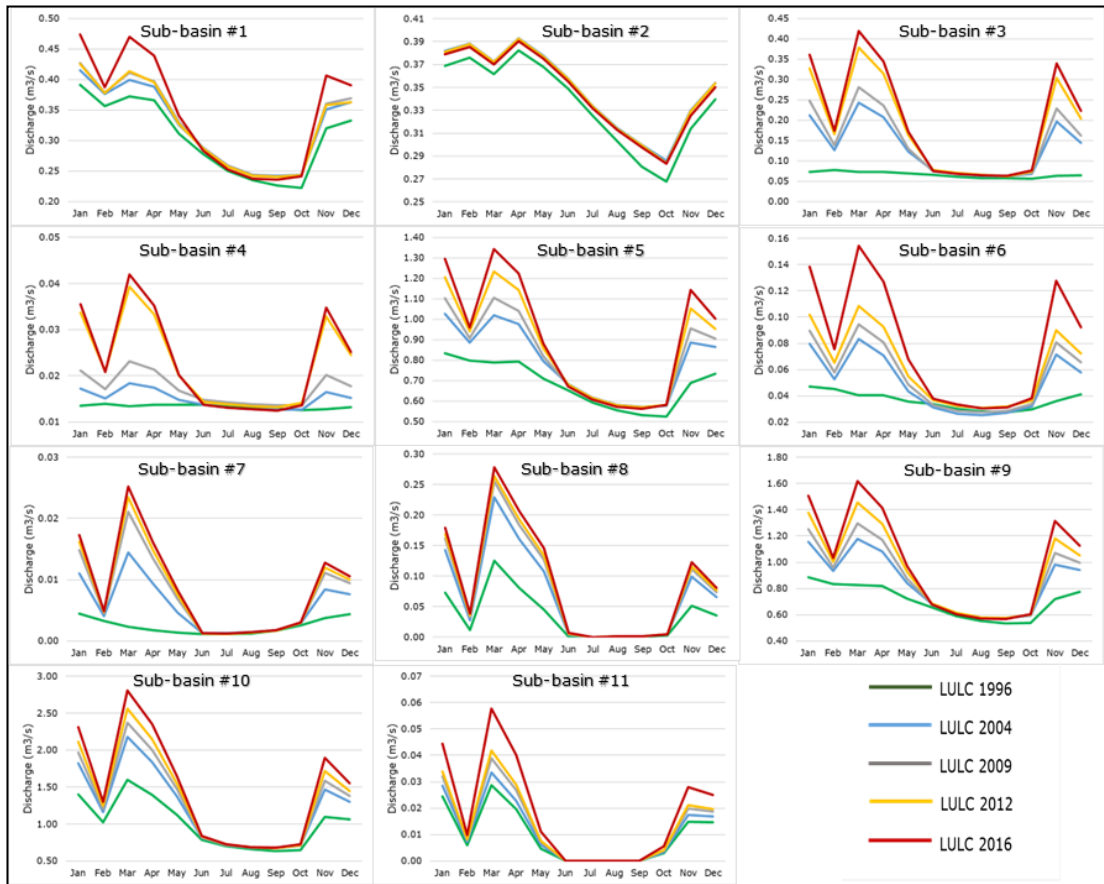


Figure 7.16: Average simulated monthly discharge using different LULC scenarios for sub-basins of the Wadi As Silayy catchment.

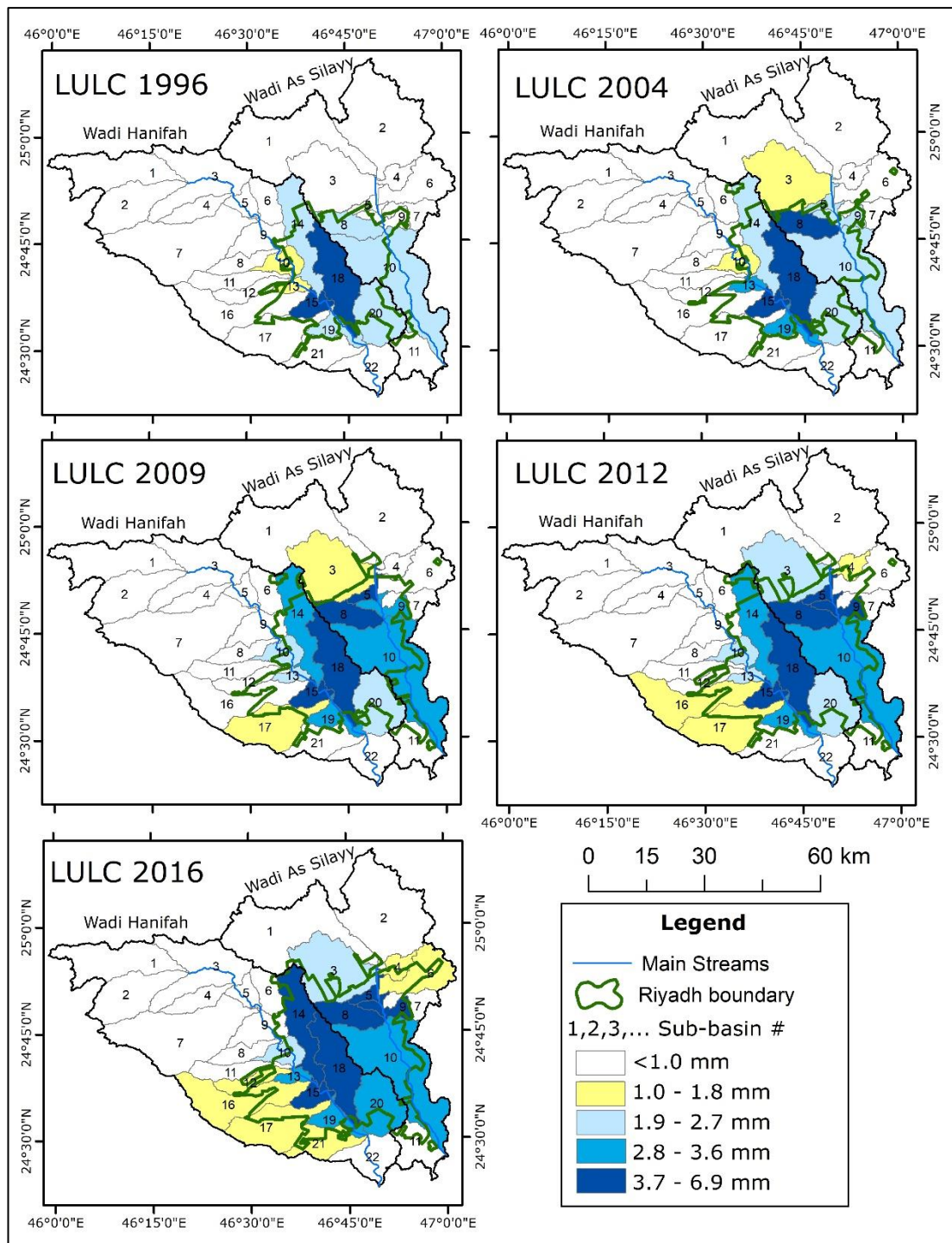


Figure 7.17: Spatial distributions of average simulated runoff for January using different LULC scenarios at Riyadh's catchments.

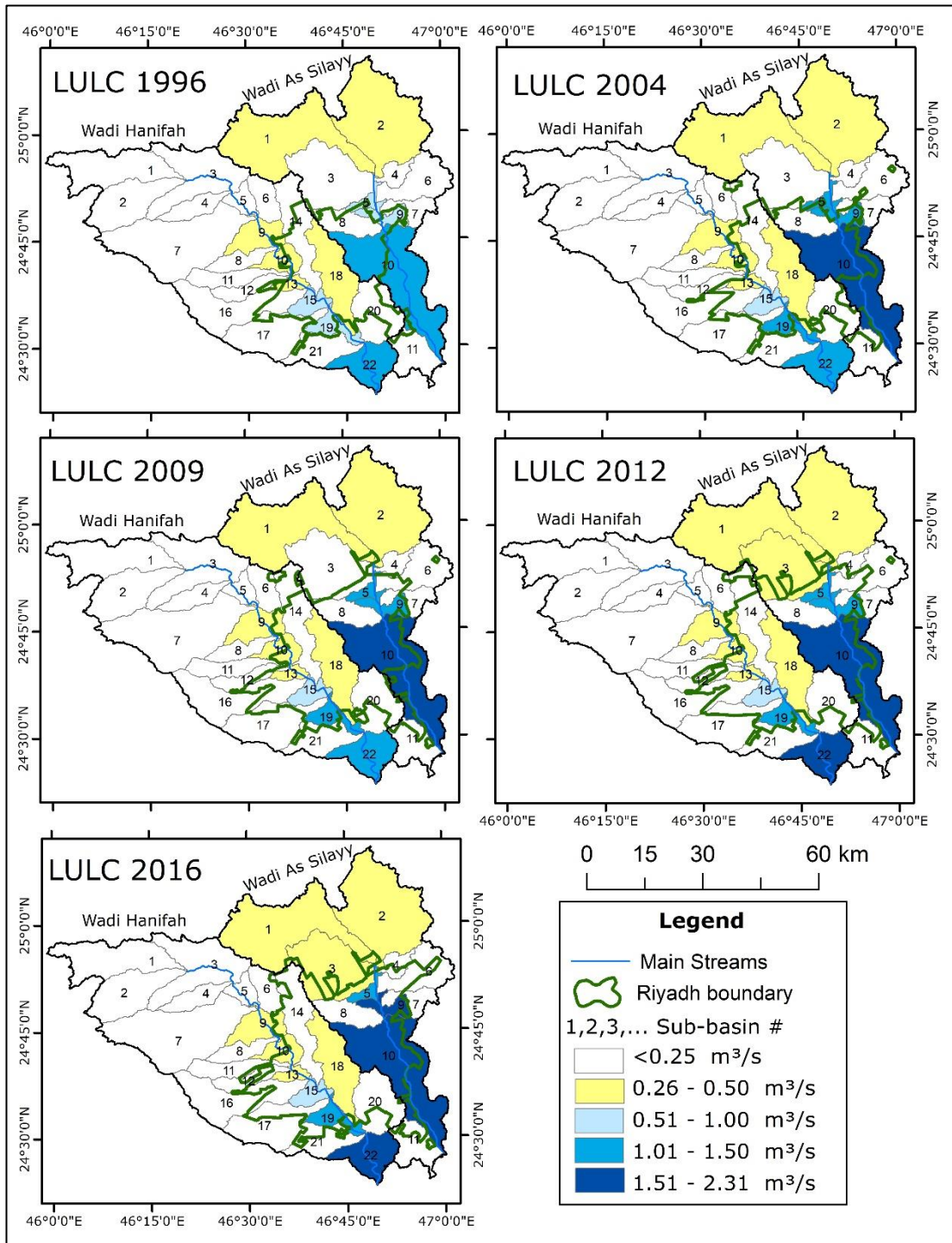


Figure 7.18: Spatial distributions of average discharge for January using different LULC scenarios at Riyadh's catchments.

7.6. Modelling annual maximum daily runoff

7.6.1. Modelling annual maximum daily runoff on catchments level

In arid regions, it is typical for relatively few rainfall events to dominate annual rainfall statistics, where a single day of rainfall can exceed half of the annual average (Warner 2004). Therefore, simulations of daily surface runoff can reveal extreme daily runoff. When short-duration, intense rainfall conditions are combined with impervious surfaces, the potential for urban flooding can be significant. To reduce the negative impacts of urbanisation on surface runoff in such an arid environment, estimation of the potential for extreme surface runoff is essential to focus on sustainable management, decreasing runoff hazards.

Since discharge rates of sub-basins in the lower reaches of the catchments represent discharge rates of the whole catchment, an explanation of discharge rates in the study area will be presented in section 7.6.2. below to avoid repetition. Table 7.15 shows simulated runoff values in the Wadi Hanifah and the Wadi As Silayy catchments for the period 1965-2000. Their return periods (recurrence intervals) were calculated. The ranked return period, in years, equals the number of years in a data set plus one, divided by the rank number of the value for which the return period is to be calculated. For both catchments of the Wadi Hanifa and the Wadi As Silayy, the highest simulated annual maximum daily runoff values were found to be in 1996 with a rank of the 37-year return period. The lowest simulated annual maximum daily runoff and discharge values were found to be in 1981 with a rank of the 1-year return period.

Figure 7.19 is a plot of simulated values of annual maximum daily runoff using the two different scenarios of LULC (1996 and 2016).

Comparison of simulated values in the Table and the plotted lines in the Figure clarify the impact of LULC change on simulated annual maximum daily surface runoff for the 20 years extending from 1996 to 2016. It is obvious that LULC changes have significantly increased runoff in the two main catchments of Riyadh city. For example, compared to runoff values when using LULC 1996 scenario, the simulated runoff increased when using the LULC 2016 scenario by a percentage ranging from 50% to 100% in the Wadi Hanifah catchment and by a percentage ranging from 100% to 200% in the Wadi As Silayy catchment (Figure 7.20).

Table 7.15: SWAT model simulations of annual maximum daily surface runoff using different LULC scenarios for Riyadh's catchments.

Year	Rank	Return Period	Rainfall (mm)	Wadi Hanifah SURQ (mm)					Wadi As Silayy SURQ (mm)				
				LULC 1996	LULC 2004	LULC 2009	LULC 2012	LULC 2016	LULC 1996	LULC 2004	LULC 2009	LULC 2012	LULC 2016
1965	3	12.3	38.2	2.4	2.9	3.3	3.6	4.1	1.7	3.0	3.4	3.9	4.4
1966	32	1.2	8.6	0.3	0.4	0.5	0.5	0.6	0.2	0.4	0.5	0.5	0.6
1967	12	3.1	23.7	1.4	1.6	1.9	2.0	2.3	1.0	1.7	1.9	2.2	2.5
1968	2	18.5	47.2	3.1	3.7	4.2	4.6	5.2	2.2	3.8	4.4	4.9	5.7
1969	14	2.6	22.2	1.3	1.5	1.7	1.9	2.1	0.9	1.6	1.8	2.0	2.3
1970	35	1.1	5.6	0.2	0.2	0.2	0.2	0.3	0.1	0.2	0.2	0.3	0.3
1971	15	2.5	22	1.2	1.5	1.7	1.9	2.1	0.9	1.5	1.8	2.0	2.3
1972	7	5.3	31	1.9	2.3	2.6	2.8	3.2	1.3	2.3	2.7	3.0	3.5
1973	30	1.2	11.4	0.5	0.6	0.7	0.8	0.9	0.4	0.6	0.7	0.8	0.9
1974	26	1.4	14	0.7	0.8	0.9	1.0	1.2	0.5	0.8	1.0	1.1	1.3
1975	8	4.6	31	1.9	2.3	2.6	2.8	3.2	1.3	2.3	2.7	3.0	3.5
1976	18	2	20	1.1	1.3	1.5	1.7	1.9	0.8	1.4	1.6	1.8	2.0
1977	34	1.1	8.3	0.3	0.4	0.4	0.5	0.5	0.2	0.4	0.5	0.5	0.6
1978	4	9.2	34.2	2.1	2.5	2.9	3.2	3.6	1.5	2.6	3.0	3.4	3.9
1979	24	1.5	14.5	0.7	0.9	1.0	1.1	1.2	0.5	0.9	1.0	1.2	1.3
1980	13	2.8	22.5	1.3	1.5	1.8	1.9	2.2	0.9	1.6	1.8	2.0	2.4
1981	36	1	5	0.1	0.2	0.2	0.2	0.2	0.1	0.2	0.2	0.2	0.2
1982	17	2.2	20.7	1.2	1.4	1.6	1.7	1.9	0.8	1.4	1.6	1.8	2.1
1983	20	1.9	19.5	1.1	1.3	1.5	1.6	1.8	0.8	1.3	1.5	1.7	2.0
1984	9	3.9	30	1.8	2.2	2.5	2.7	3.1	1.3	2.2	2.6	2.9	3.4
1985	6	6.2	32	2.0	2.4	2.7	2.9	3.3	1.4	2.4	2.8	3.1	3.6
1986	21	1.8	18.2	1.0	1.2	1.3	1.5	1.6	0.7	1.2	1.4	1.6	1.8
1987	11	3.4	28	1.7	2.0	2.3	2.5	2.8	1.2	2.1	2.4	2.7	3.1
1988	25	1.5	14.2	0.7	0.8	1.0	1.1	1.2	0.5	0.9	1.0	1.1	1.3
1989	16	2.3	21	1.2	1.4	1.6	1.8	2.0	0.8	1.4	1.7	1.9	2.2
1990	31	1.2	9	0.4	0.4	0.5	0.5	0.6	0.3	0.4	0.5	0.6	0.7
1991	29	1.3	11.6	0.5	0.6	0.7	0.8	0.9	0.4	0.7	0.8	0.8	1.0
1992	27	1.4	12.6	0.6	0.7	0.8	0.9	1.0	0.4	0.7	0.8	0.9	1.1
1993	10	3.9	30	1.8	2.1	2.5	2.6	3.0	1.2	2.2	2.5	2.8	3.2
1994	22	1.7	17.2	0.9	1.1	1.2	1.4	1.5	0.6	1.1	1.3	1.5	1.7
1995	5	7.4	33.7	2.1	2.5	2.9	3.1	3.5	1.5	2.6	3.0	3.3	3.9
1996	1	37	53	3.5	4.2	4.8	5.2	5.9	2.5	4.3	5.0	5.6	6.5
1997	19	2	20	1.1	1.3	1.5	1.7	1.9	0.8	1.4	1.6	1.8	2.0
1998	23	1.6	17	0.9	1.1	1.2	1.3	1.5	0.6	1.1	1.3	1.4	1.6
1999	28	1.3	12	0.6	0.7	0.8	0.8	0.9	0.4	0.7	0.8	0.9	1.0
2000	33	1.1	8.5	0.3	0.4	0.4	0.5	0.6	0.2	0.4	0.5	0.5	0.6

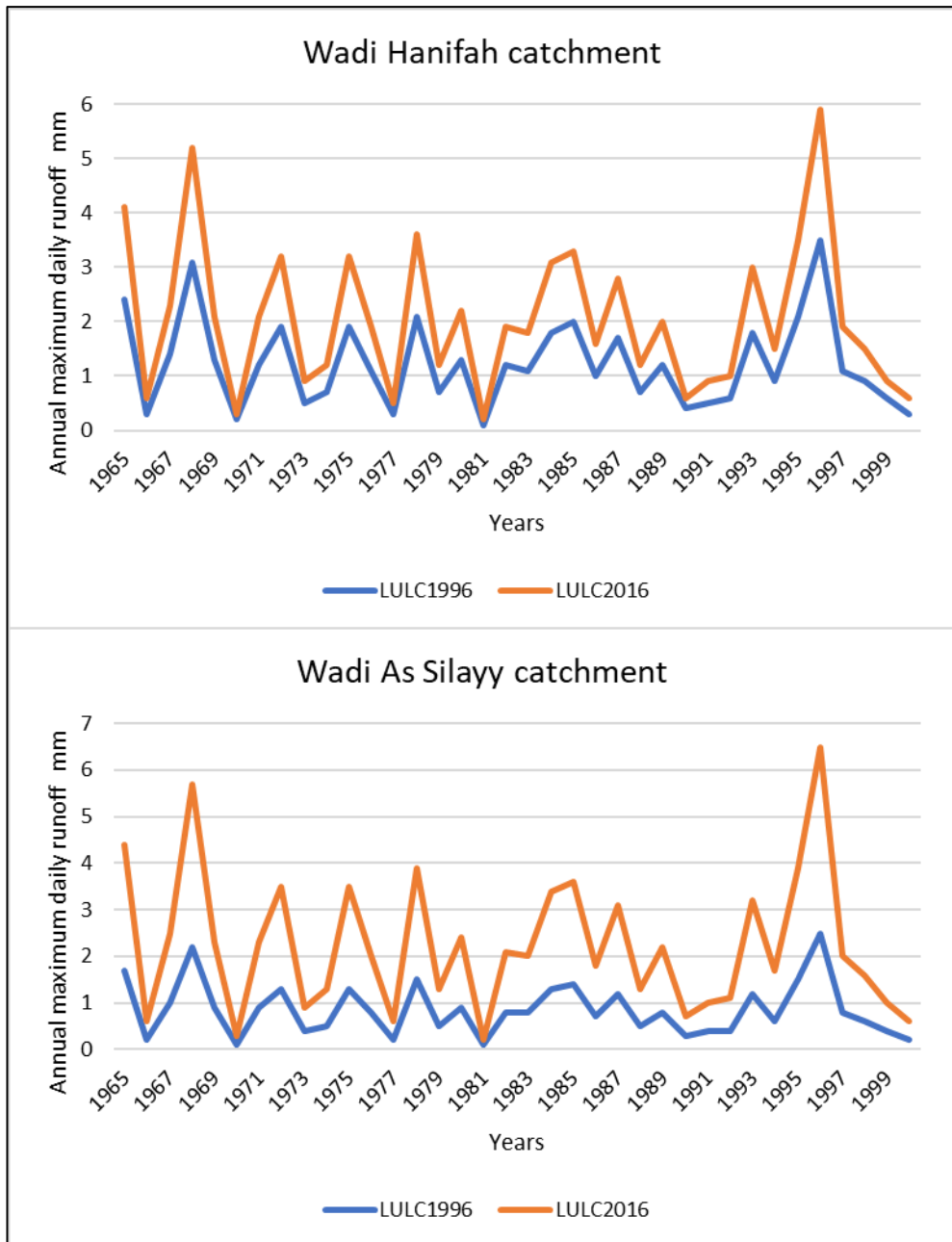


Figure 7.19: Comparison of simulated annual maximum daily runoff depths in Riyadh's catchments under LULC change for a period of 20 years using climate data 1965-2000.

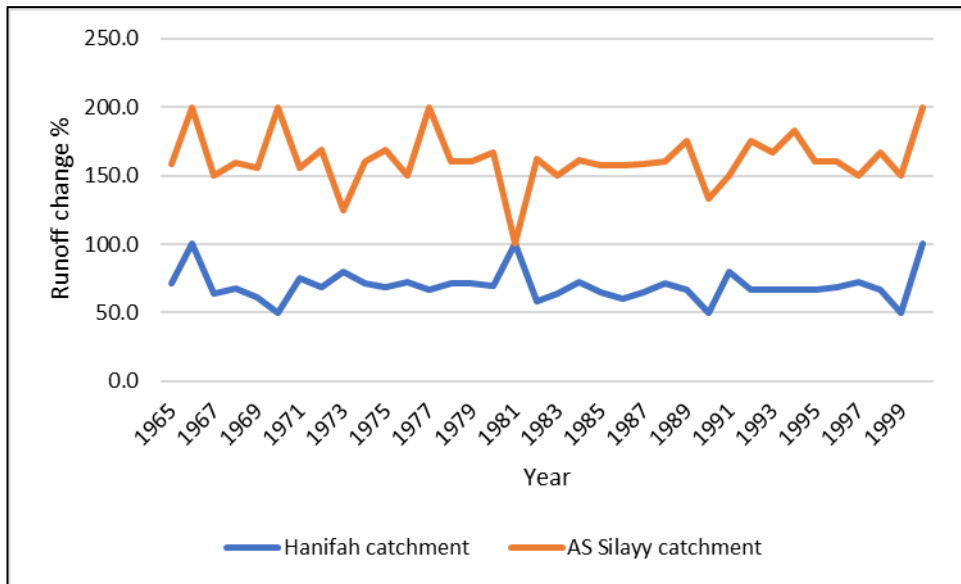


Figure 7.20: Change (%) of simulated annual maximum daily runoff values using the LULC 2016 scenario compared to their counterpart using the LULC 1996 scenario.

The EVI (Gumble) distribution was used to evaluate simulated annual maximum daily runoff and discharge on levels of main catchments and sub-basins in the study area. Frequencies of annual maximum daily runoff depths for return periods of 2-year, 5-year, 10-year, 30-year, 50-year, and 100-year were estimated in Riyadh's catchments using climate data for the period 1965-2000 and five different historical LULC scenarios (Table 7.16, Figure 7.21 and Figure 7.22). LULC change exerted a positive effect on annual maximum daily runoff depths for the various return periods. For example, the annual maximum daily runoff for the 30-year return period increased by 69% from 3.2 mm when using the LULC 1996 scenario to 5.4 mm when using the LULC 2016 scenario in the Wadi Hanifah catchment. For the same return period, the annual maximum daily runoff in the Wadi As Silayy catchment increased by 168% from 2.2 mm when using the LULC 1996 scenario to 5.9 mm when using the LULC 2016 scenario.

Table 7.16: Computed annual maximum daily runoff depth (mm) for various return periods using simulated data for the period 1965-2000 under five different historical LULC scenarios for Riyadh's catchments.

Catchment	The Wadi Hanifah catchment					The Wadi As Silayy catchment				
	2-year	10-year	30-year	50-year	100-year	2-year	10-year	30-year	50-year	100-year
LULC 1996	1.1	2.4	3.2	3.6	4.0	0.8	1.7	2.2	2.5	2.8
LULC 2004	1.3	2.9	3.8	4.3	4.9	1.3	3.0	3.9	4.4	5
LULC 2009	1.5	3.3	4.4	4.9	5.5	1.5	3.4	4.6	5.1	5.8
LULC 2012	1.6	3.6	4.8	5.3	6.1	1.7	3.8	5.1	5.7	6.5
LULC 2016	1.8	4.0	5.4	6	6.8	2.0	4.4	5.9	6.6	7.5

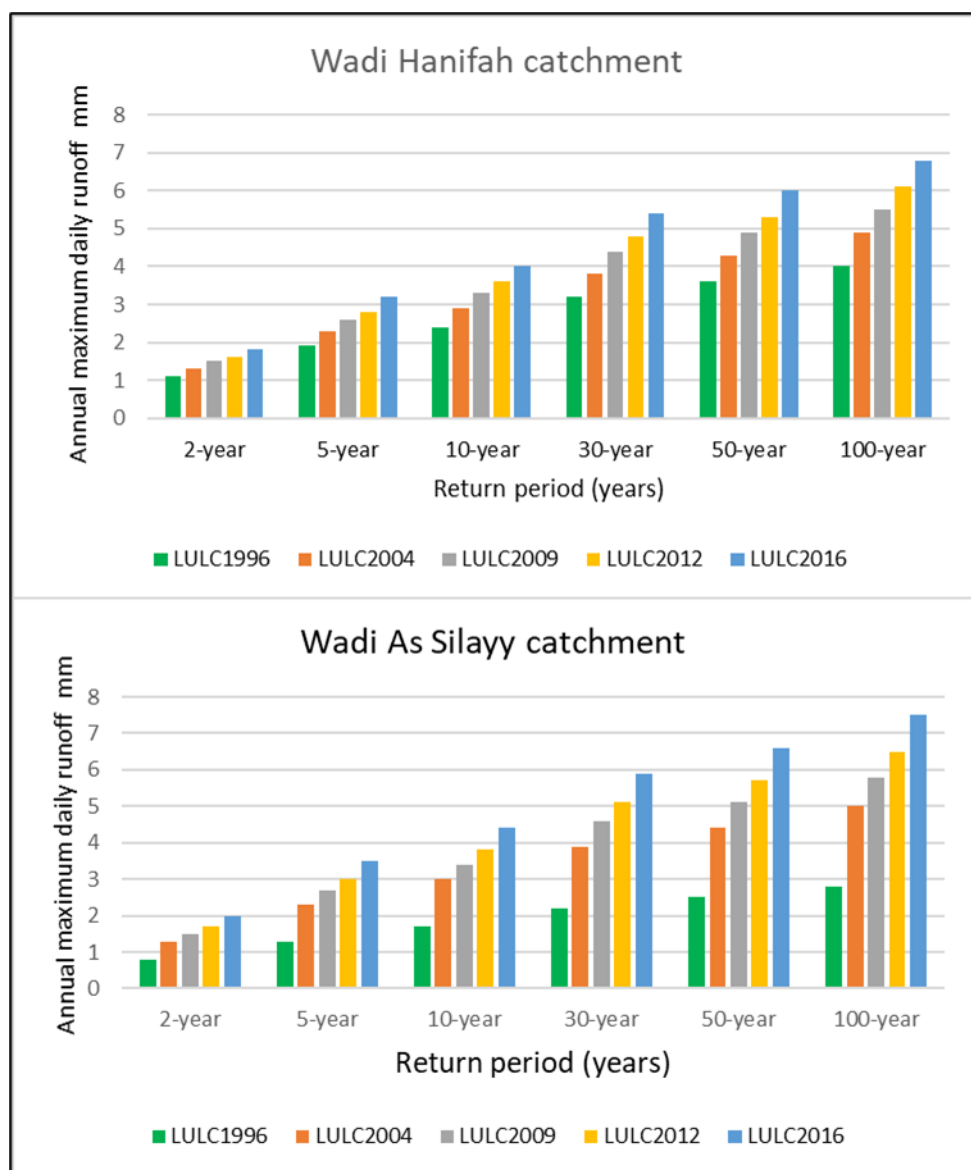


Figure 7.21: Annual maximum daily runoff depth in various return periods under five different historical LULC scenarios for Riyadh's catchments.

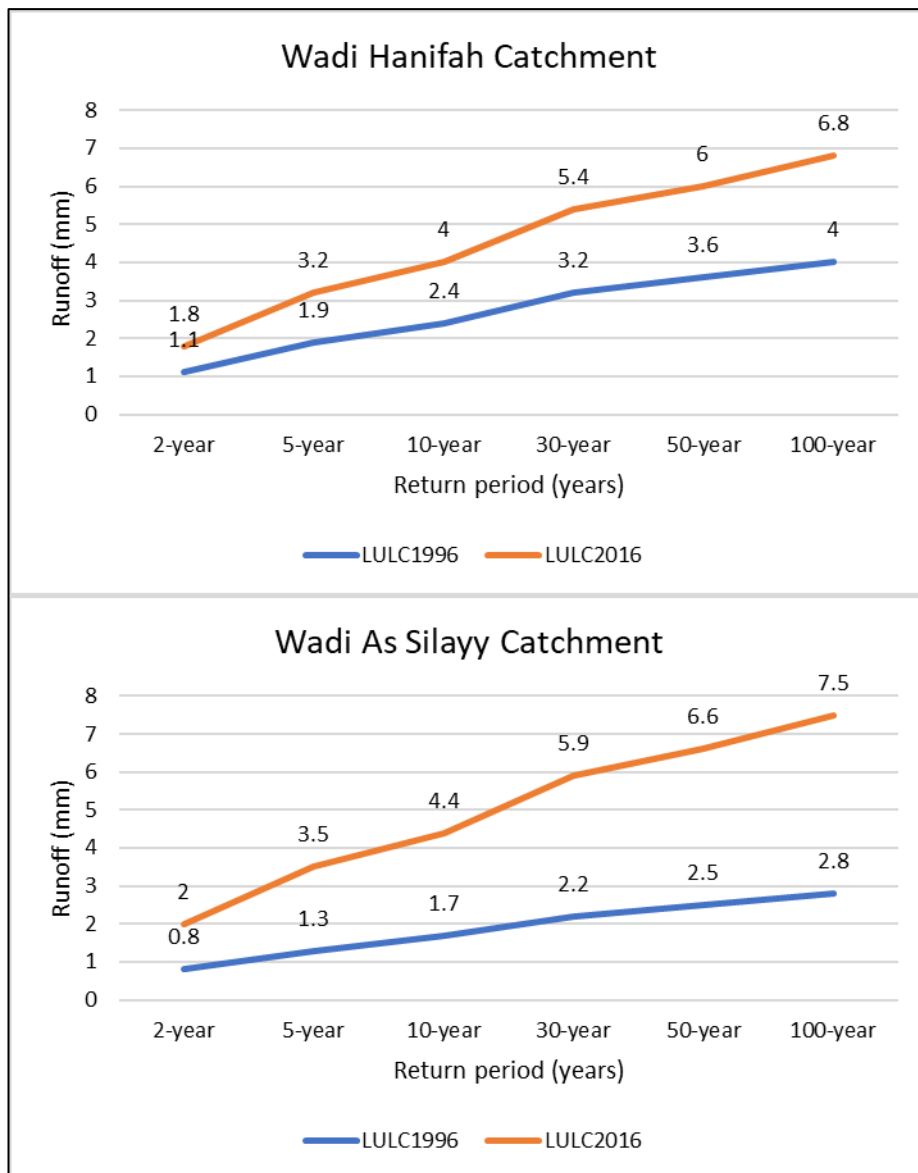


Figure 7.22: Simulated impact on runoff of LULC change between 1996 and 2016 for various return periods for Riyadh’s catchments.

The percentile was also used as an additional method to evaluate simulated annual maximum daily runoff and discharge on levels of main catchments and sub-basins in the study area. Simulated values of annual maximum daily runoff and discharge in all sub-basins of the study area were ranked in order from smallest to largest to calculate percentiles. The percentile is expressed as a certain percentage of scores that fall below that given number in the set of data. The per cent exceedance (Q_n) is obtained by subtracting the percentile scale value from 100 per cent (USGS n.d.). The percent

exceedance of Q1, Q25, Q50, Q85, and Q99 of simulated annual maximum daily runoff values were computed using data for the period 1965-2000 under five different historical LULC scenarios in Riyadh’s catchments (Table 7.17). Data in Table 7.17 were plotted to ease the visualisation of the positive impact of LULC changes on runoff in Riyadh (Figure 7.23 and Figure 7.24).

Table 7.17: Percent exceedance of simulated annual maximum daily runoff (mm) using data for the period 1965-2000 for five different historical LULC scenarios for Riyadh’s catchments.

Catchment	The Wadi Hanifah catchment					The Wadi As Silayy catchment				
	Q1	Q25	Q50	Q85	Q99	Q1	Q25	Q50	Q85	Q99
LULC 1996	3.4	1.8	1.1	0.4	0.1	2.4	1.2	0.8	0.3	0.1
LULC 2004	4.0	2.1	1.3	0.5	0.2	4.1	2.2	1.4	0.5	0.2
LULC 2009	4.6	2.5	1.5	0.6	0.2	4.8	2.5	1.6	0.6	0.2
LULC 2012	5.0	2.6	1.7	0.6	0.2	5.4	2.8	1.8	0.7	0.2
LULC 2016	5.7	3.0	1.9	0.7	0.2	6.2	3.3	2.0	0.8	0.2

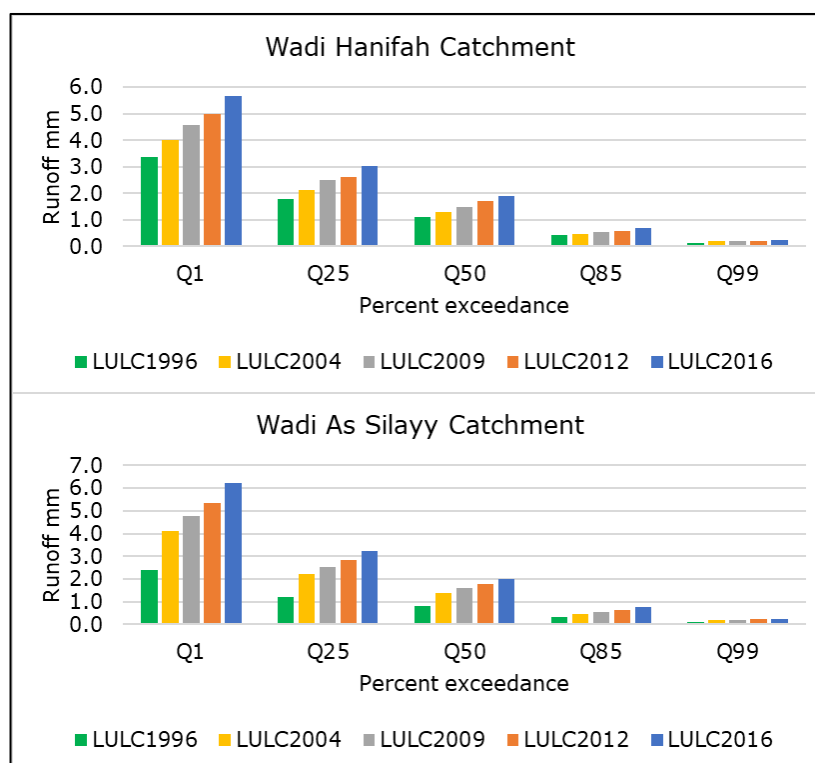


Figure 7.23: Percent exceedance of simulated annual maximum daily runoff in Riyadh’s catchments under five different historical LULC scenarios.

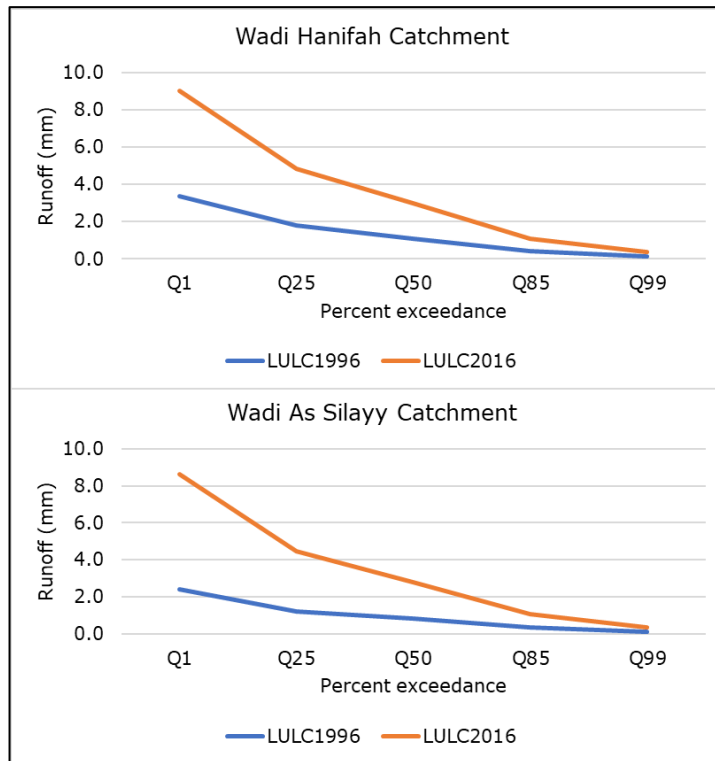


Figure 7.24: Impact of LULC change for 20 years period on percent exceedance of simulated annual maximum daily runoff in Riyadh's catchments.

Comparison of results of using the LULC 1996 and LULC 2016 scenarios can highlight the impact of LULC change for a 20-year period on simulated annual maximum daily runoff in Riyadh's catchments. A remarkable example of the impact of LULC change in the city is that the estimated runoff for the 100-year return period using LULC 1996 is equivalent to the estimated runoff for the 10-year return period using LULC 2016 in the Wadi Hanifah catchment. For the Wadi As Silayy catchment, a striking example is that the estimated 3.5 mm runoff for the 5-year return period using the LULC 2016 scenario is much greater than the runoff value (2.8 mm) for the 100-year return period using the LULC 1996.

Other examples of LULC change's impact on runoff are provided. Estimated annual maximum daily runoff values of the 2-year calculated return period in the Wadi Hanifah catchment ranged from 1.1 mm when using the LULC 1996 scenario to 1.8 mm when using

the LULC 2016 scenario, which increased by about 64%. For the Wadi As Silayy catchment, the 2-year calculated return period of annual maximum daily runoff values increased from 0.8 mm when using the LULC 1996 scenario to 2 mm when using the LULC 2016 scenario with an increase of about 150%. The annual maximum daily runoff values of the 30-year return period were estimated to be 5.4 mm for the Wadi Hanifah and 5.9 mm for the Wadi As Silayy when using the LULC 2016 scenario.

On the other hand, when using the LULC 1996 scenario, the Q99 values were 0.1 mm in the two catchments, while the Q1 values were 3.5 mm and 2.5 mm in the Wadi Hanifah catchment and the Wadi As Silayy catchment respectively. But the values of runoff of Q1 and Q99 nearly doubled in the two catchments of the study area when using the LULC 2016 scenario. It was 0.2 mm for the Q99 for the two catchments, whereas, for Q1, it was 5.9 mm in the Wadi Hanifah catchment and 6.5 mm in the Wadi As Silayy catchment. As mentioned above in section 7.2, the built-up area of Riyadh city was estimated to be 1200 km² in 2017 and reached more than 1500 km² in 2020. Thus, currently, these values of runoff depth could be much higher due to the increase of impervious surfaces in Riyadh's catchments.

7.6.2. Modelling annual maximum daily runoff on sub-basins level

Return periods and percent exceedances were also calculated for the 33 sub-basins individually, presented in Table 7.18 to 7.37. Figure 7.25 and Figure 7.26 illustrate the impact of LULC change between 1996 and 2016 on simulated annual maximum daily runoff and discharge for the 30-year return period on the sub-basins level of Riyadh's catchments. The calculated return periods and the per cent

exceedances showed a positive impact of LULC change. For example, the 2-year return period of simulated runoff in sub-basin 18 in the Wadi Hanifah catchment increased from 1.0 mm when using LULC 1996 to reach 2.9 mm when using LULC 2016. The 2-year return period of simulated runoff in sub-basin 9 in the Wadi As Silayy catchment increased from 0.4 mm when using LULC 1996 to be 2.3 mm when using LULC 2016. On the other hand, the 2-year return period of simulated discharge in sub-basin 18 in the Wadi Hanifah catchment increased from 1.7 m³/s when using LULC 1996 to reach 5.3 m³/s when using LULC 2016. The 2-year return period of simulated discharge in sub-basin 9 in the Wadi As Silayy catchment increased from 0.5 m³/s when using LULC 1996 to be 6.0 m³/s when using LULC 2016.

Table 7.18: EVI distribution estimates and the percent exceedances of annual maximum daily runoff (mm) using LULC 1996 scenario for sub-basins of the Wadi Hanifah catchment.

Sub-basin	EVI estimates of runoff frequency					Percent exceedances of runoff				
	2 Year	10 Year	30 Year	50 Year	100 Year	Q1	Q25	Q50	Q85	Q99
1	0	0	0	0	0	0	0	0	0	0
2	0	0	0	0	0	0	0	0	0	0
3	0.1	0.3	0.4	0.4	0.5	0.38	0.2	0.12	0.05	0.04
4	0	0	0	0	0	0	0	0	0	0
5	0	0	0	0	0	0	0	0	0	0
6	0.3	0.6	0.8	0.9	1.1	0.86	0.44	0.28	0.11	0.09
7	0	0	0	0	0	0	0	0	0	0
8	0	0	0	0	0	0	0	0	0	0
9	0.4	0.8	1.1	1.2	1.4	1.11	0.58	0.37	0.14	0.12
10	1.2	2.7	3.6	4.0	4.6	3.72	1.92	1.22	0.49	0.4
11	0	0	0	0	0	0	0	0	0	0
12	0.4	0.8	1.1	1.2	1.4	1.1	0.57	0.36	0.15	0.12
13	1.1	2.4	3.2	3.5	4.0	3.27	1.68	1.07	0.43	0.36
14	0.7	1.6	2.1	2.4	2.7	2.21	1.1	0.7	0.3	0.25
15	2.1	5.0	6.6	7.4	8.4	6.84	3.48	2.22	0.96	0.8
16	0.5	1.0	1.4	1.5	1.7	1.45	0.75	0.47	0.19	0.16
17	0.5	1.1	1.4	1.6	1.8	1.46	0.74	0.48	0.2	0.16
18	1.0	2.3	3.1	3.4	3.9	3.15	1.57	0.95	0.42	0.35
19	1.4	3.1	4.1	4.6	5.2	4.23	2.13	1.36	0.59	0.49
20	0.9	2.0	2.6	2.9	3.3	2.69	1.36	0.87	0.37	0.31
21	0.3	0.6	0.8	0.9	1.1	0.85	0.43	0.28	0.11	0.09
22	0	0	0	0	0	0	0	0	0	0

Table 7.19: EVI distribution estimates and percent exceedances of annual maximum daily runoff (mm) using LULC 2004 scenario for sub-basins of the Wadi Hanifah catchment.

Sub-basin	EVI estimates of runoff frequency					Percent exceedances of runoff				
	2 Year	10 Year	30 Year	50 Year	100 Year	Q1	Q25	Q50	Q85	Q99
1	0	0	0	0	0	0	0	0	0	0
2	0	0	0	0	0	0	0	0	0	0
3	0.3	0.4	0.5	0.6	0.7	0.58	0.3	0.19	0.07	0.06
4	0	0	0	0	0	0	0	0	0	0
5	0	0	0	0	0	0	0	0	0	0
6	0.6	1.3	1.7	1.9	2.2	1.81	0.9	0.6	0.24	0.2
7	0	0	0	0	0	0	0	0	0	0
8	0	0	0	0	0	0	0	0	0	0
9	0.6	1.3	1.8	2.0	2.3	1.86	0.97	0.61	0.24	0.2
10	1.4	3.2	4.2	4.7	5.3	4.36	2.23	1.43	0.58	0.48
11	0	0	0	0	0	0	0	0	0	0
12	0.3	0.8	1.0	1.1	1.3	1.07	0.55	0.35	0.14	0.12
13	2.1	4.8	6.3	7.1	8.0	6.57	3.36	2.15	0.89	0.73
14	0.8	1.8	2.4	2.6	3.0	2.43	1.21	0.77	0.33	0.28
15	2.2	5.0	6.7	7.5	8.5	6.9	3.48	2.22	0.96	0.81
16	0.6	1.4	1.9	2.1	2.4	1.97	1.01	0.65	0.26	0.22
17	0.6	1.3	1.8	2.0	2.3	1.86	0.93	0.6	0.25	0.21
18	1.0	2.4	3.1	3.5	4.0	3.24	1.62	0.99	0.43	0.37
19	1.5	3.5	4.6	5.2	5.9	4.78	2.41	1.54	0.66	0.56
20	0.9	2.1	2.8	3.1	3.5	2.87	1.45	0.93	0.4	0.33
21	0.4	0.9	1.2	1.4	1.5	1.26	0.64	0.41	0.17	0.14
22	0.2	0.3	0.4	0.5	0.6	0.47	0.24	0.16	0.06	0.05

Table 7.20: EVI distribution estimates and percent exceedances of annual maximum daily runoff (mm) using LULC 2009 scenario for sub-basins of the Wadi Hanifah catchment.

Sub-basin	EVI estimates of runoff frequency					Percent exceedances of runoff				
	2 Year	10 Year	30 Year	50 Year	100 Year	Q1	Q25	Q50	Q85	Q99
1	0	0	0	0	0	0	0	0	0	0
2	0	0	0	0	0	0	0	0	0	0
3	0.1	0.2	0.2	0.3	0.3	0.17	0.09	0.05	0.02	0.02
4	0	0	0	0	0	0	0	0	0	0
5	0	0	0	0	0	0	0	0	0	0
6	0.5	1.1	1.5	1.7	1.9	1.59	0.81	0.53	0.21	0.18
7	0	0	0	0	0	0	0	0	0	0
8	0	0	0	0	0	0	0	0	0	0
9	0.7	1.6	2.2	2.4	2.8	2.24	1.18	0.73	0.29	0.24
10	1.7	3.8	5.1	5.7	6.4	5.24	2.73	1.71	0.7	0.58
11	0	0	0	0	0	0	0	0	0	0
12	0.4	0.9	1.2	1.4	1.6	1.27	0.67	0.42	0.17	0.14
13	1.5	3.4	4.6	5.1	5.8	4.69	2.42	1.53	0.64	0.53
14	0.8	1.9	2.5	2.8	3.2	2.59	1.3	0.81	0.35	0.3
15	2.4	5.4	7.2	8.0	9.2	7.38	3.73	2.37	1.03	0.86
16	0.7	1.6	2.1	2.4	2.7	2.2	1.14	0.72	0.3	0.24
17	0.7	1.6	2.1	2.3	2.6	2.16	1.09	0.7	0.3	0.25
18	1.1	2.5	3.3	3.7	4.2	3.37	1.71	1.03	0.45	0.38
19	1.5	3.5	4.6	5.2	5.9	4.77	2.37	1.52	0.66	0.56
20	0.9	2.2	2.9	3.2	3.7	2.96	1.47	0.95	0.41	0.34
21	0.5	1.2	1.6	1.7	2.0	1.61	0.83	0.53	0.22	0.18
22	0.1	0.3	0.5	0.5	0.6	0.45	0.24	0.15	0.06	0.05

Table 7.21: EVI distribution estimates and percent exceedances of annual maximum daily runoff (mm) using LULC 2012 scenario for sub-basins of the Wadi Hanifah catchment.

Sub-basin	EVI estimates of runoff frequency					Percent exceedances of runoff				
	2 Year	10 Year	30 Year	50 Year	100 Year	Q1	Q25	Q50	Q85	Q99
1	0	0	0	0	0	0	0	0	0	0
2	0	0	0	0	0	0	0	0	0	0
3	0.1	0.2	0.2	0.3	0.3	0.17	0.09	0.05	0.02	0.02
4	0	0	0	0	0	0	0	0	0	0
5	0	0	0	0	0	0	0	0	0	0
6	0.5	1.2	1.6	1.8	2.0	1.63	0.82	0.54	0.22	0.18
7	0	0	0	0	0	0	0	0	0	0
8	0	0	0	0	0	0	0	0	0	0
9	0.8	1.8	2.4	2.7	3.1	2.51	1.29	0.82	0.32	0.27
10	1.9	4.2	5.6	6.2	7.1	5.8	2.95	1.89	0.78	0.65
11	0.2	0.5	0.6	0.7	0.8	0.66	0.34	0.22	0.09	0.07
12	0.6	1.4	1.9	2.1	2.4	1.92	0.97	0.63	0.26	0.21
13	1.7	3.8	4.9	5.4	6.2	5.05	2.54	1.64	0.69	0.57
14	0.9	2.1	2.9	3.2	3.6	2.91	1.47	0.92	0.39	0.33
15	2.4	5.4	7.2	8.0	9.1	7.4	3.74	2.38	1.03	0.86
16	0.8	1.7	2.3	2.6	2.9	2.39	1.21	0.78	0.32	0.27
17	0.8	1.7	2.3	2.5	2.9	2.33	1.18	0.76	0.32	0.27
18	1.1	2.5	3.3	3.7	4.2	3.38	1.7	1.03	0.45	0.38
19	1.5	3.5	4.7	5.2	6.0	4.83	2.4	1.54	0.66	0.56
20	1.1	2.4	3.2	3.6	4.1	3.3	1.64	1.05	0.45	0.38
21	0.6	1.3	1.8	2.0	2.2	1.81	0.92	0.59	0.24	0.2
22	0.3	0.6	0.8	0.9	1.0	0.84	0.43	0.27	0.11	0.09

Table 7.22: EVI distribution estimates and percent exceedances of annual maximum daily runoff (mm) using LULC 2016 scenario for sub-basins of the Wadi Hanifah catchment.

Sub-basin	EVI estimates of runoff frequency					Percent exceedances of runoff				
	2 Year	10 Year	30 Year	50 Year	100 Year	Q1	Q25	Q50	Q85	Q99
1	0	0	0	0	0	0	0	0	0	0
2	0	0	0	0	0	0	0	0	0	0
3	0.2	0.5	0.6	0.7	0.8	0.65	0.33	0.21	0.08	0.07
4	0	0	0	0	0	0	0	0	0	0
5	0.1	0.2	0.3	0.3	0.4	0.26	0.14	0.09	0.03	0.03
6	0.4	0.9	1.2	1.4	1.6	1.24	0.64	0.41	0.17	0.14
7	0	0	0	0	0	0	0	0	0	0
8	0	0	0	0	0	0	0	0	0	0
9	0.9	1.9	2.5	2.8	3.2	2.64	1.36	0.86	0.34	0.28
10	2.0	4.5	6.0	6.6	7.5	6.16	3.14	2.01	0.82	0.68
11	0.3	0.6	0.8	0.9	1.0	0.84	0.44	0.28	0.11	0.09
12	0.5	1.1	1.5	1.7	1.9	1.57	0.8	0.51	0.22	0.18
13	1.9	4.2	5.6	6.3	7.1	5.81	2.98	1.89	0.81	0.67
14	2.2	4.9	6.5	7.2	8.2	6.67	3.41	2.18	0.93	0.77
15	2.2	4.9	6.6	7.3	8.3	6.76	3.37	2.16	0.93	0.79
16	0.9	2.0	2.7	3.0	3.4	2.8	1.45	0.92	0.37	0.31
17	1.0	2.3	3.0	3.4	3.9	3.12	1.57	1.01	0.42	0.35
18	2.9	6.4	8.8	9.5	10.9	8.8	4.51	2.88	1.23	1.02
19	0.8	1.7	2.3	2.6	3.0	2.36	1.18	0.71	0.31	0.26
20	1.9	4.3	5.7	6.3	7.2	5.85	2.98	1.93	0.81	0.67
21	0.8	1.9	2.5	2.8	3.2	2.55	1.28	0.83	0.35	0.29
22	0.6	1.3	1.8	2.0	2.2	1.82	0.92	0.59	0.24	0.2

Table 7.23: EVI distribution estimates and percent exceedances of annual maximum daily runoff (mm) using LULC 1996 scenario for sub-basins of the Wadi As Silayy catchment.

Sub-basin	EVI estimates of runoff frequency					Percent exceedances of runoff				
	2 Year	10 Year	30 Year	50 Year	100 Year	Q1	Q25	Q50	Q85	Q99
1	0.2	0.4	0.5	0.6	0.7	0.52	0.27	0.17	0.07	0.06
2	0	0	0	0	0	0	0	0	0	0
3	0	0	0	0	0	0	0	0	0	0
4	0	0	0	0	0	0	0	0	0	0
5	0.2	0.4	0.6	0.6	0.7	0.55	0.28	0.18	0.07	0.06
6	0	0	0	0	0	0	0	0	0	0
7	0	0	0	0	0	0	0	0	0	0
8	1.1	2.4	3.3	3.6	4.2	3.33	1.7	1.08	0.46	0.38
9	0.4	0.8	1.1	1.2	1.4	1.14	0.57	0.37	0.15	0.13
10	0.8	1.8	2.3	2.6	3.0	2.42	1.21	0.78	0.33	0.28
11	0.5	1.0	1.3	1.5	1.7	1.41	0.72	0.46	0.18	0.15

Table 7.24: EVI distribution estimates and percent exceedances of annual maximum daily runoff (mm) using LULC 2004 scenario for sub-basins of the Wadi As Silayy catchment.

Sub-basin	EVI estimates of runoff frequency					Percent exceedances of runoff				
	2 Year	10 Year	30 Year	50 Year	100 Year	Q1	Q25	Q50	Q85	Q99
1	0.2	0.4	0.5	0.6	0.7	0.57	0.29	0.19	0.07	0.06
2	0	0	0	0	0	0	0	0	0	0
3	0.5	1.2	1.6	1.8	2.0	1.64	0.82	0.54	0.22	0.18
4	0.2	0.4	0.5	0.6	0.7	0.52	0.28	0.17	0.07	0.05
5	0.9	1.9	2.6	2.9	3.3	2.64	1.33	0.86	0.35	0.29
6	0.4	0.9	1.2	1.3	1.5	1.25	0.65	0.41	0.16	0.13
7	0.3	0.6	0.8	0.9	1.0	0.8	0.41	0.26	0.1	0.09
8	1.4	3.3	4.4	4.9	5.6	4.47	2.23	1.41	0.61	0.52
9	1.7	3.9	5.2	5.8	6.6	5.37	2.68	1.76	0.73	0.6
10	0.9	2.0	2.7	3.0	3.5	2.79	1.39	0.89	0.38	0.32
11	0.5	1.1	1.4	1.6	1.8	1.49	0.75	0.49	0.19	0.16

Table 7.25: EVI distribution estimates and percent exceedances of annual maximum daily runoff (mm) using LULC 2009 scenario for sub-basins of the Wadi As Silayy catchment.

Sub-basin	EVI estimates of runoff frequency					Percent exceedances of runoff				
	2 Year	10 Year	30 Year	50 Year	100 Year	Q1	Q25	Q50	Q85	Q99
1	0.2	0.5	0.6	0.7	0.8	0.67	0.34	0.22	0.09	0.07
2	0	0	0	0	0	0	0	0	0	0
3	0.7	1.5	2.0	2.3	2.6	2.09	1.04	0.68	0.28	0.23
4	0.3	0.6	0.8	0.9	1.1	0.84	0.44	0.28	0.11	0.09
5	1.6	3.7	4.9	5.4	6.2	5.04	2.58	1.66	0.7	0.58
6	0.5	1.0	1.4	1.5	1.7	1.42	0.73	0.46	0.18	0.15
7	0.3	0.8	1.0	1.1	1.3	1.06	0.53	0.35	0.14	0.12
8	1.5	3.4	4.6	5.1	5.9	4.75	2.37	1.49	0.64	0.55
9	2.0	4.4	5.8	6.5	7.4	6.05	3.04	1.99	0.83	0.68
10	0.9	2.1	2.9	3.2	3.6	2.91	1.45	0.93	0.4	0.34
11	0.5	1.2	1.6	1.8	2.0	1.7	0.86	0.55	0.22	0.18

Table 7.26: EVI distribution estimates and percent exceedances of annual maximum daily runoff (mm) using LULC 2012 scenario for sub-basins of the Wadi As Silayy catchment.

Sub-basin	EVI estimates of runoff frequency					Percent exceedances of runoff				
	2 Year	10 Year	30 Year	50 Year	100 Year	Q1	Q25	Q50	Q85	Q99
1	0.2	0.5	0.7	0.8	0.9	0.7	0.36	0.23	0.09	0.08
2	0	0	0	0	0	0	0	0	0	0
3	0.9	2.0	2.6	3.0	3.4	2.72	1.37	0.9	0.37	0.31
4	0.7	1.5	2.1	2.3	2.6	2.11	1.09	0.69	0.28	0.23
5	1.9	4.3	5.8	6.4	7.3	5.94	3.03	1.94	0.83	0.68
6	0.5	1.1	1.4	1.6	1.8	1.46	0.74	0.48	0.19	0.16
7	0.4	0.9	1.1	1.3	1.4	1.16	0.58	0.38	0.16	0.13
8	1.6	3.5	4.8	5.3	6.0	4.87	2.43	1.53	0.65	0.56
9	2.2	4.8	6.4	7.2	8.2	6.67	3.37	2.19	0.91	0.76
10	0.9	2.2	2.9	3.2	3.7	2.97	1.48	0.94	0.4	0.34
11	0.6	1.3	1.8	2.0	2.2	1.83	0.93	0.6	0.24	0.2

Table 7.27: EVI distribution estimates and percent exceedances of annual maximum daily runoff (mm) using LULC 2016 scenario for sub-basins of the Wadi As Silayy catchment.

Sub-basin	EVI estimates of runoff frequency					Percent exceedances of runoff				
	2 Year	10 Year	30 Year	50 Year	100 Year	Q1	Q25	Q50	Q85	Q99
1	0.4	0.8	1.1	1.2	1.4	1.13	0.57	0.37	0.15	0.12
2	0	0	0	0	0	0	0	0	0	0
3	1.0	2.2	3.0	3.3	3.7	3.05	1.56	1	0.42	0.35
4	0.8	1.7	2.3	2.5	2.9	2.33	1.2	0.76	0.31	0.26
5	2.1	4.8	6.4	7.2	8.2	6.62	3.38	2.16	0.92	0.76
6	0.8	1.7	2.3	2.6	2.9	2.38	1.2	0.78	0.32	0.26
7	0.4	0.9	1.2	1.3	1.5	1.23	0.61	0.4	0.17	0.14
8	1.6	3.6	4.9	5.4	6.2	5	2.5	1.57	0.67	0.58
9	2.3	5.1	6.8	7.6	8.6	7.03	3.57	2.31	0.97	0.8
10	1.0	2.3	3.0	3.4	3.9	3.12	1.55	0.99	0.42	0.36
11	0.8	1.7	2.3	2.6	2.9	2.39	1.2	0.78	0.32	0.26

Table 7.28: EVI distribution estimates and percent exceedances of annual maximum daily discharge (m³/s) using LULC 1996 scenario for sub-basins of the Wadi Hanifah catchment.

Sub-basin	EVI estimates of discharge frequency					Percent exceedances of discharge				
	2 Year	10 Year	30 Year	50 Year	100 Year	Q1	Q25	Q50	Q85	Q99
1	0	0	0	0	0	0.04	0	0	0	0
2	0	0	0	0	0	0.06	0.01	0	0	0
3	0.2	0.6	0.8	0.9	1.0	0.86	0.36	0.21	0.08	0.06
4	0	0	0	0	0	0.02	0.01	0	0	0
5	0.1	0.4	0.6	0.7	0.8	0.69	0.23	0.15	0.03	0.02
6	0.2	0.5	0.7	0.7	0.8	0.68	0.34	0.22	0.09	0.07
7	0	0.1	0.1	0.2	0.2	0.13	0.05	0.02	0	0
8	0	0	0	0	0	0.02	0.01	0	0	0
9	0.6	1.5	2.0	2.3	2.6	2.28	0.88	0.53	0.21	0.18
10	1.1	2.8	3.8	4.3	4.9	4.26	1.75	1.03	0.37	0.31
11	0	0	0	0	0	0.02	0	0	0	0
12	0.3	0.6	0.7	0.8	0.9	0.78	0.39	0.26	0.1	0.09
13	1.4	3.7	5.0	5.6	6.5	5.54	2.29	1.31	0.47	0.4
14	1.0	2.5	3.4	3.8	4.3	3.58	1.59	0.88	0.39	0.28
15	4.0	10.1	13.9	15.6	17.8	14.9	6.56	3.63	1.48	1.08
16	0.9	2.2	3.0	3.3	3.8	3.11	1.45	0.87	0.34	0.28
17	0.8	2.0	2.7	3.0	3.4	2.77	1.35	0.81	0.32	0.26
18	1.7	4.3	5.8	6.6	7.5	6.19	2.85	1.53	0.73	0.51
19	6.2	16.5	22.7	25.6	29.4	24.8	10.3	5.61	2.22	1.49
20	1.5	3.4	4.6	5.1	5.9	4.74	2.31	1.42	0.61	0.49
21	0.3	0.7	1.0	1.1	1.3	1.03	0.49	0.32	0.13	0.1
22	6.4	18.0	25.0	28.2	32.5	27.7	10.7	5.41	1.93	1.23

Table 7.29: EVI distribution estimates and percent exceedances of annual maximum daily discharge (m³/s) using LULC 2004 scenario for sub-basins of the Wadi Hanifah catchment.

Sub-basin	EVI estimates of discharge frequency					Percent exceedances of discharge				
	2 Year	10 Year	30 Year	50 Year	100 Year	Q1	Q25	Q50	Q85	Q99
1	0	0	0	0	0	0.04	0	0	0	0
2	0	0	0	0	0	0.06	0.01	0	0	0
3	0.4	0.9	1.2	1.4	1.6	1.37	0.59	0.36	0.14	0.12
4	0	0	0	0	0	0.02	0.01	0	0	0
5	0.2	0.7	1.0	1.1	1.3	1.12	0.39	0.22	0.06	0.05
6	0.5	1.0	1.4	1.5	1.7	1.42	0.71	0.46	0.19	0.16
7	0	0	0	0	0	0.13	0.05	0.02	0	0
8	0	0	0	0	0	0.02	0.01	0	0	0
9	1.1	2.7	3.7	4.2	4.8	4.05	1.69	0.99	0.39	0.32
10	1.7	4.2	5.8	6.5	7.4	6.26	2.66	1.57	0.6	0.52
11	0	0	0	0	0	0.02	0	0	0	0
12	0.2	0.5	0.7	0.8	0.9	0.75	0.38	0.25	0.1	0.08
13	2.3	5.7	7.8	8.7	1.0	8.39	3.59	2.13	0.76	0.69
14	1.1	2.7	3.7	4.2	4.8	3.99	1.79	0.97	0.43	0.31
15	5.2	13.2	18.0	20.2	23	19.2	8.63	4.84	1.91	1.51
16	1.3	3.0	4.1	4.6	5.3	4.31	2.04	1.26	0.47	0.41
17	1.1	2.6	3.5	3.9	4.4	3.59	1.72	1.06	0.41	0.35
18	1.8	4.4	6.0	6.8	7.7	6.37	2.95	1.61	0.72	0.53
19	7.8	20.3	27.9	31.4	36.0	30.1	12.9	7.06	2.8	2.03
20	1.6	3.6	4.9	5.5	6.3	5.07	2.47	1.53	0.65	0.53
21	0.5	1.1	1.5	1.7	1.9	1.55	0.75	0.48	0.2	0.16
22	8.1	22.5	31.1	35.0	40.3	34	13.8	6.97	2.7	1.75

Table 7.30: EVI distribution estimates and percent exceedances of annual maximum daily discharge (m³/s) using LULC 2009 scenario for sub-basins of the Wadi Hanifah catchment.

Sub-basin	EVI estimates of discharge frequency					Percent exceedances of discharge				
	2 Year	10 Year	30 Year	50 Year	100 Year	Q1	Q25	Q50	Q85	Q99
1	0	0	0	0	0	0.04	0	0	0	0
2	0	0	0	0	0	0.06	0.01	0	0	0
3	0.1	0.3	0.4	0.4	0.5	0.44	0.15	0.1	0.03	0.02
4	0	0	0	0	0	0.02	0.01	0	0	0
5	0	0.2	0.3	0.4	0.4	0.36	0.08	0.05	0	0
6	0.4	0.9	1.2	1.3	1.5	1.25	0.62	0.41	0.17	0.14
7	0.03	0.1	0.2	0.2	0.2	0.17	0.06	0.02	0	0
8	0	0	0	0	0	0.02	0.01	0	0	0
9	1.0	2.4	3.3	3.7	4.2	3.65	1.53	0.96	0.36	0.31
10	1.8	4.4	6.0	6.7	7.7	6.47	2.79	1.69	0.63	0.58
11	0	0	0	0	0	0.02	0	0	0	0
12	0.3	0.6	0.9	1.0	1.0	0.9	0.46	0.29	0.12	0.1
13	2.2	5.6	7.6	8.5	9.7	8.18	3.55	2.11	0.76	0.7
14	1.2	3.0	4.0	4.5	5.2	4.3	1.91	1.04	0.46	0.33
15	5.5	13.9	18.9	21.2	24.3	20	9.14	5.2	2.07	1.53
16	1.4	3.5	4.7	5.2	6.0	4.87	2.28	1.42	0.56	0.46
17	1.3	3.0	4.0	4.6	5.2	4.22	2.03	1.25	0.52	0.41
18	1.9	4.6	6.3	7.0	8.1	6.63	3.15	1.68	0.75	0.56
19	8.3	21.6	29.6	33.3	38.2	31.8	13.6	7.58	3.07	2.13
20	1.6	3.8	5.1	5.7	6.5	5.28	2.58	1.57	0.68	0.55
21	0.6	1.4	1.9	2.1	2.4	1.98	0.99	0.62	0.26	0.21
22	8.8	24.0	33.2	37.4	43.0	36.3	14.5	7.58	2.95	1.9

Table 7.31: EVI distribution estimates and percent exceedances of annual maximum daily discharge (m³/s) using LULC 2012 scenario for sub-basins of the Wadi Hanifah catchment.

Sub-basin	EVI estimates of discharge frequency					Percent exceedances of discharge				
	2 Year	10 Year	30 Year	50 Year	100 Year	Q1	Q25	Q50	Q85	Q99
1	0	0	0	0	0	0.04	0	0	0	0
2	0	0	0	0	0	0.06	0.01	0	0	0
3	0.1	0.3	0.4	0.4	0.5	0.44	0.15	0.1	0.03	0.02
4	0	0	0	0	0	0.02	0.01	0	0	0
5	0.05	0.2	0.3	0.4	0.4	0.36	0.08	0.04	0	0
6	0.4	0.9	1.2	1.4	1.6	1.28	0.64	0.42	0.17	0.14
7	0.03	0.1	0.2	0.2	0.2	0.17	0.06	0.02	0	0
8	0	0	0	0	0	0.02	0.01	0	0	0
9	1.0	2.6	3.6	4.0	4.5	3.9	1.67	1.02	0.4	0.35
10	2.0	4.9	6.6	7.4	8.4	7.06	3.12	1.86	0.68	0.64
11	0.2	0.4	0.5	0.6	0.7	0.54	0.26	0.15	0.06	0.05
12	0.4	1.0	1.3	1.5	1.6	1.35	0.68	0.44	0.18	0.15
13	2.7	6.8	9.2	10.3	11.8	9.77	4.31	2.54	0.99	0.84
14	1.3	3.4	4.6	5.1	5.9	4.85	2.19	1.2	0.54	0.38
15	6.2	15.7	21.4	23.9	27.4	22.6	10.3	5.81	2.34	1.77
16	1.6	3.8	5.0	5.7	6.5	5.33	2.53	1.54	0.62	0.51
17	1.4	3.2	4.4	4.9	5.6	4.57	2.18	1.35	0.57	0.45
18	1.9	4.7	6.3	7.0	8.0	6.66	3.15	1.69	0.75	0.56
19	9.1	23.6	32.3	36.3	41.7	34.7	15	8.33	3.35	2.34
20	1.2	4.2	5.7	6.4	7.3	5.92	2.9	1.75	0.75	0.61
21	0.7	1.6	2.2	2.4	2.7	2.24	1.1	0.71	0.29	0.24
22	9.9	26.8	37.0	41.7	48.0	40.3	16.5	8.56	3.3	2.23

Table 7.32: EVI distribution estimates and percent exceedances of annual maximum daily discharge (m³/s) using LULC 2016 scenario for sub-basins of the Wadi Hanifah catchment.

Sub-basin	EVI estimates of discharge frequency					Percent exceedances of discharge				
	2 Year	10 Year	30 Year	50 Year	100 Year	Q1	Q25	Q50	Q85	Q99
1	0	0	0	0	0	0.04	0	0	0	0
2	0	0	0	0	0	0.06	0.01	0	0	0
3	0.4	1.0	1.4	1.6	1.8	1.58	0.65	0.38	0.15	0.14
4	0	0	0	0	0	0.02	0.01	0	0	0
5	0.3	0.9	1.3	1.5	1.7	1.45	0.55	0.27	0.09	0.09
6	0.3	0.7	0.9	1.0	1.2	0.98	0.49	0.32	0.13	0.11
7	0.03	0.1	0.2	0.2	0.2	0.17	0.06	0.02	0	0
8	0	0	0	0	0	0.02	0.01	0	0	0
9	1.3	3.2	4.4	4.9	5.6	4.78	2.03	1.19	0.46	0.4
10	2.2	5.5	7.5	8.4	9.7	8.1	3.53	2.1	0.76	0.67
11	0.2	0.5	0.7	0.7	0.8	0.71	0.32	0.21	0.07	0.07
12	0.4	0.8	1.0	1.2	1.4	1.11	0.55	0.36	0.15	0.13
13	3.0	7.5	10.3	11.5	13.2	10.9	4.87	2.82	1.08	0.87
14	3.3	7.9	10.7	12.0	13.7	11.1	5.32	3.19	1.36	1.07
15	8.5	21.2	28.8	32.3	37.0	30.4	14	7.99	3.25	2.45
16	1.9	4.5	6.0	6.7	7.6	6.28	3.01	1.87	0.7	0.62
17	1.9	4.4	6.0	6.7	7.6	6.18	3.02	1.87	0.74	0.64
18	5.3	12.5	16.8	18.7	21.4	17.3	8.36	5.17	2.17	1.8
19	14.2	36.0	49.2	55.2	63.3	52.3	23.6	13.3	5.55	3.99
20	3.3	7.6	10.1	11.3	12.9	10.4	5.22	3.29	1.36	1.15
21	1.0	2.3	3.0	3.4	3.9	3.16	1.59	1.01	0.42	0.35
22	16.4	43.0	59.0	66.2	76.0	63.4	27.3	15.1	6.21	4.22

Table 7.33: EVI distribution estimates and percent exceedances of annual maximum daily discharge (m³/s) using LULC 1996 scenario for sub-basins of the Wadi As Silayy catchment.

Sub-basin	EVI estimates of discharge frequency					Percent exceedances of discharge				
	2 Year	10 Year	30 Year	50 Year	100 Year	Q1	Q25	Q50	Q85	Q99
1	0.5	1.3	1.8	2.0	2.3	1.99	0.83	0.46	0.16	0.14
2	0.03	0.1	0.2	0.2	0.2	0.21	0.07	0.03	0	0
3	0	0	0	0	0	0.05	0.01	0	0	0
4	0	0	0	0	0	0.01	0	0	0	0
5	0.4	1.2	1.7	1.9	2.2	1.93	0.67	0.37	0.11	0.1
6	0	0	0	0	0	0.02	0	0	0	0
7	0	0	0	0	0	0.01	0	0	0	0
8	1.0	2.3	3.1	3.5	4.0	3.22	1.56	0.98	0.41	0.35
9	0.5	1.4	2.0	2.2	2.6	2.29	0.76	0.43	0.11	0.11
10	5.3	12.5	16.9	18.8	21.5	17.8	8.26	5.18	2.08	1.82
11	0.3	0.7	1.0	1.1	1.3	1.09	0.45	0.25	0.09	0.07

Table 7.34: EVI distribution estimates and percent exceedances of annual maximum daily discharge (m³/s) using LULC 2004 scenario for sub-basins of the Wadi As Silayy catchment.

Sub-basin	EVI estimates of discharge frequency					Percent exceedances of discharge				
	2 Year	10 Year	30 Year	50 Year	100 Year	Q1	Q25	Q50	Q85	Q99
1	0.6	1.5	2.0	2.2	2.6	2.2	0.95	0.53	0.2	0.15
2	0.04	0.1	0.2	0.2	0.3	0.25	0.07	0.03	0	0
3	1.5	3.4	4.6	5.1	5.8	4.75	2.35	1.47	0.59	0.51
4	0.1	0.2	0.2	0.2	0.3	0.24	0.12	0.08	0.03	0.02
5	1.9	4.8	6.5	7.3	8.4	7	3.03	1.75	0.67	0.52
6	0.5	1.2	1.6	1.8	2.1	1.72	0.79	0.49	0.19	0.16
7	0.1	0.3	0.4	0.5	0.5	0.45	0.21	0.13	0.05	0.04
8	1.3	3.2	4.3	4.8	5.4	4.44	2.17	1.3	0.57	0.46
9	3.0	7.6	10.4	11.7	13.4	11.1	4.89	2.79	1.08	0.82
10	8.8	21.0	28.3	31.7	36.2	29.6	14	8.48	3.45	2.84
11	0.3	0.8	1.1	1.2	1.4	1.16	0.5	0.26	0.1	0.07

Table 7.35: EVI distribution estimates and percent exceedances of annual maximum daily discharge (m³/s) using LULC 2009 scenario for sub-basins of the Wadi As Silayy catchment.

Sub-basin	EVI estimates of discharge frequency					Percent exceedances of discharge				
	2 Year	10 Year	30 Year	50 Year	100 Year	Q1	Q25	Q50	Q85	Q99
1	0.7	1.7	2.3	2.6	3.0	2.58	1.09	0.62	0.24	0.19
2	0.04	0.1	0.2	0.2	0.3	0.25	0.07	0.03	0	0
3	1.9	4.3	5.8	6.5	7.4	6.06	3	1.91	0.76	0.65
4	0.1	0.3	0.4	0.4	0.5	0.39	0.2	0.13	0.05	0.04
5	2.6	6.4	8.7	9.8	11.2	9.29	4.13	2.39	0.96	0.72
6	0.6	1.4	1.8	2.1	2.3	1.96	0.93	0.58	0.21	0.18
7	0.2	0.4	0.6	0.7	0.7	0.62	0.3	0.18	0.07	0.06
8	1.4	3.4	4.5	5.1	5.8	4.72	2.3	1.37	0.6	0.48
9	3.9	9.7	13.3	14.9	17.0	14.1	6.32	3.64	1.43	1.07
10	10.0	23.8	32.1	36.0	41.1	33.6	15.9	9.62	3.93	3.19
11	0.3	0.9	1.3	1.4	1.6	1.37	0.59	0.31	0.12	0.09

Table 7.36: EVI distribution estimates and percent exceedances of annual maximum daily discharge (m³/s) using LULC 2012 scenario for sub-basins of the Wadi As Silayy catchment.

Sub-basin	EVI estimates of discharge frequency					Percent exceedances of discharge				
	2 Year	10 Year	30 Year	50 Year	100 Year	Q1	Q25	Q50	Q85	Q99
1	0.7	1.8	2.5	2.8	3.2	2.73	1.17	0.67	0.25	0.203
2	0.04	0.1	0.2	0.2	0.3	0.25	0.07	0.03	0	0
3	2.5	5.7	7.7	8.5	9.7	7.94	3.96	2.49	1.01	0.854
4	0.3	0.7	0.9	1.0	1.2	0.98	0.49	0.32	0.13	0.107
5	3.4	8.3	11.3	12.7	14.5	12	5.43	3.16	1.27	0.979
6	0.6	1.4	1.9	2.1	2.4	2.02	0.96	0.59	0.21	0.188
7	0.2	0.5	0.6	0.7	0.8	0.67	0.32	0.2	0.08	0.066
8	1.5	3.4	4.6	5.2	5.9	4.82	2.35	1.41	0.62	0.494
9	4.8	11.9	16.2	18.1	20.1	17.1	7.77	4.47	1.8	1.347
10	11.0	26.3	35.5	39.7	45.4	37.1	17.6	10.6	4.35	3.523
11	0.4	1.0	1.4	1.6	1.8	1.49	0.63	0.35	0.13	0.1

Table 7.37: EVI distribution estimates and percent exceedances of annual maximum daily discharge (m³/s) using LULC 2016 scenario for sub-basins of the Wadi As Silayy catchment.

Sub-basin	EVI estimates of discharge frequency					Percent exceedances of discharge				
	2 Year	10 Year	30 Year	50 Year	100 Year	Q1	Q25	Q50	Q85	Q99
1	1.2	3.0	4.1	4.6	5.3	4.43	1.98	1.15	0.44	0.37
2	0.04	0.1	0.2	0.2	0.3	0.24	0.07	0.03	0	0
3	2.8	6.4	8.6	9.6	11.0	8.95	4.46	2.8	1.14	0.99
4	0.3	0.8	1.0	1.2	1.3	1.08	0.54	0.35	0.14	0.12
5	4.2	10.3	14.0	15.7	18.0	14.8	6.82	3.92	1.59	1.23
6	1.0	2.4	3.2	3.6	4.1	3.4	1.63	1.01	0.39	0.34
7	0.2	0.5	0.7	0.8	0.9	0.72	0.34	0.21	0.08	0.07
8	1.5	3.5	4.8	5.3	6.1	4.97	2.42	1.44	0.64	0.51
9	6.0	15.0	20.3	22.7	26.1	21.5	9.85	5.62	2.28	1.73
10	12.6	30.3	40.9	45.8	52.3	42.8	20.3	12.2	5.02	4.03
11	0.5	1.4	1.9	2.1	2.4	2.02	0.89	0.49	0.19	0.14

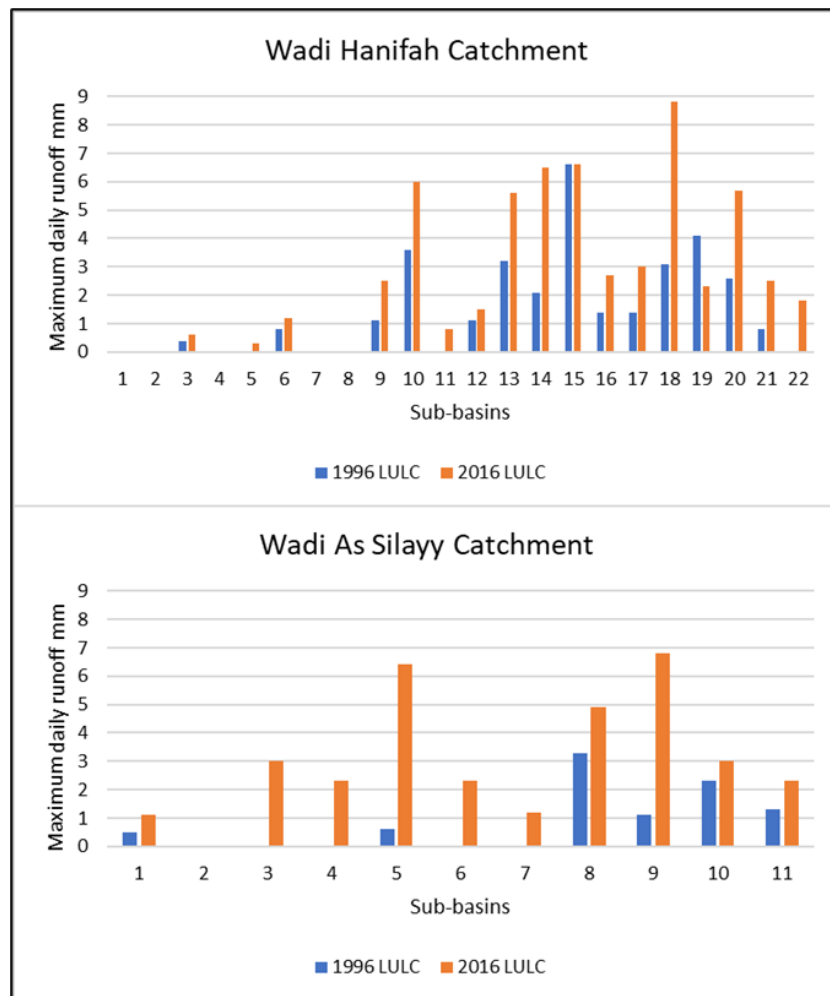


Figure 7.25: Impact of LULC change between 1996 and 2016 on simulated annual maximum daily runoff for the 30-year return period for the sub-basins of Riyadh's catchments.

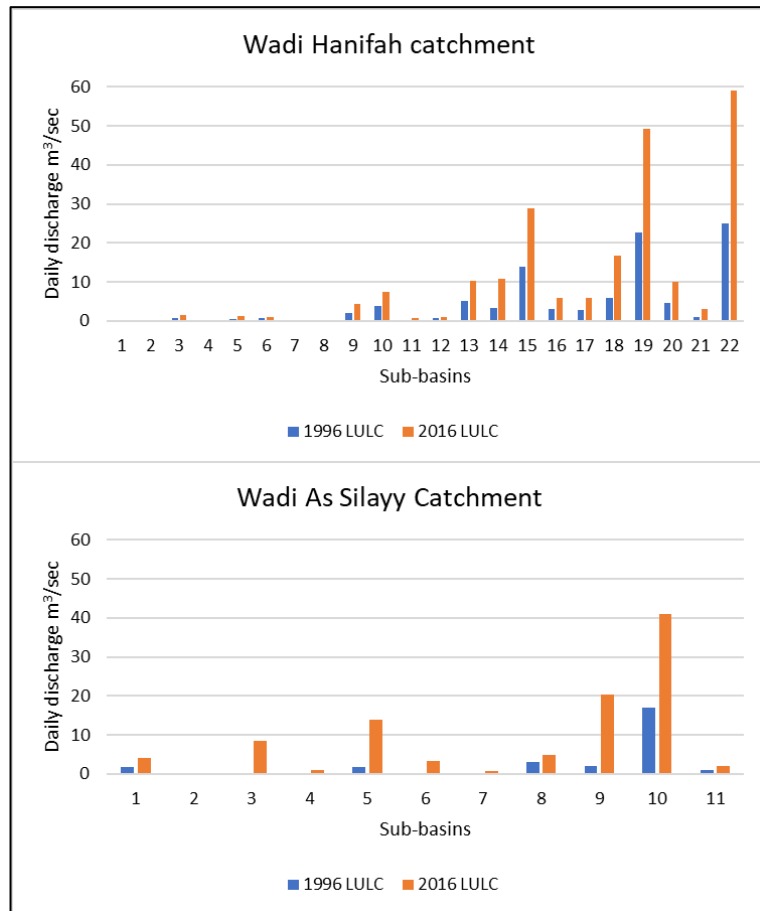


Figure 7.26: Impact of LULC change between 1996 and 2016 on simulated annual maximum daily discharge for the 30-year return period for the sub-basins of Riyadh’s catchments.

All calculated return periods and the percent exceedances for sub-basins in the study area were mapped (Appendix C). For comparison, the 2-year and 30-year return period and the per cent exceedances of Q1 and Q99 using the LULC 1996 and LULC 2016 scenarios were selected to show the spatial distribution characteristics of the simulated runoff and discharge in sub-basins of Riyadh's catchments (Figure 7.27, Figure 7.28, Figure 7.29, and Figure 7.30). These figures clearly illustrate the impact of LULC changes, in the study area, on the spatial distribution of annual maximum daily runoff and discharge. A comparison of maps indicates an increasing trend of surface runoff depths and discharge rates in the sub-basins located within the boundary of Riyadh city because of the increase of impermeable surfaces. For example, when using the LULC 1996

scenario, simulated annual maximum daily runoff greater than 4.9 mm in the 30-year return period was found only in sub-basin 15 (48 km²) of the Wadi Hanifah catchment. However, when using the LULC 2016 scenario, nine sub-basins neighbouring each other with annual maximum daily runoff greater than 4.9 mm were found covering an area of about 812 km² of the two catchments in the study area. In contrast, changes in annual maximum daily runoff in the two scenarios were not significant in sub-basins unaffected by urbanisation.

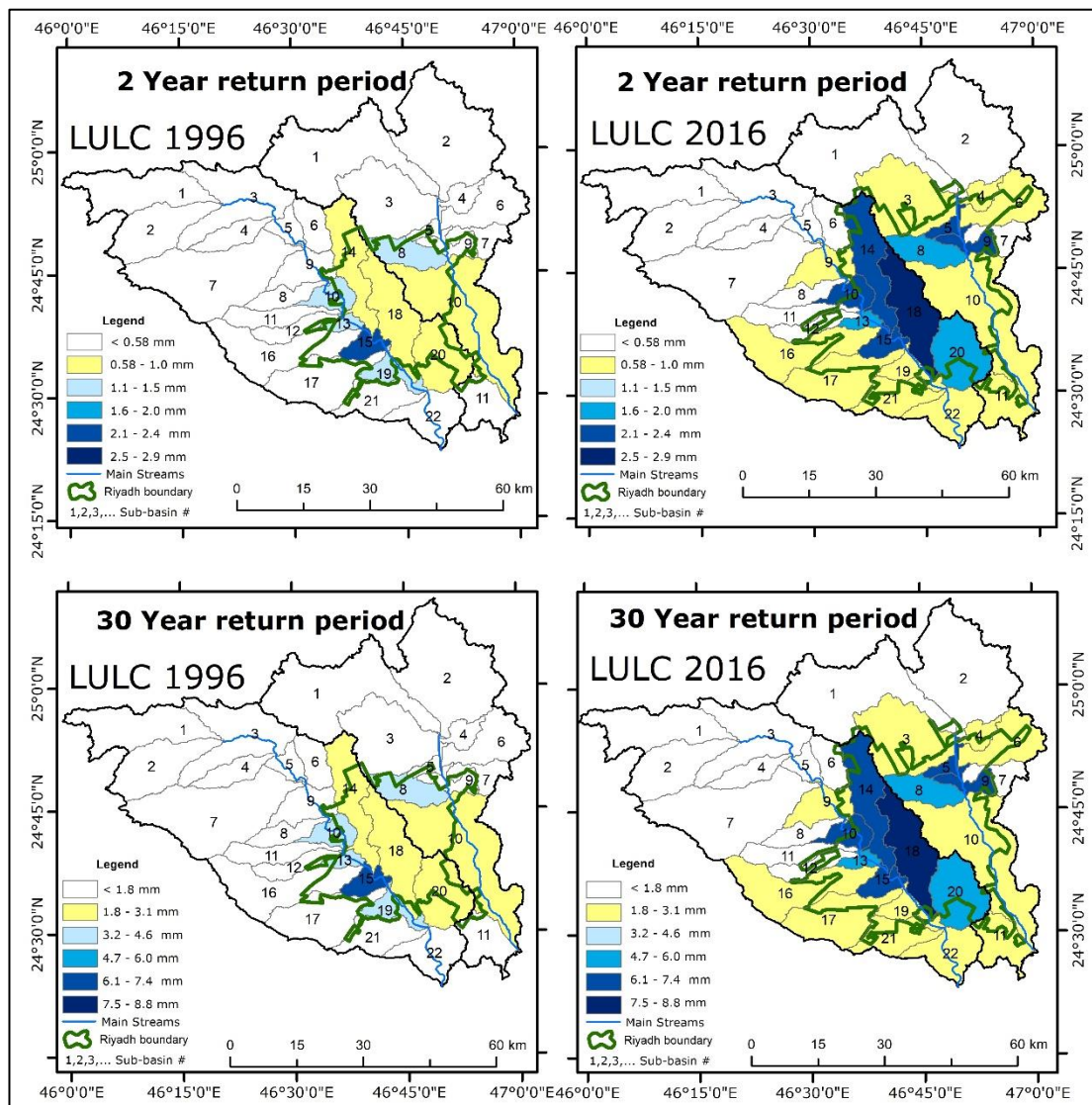


Figure 7.27: Spatial distribution of simulated annual maximum daily runoff for the 2-year and 30-year return periods under historical LULC change.

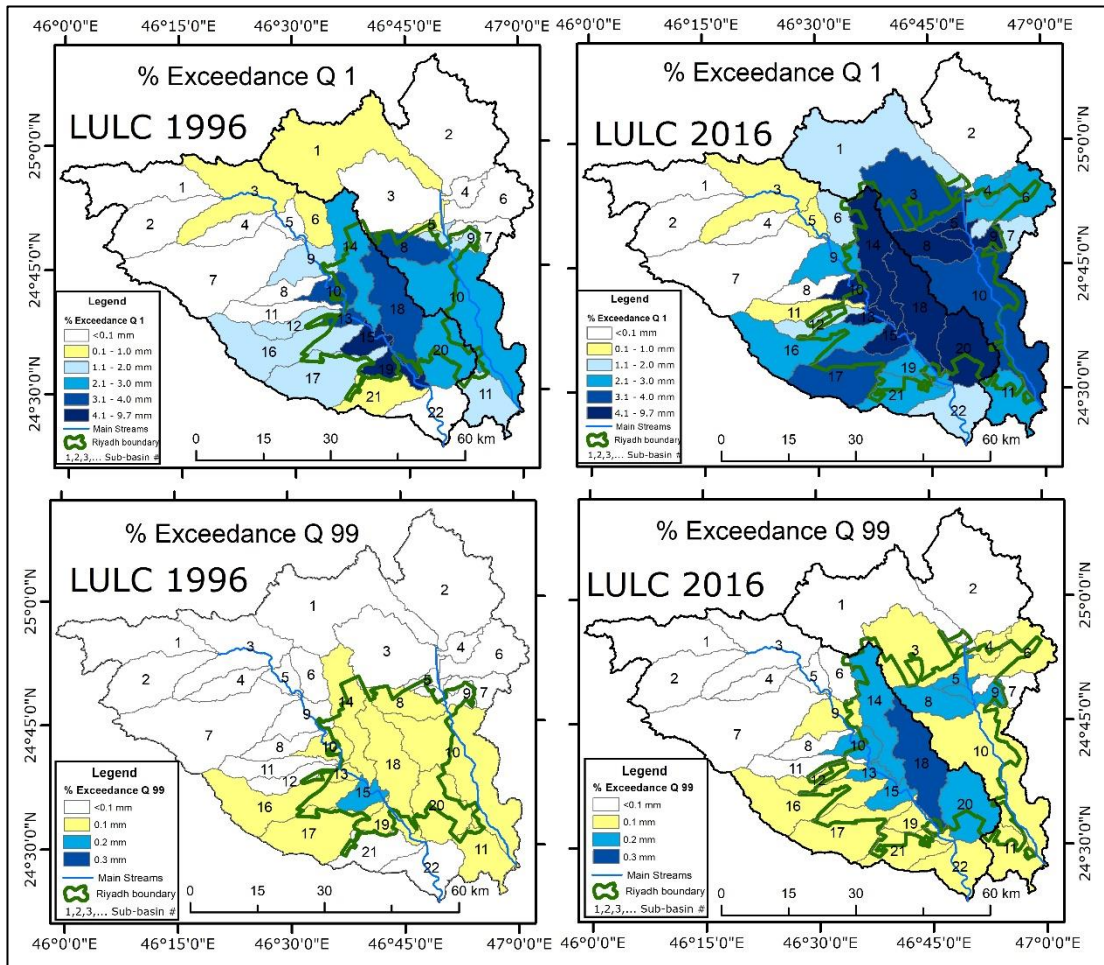


Figure 7.28: Spatial distribution comparison of simulated annual maximum daily runoff for percent exceedances of Q1 and Q99 under historical LULC change.

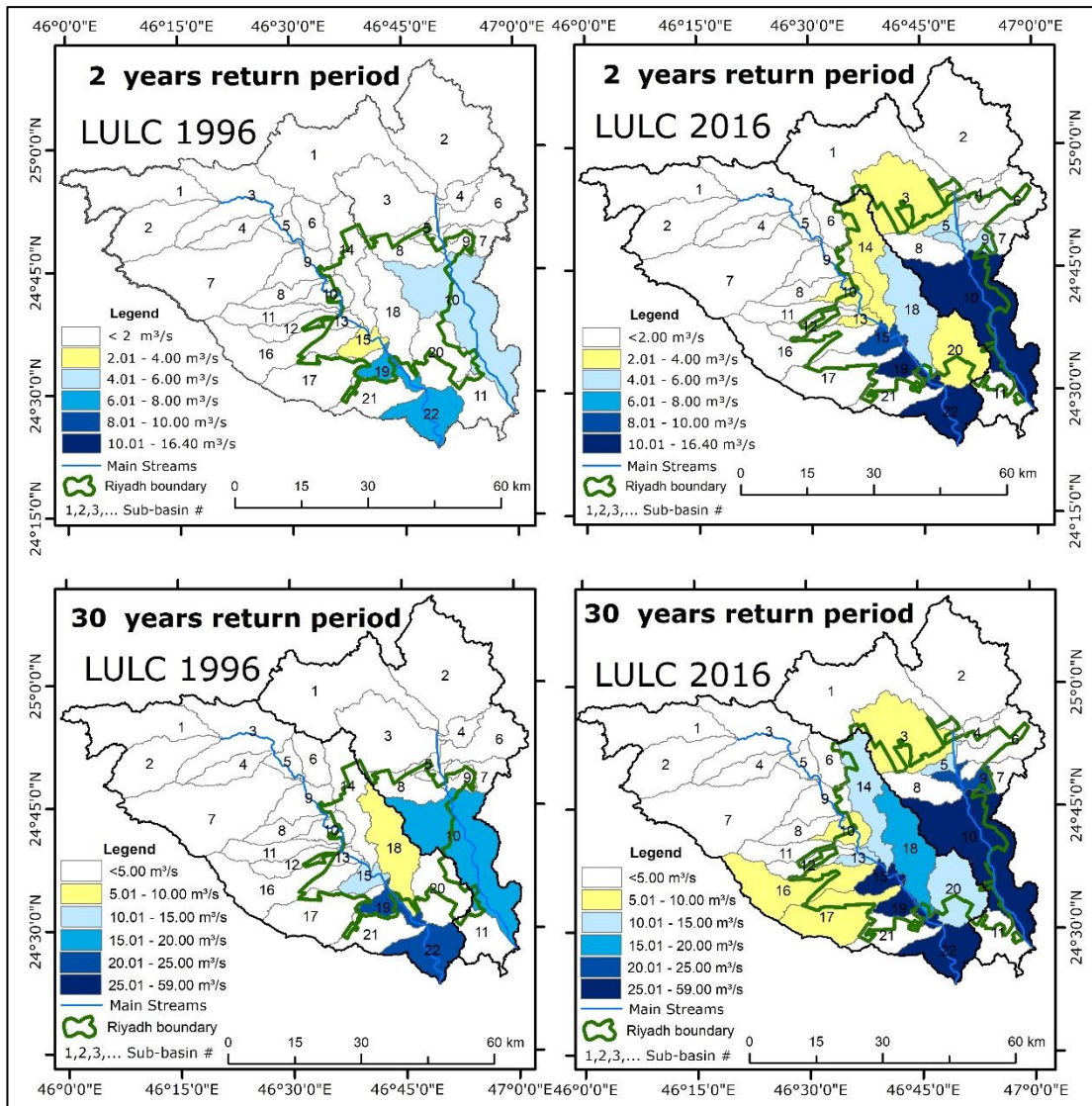


Figure 7.29: Spatial distribution comparison of simulated annual maximum daily discharge in the 2-year and 30-year return periods under historical LULC change.

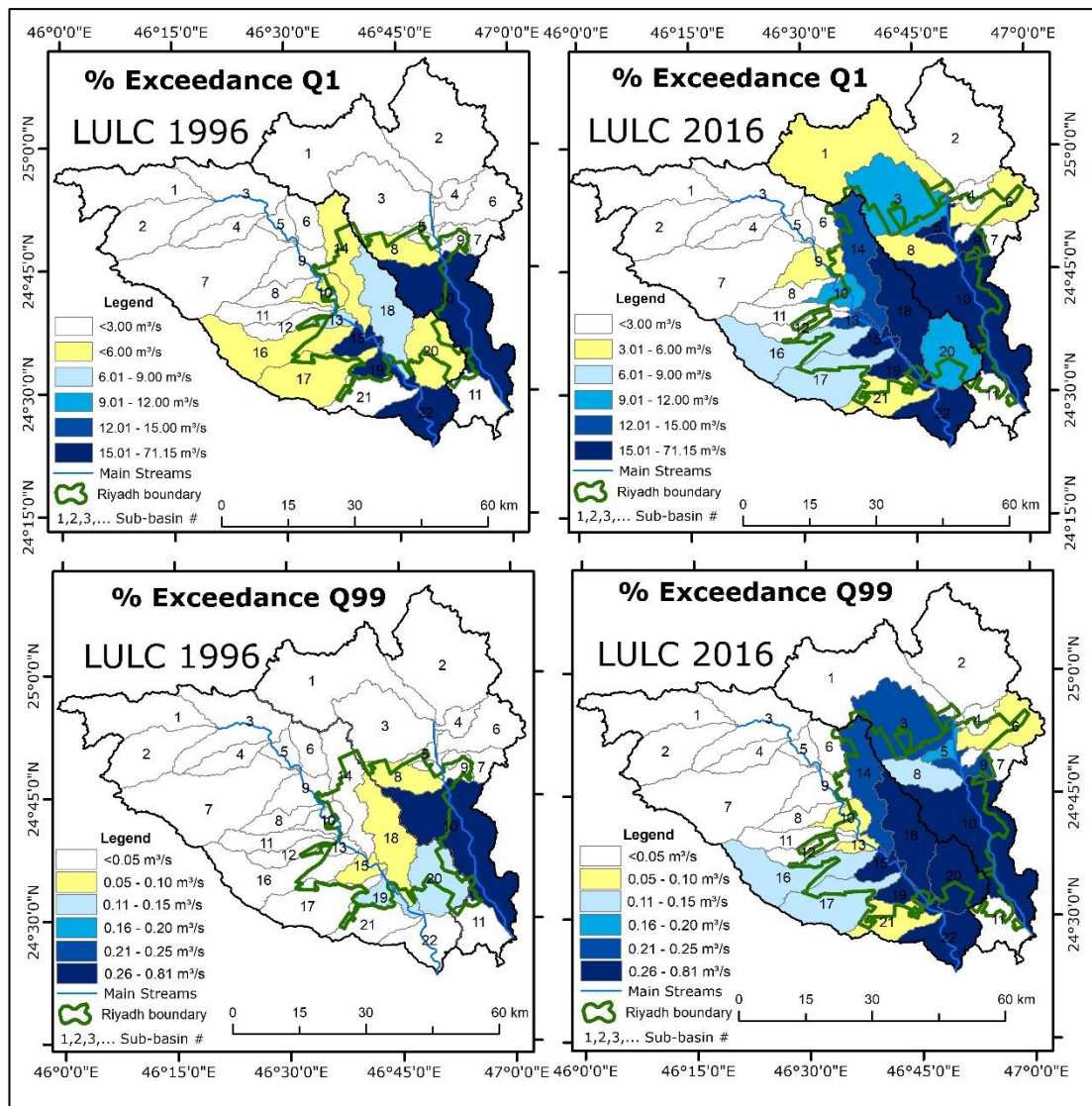


Figure 7.30: Spatial distribution comparison of simulated annual maximum daily discharge for percent exceedances of Q1 and Q99 under historical LULC change.

Based on the two scenarios' results, the increase of impermeable surfaces in the catchments of the study area increased discharge rates in the sub-basins associated with the main channel in the lower reaches of the catchments. In the LULC 1996 scenario, there was no discharge rate greater than 25 m³/s in the study area for the 30-year return period, but in the LULC 2016 scenario, many sub-basins that spread over an area of about 634 km² in the lower reaches of catchments had discharge greater than 25 m³/s, and some cases reached 59 m³/s such as sub-basin 22 in the Wadi Hanifah catchment. This means that the discharge rate for the 30-year return

period in the LULC 2016 scenario is more than twice as much as in the LULC 1996 scenario.

Percent exceedances of the simulated daily runoff and discharge were calculated and plotted for the period 1965-2000 to assess the impact of LULC change on simulated daily runoff depths and discharge rates on the sub-basin level in the study area (Figure 7.31, Figure 7.32, Figure 7.33, and Figure 7.34). These figures clearly illustrate the positive impact of the urbanisation of Riyadh on daily runoff and discharge. The increase in runoff depths and discharge rates are attributed to the conversion of permeable barren land to impervious surfaces due to the expansion of Riyadh city.

Notably, the SWAT outputs of daily runoff in the study area for the period 1965-2000 have numbers of runoff days higher than the numbers of rainy days, most likely because of simulated delayed runoff typical in humid and sub-humid areas. In arid/semi-arid regions, such behaviour is less likely because of the highly localised, intense rainfall events of short duration (Rodier and Roche 1978; Pilgrim et al. 1988; Zoccatelli et al. 2019; Aryal et al. 2020). The SWAT model requires daily runoff data to adjust the model for delayed runoff to avoid such a problem. However, the absence of such data means that this condition cannot be met for the study area.

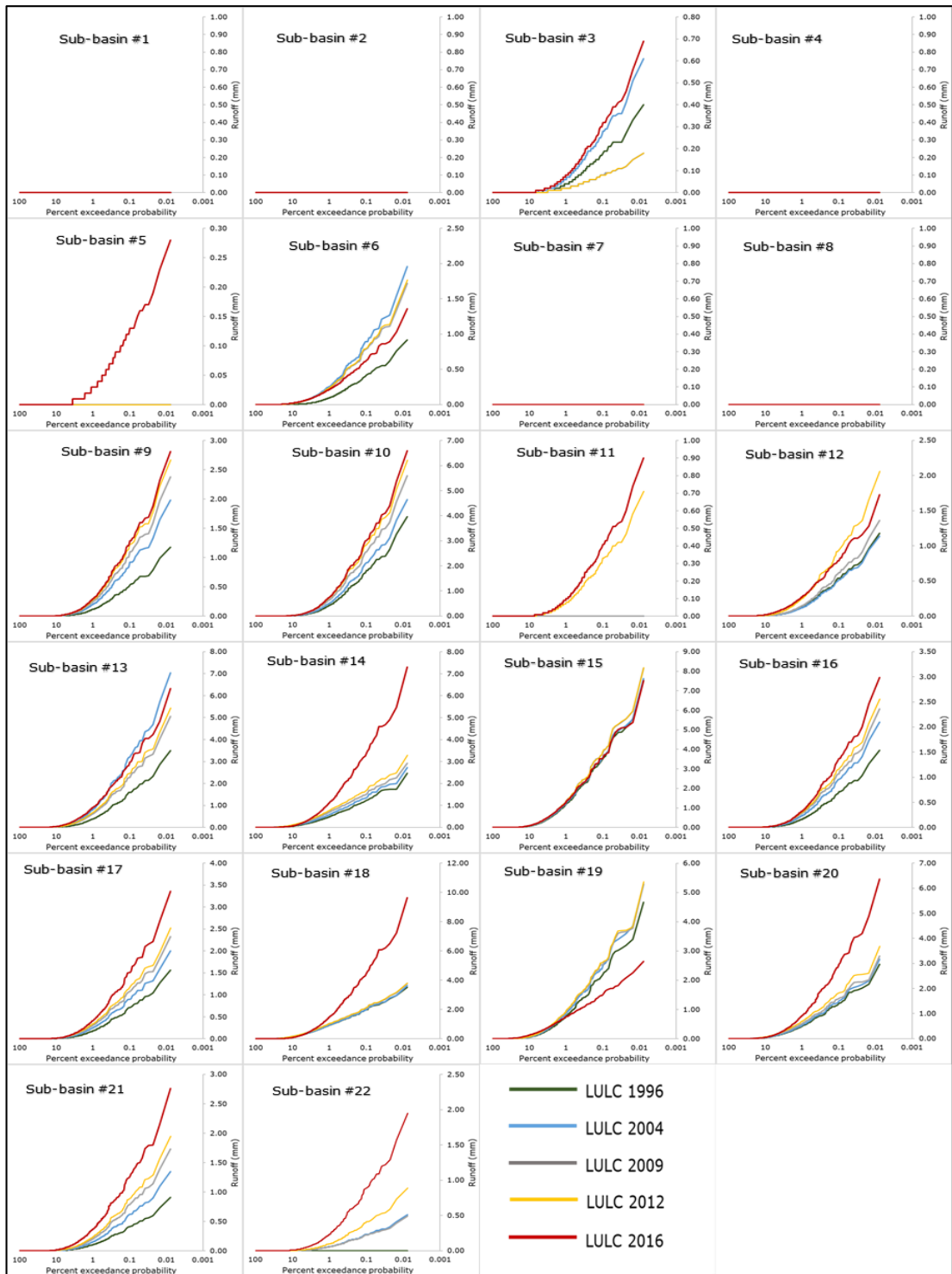


Figure 7.31: Percent exceedances of the simulated daily runoff for sub-basins of the Wadi Hanifah catchment under five different historical LULC maps.

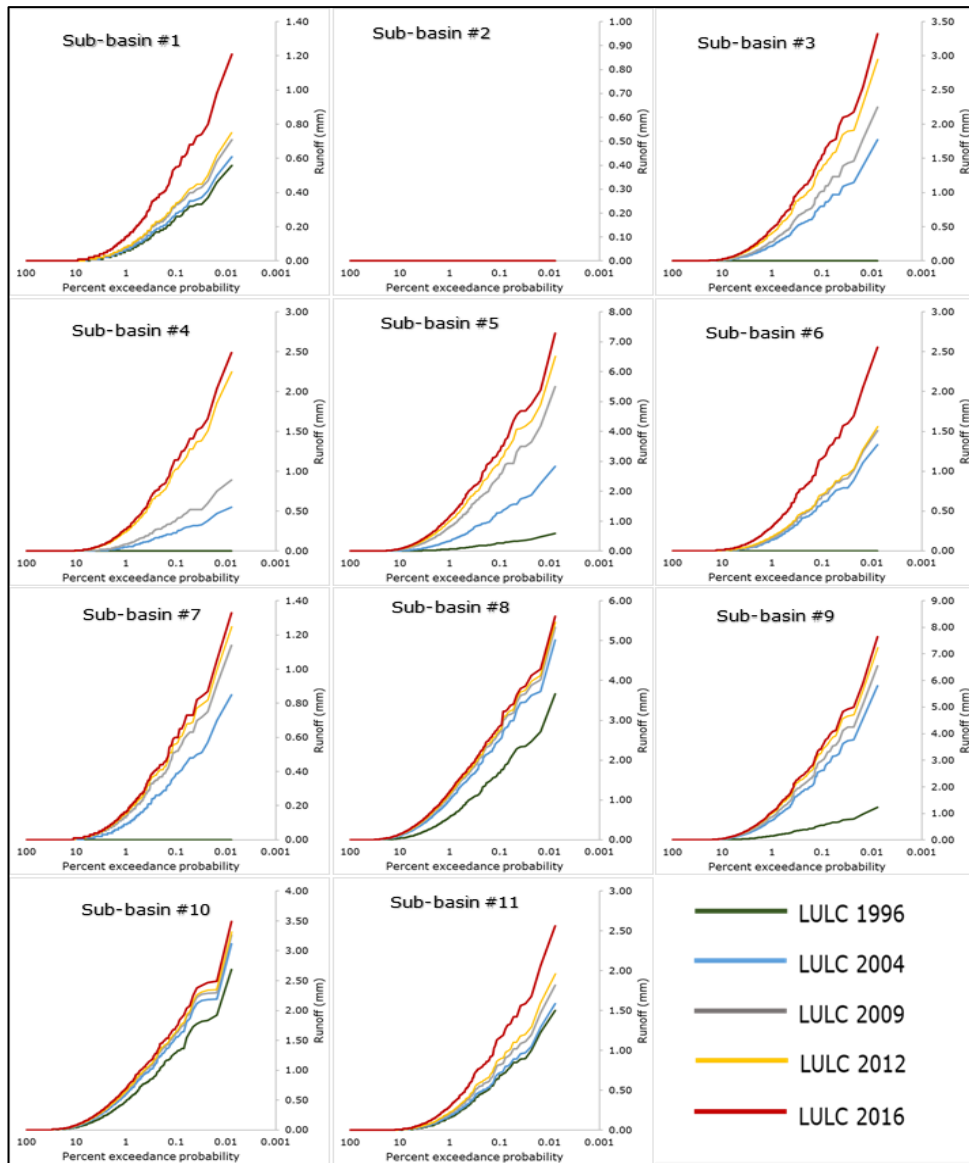


Figure 7.32: Percent exceedances of the simulated daily runoff for sub-basins of the Wadi As Silayy catchment under five different historical LULC maps.

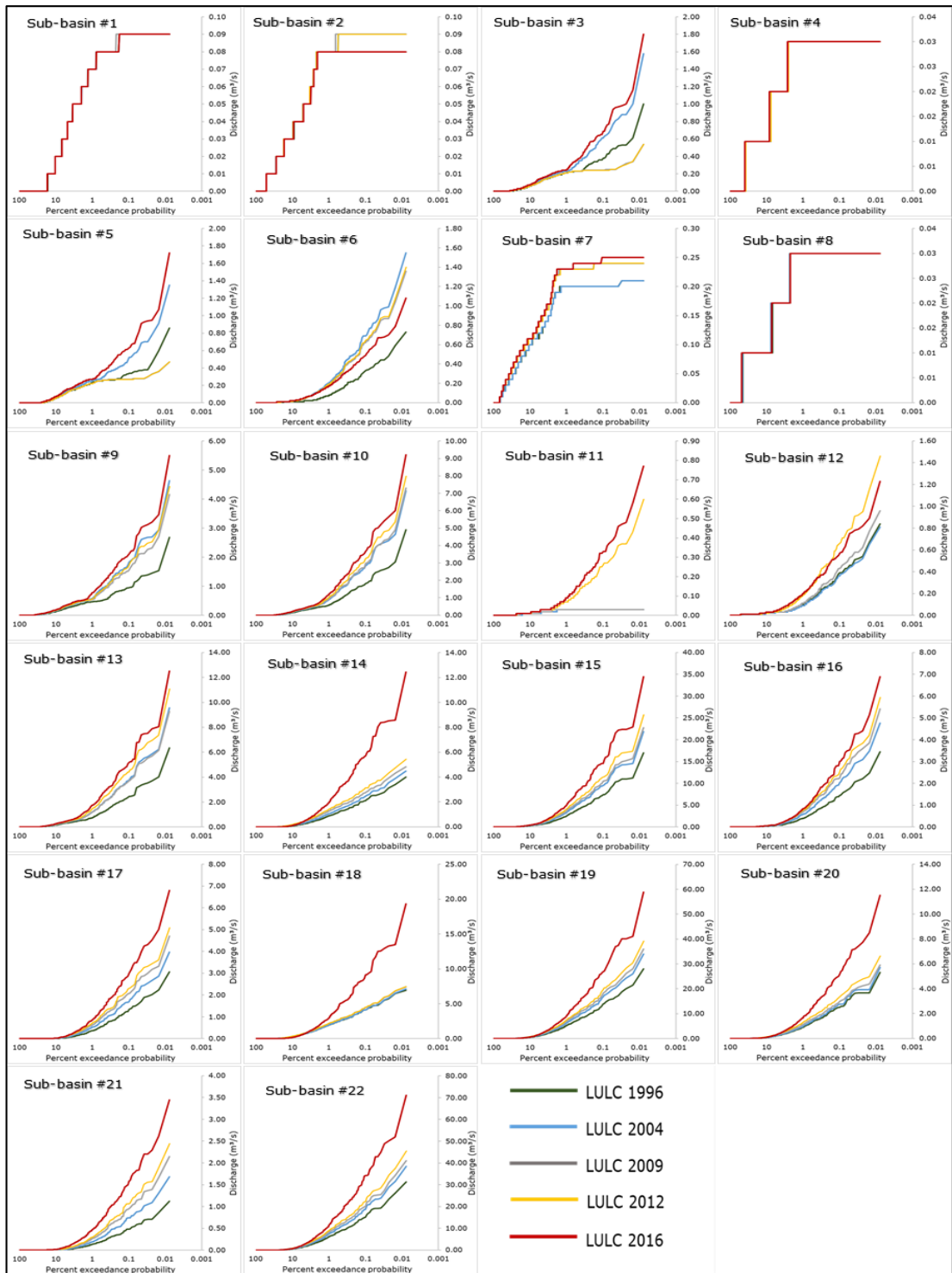


Figure 7.33: Percent exceedances of the simulated daily discharge for sub-basins of the Wadi Hanifah catchment under five different historical LULC maps.

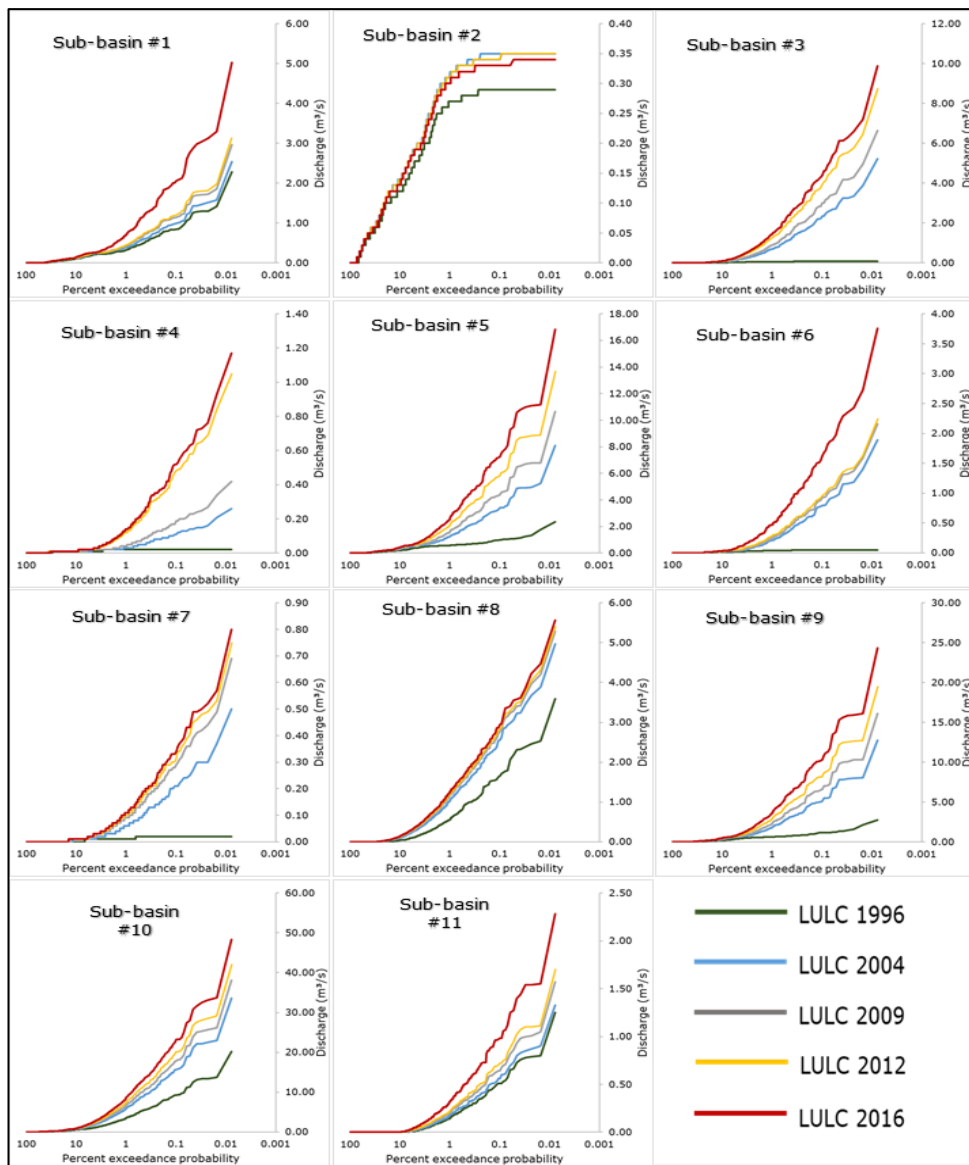


Figure 7.34: Percent exceedances of the simulated daily discharge for sub-basins of the Wadi As Silayy catchment under five different historical LULC maps.

7.7. Summary

This chapter has dealt with the effects of LULC change on runoff and discharge in Riyadh's catchments that experienced rapid urbanisation between 1996 and 2016. The chapter includes the SWAT model results of runoff depths and discharge simulations at annual, monthly, and daily temporal resolution using five historical LULC scenarios for 20 years during the period extending from 1996 to 2016. Modelling was carried out on the levels of the main catchments and sub-basins respectively.

The results indicate an increasing trend of surface runoff depths and discharge rates in the main catchments and the sub-basins located within the boundary of Riyadh city because of the increase of impermeable surfaces. The average simulated annual runoff values in the Wadi Hanifah catchment increased by about 69% in 20 years, from 4.5 mm when using LULC 1996 scenario to reach 7.6 mm when using the LULC 2016 scenario. Whilst the average simulated annual runoff values in the Wadi As Silayy catchment increased by about 175%, from 3.6 mm when using LULC 1996 scenario to reach 9.9 mm when using LULC 2016 scenario. On the other hand, the simulated results of annual runoff depths and discharge rates for sub-basins in the two catchments of the study area, varied from one sub-basin to another and varied as well in each sub-basin depending on the change rates of LULC.

Monthly runoff and discharge values varied from one sub-basin to another, between months, and across years. The graphs of average monthly runoff under different historical LULC scenarios show that sub-basins unaffected by urbanisation had no significant runoff changes. In contrast, the sub-basins, located within the urbanised area, experienced a gradual increase in runoff depths and discharge rates due to LULC change during the period from 1996 to 2016. But the increasing rates of simulated runoff were not the same for all sub-basins due to the different proportions of urbanisation in each sub-basin. Simulated runoff depths in some sub-basins increased by 25% and others such as the sub-basin 5 in the Wadi As Silayy catchment reached up to 2,025% for March.

Results of daily runoff indicated that LULC changes have significantly increased runoff on levels of main catchments and sub-basins. For example, compared to annual maximum runoff values when using LULC 1996 scenario, the simulated annual maximum daily runoff

increased when using the LULC 2016 scenario by a percentage ranging from 50% to 100% in the Wadi Hanifah catchment and by a percentage ranging from 100% to 200% in the Wadi As Silayy catchment. Moreover, LULC change exerted a positive effect on annual maximum daily runoff depths for the various return periods. A remarkable example of the impact of LULC change in Riyadh city is that the estimated annual maximum daily runoff for the 100-year return period using LULC 1996 is equivalent to the estimated runoff for the 10-year return period using LULC 2016 in the Wadi Hanifah catchment. For the Wadi As Silayy catchment, a striking example is that the estimated 3.5 mm runoff for the 5-year return period using the LULC 2016 scenario is much greater than the runoff value (2.8 mm) for the 100-year return period using the LULC 1996.

Chapter 8: Projections of runoff and discharge for Riyadh under future LULC scenario

8.1. Overview

To get a general idea of the potential impact of LULC change on runoff in the city in the near future, surface runoff projections were calculated for the year 2030 under different probabilities of future LULC change. As mentioned in Chapter 4, the probabilities of the Riyadh urban boundary by the year 2030 have been calculated and mapped by Seto et al. (2012). The 3%, 49%, 75%, 77%, and 100% probabilities of Riyadh urban expansion in 2030 have been used for projections of future runoff scenarios in Riyadh's catchments. Predicted urban areas for Riyadh were 3683 km², 3089 km², 2885 km², 2431 km² and 1902 km² for probabilities of 3%, 49%, 75%, 77%, and 100% respectively (Figure 8.1 and Figure 8.2).

This chapter deals with the projections of runoff depths and discharge rates for catchments in Riyadh under five future LULC scenarios. The calibrated and validated SWAT models from Chapter 6 were applied to simulate annual, monthly, and daily runoff and discharge. As mentioned in section 7.3., annual and monthly runoff and discharge were modelled using climate data from three weather stations and three rain gauges for the period 1991-2000. Whereas daily rainfall data for the period 1965-2000 from one rain gauge were used to model the annual maximum daily runoff aiming to relate variations of daily surface runoff either to LULC type or to the change of LULC. The interpretation and explanation of the SWAT model results were presented on two scales: the main catchments and sub-basins.

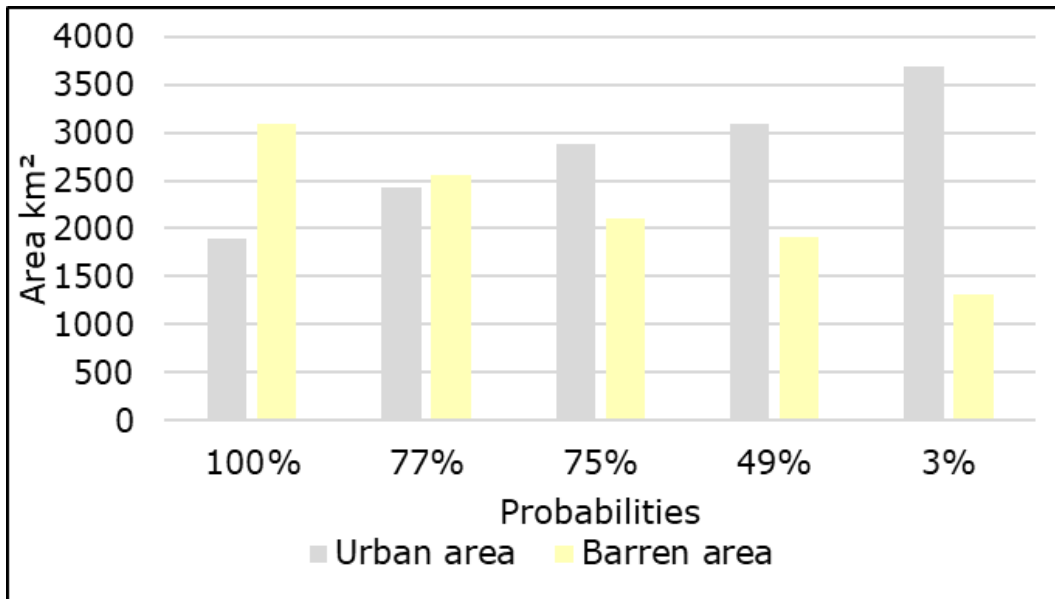


Figure 8.1: Probabilities of Riyadh Urban Expansion in 2030.

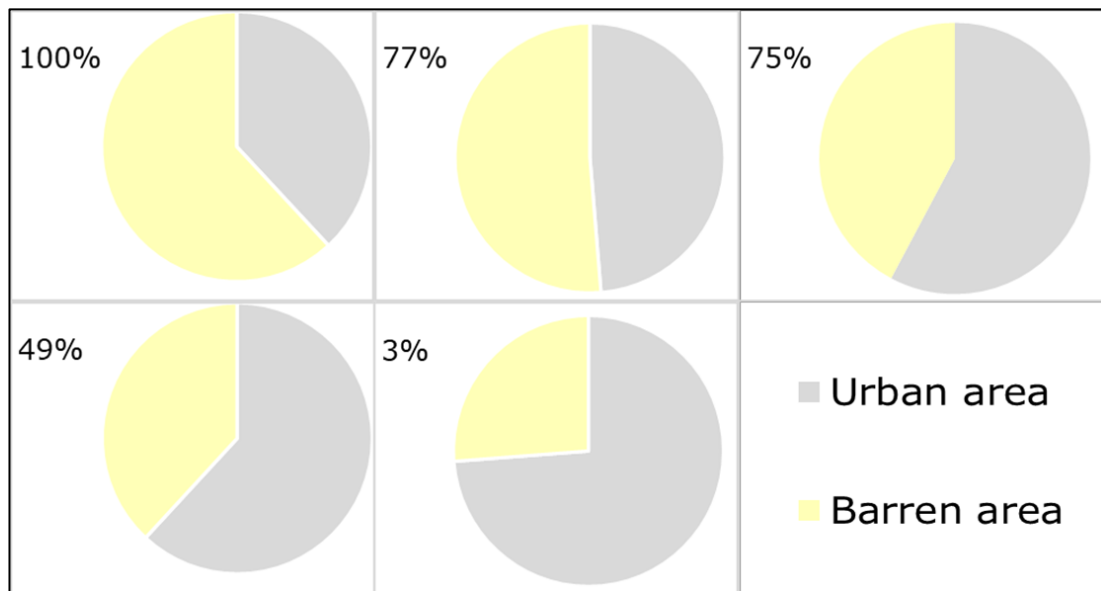


Figure 8.2: Proportions of urban area in Riyadh catchments for probabilities of urban expansion in 2030.

8.2. Modelling annual runoff

Table 8.1 and Table 8.2 show the simulated annual surface runoff depths for the Wadi Hanifah and the Wadi As Silayy catchments under five different LULC change probabilities in 2030. For the 100% probability of LULC in 2030, the average annual surface runoff depths are projected to be 12.9 mm and 13.6 mm in the Wadi Hanifah and the Wadi As Silayy catchments, respectively. It is clear

from the tables that an increasing trend in the surface runoff with a lower percentage of probabilities for LULC change in 2030 can occur. For example, the projected average annual surface runoff depths for the 49% probability of LULC change in 2030 can reach 16 mm and 25.8 mm in the Wadi Hanifah and the Wadi As Silayy catchments respectively (Figure 8.3). Additionally, changes in runoff coefficient and discharge rate in the two main catchments of Riyadh city are proportionate with increments of projected surface runoff depths for the different probabilities of LULC change in 2030.

Compared to the results when using the 2016 LULC scenario, runoff depth will increase by about 71% and 37% when using the 100% probability scenario for the Wadi Hanifah and the Wadi As Silayy catchments, respectively. But when using the 49% scenario, the positive change in runoff depth will be about 112% in the Wadi Hanifah catchment and 160% in the Wadi As Silayy catchment. The increase of projected surface runoff depths for the different probabilities of LULC change in 2030 can mainly be attributed to the potential decrease of relatively permeable barren lands and the increase of impervious surfaces.

Table 8.1: The projected effect of LULC change on annual surface runoff (mm) in the Wadi Hanifah catchment under five probabilities of LULC 2030 change.

Year	Rainfall (mm)	Probabilities of LULC 2030				
		100%	77%	75%	49%	3%
1991	38.1	3.0	3.3	3.5	3.7	4.4
1992	76.2	8.8	9.4	10.2	10.5	12.0
1993	161.4	21.9	23.6	25.7	26.7	30.7
1994	35.2	4.3	4.5	4.8	4.9	5.3
1995	176.4	30.0	31.5	33.8	34.8	39.2
1996	175.3	25.7	28.1	31.3	32.9	38.4
1997	209.7	21.4	24.3	28.1	30.0	35.9
1998	51.5	8.6	8.9	9.3	9.5	10.4
1999	12.8	1.3	1.4	1.4	1.5	1.6
2000	43.9	3.9	4.5	5.2	5.6	6.8
Average	98.1	12.9	13.9	15.3	16.0	18.4
Runoff Coefficient	-	0.1315	0.1422	0.1562	0.1633	0.1882

Table 8.2: The projected effect of LULC change on annual surface runoff (mm) in the Wadi As Silayy catchment under five probabilities of LULC 2030 change.

Year	Rainfall (mm)	Probabilities of LULC 2030				
		100%	77%	75%	49%	3%
1991	80.3	4.8	8.6	11.0	11.9	15.0
1992	159.0	10.6	17.8	22.2	24.1	29.8
1993	229.0	21.9	32.4	39.2	42.2	50.5
1994	57.3	5.3	6.6	7.7	8.1	9.2
1995	254.0	31.9	42.7	50.5	53.9	62.5
1996	199.9	23.5	32.5	38.7	41.4	48.6
1997	273.7	24.6	37.8	46.3	49.9	60.5
1998	73.0	7.6	10.5	12.5	13.4	15.6
1999	27.4	1.7	2.9	3.6	4.0	4.9
2000	68.4	4.6	7.1	8.7	9.4	11.4
Average	142.2	13.6	19.9	24.0	25.8	30.8
Runoff Coefficient	-	0.0959	0.1398	0.1689	0.1816	0.2167

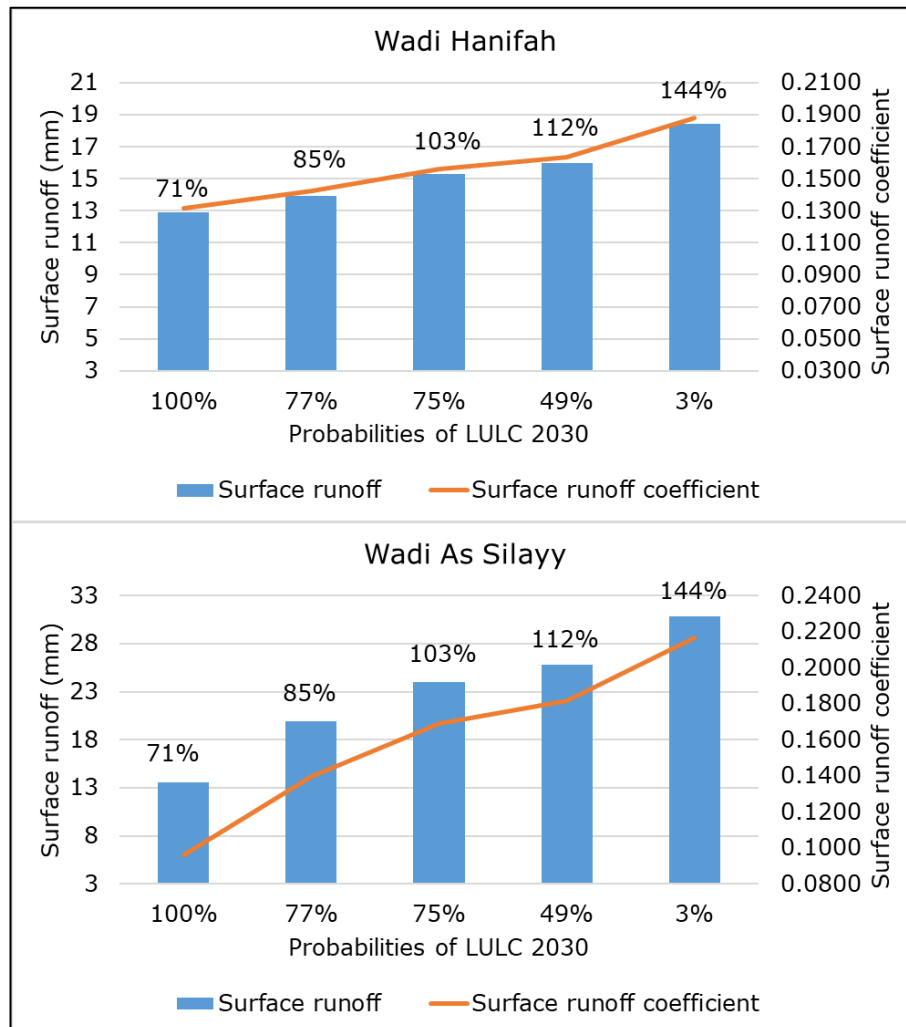


Figure 8.3: Projected annual runoff for 2030 for five LULC change probabilities in Riyadh's catchments (percentages indicate to the comparison of runoff depth with the results of the 2016 LULC scenario).

Table 8.3, Table 8.4, Table 8.5, Table 8.6, Table 8.7, and Table 8.8 show average projected simulations of surface runoff depths, runoff coefficients, and discharge rates sub-basins in Riyadh's catchments under different probabilities of LULC change in 2030. It is evident that predicted results of each variable vary greatly from one sub-basin to another. For example, under 100%-probability of LULC change in 2030 and with the same amount of rainfall, projected surface runoff depths are 0.8 mm in sub-basins 2 and 38.1 mm in sub-basin 5 in the Wadi As Silayy catchment. Simulated average surface runoff values in sub-basin 5 at the Wadi As Silayy catchment are 38.1 mm with 100%-probability of LULC change and 52.6 mm with 49%-probability of LULC change.

Table 8.3: Average simulated annual surface runoff (mm) for the sub-basins in the Wadi Hanifah catchment under five probabilities of LULC 2030 change.

Sub-basin	Rainfall (mm)	Probabilities of LULC 2030				
		100%	77%	75%	49%	3%
1	77.0	0.0	0.0	0.0	0.0	6.3
2	77.0	0.0	0.0	0.4	0.4	3.7
3	82.6	0.6	4.8	10.6	10.6	15.1
4	82.6	0.0	4.8	5.4	5.6	5.6
5	82.6	0.0	11.0	11.3	12.9	18.2
6	82.6	2.7	5.1	21.7	21.7	23.0
7	82.6	0.0	0.0	0.0	1.2	4.4
8	111.5	4.3	4.3	4.3	9.9	16.2
9	82.6	10.7	10.7	11.0	19.1	19.5
10	111.5	27.6	27.6	27.6	27.6	27.6
11	111.5	4.5	4.5	4.5	4.5	8.5
12	111.5	12.8	13.0	13.0	13.0	13.0
13	111.5	30.8	30.8	30.8	30.8	30.8
14	120.6	30.2	30.2	35.3	35.3	35.3
15	110.3	30.6	30.6	30.6	30.6	30.6
16	111.5	13.1	17.6	17.6	17.6	22.4
17	111.5	25.8	25.8	28.1	28.1	29.5
18	120.6	36.4	36.4	36.4	36.4	36.4
19	110.3	28.3	28.3	28.3	28.3	28.3
20	110.3	27.9	27.9	27.9	27.9	27.9
21	110.3	25.6	25.6	26.2	26.1	26.1
22	110.3	19.9	19.9	19.9	22.4	23.6

Table 8.4: Simulated average annual surface runoff (mm) for the sub-basins in the Wadi As Silayy catchment under five probabilities of LULC 2030 change.

Sun-basin	Rainfall (mm)	Probabilities of LULC 2030				
		100%	77%	75%	49%	3%
1	154.4	2.6	9.4	12.7	13.3	22.4
2	154.4	0.8	7.4	8.0	12.5	24.3
3	154.4	9.6	32.2	39.2	41.9	42.8
4	154.4	8.8	11.9	42.2	42.4	42.4
5	154.4	38.1	47.2	52.6	52.6	52.6
6	154.4	17.4	20.9	35.5	35.9	42.7
7	120.7	12.7	13.2	29.3	29.7	29.7
8	120.7	35.0	35.0	37.9	37.9	37.9
9	120.7	28.4	28.6	34.5	34.5	34.5
10	120.7	32.1	32.2	32.2	32.7	32.7
11	110.3	17.4	17.7	17.7	21.6	21.6

Table 8.5: Simulated average annual runoff coefficients for the sub-basins in the Wadi Hanifah catchment under five probabilities of LULC 2030 change.

Sub-basin	Rainfall (mm)	Probabilities of LULC 2030				
		100%	77%	75%	49%	3%
1	77.0	0.0000	0.0000	0.0000	0.0000	0.0814
2	77.0	0.0000	0.0000	0.0047	0.0047	0.0475
3	82.6	0.0077	0.0587	0.1284	0.1284	0.1832
4	82.6	0.0000	0.0586	0.0653	0.0678	0.0678
5	82.6	0.0000	0.1337	0.1366	0.1556	0.2202
6	82.6	0.0332	0.0615	0.2627	0.2627	0.2781
7	82.6	0.0000	0.0000	0.0000	0.0145	0.0536
8	111.5	0.0383	0.0383	0.0383	0.0888	0.1453
9	82.6	0.1291	0.1291	0.1329	0.2315	0.2367
10	111.5	0.2474	0.2474	0.2474	0.2474	0.2474
11	111.5	0.0406	0.0406	0.0406	0.0406	0.0761
12	111.5	0.1150	0.1164	0.1164	0.1164	0.1164
13	111.5	0.2761	0.2761	0.2761	0.2761	0.2761
14	120.6	0.2501	0.2501	0.2928	0.2927	0.2927
15	110.3	0.2774	0.2774	0.2774	0.2775	0.2775
16	111.5	0.1177	0.1581	0.1581	0.1581	0.2009
17	111.5	0.2315	0.2315	0.2521	0.2521	0.2651
18	120.6	0.3022	0.3022	0.3022	0.3022	0.3022
19	110.3	0.2565	0.2565	0.2565	0.2565	0.2565
20	110.3	0.2529	0.2529	0.2529	0.2529	0.2529
21	110.3	0.2321	0.2321	0.2371	0.2370	0.2370
22	110.3	0.1806	0.1806	0.1806	0.2030	0.2136

Table 8.6: Simulated average annual runoff coefficients for sub-basins in the Wadi As Silayy catchment under five probabilities of LULC 2030 change.

Sub-basin	Rainfall (mm)	Probabilities of LULC 2030				
		100%	77%	75%	49%	3%
1	154.4	0.0169	0.0610	0.0820	0.0860	0.1449
2	154.4	0.0053	0.0477	0.0519	0.0810	0.1577
3	154.4	0.0625	0.2085	0.2536	0.2716	0.2768
4	154.4	0.0569	0.0770	0.2735	0.2743	0.2743
5	154.4	0.2465	0.3057	0.3407	0.3408	0.3408
6	154.4	0.1127	0.1353	0.2298	0.2328	0.2764
7	120.7	0.1051	0.1092	0.2431	0.2460	0.2460
8	120.7	0.2900	0.2900	0.3142	0.3142	0.3142
9	120.7	0.2353	0.2371	0.2861	0.2861	0.2861
10	120.7	0.2661	0.2666	0.2666	0.2709	0.2709
11	110.3	0.1580	0.1604	0.1604	0.1955	0.1955

Table 8.7: Simulated average annual discharge (m³/s) for the sub-basins in the Wadi Hanifah catchment under five probabilities of LULC 2030 change.

Sub-basin	Rainfall (mm)	Probabilities of LULC 2030				
		100%	77%	75%	49%	3%
1	77.0	0.2	0.2	0.2	0.2	0.8
2	77.0	0.3	0.3	0.4	0.4	0.7
3	82.6	0.9	1.5	2.0	2.0	3.3
4	82.6	0.1	0.2	0.3	0.3	0.3
5	82.6	0.8	1.7	2.2	2.3	3.6
6	82.6	0.1	0.2	0.6	0.6	0.6
7	82.6	1.8	1.8	1.8	2.1	2.9
8	111.5	0.3	0.3	0.3	0.4	0.5
9	82.6	2.8	3.7	4.6	5.3	7.4
10	111.5	3.3	4.3	5.2	5.9	8.2
11	111.5	0.3	0.3	0.3	0.3	0.4
12	111.5	0.4	0.4	0.4	0.4	0.4
13	111.5	4.2	5.1	6.1	6.8	9.1
14	120.6	1.7	1.7	2.0	2.0	2.0
15	110.3	7.9	9.2	10.4	11.1	13.8
16	111.5	1.8	2.1	2.1	2.1	2.5
17	111.5	1.9	1.9	2.0	2.0	2.1
18	120.6	2.5	2.5	2.5	2.5	2.5
19	110.3	12.2	13.5	14.9	15.6	18.4
20	110.3	1.8	1.8	1.8	1.8	1.8
21	110.3	1.1	1.1	1.1	1.1	1.1
22	110.3	15.4	16.7	18.1	18.8	21.7

Table 8.8: Simulated average annual discharge (m³/s) for the sub-basins in the Wadi As Silayy catchment under five probabilities of LULC 2030 change.

Sub-basin	Rainfall (mm)	Probabilities of LULC 2030				
		100%	77%	75%	49%	3%
1	154.4	4.0	4.4	4.9	5.0	6.3
2	154.4	4.3	4.9	5.0	5.6	7.0
3	154.4	1.8	4.0	4.5	4.6	4.7
4	154.4	0.3	0.3	0.7	0.7	0.7
5	154.4	10.3	13.6	15.1	16.0	18.7
6	154.4	1.4	1.5	2.1	2.1	2.4
7	120.7	0.3	0.3	0.6	0.6	0.6
8	120.7	1.2	1.2	1.3	1.3	1.3
9	120.7	12.2	15.5	18.1	19.1	22.0
10	120.7	19.3	22.8	25.4	26.5	29.5
11	110.3	0.7	0.7	0.7	0.8	0.8

Figure 8.4, Figure 8.5, and Figure 8.6 show the spatial distribution of the projected average annual runoff amount, runoff coefficient, and discharge rate at different probabilities of LULC change in 2030. The highest values of these variables are mainly confined to the sub-basins located within the urban areas reflecting the high impact of the urbanisation process on water flow in the study area.

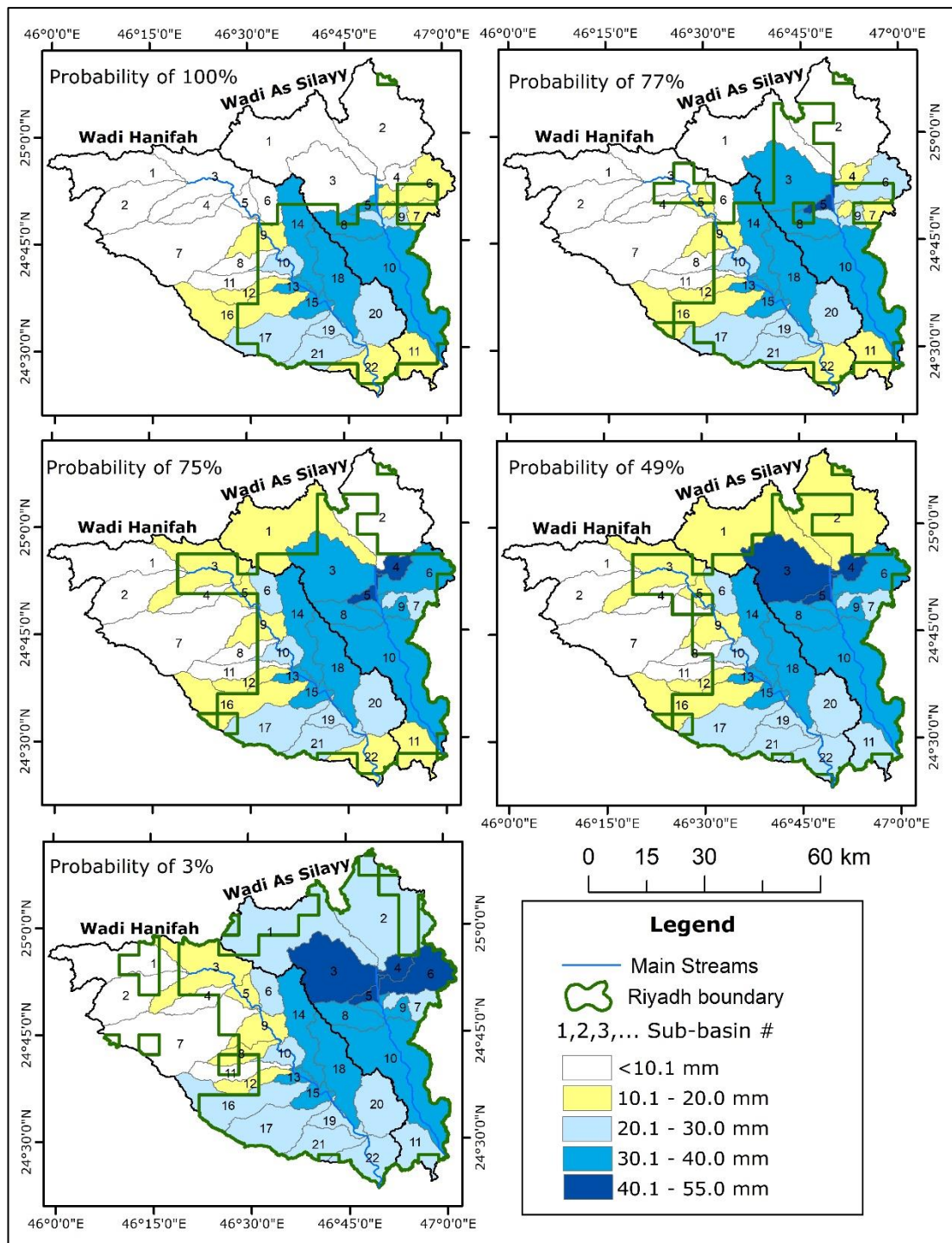


Figure 8.4: Spatial distribution of projected average annual runoff in 2030 for five LULC change probabilities in Riyadh's catchments.

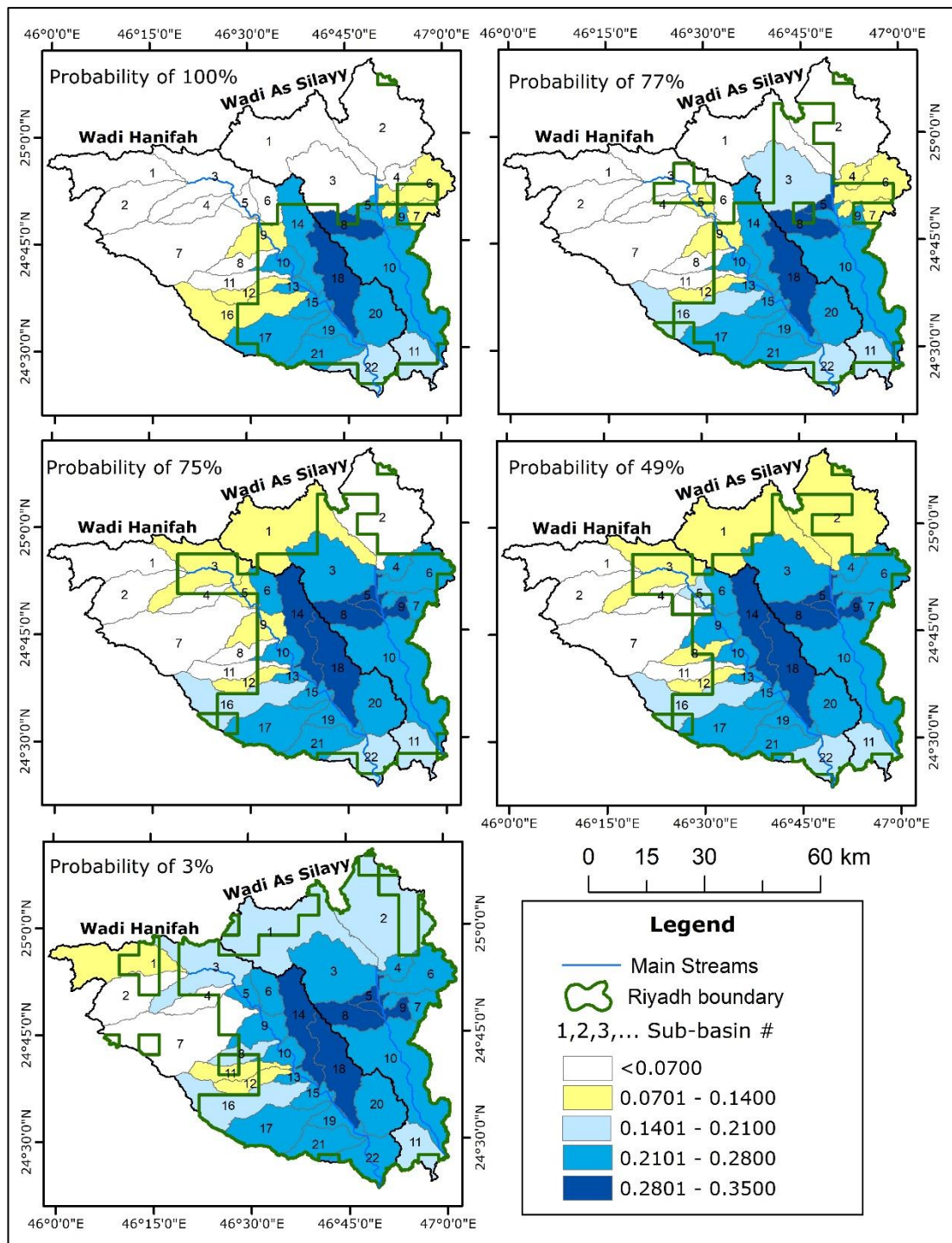


Figure 8.5: Spatial distribution of projected average annual runoff coefficients in 2030 for five LULC change probabilities in Riyadh's catchments.

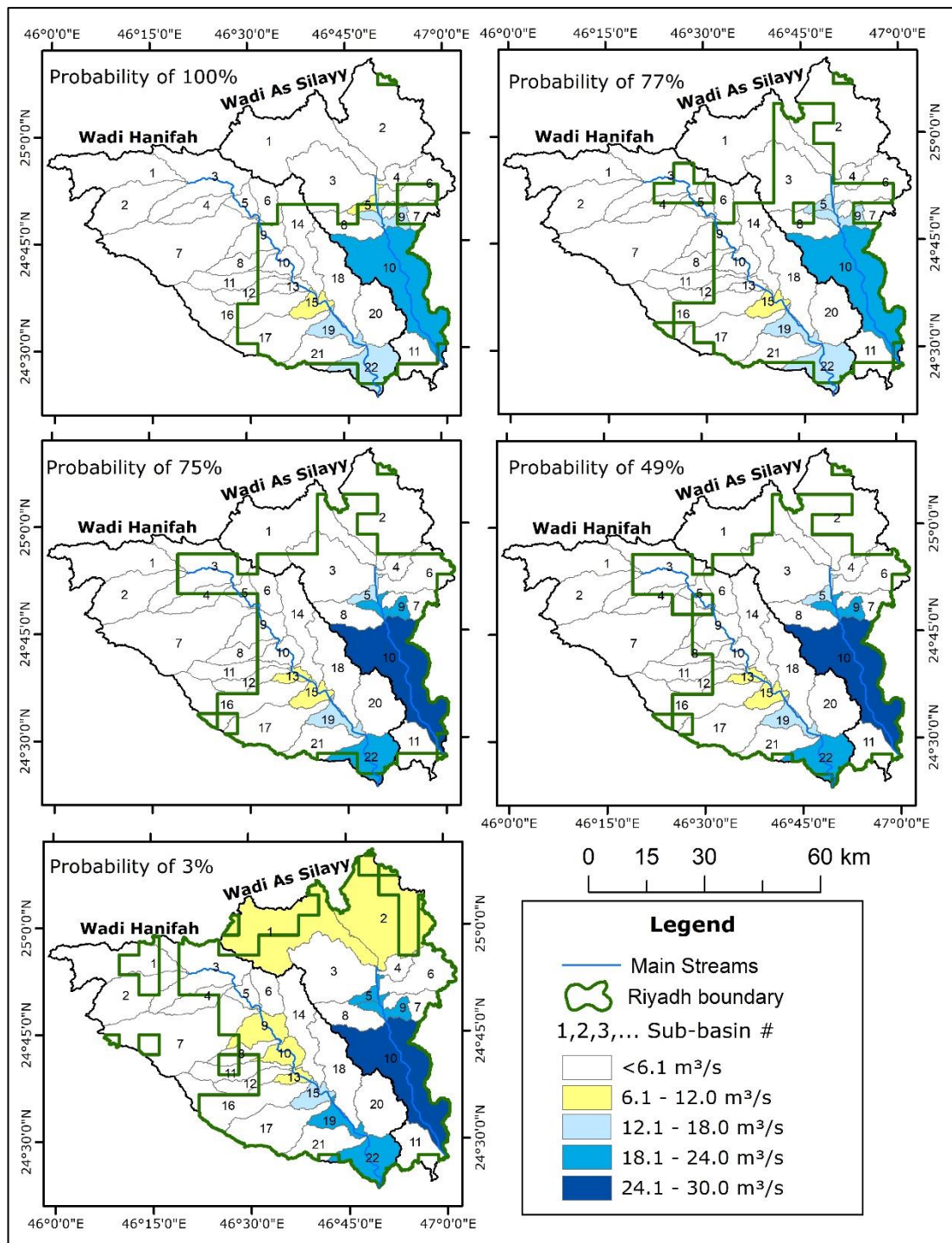


Figure 8.6: Spatial distribution of projected average annual discharge rates in 2030 for five LULC change probabilities in Riyadh's catchments.

8.3. Modelling monthly runoff

Table 8.9 and

Table 8.10 present projected average monthly surface runoff depths in the catchments of the study area under five probabilities of LULC 2030 change. The highest values of projected average monthly surface runoff were found in March in Riyadh's catchments in the LULC 2030 scenario, with the lowest in October. Based on the prediction of 100% probability, the potential average surface runoff depth in March could reach 4.1 mm in the Wadi Hanifah and Wadi As Silayy catchments. Comparing these results to the results of the LULC 2016 scenario, the increase of runoff in the Wadi Hanifah and the Wadi As Silayy catchments will be 71% and 41%, respectively (Figure 8.7). Simultaneously, runoff coefficients and discharge rates increase in the catchments.

Table 8.9: The projected average monthly surface runoff depths (mm) in the Wadi Hanifah catchment under five probabilities of LULC 2030 change.

Month	Average rainfall (mm)	Probabilities of LULC 2030				
		100%	77%	75%	49%	3%
January	15.9	2.3	2.5	2.7	2.9	3.2
February	3.8	0.3	0.3	0.4	0.4	0.5
March	28.3	4.1	4.4	4.8	5.0	5.8
April	19.2	2.6	2.8	3.0	3.1	3.5
May	3.2	0.6	0.6	0.6	0.7	0.7
June	0.0	0.0	0.0	0.0	0.0	0.0
July	0.0	0.0	0.0	0.0	0.0	0.0
August	0.1	0.0	0.0	0.0	0.0	0.0
September	0.0	0.0	0.0	0.0	0.0	0.0
October	3.9	0.4	0.4	0.5	0.5	0.6
November	14.5	1.4	1.6	1.9	2.0	2.5
December	9.3	1.2	1.3	1.4	1.4	1.6

Table 8.10: The projected average monthly surface runoff depths (mm) in the Wadi As Silayy catchment under five probabilities of LULC 2030 change.

Month	Average rainfall (mm)	Probabilities of LULC 2030				
		100%	77%	75%	49%	3%
January	24.9	2.4	3.6	4.3	4.7	5.6
February	8.2	0.4	0.8	1.0	1.1	1.3
March	34.4	4.1	5.6	6.7	7.2	8.4
April	28.4	2.7	3.8	4.5	4.8	5.7
May	7.3	0.8	1.1	1.3	1.4	1.6
June	0.0	0.0	0.0	0.0	0.0	0.0
July	0.0	0.0	0.0	0.0	0.0	0.0
August	0.2	0.0	0.0	0.0	0.0	0.0
September	0.0	0.0	0.0	0.0	0.0	0.0
October	2.8	0.2	0.2	0.3	0.3	0.4
November	21.6	1.8	3.0	3.7	4.0	4.9
December	14.7	1.2	1.9	2.3	2.5	3.0

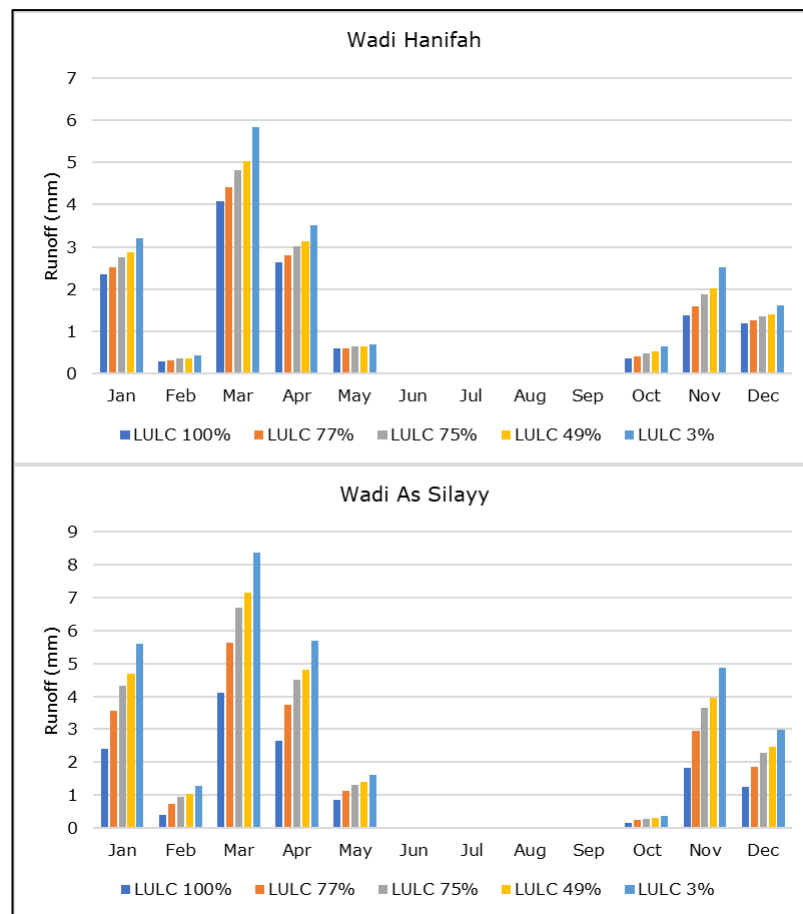


Figure 8.7: Projections of the impact of LULC changes on the average simulated monthly runoff for Riyadh's catchments using different LULC 2030 scenarios.

On the sub-basins level, the monthly runoff depths and discharge rates for the probabilities of LULC 2030 change were simulated in the catchments of the study area, under five different future LULC scenarios (Appendix D). Average simulated monthly runoff and discharge are plotted in Figure 8.8, Figure 8.9, Figure 8.10, and Figure 8.11 to assess the impact of expected LULC 2030 change on simulations of monthly runoff and discharge on the sub-basins level for the two main catchments. Potential runoff depths and discharge rates in sub-basins within urban boundaries have high increases for all probabilities of LULC 2030 change. From the graphs, it can be noticed that the average monthly runoff and discharge values varied from one sub-basin to another and from month to another in the study area. The line charts reveal an increasing trend of monthly simulated runoff depths and discharge rates that occurred in the sub-basins within the city's boundary. The potential increases in runoff depths and discharge rates in most sub-basins were due to the potential increase of impervious surfaces. For the 100% probability of LULC 2030 change, it can be seen that the highest average potential runoff depth was 9.1 mm found in sub-basin 8 of the Wadi As Silayy catchment for March. The comparison of this result with the result of the SWAT model when using the LULC 1996 scenario, the potential increase of runoff is about 7% in this sub-basin.

As an example, to show the effect of potential LULC change on the spatial distribution characteristics of the average simulated runoff and discharge in the study area, the simulations for January using five different LULC 2030 scenarios were mapped (Figure 8.12 and Figure 8.13). The maps clearly illustrate the potential positive effect of the urbanisation process in Riyadh on runoff depths and discharge rates. These maps show that runoff depths and discharge rates in sub-basins outside boundaries of the probable built-up areas of

Riyadh will have no significant changes when using the LULC 2030 scenarios. For example, simulated discharge rates for sub-basin 1 in the Wadi Hanifah catchment in January were in the category of $<0.50 \text{ m}^3/\text{s}$ for all LULC 2030 scenarios. On the other hand, the maps show that runoff depths and discharge rates will increase in the sub-basins that will be within the boundary of built-up areas for the LULC 2030 scenarios. For example, simulated discharge rates for sub-basin 10 in the Wadi As Silayy catchment for January will increase by about 15%, from $2.31 \text{ m}^3/\text{s}$ when using the LULC 2016 scenario to $2.66 \text{ m}^3/\text{s}$ when using the 100% probability scenario.

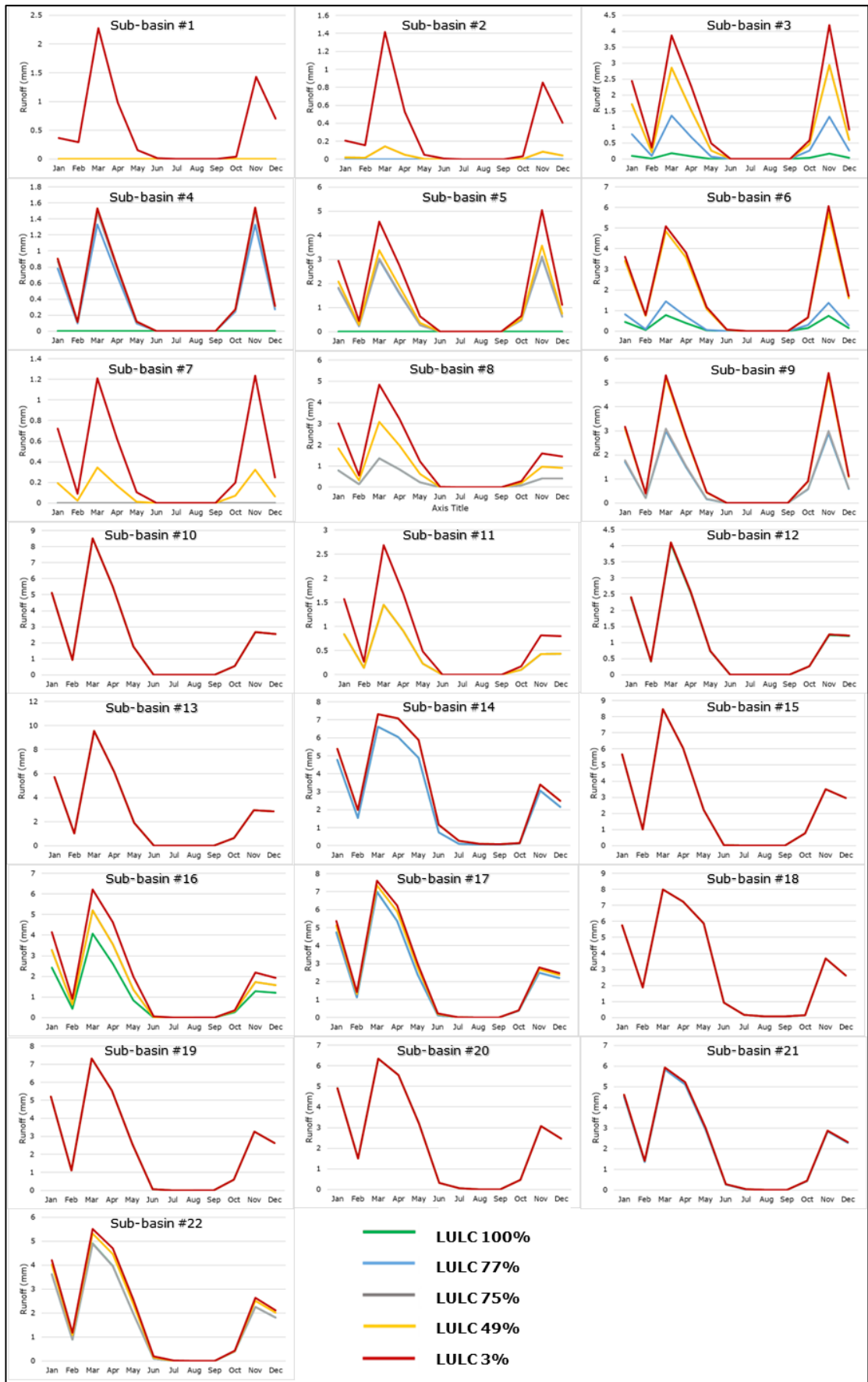


Figure 8.8: Average simulated monthly runoff using different LULC 2030 scenarios for sub-basins of the Wadi Hanifah catchment.

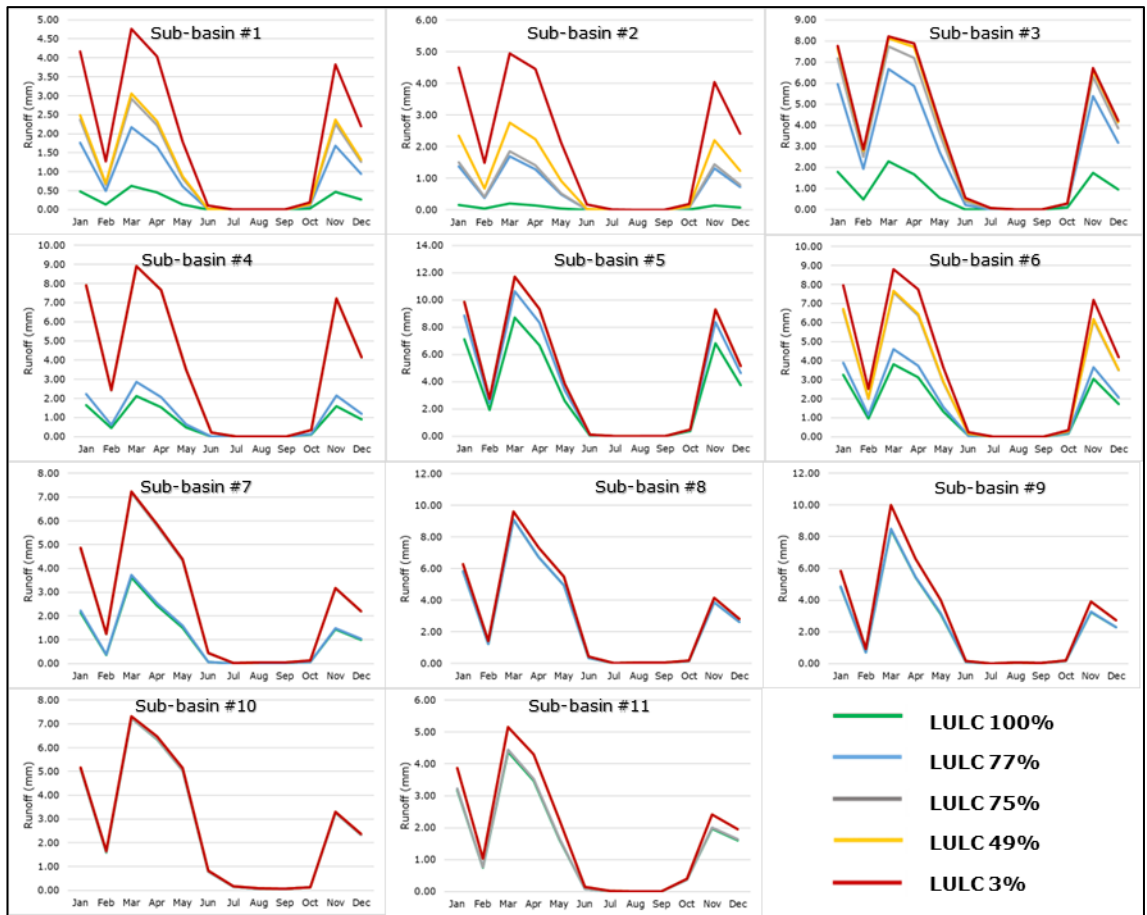


Figure 8.9: Average simulated monthly runoff using different LULC 2030 scenarios for sub-basins of the As Silay catchment.

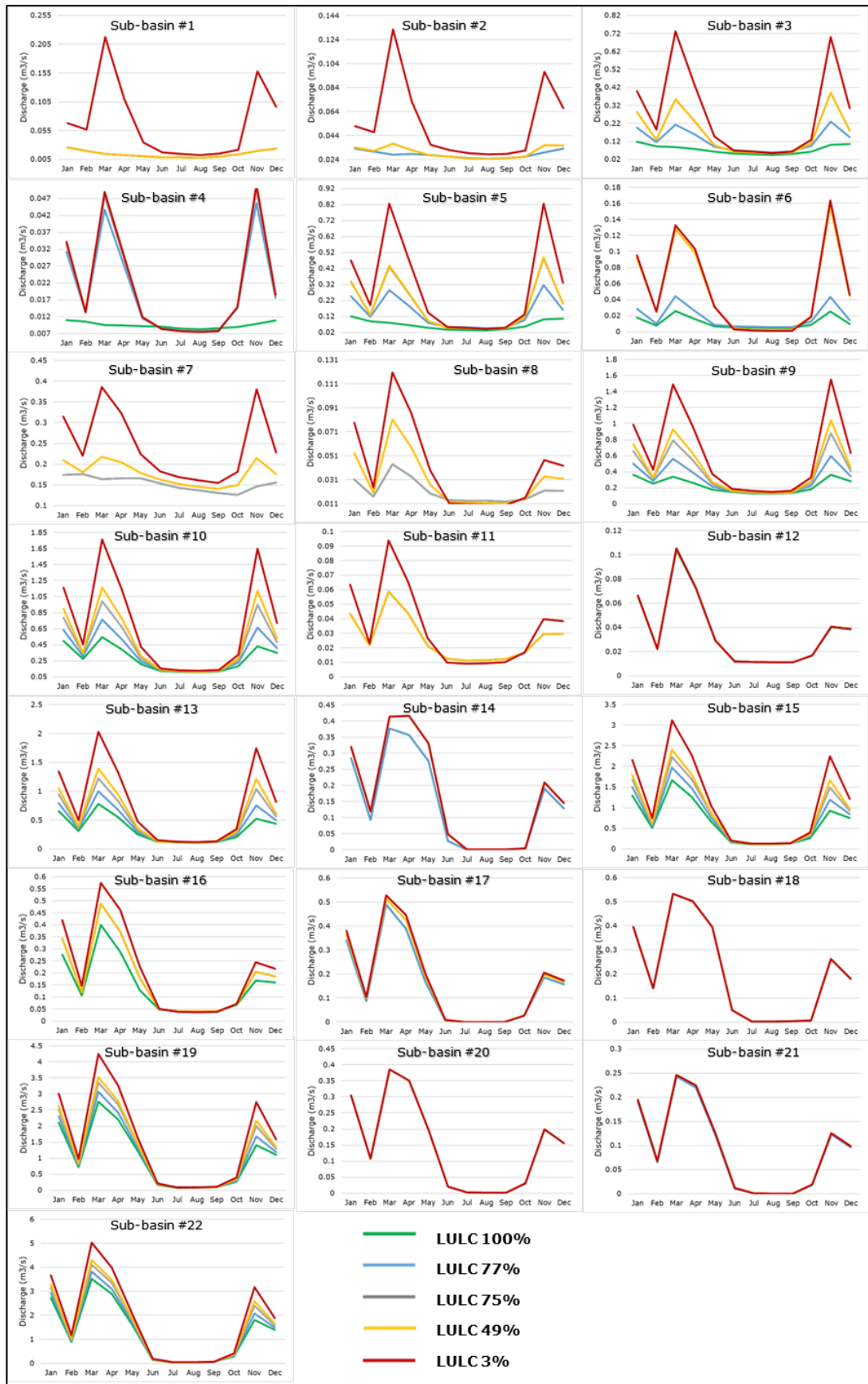


Figure 8.10: Average simulated monthly discharge using different LULC 2030 scenarios for sub-basins of the Wadi Hanifah catchment.

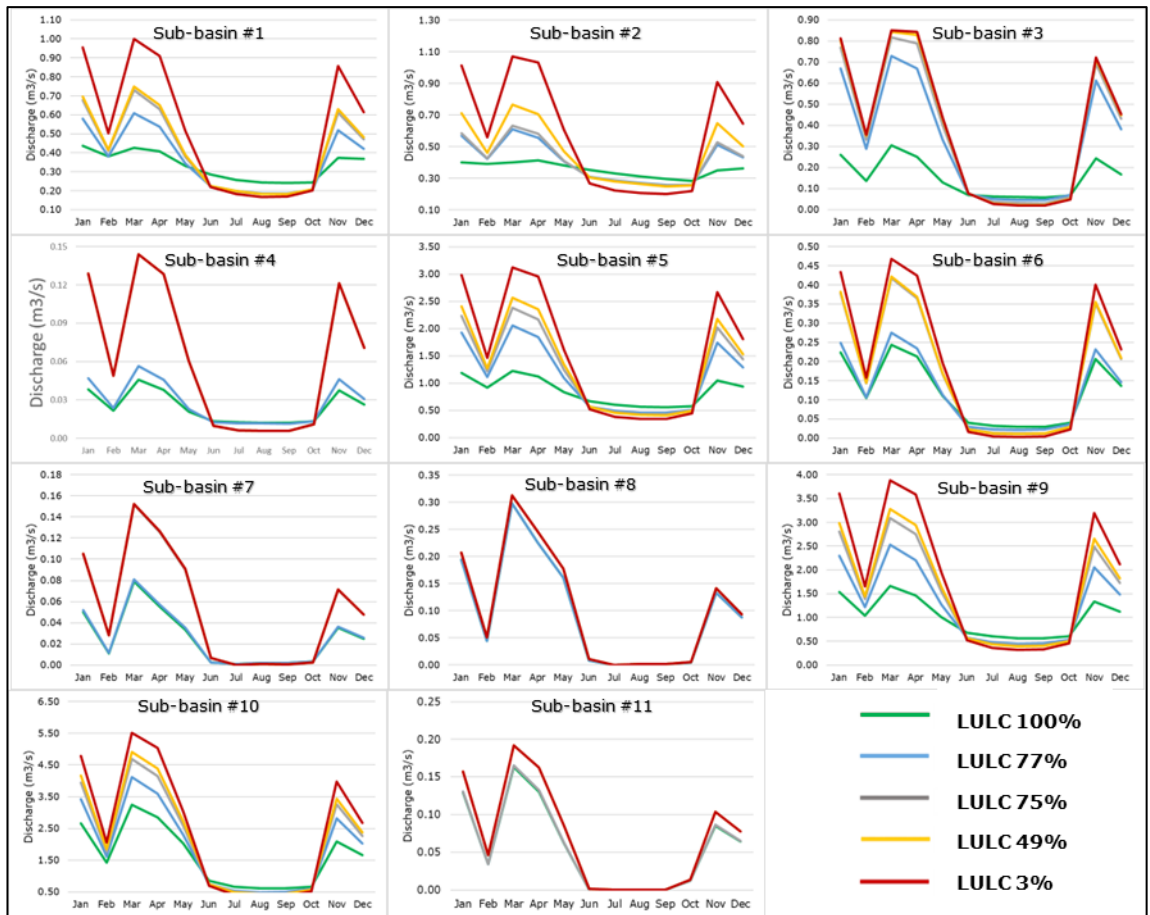


Figure 8.11: Average simulated monthly discharge using different LULC 2030 scenarios for sub-basins of the As Silay catchment.

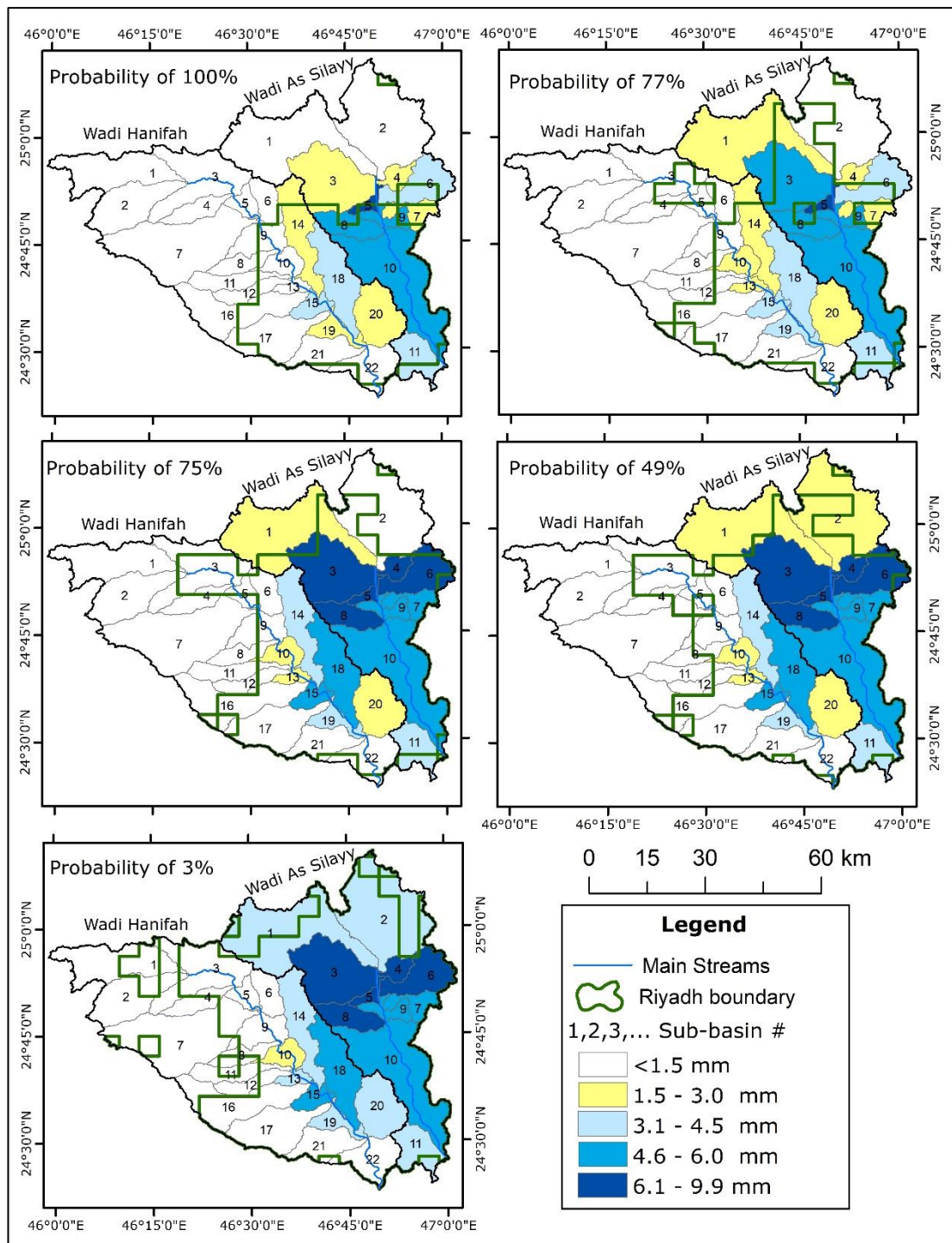


Figure 8.12: Spatial distributions of projected average simulated runoff for January in Riyadh's catchments using five probabilities of LULC 2030.

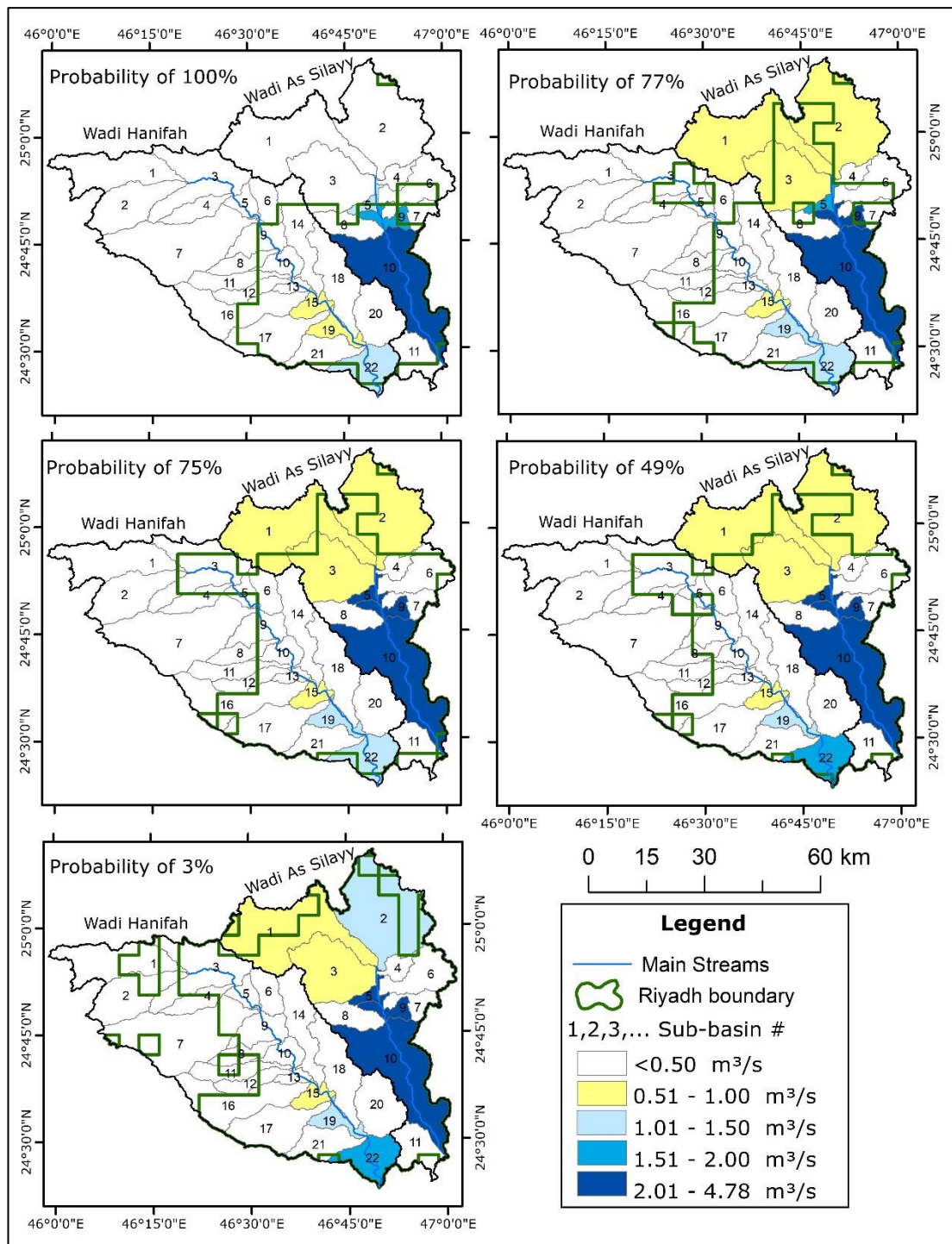


Figure 8.13: Spatial distributions of projected average discharge for January in Riyadh's catchments using five probabilities of LULC 2030.

8.4. Modelling daily extreme runoff

Table 8.11 shows simulations of annual maximum daily runoff and Figure 8.14 is a plot of annual maximum daily runoff values simulated using LULC 2016 and its corresponding values projected using 100%-probability LULC 2030 scenarios. This Figure indicates a high potential positive impact of LULC change on simulated annual maximum daily surface runoff by 2030. The simulated data of maximum daily runoff and discharge for 2030 were used to compute various return periods (Table 8.12 and Table 8.13). Runoff forecasting for LULC 2030 scenarios reveals that the 100-year event (10.7 mm) in the 100% probability scenario for the Wadi As Silayy catchment becomes a 10-year event (10.2 mm) in the 75% probability scenario. It means that this large event will be 10 times more common in the 75% probability scenario than in the 100% probability scenario. It should be noted that the runoff value of the 100-year event in the 100% probability scenario for the Wadi As Silayy catchment is more than 3 times of the 100-year event (2.8 mm) in the LULC 1996 scenario.

From Table 8.13, it can be seen that the difference between estimated values of discharge using the 49% probability scenario and 75% probability scenario is not large compared with the difference between estimated values when using the 75% probability scenario and 100% probability map. These interesting results can be attributed to the differences in estimated urbanised areas which are 1,902 km² for 100% probability, 2,855 km² for 75% probability, and 3,089 km² for 49% probability. The continual significant positive impacts of historical and future LULC changes on computed annual maximum daily runoff and discharge can be seen by comparing 2-year and 30-year return periods in the study area as plotted in Figure 8.15 and Figure 8.16.

Table 8.11: SWAT model simulations of annual maximum daily surface runoff using different probabilities of LULC 2030 scenarios for Riyadh's catchments.

Year	Rank	Return Period	Rainfall (mm)	Wadi Hanifah SURQ (mm)					Wadi As Silayy SURQ (mm)				
				Probabilities of LULC 2030					Probabilities of LULC 2030				
				LULC 100%	LULC 77%	LULC 75%	LULC 49%	LULC 3%	LULC 100%	LULC 77%	LULC 75%	LULC 49%	LULC 3%
1965	3	12.3	38.2	7.01	7.63	8.44	8.86	10.34	6.36	8.61	10.2	10.91	12.7
1966	32	1.2	8.6	0.97	1.05	1.16	1.22	1.43	0.88	1.19	1.41	1.5	1.75
1967	12	3.1	23.7	3.96	4.31	4.78	5.01	5.85	3.6	4.87	5.77	6.17	7.19
1968	2	18.5	47.2	8.93	9.72	10.76	11.29	13.18	8.11	10.97	13	13.91	16.19
1969	14	2.6	22.2	3.66	3.98	4.41	4.63	5.4	3.32	4.5	5.33	5.7	6.63
1970	35	1.1	5.6	0.46	0.5	0.55	0.58	0.68	0.42	0.57	0.67	0.72	0.83
1971	15	2.5	22	3.6	3.92	4.34	4.56	5.32	3.27	4.43	5.25	5.61	6.53
1972	7	5.3	31	5.5	5.98	6.62	6.95	8.12	4.99	6.76	8	8.56	9.97
1973	30	1.2	11.4	1.49	1.62	1.79	1.88	2.19	1.35	1.83	2.16	2.32	2.7
1974	26	1.4	14	1.99	2.17	2.4	2.52	2.94	1.81	2.45	2.9	3.1	3.61
1975	8	4.6	31	5.49	5.98	6.62	6.95	8.11	4.99	6.75	8	8.56	9.96
1976	18	2	20	3.2	3.49	3.86	4.05	4.73	2.91	3.94	4.67	4.99	5.81
1977	34	1.1	8.3	0.91	0.99	1.1	1.15	1.34	0.83	1.12	1.33	1.42	1.65
1978	4	9.2	34.2	6.17	6.72	7.44	7.81	9.11	5.6	7.59	8.99	9.61	11.19
1979	24	1.5	14.5	2.09	2.28	2.52	2.64	3.09	1.9	2.57	3.04	3.26	3.79
1980	13	2.8	22.5	3.72	4.05	4.48	4.71	5.49	3.38	4.57	5.42	5.79	6.74
1981	36	1	5	0.37	0.4	0.45	0.47	0.55	0.34	0.45	0.54	0.58	0.67
1982	17	2.2	20.7	3.35	3.64	4.04	4.24	4.94	3.04	4.12	4.88	5.21	6.07
1983	20	1.9	19.5	3.1	3.38	3.74	3.92	4.58	2.82	3.81	4.52	4.83	5.62
1984	9	3.9	30	5.29	5.75	6.37	6.69	7.8	4.8	6.5	7.7	8.23	9.58
1985	6	6.2	32	5.71	6.21	6.88	7.22	8.43	5.18	7.01	8.31	8.89	10.35
1986	21	1.8	18.2	2.84	3.09	3.42	3.59	4.19	2.58	3.49	4.13	4.42	5.14
1987	11	3.4	28	4.86	5.3	5.86	6.15	7.18	4.42	5.98	7.08	7.58	8.82
1988	25	1.5	14.2	2.03	2.21	2.45	2.57	3	1.84	2.5	2.96	3.16	3.68
1989	16	2.3	21	3.41	3.71	4.11	4.31	5.03	3.09	4.19	4.96	5.31	6.18
1990	31	1.2	9	1.04	1.13	1.25	1.31	1.53	0.94	1.28	1.51	1.62	1.88
1991	29	1.3	11.6	1.52	1.66	1.84	1.93	2.25	1.38	1.87	2.22	2.37	2.76
1992	27	1.4	12.6	1.72	1.87	2.07	2.17	2.54	1.56	2.11	2.5	2.68	3.11
1993	10	3.9	30	5.1	5.56	6.15	6.46	7.54	4.64	6.28	7.43	7.95	9.25
1994	22	1.7	17.2	2.63	2.87	3.17	3.33	3.89	2.39	3.24	3.83	4.1	4.77
1995	5	7.4	33.7	6.06	6.6	7.31	7.67	8.96	5.51	7.46	8.83	9.45	11
1996	1	37	53	10.16	11.06	12.25	12.86	15.01	9.23	12.49	14.8	15.83	18.43
1997	19	2	20	3.2	3.49	3.86	4.05	4.73	2.91	3.94	4.67	4.99	5.81
1998	23	1.6	17	2.59	2.82	3.12	3.28	3.83	2.35	3.19	3.78	4.04	4.7
1999	28	1.3	12	1.6	1.74	1.93	2.03	2.36	1.45	1.97	2.33	2.49	2.9
2000	33	1.1	8.5	0.95	1.03	1.14	1.2	1.4	0.86	1.16	1.38	1.48	1.72

Many datasets of projected annual maximum daily runoff and discharge were obtained for the 33 sub-basins based on the results of the five SWAT models. By applying EVI distribution, the 2-year and 30-year return periods using the 100%-probability and 49% probability maps of LULC 2030 were computed to give examples of the spatial distribution characteristics of the projected runoff and discharge in sub-basins of Riyadh's catchments (Figure 8.17 and Figure 8.18). All results showed considerable increases in runoff and discharge. By comparing the built-up boundaries of the city and the simulated and calculated values of annual maximum daily runoff based on the various historical and future LULC scenarios, it is apparent that the increase in runoff depths and discharge rates in

the sub-basins of the study area is affected significantly by the increase of impermeable the built-up area within each sub-basin.

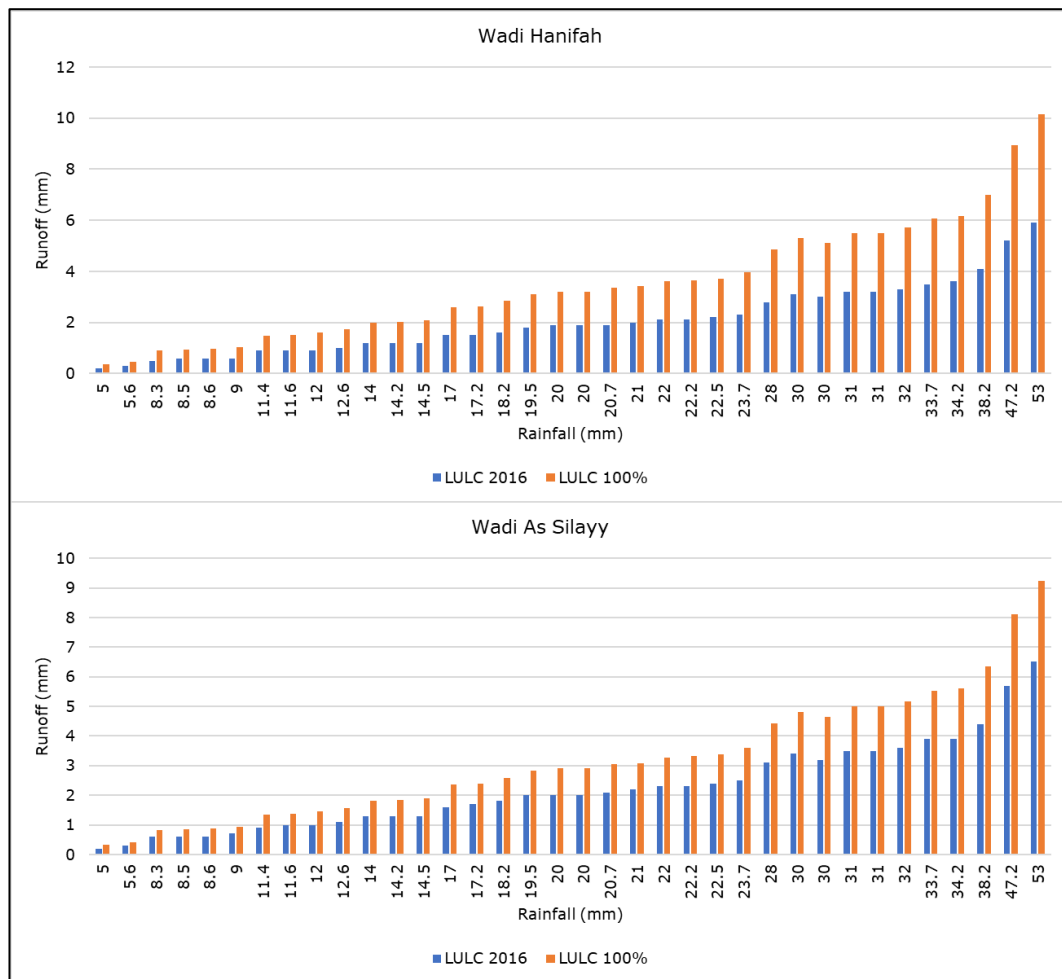


Figure 8.14: A comparison between simulated annual maximum daily runoff values using LULC 2016 and 100% probability LULC 2030 scenarios.

Table 8.12: Computed annual maximum daily runoff depth (mm) in various return periods using simulated data for the period 1965-2000 under five different probabilities of LULC in 2030 of Riyadh's catchments.

Catchment	The Wadi Hanifah catchment					The Wadi As Silayy catchment				
	2-year	10-year	30-year	50-year	100-year	2-year	10-year	30-year	50-year	100-year
LULC 100%	3.16	7.00	9.31	10.37	11.79	2.87	6.36	8.46	9.42	10.71
LULC 77%	3.44	7.62	10.14	11.29	12.84	3.88	8.61	11.45	12.75	14.50
LULC 75%	3.81	8.44	11.23	12.50	14.22	4.6	10.20	13.57	15.10	17.18
LULC 49%	4.00	8.86	11.78	13.12	14.92	4.92	10.91	14.51	16.16	18.37
LULC 3%	4.67	10.34	13.76	15.32	17.42	5.73	12.70	16.89	18.81	21.39

Table 8.13: Computed annual maximum daily discharge rate (m³/s) in various return periods using simulated data for the period 1965-2000 under five different probabilities of LULC in 2030 of Riyadh's catchments.

Catchment	The Wadi Hanifah catchment					The Wadi As Silayy catchment				
	2-year	10-year	30-year	50-year	100-year	2-year	10-year	30-year	50-year	100-year
LULC 100%	18.09	47.31	64.90	72.93	83.76	14.09	34.31	46.49	52.04	59.54
LULC 77%	19.81	52.12	71.56	80.44	92.41	19.00	46.64	63.28	70.87	81.12
LULC 75%	21.04	55.51	76.26	85.73	98.51	21.44	52.64	71.43	80.00	91.57
LULC 49%	22.26	58.85	80.87	90.92	104.48	22.23	54.60	74.09	82.98	94.98
LULC 3%	25.06	66.71	91.78	103.22	118.65	24.38	59.98	81.41	91.19	104.38

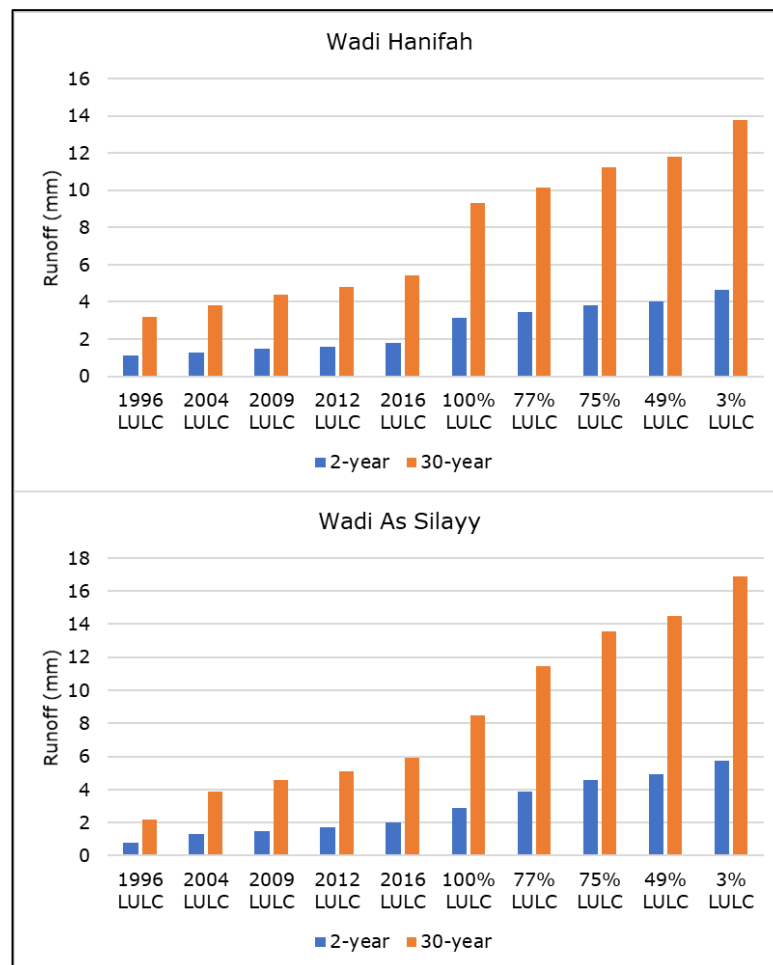


Figure 8.15: Impact of LULC changes on computed annual maximum daily runoff for various return periods using different historical and future scenarios.

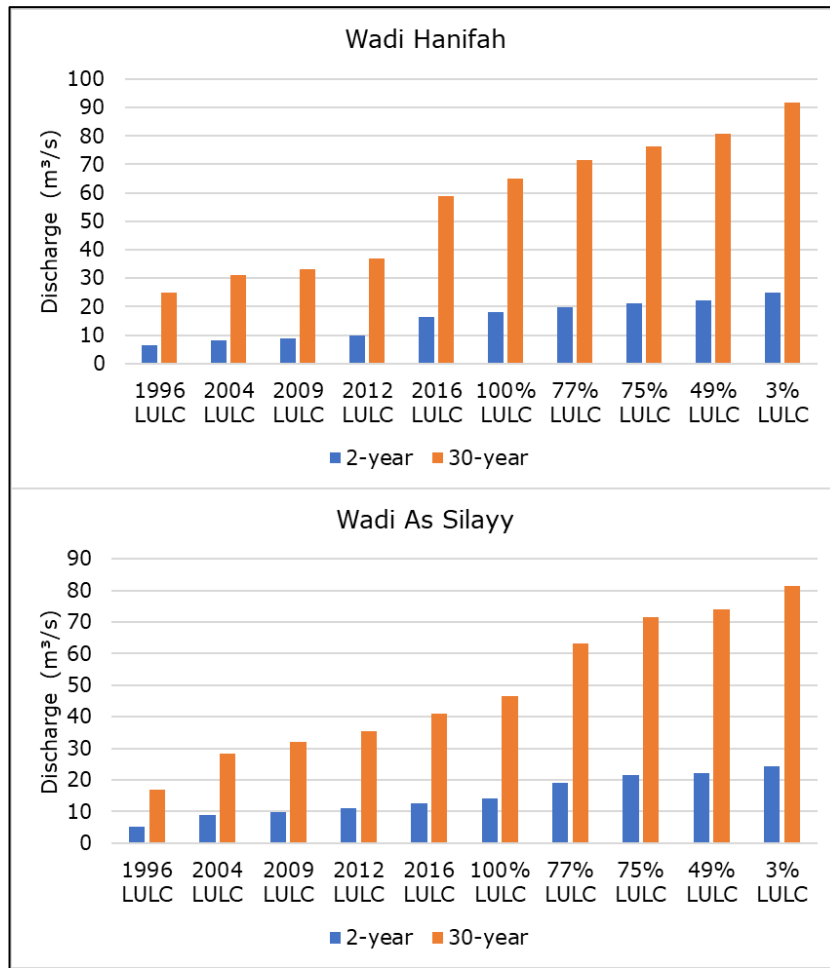


Figure 8.16: Impact of LULC changes on computed annual maximum daily discharge for various return periods using different historical and future scenarios.

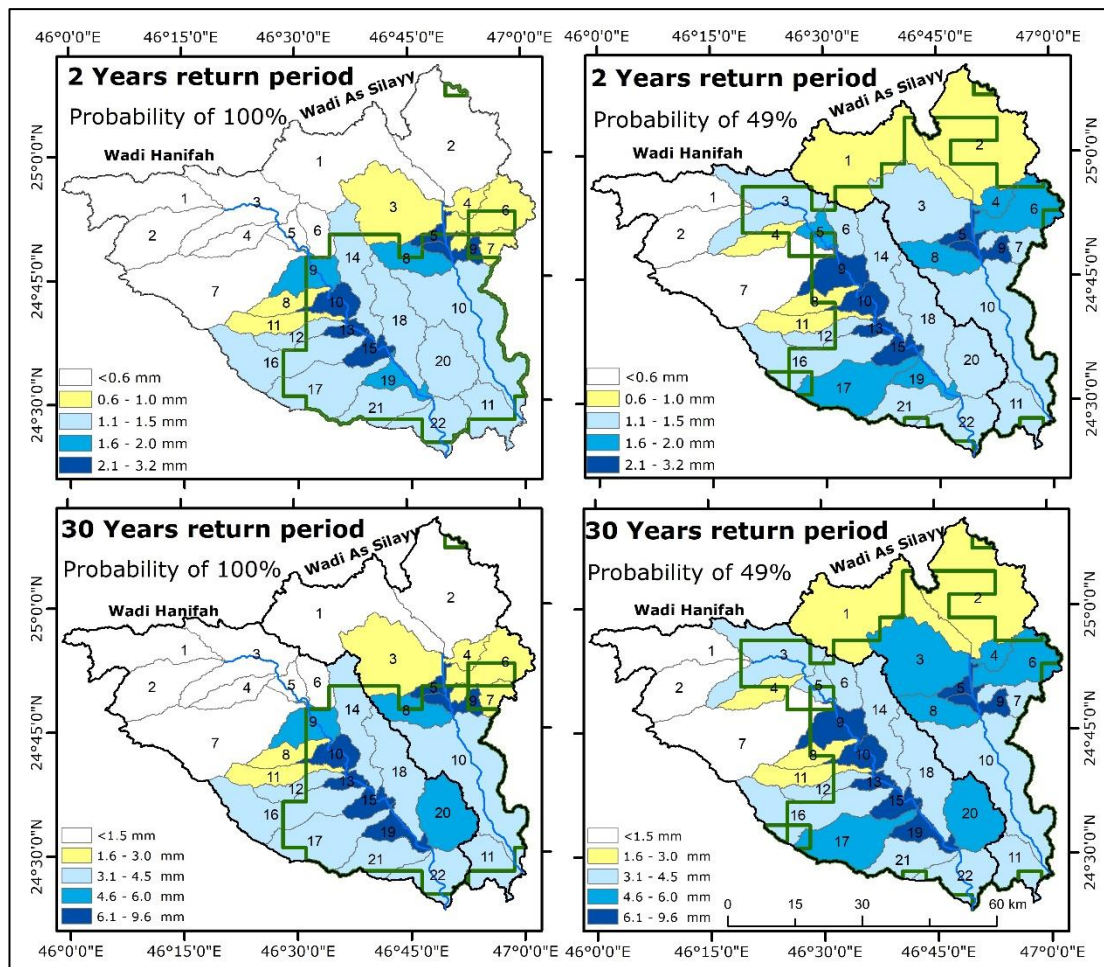


Figure 8.17: Spatial distributions of computed maximum daily runoff for the 2-year (top panels) and 30-year (bottom) return period using 100% (left panels) and 49% (right) probabilities of LULC 2030.

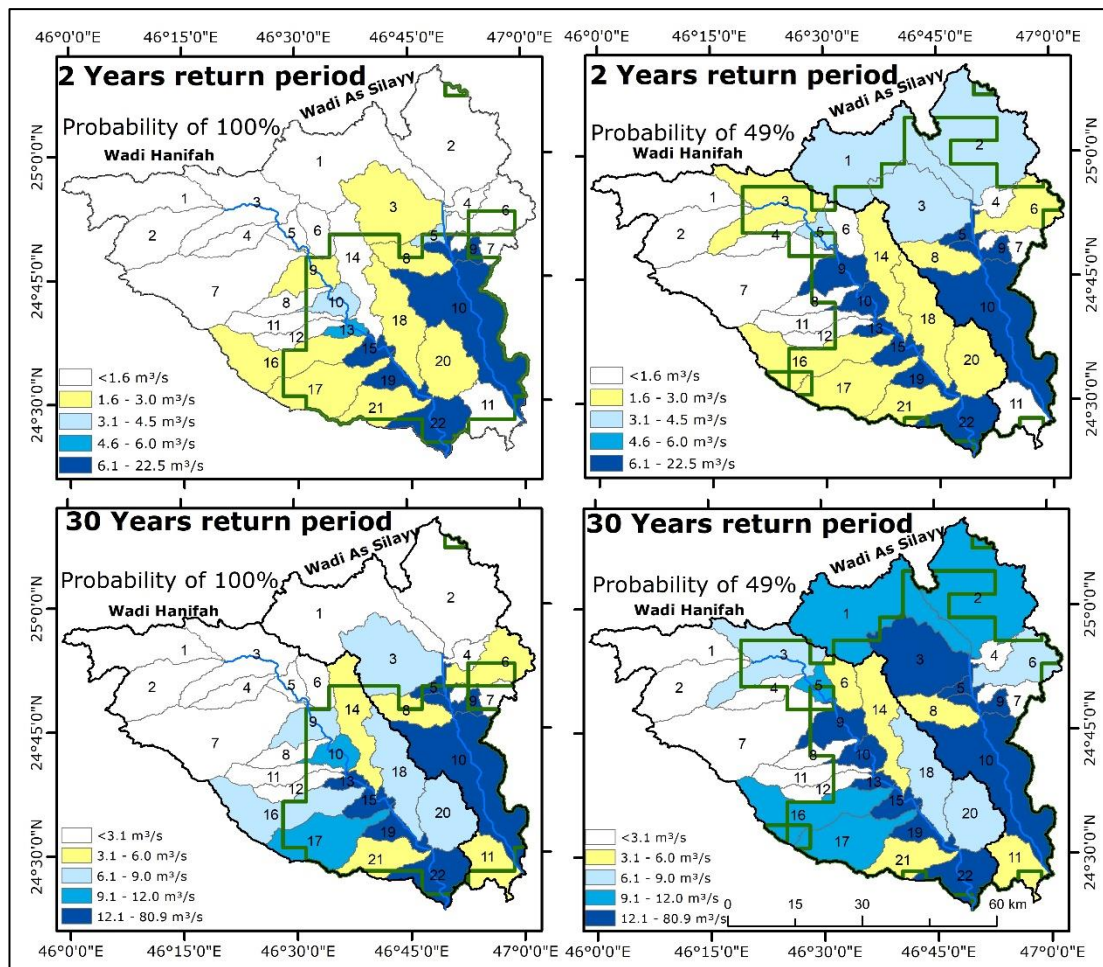


Figure 8.18: Spatial distributions of computed maximum daily discharge for the 2-year (top panels) and 30-year (bottom) return period using 100% (left panels) and 49% (right) probabilities of LULC 2030.

8.5. Summary

Annual, monthly, and annual maximum daily surface runoff and discharge were projected and mapped for the near future in the study area on catchment and sub-basin levels using five different scenarios of LULC 2030 probabilities. Outputs of SWAT models demonstrate the potential positive effect of the urbanisation process in Riyadh on runoff depths and discharge rates for LULC 2030 probabilities scenarios. On the contrary, simulation results show that runoff depths and discharge rates in sub-basins outside the boundaries of the probable built-up areas of Riyadh will have no significant changes when using the LULC 2030 scenarios. The

projected surface runoff and discharge increase for the different LULC 2030 probabilities scenarios can be attributed to the potential decrease of relatively permeable barren lands and the increase of impervious urban surfaces.

Simulation results show that the average annual surface runoff depths, for the 100% probability of LULC in 2030, are 12.9 mm and 13.6 mm in the Wadi Hanifah and the Wadi As Silayy catchments, respectively. The results also show an increasing trend in the surface runoff with a lower percentage of probabilities for LULC change in 2030 can occur. For example, the projected average annual surface runoff depths for the 49% probability of LULC change in 2030 can reach 16 mm and 25.8 mm in the Wadi Hanifah and the Wadi As Silayy catchments respectively. Besides, results indicate that changes in runoff coefficient and discharge rate in the two main catchments of Riyadh city are proportionate with increments of projected surface runoff depths for the different probabilities of LULC change in 2030.

The results reveal that runoff depths in March are highest in the study area under the LULC 2030 scenarios, and runoff values in October are the lowest. Based on the prediction of 100% probability, the potential average surface runoff depths in March could reach 4.1 mm in the Wadi Hanifah and Wadi As Silayy catchments. Compared these results to the results of the LULC 2016 scenario, the increase of runoff in the Wadi Hanifah and the Wadi As Silayy catchments will be 71% and 41%, respectively. Simultaneously, runoff coefficients and discharge rates increase in the catchments.

The results indicate a high potential positive impact of LULC 2030 scenarios on simulated annual maximum daily surface runoff and discharge rates. Return periods computation of annual maximum

daily runoff for LULC 2030 scenarios reveals that the 100-year event in the 100% probability scenario for the Wadi As Silayy catchment becomes a 10-year event in the 75% probability scenario. It means that this large event will be 10 times more common in the 75% probability scenario than in the 100% probability scenario. Compared to a historical LULC scenario, the runoff value of the 100-year event in the 100% probability scenario for the Wadi As Silayy catchment is more than 3 times the 100-year event in the LULC 1996 scenario.

Chapter 9: Discussion

9.1. Overview

Since the oil boom in the mid-seventies of the last century, Riyadh city has been growing rapidly. The rapid development has been associated with serious environmental problems in Riyadh city, including repeated urban flooding (Al Saud, 2010; Alamri 2011; Abosuliman et al. 2013; Almazroui, 2013; Al-Momani and Shawaqfah, 2013; Qari et al., 2014; Al Saud 2015; Hijji et al. 2015; Rahman et al., 2016), groundwater level rise (Al-Othman and Ahmed 2012, Riyadh Environment 2017), and wastewater perennial streams (Al-Samhuri and Al-Naim 2007; Al-Othman 2008; Al-Jasser 2011; Al-Othman 2015; Al-Hammad and Abd El-Salam 2017; Al-Nuwaysir et al. 2019; Bacha et al. 2019). Because of the lack of proper sewage disposal and other sanitary services in several neighbourhoods of Riyadh city and the leakage from water supply systems, the city has faced a groundwater level rise problem (Figure 9.1). Commonly, urban areas reduce infiltration rates and increase runoff volumes and peak discharges (Leopold 1968; Graf 1975; USDA 1986; Fitzpatrick et al. 2005).

In addition to the role of impervious surfaces in Riyadh, urban runoff has been affected directly or indirectly by other factors. Leakages from public water supply systems and discharge of wastewater effluents from septic systems resulted in an increase in soil moisture, rise in groundwater levels, waterlogging, and creation of water ponds in some neighbourhoods of the city (Arriyadh Environment, n.d.; Alahmari 2018; Aljammaz et al. 2021). Moreover, the development of Riyadh city ignored the geomorphological factor (Mubarak 2004; AlQahtany et al. 2014). Although green and open spaces are significant for minimizing flood risk (Yao et al. 2015; Kim et al. 2016; Müller et al. 2020), city landscaping has been neglected,

to a high degree, during the urbanisation process of Riyadh city (Alqahtany 2014). Besides, the infrastructure of Riyadh city has lagged far behind its dramatic growth (Garba, 2004). In 2010, for instance, stormwater drainage networks covered only 30% of the city (Alhaddan, 2010; Al-Fawzan 2016). After the 9 November 2018 flood, the Mayor of Riyadh revealed that 40% of stormwater drainage networks in Riyadh were completed, indicating that the target of the Municipality of Riyadh was to cover 58% of the city by 2020 (Akhbaar24 2019).



Figure 9.1: Problem of groundwater level rise in some neighbourhoods of the Riyadh city.
Source: Riyadh Environment (2017).

This chapter provides a discussion of the challenge to model surface runoff in ungauged arid catchments having a scarcity of climate data and uneven distribution of weather stations. Also, it includes a discussion of the evaluation of LULC change's impact on surface runoff. Besides, it contains a discussion of the direct or indirect effects of other anthropogenic factors on runoff such as the impact of the rapid and not properly planned expansion of Riyadh, the

impact of the shortage of public green spaces in Riyadh, and the impact of Riyadh's development on flood occurrence potential.

9.2. The challenges in setting-up SWAT models for Riyadh

Due to the absence of runoff measurements and limitations and deficiencies in the few previous studies on runoff and flood in Riyadh city, there is an urgent need to estimate surface runoff and how it is affected by LULC change in the main catchments of the city, which can help policymakers to take necessary actions to mitigate and prevent flood problems. Two previous studies were found applying the SWAT to estimate runoff in Saudi Arabia. SWAT models in both studies were unvalidated and applied regionalisation techniques for the SWAT model calibration by extrapolating catchment-specific parameters from the Wadi Girafi catchment (3,350 km²) in the Sinai Peninsula, Egypt.

The use of an uncalibrated SWAT model to simulate runoff in Riyadh catchments can overestimate the simulations. Saleh et al. (2009) reported that the uncalibrated SWAT model overestimated daily streamflow values for the Mustang Creek basin, California by about 423%. Abaho et al. (2009) applied an uncalibrated SWAT model to evaluate the impacts of climate change on river flows and groundwater recharge in the Sezibwa catchment, Uganda. The authors found a 47 % increase in average river flow for the period of 2070–2100. Odusanya et al. (2019) draw the attention that there are high levels of uncertainty associated with uncalibrated model predictions. Although simulation outputs of the uncalibrated SWAT models were reported to be highly overestimated, in a recently published paper, Doulabian et al. (2021) applied an uncalibrated SWAT model to locate potential rainwater harvesting sites in an area that was categorised as semi-arid to arid. The authors neglected calibration and validation processes and mentioned two reasons to

justify it which were the inadequacy of observed runoff data and in the comparative environment, calibration and validation processes are not necessary.

Setting up the SWAT model for Riyadh's catchments to fill this research gap and help researchers to better understand urban development and environmental response in this arid environment was a challenge because of many factors (Huang et al. 2016; Mengistu et al. 2019).

Calibration and validation of physics-based hydrological models have been always difficult tasks in arid environments (Xue et al. 2018). The unique characteristics of arid lands such as low vegetation coverage, thick aeration zone, and climatic conditions, contribute to complicating the hydrological processes in this environment. The performance of hydrological models varies considerably in arid and semi-arid environments because the models have mainly been developed for humid and sub-humid environments (Cirilo et al. 2020).

Unavailability or scarcity of data is an additional factor where most catchments in these environments are ungauged or have limited observed data, are not spatially well distributed, and are sometimes of poor quality. In addition, hydrological and climatological variables in arid environments are characterised by high spatial and temporal variability (Wheater and Al-Weshah 2002). Thus, modelling large catchments in arid lands having representative reliable observed hydrological and climatological data can perform satisfactory accuracies, while catchments with limited observed data can make the use of physics-based models a challenging task. Therefore, several procedures and tests were performed to assess the performance of the SWAT model and its accuracy to estimate runoff in the study area.

9.2.1. Initial calibration and validation of the SWAT model

A major limitation to developing the SWAT model for the study area was the absence of runoff data to calibrate and validate the models. To overcome this problem ET was used as an alternative option for calibration and validation of models for Riyadh's catchments.

Immerzeel and Droogers (2008) presented an innovative approach to calibrate a SWAT model that incorporated satellite-based ET. Since then, a growing number of studies have used derived ET to calibrate the SWAT model at data-scarce areas (Cheema et al. 2014; Emam et al. 2017; Franco and Bonumá 2017; Roy et al., 2017; Ha et al. 2018; Mengistu et al. 2019; Odusanya et al. 2019; Herman et al. 2020; Jin and Jin 2020). These studies successfully calibrated and validated SWAT models, achieving adequate performance of the models and demonstrated the potential to use remotely sensed ET data for the hydrological model calibration and validation in ungauged large catchments. To develop the SWAT model for Riyadh's catchments, ET data sets were used for the calibrations and validations of the models.

Most previous studies have successfully used satellite-based ET, especially the datasets of GLEAM and MODIS. But the GLEAM global ET datasets did not cover the catchments of Riyadh and attempts using MODIS ET did not yield good SWAT model performance for Riyadh. Unlike most previous studies, the development of the SWAT model for the study area successfully used the recently developed Terraclimate global ET dataset for the calibration and validation of the SWAT model. Terraclimate ET data for the study area were available only at a monthly time step for the periods 1991-2000. Hence, the time step was monthly to set up the SWAT model for Riyadh's catchments. The literature review revealed that the use of

Terraclimate ET to calibrate SWAT models is still very limited so far. Therefore, this study is fairly unique in that it uses Terraclimate ET to successfully calibrate and validate a SWAT model. The only previous study found is Herman et al. (2020) (see section 2.5).

Initially, the SWAT model was developed for the main catchments using climate data for 1991-2000 for calibration and 2001-2010 for validation. But statistical results demonstrated satisfactory performance of SWAT for the calibration period and unsatisfactory for the validation period. The comparison between rainfall data from the different sources in Riyadh city indicated significant relationships for the 10-year monthly rainfall records from 1991 to 2000. On the contrary, the analysis results for the validation period (2001-2010) of monthly rainfall from Riyadh Weather Station versus other sources showed that there was no relationship. The key difference between the two periods is that 2000-2010 was a very dry decade (see Figure 5.11), which may explain the discrepancy in measurement values and also why a model calibrated using 1991 – 2000 climate data is not able to accurately predict ET in this unusually dry decade.

The relative dryness of the first decade of the 21st century may be due to anthropogenic climate change. Gosling et al. (2011) showed that there has been strong warming over the Arabian Peninsula from 1960 to 2010. Other previous studies reported that the rainfall trend was generally decreasing throughout the first decade of the 21st century in Saudi Arabia. Presidency of Meteorology and Environment (2011) indicated that the period 2004-2008, showed that, from 26 weather stations spread in Saudi Arabia, six stations were having a positive trend, thirteen stations had a negative trend, and seven stations showed a steady trend. Hasanean and Almazroui (2015) reported that analysis of observed rainfall data from 26 stations in Saudi Arabia revealed a decreasing linear trend of 6.2 mm per

decade during the period 1978–2009, emphasizing that the period 1994-2009 was having a statistically significant decreasing trend of 47.8 mm per decade.

Recent studies of climate change in Saudi Arabia found an increase in the frequency and intensity of rainfall events. Based on rainfall data for the period 1971-2012, Subyani and Hajjar (2016) analysed rainfall in the Jeddah region and concluded that rainy months had more intense rainfall and drier months had less rainfall due to the impact of climate change. Abu Abdullah et al. (2019) reported that Saudi Arabia has been facing significant changes in rainstorm intensities, frequencies, and distributions leading to flash flood events over the last decade. Almazroui (2020) emphasised that the frequency of intense rainfall events was increasing, and the frequency of weak events was decreasing for most meteorological stations in Saudi Arabia. Luong et al. (2020) investigated changes in large-scale weather patterns associated with extreme precipitation events over Jeddah and concluded that extreme precipitation events are becoming less frequent but more intense.

9.2.2. Performance of the SWAT model in the study area

To overcome the problem of using climate data for the period 2001-2010 to validate the SWAT model, it was decided to use data measured before 2000 for both the calibration and validation of the model. The statistical results of the model performance were much better than the previous attempt when using 2001-2010, with model indicators showing similar performance between the calibration and validation periods. Like the calibration statistical results, the NSE, R^2 , and RSR model performance indicators, for the validation, yielded satisfactory results while the PBIAS index revealed an unsatisfactory result for the Wadi Hanifah catchment. In comparison,

all statistical results of the calibration and validation yielded satisfactory or good model performance for the Wadi As Silayy catchment. Comparing these results with the result obtained by Herman et al. (2020) using TerraClimate ET data, seems to be reasonable, especially when considering the differences in environments and the limitations of the study area. In addition, the results of the current study agree with some previous studies that the NSE and R^2 indicated a satisfactory performance of SWAT models and unsatisfactory PBIAS results (Niraula et al. 2012; Paul and Negahban 2018).

To test the ability of the model to simulate monthly ET in the study area for the period before the year 2000, the model was run using the climate data for 36 years from 1965 to 2000. Monthly simulated and TerraClimate ET values revealed an acceptable fit of data for this period. The TerraClimate ET values were greater than the SWAT model simulated ET values. A possible explanation is that the SWAT model can underestimate monthly ET, especially in arid areas. Wang et al. (2006) stated the SWAT tends to underestimate the ET for dry hydrologic conditions. Marek et al. (2016) note that SWAT underestimates ET at both the daily and monthly resolution in a semi-arid area. Odusanya et al. (2019) found that the SWAT simulations tend to underestimate monthly ET. Statistically, the degree of agreement between the simulated and the measured data for the two main catchments was evaluated by the NSE, R^2 , PBIAS, and RSR. The results of the NSE and R^2 indicate an acceptable performance.

Since the key goal behind the setup of the SWAT models for the study area has been to simulate surface runoff, a one-by-one sensitivity analysis was performed to evaluate the impact of parameter values' change on runoff simulations in Riyadh's catchments. The plotted error bar curves as shown in Chapter 6 were

highly matching indicating that simulated runoff sensitivity to selected parameter values in the developed SWAT models was minimal in the study area. Consequently, the change in simulated runoff in different modelling scenarios in the study area is attributed to the change in LULC. All reviewed previous studies that setup the SWAT model to simulate runoff did not test runoff sensitivity to the SWAT parameters values.

To verify the accuracy of simulated surface runoff of the calibrated SWAT model for the Wadi Hanifah catchment, the model was run using climate data for the period 1965-2000. Then, the simulated annual surface runoff results were compared with their counterparts from measured historical data found in the literature for the period 1965-1983, for the Wadi Hanifah catchment. The line charts of simulated annual and historical measured annual runoff data are broadly similar except for the years 1965 and 1968. To assess statistically the degree of agreement between the simulated surface runoff values and measured data, the NSE, R^2 , PBIAS, and RSR were calculated. The statistical results were 0.28, 0.30, 12.53, and 0.85, respectively. These values indicate a poor agreement, except for the PBIAS which gave a good positive agreement. The positive value of PBIAS may indicate surface runoff underestimations of the SWAT model for the Wadi Hanifah catchment.

Rainfall variability is a factor that may contribute to the causes of the relatively weak agreement between the simulated annual surface runoff values and the measured ones in this arid environment large catchment. Spatial and temporal variability of rainfall is a characteristic of arid environments that consequently influences runoff distribution within the catchment, especially in large catchments. Thus, measurements from a single runoff gauge in an arid, large catchment are unlikely to represent the whole catchment area. Certainly, accurate modelling requires representative rainfall

and runoff data that considers the adequate distribution of rainfall and runoff gauges.

9.2.3. Rainfall characteristics in arid areas.

The available climate data was obtained from three weather stations and three rain gauges but with missing values, uneven records, and not spatially well distributed. Rainfall data for the study area may not be considered representative to some degree because of rainfall spatial variability. Precipitation in arid zones is characterised by temporal and spatial variabilities, where rainfall is often described as being spotty (Goudie and Wilkinson 1977). The spottiness characteristic associates with convective precipitation in arid environment (Maliva and Missimer 2012). Among the important features of rainfall in Saudi Arabia, and no exception for the catchments of Riyadh, are the irregularity, low annual rainfall, falls in 24 hours may represent large portions of annual values, relatively high spatial and temporal variability, short-duration showers, limited areal extent and the small number of rainy days each year (Schyfsma 1978; Jones et al. 1981; Abouammoh 1991; Wheeler et al. 1991; Alyamani and Sen 1993; Al-Saleh 1997; Subyani 2004; Mashat and Abdel Basset 2011 ; El Kenawy et al. 2014; Hasanean and Almazroui 2015; Subyani and Hajjar 2016). For instance, Wheeler (2008) reported that the result of an intensive five-year study of the Wadi Yiba catchment (2,869 km²) in southwestern Saudi Arabia confirming the extreme spatial variability of the rainfall. To test the variability of rainfall a uniform network of 20 rain gauges was installed having an inner-gauge distance of about 8-10 km, and rainfall was recorded only in one or two rain gauges out of 20 on 51% of rain days. Wheeler emphasised the dangerousness to generalize from samples of limited record length, but it was found that most events observed in the experimental study were

characterised by extremely spotty rainfall. He reported that there were examples of wadi flows generated from zero observed rainfall.

Precipitation in Saudi Arabia is reported to exhibit high spatial variability and Riyadh, as an arid environment, is no exception. Al-Saleh (1997) emphasised that statistical analysis of rainfall data resulted in high spatial and temporal variabilities. The author gave an example of two stations 15 km apart where on 22 March 1972 the Riyadh station had 15 mm and the Riyadh Old Airport station received more than 56 mm. Additionally, ground radar images show extreme spatial variability of rainstorms in central Saudi Arabia in the vicinity of Riyadh city (see Figure 3.4). Definitely, the high spatial variability of rainfall in an area requires an adequate density of rain gauges to avoid serious deficiencies in hydrological modelling. Moreover, rainfall measurements by rain gauges are normally affected by systematic errors that lead to an underestimation of the real value. For example, the wind is the major source of error because it can affect the trajectory of falling water droplets (Grossi et al. 2017; Jimeno-Sáez et al. 2020).

Leta et al. (2018) examined the performance of the SWAT model for two small catchments experiencing high spatial variability of rainfall. One catchment had well-distributed rainfall gauging stations and the other catchment lacked data records of rainfall. The authors concluded that the daily observed streamflow hydrographs were well-represented by the SWAT model in the catchment having well-distributed rain gauge data. But the SWAT model showed an overall low performance in the catchment that used spatially interpolated daily rainfall data from the neighbouring catchments.

The high spatial variability of rainfall within an arid catchment means that the uneven distribution would lead to variations of surface runoff

depths in the sub-basins of the catchment. Niraula et al. (2012) emphasised that runoff in arid and semi-arid basins is spatially heterogeneous because of the high spatial variability of precipitation. The authors noted that the flow characteristics at the outlet of an arid basin do not necessarily represent the entire basin. Certainly, the mentioned above limitations could influence the performance of the hydrological model for arid catchments. The development of the SWAT models for the catchments of the study area is no exception.

9.3. Impact of LULC change on surface runoff

The surface runoff scenarios of Riyadh's catchments showed an increasing trend, which was consistent with the rapid development of Riyadh city. The increase of simulated surface runoff in the catchments of the city was mainly associated with the transformation of barren land into impervious urban land. Urbanisation replaces the natural permeable surfaces with impervious surfaces such as rooftops, roads, and parking areas. Consequently, urban impervious surfaces impose changes on hydrological processes. Hu et al. (2020) reported that urban impervious areas influence hydrological elements such as infiltration rates, surface runoff volumes, peak discharge, groundwater recharge, evaporation rates, and runoff response time. For example, urbanisation can have a great effect on peak discharge.

An example of the effect of well-planned urban development on runoff has been provided by the USGS. Water Science School (2019) presented hydrographs for nine days in rural and urban streams in Washington State, USA which have the same catchment area and total water volume (Figure 9.2). However, the peak discharge in the urban stream was much higher than the peak discharge in the rural stream. Thus, the steep rising limb of the urban stream hydrograph indicates that the potential for flooding in urban areas are much

higher than in rural areas. Certainly, the problem of increased surface runoff due to urbanisation would be magnified when not well-planned urban development occurred coupled with deficiencies in stormwater and sewage networks. The case of Riyadh city is not far from such a situation as a result of the continuation of increasing impervious surfaces, inconsiderateness of landforms i.e. destruction of hills and filling of some natural valleys (see Figure 5.6), insufficient drainage systems of stormwater and wastewater, and shortage of public green spaces (Arriyadh Environment, n.d.; Garba, 2004; Mubarak 2004; Alhaddan, 2010; AlQahtany et al. 2014; Al-Fawzan 2016; Alahmari 2018; Akhbaar24 2019; Aljammaz et al. 2021).

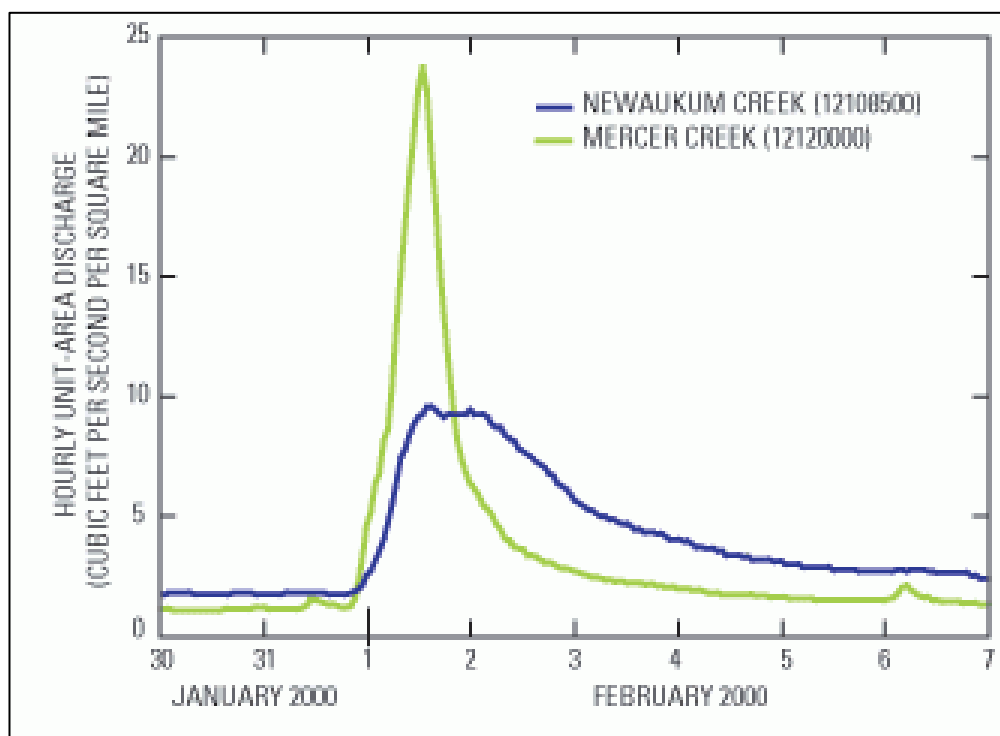


Figure 9.2: Peak discharge in an urban stream and rural stream having the same area and total volume of water. Source: Konrad (2016); Water Science School (2019).

9.3.1. Time steps for model calibration and validation

Since Terraclimate ET data was available only at a monthly time step, the calibrations and validations of SWAT models for Riyadh's

catchments were conducted on a monthly time step. Only daily climate data were available for the study area. Therefore, SWAT models set up for the catchments in the study area were run monthly and daily time steps to simulate runoff and assess the impact of LULC change on surface runoff. In arid regions, it is typical for relatively few rainfall events to dominate annual rainfall statistics, where a single day of rainfall can exceed half of the annual average (Warner 2004). Although not available for the study area, it must be emphasised that sub-daily data is ideal to estimate extreme events because some of the most damaging floods occur over a few hours. Simulated flow peaks are sensitive to the model time step. Large time steps in flow modelling yield fewer and lower peaks (Cherkauer, n.d.; US Army Corps of Engineers, n.d;).

Two previous studies were found that question the efficiency of using the monthly calibrated models for the daily simulations (Sudheer et al. 2007; Adla et al. 2019). The study of Adla et al. (2019) drew its motivation from Sudheer et al. (2007). A model calibrated with monthly or annual time steps might not guarantee a good performance of daily modelling (Sudheer et al. 2007). Adla et al. (2019) reported that a large fraction of SWAT models has been calibrated at time-steps coarser than the daily time-step. The authors mentioned that an overview of many SWAT simulation modelling studies in varied conditions revealed that out of the 114 studies only 42 (37%) were calibrated and validated on a daily time step and 14 (12%) studies were daily calibrated but not validated. In addition, they reported that the calibration of the SWAT model at a daily time-step is even rarer for developing countries. The authors indicated that hydrological models are frequently used to address problems beyond the time-step range of their calibration and validation, but the results for the agricultural catchment of Punpun

River in India challenge the existing practice of using different calibration and computation time-steps in hydrological modelling.

9.3.2. LULC scenarios

The effects on catchment hydrology of the urbanisation scenarios were explored at annual and monthly temporal resolution, and by calculating annual maximum daily runoff, both at the catchment and sub-basin spatial scales using different historical LULC scenarios and different probabilities scenarios for the near future of 2030. Taking into account recent studies that show an increase of intense rainfall events frequency over Saudi Arabia the positive influence of LULC change in Riyadh on surface runoff, and the insufficient drainage systems (Ouda 2015; Al-Fawzan 2016; Ministry of Municipal and Rural Affairs 2016), logically, the areas with high simulated values of surface runoff could have a higher potential of flooding/inundation risks under heavy rainfall conditions.

The rainfall-runoff relationship is well-established in hydrological studies and is influenced by several factors related to catchment characteristics, climate conditions, and land use types. Thus, some of the previous studies, especially performed in large catchments, have shown that the rainfall-runoff transformation is a nonlinear process (Rodríguez-Blanco et al. 2012). Since all input data for the SWAT model are unchanged for runoff simulations except LULC data, it is assumed that the change of runoff is related to the change of LULC; and consequently, the change in coefficients of determination for the relationship between rainfall and runoff in the study area should not be high when using different LULC maps.

The results of SWAT models of the main catchments and sub-basins located within the built-up areas demonstrated the positive effect of

Riyadh's development on runoff and discharge values for historical LULC scenarios and LULC 2030 probabilities scenarios. But the increasing rates of simulated runoff were not the same for all sub-basins due to the different proportions of urbanisation in each sub-basin. On the contrary, simulation results showed that runoff depths and discharge rates in sub-basins outside the boundaries of the built-up areas of Riyadh did not have significant changes when using historical LULC scenarios or LULC 2030 probabilities scenarios. The increase in runoff depths and discharge rates in the sub-basins reflected the direct influence of the urbanisation process on surface runoff. The increase in simulated surface runoff and discharge can be attributed mainly to the potential decrease of relatively permeable barren lands and the increase of impervious urban surfaces.

A comparison of results using the LULC 1996 and LULC 2016 scenarios can highlight the impact of LULC change in 20 years on simulated annual maximum daily runoff in Riyadh's catchments. A remarkable example of the impact of LULC change in the city is that the estimated runoff for the 100-year return period using LULC 1996 is equivalent to the estimated runoff for the 10-year return period using LULC 2016 in the Wadi Hanifah catchment. For the Wadi As Silayy catchment, a striking example is that the estimated 3.5 mm runoff for the 5-year return period using the LULC 2016 scenario is much greater than the runoff value (2.8 mm) for the 100-year return period using the LULC 1996 scenario. It should be noted that the values of runoff are still quite small, but these may cause damage in the city because of the inconsiderateness of landforms during the planning and development stages, deficiency of drainage systems of stormwater and wastewater, and shortage of public green spaces as a permeable surface (Arriyadh Environment, n.d.; Garba, 2004;

Mubarak 2004; Alhaddan, 2010; AlQahtany et al. 2014; Al-Fawzan 2016; Alahmari 2018; Akhbaar24 2019; Aljammaz et al. 2021).

The significant positive impacts of historical and future LULC changes on computed annual maximum daily runoff and discharge can be seen by comparing return periods in the study area. The estimated annual maximum daily runoff for the 100-year return period (6.8 mm) using the LULC 2016 scenario is equivalent to the estimated annual maximum daily runoff for the 10-year return period (7 mm) using LULC 2030 100% probability scenario in the Wadi Hanifah catchment. This means that this large event will be 10 times more common in the LULC 2030 100% probability scenario than in the LULC 2016 scenario. Moreover, the 100-year event (10.7 mm) in the LULC 2030 100% probability scenario for the Wadi As Silayy catchment becomes a 10-year event (10.2 mm) in the LULC 2030 75% probability scenario. The continual significant increase in surface runoff because of urbanisation would magnify the problem of flooding in the city if a sufficient stormwater drainage system is absent.

A significant body of published research supports the findings presented in previous Chapters, demonstrating that rapid urbanisation processes in Riyadh's catchments considerably increase surface runoff depths, runoff coefficients, and discharge rates. The increases of simulated surface runoff depths due to the increases of impervious built-up area in Riyadh city agree with the results of previous studies. Some examples of previous studies that assessed the impact of LULC on surface runoff are provided here. Coutu and Vega (2007) applied the SWAT model to assess the impacts of LULC changes on runoff in the East Branch Brandywine Creek catchment (316 km²), Pennsylvania, USA indicating surface runoff rose 12.15% from an equivalent to 20.8% to an equivalent to 32.94% of rainfall

water under LULC 1992 map and LULC 2000 map respectively. Sun et al. (2011) reported that urban areas in Beijing city, China increased from 4.18% in 1986 to reach 12.78% in 2009 of the whole study area. They indicated that surface runoff in their study area increased 25% and was highly correlated with urban expansion with R^2 0.91. Zhu and Li (2014) mentioned that simulation of streamflow in the Little River catchment (981 km²), Tennessee, USA using the SWAT model resulted in a total 3% increase from 1984 to 2010 for the whole catchment. Although urban areas only account for <12% of the catchment, the regression analysis showed a statistically significant and positive relationship ($R^2 = 0.94$, $P < 0.001$) between streamflow and the percentage of urban areas. Bansal et al. (2015) reported that high urbanisation occurred in Dehradun city, India in the period from 1991 to 2011 due to the growth of its population was about 114%. Surface runoff increased considerably in the city as the impervious layer has increased. They emphasised that inabilities to deal with increased runoff have been one of the causes of increasing floods in the city. Li et al. (2018) analysed trends of direct runoff from 1984 to 2015 in Shenyang city, China. They found that runoff depth, in Zone 3 located between the second and third ring roads in the city increased about 42% due to the increase of urban impermeable surfaces. In the central area of Beijing, China, Hu et al. (2020) reported that the average surface runoff of a 1-year return period increased about 32% between 1985 and 1999 and 17% between 1999 to 2009 due to the increase of impervious surfaces in the city. Also, they stated that changes in surface runoff were strongly correlated with changes in impervious surfaces in Beijing's central area. Hussein et al. (2020) assessed the potential impact of land-use change on flood risk on the east coast of the United Arab Emirates (UAE) for the period from 1996 to 2016. They reported that flooding caused by more frequent rainfall events having small return periods is exacerbated more by urbanisation and

stated that one catchment in their study area may see a 290% increase in the discharge caused by the 5-year storms if fully urbanised. The authors added that the current level of urbanisation of the southern catchment increased the pre-development peak discharge by about 222%, 175%, and 150% for the 5-year, 25-year, and 100-year return period storms respectively. Zheng et al. (2020) stated that a 175% expansion of urban areas from 2000 to 2011 throughout the Qinhuai River catchment (about 2,631 km²) in China led to a 23% increase in annual runoff depths.

9.4. Research limitations

Although this study provides the first calibrated and validated SWAT models to simulate surface runoff for arid ungauged urbanised catchments in Saudi Arabia and has significantly contributed to the research on surface runoff and its vulnerability to LULC change in Riyadh's catchments, it must be confirmed that some hindrances that were faced during the development of this thesis might influence its results. The limitations can be attributed mainly to the nature of the studied region, the data availability and quality, time and funding. These limitations include rainfall characteristics in this arid area, distribution of weather stations and rain gauges, unavailability of measured runoff data, results in this research were based on just one hydrological model, the calibration and validation performed on monthly time steps as mentioned in section 9.3.1., the statistical results were based on the SUFI-2 algorithm, modelling disregarded a changing climate in 2030, and the LULC projections for 2030 considered only a few LULC types and ignored how the amount of vegetation might change.

The unique characteristics of arid lands contribute to complicating the hydrological processes in this environment. Thus, Hydrologic modelling is challenging in arid and semi-arid environments (Huang

et al. 2016; Mengistu et al. 2019). Calibration and validation of physics-based hydrological models have been always difficult tasks in arid environments (Xue et al. 2018). The performance of hydrological models varies considerably in arid and semi-arid environments because they are mainly developed for humid and subhumid environments (Cirilo et al. 2020).

At the forefront of the limitations in this study is the absence of measured runoff data to calibrate and validate the SWAT models. Besides, the available climate data were obtained from three weather stations and three rain gauges but with missing values, uneven records, and not spatially well distributed. Since the study area consists of two main arid catchments covering an area of about 5,000 km² and due to high rainfall spatial variability, the used rainfall data to develop the SWAT model may not represent the study area well. Precipitation in arid zones is characterised by temporal and spatial variabilities, where rainfall is often described as being spotty. Among the important features of rainfall in Saudi Arabia, and no exception for the catchments of Riyadh, are the irregularity, low annual rainfall, falls in 24 hours that may represent large portions of annual values, relatively high spatial and temporal variability, short-duration showers, limited areal extent and the small number of rainy days each year (Schyfsma 1978; Jones et al. 1981; Abouammoh 1991; Wheeler et al. 1991; Alyamani and Sen 1993; Al-Saleh 1997; Subyani 2004; Mashat and Abdel Basset 2011 ; El Kenawy et al. 2014; Hasanean and Almazroui 2015; Subyani and Hajjar 2016).

Another obstacle of data is that the calibrations and validation of the SWAT models for the study area performed satisfactorily only when using climate data for the period 1991-2000. Initially, climate data for the period 1991-2000 was intended for calibration and 2001-2010 for validation. The performance of the SWAT model was

unsatisfactory when using climate data for the period 2001-2010. Therefore, comparisons of precipitation from different climate data sources were performed to examine rainfall data relationships in the two periods. The key difference between the two periods is that 2000-2010 was a very dry decade, which may explain the discrepancy in measurement values and also why a model calibrated on 1991 – 2000 data is not able to accurately predict ET in this unusually dry decade.

An additional limitation of this research is that the LULC projections for 2030 considered only two LULC types and ignored how the amount of vegetation might change because of data deficiency. Moreover, modelling runoff in 2030 disregarded a changing climate.

Because of the time and funding for this research, the results in this thesis were based only on SWAT hydrological model and SUFI-2 algorithm. A hydrological model is a set of equations to estimate certain hydrological variables as a function of various parameters used for describing watershed characteristics. The best model is the one that gives results close to reality with the use of the least parameters and model complexity (Devi et al. 2015). The application of different hydrological models and different algorithms may give different model performances and results in an area (Gosling et al. 2016; Tegegne et al. 2017). Golmohammadi et al. (2014) compared the results of three hydrological distributed watershed models (MIKE-SHE, APEX, and SWAT) with measured data for the Canagagigue Watershed in Canada and found the simulated flows generated by the three models were quite similar and closely match the observed flow. Wu et al. (2013) compared the SUFI-2 and the parameter solution (ParaSol) algorithms and found that SUFI-2 was able to provide more reasonable predictive results than ParaSol.

9.5. Impact of the rapid and not properly planned expansion of Riyadh

The main cause of changes in the LULC in the two catchments of Riyadh city has been continuous urbanisation since the start of the last century. The historical settlement of Riyadh covered about 1 km² in 1900 with a population of about 8,000 (AlQahtany et al. 2014). In 2017, the built-up area of the city increased to be more than 1200 km² and had a population of about 6.5 million (Al-Hathloul 2017; Altuwajri et al. 2019). In 2022, the built-up area of the city was about 1,600 km² (see Figure 1.1).

The consideration of environmental matters is a very important issue in city planning and development, but it has not been applied properly for Riyadh during its development. Alqahtany et al. (2014) argued that past plans for the city of Riyadh have failed because the urban expansion of the city has been achieved with minimum understanding and recognition of social, economic, and environmental issues that play a major role in shaping the city. The author suggested that the gridiron pattern with associated negative impacts should be replaced by a new urban planning strategy in accordance with the principles of sustainable development and emphasising local customs and traditions and considering local climate. In particular, gridded development treats the landscape as homogenous without consideration of geomorphological features and landforms (AlQahtany et al. 2014).

The expansions of Riyadh city were mainly based on grid street plans. Ministry of Municipal and Rural Affairs (2018) indicated that the Doxiadis Master Plan was composed of a supergrid extending from east-west to north-south direction. This plan divided Riyadh city into six large divisions each division composed of eight to twelve localities of 2 km × 2 km. Previous studies revealed that the Saudi

urban planners have had different opinions about the use of the grid system in the urban development of Riyadh city. Al-Hathloul (2017) considered the supergrid system of the Doxiadis plan with its superblock of 2 km × 2 km provided a rational logical system for the city to expand endlessly. Unlike Al-Hathloul, Mubarak (2004) criticised the use of the grid system for Riyadh city development. He considered that the application of the supergrid system of the Doxiadis plan proven negative attributes and inappropriateness for a harsh desert climate. Mubarak emphasised that the Saudi suburbanisation model has been an accumulation of grids of subdivisions at the outer edges that was fueled by greedy land speculation and government free-land grants and achieved with minimum appreciation to social and economic and environmental factors. He highlighted that the application of the supergrid system has treated the land as homogenous without consideration of landforms. In addition, AlQahtany et al. (2014) emphasised that the land was considered as homogenous without regard to geomorphological features during the development process of Riyadh city.

The infrastructure of Riyadh city has lagged far behind its dramatic growth (Garba, 2004). In 2010, for instance, storm water drainage networks covered only 30% of the city (Alhaddan, 2010; Al-Fawzan 2016). After the 9 November 2018 flood, the Mayor of Riyadh revealed that 40% of stormwater drainage networks in Riyadh were completed, indicating that the target of the Municipality of Riyadh was to cover 58% of the city by 2020 (AkhbaaR24 2019). The sewage networks covered about 50% of urban areas in 2010 and about 57% in 2014 (Ministry of Water and Electricity 2014; Ouda 2015; Ministry of Municipal and Rural Affairs 2016). Due to the lack of sewage networks, the in-situ cesspit is constructed for each building to dispose of the sewage (Alahmari 2018). Discharge of

wastewater effluents from in-situ cesspits has led to a general rise in groundwater levels in Riyadh, an increase in soil moisture, ponds creation in some locations, and the discharge of groundwater into lowlands and wadis channels (Aljammaz et al. 2021).

9.6. Impact of shortage of public green spaces in Riyadh

The LULC categories used to assess LULC change on surface runoff in Riyadh are barren land, vegetation, urban, and roads. Vegetation class is mainly composed of public green spaces in the city. Urban green spaces are of various forms and sizes, ranging from grass, and trees within streets to private gardens, neighbourhood gardens, various sports fields, and central parks. The accessibility target of public urban green space varied not only from one country to another but from city to city. Wüstemann and Kalisch (2016) reported the provision of a sufficient amount of urban green space in some European countries. The European Environment Agency (EEA) defines the green space provision target that people can reach green space within 15 minutes of walking distance, i.e., about 900-1,000 m. Urban residents in the United Kingdom should have access to 2ha of urban green within a 300 m distance from the place of residence. The Netherlands targets a minimum green provision of 60 m² per capita within 500 m distance from the resident house.

Although green and open spaces are extremely significant for improving the urban environment, obtaining the satisfaction of the inhabitants, and minimizing flood risk, city landscaping has been neglected, to a high degree, during the urbanisation process of Riyadh city (Alqahtany 2014). The Green Riyadh project launched in 2019 will improve green spaces in the city. The first objective of this project is to increase the green space per capita in the city from 1.7 to 28 m² which is equivalent to about 16 times the current situation (Vision 2030, n.d.). The application of the NDVI on the Landsat OLI

image acquired in February 2022 resulted in a vegetation cover within the built-up area of Riyadh of about 49,000,000 m² which represents 3% of the total area of the city. Regarding the public green space area per capita in Riyadh city, Almayouf (2013) compared green areas in Riyadh city with WHO standard and selected world cities and found that Riyadh city was one of the lowest green services per capita at about 0.86 m² (Figure 9.3). Addas and Maghrabi (2020) reported that the total area of public gardens and parks (public green spaces) in Riyadh was 6,161,567 m² and the population of Riyadh was 5,236,901. They revealed that the provision of the public open space in the city was 1.18 m²/capita. Addas and Maghrabi found the provision of the public open space in Riyadh was very far from achieving United Nations Standard (30 m²/capita) with a high shortage of about 151 km² of the city's public open space. The relatively small fraction of public green space in Riyadh city may increase surface runoff in the city.

The relationships between surface runoff and vegetation class changes obtained from historical LULC maps were evaluated in the two catchments of Riyadh city. The correlation result of surface runoff versus vegetation class was positive in Riyadh's catchments deviating from what is usual. The result was not consistent with the expectation that increasing vegetation leads to a decrease in surface runoff. The explanation for this can be attributed to the small ratio of increases in the vegetation class compared to the ratio of impervious urban and road classes. The total increases of vegetation class for the period 1996-2016 were about 117 km² while the total increases of urban and road classes were about 505 km². This means that although the areas of vegetation class increased during the development of Riyadh, the direct driver of increasing surface runoff rates in Riyadh mainly urban and road classes increased more. Consequently, the relationship between annual runoff values and the

vegetation class changes has been masked by the stronger influence of changes in urban and road classes.

Contemporary urban planning emphasises the importance and benefits of sustaining or expanding green spaces in cities. The urbanisation process, in any area, greatly affects the hydrology by reducing the amount of infiltration into the soil and increasing the speed at which water travels over the surface leading to the increase of both surface water runoff and peak discharge rates (Armson et al. 2013). Urban green spaces contribute to the mitigation of urbanisation impacts on the water cycle, local microclimate, air pollution, noise, urban ecology, and carbon footprint, which consequently contribute to the health and general well-being of the urban inhabitants (Müller et al. 2020). O'Donnell et al. (2020) indicated that the development of Blue-Green systems is key to creating future flood-resilient cities. Normally, well-planned urban development includes an acceptable ratio of public urban green areas. Axiomatically, green spaces can be considered as permeable surfaces. Thus, a higher ratio of green space within an urbanised area may substantially reduce urban surface runoff.

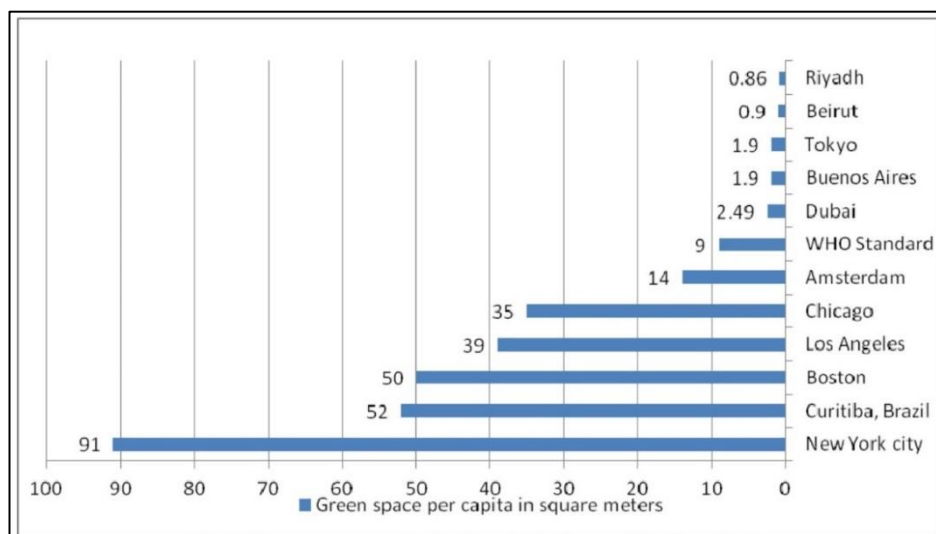


Figure 9.3: Green area per capita in Riyadh city compared to WHO standard and selected cities.

Source: Almayouf (2013).

The investigation of urban green spaces on runoff has been an interest in the urban water management field, and its effectiveness has been highlighted in notable studies. For example, Armson et al. (2013) assessed the impact of street green spaces upon urban surface runoff in Manchester, UK, and found grass space almost totally eliminated surface runoff and tree pits reduced runoff from asphalt by as much as 62%. Inkiläinen et al. (2013) evaluated the role of the residential urban forest in regulating throughfall in Raleigh, North Carolina, USA indicating that a significant influence found of vegetation on the regulation of throughfall and potential stormwater runoff. They stated that urban residential forests reduced potential stormwater runoff by 9.1–21.4%.

The urban green zones in Beijing, China, contributed about 31% of runoff reduction (Yao et al. 2015). Zhang et al. (2015a) investigated the impact of the decrease of green spaces in Beijing, China on surface runoff for the period 2000-2010 concluding that the runoff reduction rate continuously decreased from 23% in 2000 to 17% in 2010 due to changes in urban green spaces. Kim et al. (2016) found a considerable influence of green spaces on urban flooding probabilities in Seoul, Korea, where flooding probabilities could be reduced by over 50% depending on the green space area and its location. Moreover, Kim et al. (2016) reported that the urban green spaces approach has emerged as a potential option to decrease urban surface runoff. Expansion of urban green spaces is an economical and environmentally friendly approach to reduce surface runoff. Therefore, the preservation and expansion of green spaces may represent a potentially effective option to reduce urban surface runoff. However, effective mitigation of surface runoff using the urban green spaces approach requires evaluation of how increases in urban green spaces will reduce surface runoff in different

neighbouring areas because it is highly dependent on the physical factors and characteristics present in different neighbourhoods.

9.7. Impact of Riyadh development on flood occurrence potential

It appears from the above-mentioned information that undue environmental problems have not been avoided by proper planning for urban growth in the city of Riyadh. Actually, the environmental problems caused by rapid urban development are treated after its occurrence through giant projects such as restoration of Wadi Hanifah (Trottier and Wensley 2015), lowering groundwater levels in the city (Al-Othman 2011) and restoration the main channel of Wadi As Silayy (Royal Commission for Riyadh City 2018). One particular issue is repeated urban flooding in Riyadh which has occurred in 1995, 1997, 2005, 2010, 2011, 2012, 2013, 2014, 2015, and 2016 (Al Saud, 2010; Alamri, 2011; Abosuliman et al., 2013; Almazroui, 2013; Al-Momani and Shawaqfah, 2013; Hadadin et al., 2013; Qari et al., 2014; Al Saud, 2015; Rahman et al., 2016).

In the case of lacking reliable data and information on flood events in Riyadh city where the urban area has expanded, it would be an appropriate way to show some documentary evidence from media reports and social media. This would be circumstantial evidence and not solid proof that LULC change has affected flooding, but it could provide a good context.

Following the flood on 3rd May 2010, Riyadh's mayor said in a press conference that 70% of Riyadh city has no stormwater drainage networks (Alhaddan, 2010), which likely contributes substantially to the propensity to flood (see Figure 1.2). Official authorities of Riyadh city have realised the main cause of flooding in the city, where Riyadh's mayor pointed out during the same press conference that

no flooding occurred in neighbourhoods with efficient stormwater drainage networks, such as Al Malaz and Al Maather residential neighbourhoods (Alhaddan, 2010).

Floods can occur in Riyadh city due to extreme rainfall events; but the flood problem in the city is mainly due to human causes. Although not directly modelled in this thesis, the vulnerability of Riyadh city to flood hazards is also linked to anthropogenic blocking and filling of ephemeral stream channels and the absence of proper stormwater drainage networks. Alassaf (2013) emphasised that ancestors did not block wadi channels or transgress on them because they were aware of the dangers of torrential floods that occur infrequently in this arid environment. Al-Fawzan (2016) in a newspaper article entitled "blame poor drainage systems, not the weather" highlighted the deficiency of effective storm drainage systems, which serve only 45% of the city. He asserted that the causes are mainly human, stating "instead of continuously saying it's the bad weather, we should say it's the bad drainage system. This is the bitter truth that we should come to grips with". Moreover, movement of surface water could be slowed down due to the flattening of naturally rugged terrain, changing local slopes in some areas. Other potential contributing factors include naturally very low surface slopes in some areas, especially eastern areas of the city; naturally permeable surfaces have been replaced by impervious surfaces, which decrease infiltration rates and increase water flows; and the common grid street pattern in the city which may have a negative influence on water movement when orientation of a street deviates from the slope direction. Rainwater may accumulate when a street orientation intersects with the tendency of a stream.

The flooding of road tunnels in Riyadh (Figure 9.4) also frequently happens due to accumulation of runoff water, such as the Al-Suwaidi

neighbourhood tunnel in February 2005 and November 2015; the Western Ring Road in Riyadh near Exit 33; and the Dirab Tunnel November 2018 (Saudi News 2013, Alriyadh Newspaper 2015; Akhbaar24, 2019). The official justification of the Ministry of Transport and Municipality of Riyadh for this problem is that rainwater was transmitted from neighbouring areas to the tunnels due to a lack of stormwater drainage networks (Riyadh Municipality 2015, Hourpress 2018). Flooding of Riyadh streets by rainfall is still taking place. For instance, Riyadh had rainfall on 31 July 2022 which resulted in flooding of some streets (Figure 9.5).



Figure 9.4: Accumulation of runoff water in the Western Ring Road in Riyadh near Exit 33 after the 25 November 2015 storm.
Source: Alriyadh Newspaper (2015).



Figure 9.5: Accumulation of runoff water in the Al Aziziyah and Al Fayha neighbourhoods in Riyadh after the rain storm on 31st July 2022.

Source: Abu Hamad (2022); Al-Wsabi (2022)

9.8. Summary

This chapter discussed the challenge to setup a SWAT model in ungauged arid catchments which have a scarcity of climate data and uneven distribution of weather stations. TerraClimate ET data sets were used for calibration and validation of models for Riyadh's catchments due to the absence of runoff data. Initially, the SWAT model was performed on the main catchments using climate data 1991-2000 for calibration and 2001-2010 for validation. The SWAT model performance was acceptable for calibration but unsatisfactory for validation. To overcome this problem climate data measured before 2000 were used for both the calibration and validation of the SWAT model. The performance of SWAT models was satisfactory for both calibration and validation.

The impact of LULC change on simulated runoff was discussed in this chapter. The LULC impact scenarios of urbanisation on simulated runoff and discharge were examined using different historical LULC scenarios and different probabilities maps for the near future of 2030. The simulated runoff scenarios of Riyadh's catchments showed a trend of increase, which was consistent with the rapid development of Riyadh city. The increase of simulated runoff in the catchments of the city was mainly caused by the transformation of barren land into impervious urban land. The increases in simulated surface runoff depths due to the increases in the impervious built-up area in Riyadh city agree with the results of previous studies.

Chapter 10: Conclusion

10.1. Overview

Riyadh city spreads on vast areas of two ungauged catchments. The rapid expansion of the city has caused serious environmental problems in the city including repeated urban flooding. Urban expansion of Riyadh city has had a profound influence on runoff. Undertaking a literature review of previous studies revealed there is still an urgent need to study surface runoff and how it is affected by the LULC change in the main catchments in Riyadh city which can help policymakers to take necessary actions to mitigate and prevent its environmental problems. However, the absence of runoff data presents a major challenge for developing hydrological models for the city. This study addressed that knowledge gap and was the first attempt to calibrate, validate, and run a semi-distributed model to simulate runoff depths and discharge rates for Riyadh's main catchments and sub-basins using five historical and five future scenarios.

This chapter has been divided into three major parts. It includes the main findings of the thesis. In addition, the chapter provides general recommendations for the application of the calibrated models for the catchments of Riyadh and further research.

10.2. Calibrated SWAT models and runoff sensitivity to LULC change

The statistical results of SWAT models for the catchments in the study area showed similar performance between the calibration and validation periods. Like the statistical calibration results, the NSE, R^2 , and RSR model performance indicators, for the validation, yielded satisfactory results, whereas the PBIAS index revealed an unsatisfactory outcome for the Wadi Hanifah catchment. In

comparison, all the calibration and validation statistical results yielded satisfactory or good model performance for the Wadi As Silayy catchment.

Surface runoff sensitivity to parameter values of the calibrated and validated SWAT models was assessed using a one-by-one sensitivity analysis method. Using the highest and lowest parameter range values for the one-by-one sensitivity analysis, led to the generation of 24 and 18 SWAT models for the two catchments. The error bar curves that result from plotting the maximum and minimum values of surface runoff obtained from the models of one-by-one sensitivity analyses showed nearly match lines. Besides, relationships between simulated annual runoff and max and min runoff for the period 1991-2000 resulted in very high R^2 . These relationships were strong with R^2 values of nearly 1. These results show that surface runoff sensitivity to the selected parameter values is minimal for the study area.

The simulated annual surface runoff for the Wadi Hanifah catchment was compared with the annual measured runoff for the period 1965-1983 found in the literature and the values tend to be close to some degree to each other. To assess statistically the degree of agreement between the simulated surface runoff values and measured data, the NSE, R^2 , PBIAS, and RSR were calculated. The statistical results were 0.28, 0.30, 12.53, and 0.85, respectively. This indicates a poor agreement, except for the PBIAS which gave a good, positive agreement. The positive value of PBIAS may indicate surface runoff underestimations of the SWAT model for the Wadi Hanifah catchment.

The calibrated and validated SWAT models for the catchments in the study area were run monthly and daily to simulate runoff and assess

the impact of LULC change on surface runoff. The LULC impact scenarios of urbanisation on simulated runoff and discharge were examined using five historical LULC scenarios for the period 1996-2016 and five probabilities scenarios for the near future of 2030. The simulated runoff scenarios of Riyadh's catchments showed a trend of increase, which was consistent with the rapid development of Riyadh city. The increase of simulated runoff in the catchments of the city was mainly caused by the transformation of barren land into impervious urban land. During 1996–2016, the sub-basins within the boundary of the city revealed an increasing trend of surface runoff. The increase of runoff depths in these sub-basins reflected the direct influence of the urbanisation process on surface runoff.

A significant body of published research worldwide supports the findings presented in Chapter 7, demonstrating that rapid urbanisation processes in Riyadh's catchments considerably increase surface runoff depths, runoff coefficients, and discharge rates. The increases in simulated surface runoff depths due to the increases in an impervious built-up area in Riyadh city agree with the results of previous studies.

This study contributes to addressing the knowledge gap resulting from the absence of runoff measurements and limitations and deficiencies in the few previous studies on runoff and flooding in Riyadh city. The application of the calibrated SWAT models can help to improve the current situation of the city. These models can provide approximate estimates of runoff in the main catchments and sub-basins. This research also provides information on the impact of historical and future LULC scenarios on runoff in the city. These results can be used by policymakers to take necessary actions to mitigate environmental problems in Riyadh.

As discussed in Chapter 9, it must be confirmed that some caveats can influence the results of this research. These include the nature of the studied region, scarcity of data, results in this research were based on just one hydrological model, the calibration and validation performed on monthly time step, the statistical results were based on the SUFI-2 algorithm, modelling disregarded a changing climate in 2030, and the LULC projections for 2030 considered only a few LULC types and ignored how the amount of vegetation might change. Considering the above facts, rainfall variability in the study area, the SWAT hydrological model developed in humid areas, and the application of different hydrological models and different algorithms may give different results, the ambition of the calibrated SWAT models in this study was to obtain approximate estimates of surface runoff in the catchments of Riyadh and to assess LULC change on surface runoff. Due to the absence of measured runoff data and the deficiency and limitations in the few previous studies on runoff and flood in Riyadh city, the results of runoff simulations for LULC scenarios are still useful for decision-making in this rapidly expanding city.

10.3. Recommendations

Due to repeated flooding problems in Riyadh city and the absence of observed runoff data or good estimations, there is an urgent need for surface runoff estimations and how it is affected by the LULC change in the main catchments in Riyadh city. This research provides the first calibrated and validated semi-distributed models to simulate runoff depths and discharge rates for ungauged catchments and sub-basins in Riyadh. Therefore, the application of the developed satisfactory SWAT models will help to improve the current situation of the city by providing approximate estimates of runoff for policymakers to take necessary actions to mitigate its environmental problems. Besides, it can give runoff estimates for the scenarios of

future growth to implement efficient plans to prevent the occurrence of undue environmental problems.

This study has significantly contributed to the research on the surface runoff and its vulnerability to LULC change in Riyadh's catchments but future studies for better performance of the SWAT model and accurate runoff estimates are still needed. The previous section presents some limitations that were faced in this research study. Undoubtedly, these limitations provide a guideline for further research to be performed. Detailed and accurate runoff estimates in Riyadh city are still needed to assist decision-makers and city officials to adopt runoff and flood hazards management schemes in the city. The knowledge gained from conducting this research work with its associated techniques can be useful as a preliminary scientific base for future research on the surface hydrology of Riyadh city. Since this research provides the first calibrated and validated SWAT models to simulate surface runoff for arid ungauged urbanised catchments in Saudi Arabia, it is recommended that SWAT is applied in further catchments of the country for better evaluation of SWAT performance under arid catchment conditions.

References

- Abaho, P., Amanda, B., Kigobe, M., Kizza, M. and Rugumayo, A., 2009. Climate change and its impact on river flows and recharge in the Sezibwa catchment, Uganda. In *Second International Conference on Advanced in Engineering and Technology* (pp. 572-578).
- Abatzoglou, J.T., Dobrowski, S.Z., Parks, S.A. and Hegewisch, K.C., 2018. TerraClimate, a high-resolution global dataset of monthly climate and climatic water balance from 1958–2015. *Scientific data*, 5(1), pp.1-12.
- Abbaspour, K.C., 2015. SWAT-CUP: SWAT calibration and uncertainty programs—a user manual. *Eawag: Dübendorf, Switzerland*, pp.16-70.
- Abbaspour, K.C., Rouholahnejad, E., Vaghefi, S.R.I.N.I.V.A.S.A.N.B., Srinivasan, R., Yang, H. and Kløve, B., 2015. A continental-scale hydrology and water quality model for Europe: Calibration and uncertainty of a high-resolution large-scale SWAT model. *Journal of hydrology*, 524, pp.733-752.
- Abbaspour, K.C., Vaghefi, S.A., Lehmann, A., and Srinivasan, R., 2019. Monthly actual evapotranspiration satellite data with SWAT and SWAT-CUP format. PANGAEA.
- Abbaspour, K.C., Yang, J., Maximov, I., Siber, R., Bogner, K., Mieleitner, J., Zobrist, J. and Srinivasan, R., 2007. Modelling hydrology and water quality in the pre-alpine/alpine Thur watershed using SWAT. *Journal of hydrology*, 333(2-4), pp.413-430.
- Abd Rahman, N., Alahmadi, F., Sen, Z. and Taher, S., 2016. Frequency Analysis Of Annual Maximum Daily Rainfall In Wadi Alaqiq, Saudi Arabia. *Malaysian Journal of Civil Engineering*, 28(2).
- Abdeen, W.M., Awadallah, A.G. and Hassan, N.A., 2020. Investigating regional distribution for maximum daily rainfall in arid regions: case study in Saudi Arabia. *Arabian Journal of Geosciences*, 13(13), pp.1-18.

- Abdel-Lattif, A. and Al-Shamrani, M., 2013. A comparison of methods for estimating the mean annual runoff coefficient at ungauged stream in southwestern region, Kingdom of Saudi Arabia. *International Journal of Environmental Science and Toxicology Research*, 1(1), pp.12-20.
- Abdullah, M.A. and Al-Mazroui, M.A., 1998. Climatological study of the southwestern region of Saudi Arabia. I. Rainfall analysis. *Climate Research*, 9(3), pp.213-223.
- Abo Zuhair, M., 2010. *he An Nazim flood disaster rings alarm bells and families are still being held*. [online] Alriyadh newspaper. Available at: <<https://www.alriyadh.com/523508>> [Accessed 20 June 2021].
- Abosuliman, S.S., Kumar, A. and Alam, F., 2013. Disaster preparedness and management in Saudi Arabia: an empirical investigation. *International Journal of Social, Human Science and Engineering*, 7(12), pp.295-299.
- Abouammoh, A.M., 1991. The distribution of monthly rainfall intensity at some sites in Saudi Arabia. *Environmental monitoring and assessment*, 17(2), pp.89-100.
- Abteu, W. and Melesse, A., 2013. *Evaporation and evapotranspiration: measurements and estimations*. Springer Science & Business Media.
- Abu Abdullah, M.M., Youssef, A.M., Nashar, F. and AlFadail, E.A., 2019. Statistical Analysis of Rainfall Patterns in Jeddah City, KSA: Future Impacts. In *Rainfall-Extremes, Distribution and Properties*. IntechOpen.
- Abu Hamad, 2022. [Twitter] *Al Fayha Neighbourhood*. [video] Available at: <<https://twitter.com/E3jCp/status/1553974248191959043?t=RV2yY7FNSncYntr6JDZ87A&s=08>> [Accessed 30 August 2022].
- Abu-Zreig, M. and Hani, L.B., 2021. Assessment of the SWAT model in simulating watersheds in arid regions: Case study of the

Yarmouk River Basin (Jordan). *Open Geosciences*, 13(1), pp.377-389.

Addas, A. and Maghrabi, A., 2020. A Proposed Planning Concept for Public Open Space Provision in Saudi Arabia: A Study of Three Saudi Cities. *International Journal of Environmental Research and Public Health*, 17(16), p.5970.

Adla, S., Tripathi, S. and Disse, M., 2019. Can we calibrate a daily time-step hydrological model using monthly time-step discharge data?. *Water*, 11(9), p.1750.

Afinowicz, J.D., Munster, C.L. and Wilcox, B.P., 2005. MODELING EFFECTS OF BRUSH MANAGEMENT ON THE RANGELAND WATER BUDGET: EDWARDS PLATEAU, TEXAS 1. *JAWRA Journal of the American Water Resources Association*, 41(1), pp.181-193.

Afrifa-Yamoah, E., Mueller, U.A., Taylor, S.M. and Fisher, A.J., 2020. Missing data imputation of high-resolution temporal climate time series data. *Meteorological Applications*, 27(1), p.e1873.

Aghakhani Afshar, A., Hassanzadeh, Y., Pourreza-Bilondi, M. and Ahmadi, A., 2018. Analyzing long-term spatial variability of blue and green water footprints in a semi-arid mountainous basin with MIROC-ESM model (case study: Kashafrood River Basin, Iran). *Theoretical and Applied Climatology*, 134(3), pp.885-899.

Ahmadi, M., Moeini, A., Ahmadi, H., Motamedvaziri, B. and Zehtabiyan, G.R., 2019. Comparison of the performance of SWAT, IHACRES and artificial neural networks models in rainfall-runoff simulation (case study: Kan watershed, Iran). *Physics and Chemistry of the Earth, Parts A/B/C*, 111, pp.65-77.

Ahn, S., Abudu, S., Sheng, Z. and Mirchi, A., 2018. Hydrologic impacts of drought-adaptive agricultural water management in a semi-arid river basin: Case of Rincon Valley, New Mexico. *Agricultural Water Management*, 209, pp.206-218.

Akhbaar24, 2019. *The mayor of Riyadh explains the reason flooding of some neighborhoods and road tunnels*. [online] Akhbaar24

Website. Available at:
<<https://akhbaar24.argaam.com/article/detail/427316>>
[Accessed 24 July 2021].

Akoko, G., Le, T.H., Gomi, T. and Kato, T., 2021. A review of SWAT model application in Africa. *Water*, 13(9), p.1313.

Al Saud, M., 2010. Assessment of Flood Hazard of Jeddah Area 2009, Saudi Arabia. *Journal of Water Resource and Protection*, 02(09), pp.839-847.

Al Saud, M., 2015. *Flood control management for the city and surroundings of Jeddah, Saudi Arabia*. Springer.

Alahmadi, F., 2017. Regional rainfall frequency analysis by L-moments approach for Madina Region, Saudi Arabia. *Int. J. Eng. Res. Dev*, 13(7), pp.39-48.

Al-Ahmadi, K. and Al-Ahmadi, S., 2013. Rainfall-Altitude Relationship in Saudi Arabia. *Advances in Meteorology*, 2013, pp.1-14.

Al-Ahmadi, K. and Al-Ahmadi, S., 2014. Spatiotemporal variations in rainfall-topographic relationships in southwestern Saudi Arabia. *Arabian Journal of Geosciences*, 7(8), pp.3309-3324.

Alahmari, A., 2018. *The role of knowledge and institutional challenges to the adoption of sustainable urban drainage in Saudi Arabia: implications for sustainable environmental development* (Doctoral dissertation, Middlesex University).

Alamri, Y.A., 2011. Rains and floods in Saudi Arabia. Crying of the sky or of the people?. *Saudi medical journal*, 32(3), pp.311-313.

Alassaf, M., 2013. *Our ancestors knew the "wadi channel" and did not destruct it*. [online] Available at: <<http://www.alriyadh.com/886269>> [Accessed 6 September 2020].

- Alawi, I., 2018. *The deputy Minister for water affairs transfers automatic weather stations to GAMEP*. [online] Okaz Newspaper. Available at: <<https://www.okaz.com.sa/local/na/1637664>> [Accessed 18 May 2021].
- Al-Dousari, A., Milewski, A., Din, S.U. and Ahmed, M., 2010. Remote sensing inputs to SWAT model for groundwater recharge estimates in Kuwait. *Advances in Natural and Applied Sciences*, 4(1), pp.71-77.
- Al-Fawzan, R., 2016. *Blame poor drainage systems, not the weather*. [online] Saudi Gazette Newspaper. Available at: <<https://saudigazette.com.sa/article/145653>> [Accessed 25 October 2021].
- Al-Fuhaid, A., 2013. *The Transportation Ministry connects the drainage of the Al-Amariah tunnel to the Wadi Al-Aysen channel*. [online] Al-Jazirah Newspaper. Available at: <<https://www.al-jazirah.com/2013/20131120/fe31.htm>> [Accessed 29 November 2019].
- Al-Gabbani, M., 1991. Population density pattern and change in the city of Riyadh, Saudi Arabia. *GeoJournal*, 24(4), pp.375-385.
- Alghamdi, A.S. and Moore, T.W., 2014. Analysis and comparison of trends in extreme temperature indices in Riyadh City, Kingdom of Saudi Arabia, 1985–2010. *Journal of Climatology*, 2014.
- Al-Ghamdi, K. A., Elzahrany, R. A., Mirza, M. N. and Dawod, G. M., 2012. Impacts of urban growth on flood hazards in Makkah City, Saudi Arabia. *International Journal of Water Resources and Environmental Engineering*, 4(2), pp.23-34.
- Al-Ghobari, H., Dewidar, A. and Alataway, A., 2020. Estimation of surface water runoff for a semi-arid area using RS and GIS-based SCS-CN method. *Water*, 12(7), p.1924.
- Alhaddan, A., 2010. *Riyadh was not ready for large amounts of rainfall and stormwater drainage networks do not exceed 30%*. [online] Alriyadh newspaper. Available at:

<<http://www.alriyadh.com/523408>> [Accessed 25 March 2019].

- Al-Hammad, B.A., El-Salam, A. and Magdy, M., 2017. Monitoring water pollution levels in Wadi Hanifa, Riyadh, Saudi Arabia and its pub
- Alhamid, A.A., Alfayzi, S.A. and Hamadto, M.A., 2007. A sustainable water resources management plan for Wadi Hanifa in Saudi Arabia. *Journal of King Saud University-Engineering Sciences*, 19(2), pp.209-221.
- Alharbi, M.M.E.A., 2018. *Analysis of extreme precipitation events over the Eastern Red Sea Coast for recent and future climate conditions* (Doctoral dissertation, University of Birmingham).
- Al-Hasan, A.A.S. and Mattar, Y.E.S., 2014. Mean runoff coefficient estimation for ungauged streams in the Kingdom of Saudi Arabia. *Arabian Journal of Geosciences*, 7(5), pp.2019-2029.
- AlHassoun, S.A., 2011. Developing an empirical formulae to estimate rainfall intensity in Riyadh region. *Journal of King Saud university-engineering sciences*, 23(2), pp.81-88.
- Al-Hathloul, S., 2017. Riyadh development plans in the past fifty years (1967-2016). *Current Urban Studies*, 5(01), p.97.
- Alhawas, A.A., 2011. Towards sustainable water resources for arid land cities: the case of Riyadh. *WIT Transactions on Ecology and the Environment*, 145, pp.87-98.
- Alhumimidi, M.S., 2020. Estimation of potential runoff in Wadi Damad watershed, Jazan Province, southwestern Saudi Arabia. *Arabian Journal of Geosciences*, 13(7), pp.1-12.
- Aljammaz, A., Sultan, M., Izadi, M., Abotalib, A.Z., Elhebiry, M.S., Emil, M.K., Abdelmohsen, K., Saleh, M. and Becker, R., 2021. Land subsidence induced by rapid urban in arid environments: A remote sensing-based investigation. *Remote Sensing*, 13(6), p.1109.

- Al-Jasser, A.O., 2011. Saudi wastewater reuse standards for agricultural irrigation: Riyadh treatment plants effluent compliance. *Journal of King Saud University-Engineering Sciences*, 23(1), pp.1-8.
- Al-Juaidi, A.E. and Attiah, A.S., 2020. Evaluation of desalination and groundwater supply sources for future water resources management in Riyadh city. *Desalination and Water Treatment*, 175, pp.11-23.
- Almayouf, A., 2013. Preserving the Green in Hot-arid Desert Environments: The Case of Riyadh, Saudi Arabia, *J. King Saud University*, 25, pp.39-49.
- Almazroui, M., 2011. Calibration of TRMM rainfall climatology over Saudi Arabia during 1998–2009. *Atmospheric Research*, 99(3-4), pp.400-414.
- Almazroui, M., 2012a. Temperature variability over Saudi Arabia and its association with global climate indices. *JKAU Met. Env. Arid. Land. Agric. Sci*, 23(1), pp.85-108.
- Almazroui, M., 2012b. The life cycle of extreme rainfall events over western Saudi Arabia simulated by a regional climate model: Case study of November 1996. *Atmósfera*, 25(1), pp.23-41.
- Almazroui, M., 2013. Simulation of present and future climate of Saudi Arabia using a regional climate model (PRECIS). *International journal of climatology*, 33(9), pp.2247-2259.
- Almazroui, M., 2019. Assessment of meteorological droughts over Saudi Arabia using surface rainfall observations during the period 1978–2017. *Arabian Journal of Geosciences*, 12(22), pp.1-16.
- Almazroui, M., 2020. Rainfall trends and extremes in Saudi Arabia in recent decades. *Atmosphere*, 11(9), p.964.
- Almazroui, M., Kamil, S., Ammar, K., Keay, K. and Alamoudi, A.O., 2016. Climatology of the 500-hPa Mediterranean storms

associated with Saudi Arabia wet season precipitation. *Climate Dynamics*, 47(9), pp.3029-3042.

Al-Momani, A. and Shawaqfah, M.A., 2013. Assessment and management of flood risks at the city of Tabuk, Saudi Arabia. *The holistic approach to environment*, 3(1), pp.15-31.

Al-Mutaz, I.S., 1987. Water resources development in Riyadh, Saudi Arabia. *Desalination*, 64, pp.193-202.

Al-Nuwaysir, H., Moubayed, N., Al-Othman, M., Bacha, A.B. and Abid, I., 2019. Molecular detection of Escherichia coli in Wadi Hanifa, Saudi Arabia. *Biomedical Research*, 30(2), pp.253-258.

ALOS, n.d. *Global Digital Surface Model*. [online] ALOS. Available at: <https://www.eorc.jaxa.jp/ALOS/en/dataset/aw3d30/aw3d30_e.htm> [Accessed 14 April 2019].

Al-Othman, A. A., 2011. Implication of Gravity drainage plan on shallow rising groundwater conditions in parts of ArRiyadh City, Saudi Arabia. *International Journal of Physical Sciences*, 6(7), pp.1611-1619.

Al-Othman, A.A. and Ahmed, I., 2012. Hydrogeological framework and its implication on water level rise in Eastern ArRiyadh, Saudi Arabia. *Environmental Earth Sciences*, 67(5), pp.1493-1502.

Al-Othman, A.A., 2008. Evaluation of drainage water quality to be reused for irrigation purposes in Riyadh area, Saudi Arabia. *Misr Journal of Agricultural Engineering*, 25(4), pp.1323-1342.

Al-Othman, A.A., 2015. Evaluation of the suitability of surface water from Riyadh Mainstream Saudi Arabia for a variety of uses. *Arabian Journal of Chemistry*, 12(8), pp.2104-2110.

AlQahtany, A., Rezgui, Y. and Li, H., 2014. A consensus-based framework for the sustainable urban planning development: as an approach for Saudi Arabian cities. *International Journal of Environmental Science and Development*, 5(2), pp.124-131.

- Al-Qahtany, A.M., 2014. *The development of a consensus-based framework for a sustainable urban planning of the city of Riyadh* (Doctoral dissertation, Cardiff University).
- Alriyadh Newspaper, 2015. *Transportation: Our network is designed to drain road water and not what coming from neighboring areas.* [online] Alriyadh Newspaper. Available at: <<https://www.alriyadh.com/1104044>> [Accessed 23 September 2021].
- Alsaaran, N.A. and Alghamdi, A.S., 2022. Precipitation climatology and spatiotemporal trends over the Arabian Peninsula. *Theoretical and Applied Climatology*, 147(3), pp.1133-1149.
- Al-Saleh, M.A., 1997. Variability and frequency of daily rainfall in Riyadh, Saudi Arabia. *The Geographical Bulletin*, 39(1), p.48.
- Al-Samhoury, W. and Al-Naim, M., 2007. Wadi Hanifah Wetlands Riyadh, Saudi Arabia.
- Al-Shareef, O.H., Ezzeldin, M. and Gutub, S.A., 2013. Comparison of peak discharge estimation methods in northern Jeddah in western Saudi Arabia. *Advances and Applications in Fluid Mechanics*, 14(2), p.219.
- Al-Sobaihi, S.M., 1976. *Water resources of Wadi Hanifah, Saudi Arabia: a case study* (Masters dissertation, Durham University).
- Altuwaijri, H.A., Alotaibi, M.H., Almudlaj, A.M. and Almalki, F.M., 2019. Predicting urban growth of Arriyadh city, capital of the Kingdom of Saudi Arabia, using Markov cellular automata in TerrSet geospatial system. *Arabian Journal of Geosciences*, 12(4), pp.1-15.
- Al-Wsabi, R., 2022. [Twitter] *Al Aziziyah Neighbourhood*. [video] Available at: <https://twitter.com/r_1410/status/1553814705868865536> [Accessed 30 August 2022].

- ALYAMANI, M.S. and SEN, Z., 1993. Regional variations of monthly rainfall amounts in the Kingdom of Saudi Arabia. *Earth Sciences*, 6(1).
- Alyamani, M.S., 2001. Isotopic composition of rainfall and ground-water recharge in the western province of Saudi Arabia. *Journal of Arid Environments*, 49(4), pp.751-760.
- Al-Zahrani, M., Al-Areeq, A. and Sharif, H.O., 2016. Estimating urban flooding potential near the outlet of an arid catchment in Saudi Arabia. *Geomatics, Natural Hazards and Risk*, 8(2), pp.672-688.
- Andaryani, S., Trolle, D., Nikjoo, M.R., Moghadam, M.H. and Mokhtari, D., 2019. Forecasting near-future impacts of land use and climate change on the Zilbier river hydrological regime, northwestern Iran. *Environmental Earth Sciences*, 78(6), pp.1-14.
- Aqnouy, M., El Messari, J.E.S., Ismail, H., Bouadila, A., Moreno Navarro, J.G., Loubna, B. and Mansour, M.R.A., 2019. Assessment of the SWAT model and the parameters affecting the flow simulation in the watershed of Oued Laou (Northern Morocco). *Journal of Ecological Engineering*, 20(4).
- Argaam, 2019. *Saudi Arabia's drinking water consumption rises 8% in 2018*. [online] Argaam Website. Available at: <<https://www.argaam.com/en/article/articledetail/id/1312492>> [Accessed 25 August 2021].
- Armson, D., Stringer, P. and Ennos, A.R., 2013. The effect of street trees and amenity grass on urban surface water runoff in Manchester, UK. *Urban Forestry & Urban Greening*, 12(3), pp.282-286.
- Arnold, J.G., Kiniry, J.R., Srinivasan, R., Williams, J.R., Haney, E.B. and Neitsch, S.L., 2012a. SWAT input/output documentation version 2012. *Texas Water Resources Institute: College Station, TX, USA*, p.654.
- Arnold, J.G., Moriasi, D.N., Gassman, P.W., Abbaspour, K.C., White, M.J., Srinivasan, R., Santhi, C., Harmel, R.D., Van Griensven,

A., Van Liew, M.W. and Kannan, N., 2012b. SWAT: Model use, calibration, and validation. *Transactions of the ASABE*, 55(4), pp.1491-1508.

Arriyadh Environment, n.d. *High groundwater level problem*. [online] Arriyadh Environment Website. Available at: <<https://www.riyadhenv.gov.sa/achievement/%d8%a7%d8%b1%d8%aa%d9%81%d8%a7%d8%b9-%d9%85%d9%86%d8%b3%d9%88%d8%a8-%d8%a7%d9%84%d9%85%d9%8a%d8%a7%d9%87/>> [Accessed 5 January 2021].

Aryal, S.K., Silberstein, R.P., Fu, G., Hodgson, G., Charles, S.P. and McFarlane, D., 2020. Understanding spatio-temporal rainfall-runoff changes in a semi-arid region. *Hydrological Processes*, 34(11), pp.2510-2530.

Assiri, M.E., 2017. Assessing MODIS Land Surface Temperature (LST) Over Jeddah. *Polish Journal of Environmental Studies*, 26(4).

Ayele, G.T., Teshale, E.Z., Yu, B., Rutherford, I.D. and Jeong, J., 2017. Streamflow and sediment yield prediction for watershed prioritization in the Upper Blue Nile River Basin, Ethiopia. *Water*, 9(10), p.782.

Azgin, S.T. and Celik, F.D., 2020. Evaluating surface runoff responses to land use changes in a data scarce basin: A case study in Palas basin, Turkey. *Water Resources*, 47(5), pp.828-834.

Bacha, A.B., Abid, I., Nehdi, I. and Horchani, H., 2019. Hydrolysis of oils in the Wadi Hanifah River in Saudi Arabia by free and immobilized *Staphylococcus aureus* ALA1 lipase. *Environmental Progress & Sustainable Energy*, 38(3), p.e13000.

Baddoo, T.D., Li, Z., Guan, Y., Boni, K.R.C. and Noonni, I.K., 2020. Data-Driven Modeling and the Influence of Objective Function Selection on Model Performance in Limited Data Regions. *International Journal of Environmental Research and Public Health*, 17(11), p.4132.

- Bansal, N., Mukherjee, M. and Gairola, A., 2015. Causes and impact of urban flooding in Dehradun. *International Journal of Current Research*, 7(2), pp.12615-12627.
- Barth, H.K. and Quiel, F., 1987. Riyadh and its Development. *GeoJournal*, 15(1), pp.39-46.
- Birkinshaw, S.J., O'Donnell, G., Glenis, V. and Kilsby, C., 2021. Improved hydrological modelling of urban catchments using runoff coefficients. *Journal of Hydrology*, 594, p.125884.
- Boskidis, I., Gikas, G.D., Sylaios, G.K. and Tsihrintzis, V.A., 2012. Hydrologic and water quality modeling of lower Nestos river basin. *Water resources management*, 26(10), pp.3023-3051.
- Bouslihim, Y., Rochdi, A., Paaza, N.E.A. and Liuzzo, L., 2019. Understanding the effects of soil data quality on SWAT model performance and hydrological processes in Tamedroust watershed (Morocco). *Journal of African Earth Sciences*, 160, p.103616.
- Bramkamp, R.A. and Ramirez, L.F., 1958. *Geology Map of the Northern Tuwayq Quadrangle, Kingdom of Saudi Arabia*. Ministry of Petroleum and Mineral Resources, Directorate General of Mineral Resources.
- Brouwer, C., Goffeau, A. and Heibloem, M., 1985. Irrigation Water Management: Training manual no. 1-Introduction into Irrigation. Food and Agriculture Organization of the United Nations. *Land and Water Development Division*.
- Brouziyne, Y., Abouabdillah, A., Bouabid, R., Benaabidate, L. and Oueslati, O., 2017. SWAT manual calibration and parameters sensitivity analysis in a semi-arid watershed in North-western Morocco. *Arabian Journal of Geosciences*, 10(19), pp.1-13.
- Buchhorn, M., Smets, B., Bertels, L., De Roo, B., Lesiv, M., Tsendbazar, N.E., Herold, M. and Fritz, S., 2020. Copernicus global land service: Land cover 100m: collection 3: epoch 2019: Globe. *Version V3. 0.1*[Data set].

- Carlos Mendoza, J.A., Chavez Alcazar, T.A. and Zuñiga Medina, S.A., 2021. Calibration and uncertainty analysis for modelling runoff in the Tambo River Basin, Peru, using Sequential Uncertainty Fitting Ver-2 (SUF2) algorithm. *Air, Soil and Water Research*, 14, p.1178622120988707.
- Chapman, R.W. (1978). Geology. In: Al-Sayari, S.S., Zötl, J.G. (eds) Quaternary Period in Saudi Arabia. Springer, Vienna.
- Chaponnière, A., Boulet, G., Chehbouni, A. and Aresmouk, M., 2008. Understanding hydrological processes with scarce data in a mountain environment. *Hydrological Processes: An International Journal*, 22(12), pp.1908-1921.
- Chaponniere, A., Maisongrande, P., Escadafal, R., de Solan, B. and Chehbouni, G., 2003, July. Satellite driven modeling of snow runoff in a small semi-arid mountainous watershed in Morocco. In *IGARSS 2003. 2003 IEEE International Geoscience and Remote Sensing Symposium. Proceedings (IEEE Cat. No. 03CH37477)* (Vol. 2, pp. 1181-1183). IEEE.
- Cheema, M.J.M., Immerzeel, W.W. and Bastiaanssen, W.G.M., 2014. Spatial quantification of groundwater abstraction in the irrigated Indus basin. *Groundwater*, 52(1), pp.25-36.
- Chen, H., Zhu, G., Zhang, K., Bi, J., Jia, X., Ding, B., Zhang, Y., Shang, S., Zhao, N. and Qin, W., 2020. Evaluation of evapotranspiration models using different LAI and meteorological forcing data from 1982 to 2017. *Remote Sensing*, 12(15), p.2473.
- Cherkauer, K., n.d. *Notes about Model Time Steps*. [online] VIC Website. Available at: <<https://vic.readthedocs.io/en/vic.4.2.d/Documentation/TechnicalNotes/Timestep/>> [Accessed 29 September 2022].
- Chorley, R. J., Schumm, S. A. and Sugden, D. E., 1984. *Geomorphology*, Methuen & Co Ltd, London.
- Chow, V. T., Maidment, D.R., and Mays, L.W., 1988. *Applied Hydrology*, McGraw-Hill, Inc., New York, USA.

- Cirilo, J.A., Verçosa, L.F.D.M., Gomes, M.M.D.A., Feitoza, M.A.B., Ferraz, G.D.F. and Silva, B.D.M., 2020. Development and application of a rainfall-runoff model for semi-arid regions. *RBRH*, 25.
- Coutu, G.W. and Vega, C., 2007. Impacts of landuse changes on runoff generation in the east branch of the Brandywine creek watershed using a GIS-based hydrologic model. *Middle States Geogr*, 40, pp.142-149.
- Cronshey, R., 1986. 2nd edition. *Urban hydrology for small watersheds*. US Dept. of Agriculture, Soil Conservation Service, Engineering Division.
- Daoudi, M. and Niang, A.J., 2019. Flood Risk and Vulnerability of Jeddah City, Saudi Arabia. *Recent Advances in Flood Risk Management*, pp.634-654.
- Dawod, G.M. and Koshak, N.A., 2011. Developing GIS-based unit hydrographs for flood management in Makkah metropolitan area, Saudi Arabia. *Journal of Geographic Information System*, 3(2), p.153.
- De Vries, A.J., Feldstein, S.B., Riemer, M., Tyrlis, E., Sprenger, M., Baumgart, M., Fnais, M. and Lelieveld, J., 2016. Dynamics of tropical-extratropical interactions and extreme precipitation events in Saudi Arabia in autumn, winter and spring. *Quarterly Journal of the Royal Meteorological Society*, 142(697), pp.1862-1880.
- Deb, P., Kiem, A.S. and Willgoose, G., 2019. A linked surface water-groundwater modelling approach to more realistically simulate rainfall-runoff non-stationarity in semi-arid regions. *Journal of Hydrology*, 575, pp.273-291.
- Desai, S., Singh, D.K., Islam, A. and Sarangi, A., 2021. Multi-site calibration of hydrological model and assessment of water balance in a semi-arid river basin of India. *Quaternary International*, 571, pp.136-149.
- Devia, G.K., Ganasri, B.P. and Dwarakish, G.S., 2015. A review on hydrological models. *Aquatic procedia*, 4, pp.1001-1007.

- DMS Projects, n.d., NWC - Yabreen Water Field. <https://www.dmsprojects.net/saudi-arabia/projects/nwc-riyadh-yabreen-water-field/PRJ00024610>
- Donahue, R.L., Miller, R.W. and Shickluna, J.C., 1983. *Soils. An introduction to soils and plant growth*. Prentice-Hall, Inc..
- Dong, W., Cui, B., Liu, Z. and Zhang, K., 2014. Relative effects of human activities and climate change on the river runoff in an arid basin in northwest China. *Hydrological processes*, 28(18), pp.4854-4864.
- Doulabian, S., Ghasemi Tousi, E., Aghlmand, R., Alizadeh, B., Ghaderi Bafti, A. and Abbasi, A., 2021. Evaluation of integrating swat model into a multi-criteria decision analysis towards reliable rainwater harvesting systems. *Water*, 13(14), p.1935.
- Earthdata, n.d., NASA. <https://urs.earthdata.nasa.gov/>
- EarthExplorer, n.d., UUGS. <https://earthexplorer.usgs.gov/>
- Eini, M.R., Javadi, S., Delavar, M., Monteiro, J.A. and Darand, M., 2019. High accuracy of precipitation reanalyses resulted in good river discharge simulations in a semi-arid basin. *Ecological engineering*, 131, pp.107-119.
- El Kenawy, A.M., McCabe, M.F., Stenchikov, G.L. and Raj, J., 2014. Multi-decadal classification of synoptic weather types, observed trends and links to rainfall characteristics over Saudi Arabia. *Frontiers in Environmental Science*, 2, p.37.
- El Maghraby, M., Masoud, M.H.Z. and Niyazi, B., 2014. Assessment of surface runoff in arid, data scarce regions; an approach applied in. *Life Science Journal*, 11(4).
- Elquliti, S., Alfalatah, S.M., Alghamdi, M., Alabdali, Y. and Ahmed, A., 2016. Assessment of the Frequency and Return Period for Extreme rainfall Causing Floods Inmecca, Saudi Arabia. *Int. J. Sci. Technol. Res. Eng*, 1 (2), pp.1-5.

- Elsebaie, I.H., 2012. Developing rainfall intensity–duration–frequency relationship for two regions in Saudi Arabia. *Journal of King Saud University-Engineering Sciences*, 24(2), pp.131-140.
- El-Sharif, A.R., 1985. Water supply problems of Riyadh, Saudi Arabia. *GeoJournal*, Vol. 11, pp. 239–243.
- Emam, A.R., Kappas, M., Linh, N.H.K. and Renchin, T., 2017. Hydrological modeling and runoff mitigation in an ungauged basin of central Vietnam using SWAT model. *Hydrology*, 4(1), p.16.
- Eshtawi, T., Evers, M. and Tischbein, B., 2016. Quantifying the impact of urban area expansion on groundwater recharge and surface runoff. *Hydrological Sciences Journal*, 61(5), pp.826-843.
- Esmali, A., Golshan, M. and Kavian, A., 2021. Investigating the performance of SWAT and IHACRES in simulation streamflow under different climatic regions in Iran. *Atmósfera*, 34(1), pp.79-96.
- Ewea, H.A., Elfeki, A.M. and Al-Amri, N.S., 2017. Development of intensity–duration–frequency curves for the Kingdom of Saudi Arabia. *Geomatics, Natural Hazards and Risk*, 8(2), pp.570-584.
- Fadil, A., Rhinane, H., Kaoukaya, A., Kharchaf, Y. and Bachir, O.A., 2011. Hydrologic modeling of the Bouregreg watershed (Morocco) using GIS and SWAT model. *Journal of Geographic Information System*, 3(04), p.279.
- Fallatah, O.A., Ahmed, M., Cardace, D., Boving, T. and Akanda, A.S., 2019. Assessment of modern recharge to arid region aquifers using an integrated geophysical, geochemical, and remote sensing approach. *Journal of Hydrology*, 569, pp.600-611.
- Fang, G., Yang, J., Chen, Y., Li, Z. and De Maeyer, P., 2018. Impact of GCM structure uncertainty on hydrological processes in an arid area of China. *Hydrology Research*, 49(3), pp.893-907.

FAO, 1974. *Soil Map of the World, 1: 5 000 000: Volume I: Legend*.

FAO, 1988. Soil map of the world: revised legend with corrections and updates. FAO, Rome.

FAO, n.d., Digital soil map of the World. FAO Website.

Fett, R.W., Bohan, W.A. and Englebretson, R.E., 1983. *Navy Tactical Applications Guide. Volume 5, Part 1. Indian Ocean (Red Sea/Persian Gulf) Weather Analysis and Forecast Applications*. BOHAN (WALTER A) CO PARK RIDGE IL.

Fisher, M., Mambery, D.A. 1998. Climate. In: Ghazanfar, S.A., Fisher, M. (eds) *Vegetation of the Arabian Peninsula. Geobotany*, vol 25. Springer, Dordrecht.

Fitzpatrick, F.A., Diebel, M.W., Harris, M.A., Arnold, T.L., Lutz, M.A. and Richards, K.D., 2005. Effects of urbanization on the geomorphology, habitat, hydrology, and fish index of biotic integrity of streams in the Chicago area, Illinois and Wisconsin. In *American Fisheries Society Symposium* (Vol. 47, pp. 87-115).

Foglia, L., Hill, M.C., Mehl, S.W. and Burlando, P., 2009. Sensitivity analysis, calibration, and testing of a distributed hydrological model using error-based weighting and one objective function. *Water Resources Research*, 45(6).

Foth, H.D., 1990. *Fundamentals of soil science*. John Wiley and Sons, New York. NY. 360p.

Franco, A.C.L. and Bonumá, N.B., 2017. Multi-variable SWAT model calibration with remotely sensed evapotranspiration and observed flow. *RBRH*, 22.

Gao, X., Chen, X., Biggs, T.W. and Yao, H., 2018. Separating wet and dry years to improve calibration of SWAT in Barrett Watershed, Southern California. *Water*, 10(3), p.274.

- Garba, S.B., 2004. Managing urban growth and development in the Riyadh metropolitan area, Saudi Arabia. *Habitat international*, 28(4), pp.593-608.
- Garg, K.K. and Wani, S.P., 2013. Opportunities to build groundwater resilience in the semi-arid tropics. *Groundwater*, 51(5), pp.679-691.
- Gassman, P.W., Reyes, M.R., Green, C.H. and Arnold, J.G., 2007. The soil and water assessment tool: historical development, applications, and future research directions. *Transactions of the ASABE*, 50(4), pp.1211-1250.
- General Authority for Statistics, n.d., Annual Year Book.
- Ghadei, S., Singh, P. and Mishra, S., 2018. Hydrological Modeling in the Ong River Basin, India using SWAT Model. *Journal of Spatial Hydrology*, 14(2).
- Githui, F., Selle, B. and Thayalakumaran, T., 2012. Recharge estimation using remotely sensed evapotranspiration in an irrigated catchment in southeast Australia. *Hydrological Processes*, 26(9), pp.1379-1389.
- GLEAM, n.d. *GLEAM | Global Land Evaporation Amsterdam Model*. [online] GLEAM. Available at: <<https://www.gleam.eu/>> [Accessed 9 January 2019].
- Golmohammadi, G., Prasher, S., Madani, A. and Rudra, R., 2014. Evaluating three hydrological distributed watershed models: MIKE-SHE, APEX, SWAT. *Hydrology*, 1(1), pp.20-39.
- Gosling, S.N., Dunn, R., Carrol, F., Christidis, N., Fullwood, J., Gusmao, D.D., Golding, N., Good, L., Hall, T., Kendon, L. and Kennedy, J., 2011. Climate: observations, projections and impacts: Saudi Arabia. *The Met Office, UK*.
- Gosling, S.N., Zaherpour, J., Mount, N.J., Hattermann, F.F., Dankers, R., Arheimer, B., Breuer, L., Ding, J., Haddeland, I., Kumar, R. and Kundu, D., 2016. A comparison of changes in river runoff from multiple global and catchment-scale

hydrological models under global warming scenarios of 1 C, 2 C and 3 C. *Climatic Change*, 141(3), pp.577-595.

Goudie, A. and Wilkinson, J.C., 1977. *The warm desert environment*. Cambridge University Press.

Graf, W.L., 1975. The impact of suburbanization on fluvial geomorphology. *Water Resources Research*, 11(5), pp.690-692.

Gregory, P.J., and Nortcliff, S., 2013. Soil conditions and plant growth. Blackwell Publishing Ltd.

Grossi, G., Lendvai, A., Peretti, G. and Ranzi, R., 2017. Snow precipitation measured by gauges: Systematic error estimation and data series correction in the central Italian Alps. *Water*, 9(7), p.461.

Gu, X., Yang, G., He, X., Zhao, L., Li, X., Li, P., Liu, B., Gao, Y., Xue, L. and Long, A., 2020. Hydrological process simulation in Manas River Basin using CMADS. *Open Geosciences*, 12(1), pp.946-957.

Gungor, K., 2014. SWAT: Soil Data for non-US Study Areas. [Blog] *Dr. Kerem Gungor's Environmental Science and Engineering Blog*, Available at: <<http://drgungorese.blogspot.com/2014/04/swat-using-soil-data-for-non-us-study.html>> [Accessed 28 April 2019].

Gyamfi, C., Ndambuki, J.M. and Salim, R.W., 2016. Simulation of sediment yield in a semi-arid river basin under changing land use: an integrated approach of hydrologic modelling and principal component analysis. *Sustainability*, 8(11), p.1133.

Ha, L.T., Bastiaanssen, W.G., Van Griensven, A., Van Dijk, A.I. and Senay, G.B., 2018. Calibration of spatially distributed hydrological processes and model parameters in SWAT using remote sensing data and an auto-calibration procedure: A case study in a Vietnamese river basin. *Water*, 10(2), p.212.

Hadadin, N., Tarawneh, Z., Shatanawi, K., Banihani, Q. and Hamdi, M.R., 2013. Hydrological analysis for floodplain hazard of

Jeddah's drainage Basin, Saudi Arabia. *Arabian Journal for Science and Engineering*, 38(12), pp.3275-3287.

Halefom, A., Sisay, E., Worku, T., Khare, D., Dananto, M. and Narayanan, K., 2018. Precipitation and runoff modelling in Megech watershed, Tana Basin, Amhara region of Ethiopia. *American Journal of Environmental Engineering*, 8(3), pp.45-53.

Harrigan, P., 2017. Riyadh: Oasis of Heritage and Vision, High Commission for the Development of Arriyadh.

Hasanean, H. and Almazroui, M., 2015. Rainfall: features and variations over Saudi Arabia, a review. *Climate*, 3(3), pp.578-626.

Hassan, A.A.A., 2018. Accuracy assessment of open source digital elevation models. *Journal of University of Babylon for Engineering Sciences*, 26(3), pp.23-33.

Her, Y., Frankenberger, J., Chaubey, I. and Srinivasan, R., 2015. Threshold effects in HRU definition of the soil and water assessment tool. *Transactions of the ASABE*, 58(2), pp.367-378.

Herman, M.R., Hernandez-Suarez, J.S., Nejadhashemi, A.P., Kropp, I. and Sadeghi, A.M., 2020. Evaluation of multi-and many-objective optimization techniques to improve the performance of a hydrologic model using evapotranspiration remote-sensing data. *Journal of Hydrologic Engineering*, 25(4),

Herman, M.R., Nejadhashemi, A.P., Abouali, M., Hernandez-Suarez, J.S., Daneshvar, F., Zhang, Z., Anderson, M.C., Sadeghi, A.M., Hain, C.R. and Sharifi, A., 2018. Evaluating the role of evapotranspiration remote sensing data in improving hydrological modeling predictability. *Journal of Hydrology*, 556, pp.39-49.

Hijji, M., Amin, S., Iqbal, R. and Harrop, W., 2015. The significance of using "expert system" to assess the preparedness of training capabilities against different flash flood scenarios. *Lecture Notes on Software Engineering*, 3(3), p.214.

Holden, J., 2005. Surface Runoff and Subsurface Drainage. *Water Encyclopedia*, 3, pp.451-454.

Hourpress, 2018. *A number of cars sank today, Friday, in the Dirab tunnel in the Saudi capital, Riyadh*. [online] Hourpress website. Available at: <<https://hourpress.net/91816/%D8%B4%D8%A7%D9%87%D8%AF-%D8%A8%D8%A7%D9%84%D9%81%D9%8A%D8%AF%D9%8A%D9%88..-%D8%BA%D8%B1%D9%82-%D8%B9%D8%AF%D8%AF-%D9%85%D9%86-%D8%A7%D9%84%D8%B3%D9%8A%D8%A7%D8%B1%D8%A7%D8%AA-%D8%A7%D9%84%D9%8A%D9%88%D9%85-%D8%A7%D9%84%D8%AC%D9%85%D8%B9%D8%A9-%D9%81%D9%8A-%D9%86%D9%81%D9%82-%D8%AF%D9%8A%D8%B1%D8%A7%D8%A8-%D8%A8%D8%A7%D9%84%D8%B9%D8%A7%D8%B5%D9%85%D8%A9-%D8%A7%D9%84%D8%B3%D8%B9%D9%88%D8%AF%D9%8A%D8%A9-%D8%A7%D9%84%D8%B1%D9%8A%D8%A7%D8%B6>> [Accessed 14 August 2021].

Hu, S., Fan, Y. and Zhang, T., 2020. Assessing the effect of land use change on surface runoff in a rapidly urbanized city: A case study of the central area of Beijing. *Land*, 9(1), p.17.

Huang, P., Li, Z., Chen, J., Li, Q. and Yao, C., 2016. Event-based hydrological modeling for detecting dominant hydrological process and suitable model strategy for semi-arid catchments. *Journal of Hydrology*, 542, pp.292-303.

Huang, P.M., Li, Y. and Sumner, M.E. eds., 2012. *Handbook of soil sciences: properties and processes*. CRC Press.

Huffman, R.L., Fangmeier, D.D., Elliot, W.J., and Workman, S.R., 2013. Chapter 4: Evaporation and Evapotranspiration. pp. 55-79. in: *Soil and Water conservation engineering*, Soil and Water conservation engineering, 7th edition, American Society of Agricultural and Biological Engineering.

Hussein, K., Alkaabi, K., Ghebreyesus, D., Liaqat, M.U. and Sharif, H.O., 2020. Land use/land cover change along the Eastern

Coast of the UAE and its impact on flooding risk. *Geomatics, Natural Hazards and Risk*, 11(1), pp.112-130.

ICAR e-Course, n.d., Introduction to Soil Science. AgriMoon Website.

ICOMOS Consultant, 2010. At-Turaif District in ad-Dir'iyah (Saudi Arabia), Report No 1329.

Immerzeel, W.A. and Droogers, P., 2008. Calibration of a distributed hydrological model based on satellite evapotranspiration. *Journal of hydrology*, 349(3-4), pp.411-424.

Inkiläinen, E.N., McHale, M.R., Blank, G.B., James, A.L. and Nikinmaa, E., 2013. The role of the residential urban forest in regulating throughfall: A case study in Raleigh, North Carolina, USA. *Landscape and urban planning*, 119, pp.91-103.

Institute of Hydrology, 1984. *Flood estimates for Mushwab Dam, Jeddah*. NERC Institute of Hydrology. (Unpublished)

Iskender, I. and Sajikumar, N., 2016. Evaluation of surface runoff estimation in ungauged watersheds using SWAT and GIUH. *Procedia Technology*, 24, pp.109-115.

Jajarmizadeh, M., Harun, S., Abdullah, R. and Salarpour, M., 2016a. An evaluation of blue water prediction in southern part of Iran using the Soil and Water Assessment Tool (SWAT). *Environmental Engineering & Management Journal (EEMJ)*, 15(1).

Jajarmizadeh, M., Harun, S.B., Shahid, S., Akib, S. and Salarpour, M., 2014. Impact of direct soil moisture and revised soil moisture index methods on hydrologic predictions in an arid climate. *Advances in Meteorology*, 2014.

Jajarmizadeh, M., Kakaei Lafdani, E., Harun, S. and Ahmadi, A., 2015. Application of SVM and SWAT models for monthly streamflow prediction, a case study in South of Iran. *KSCE Journal of Civil Engineering*, 19(1), pp.345-357.

- Jajarmizadeh, M., Sidek, L.M., Mirzai, M., Alaghmand, S., Harun, S. and Majid, M.R., 2016b. Prediction of surface flow by forcing of climate forecast system reanalysis data. *Water resources management*, 30(8), pp.2627-2640.
- Jimeno-Sáez, P., Pulido-Velazquez, D., Collados-Lara, A.J., Pardo-Igúzquiza, E., Senent-Aparicio, J. and Baena-Ruiz, L., 2020. A preliminary assessment of the “Undercatching” and the precipitation pattern in an alpine basin. *Water*, 12(4), p.1061.
- Jin, X. and Jin, Y., 2020. Calibration of a distributed hydrological model in a data-scarce basin based on GLEAM datasets. *Water*, 12(3), p.897.
- Jin, X., He, C., Zhang, L. and Zhang, B., 2018. A modified groundwater module in SWAT for improved streamflow simulation in a large, arid endorheic river watershed in Northwest China. *Chinese Geographical Science*, 28(1), pp.47-60.
- Jin, X., Jin, Y. and Mao, X., 2019. Land use/cover change effects on river basin hydrological processes based on a modified soil and water assessment tool: A case study of the Heihe river basin in northwest China’s arid region. *Sustainability*, 11(4), p.1072.
- Jones, K.R., Berney, O., Carr, D.P. and Barrett, E.C., 1981. *Arid zone hydrology for agricultural development*. FAO Irrigation and Drainage Papers (FAO). no. 37.
- Kanda, N., Negi, H.S., Rishi, M.S. and Shekhar, M.S., 2018. Performance of various techniques in estimating missing climatological data over snowbound mountainous areas of Karakoram Himalaya. *Meteorological Applications*, 25(3), pp.337-349.
- Kane, F., 2021. *Saudi crown prince unveils plan to make Riyadh one of world’s 10 largest city economies*. [online] Arab News. Available at: <<https://www.arabnews.com/node/1800231/business-economy>> [Accessed 23 June 2021].

- Khalil, R., 2017. Determination of Potential Runoff Coefficient Using GIS and Remote Sensing. *Journal of Geographic Information System*, 9(6), pp.752-762.
- Khan, J.N., Ali, S.R., Jillani, A. and Ashraf, I., 2020. Application of rs/gis in conservation studies for surface and groundwater harvesting in cold arid regions of northwestern himalayas. *Applied engineering in agriculture*, 36(1), pp.105-114.
- Kheimi, M.M. and Gutub, S., 2014, December. Assessment of remotely sensed precipitation products across the Saudi Arabia region. In *6th International conference on water resources and arid environments* (Vol. 1617).
- Khelifa, W.B., Hermassi, T., Strohmeier, S., Zucca, C., Ziadat, F., Boufaroua, M. and Habaieb, H., 2017. Parameterization of the effect of bench terraces on runoff and sediment yield by SWAT modeling in a small semi-arid watershed in Northern Tunisia. *Land Degradation & Development*, 28(5), pp.1568-1578.
- Kim, H., Lee, D.K. and Sung, S., 2016. Effect of urban green spaces and flooded area type on flooding probability. *Sustainability*, 8(2), p.134.
- Kiros, G., Shetty, A. and Nandagiri, L., 2015. Performance evaluation of SWAT model for land use and land cover changes in semi-arid climatic conditions: a review. *Hydrology: Current Research*, 6(3), p.7.
- Komurcu, M., Schlosser, C.A., Alshehri, I., Alshahrani, T., Alhayaza, W., AlSaati, A. and Strzepek, K., 2020. Mid-Century Changes in the Mean and Extreme Climate in the Kingdom of Saudi Arabia and Implications for Water Harvesting and Climate Adaptation. *Atmosphere*, 11(10), p.1068.
- Konrad, C., 2016. *Effects of Urban Development on Floods*. [online] USGS. Available at: <<https://pubs.usgs.gov/fs/fs07603/>> [Accessed 10 October 2022].

- Koycegiz, C., Buyukyildiz, M. and Kumcu, S.Y., 2021. Spatio-temporal analysis of sediment yield with a physically based model for a data-scarce headwater in Konya Closed Basin, Turkey. *Water Supply*, 21(4), pp.1752-1763.
- Koycegiz, C. and Buyukyildiz, M., 2019. Calibration of SWAT and two data-driven models for a data-scarce mountainous headwater in semi-arid Konya closed basin. *Water*, 11(1), p.147.
- Kumar, R., 2011. *Research methodology*. London, England: Sage.
- Kunnath-Poovakka, A., Ryu, D., Renzullo, L.J. and George, B., 2016. The efficacy of calibrating hydrologic model using remotely sensed evapotranspiration and soil moisture for streamflow prediction. *Journal of hydrology*, 535, pp.509-524.
- Kunnath-Poovakka, A., Ryu, D., Renzullo, L., Pipunic, R.C. and George, B., 2013. Calibration of land surface model using remotely sensed evapotranspiration and soil moisture predictions. In *Proceedings of the 20th international congress on modelling and simulation MODSIM2013*. <http://www.mssanzorg.au/modsim2013> L (Vol. 19).
- Lee, S., Wallace, C.W., Sadeghi, A.M., McCarty, G.W., Zhong, H. and Yeo, I.Y., 2018. Impacts of Global Circulation Model (GCM) bias and WXGEN on modeling hydrologic variables. *Water*, 10(6), p.764.
- Leopold, L.B., 1968. *Hydrology for urban land planning: A guidebook on the hydrologic effects of urban land use* (Vol. 554). US Geological Survey.
- Leta, O.T., El-Kadi, A.I., Dulai, H. and Ghazal, K.A., 2018. Assessment of SWAT model performance in simulating daily streamflow under rainfall data scarcity in Pacific island watersheds. *Water*, 10(11), p.1533.
- Li, C., Liu, M., Hu, Y., Shi, T., Zong, M. and Walter, M.T., 2018. Assessing the impact of urbanization on direct runoff using improved composite CN method in a large urban area. *International journal of environmental research and public health*, 15(4), p.775.

- Li, C., Qi, J., Feng, Z., Yin, R., Zou, S. and Zhang, F., 2010. Parameters optimization based on the combination of localization and auto-calibration of SWAT model in a small watershed in Chinese Loess Plateau. *Frontiers of earth science in china*, 4(3), pp.296-310.
- Li, E., Mu, X., Zhao, G., Gao, P. and Sun, W., 2017. Effects of check dams on runoff and sediment load in a semi-arid river basin of the Yellow River. *Stochastic Environmental Research and Risk Assessment*, 31(7), pp.1791-1803.
- Li, Q., Yu, X., Xin, Z. and Sun, Y., 2013. Modeling the effects of climate change and human activities on the hydrological processes in a semiarid watershed of loess plateau. *Journal of Hydrologic Engineering*, 18(4), pp.401-412.
- Li, X. and Lu, M., 2012. Multi-step optimization of parameters in the Xinanjiang model taking into account their time scale dependency. *Journal of Japan Society of Civil Engineers, Ser. B1 (Hydraulic Engineering)*, 68(4), pp.I_145-I_150.
- Li, Z., Deng, X., Wu, F. and Hasan, S.S., 2015. Scenario analysis for water resources in response to land use change in the middle and upper reaches of the Heihe River Basin. *Sustainability*, 7(3), pp.3086-3108.
- Licciardello, F., Toscano, A., Cirelli, G.L., Consoli, S. and Barbagallo, S., 2017. Evaluation of sediment deposition in a Mediterranean reservoir: Comparison of long term bathymetric measurements and SWAT estimations. *Land Degradation & Development*, 28(2), pp.566-578.
- Lin, F., Chen, X. and Yao, H., 2017. Evaluating the use of Nash-Sutcliffe efficiency coefficient in goodness-of-fit measures for daily runoff simulation with SWAT. *Journal of Hydrologic Engineering*, 22(11), p.05017023.
- Liu, J., Liu, T., Bao, A., De Maeyer, P., Feng, X., Miller, S.N. and Chen, X., 2016. Assessment of different modelling studies on the spatial hydrological processes in an arid alpine catchment. *Water resources management*, 30(5), pp.1757-1770.

- Liu, Z., Zhu, J., Fu, H., Zhou, C. and Zuo, T., 2020. Evaluation of the vertical accuracy of open global dems over steep terrain regions using icesat data: A case study over hunan province, china. *Sensors*, 20(17), p.4865.
- López-Lambraño, A.A., Martínez-Acosta, L., Gámez-Balmaceda, E., Medrano-Barboza, J.P., Remolina López, J.F. and López-Ramos, A., 2020. Supply and demand analysis of water resources. Case study: Irrigation water demand in a semi-arid zone in Mexico. *Agriculture*, 10(8), p.333.
- Luo, K. and Li, Y., 2021. Assessing rainwater harvesting potential in a humid and semi-humid region based on a hydrological model. *Journal of Hydrology: Regional Studies*, 37, p.100912.
- Luo, Y., Arnold, J., Allen, P. and Chen, X., 2012. Baseflow simulation using SWAT model in an inland river basin in Tianshan Mountains, Northwest China. *Hydrology and Earth System Sciences*, 16(4), pp.1259-1267.
- Luong, T.M., Dasari, H.P. and Hoteit, I., 2020. Extreme precipitation events are becoming less frequent but more intense over Jeddah, Saudi Arabia. Are shifting weather regimes the cause?. *Atmospheric Science Letters*, 21(8), p.e981.
- Mahmoodi, N., Kiesel, J., Wagner, P.D. and Fohrer, N., 2020. Integrating water use systems and soil and water conservation measures into a hydrological model of an Iranian Wadi system. *Journal of Arid Land*, 12(4), pp.545-560.
- Mahmoud, M.T., Al-Zahrani, M.A. and Sharif, H.O., 2018. Assessment of global precipitation measurement satellite products over Saudi Arabia. *Journal of Hydrology*, 559, pp.1-12.
- Makwana, J.J. and Tiwari, M.K., 2017. Hydrological stream flow modelling using soil and water assessment tool (SWAT) and neural networks (NNs) for the Limkheda watershed, Gujarat, India. *Modeling Earth Systems and Environment*, 3(2), pp.635-645.

- Maliva, R. and Missimer, T., 2012. *Arid lands water evaluation and management*. Springer Science & Business Media.
- Mapes, K.L. and Pricope, N.G., 2020. Evaluating SWAT model performance for runoff, percolation, and sediment loss estimation in low-gradient watersheds of the Atlantic coastal plain. *Hydrology*, 7(2), p.21.
- Marcella, M.P. and Eltahir, E.A., 2008. The hydroclimatology of Kuwait: explaining the variability of rainfall at seasonal and interannual time scales. *Journal of hydrometeorology*, 9(5), pp.1095-1105.
- Marek, G.W., Gowda, P.H., Evett, S.R., Baumhardt, R.L., Brauer, D.K., Howell, T.A., Marek, T.H. and Srinivasan, R., 2016. Estimating evapotranspiration for dryland cropping systems in the semiarid Texas High Plains using SWAT. *JAWRA Journal of the American Water Resources Association*, 52(2), pp.298-314.
- Markhi, A., Laftouhi, N., Grusson, Y. and Soulaïmani, A., 2019. Assessment of potential soil erosion and sediment yield in the semi-arid N' fis basin (High Atlas, Morocco) using the SWAT model. *Acta Geophysica*, 67(1), pp.263-272.
- Mashat, A. and Abdel Basset, H.A., 2011. Analysis of rainfall over Saudi Arabia. *Journal of King Abdulaziz University: Metrology, Environment and Arid Land Agricultural Sciences*, 22(2), pp.59-78.
- Masih, I., Maskey, S., Uhlenbrook, S. and Smakhtin, V., 2011. Impact of upstream changes in rain-fed agriculture on downstream flow in a semi-arid basin. *Agricultural Water Management*, 100(1), pp.36-45.
- Matin, M.A. and Bourque, C.P.A., 2015. Mountain-river runoff components and their role in the seasonal development of desert-oases in northwest China. *Journal of Arid Environments*, 122, pp.1-15.
- Me, W., Abell, J.M. and Hamilton, D.P., 2015. Effects of hydrologic conditions on SWAT model performance and parameter sensitivity for a small, mixed land use catchment in New

Zealand. *Hydrology and Earth System Sciences*, 19(10), pp.4127-4147.

Meng, F., Sa, C., Liu, T., Luo, M., Liu, J. and Tian, L., 2020. Improved model parameter transferability method for hydrological simulation with SWAT in Ungauged Mountainous Catchments. *Sustainability*, 12(9), p.3551.

Mengistu, A.G., Tesfahuney, W.A., Woyessa, Y.E. and van Rensburg, L.D., 2020. Analysis of the spatio-temporal variability of precipitation and drought intensity in an arid catchment in South Africa. *Climate*, 8(6), p.70.

Mengistu, A.G., van Rensburg, L.D. and Woyessa, Y.E., 2019. Techniques for calibration and validation of SWAT model in data scarce arid and semi-arid catchments in South Africa. *Journal of Hydrology: Regional Studies*, 25, p.100621.

Menking, K.M., Syed, K.H., Anderson, R.Y., Shafike, N.G. and Arnold, J.G., 2003. Model estimates of runoff in the closed, semiarid Estancia basin, central New Mexico, USA. *Hydrological sciences journal*, 48(6), pp.953-970.

Milewski, A., Sultan, M., Al-Dousari, A. and Yan, E., 2014. Geologic and hydrologic settings for development of freshwater lenses in arid lands. *Hydrological Processes*, 28(7), pp.3185-3194.

Milewski, A., Sultan, M., Yan, E., Becker, R., Abdeldayem, A., Soliman, F. and Gelil, K.A., 2009. A remote sensing solution for estimating runoff and recharge in arid environments. *Journal of Hydrology*, 373(1-2), pp.1-14.

Minister of Municipal and Rural Affairs, 2019. Saudi Cities Report 2019, Minister of Municipal and Rural Affairs, Riyadh, Saudi Arabia.

Ministry of Agriculture and Water, 1984. Water Atlas of Saudi Arabia. Ministry of Environment, Water, and Agriculture, Riyadh, Saudi Arabia.

- Ministry of Agriculture and Water, 1986. General soil map of the Kingdom of Saudi Arabia. Ministry of Environment, Water, and Agriculture, Riyadh, Saudi Arabia.
- Ministry of Municipal and Rural Affairs, 2016. Saudi 2016 National report. Third United Nations Conference on Housing and Sustainable Urban Development, HABITAT III.
- Ministry of Municipal and Rural Affairs, 2018. CPI Profile for Riyadh 2018. UN-HABITAT.
- Ministry of Municipal and Rural Affairs, 2019. CPI Profile for Riyadh. UNHABITAT.
- Ministry of Water and Electricity, 2014. Annual Report 2014: Water. Ministry of Environment, Water, and Agriculture, Riyadh, Saudi Arabia.
- Miralles, D.G., Jiménez, C., Jung, M., Michel, D., Ershadi, A., McCabe, M.F., Hirschi, M., Martens, B., Dolman, A.J., Fisher, J.B. and Mu, Q., 2016. The WACMOS-ET project–Part 2: Evaluation of global terrestrial evaporation data sets. *Hydrology and Earth System Sciences*, 20(2), pp.823-842.
- Moderate Resolution Imaging Spectroradiometer, n.d. *MODIS Web*. [online] Modis.gsfc.nasa.gov. Available at: <<https://modis.gsfc.nasa.gov/about/>> [Accessed 20 July 2021].
- Moreira, L.L., Schwaback, D. and Rigo, D., 2018. Sensitivity analysis of the Soil and Water Assessment Tools (SWAT) model in streamflow modeling in a rural river basin. *Revista Ambiente & Água*, 13.
- Moriasi, D.N., Arnold, J.G., Van Liew, M.W., Bingner, R.L., Harmel, R.D. and Veith, T.L., 2007. Model evaluation guidelines for systematic quantification of accuracy in watershed simulations. *Transactions of the ASABE*, 50(3), pp.885-900.
- Moriasi, D.N., Gitau, M.W., Pai, N. and Daggupati, P., 2015. Hydrologic and water quality models: Performance measures

and evaluation criteria. *Transactions of the ASABE*, 58(6), pp.1763-1785.

Mosbahi, M. and Benabdallah, S., 2020. Assessment of land management practices on soil erosion using SWAT model in a Tunisian semi-arid catchment. *Journal of Soils and Sediments*, 20(2), pp.1129-1139.

Mosbahi, M., Benabdallah, S. and Boussema, M.R., 2015. Sensitivity analysis of a GIS-based model: A case study of a large semi-arid catchment. *Earth Science Informatics*, 8(3), pp.569-581.

Mubarak, F.A., 2004. Urban growth boundary policy and residential suburbanization: Riyadh, Saudi Arabia. *Habitat international*, 28(4), pp.567-591.

Mukherjee, S., Joshi, P.K., Mukherjee, S., Ghosh, A., Garg, R.D. and Mukhopadhyay, A., 2013. Evaluation of vertical accuracy of open source Digital Elevation Model (DEM). *International Journal of Applied Earth Observation and Geoinformation*, 21, pp.205-217.

Müller, A., Österlund, H., Marsalek, J. and Viklander, M., 2020. The pollution conveyed by urban runoff: A review of sources. *Science of the Total Environment*, 709, p.136125.

Muttiah, R.S. and Wurbs, R.A., 2002. Scale-dependent soil and climate variability effects on watershed water balance of the SWAT model. *Journal of hydrology*, 256(3-4), pp.264-285.

Naderi, M., 2020. Assessment of water security under climate change for the large watershed of Dorudzan Dam in southern Iran. *Hydrogeology Journal*, 28(5), pp.1553-1574.

Nasiri, S., Ansari, H. and Ziaei, A.N., 2020. Simulation of water balance equation components using SWAT model in Samalqan Watershed (Iran). *Arabian Journal of Geosciences*, 13(11), pp.1-15.

Naval Intelligence Division, 2005. Western Arabia and The Red Sea, Kegan Paul Limited, London, UK.

- Nicholson, S. E., 2011. *Dryland Climatology*. Cambridge University Press, Cambridge, UK.
- Niraula, R., Norman, L.M., Meixner, T. and Callegary, J.B., 2012. Multi-gauge calibration for modeling the semi-arid Santa Cruz Watershed in Arizona-Mexico border area using SWAT. *Air, Soil and Water Research*, 5, pp.ASWR-S9410.
- O'Donnell, E., Thorne, C., Ahilan, S., Arthur, S., Birkinshaw, S., Butler, D., Dawson, D., Everett, G., Fenner, R., Glenis, V. and Kapetas, L., 2020. The blue-green path to urban flood resilience. *Blue-Green Systems*, 2(1), pp.28-45.
- Odusanya, A.E., Mehdi, B., Schürz, C., Oke, A.O., Awokola, O.S., Awomeso, J.A., Adejuwon, J.O. and Schulz, K., 2019. Multi-site calibration and validation of SWAT with satellite-based evapotranspiration in a data-sparse catchment in southwestern Nigeria. *Hydrology and Earth System Sciences*, 23(2), pp.1113-1144.
- Odusanya, A.E., Schulz, K., Biao, E.I., Degan, B.A. and Mehdi-Schulz, B., 2021. Evaluating the performance of streamflow simulated by an eco-hydrological model calibrated and validated with global land surface actual evapotranspiration from remote sensing at a catchment scale in West Africa. *Journal of Hydrology: Regional Studies*, 37, p.100893.
- Olivera, F., Valenzuela, M., Srinivasan, R., Choi, J., Cho, H., Koka, S. and Agrawal, A., 2006. ARCGIS-swat: a geodata model and GIS interface for swat 1. *JAWRA Journal of the American Water Resources Association*, 42(2), pp.295-309.
- Omuto, C., Nachtergaele, F. and Rojas, R.V., 2013. *State of the Art Report on Global and regional Soil Information: Where are we? Where to go?* (p. 81). Rome, Italy: Food and Agriculture Organization of the United Nations.
- Oosterbaan, R.J., n.d. *Software and mathematical (numerical) simulation models for hydrology, salinity and statistics*. [online] waterlog.info. Available at: <<https://www.waterlog.info/software.htm>> [Accessed 26 May 2021].

- Ouda, O.K., 2015. Treated wastewater use in Saudi Arabia: challenges and initiatives. *International Journal of Water Resources Development*, 32(5), pp.799-809.
- Ouessar, M., Bruggeman, A., Abdelli, F., Mohtar, R.H., Gabriels, D. and Cornelis, W.M., 2009. Modelling water-harvesting systems in the arid south of Tunisia using SWAT. *Hydrology and Earth System Sciences*, 13(10), pp.2003-2021.
- Parajuli, P.B., Jayakody, P. and Ouyang, Y., 2018. Evaluation of using remote sensing evapotranspiration data in SWAT. *Water resources management*, 32(3), pp.985-996.
- Park, G., Park, J.Y., Joh, H.K., Lee, J.W., Ahn, S.R. and Kim, S.J., 2014. Evaluation of mixed forest evapotranspiration and soil moisture using measured and swat simulated results in a hillslope watershed. *KSCE Journal of Civil Engineering*, 18(1), pp.315-322.
- Paul, M. and Negahban-Azar, M., 2018. Sensitivity and uncertainty analysis for streamflow prediction using multiple optimization algorithms and objective functions: San Joaquin Watershed, California. *Modeling Earth Systems and Environment*, 4(4), pp.1509-1525.
- Peng, J., Liu, T., Huang, Y., Ling, Y., Li, Z., Bao, A., Chen, X., Kurban, A. and De Maeyer, P., 2021. Satellite-based precipitation datasets evaluation using gauge observation and hydrological modeling in a typical arid land watershed of Central Asia. *Remote Sensing*, 13(2), p.221.
- Perrin, J., Ferrant, S., Massuel, S., Dewandel, B., Maréchal, J.C., Aulong, S. and Ahmed, S., 2012. Assessing water availability in a semi-arid watershed of southern India using a semi-distributed model. *Journal of Hydrology*, 460, pp.143-155.
- Pilgrim, D.H., Chapman, T.G. and Doran, D.G., 1988. Problems of rainfall-runoff modelling in arid and semiarid regions. *Hydrological Sciences Journal*, 33(4), pp.379-400.

- Powers, R.W., Ramirez, L.F., Redmond, C.D. and Elberg, E.L., 1966. *Geology of the Arabian Peninsula*: (p. 147). United States Department of the Interior, Geological Survey.
- Pradhan, P., Tingsanchali, T. and Shrestha, S., 2020. Evaluation of Soil and Water Assessment Tool and Artificial Neural Network models for hydrologic simulation in different climatic regions of Asia. *Science of the Total Environment*, 701, p.134308.
- Presidency of Meteorology and Environment, 2011. Second National Communication: Kingdom of Saudi Arabia. In *A Report Prepared, Coordinated by the Presidency of Meteorology and Environment (PME), Riyadh, Saudi Arabia, and submitted to the United Nations Framework Convention on Climate Change [UNFCCC]*.
- Pulighe, G., Bonati, G., Colangeli, M., Traverso, L., Lupia, F., Altobelli, F., Dalla Marta, A. and Napoli, M., 2020. Predicting streamflow and nutrient loadings in a semi-arid Mediterranean watershed with ephemeral streams using the SWAT model. *Agronomy*, 10(1), p.2.
- Qari, H.A., Jomoah, I. and Mambretti, S., 2014. Flood management in highly developed areas: problems and proposed solutions. *Journal of American Science*, 10(3), p.10.
- Qhtani, A.M. and Al Fassam, A.N., 2011, July. Ar Riyadh Geospatial urban information system and metropolitan development strategy for Ar Riyadh. In *ESRI international user conference* (pp. 1-26).
- Qi, Z., Kang, G., Chu, C., Qiu, Y., Xu, Z. and Wang, Y., 2017. Comparison of SWAT and GWLF model simulation performance in humid south and semi-arid north of China. *Water*, 9(8), p.567.
- Radwan, F., Alazba, A.A. and Mossad, A., 2018. Estimating potential direct runoff for ungauged urban watersheds based on RST and GIS. *Arabian Journal of Geosciences*, 11(23), pp.1-12.

Rahman, M.T., Aldosary, A.S., Nahiduzzaman, K.M. and Reza, I., 2016. Vulnerability of flash flooding in Riyadh, Saudi Arabia. *Natural Hazards*, 84(3), pp.1807-1830.

Reynolds, R., 2015. Synoptic Meteorology - Weather Maps. In *Encyclopedia of Atmospheric Sciences*, pp. 289-298.

Riyadh Environment, n.d.a. *Environmental rehabilitation of Wadi As Silayy and its tributaries*. [online] Riyadh Environment. Available at: <<https://www.riyadhenv.gov.sa/plan/%D8%A7%D9%84%D8%AA%D8%A3%D9%87%D9%8A%D9%84-%D8%A7%D9%84%D8%A8%D9%8A%D8%A6%D9%8A-%D9%84%D9%88%D8%A7%D8%AF%D9%8A-%D8%A7%D9%84%D8%B3%D9%84%D9%8A-%D9%88%D8%B1%D9%88%D8%A7%D9%81%D8%AF%D9%87/?tab=2,137>> [Accessed 22 March 2020].

Riyadh Environment, 2017 *Water Level Rise*. [online] Riyadh Environment. Available at: <<https://www.riyadhenv.gov.sa/en/achievement/%d8%a7%d8%b1%d8%aa%d9%81%d8%a7%d8%b9-%d9%85%d9%86%d8%b3%d9%88%d8%a8-%d8%a7%d9%84%d9%85%d9%8a%d8%a7%d9%87/>> [Accessed 16 March 2020].

Riyadh Green, n.d. *Riyadh Four Wellbeing Projects: Enhancing Life*. [online] Riyadhgreen.sa. Available at: <<https://riyadhgreen.sa/en/>> [Accessed 16 April 2021].

Riyadh High Commission for the development of Arriyadh, 2014. *Landscape Plants for Arriyadh Region: A Reference Manual*. Royal Commission for Riyadh City, Riyadh, Saudi Arabia.

Riyadh Municipality, 2015. *Transportation: Our network is designed to drain road water and not what coming from neighboring areas*. Riyadh Municipality Website, Riyadh, Saudi Arabia.

Riyadh Municipality, n.d. *Riyadh Population Development*. Riyadh Municipality, Riyadh, Saudi Arabia.

- Rodier, J. and Roche, M., 1978. Chapter 13: River flow in arid regions. In Herschy, R.W., edr, *Hydrometry: Principles and Practices*, pp. 453-472.
- Rodríguez-Blanco, M.L., Taboada-Castro, M.M. and Taboada-Castro, M.T., 2012. Rainfall–runoff response and event-based runoff coefficients in a humid area (northwest Spain). *Hydrological Sciences Journal*, 57(3), pp.445-459.
- Ropelewski, C.F., and Arkin, P.A., 2019 *Climate Analysis*. Cambridge University Press, Cambridge, UK.
- Rostamian, R., Jaleh, A., Afyuni, M., Mousavi, S.F., Heidarpour, M., Jalalian, A. and Abbaspour, K.C., 2008. Application of a SWAT model for estimating runoff and sediment in two mountainous basins in central Iran. *Hydrological sciences journal*, 53(5), pp.977-988.
- Roy, T., Gupta, H.V., Serrat-Capdevila, A. and Valdes, J.B., 2017. Using satellite-based evapotranspiration estimates to improve the structure of a simple conceptual rainfall–runoff model. *Hydrology and Earth System Sciences*, 21(2), pp.879-896.
- Royal Commission for Riyadh City, 2002. The natural environment of the city of Riyadh. *Tatweer Magazine*, Issue 33
- Royal Commission for Riyadh City, 2006. Rationalizing water consumption: the basis for sustainable development in the desert metropolis. *Tatweer Magazine*, Issue 46, pp. 40-41.
- Royal Commission for Riyadh City, 2018. Adoption of the comprehensive plan for Wadi As Silayy. *Tatweer Magazine*, Issue 79, pp. 10-13.
- Royal Commission for Riyadh City, 2020. Factsheet: Riyadh, Saudi Arabia.
- Safe Drinking Water Foundation, n.d. *Water Consumption — Safe Drinking Water Foundation*. [online] Safe Drinking Water

Foundation. Available at: <<https://www.safewater.org/fact-sheets-1/2017/1/23/water-consumption#:~:text=The%20Safe%20Drinking%20Water%20Foundation's,amount%20of%20water%20to%20use>> [Accessed 28 July 2021].

Saleh, D.K., Kratzer, C.R., Green, C.H. and Evans, D.G., 2009. *Using the soil and water assessment tool (SWAT) to simulate runoff in Mustang Creek Basin, California*. U. S. Geological Survey.

Samimi, M., Mirchi, A., Moriasi, D., Ahn, S., Alian, S., Taghvaeian, S. and Sheng, Z., 2020. Modeling arid/semi-arid irrigated agricultural watersheds with SWAT: Applications, challenges, and solution strategies. *Journal of Hydrology*, 590, p.125418.

Samman, A.E. and Gallus Jr, W.A., 2018. A classification of synoptic patterns inducing heavy precipitation in Saudi Arabia during the period 2000-2014. *Atmósfera*, 31(1), pp.47-67.

Sao, D., Kato, T., Tu, L.H., Thouk, P., Fitriyah, A. and Oeurng, C., 2020. Evaluation of different objective functions used in the sufi-2 calibration process of swat-cup on water balance analysis: A case study of the Pursat river basin, Cambodia. *Water*, 12(10), p.2901.

Sattari, M.T., Rezazadeh-Joudi, A. and Kusiak, A., 2017. Assessment of different methods for estimation of missing data in precipitation studies. *Hydrology Research*, 48(4), pp.1032-1044.

Saudi Geological Survey, 2012. Kingdom of Saudi Arabia: facts and figures. Saudi Geological Survey, Riyadh, Saudi Arabia.

Saudi National Center for Meteorology, n.d. *Infrared Images and Radar Images*. [online] Ncm.gov.sa. Available at: <<https://ncm.gov.sa/Ar/Weather/SatelliteImages/Pages/SatelliteIR.aspx#3>> [Accessed 26 November 2021].

Saudi News, 2013. [Twitter] Al-Suwaidi Tunnel in Riyadh flooded. [image] Available at: <https://twitter.com/saudinews50/status/401884936137113600?lang=ar> (Accessed: 10 January 2020).

- Saudi Press Agency, 2014. *Prince Turki bin Abdullah meets the needs of the residents of Riyadh for water and electricity*. [online] Spa.gov.sa. Available at: <<https://www.spa.gov.sa/1265162>> [Accessed 3 August 2021].
- Schyfsma, E., 1978. *Climate*. In: Al-Sayari, S.S. and Zötl, J.G. eds., 2012. *Quaternary period in Saudi Arabia*. Springer, Vienna.
- Sen, Z. and Al-Suba'i, K., 2002. Hydrological considerations for dam siting in arid regions: a Saudi Arabian study. *Hydrological sciences journal*, 47(2), pp.173-186.
- Sendil, U., Salih, A.M.A. 1987. *Rainfall Frequency Studies for Central Saudi Arabia*. In: Singh, V.P. (eds) *Hydrologic Frequency Modeling*. Springer, Dordrecht.
- Seto, K.C., Güneralp, B. and Hutyrá, L.R., 2012. Global forecasts of urban expansion to 2030 and direct impacts on biodiversity and carbon pools. *Proceedings of the National Academy of Sciences*, 109(40), pp.16083-16088.
- Shah, S., Duan, Z., Song, X., Li, R., Mao, H., Liu, J., Ma, T. and Wang, M., 2021. Evaluating the added value of multi-variable calibration of SWAT with remotely sensed evapotranspiration data for improving hydrological modeling. *Journal of Hydrology*, 603, p.127046.
- Sharif, H. O., Al-Juaidi, F. H., Al-Othman, A., Al-Dousary, I., Fadda, E., Jamal-Uddeen, S. and Elhassan, A., 2016. Flood hazards in an urbanizing watershed in Riyadh, Saudi Arabia, *Geomatics, Natural Hazards and Risk*, Vol. 7:2, pp. 702-720.
- Shivhare, N., Dikshit, P.K.S. and Dwivedi, S.B., 2018. A comparison of SWAT model calibration techniques for hydrological modeling in the Ganga river watershed. *Engineering*, 4(5), pp.643-652.
- Shukla, S. and Gedam, S., 2018. Assessing the impacts of urbanization on hydrological processes in a semi-arid river basin of Maharashtra, India. *Modeling Earth Systems and Environment*, 4(2), pp.699-728.

- Shukla, S. and Gedam, S., 2019. Evaluating hydrological responses to urbanization in a tropical river basin: A water resources management perspective. *Natural Resources Research*, 28(2), pp.327-347.
- Singh, V.V., Sharma, A. and Joshi, P.C., 2015. Modelling of runoff response in a semi-arid coastal watershed using SWAT. *International Journal of Engineering Research and Applications*. Vol, 5, pp.50-57.
- Sirisena, T.J.G., Maskey, S. and Ranasinghe, R., 2020. Hydrological model calibration with streamflow and remote sensing based evapotranspiration data in a data poor basin. *Remote sensing*, 12(22), p.3768.
- Small, R. J. and Clark, M. J., 1982. Slopes and Weathering, Cambridge University Press, Cambridge.
- Srinivas, J.S., Kumar, T.K.S. and Reshma, T., 2016. Simulation of runoff for an experimental watershed using SWAT. *Int J Technol Res Appl*, 4, pp.364-369.
- Subyani, A.M. and Hajjar, A.F., 2016. Rainfall analysis in the contest of climate change for Jeddah area, Western Saudi Arabia. *Arabian Journal of Geosciences*, 9(2), pp.1-15.
- Subyani, A.M., 2004. Geostatistical study of annual and seasonal mean rainfall patterns in southwest Saudi Arabia/Distribution géostatistique de la pluie moyenne annuelle et saisonnière dans le Sud-Ouest de l'Arabie Saoudite. *Hydrological Sciences Journal*, 49(5).
- Subyani, A.M. and Al-Amri, N.S., 2015. IDF curves and daily rainfall generation for Al-Madinah city, western Saudi Arabia. *Arabian Journal of Geosciences*, 8(12), pp.11107-11119.
- Sudheer, K.P., Chaubey, I., Garg, V. and Migliaccio, K.W., 2007. Impact of time-scale of the calibration objective function on the performance of watershed models. *Hydrological Processes: An International Journal*, 21(25), pp.3409-3419.

- Suliman, A.H.A., Jajarmizadeh, M., Harun, S. and Mat Darus, I.Z., 2015. Comparison of semi-distributed, GIS-based hydrological models for the prediction of streamflow in a large catchment. *Water resources management*, 29(9), pp.3095-3110.
- Sultan, M., Sefry, S., AbuAbdallah, M., 2015. Impacts of Climate Change on the Red Sea Region and its Watersheds, Saudi Arabia. In: Rasul, N., Stewart, I. (eds) *The Red Sea*. Springer Earth System Sciences. Springer, Berlin, Heidelberg
- Sultana, R. and Nasrollahi, N., 2018. Evaluation of remote sensing precipitation estimates over Saudi Arabia. *Journal of Arid Environments*, 151, pp.90-103.
- Sun, Z., Guo, H., Li, X., Huang, Q. and Zhang, D., 2011, May. Effect of LULC change on surface runoff in urbanization area. In *Proceedings of the ASPRS 2011 Annual Conference, Milwaukee, Wisconsin, May* (Vol. 1, No. 5).
- SWAT Literature Database, n.d. *SWAT Literature Database for Peer-Reviewed Journal Articles*. [online] Card.iastate.edu. Available at: <https://www.card.iastate.edu/swat_articles/> [Accessed 29 November 2021].
- SWAT, n.d.a. *Global Data*. [online] Swat.tamu.edu. Available at: <<https://swat.tamu.edu/data/>> [Accessed 11 February 2019].
- SWAT, n.d.b. *SWAT | Soil & Water Assessment Tool*. [online] Swat.tamu.edu. Available at: <<https://swat.tamu.edu/>> [Accessed 11 February 2019].
- Taghvaye Salimi, E., Nohegar, A., Malekian, A., Hosseini, M. and Holisaz, A., 2016. Runoff simulation using SWAT model and SUFI-2 algorithm (Case study: Shafaroud watershed, Guilan Province, Iran). *Caspian Journal of Environmental Sciences*, 14(1), pp.69-80.
- Tahir Hussein, M., Awad, H., Allafouza, O. and Al Ahmadi, F., 2009. Assessing elements of surface hydrology for environmental quality characterisation of a site northwest of Riyadh, Saudi

Arabia. *Management of Environmental Quality: An International Journal*.

- Talebi, A., Zahedi, E., Hassan, M.A. and Lesani, M.T., 2019. Locating suitable sites for the construction of underground dams using the subsurface flow simulation (SWAT model) and analytical network process (ANP)(case study: Daroongar watershed, Iran). *Sustainable water resources management*, 5(3), pp.1369-1378.
- Tanksali, A. and Soraganvi, V.S., 2021. Assessment of impacts of land use/land cover changes upstream of a dam in a semi-arid watershed using QSWAT. *Modeling Earth Systems and Environment*, 7(4), pp.2391-2406.
- Tapia-Arenas, C.A., Feger, K.H. and Julich, S., 2020. Remote sensing data for calibrating hydrologic modeling: Hydrological impacts of land use change of the Reventado river sub-basin, Costa Rica. *Revista Forestal Mesoamericana Kurú*, 17(41), pp.16-28.
- Tegegne, G., Park, D.K. and Kim, Y.O., 2017. Comparison of hydrological models for the assessment of water resources in a data-scarce region, the Upper Blue Nile River Basin. *Journal of Hydrology: Regional Studies*, 14, pp.49-66.
- Tekeli, A.E. and Fouli, H., 2016. Evaluation of TRMM satellite-based precipitation indexes for flood forecasting over Riyadh City, Saudi Arabia. *Journal of Hydrology*, 541, pp.471-479.
- Thomas, J. 2011. Plant Diversity in Saudi Arabia: an introduction. The Website of Dr. Jacob Thomas, Herbarium (KSU), Dept. of Botany & Microbiology, King Saud University, Riyadh.
- Tian, F., Lü, Y.H., Fu, B.J., Yang, Y.H., Qiu, G., Zang, C. and Zhang, L., 2016. Effects of ecological engineering on water balance under two different vegetation scenarios in the Qilian Mountain, northwestern China. *Journal of Hydrology: Regional Studies*, 5, pp.324-335.
- Toosi, A.S., Doulabian, S., Tousi, E.G., Calbimonte, G.H. and Alaghmand, S., 2020. Large-scale flood hazard assessment

under climate change: A case study. *Ecological Engineering*, 147, p.105765.

Trottier, J. and Wensley, D., 2015. Wadi Hanifah - Urban Landscape Infrastructure for the 21st Century.

Tsvieli, Y. and Zangvil, A., 2005. Synoptic climatological analysis of 'wet' and 'dry' Red Sea troughs over Israel. *International Journal of Climatology: A Journal of the Royal Meteorological Society*, 25(15), pp.1997-2015.

US Army Corps of Engineers, n.d. *HEC-RAS Hydraulic Reference Manual*. Version 6.2, [online] US Army Corps of Engineers Website. Available at: <<https://www.hec.usace.army.mil/confluence/rasdocs/ras1dtechref/latest/performing-a-dam-break-study-with-hec-ras/computational-time-step>> [Accessed 29 September 2022].

US National Weather Service, n.d. *NWS JetStream - NWS Radar Images: Reflectivity*. [online] Weather.gov. Available at: <<https://www.weather.gov/jetstream/refl#:~:text=The%20color>> [Accessed 22 December 2021].

USDA ARS, 2018. *SWAT - Soil and Water Assessment Tool*. [online] Available at: <<https://data.nal.usda.gov/dataset/swat-soil-and-water-assessment-tool>> [Accessed 16 November 2019].

USDA, 1975. *Soil Taxonomy: A Basic System of Soil Classification for Making and Interpreting Soil Surveys*. Soil Conservation Service, United States Department of Agriculture, Agricultural Handbook No. 436.

USDA, 1986. *Urban Hydrology for Small Watersheds TR-55*. Conservation Engineering Division, United States Department of Agriculture.

USDA, 2007. *Stream Restoration Design*, Natural Resources Conservation Service, United States Department of Agriculture, USA.

USGS, n.d. *What is a percentile? – USGS Water Data for the Nation Help System*. [online] waterdata.usgs.gov. Available at: <<https://help.waterdata.usgs.gov/faq/surface-water/what-is-a-percentile>> [Accessed 12 June 2021].

Uuemaa, E., Ahi, S., Montibeller, B., Muru, M. and Kmoch, A., 2020. Vertical accuracy of freely available global digital elevation models (ASTER, AW3D30, MERIT, TanDEM-X, SRTM, and NASADEM). *Remote Sensing*, 12(21), p.3482.

Verma, N., 2016. Simulation of hydrologic processes through SWAT and MODIS ET for Sirsa River Basin in Western Himalaya. Proceedings of 7th International Conference on Water Resources and Arid Environments (ICWRAE 7) 4-6 December 2016, Riyadh, Saudi Arabia, pp. 629-643.

Vision 2030, n.d. *Green Riyadh*. [online] Vision 2030. Available at: <<https://www.vision2030.gov.sa/v2030/v2030-projects/green-riyadh/>> [Accessed 29 September 2022].

Wang, X., Melesse, A.M. and Yang, W., 2006. Influences of potential evapotranspiration estimation methods on SWAT's hydrologic simulation in a northwestern Minnesota watershed. *Transactions of the ASABE*, 49(6), pp.1755-1771.

Warner, T.T., 2004. *Desert Meteorology*. Cambridge University Press.

Water Science School, 2019. *Surface Runoff and the Water Cycle | U.S. Geological Survey*. [online] Usgs.gov. Available at: <<https://www.usgs.gov/special-topics/water-science-school/science/surface-runoff-and-water-cycle>> [Accessed 16 June 2021].

Welderufael, W.A., Woyessa, Y.E. and Edossa, D.C., 2013. Impact of rainwater harvesting on water resources of the modder river basin, central region of South Africa. *Agricultural water management*, 116, pp.218-227.

Wheater, H.S., 2008. G-WADI – UNESCO's Global Network for Water and Development Information for Arid Lands. In: Lee, C., Schaaf, T. (eds) *The Future of Drylands*. Springer, Dordrecht.

- Wheater, H.S., and Al-Weshah, R.A., 2002. Hydrology of wadi systems. HP-V, Technical Documents in Hydrology, No. 55, UNESCO, Paris.
- Wheater, H.S., Butler, A.P., Stewart, E.J. and Hamilton, G.S., 1991. A multivariate spatial-temporal model of rainfall in southwest Saudi Arabia. I. Spatial rainfall characteristics and model formulation. *Journal of Hydrology*, 125(3-4), pp.175-199.
- WMO, 2008. Guide to Hydrological Practices–Volume I: Hydrology–From Measurements to Hydrological Information (WMO-No. 168).
- Wu, H., Chen, B. and Li, P., 2013. Comparison of Sequential Uncertainty Fitting Algorithm (SUFI-2) and Parameter Solution (ParaSol) Method for Analyzing Uncertainties in Distributed Hydrological Modeling–A Case Study. *GEN*, 309, p.1.
- Wüstemann, H. and Kalisch, D., 2016. *Towards a national indicator for urban green space provision and environmental inequalities in Germany: Method and findings* (No. 2016-022). SFB 649 Discussion Paper.
- Xu, Z.X., Pang, J.P., Liu, C.M. and Li, J.Y., 2009. Assessment of runoff and sediment yield in the Miyun Reservoir catchment by using SWAT model. *Hydrological Processes: An International Journal*, 23(25), pp.3619-3630.
- Xue, L., Yang, F., Yang, C., Wei, G., Li, W. and He, X., 2018. Hydrological simulation and uncertainty analysis using the improved TOPMODEL in the arid Manas River basin, China. *Scientific reports*, 8(1), pp.1-12.
- Yan, Y., Xue, B., Sun, W. and Zhang, H., 2020. Quantification of climate change and land cover/use transition impacts on runoff variations in the upper Hailar Basin, NE China. *Hydrology Research*, 51(5), pp.976-993.
- Yanbuweather, n.d. *Rain Radar*. [online] Available at: <<https://www.yanbuweather.com/pages/RainRadar/>> [Accessed 29 November 2020].

- Yao, L., Chen, L., Wei, W. and Sun, R., 2015. Potential reduction in urban runoff by green spaces in Beijing: A scenario analysis. *Urban Forestry & Urban Greening*, 14(2), pp.300-308.
- Yin, J., He, F., Xiong, Y.J. and Qiu, G.Y., 2017. Effects of land use/land cover and climate changes on surface runoff in a semi-humid and semi-arid transition zone in northwest China. *Hydrology and Earth System Sciences*, 21(1), pp.183-196.
- Youssef, A.M., Sefry, S.A., Pradhan, B. and Alfadail, E.A., 2015. Analysis on causes of flash flood in Jeddah city (Kingdom of Saudi Arabia) of 2009 and 2011 using multi-sensor remote sensing data and GIS. *Geomatics, Natural Hazards and Risk*, 7(3), pp.1018-1042.
- Yuan, L. and Forshay, K.J., 2019. Using SWAT to evaluate streamflow and lake sediment loading in the Xinjiang River Basin with limited data. *Water*, 12(1), p.39.
- Yuan, Y., W. Nie, and E. Sanders, 2014. Problems and Prospects of SWAT Model Application on an Arid/Semi-arid Watershed in Arizona. Presented at SEDHYD 2014 Joint Conference, Reno, NV, March 23 - 27, 2014.
- Zende, A.M. and Nagarajan, R., 2015. Sediment Yield Estimate of River Basin Using SWAT Model in Semi-arid Region of Peninsular India. In: Lollino, G., Arattano, M., Rinaldi, M., Giustolisi, O., Marechal, J.C., Grant, G. (eds) *Engineering Geology for Society and Territory - Volume 3*. Springer, Cham.
- Zettam, A., Taleb, A., Sauvage, S., Boithias, L., Belaidi, N. and Sánchez-Pérez, J.M., 2017. Modelling hydrology and sediment transport in a semi-arid and anthropized catchment using the SWAT model: The case of the Tafna river (northwest Algeria). *Water*, 9(3), p.216.
- Zhang, B., Li, N. and Wang, S., 2015a. Effect of urban green space changes on the role of rainwater runoff reduction in Beijing, China. *Landscape and Urban Planning*, 140, pp.8-16.

- Zhang, L., Jin, X., He, C., Zhang, B., Zhang, X., Li, J., Zhao, C., Tian, J. and DeMarchi, C., 2016a. Comparison of SWAT and DLBRM for hydrological modeling of a mountainous watershed in arid northwest China. *Journal of Hydrologic Engineering*, 21(5), p.04016007.
- Zhang, L., Nan, Z., Xu, Y. and Li, S., 2016b. Hydrological impacts of land use change and climate variability in the headwater region of the Heihe River Basin, Northwest China. *PloS one*, 11(6), p.e0158394.
- Zhang, L., Nan, Z., Yu, W. and Ge, Y., 2015b. Modeling land-use and land-cover change and hydrological responses under consistent climate change scenarios in the Heihe River Basin, China. *Water Resources Management*, 29(13), pp.4701-4717.
- Zhang, S., Wu, Y., Sivakumar, B., Mu, X., Zhao, F., Sun, P., Sun, Y., Qiu, L., Chen, J., Meng, X. and Han, J., 2019. Climate change-induced drought evolution over the past 50 years in the southern Chinese Loess Plateau. *Environmental Modelling & Software*, 122, p.104519.
- Zhang, Y., Zhang, L., Hou, J., Gu, J. and Huang, C., 2017. Development of an evapotranspiration data assimilation technique for streamflow estimates: a case study in a semi-arid region. *Sustainability*, 9(10), p.1658.
- Zheng, Q., Hao, L., Huang, X., Sun, L. and Sun, G., 2020. Effects of urbanization on watershed evapotranspiration and its components in southern China. *Water*, 12(3), p.645.
- Zhou, Q., 2017. Digital elevation model and digital surface model. *International Encyclopedia of Geography: People, the Earth, Environment and Technology*, pp.1-17.
- Zhou, Q., Lees, B. and Tang, G.A. eds., 2008. *Advances in digital terrain analysis*. Springer Science & Business Media.
- Zhu, C. and Li, Y., 2014. Long-term hydrological impacts of land use/land cover change from 1984 to 2010 in the Little River Watershed, Tennessee. *International Soil and Water Conservation Research*, 2(2), pp.11-21.

- Zoccatelli, D., Marra, F., Armon, M., Rinat, Y., Smith, J.A. and Morin, E., 2019. Contrasting rainfall-runoff characteristics of floods in desert and Mediterranean basins. *Hydrology and Earth System Sciences*, 23(6), pp.2665-2678.
- Zou, M., Niu, J., Kang, S., Li, X. and Lu, H., 2017. The contribution of human agricultural activities to increasing evapotranspiration is significantly greater than climate change effect over Heihe agricultural region. *Scientific reports*, 7(1), pp.1-14.
- Zou, S., Ruan, H., Lu, Z., Yang, D., Xiong, Z. and Yin, Z., 2016. Runoff simulation in the upper reaches of Heihe River basin based on the RIEMS-SWAT model. *Water*, 8(10), p.455.

Appendix A

Initial sensitivity analysis results

Initial sensitivity analysis of the Wadi Hanifah catchment (runs from 38 parameters to 11 parameters)

Parameter Name	38		32		29		26		23		21		19		14		11	
	Rank	P-Value																
CN2.mgt	1	2E-129	1	3E-126	2	8E-127	1	1E-132	1	8E-121	1	1E-123	1	6E-129	1	5E-127	1	2E-127
ESCO.hru	2	2E-103	2	2E-123	1	5E-130	2	4E-120	2	9E-111	2	3E-113	2	1E-105	2	6E-99	2	3E-116
SOL_Z(..).sol	3	1E-44	3	9E-59	3	3E-62	4	4E-45	3	2E-48	3	2E-49	3	3E-52	3	4E-61	3	4E-58
ICN.bsn	4	2E-41	4	8E-44	4	1E-43	3	4E-46	4	1E-40	4	5E-41	4	5E-46	4	1E-43	4	3E-44
SOL_K(..).sol	5	1E-09	6	5E-07	7	4E-06	5	2E-11	7	0.0002	7	3E-04	5	1E-06	6	1E-05	7	0.0007
SOL_BD(..).sol	6	2E-09	5	2E-11	5	1E-07	6	6E-07	5	3E-07	5	5E-06	6	6E-05	5	8E-10	5	3E-05
SOL_AWC(..).sol	7	8E-06	7	3E-06	6	4E-06	8	0.0001	9	0.0098	9	0.013	7	0.0004	8	0.01	8	0.0084
EPCO.hru	8	0.005	8	8E-05	8	0.0006	10	0.0016	17	0.4755	18	0.394	14	0.6418	7	0.001	9	0.01
SOL_CRK.sol	9	0.018	32	0.894														
ESCO.bsn	10	0.023	18	0.385	11	0.0407	18	0.5257	16	0.3981	17	0.336	12	0.5922	12	0.571		
SLSOIL.hru	11	0.041	11	0.028	14	0.0895	23	0.752	22	0.823								
CNCOEF.bsn	12	0.06	9	0.009	9	0.0014	13	0.0628	8	0.002	8	0.001	9	0.1165	10	0.014	6	0.0004
GW_REVAP.gw	13	0.177	16	0.27	28	0.6668												
SLSUBBSN.hru	14	0.196	23	0.477	19	0.3195	11	0.0171	11	0.0468	11	0.056	19	0.9986				
CANMX.hru	15	0.235	17	0.365	18	0.2979	7	2E-05	6	4E-05	6	2E-05	15	0.8419				
GSI{..}.plant.dat	16	0.238	29	0.738	17	0.2316	24	0.8134										
SURLAG.bsn	17	0.392	21	0.44	27	0.6496												
CH_L1.sub	18	0.427	24	0.482	21	0.3366	14	0.132	13	0.1529	14	0.195	16	0.9523				
CNOP{..}.mgt	19	0.455	13	0.058	15	0.0952	19	0.5531	19	0.6149	19	0.533	11	0.1683	14	0.807		
WUDEEP(..).wus	20	0.488	26	0.574	16	0.1799	20	0.6586	23	0.9096								
BLAI{..}.plant.dat	21	0.488	28	0.723	26	0.5999												
ALAI_MIN{..}.plant.dat	22	0.519	22	0.467	29	0.6818	25	0.8504										
SHALLST.gw	23	0.556	12	0.051	25	0.5125	17	0.3343	12	0.1246	12	0.068	10	0.1402	13	0.705		

Initial sensitivity analysis of the Wadi Hanifah catchment (runs from 38 parameters to 11 parameters) (Continued)

Parameter Name	38		32		29		26		23		21		19		14		11	
	Rank	P-Value																
CH_N1.sub	24	0.576	30	0.814														
OV_N.hru	25	0.65	14	0.12	23	0.4088	26	0.9792										
DEEPST.gw	26	0.652	27	0.625	20	0.3308	12	0.035	14	0.2379	13	0.092	8	0.0458	9	0.013	11	0.7369
WUSHAL(..).wus	27	0.656	20	0.421	22	0.3743	22	0.7321	18	0.5994	16	0.326	18	0.9834				
SOL_ALB(..).sol	28	0.703	10	0.021	10	0.0052	21	0.693	20	0.7271	21	0.702						
EPCO.bsn	29	0.705	19	0.398	24	0.5019	9	0.0008	10	0.0225	10	0.02	17	0.9674				
CNOP{..}.mgt	30	0.712	15	0.243	12	0.0433	15	0.1494	21	0.7278	20	0.686						
GW_DELAY.gw	31	0.738	25	0.497	13	0.082	16	0.2738	15	0.3817	15	0.271	13	0.6376	11	0.117	10	0.0606
RCHRG_DP.gw	32	0.789	31	0.867														
CNOP{..}.mgt	33	0.854																
CH_S1.sub	34	0.861																
REVAPMN.gw	35	0.861																
ALPHA_BF.gw	36	0.886																
FFCB.bsn	37	0.93																
GWQMN.gw	38	0.97																

Initial sensitivity analysis of the Wadi As Silayy catchment (runs from 38 parameters to 13 parameters).

Parameter Name	38		32		29		22		20		18		16		13	
	Rank	P-Value														
SOL_Z(..).sol	1	0	32	0	1	0	1	0	1	7E-306	1	0	1	0	1	0
ESCO.hru	2	1E-112	31	8E-124	2	1E-111	2	3E-104	2	9E-94	2	4E-122	2	2E-122	2	9E-103
SOL_AWC(..).sol	3	2E-112	30	2E-89	25	0.8898	3	6E-86	3	2E-71	3	5E-100	3	3E-100	3	4E-91
CN2.mgt	4	4E-33	29	2E-27	4	8E-28	4	2E-30	4	8E-38	4	4E-28	4	3E-28	4	2E-30
ICN.bsn	5	1E-14	28	2E-11	5	9E-10	5	5E-13	5	3E-11	5	1E-11	5	1E-11	5	2E-13
SOL_K(..).sol	6	0.0034	18	0.2896												
ESCO.bsn	7	0.041	16	0.3591	17	0.5706	13	0.2438	20	0.8743						
CNOP{..}.mgt	8	0.053	15	0.3739	11	0.4433	8	0.0664	12	0.3149	9	0.0788	9	0.0769	9	0.3246
SLSOIL.hru	9	0.068	24	0.0582	24	0.8736										
GW_REVAP.gw	10	0.0845	17	0.2964	12	0.452	16	0.4394	17	0.4619	11	0.2426	11	0.2431	12	0.7106
SOL_ALB(..).sol	11	0.1264	9	0.4754	3	1E-87	9	0.1177	16	0.3686	12	0.3504	12	0.3282	6	0.03
SURLAG.bsn	12	0.1693	14	0.4265	28	0.9603										
GWQMN.gw	13	0.1979	10	0.4502	22	0.7552	12	0.22	10	0.2476	18	0.9966				
CNOP{..}.mgt	14	0.1998	20	0.1641	14	0.5464	18	0.6211	14	0.3554	10	0.236	10	0.2308	13	0.8667
CNOP{..}.mgt	15	0.2097	26	0.0318	18	0.6634	22	0.9727								
SHALLST.gw	16	0.2608	23	0.1303	19	0.6832	15	0.3575	7	0.113	14	0.6216	13	0.5955	8	0.2758
CH_N1.sub	17	0.2732	11	0.4425	6	0.1641	20	0.687	18	0.6301	8	0.0509	8	0.0476	11	0.6492
ALPHA_BF.gw	18	0.2768	6	0.5043	20	0.702	7	0.0197	13	0.3474	13	0.5493	16	0.9903		
CANMX.hru	19	0.3566	25	0.0513	16	0.5647	10	0.1718	6	0.0976	6	0.0012	6	0.0011	7	0.1086
GSI{..}.plant.dat	20	0.3774	7	0.5014	26	0.9019										
SOL_BD(..).sol	21	0.3801	27	0.0242	29	0.9783										

Initial sensitivity analysis of the Wadi As Silayy catchment (runs from 38 parameters to 13 parameters.
(Continued)

Parameter Name	38		32		29		22		20		18		16		13	
	Rank	P-Value														
REVAPMN.gw	22	0.399	19	0.254	23	0.8624										
WUDEEP(..).wus	23	0.4107	4	0.7318	13	0.4817	14	0.2933	8	0.1268	17	0.8113				
CNCOEF.bsn	24	0.4496	2	0.8483												
SOL_CRK.sol	25	0.4791	21	0.1557	27	0.9096										
FFCB.bsn	26	0.5423	8	0.4886	7	0.2743	6	0.0013	19	0.7795						
SLSUBBSN.hru	27	0.5662	1	0.9312	10	0.399										
RCHRG_DP.gw	28	0.6412	3	0.8081												
OV_N.hru	29	0.6781	12	0.4424	15	0.5505	21	0.7059								
EPCO.hru	30	0.7462	5	0.5977	21	0.7038	19	0.6353	15	0.3684	16	0.6896	14	0.6689		
BLAI{..}.plant.dat	31	0.7567	13	0.4406	8	0.3221	17	0.559	11	0.2859	15	0.6341	15	0.7876		
CH_L1.sub	32	0.7962	22	0.1321	9	0.3598	11	0.1847	9	0.1501	7	0.0029	7	0.0031	10	0.5262
EPCO.bsn	33	0.8297														
WUSHAL(..).wus	34	0.8333														
ALAI_MIN{..}.plant.dat	35	0.917														
GW_DELAY.gw	36	0.9495														
DEEPST.gw	37	0.9639														
CH_S1.sub	38	0.9671														

Statistical results of model performance indices of the initial sensitivity analysis for the Wadi Hanifah catchment.

ID	Parameters	NSE	R ²	PBIAS	RSR
1	38	0.51	0.63	41.89	0.7
2	32	0.49	0.61	42.92	0.71
3	29	0.48	0.57	37.59	0.72
4	26	0.47	0.57	38.34	0.73
5	23	0.49	0.6	41.51	0.71
6	21	0.49	0.6	41.49	0.71
7	19	0.48	0.59	40.56	0.72
8	14	0.47	0.58	41.17	0.73
9	11	0.48	0.57	38.09	0.72

Statistical results of model performance indices of the initial sensitivity analysis for the Wadi As Silayy catchment.

ID	Parameters	NSE	R ²	PBIAS	RSR
1	38	0.63	0.65	13.65	0.61
2	32	0.62	0.66	18.98	0.62
3	29	0.61	0.66	22.06	0.62
4	22	0.59	0.61	15.88	0.64
5	20	0.59	0.62	20.47	0.65
6	18	0.59	0.65	23.27	0.64
7	16	0.59	0.65	23.27	0.64
8	13	0.6	0.62	17.16	0.64

Appendix B

Simulated average monthly runoff and discharge under five different historical LULC scenarios.

Average monthly runoff (mm) under five different historical LULC scenarios for the Wadi Hanifah catchment.

Month	LULC	1	2	3	4	5	6	7	8	9	10	11	12	13	14	15	16	17	18	19	20	21	22
Jan	LULC 1996	0.0	0.0	0.1	0.0	0.0	0.2	0.0	0.0	0.3	1.4	0.0	0.5	1.3	2.1	4.0	0.6	0.6	4.4	2.7	1.9	0.3	0.0
	LULC 2004	0.0	0.0	0.2	0.0	0.0	0.7	0.0	0.0	0.5	1.8	0.0	0.4	2.9	2.6	4.3	0.8	0.9	4.5	3.1	2.0	0.5	0.2
	LULC 2009	0.0	0.0	0.0	0.0	0.0	0.7	0.0	0.0	0.6	2.2	0.0	0.5	2.2	3.2	4.7	1.0	1.1	5.0	3.4	2.4	0.7	0.2
	LULC 2012	0.0	0.0	0.0	0.0	0.0	0.7	0.0	0.0	0.7	2.5	0.3	0.9	2.4	3.6	4.7	1.1	1.2	5.1	3.5	2.7	0.8	0.3
	LULC 2016	0.0	0.0	0.2	0.0	0.1	0.7	0.0	0.0	0.7	2.6	0.3	1.1	3.4	4.2	4.7	1.1	1.5	5.5	3.5	3.2	1.2	0.8
Feb	LULC 1996	0.0	0.0	0.0	0.0	0.0	0.0	0.0	0.0	0.0	0.2	0.0	0.1	0.2	0.4	0.6	0.1	0.1	1.2	0.5	0.4	0.0	0.0
	LULC 2004	0.0	0.0	0.0	0.0	0.0	0.1	0.0	0.0	0.1	0.3	0.0	0.1	0.5	0.5	0.7	0.1	0.1	1.2	0.5	0.4	0.1	0.0
	LULC 2009	0.0	0.0	0.0	0.0	0.0	0.1	0.0	0.0	0.1	0.4	0.0	0.1	0.4	0.8	0.8	0.2	0.2	1.5	0.6	0.5	0.1	0.0
	LULC 2012	0.0	0.0	0.0	0.0	0.0	0.1	0.0	0.0	0.1	0.4	0.0	0.2	0.4	0.9	0.8	0.2	0.2	1.5	0.6	0.6	0.1	0.0
	LULC 2016	0.0	0.0	0.0	0.0	0.0	0.1	0.0	0.0	0.1	0.4	0.1	0.2	0.6	0.6	0.8	0.2	0.2	0.8	1.1	0.5	0.2	0.1

Average monthly runoff (mm) under five different historical LULC scenarios for the Wadi Hanifah catchment.
(Continued)

Month	LULC	1	2	3	4	5	6	7	8	9	10	11	12	13	14	15	16	17	18	19	20	21	22
Mar	LULC 1996	0.0	0.0	0.2	0.0	0.0	0.4	0.0	0.0	0.5	2.5	0.0	0.8	2.3	3.4	6.2	1.0	1.1	6.5	4.1	2.7	0.5	0.0
	LULC 2004	0.0	0.0	0.3	0.0	0.0	1.2	0.0	0.0	0.9	3.1	0.0	0.7	5.0	4.1	6.6	1.4	1.5	6.6	4.6	2.9	0.8	0.3
	LULC 2009	0.0	0.0	0.1	0.0	0.0	1.1	0.0	0.0	1.1	3.9	0.0	0.9	3.8	4.8	7.1	1.7	1.9	7.2	5.0	3.3	1.0	0.3
	LULC 2012	0.0	0.0	0.1	0.0	0.0	1.2	0.0	0.0	1.2	4.4	0.4	1.5	4.2	5.4	7.1	1.8	2.1	7.3	5.2	3.8	1.2	0.5
	LULC 2016	0.0	0.0	0.3	0.0	0.1	1.1	0.0	0.0	1.3	4.5	0.6	1.8	5.7	7.4	7.1	2.0	2.5	9.8	4.2	4.8	1.9	1.2
Apr	LULC 1996	0.0	0.0	0.1	0.0	0.0	0.2	0.0	0.0	0.2	1.6	0.0	0.5	1.4	2.3	4.3	0.6	0.7	5.3	2.9	2.0	0.4	0.0
	LULC 2004	0.0	0.0	0.1	0.0	0.0	0.7	0.0	0.0	0.4	1.9	0.0	0.5	3.1	2.9	4.6	0.9	0.9	5.4	3.3	2.2	0.5	0.2
	LULC 2009	0.0	0.0	0.0	0.0	0.0	0.6	0.0	0.0	0.5	2.4	0.0	0.6	2.4	3.8	5.1	1.1	1.2	6.2	3.7	2.6	0.7	0.2
	LULC 2012	0.0	0.0	0.0	0.0	0.0	0.6	0.0	0.0	0.6	2.7	0.3	1.0	2.6	4.3	5.0	1.1	1.3	6.3	3.7	3.0	0.8	0.3
	LULC 2016	0.0	0.0	0.2	0.0	0.1	0.7	0.0	0.0	0.6	2.8	0.4	1.2	3.6	4.6	5.0	1.2	1.6	6.1	3.9	3.4	1.3	0.8

Average monthly runoff (mm) under five different historical LULC scenarios for the Wadi Hanifah catchment.
(Continued)

Month	LULC	1	2	3	4	5	6	7	8	9	10	11	12	13	14	15	16	17	18	19	20	21	22
May	LULC 1996	0.0	0.0	0.0	0.0	0.0	0.0	0.0	0.0	0.0	0.4	0.0	0.1	0.4	1.6	1.4	0.1	0.2	4.1	1.0	0.8	0.1	0.0
	LULC 2004	0.0	0.0	0.0	0.0	0.0	0.1	0.0	0.0	0.0	0.5	0.0	0.1	0.8	2.1	1.5	0.2	0.2	4.3	1.2	0.9	0.1	0.0
	LULC 2009	0.0	0.0	0.0	0.0	0.0	0.1	0.0	0.0	0.0	0.6	0.0	0.1	0.7	3.0	1.8	0.3	0.3	5.1	1.4	1.2	0.2	0.0
	LULC 2012	0.0	0.0	0.0	0.0	0.0	0.1	0.0	0.0	0.0	0.7	0.1	0.3	0.7	3.3	1.7	0.3	0.4	5.0	1.4	1.4	0.2	0.1
	LULC 2016	0.0	0.0	0.0	0.0	0.0	0.2	0.0	0.0	0.0	0.7	0.1	0.4	1.1	2.6	1.9	0.3	0.4	3.5	2.5	1.1	0.4	0.2
Jun	LULC 1996	0.0	0.0	0.0	0.0	0.0	0.0	0.0	0.0	0.0	0.0	0.0	0.0	0.0	0.1	0.0	0.0	0.0	0.4	0.0	0.0	0.0	0.0
	LULC 2004	0.0	0.0	0.0	0.0	0.0	0.0	0.0	0.0	0.0	0.0	0.0	0.0	0.0	0.1	0.0	0.0	0.0	0.5	0.0	0.0	0.0	0.0
	LULC 2009	0.0	0.0	0.0	0.0	0.0	0.0	0.0	0.0	0.0	0.0	0.0	0.0	0.0	0.3	0.0	0.0	0.0	0.7	0.0	0.0	0.0	0.0
	LULC 2012	0.0	0.0	0.0	0.0	0.0	0.0	0.0	0.0	0.0	0.0	0.0	0.0	0.0	0.3	0.0	0.0	0.0	0.7	0.0	0.0	0.0	0.0
	LULC 2016	0.0	0.0	0.0	0.0	0.0	0.0	0.0	0.0	0.0	0.0	0.0	0.0	0.0	0.1	0.0	0.0	0.0	0.1	0.2	0.0	0.0	0.0

Average monthly runoff (mm) under five different historical LULC scenarios for the Wadi Hanifah catchment.
(Continued)

Month	LULC	1	2	3	4	5	6	7	8	9	10	11	12	13	14	15	16	17	18	19	20	21	22	
Jul	LULC 1996	0.0	0.0	0.0	0.0	0.0	0.0	0.0	0.0	0.0	0.0	0.0	0.0	0.0	0.0	0.0	0.0	0.0	0.0	0.0	0.0	0.0	0.0	
	LULC 2004	0.0	0.0	0.0	0.0	0.0	0.0	0.0	0.0	0.0	0.0	0.0	0.0	0.0	0.0	0.0	0.0	0.0	0.0	0.0	0.0	0.0	0.0	
	LULC 2009	0.0	0.0	0.0	0.0	0.0	0.0	0.0	0.0	0.0	0.0	0.0	0.0	0.0	0.0	0.0	0.0	0.0	0.0	0.1	0.0	0.0	0.0	0.0
	LULC 2012	0.0	0.0	0.0	0.0	0.0	0.0	0.0	0.0	0.0	0.0	0.0	0.0	0.0	0.0	0.0	0.0	0.0	0.0	0.1	0.0	0.0	0.0	0.0
	LULC 2016	0.0	0.0	0.0	0.0	0.0	0.0	0.0	0.0	0.0	0.0	0.0	0.0	0.0	0.0	0.0	0.0	0.0	0.0	0.0	0.0	0.0	0.0	0.0
Aug	LULC 1996	0.0	0.0	0.0	0.0	0.0	0.0	0.0	0.0	0.0	0.0	0.0	0.0	0.0	0.0	0.0	0.0	0.0	0.0	0.0	0.0	0.0	0.0	0.0
	LULC 2004	0.0	0.0	0.0	0.0	0.0	0.0	0.0	0.0	0.0	0.0	0.0	0.0	0.0	0.0	0.0	0.0	0.0	0.0	0.0	0.0	0.0	0.0	0.0
	LULC 2009	0.0	0.0	0.0	0.0	0.0	0.0	0.0	0.0	0.0	0.0	0.0	0.0	0.0	0.0	0.0	0.0	0.0	0.0	0.1	0.0	0.0	0.0	0.0
	LULC 2012	0.0	0.0	0.0	0.0	0.0	0.0	0.0	0.0	0.0	0.0	0.0	0.0	0.0	0.0	0.0	0.0	0.0	0.0	0.1	0.0	0.0	0.0	0.0
	LULC 2016	0.0	0.0	0.0	0.0	0.0	0.0	0.0	0.0	0.0	0.0	0.0	0.0	0.0	0.0	0.1	0.0	0.0	0.0	0.1	0.0	0.0	0.0	0.0

Average monthly runoff (mm) under five different historical LULC scenarios for the Wadi Hanifah catchment.
(Continued)

Month	LULC	1	2	3	4	5	6	7	8	9	10	11	12	13	14	15	16	17	18	19	20	21	22	
Sep	LULC 1996	0.0	0.0	0.0	0.0	0.0	0.0	0.0	0.0	0.0	0.0	0.0	0.0	0.0	0.0	0.0	0.0	0.0	0.0	0.0	0.0	0.0	0.0	0.0
	LULC 2004	0.0	0.0	0.0	0.0	0.0	0.0	0.0	0.0	0.0	0.0	0.0	0.0	0.0	0.0	0.0	0.0	0.0	0.0	0.1	0.0	0.0	0.0	0.0
	LULC 2009	0.0	0.0	0.0	0.0	0.0	0.0	0.0	0.0	0.0	0.0	0.0	0.0	0.0	0.0	0.0	0.0	0.0	0.0	0.1	0.0	0.0	0.0	0.0
	LULC 2012	0.0	0.0	0.0	0.0	0.0	0.0	0.0	0.0	0.0	0.0	0.0	0.0	0.0	0.0	0.0	0.0	0.0	0.0	0.1	0.0	0.0	0.0	0.0
	LULC 2016	0.0	0.0	0.0	0.0	0.0	0.0	0.0	0.0	0.0	0.0	0.0	0.0	0.0	0.0	0.0	0.0	0.0	0.0	0.0	0.0	0.0	0.0	0.0
Oct	LULC 1996	0.0	0.0	0.0	0.0	0.0	0.1	0.0	0.0	0.1	0.2	0.0	0.1	0.2	0.1	0.6	0.1	0.1	0.1	0.4	0.2	0.1	0.0	0.0
	LULC 2004	0.0	0.0	0.1	0.0	0.0	0.2	0.0	0.0	0.2	0.2	0.0	0.1	0.4	0.1	0.6	0.1	0.1	0.1	0.4	0.3	0.1	0.0	0.0
	LULC 2009	0.0	0.0	0.0	0.0	0.0	0.2	0.0	0.0	0.2	0.3	0.0	0.1	0.3	0.1	0.6	0.1	0.1	0.1	0.4	0.3	0.1	0.0	0.0
	LULC 2012	0.0	0.0	0.0	0.0	0.0	0.2	0.0	0.0	0.3	0.3	0.0	0.1	0.3	0.1	0.7	0.1	0.1	0.1	0.4	0.3	0.1	0.1	0.1
	LULC 2016	0.0	0.0	0.1	0.0	0.0	0.2	0.0	0.0	0.3	0.3	0.0	0.1	0.4	0.2	0.6	0.1	0.2	0.2	0.3	0.5	0.2	0.1	0.1

Average monthly runoff (mm) under five different historical LULC scenarios for the Wadi Hanifah catchment.
(Continued)

Month	LULC	1	2	3	4	5	6	7	8	9	10	11	12	13	14	15	16	17	18	19	20	21	22
Nov	LULC 1996	0.0	0.0	0.2	0.0	0.0	0.4	0.0	0.0	0.5	0.7	0.0	0.2	0.7	1.4	2.5	0.3	0.3	2.9	1.7	1.2	0.2	0.0
	LULC 2004	0.0	0.0	0.3	0.0	0.0	1.3	0.0	0.0	0.8	0.9	0.0	0.2	1.5	1.7	2.7	0.4	0.5	3.0	1.9	1.3	0.3	0.1
	LULC 2009	0.0	0.0	0.1	0.0	0.0	1.2	0.0	0.0	1.0	1.1	0.0	0.3	1.1	2.1	2.9	0.5	0.6	3.3	2.1	1.5	0.4	0.1
	LULC 2012	0.0	0.0	0.1	0.0	0.0	1.2	0.0	0.0	1.1	1.3	0.1	0.5	1.2	2.4	2.9	0.5	0.6	3.3	2.2	1.7	0.5	0.2
	LULC 2016	0.0	0.0	0.3	0.0	0.1	1.2	0.0	0.0	1.2	1.3	0.2	0.6	1.7	2.8	2.9	0.6	0.8	3.7	2.2	1.9	0.7	0.4
Dec	LULC 1996	0.0	0.0	0.0	0.0	0.0	0.1	0.0	0.0	0.1	0.7	0.0	0.2	0.7	0.9	2.1	0.3	0.3	2.0	1.4	1.0	0.2	0.0
	LULC 2004	0.0	0.0	0.1	0.0	0.0	0.3	0.0	0.0	0.2	0.9	0.0	0.2	1.5	1.2	2.3	0.4	0.5	2.0	1.6	1.0	0.3	0.1
	LULC 2009	0.0	0.0	0.0	0.0	0.0	0.2	0.0	0.0	0.2	1.2	0.0	0.3	1.1	1.4	2.5	0.5	0.6	2.3	1.8	1.2	0.4	0.1
	LULC 2012	0.0	0.0	0.0	0.0	0.0	0.2	0.0	0.0	0.2	1.3	0.1	0.5	1.2	1.6	2.5	0.5	0.6	2.3	1.8	1.4	0.4	0.2
	LULC 2016	0.0	0.0	0.1	0.0	0.0	0.3	0.0	0.0	0.2	1.3	0.2	0.5	1.7	2.0	2.5	0.6	0.8	2.6	1.7	1.7	0.7	0.4

Average monthly discharge (m³/s) under five different historical LULC scenarios for the Wadi Hanifah catchment.

Month	LULC	1	2	3	4	5	6	7	8	9	10	11	12	13	14	15	16	17	18	19	20	21	22
Jan	LULC 1996	0.03	0.03	0.10	0.01	0.10	0.01	0.16	0.01	0.27	0.31	0.01	0.02	0.35	0.12	0.62	0.09	0.05	0.31	1.00	0.13	0.02	1.12
	LULC 2004	0.03	0.03	0.11	0.01	0.11	0.02	0.16	0.01	0.30	0.35	0.01	0.02	0.40	0.15	0.72	0.11	0.07	0.32	1.15	0.14	0.03	1.29
	LULC 2009	0.03	0.03	0.11	0.01	0.11	0.02	0.17	0.01	0.32	0.38	0.01	0.02	0.43	0.19	0.81	0.13	0.08	0.35	1.29	0.16	0.03	1.46
	LULC 2012	0.03	0.03	0.11	0.01	0.11	0.02	0.17	0.01	0.32	0.39	0.02	0.03	0.45	0.22	0.87	0.14	0.09	0.36	1.37	0.18	0.04	1.57
	LULC 2016	0.03	0.03	0.13	0.01	0.13	0.02	0.17	0.01	0.35	0.41	0.03	0.04	0.50	0.25	0.96	0.14	0.11	0.39	1.50	0.21	0.06	1.77
Feb	LULC 1996	0.02	0.03	0.07	0.01	0.07	0.01	0.16	0.01	0.22	0.22	0.01	0.01	0.23	0.02	0.29	0.05	0.01	0.09	0.36	0.04	0.01	0.37
	LULC 2004	0.02	0.03	0.08	0.01	0.08	0.01	0.16	0.01	0.22	0.23	0.01	0.01	0.25	0.03	0.32	0.05	0.01	0.10	0.40	0.04	0.01	0.41
	LULC 2009	0.02	0.03	0.09	0.01	0.08	0.01	0.17	0.01	0.24	0.25	0.01	0.01	0.27	0.04	0.36	0.06	0.02	0.11	0.47	0.05	0.01	0.49
	LULC 2012	0.02	0.03	0.09	0.01	0.08	0.01	0.17	0.01	0.24	0.25	0.01	0.02	0.27	0.05	0.38	0.06	0.02	0.12	0.49	0.06	0.01	0.52
	LULC 2016	0.02	0.03	0.09	0.01	0.09	0.01	0.18	0.01	0.26	0.27	0.02	0.02	0.29	0.03	0.38	0.06	0.02	0.06	0.45	0.05	0.01	0.49
Mar	LULC 1996	0.01	0.03	0.07	0.01	0.06	0.02	0.15	0.01	0.21	0.26	0.01	0.03	0.30	0.19	0.68	0.11	0.08	0.44	1.22	0.17	0.03	1.34
	LULC 2004	0.01	0.03	0.09	0.01	0.08	0.04	0.15	0.01	0.26	0.32	0.01	0.03	0.38	0.23	0.84	0.15	0.11	0.45	1.43	0.19	0.04	1.59
	LULC 2009	0.01	0.03	0.08	0.01	0.07	0.03	0.15	0.01	0.26	0.34	0.01	0.03	0.40	0.28	0.94	0.18	0.13	0.48	1.60	0.21	0.05	1.79
	LULC 2012	0.01	0.03	0.08	0.01	0.07	0.03	0.15	0.01	0.27	0.36	0.02	0.05	0.45	0.31	1.04	0.19	0.15	0.49	1.71	0.24	0.05	1.95
	LULC 2016	0.01	0.03	0.10	0.01	0.10	0.03	0.16	0.01	0.31	0.40	0.03	0.05	0.52	0.43	1.24	0.20	0.18	0.67	2.11	0.30	0.08	2.47

Average monthly discharge (m³/s) under five different historical LULC scenarios for the Wadi Hanifah catchment.
(Continued)

Month	LULC	1	2	3	4	5	6	7	8	9	10	11	12	13	14	15	16	17	18	19	20	21	22
Apr	LULC 1996	0.01	0.03	0.06	0.01	0.05	0.01	0.15	0.01	0.18	0.21	0.01	0.02	0.24	0.13	0.49	0.08	0.05	0.37	0.91	0.14	0.02	1.00
	LULC 2004	0.01	0.03	0.07	0.01	0.06	0.02	0.15	0.01	0.21	0.24	0.01	0.02	0.29	0.17	0.61	0.10	0.07	0.38	1.07	0.15	0.03	1.19
	LULC 2009	0.01	0.03	0.07	0.01	0.06	0.02	0.16	0.01	0.22	0.27	0.01	0.03	0.31	0.22	0.71	0.13	0.09	0.44	1.25	0.17	0.04	1.40
	LULC 2012	0.01	0.03	0.07	0.01	0.06	0.02	0.16	0.01	0.22	0.28	0.02	0.03	0.34	0.25	0.78	0.13	0.10	0.44	1.33	0.20	0.04	1.51
	LULC 2016	0.01	0.03	0.09	0.01	0.08	0.02	0.17	0.01	0.25	0.30	0.02	0.04	0.38	0.27	0.85	0.14	0.11	0.43	1.41	0.23	0.06	1.66
May	LULC 1996	0.01	0.03	0.05	0.01	0.04	0.01	0.16	0.01	0.15	0.14	0.01	0.01	0.15	0.08	0.27	0.04	0.01	0.28	0.53	0.06	0.01	0.55
	LULC 2004	0.01	0.03	0.05	0.01	0.04	0.01	0.16	0.01	0.16	0.15	0.01	0.01	0.16	0.11	0.32	0.05	0.02	0.29	0.60	0.07	0.01	0.63
	LULC 2009	0.01	0.03	0.06	0.01	0.04	0.01	0.16	0.01	0.17	0.17	0.01	0.02	0.18	0.16	0.40	0.06	0.02	0.35	0.75	0.09	0.01	0.80
	LULC 2012	0.01	0.03	0.06	0.01	0.04	0.01	0.16	0.01	0.17	0.17	0.01	0.02	0.19	0.18	0.43	0.06	0.03	0.34	0.77	0.10	0.01	0.83
	LULC 2016	0.01	0.03	0.06	0.01	0.05	0.01	0.17	0.01	0.18	0.18	0.01	0.02	0.21	0.15	0.42	0.06	0.03	0.24	0.70	0.08	0.02	0.77
Jun	LULC 1996	0.01	0.03	0.04	0.01	0.03	0.01	0.14	0.01	0.13	0.11	0.01	0.01	0.11	0.00	0.11	0.02	0.00	0.02	0.09	0.01	0.00	0.06
	LULC 2004	0.01	0.03	0.04	0.01	0.03	0.00	0.14	0.01	0.13	0.11	0.01	0.01	0.11	0.00	0.11	0.02	0.00	0.03	0.10	0.01	0.00	0.07
	LULC 2009	0.01	0.03	0.05	0.01	0.04	0.00	0.15	0.01	0.14	0.13	0.01	0.01	0.12	0.01	0.13	0.03	0.00	0.04	0.12	0.01	0.00	0.09
	LULC 2012	0.01	0.03	0.05	0.01	0.04	0.00	0.15	0.01	0.14	0.13	0.01	0.01	0.12	0.01	0.13	0.03	0.00	0.04	0.12	0.01	0.00	0.09
	LULC 2016	0.01	0.03	0.05	0.01	0.04	0.01	0.15	0.01	0.15	0.13	0.01	0.01	0.13	0.00	0.13	0.03	0.00	0.00	0.10	0.01	0.00	0.07

Average monthly discharge (m³/s) under five different historical LULC scenarios for the Wadi Hanifah catchment.
(Continued)

Month	LULC	1	2	3	4	5	6	7	8	9	10	11	12	13	14	15	16	17	18	19	20	21	22
Jul	LULC 1996	0.01	0.03	0.04	0.01	0.03	0.01	0.13	0.01	0.12	0.10	0.01	0.01	0.10	0.00	0.09	0.02	0.00	0.00	0.05	0.01	0.00	0.02
	LULC 2004	0.01	0.03	0.04	0.01	0.03	0.00	0.13	0.01	0.12	0.10	0.01	0.01	0.10	0.00	0.09	0.02	0.00	0.00	0.05	0.01	0.00	0.02
	LULC 2009	0.01	0.03	0.05	0.01	0.03	0.00	0.14	0.01	0.13	0.11	0.01	0.01	0.11	0.00	0.10	0.02	0.00	0.00	0.07	0.01	0.00	0.03
	LULC 2012	0.01	0.03	0.05	0.01	0.03	0.00	0.14	0.01	0.13	0.11	0.01	0.01	0.11	0.00	0.10	0.02	0.00	0.00	0.07	0.01	0.00	0.03
	LULC 2016	0.01	0.03	0.05	0.01	0.04	0.00	0.14	0.01	0.14	0.12	0.01	0.01	0.12	0.00	0.11	0.02	0.00	0.00	0.07	0.01	0.00	0.03
Aug	LULC 1996	0.01	0.02	0.03	0.01	0.02	0.01	0.11	0.01	0.10	0.09	0.01	0.01	0.09	0.00	0.08	0.02	0.00	0.00	0.05	0.01	0.00	0.02
	LULC 2004	0.01	0.02	0.03	0.01	0.03	0.00	0.11	0.01	0.10	0.09	0.01	0.01	0.09	0.00	0.09	0.02	0.00	0.00	0.05	0.01	0.00	0.02
	LULC 2009	0.01	0.02	0.04	0.01	0.03	0.00	0.13	0.01	0.12	0.11	0.01	0.01	0.11	0.00	0.10	0.02	0.00	0.00	0.07	0.01	0.00	0.03
	LULC 2012	0.01	0.02	0.04	0.01	0.03	0.00	0.13	0.01	0.12	0.11	0.01	0.01	0.11	0.00	0.10	0.02	0.00	0.00	0.07	0.01	0.00	0.03
	LULC 2016	0.01	0.02	0.04	0.01	0.04	0.00	0.14	0.01	0.13	0.11	0.01	0.01	0.11	0.00	0.11	0.02	0.00	0.00	0.08	0.01	0.00	0.04
Sep	LULC 1996	0.01	0.03	0.04	0.01	0.03	0.01	0.10	0.01	0.10	0.09	0.01	0.01	0.09	0.00	0.09	0.02	0.00	0.00	0.06	0.01	0.00	0.03
	LULC 2004	0.01	0.03	0.04	0.01	0.03	0.00	0.10	0.01	0.10	0.09	0.01	0.01	0.09	0.00	0.09	0.02	0.00	0.00	0.06	0.01	0.00	0.04
	LULC 2009	0.01	0.03	0.05	0.01	0.04	0.00	0.13	0.01	0.13	0.12	0.01	0.01	0.12	0.00	0.12	0.03	0.00	0.00	0.09	0.01	0.00	0.06
	LULC 2012	0.01	0.03	0.05	0.01	0.04	0.00	0.13	0.01	0.13	0.12	0.01	0.01	0.12	0.00	0.12	0.03	0.00	0.00	0.09	0.01	0.00	0.06
	LULC 2016	0.01	0.03	0.05	0.01	0.04	0.00	0.13	0.01	0.14	0.12	0.01	0.01	0.13	0.00	0.12	0.03	0.00	0.00	0.09	0.01	0.00	0.06

Average monthly discharge (m³/s) under five different historical LULC scenarios for the Wadi Hanifah catchment.
(Continued)

Month	LULC	1	2	3	4	5	6	7	8	9	10	11	12	13	14	15	16	17	18	19	20	21	22
Oct	LULC 1996	0.01	0.03	0.05	0.01	0.04	0.01	0.10	0.01	0.13	0.13	0.01	0.01	0.14	0.00	0.16	0.04	0.01	0.01	0.15	0.02	0.01	0.13
	LULC 2004	0.01	0.03	0.06	0.01	0.05	0.01	0.10	0.01	0.14	0.14	0.01	0.01	0.15	0.00	0.18	0.04	0.01	0.01	0.16	0.02	0.01	0.15
	LULC 2009	0.01	0.03	0.06	0.01	0.05	0.01	0.12	0.01	0.16	0.16	0.01	0.01	0.17	0.00	0.20	0.04	0.01	0.01	0.19	0.03	0.01	0.18
	LULC 2012	0.01	0.03	0.06	0.01	0.05	0.01	0.12	0.01	0.16	0.16	0.01	0.01	0.18	0.00	0.21	0.04	0.01	0.01	0.19	0.03	0.01	0.19
	LULC 2016	0.01	0.03	0.07	0.01	0.06	0.01	0.12	0.01	0.18	0.18	0.01	0.01	0.19	0.01	0.23	0.04	0.01	0.01	0.22	0.04	0.01	0.22
Nov	LULC 1996	0.02	0.03	0.09	0.01	0.08	0.02	0.13	0.01	0.23	0.25	0.01	0.02	0.27	0.09	0.45	0.06	0.03	0.21	0.69	0.09	0.01	0.76
	LULC 2004	0.02	0.03	0.10	0.01	0.10	0.04	0.13	0.01	0.28	0.30	0.01	0.02	0.33	0.11	0.54	0.07	0.04	0.21	0.81	0.09	0.02	0.89
	LULC 2009	0.02	0.03	0.09	0.01	0.09	0.04	0.14	0.01	0.29	0.32	0.01	0.02	0.35	0.13	0.60	0.08	0.05	0.24	0.90	0.11	0.02	1.00
	LULC 2012	0.02	0.03	0.09	0.01	0.09	0.04	0.14	0.01	0.30	0.33	0.02	0.02	0.37	0.15	0.64	0.09	0.05	0.24	0.95	0.12	0.02	1.07
	LULC 2016	0.02	0.03	0.12	0.01	0.12	0.04	0.15	0.01	0.33	0.37	0.02	0.03	0.42	0.17	0.72	0.09	0.06	0.27	1.07	0.13	0.04	1.23
Dec	LULC 1996	0.02	0.03	0.09	0.01	0.09	0.01	0.14	0.01	0.23	0.25	0.01	0.02	0.28	0.06	0.42	0.06	0.03	0.14	0.59	0.07	0.01	0.64
	LULC 2004	0.02	0.03	0.09	0.01	0.10	0.01	0.14	0.01	0.24	0.27	0.01	0.02	0.30	0.07	0.47	0.07	0.04	0.14	0.65	0.08	0.02	0.72
	LULC 2009	0.02	0.03	0.10	0.01	0.10	0.01	0.15	0.01	0.27	0.30	0.01	0.02	0.33	0.09	0.53	0.08	0.04	0.16	0.74	0.09	0.02	0.81
	LULC 2012	0.02	0.03	0.10	0.01	0.10	0.01	0.15	0.01	0.27	0.30	0.02	0.02	0.34	0.10	0.55	0.09	0.05	0.16	0.77	0.10	0.02	0.87
	LULC 2016	0.02	0.03	0.11	0.01	0.11	0.01	0.16	0.01	0.28	0.32	0.02	0.02	0.37	0.12	0.60	0.09	0.06	0.19	0.85	0.11	0.03	0.99

Average monthly runoff (mm) under five different historical LULC scenarios for the Wadi As Silayy catchment.

Month	LULC	1	2	3	4	5	6	7	8	9	10	11
Jan	LULC 1996	0.3	0.0	0.0	0.0	0.3	0.0	0.0	2.2	0.6	2.0	0.5
	LULC 2004	0.3	0.0	1.3	0.2	1.9	0.7	0.3	4.3	2.7	2.6	0.6
	LULC 2009	0.4	0.0	1.6	0.4	4.7	0.8	0.5	4.9	3.2	2.8	0.7
	LULC 2012	0.4	0.0	2.4	1.3	5.9	0.9	0.6	5.1	3.7	2.9	0.7
	LULC 2016	0.7	0.0	2.7	1.4	6.9	1.6	0.6	5.4	3.9	3.2	1.0
Feb	LULC 1996	0.1	0.0	0.0	0.0	0.1	0.0	0.0	0.3	0.1	0.3	0.1
	LULC 2004	0.1	0.0	0.3	0.1	0.5	0.2	0.0	0.8	0.4	0.5	0.1
	LULC 2009	0.1	0.0	0.4	0.1	1.3	0.2	0.1	0.9	0.4	0.5	0.1
	LULC 2012	0.1	0.0	0.7	0.3	1.6	0.3	0.1	1.0	0.5	0.6	0.1
	LULC 2016	0.2	0.0	0.7	0.4	1.9	0.4	0.1	1.1	0.5	0.7	0.1
Mar	LULC 1996	0.4	0.0	0.0	0.0	0.4	0.0	0.0	3.8	1.0	3.4	0.8
	LULC 2004	0.4	0.0	1.6	0.3	2.4	0.9	0.6	7.0	4.9	4.2	0.9
	LULC 2009	0.5	0.0	2.0	0.6	5.8	1.1	0.9	7.8	5.8	4.5	1.1
	LULC 2012	0.5	0.0	2.9	1.6	7.3	1.2	1.0	8.1	6.6	4.6	1.1
	LULC 2016	0.9	0.0	3.4	1.8	8.5	2.1	1.1	8.5	7.0	5.0	1.6
Apr	LULC 1996	0.3	0.0	0.0	0.0	0.3	0.0	0.0	2.4	0.6	2.2	0.6
	LULC 2004	0.3	0.0	1.2	0.2	1.8	0.6	0.4	4.8	3.1	2.9	0.6
	LULC 2009	0.4	0.0	1.5	0.4	4.3	0.8	0.6	5.5	3.6	3.2	0.7
	LULC 2012	0.4	0.0	2.2	1.2	5.5	0.9	0.6	5.7	4.1	3.3	0.8
	LULC 2016	0.7	0.0	2.5	1.3	6.5	1.5	0.7	6.1	4.4	3.6	1.1
May	LULC 1996	0.1	0.0	0.0	0.0	0.1	0.0	0.0	1.4	0.3	1.5	0.1
	LULC 2004	0.1	0.0	0.4	0.1	0.6	0.2	0.2	3.3	1.6	2.0	0.1
	LULC 2009	0.1	0.0	0.5	0.1	1.6	0.2	0.3	3.9	1.9	2.2	0.2
	LULC 2012	0.1	0.0	0.8	0.4	2.1	0.3	0.3	4.1	2.3	2.3	0.2
	LULC 2016	0.2	0.0	0.9	0.4	2.5	0.5	0.3	4.5	2.4	2.6	0.3

Average monthly runoff (mm) under five different historical LULC scenarios for the Wadi As Silayy catchment. (Continued)

Month	LULC	1	2	3	4	5	6	7	8	9	10	11
Jun	LULC 1996	0.0	0.0	0.0	0.0	0.0	0.0	0.0	0.0	0.0	0.1	0.0
	LULC 2004	0.0	0.0	0.0	0.0	0.0	0.0	0.0	0.1	0.0	0.1	0.0
	LULC 2009	0.0	0.0	0.0	0.0	0.0	0.0	0.0	0.2	0.0	0.1	0.0
	LULC 2012	0.0	0.0	0.0	0.0	0.0	0.0	0.0	0.2	0.0	0.1	0.0
	LULC 2016	0.0	0.0	0.0	0.0	0.0	0.0	0.0	0.3	0.0	0.2	0.0
Jul	LULC 1996	0.0	0.0	0.0	0.0	0.0	0.0	0.0	0.0	0.0	0.0	0.0
	LULC 2004	0.0	0.0	0.0	0.0	0.0	0.0	0.0	0.0	0.0	0.0	0.0
	LULC 2009	0.0	0.0	0.0	0.0	0.0	0.0	0.0	0.0	0.0	0.0	0.0
	LULC 2012	0.0	0.0	0.0	0.0	0.0	0.0	0.0	0.0	0.0	0.0	0.0
	LULC 2016	0.0	0.0	0.0	0.0	0.0	0.0	0.0	0.0	0.0	0.0	0.0
Aug	LULC 1996	0.0	0.0	0.0	0.0	0.0	0.0	0.0	0.0	0.0	0.0	0.0
	LULC 2004	0.0	0.0	0.0	0.0	0.0	0.0	0.0	0.0	0.0	0.0	0.0
	LULC 2009	0.0	0.0	0.0	0.0	0.0	0.0	0.0	0.1	0.0	0.0	0.0
	LULC 2012	0.0	0.0	0.0	0.0	0.0	0.0	0.0	0.1	0.1	0.0	0.0
	LULC 2016	0.0	0.0	0.0	0.0	0.0	0.0	0.0	0.1	0.1	0.0	0.0
Sep	LULC 1996	0.0	0.0	0.0	0.0	0.0	0.0	0.0	0.0	0.0	0.0	0.0
	LULC 2004	0.0	0.0	0.0	0.0	0.0	0.0	0.0	0.0	0.0	0.0	0.0
	LULC 2009	0.0	0.0	0.0	0.0	0.0	0.0	0.0	0.0	0.0	0.0	0.0
	LULC 2012	0.0	0.0	0.0	0.0	0.0	0.0	0.0	0.0	0.0	0.0	0.0
	LULC 2016	0.0	0.0	0.0	0.0	0.0	0.0	0.0	0.0	0.0	0.0	0.0
Oct	LULC 1996	0.0	0.0	0.0	0.0	0.0	0.0	0.0	0.1	0.0	0.1	0.1
	LULC 2004	0.0	0.0	0.1	0.0	0.1	0.0	0.0	0.1	0.1	0.1	0.1
	LULC 2009	0.0	0.0	0.1	0.0	0.3	0.1	0.0	0.1	0.1	0.1	0.1
	LULC 2012	0.0	0.0	0.1	0.1	0.3	0.1	0.0	0.2	0.1	0.1	0.1
	LULC 2016	0.0	0.0	0.1	0.1	0.4	0.1	0.0	0.2	0.1	0.1	0.2

Average monthly runoff (mm) under five different historical LULC scenarios for the Wadi As Silayy catchment. (Continued)

Month	LULC	1	2	3	4	5	6	7	8	9	10	11
Nov	LULC 1996	0.3	0.0	0.0	0.0	0.3	0.0	0.0	1.5	0.4	1.4	0.3
	LULC 2004	0.3	0.0	1.2	0.2	1.8	0.7	0.2	2.9	1.8	1.7	0.3
	LULC 2009	0.4	0.0	1.5	0.4	4.5	0.8	0.3	3.2	2.2	1.9	0.4
	LULC 2012	0.4	0.0	2.3	1.2	5.7	0.9	0.4	3.4	2.5	1.9	0.4
	LULC 2016	0.7	0.0	2.6	1.4	6.6	1.6	0.4	3.6	2.6	2.1	0.6
Dec	LULC 1996	0.2	0.0	0.0	0.0	0.2	0.0	0.0	1.0	0.3	0.9	0.3
	LULC 2004	0.2	0.0	0.7	0.1	1.0	0.4	0.2	2.0	1.3	1.2	0.3
	LULC 2009	0.2	0.0	0.9	0.2	2.5	0.4	0.2	2.2	1.5	1.3	0.4
	LULC 2012	0.2	0.0	1.3	0.7	3.1	0.5	0.3	2.3	1.8	1.3	0.4
	LULC 2016	0.4	0.0	1.4	0.8	3.7	0.9	0.3	2.4	1.9	1.4	0.5

Average monthly discharge (m³/s) under five different historical LULC scenarios for the Wadi As Silayy catchment.

Month	LULC	1	2	3	4	5	6	7	8	9	10	11
Jan	LULC 1996	0.39	0.37	0.07	0.01	0.83	0.05	0.00	0.07	0.89	1.40	0.02
	LULC 2004	0.41	0.38	0.21	0.02	1.03	0.08	0.01	0.14	1.15	1.82	0.03
	LULC 2009	0.43	0.38	0.25	0.02	1.10	0.09	0.01	0.16	1.25	1.97	0.03
	LULC 2012	0.43	0.38	0.33	0.03	1.21	0.10	0.02	0.17	1.38	2.12	0.03
	LULC 2016	0.47	0.38	0.36	0.04	1.30	0.14	0.02	0.18	1.51	2.31	0.04
Feb	LULC 1996	0.36	0.38	0.08	0.01	0.80	0.05	0.00	0.01	0.83	1.02	0.01
	LULC 2004	0.38	0.39	0.13	0.02	0.89	0.05	0.00	0.03	0.93	1.16	0.01
	LULC 2009	0.38	0.39	0.14	0.02	0.91	0.06	0.00	0.03	0.96	1.20	0.01
	LULC 2012	0.38	0.39	0.17	0.02	0.94	0.07	0.00	0.04	1.00	1.25	0.01
	LULC 2016	0.39	0.39	0.17	0.02	0.96	0.08	0.00	0.04	1.03	1.30	0.01
Mar	LULC 1996	0.37	0.36	0.07	0.01	0.79	0.04	0.00	0.12	0.83	1.60	0.03
	LULC 2004	0.40	0.37	0.24	0.02	1.02	0.08	0.01	0.23	1.18	2.18	0.03
	LULC 2009	0.41	0.37	0.28	0.02	1.11	0.09	0.02	0.25	1.30	2.37	0.04
	LULC 2012	0.41	0.37	0.38	0.04	1.23	0.11	0.02	0.26	1.45	2.56	0.04
	LULC 2016	0.47	0.37	0.42	0.04	1.34	0.15	0.03	0.28	1.62	2.81	0.06
Apr	LULC 1996	0.37	0.38	0.07	0.01	0.79	0.04	0.00	0.08	0.82	1.39	0.02
	LULC 2004	0.39	0.39	0.21	0.02	0.98	0.07	0.01	0.16	1.08	1.84	0.02
	LULC 2009	0.40	0.39	0.24	0.02	1.04	0.08	0.01	0.18	1.17	2.00	0.03
	LULC 2012	0.40	0.39	0.31	0.03	1.14	0.09	0.01	0.19	1.29	2.15	0.03
	LULC 2016	0.44	0.39	0.34	0.04	1.23	0.13	0.02	0.21	1.41	2.35	0.04
May	LULC 1996	0.31	0.37	0.07	0.01	0.71	0.04	0.00	0.04	0.72	1.12	0.00
	LULC 2004	0.33	0.38	0.12	0.01	0.80	0.04	0.00	0.11	0.84	1.38	0.01
	LULC 2009	0.33	0.38	0.13	0.02	0.82	0.05	0.01	0.13	0.88	1.47	0.01
	LULC 2012	0.33	0.38	0.16	0.02	0.86	0.05	0.01	0.13	0.93	1.54	0.01
	LULC 2016	0.34	0.38	0.17	0.02	0.88	0.07	0.01	0.15	0.97	1.64	0.01
Jun	LULC 1996	0.28	0.35	0.07	0.01	0.65	0.03	0.00	0.00	0.65	0.79	0.00
	LULC 2004	0.29	0.36	0.08	0.01	0.68	0.03	0.00	0.00	0.68	0.81	0.00
	LULC 2009	0.29	0.36	0.07	0.01	0.68	0.03	0.00	0.01	0.68	0.82	0.00
	LULC 2012	0.29	0.36	0.08	0.01	0.68	0.04	0.00	0.01	0.69	0.83	0.00
	LULC 2016	0.28	0.36	0.08	0.01	0.67	0.04	0.00	0.01	0.68	0.83	0.00

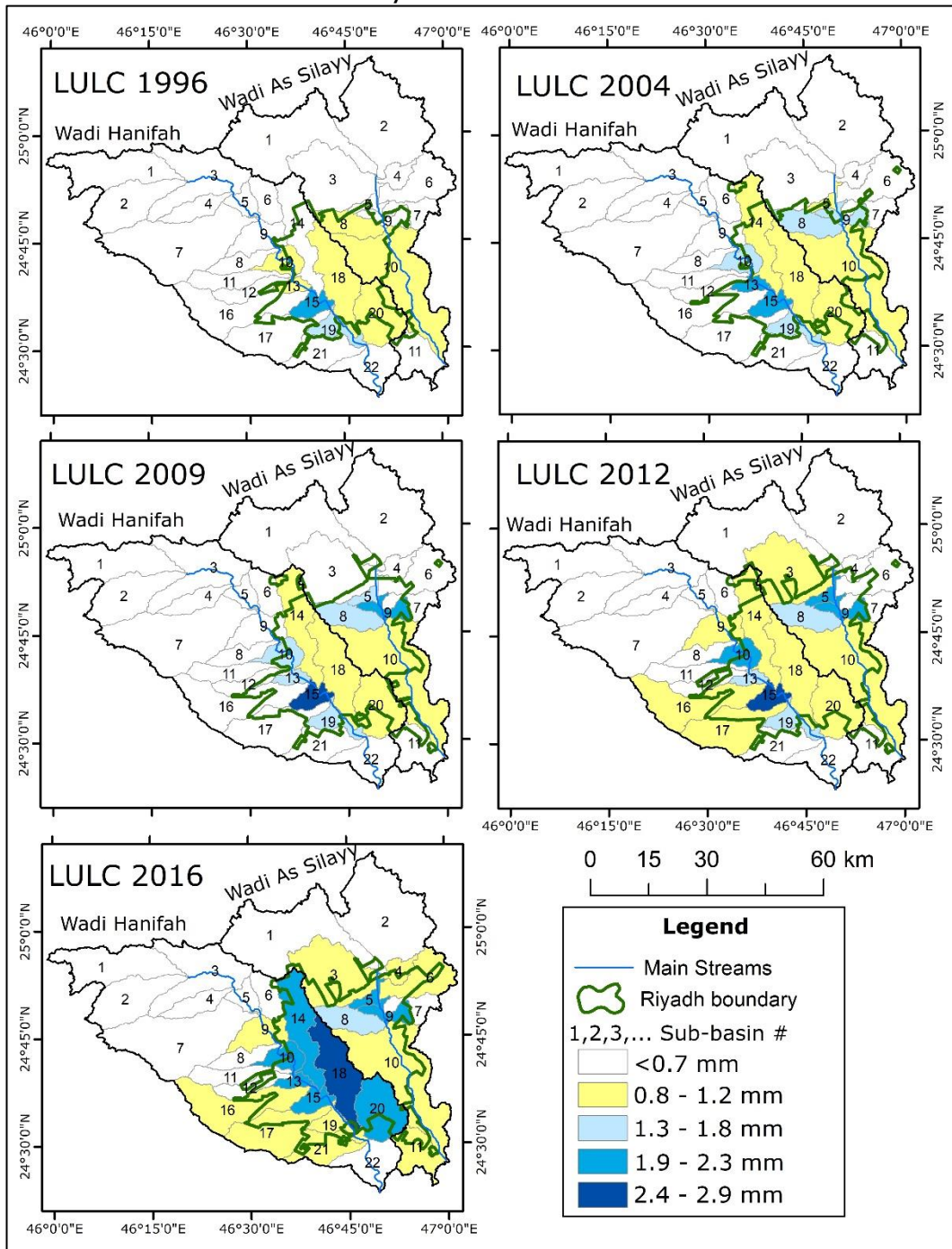
Average monthly discharge (m³/s) under five different historical LULC scenarios for the Wadi As Silayy catchment. (Continued)

Month	LULC	1	2	3	4	5	6	7	8	9	10	11
Jul	LULC 1996	0.25	0.33	0.06	0.01	0.59	0.03	0.00	0.00	0.59	0.70	0.00
	LULC 2004	0.26	0.33	0.07	0.01	0.62	0.03	0.00	0.00	0.61	0.72	0.00
	LULC 2009	0.26	0.33	0.07	0.01	0.62	0.03	0.00	0.00	0.61	0.71	0.00
	LULC 2012	0.26	0.33	0.07	0.01	0.62	0.03	0.00	0.00	0.61	0.73	0.00
	LULC 2016	0.25	0.33	0.07	0.01	0.61	0.03	0.00	0.00	0.61	0.72	0.00
Aug	LULC 1996	0.24	0.30	0.06	0.01	0.56	0.03	0.00	0.00	0.55	0.66	0.00
	LULC 2004	0.24	0.31	0.06	0.01	0.58	0.03	0.00	0.00	0.57	0.68	0.00
	LULC 2009	0.24	0.31	0.06	0.01	0.58	0.03	0.00	0.00	0.58	0.68	0.00
	LULC 2012	0.24	0.31	0.07	0.01	0.58	0.03	0.00	0.00	0.58	0.69	0.00
	LULC 2016	0.24	0.31	0.06	0.01	0.57	0.03	0.00	0.00	0.57	0.69	0.00
Sep	LULC 1996	0.23	0.28	0.06	0.01	0.53	0.03	0.00	0.00	0.53	0.63	0.00
	LULC 2004	0.24	0.30	0.06	0.01	0.57	0.03	0.00	0.00	0.57	0.67	0.00
	LULC 2009	0.24	0.30	0.06	0.01	0.57	0.03	0.00	0.00	0.57	0.67	0.00
	LULC 2012	0.24	0.30	0.06	0.01	0.57	0.03	0.00	0.00	0.57	0.67	0.00
	LULC 2016	0.24	0.30	0.06	0.01	0.56	0.03	0.00	0.00	0.57	0.68	0.00
Oct	LULC 1996	0.22	0.27	0.06	0.01	0.53	0.03	0.00	0.00	0.54	0.65	0.00
	LULC 2004	0.24	0.29	0.07	0.01	0.58	0.03	0.00	0.00	0.59	0.70	0.00
	LULC 2009	0.24	0.28	0.07	0.01	0.58	0.03	0.00	0.00	0.60	0.71	0.00
	LULC 2012	0.24	0.28	0.07	0.01	0.58	0.04	0.00	0.00	0.60	0.71	0.00
	LULC 2016	0.24	0.28	0.08	0.01	0.58	0.04	0.00	0.00	0.60	0.73	0.01
Nov	LULC 1996	0.32	0.31	0.06	0.01	0.69	0.04	0.00	0.05	0.72	1.10	0.01
	LULC 2004	0.35	0.33	0.20	0.02	0.89	0.07	0.01	0.10	0.98	1.47	0.02
	LULC 2009	0.36	0.33	0.23	0.02	0.96	0.08	0.01	0.11	1.07	1.59	0.02
	LULC 2012	0.36	0.33	0.30	0.03	1.05	0.09	0.01	0.12	1.18	1.71	0.02
	LULC 2016	0.41	0.33	0.34	0.03	1.14	0.13	0.01	0.12	1.32	1.89	0.03
Dec	LULC 1996	0.33	0.34	0.06	0.01	0.73	0.04	0.00	0.04	0.77	1.07	0.01
	LULC 2004	0.36	0.35	0.14	0.02	0.87	0.06	0.01	0.07	0.94	1.30	0.02
	LULC 2009	0.37	0.35	0.16	0.02	0.91	0.07	0.01	0.07	1.00	1.38	0.02
	LULC 2012	0.36	0.35	0.20	0.02	0.95	0.07	0.01	0.08	1.05	1.44	0.02
	LULC 2016	0.39	0.35	0.22	0.03	1.00	0.09	0.01	0.08	1.12	1.55	0.03

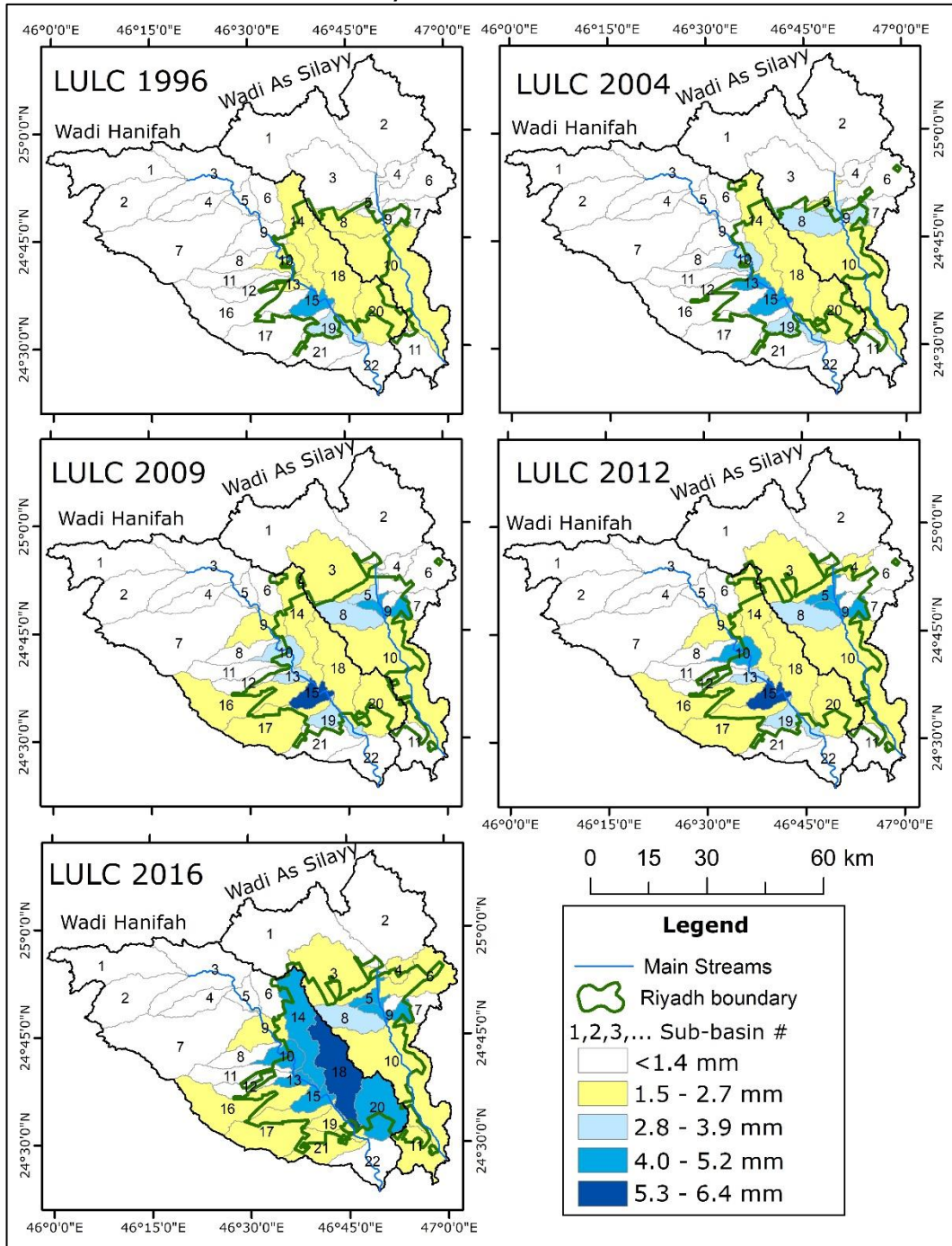
Appendix C

Distribution maps of calculated return periods and the percent exceedances

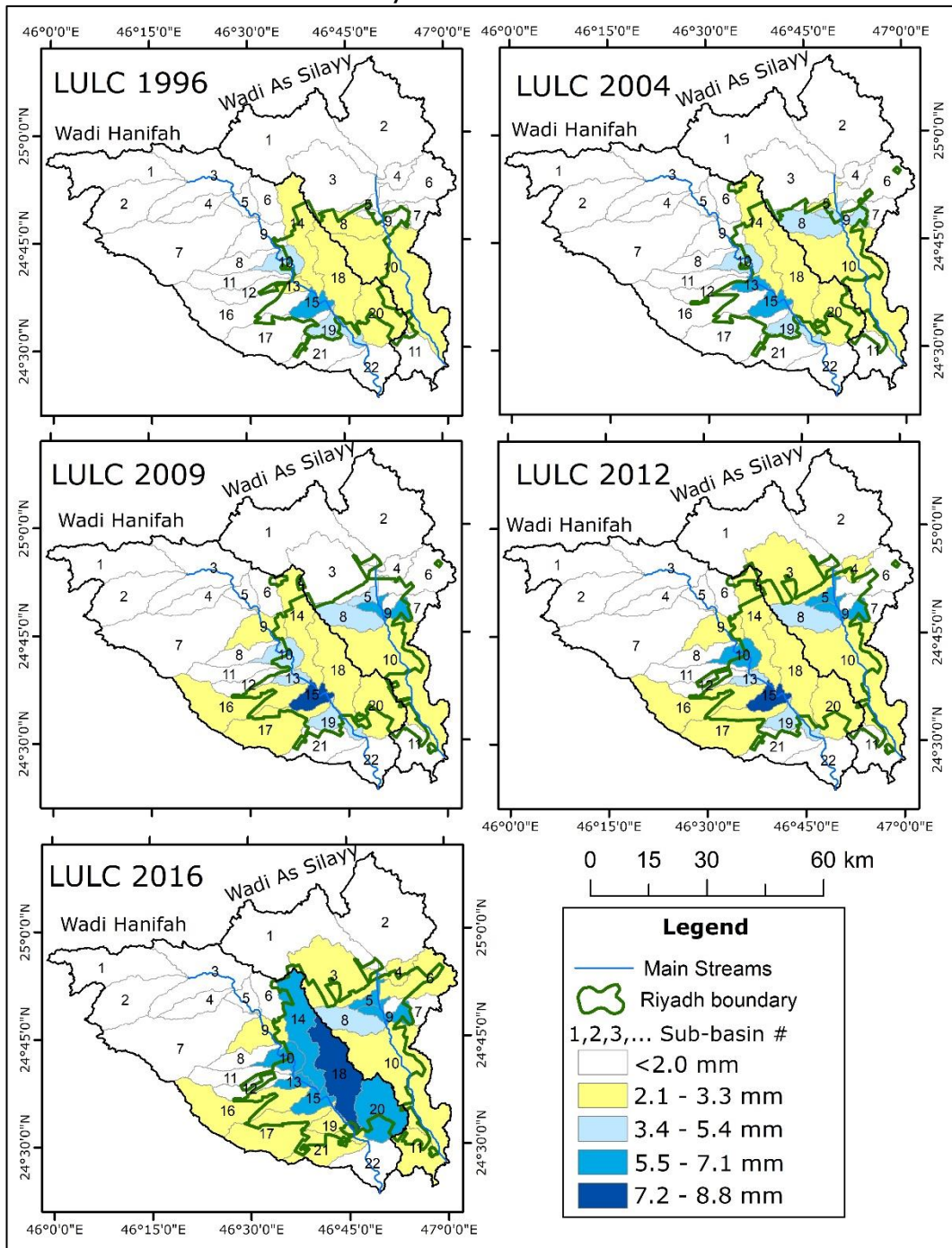
Spatial distributions of simulated annual maximum daily runoff (mm) in the 2-year return periods using different LULC conditions at Riyadh's catchments.



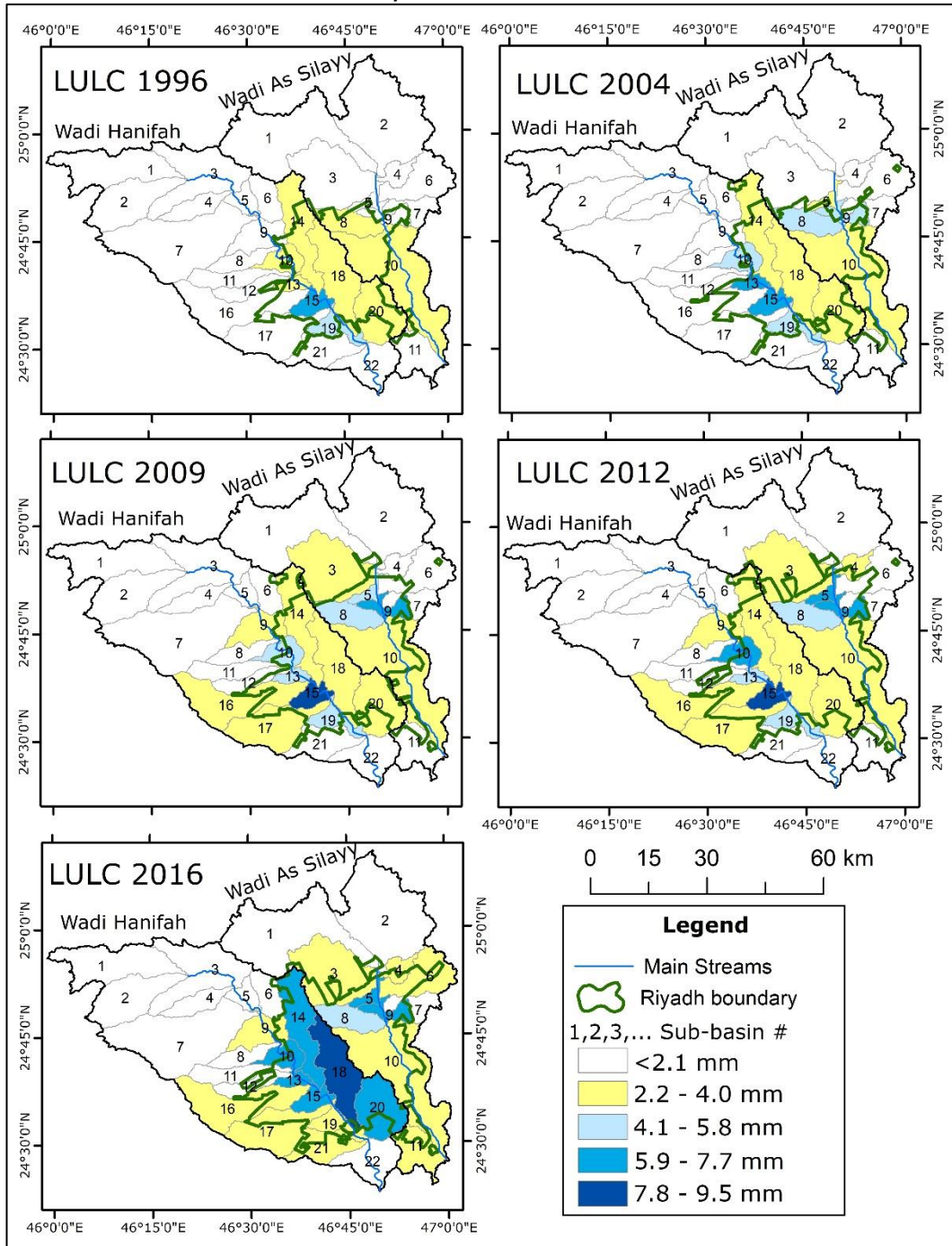
Spatial distributions of simulated annual maximum daily runoff (mm) in the 10-year return periods using different LULC conditions at Riyadh's catchments.



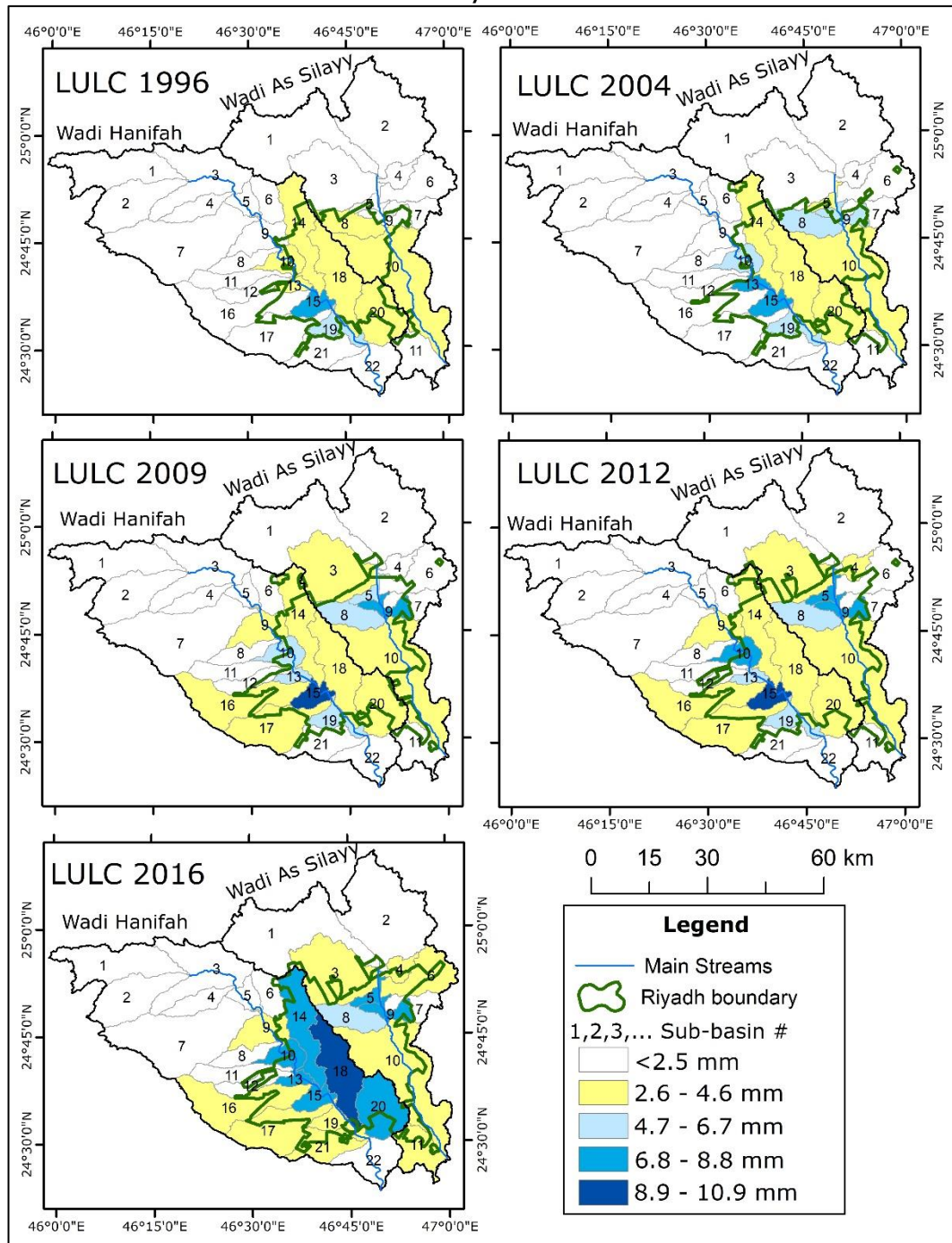
Spatial distributions of simulated annual maximum daily runoff (mm) in the 30-year return periods using different LULC conditions at Riyadh's catchments.



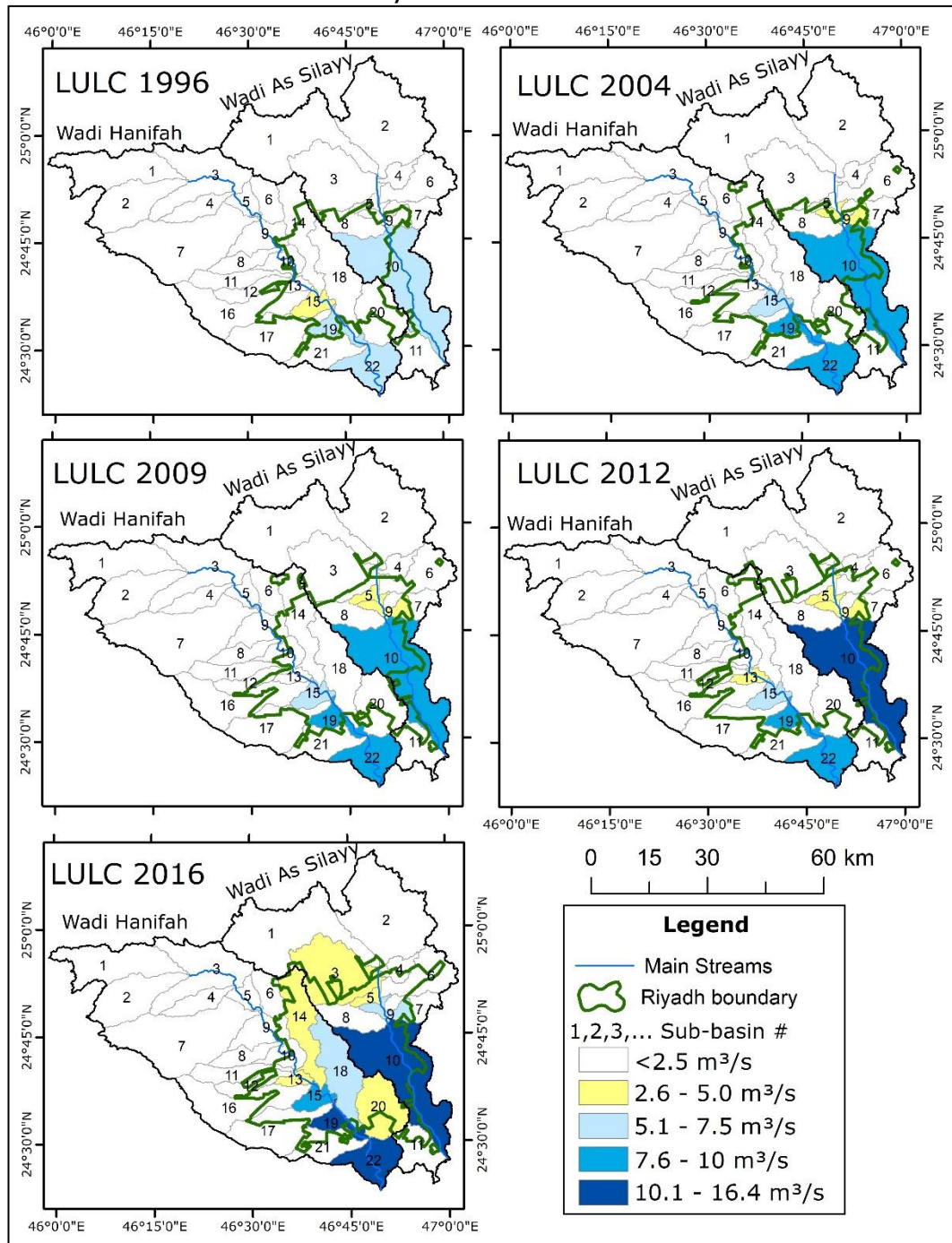
Spatial distributions of simulated annual maximum daily runoff (mm) in the 50-year return periods using different LULC conditions at Riyadh's catchments.



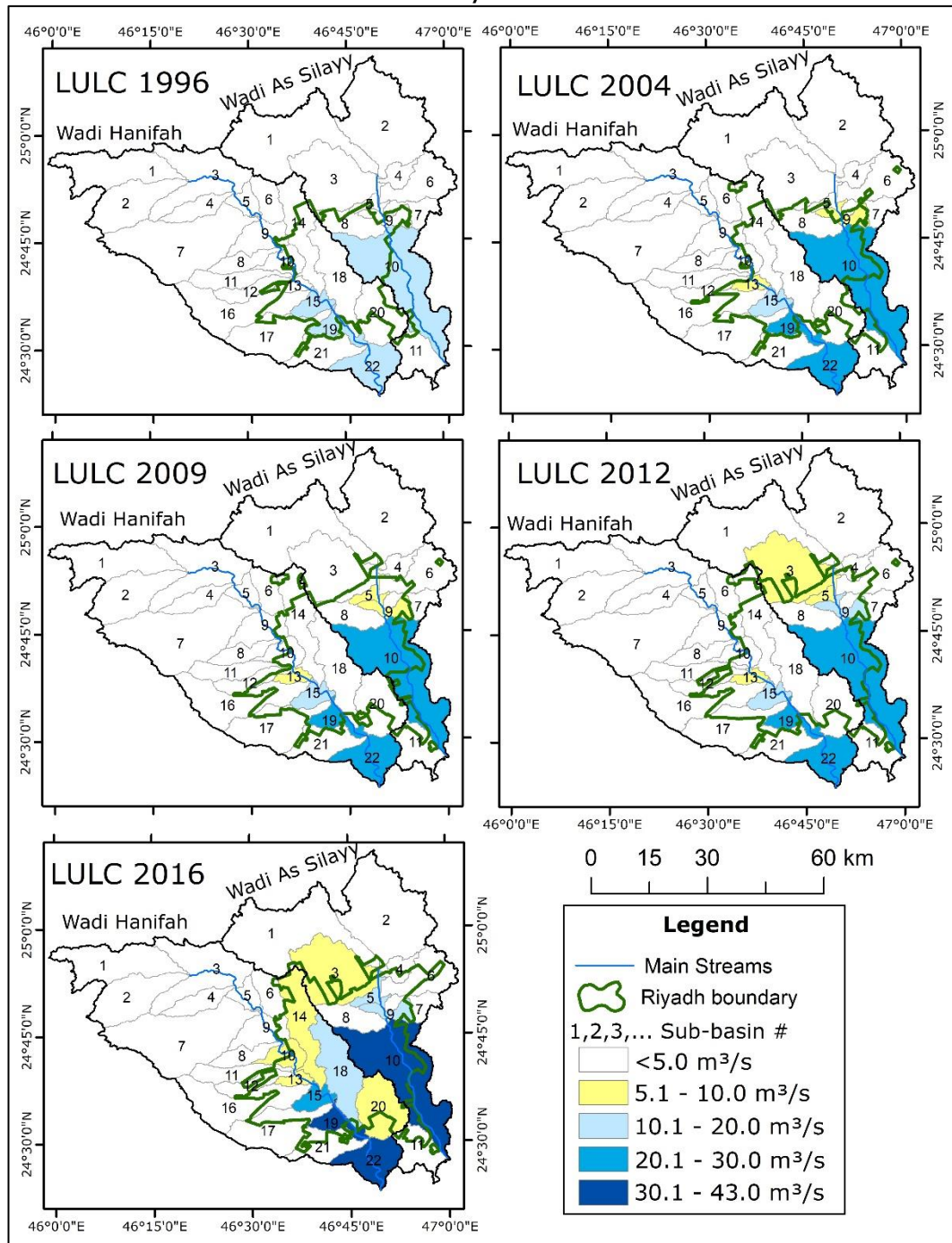
Spatial distributions of simulated annual maximum daily runoff (mm) in the 100-year return periods using different LULC conditions at Riyadh's catchments.



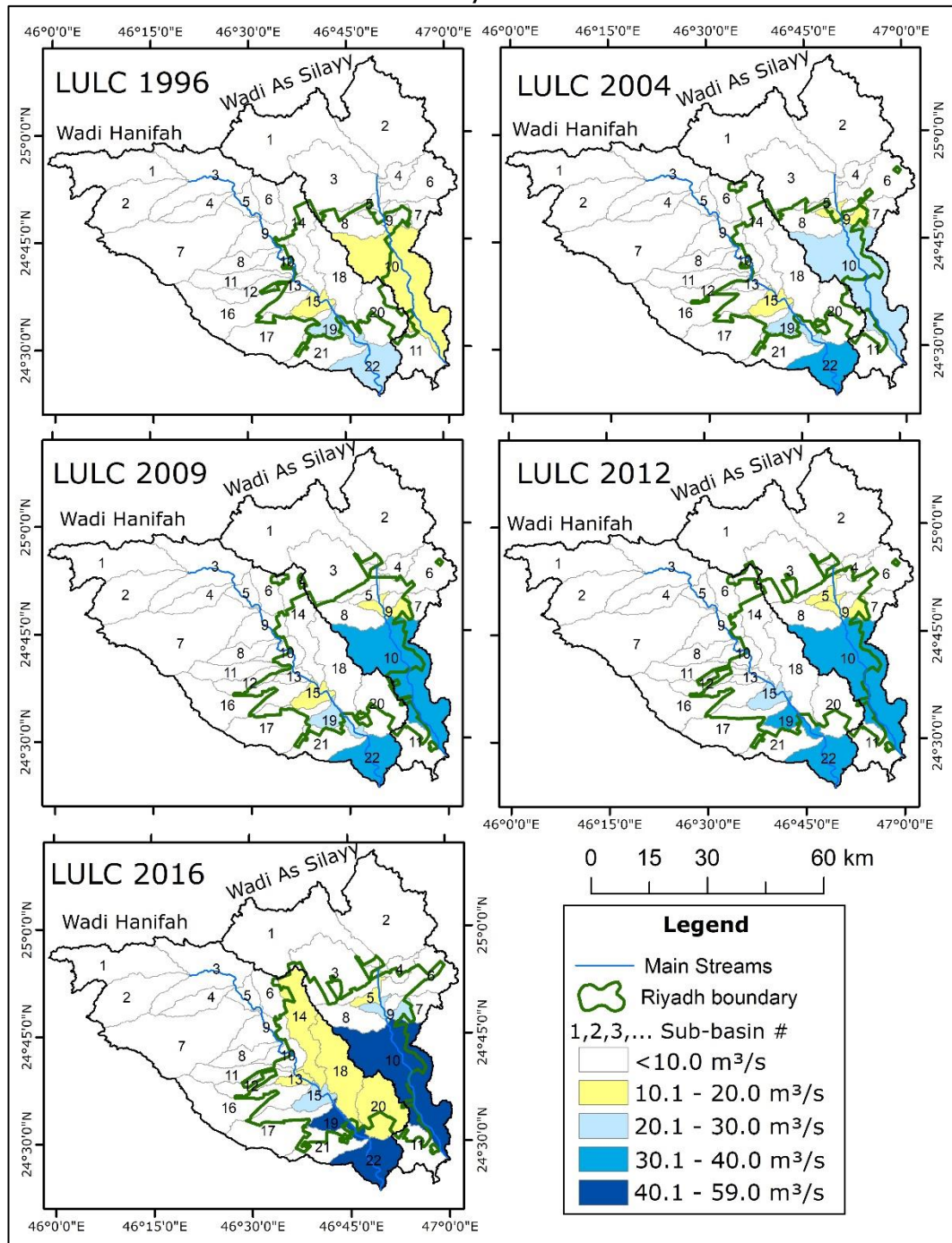
Spatial distributions of simulated annual maximum daily discharge (m^3/s) in the 2-year return periods using different LULC conditions at Riyadh's catchments.



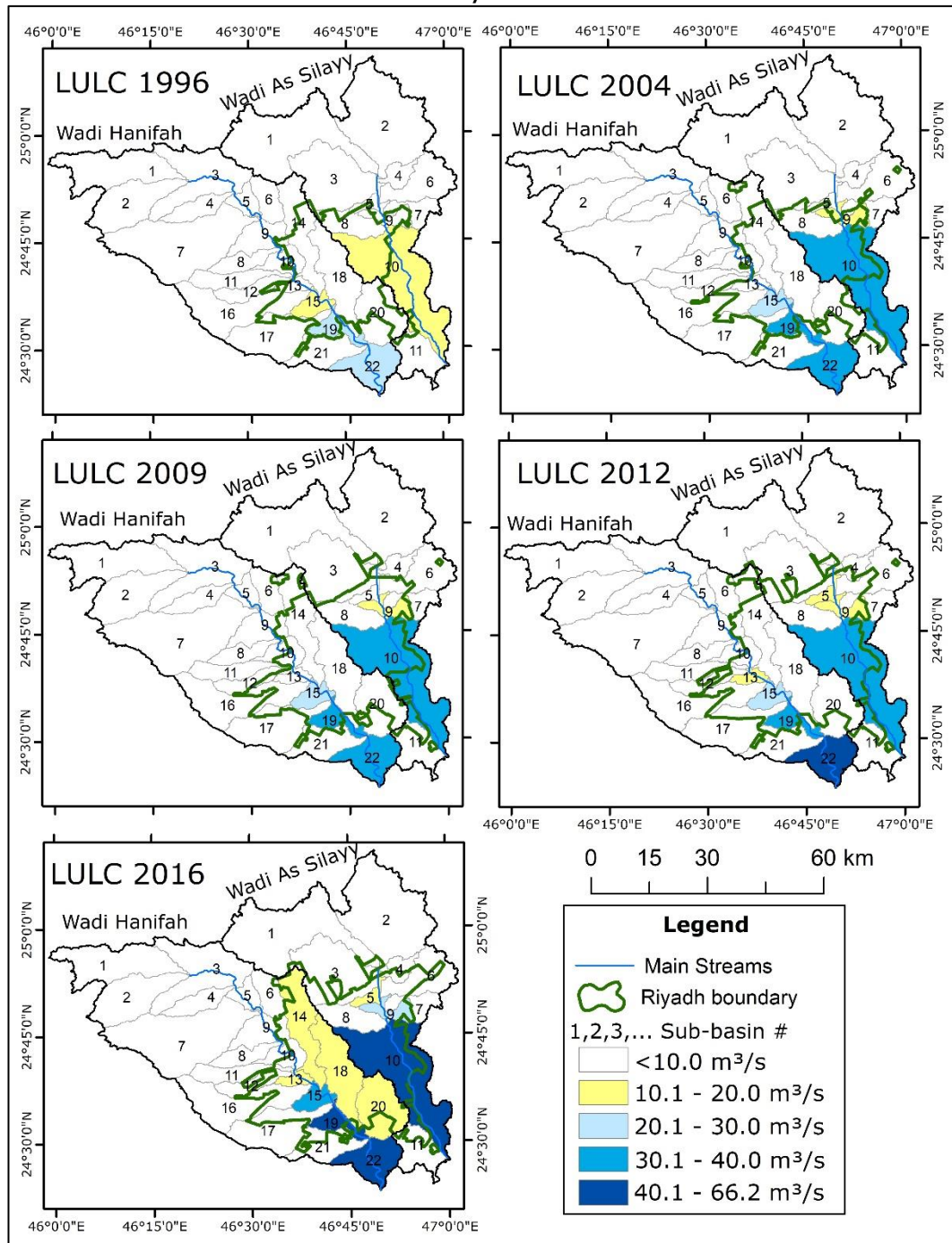
Spatial distributions of simulated annual maximum daily discharge (m^3/s) in the 10-year return periods using different LULC conditions at Riyadh's catchments.



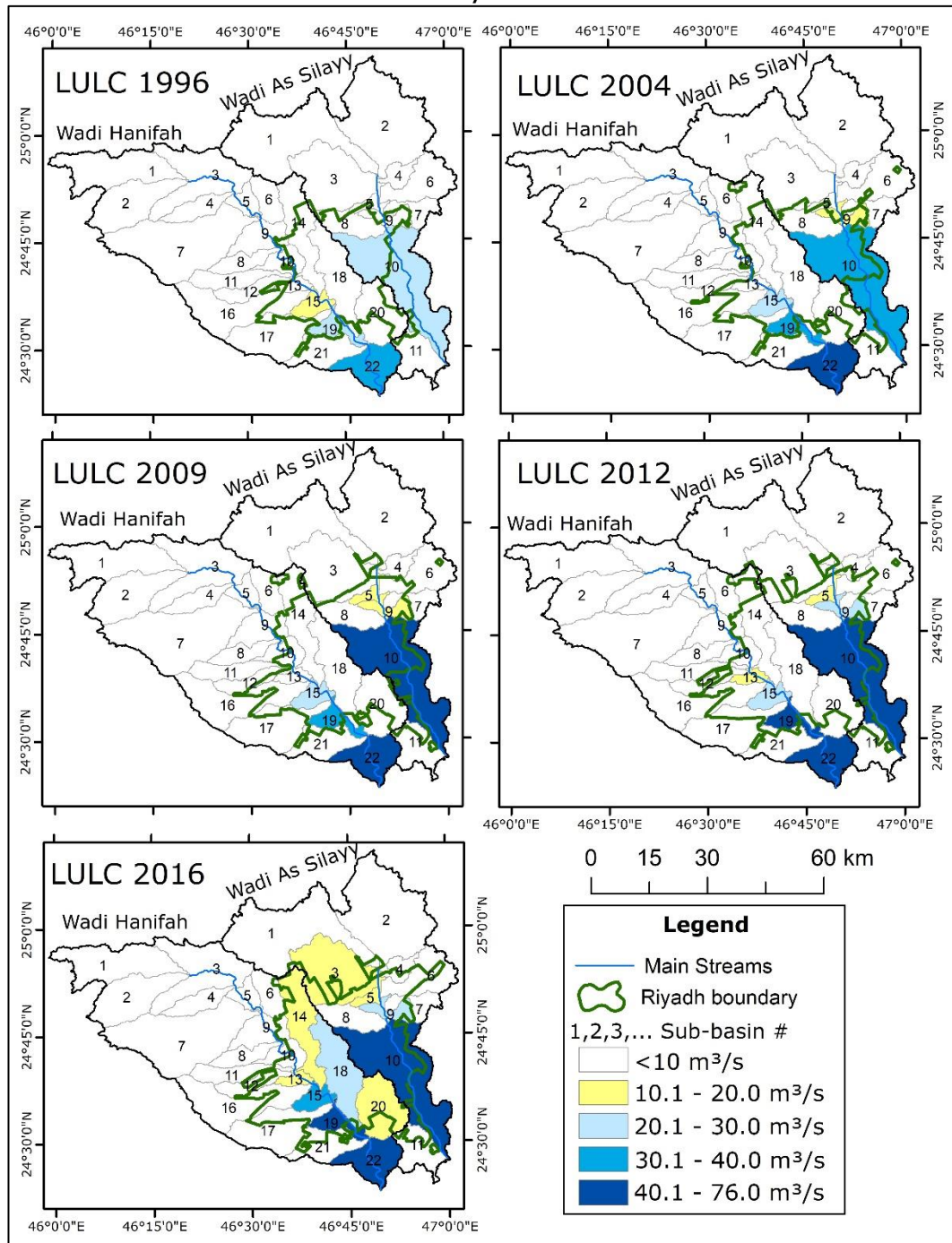
Spatial distributions of simulated annual maximum daily discharge (m^3/s) in the 30-year return periods using different LULC conditions at Riyadh's catchments.



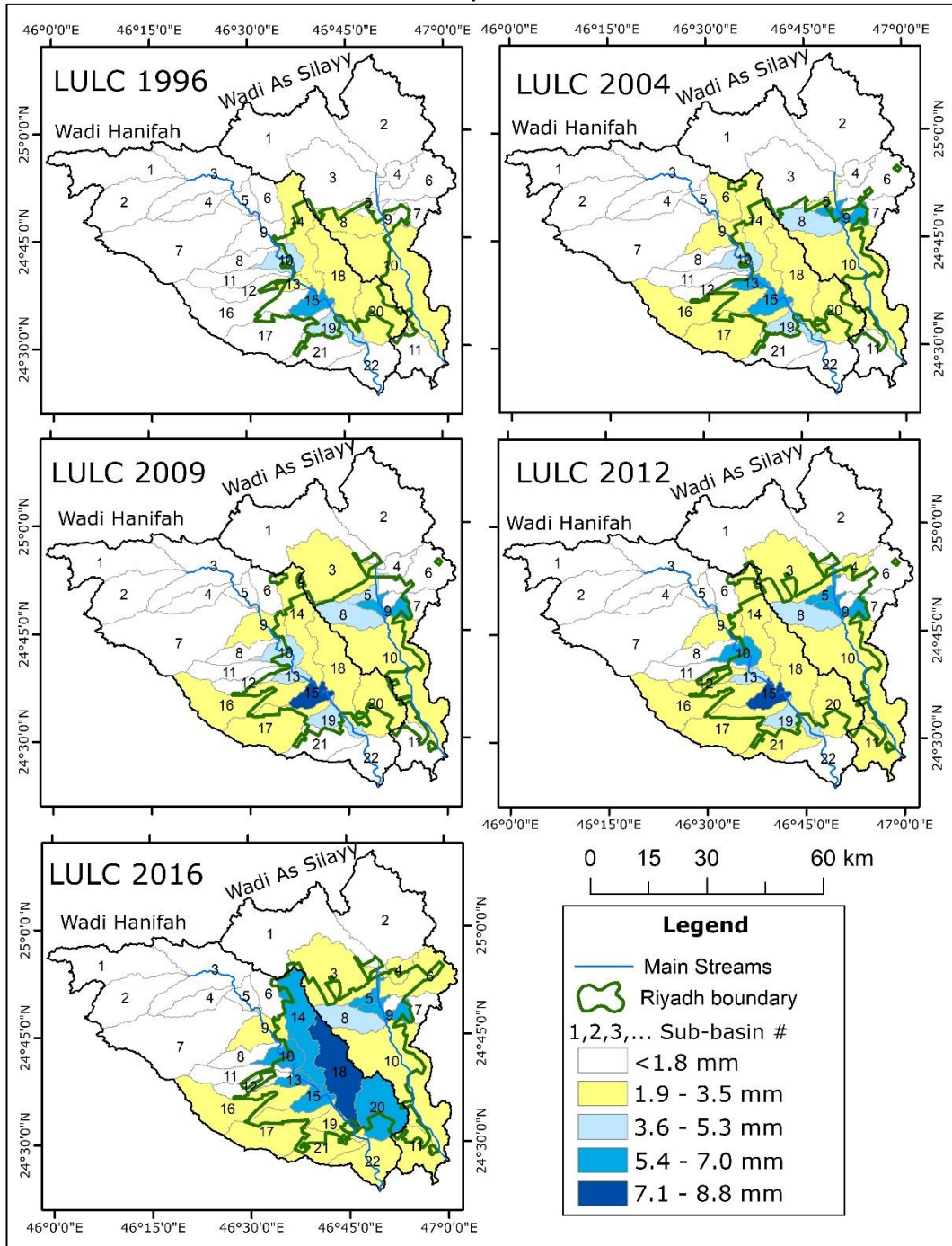
Spatial distributions of simulated annual maximum daily discharge (m^3/s) in the 50-year return periods using different LULC conditions at Riyadh's catchments.



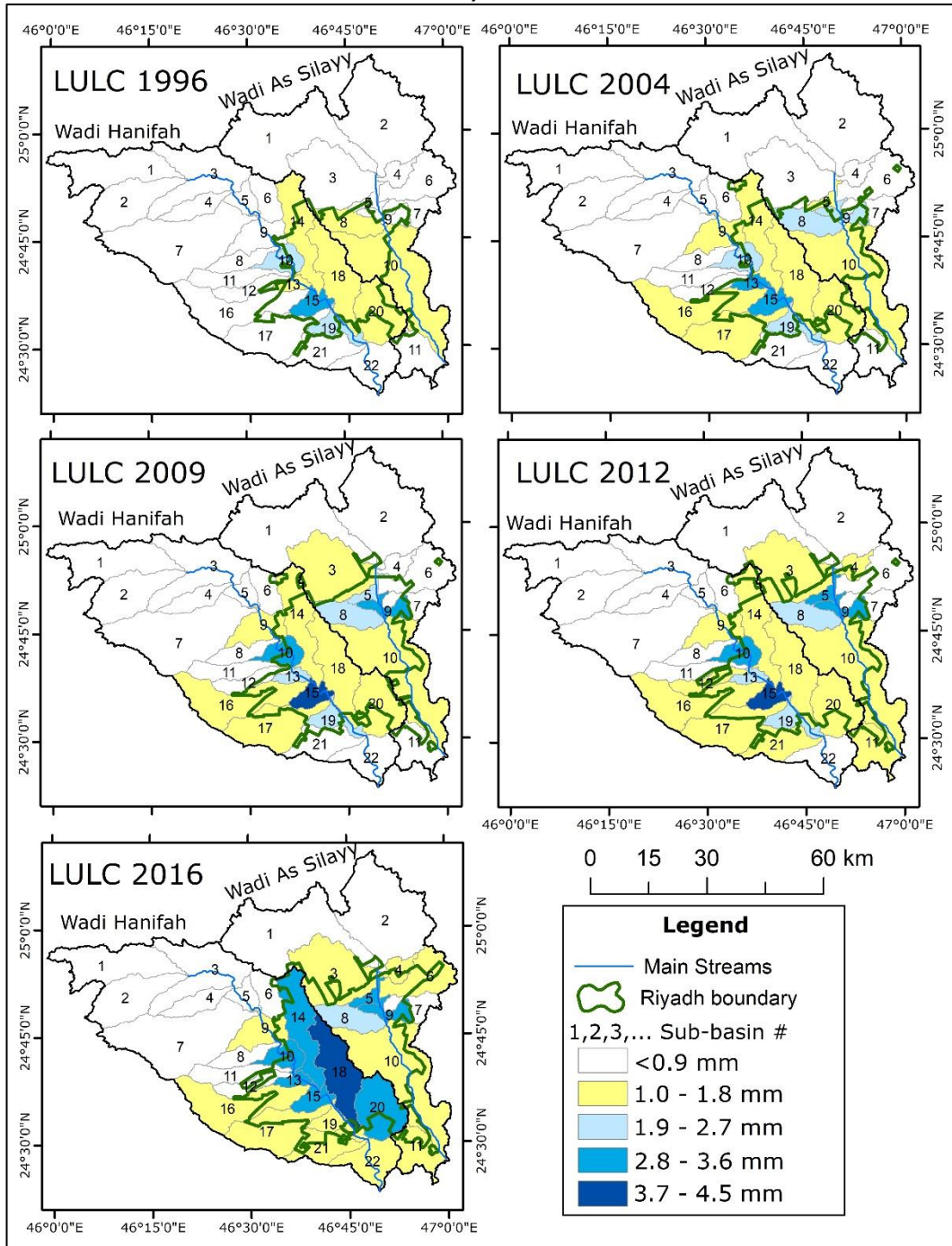
Spatial distributions of simulated annual maximum daily discharge (m^3/s) in the 100-year return periods using different LULC conditions at Riyadh's catchments.



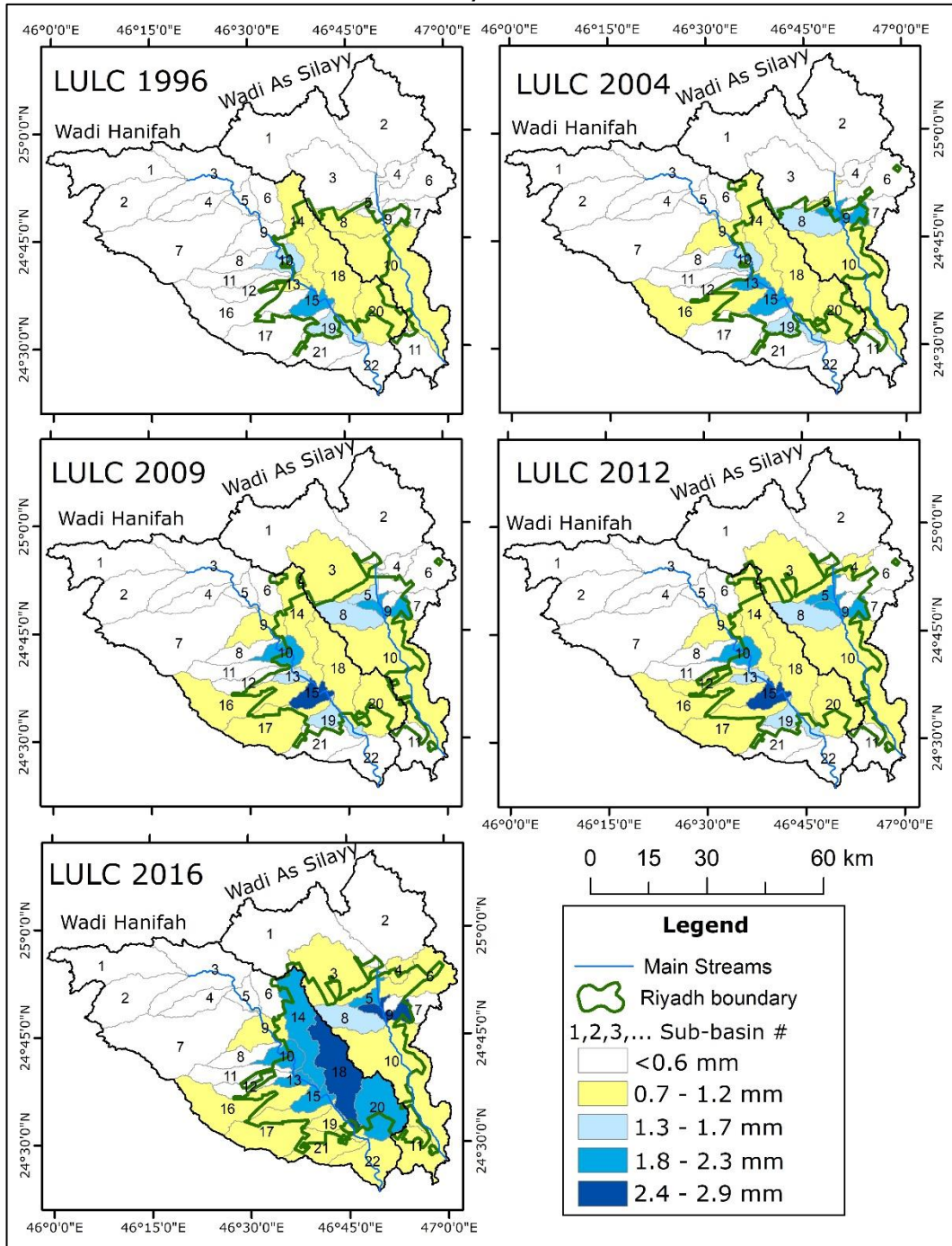
Spatial distributions of simulated annual maximum daily runoff (mm) for percent exceedances of Q1 using different LULC conditions at Riyadh's catchments.



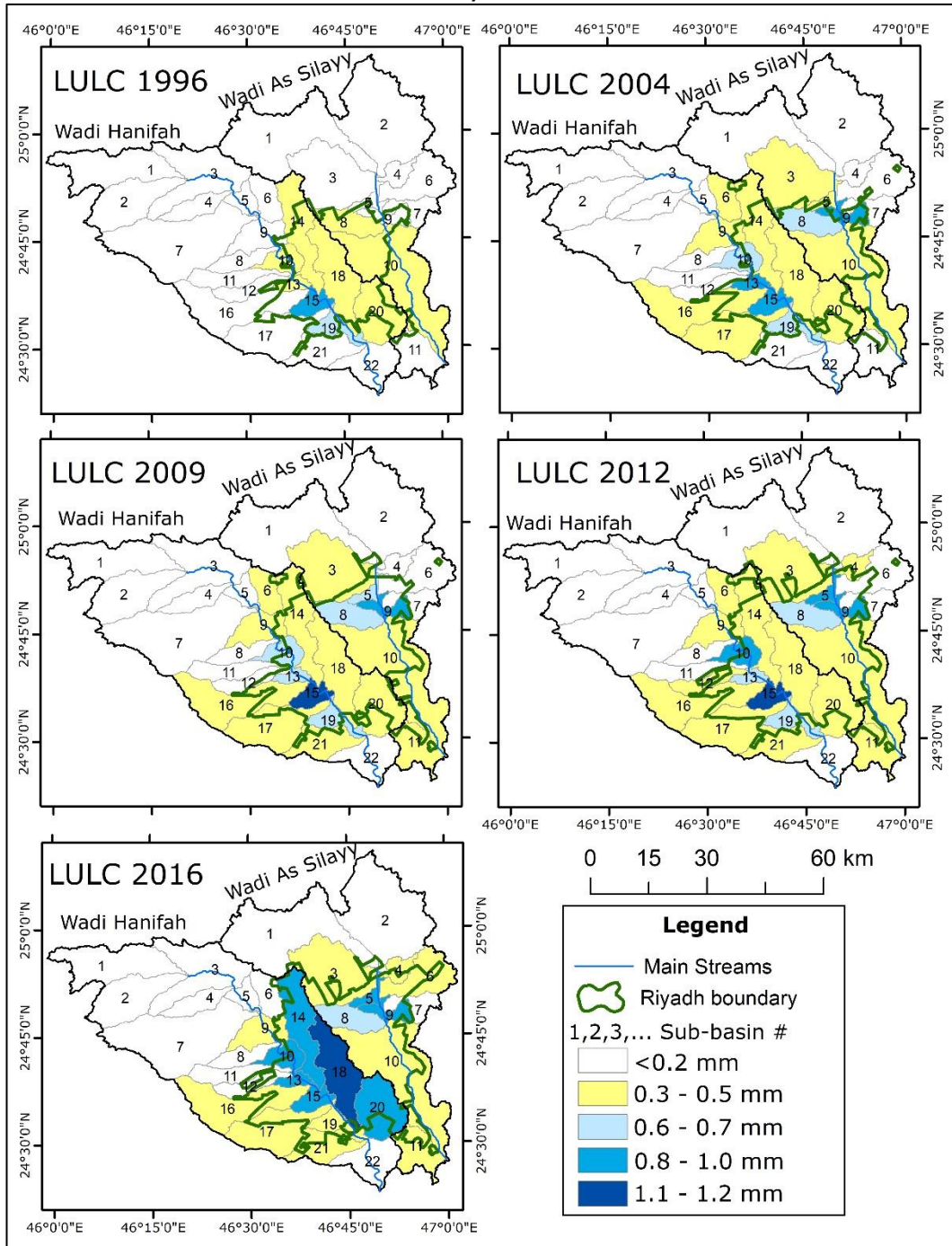
Spatial distributions of simulated annual maximum daily runoff (mm) for percent exceedances of Q25 using different LULC conditions at Riyadh's catchments.



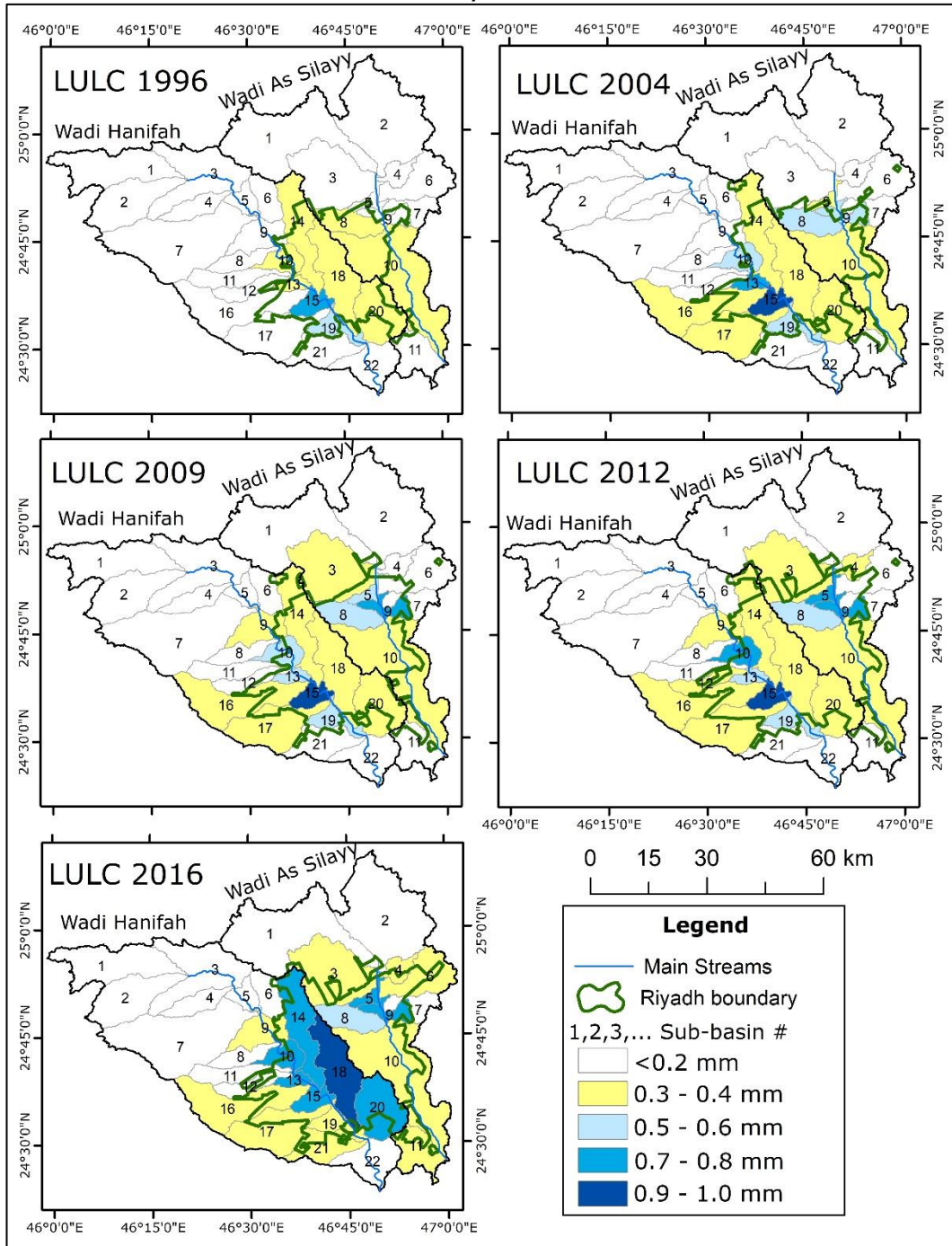
Spatial distributions of simulated annual maximum daily runoff (mm) for percent exceedances of Q50 using different LULC conditions at Riyadh's catchments.



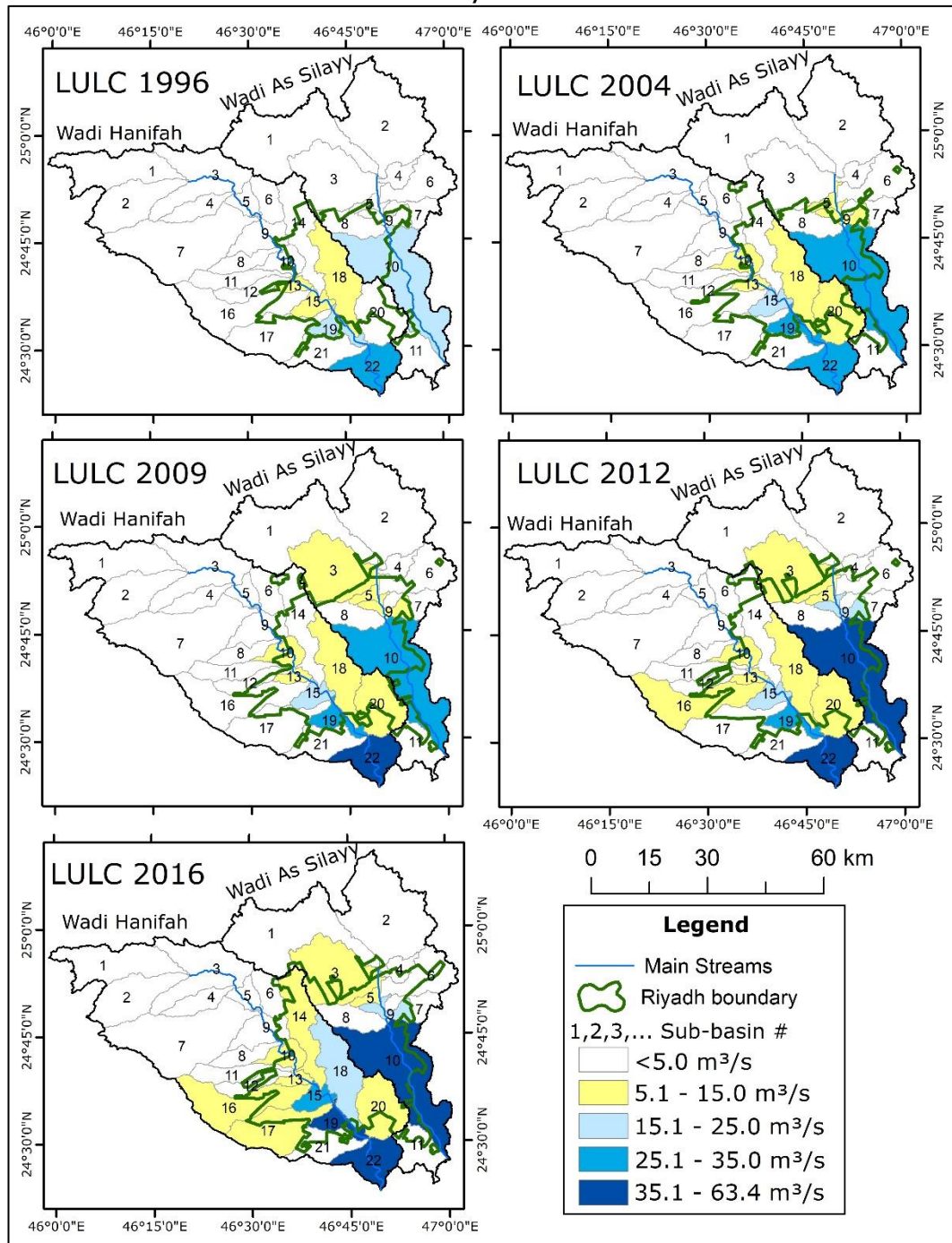
Spatial distributions of simulated annual maximum daily runoff (mm) for percent exceedances of Q85 using different LULC conditions at Riyadh's catchments.



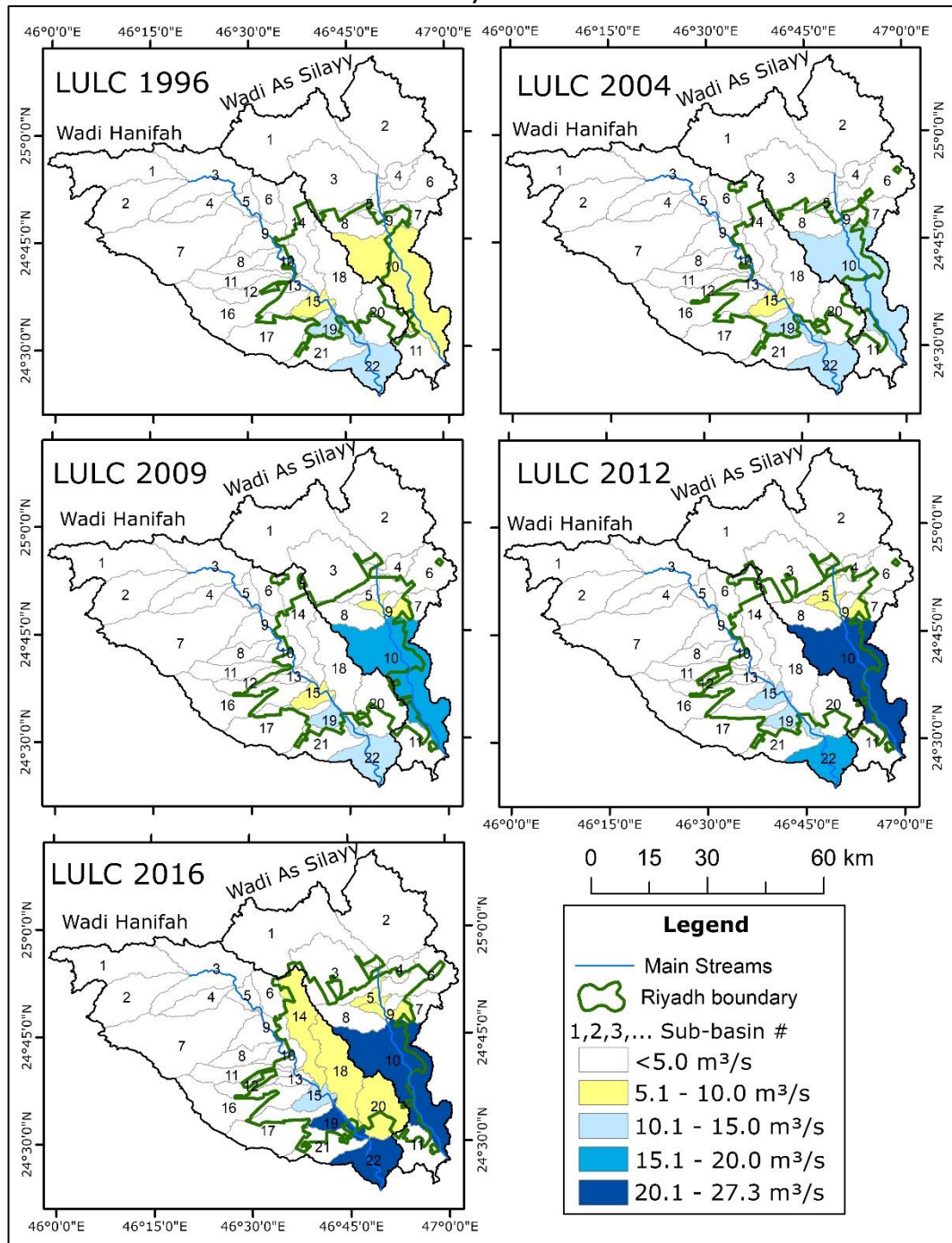
Spatial distributions of simulated annual maximum daily runoff (mm) for percent exceedances of Q99 using different LULC conditions at Riyadh's catchments.



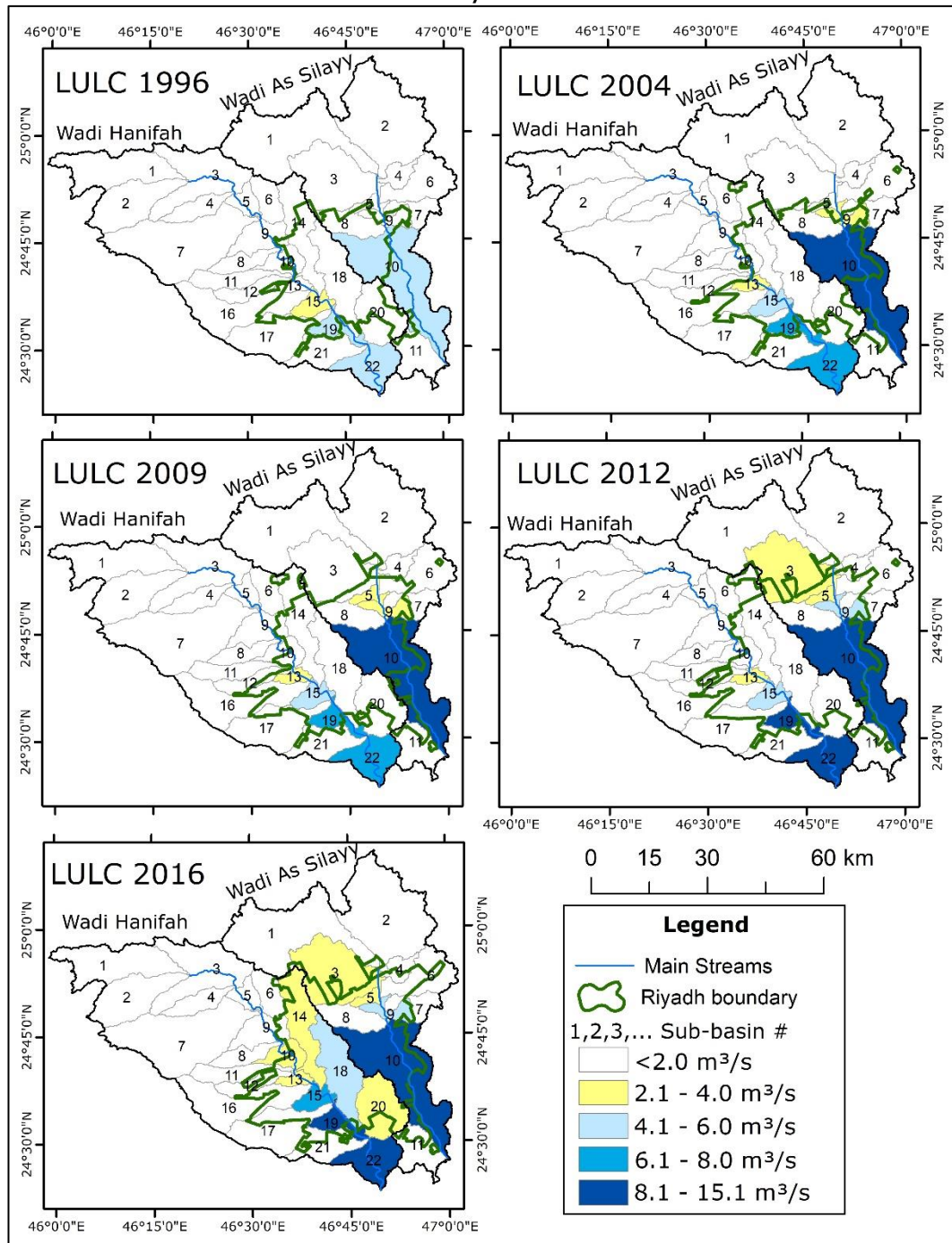
Spatial distributions of simulated annual maximum daily discharge (m^3/s) for percent exceedances of Q1 using different LULC conditions at Riyadh's catchments.



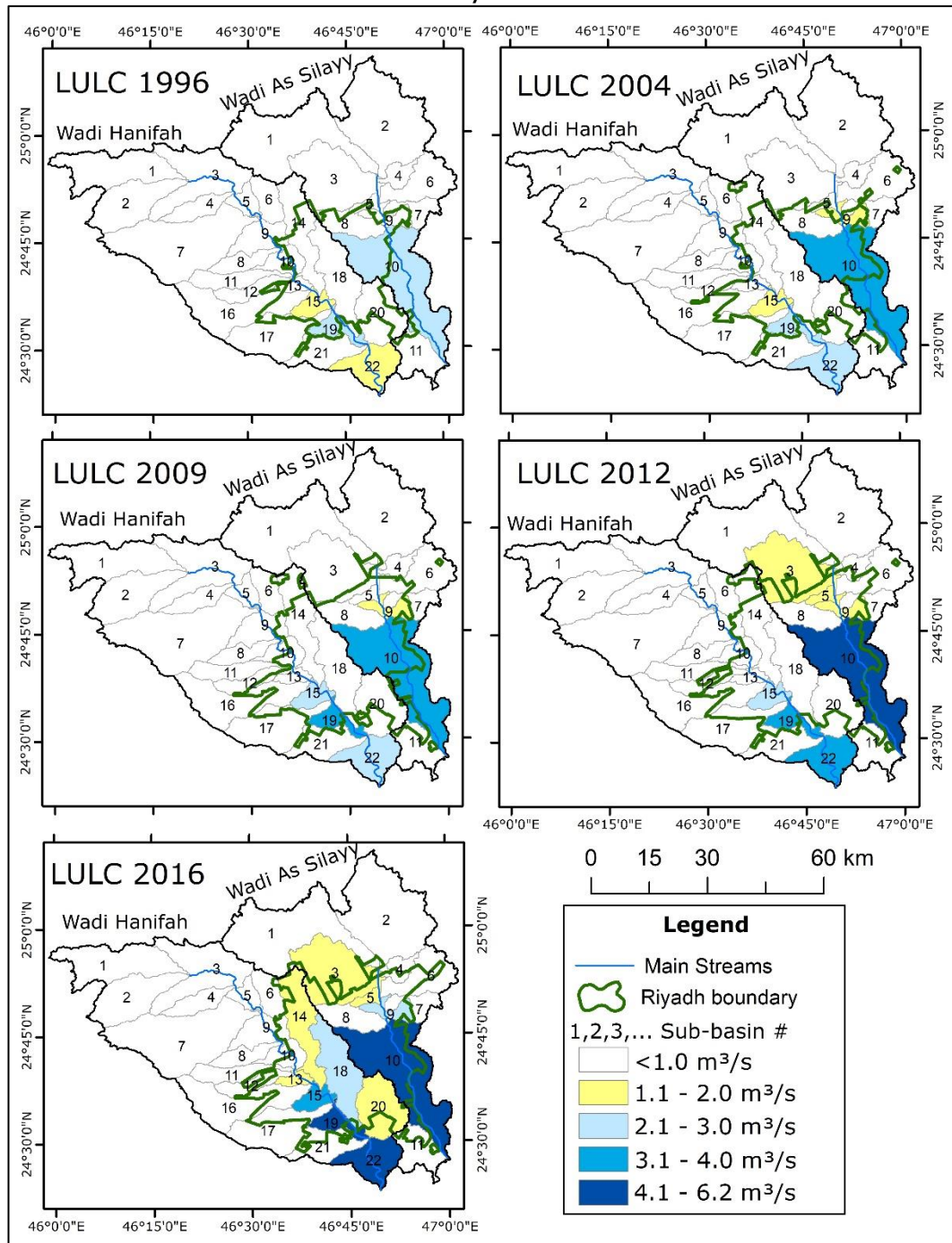
Spatial distributions of simulated annual maximum daily discharge (m³/s) for percent exceedances of Q25 using different LULC conditions at Riyadh's catchments.



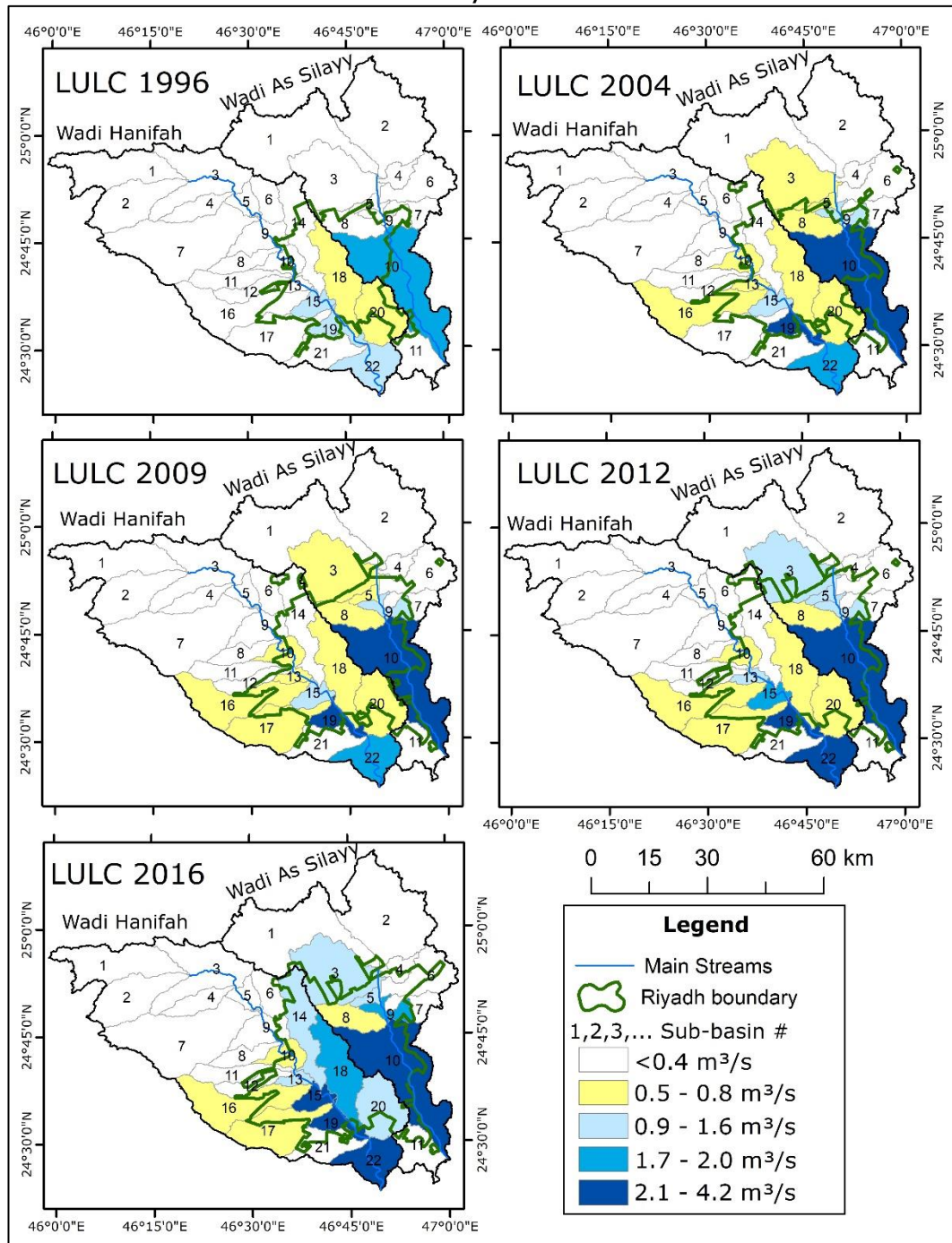
Spatial distributions of simulated annual maximum daily discharge (m^3/s) for percent exceedances of Q50 using different LULC conditions at Riyadh's catchments.



Spatial distributions of simulated annual maximum daily discharge (m^3/s) for percent exceedances of Q85 using different LULC conditions at Riyadh's catchments.



Spatial distributions of simulated annual maximum daily discharge (m³/s) for percent exceedances of Q99 using different LULC conditions at Riyadh's catchments.



Appendix D

Simulated average monthly runoff and discharge under five different probabilities of LULC 2030 scenarios

Average monthly runoff (mm) for the Wadi Hanifah under five different probabilities of LULC 2030 scenarios for the Wadi Hanifah catchment.

Month	Probabilities %	1	2	3	4	5	6	7	8	9	10	11	12	13	14	15	16	17	18	19	20	21	22
Jan	100	0.0	0.0	0.1	0.0	0.0	0.4	0.0	0.8	1.7	5.1	0.8	2.4	5.7	4.8	5.7	2.4	4.7	5.8	5.2	4.9	4.5	3.6
	77	0.0	0.0	0.8	0.8	1.8	0.8	0.0	0.8	1.7	5.1	0.8	2.4	5.7	4.8	5.7	3.3	4.7	5.8	5.2	4.9	4.5	3.6
	75	0.0	0.0	1.7	0.9	1.8	3.4	0.0	0.8	1.8	5.1	0.8	2.4	5.7	5.4	5.7	3.3	5.1	5.8	5.2	4.9	4.6	3.6
	49	0.0	0.0	1.7	0.9	2.1	3.4	0.2	1.8	3.1	5.1	0.8	2.4	5.7	5.4	5.7	3.3	5.1	5.8	5.2	4.9	4.6	4.0
	3	0.4	0.2	2.4	0.9	2.9	3.6	0.7	3.0	3.2	5.1	1.6	2.4	5.7	5.4	5.7	4.1	5.4	5.8	5.2	4.9	4.6	4.2
Feb	100	0.0	0.0	0.0	0.0	0.0	0.1	0.0	0.1	0.2	0.9	0.1	0.4	1.0	1.5	1.0	0.4	1.1	1.9	1.1	1.5	1.4	0.9
	77	0.0	0.0	0.1	0.1	0.2	0.1	0.0	0.1	0.2	0.9	0.1	0.4	1.0	1.5	1.0	0.6	1.1	1.9	1.1	1.5	1.4	0.9
	75	0.0	0.0	0.2	0.1	0.2	0.7	0.0	0.1	0.2	0.9	0.1	0.4	1.0	2.0	1.0	0.6	1.3	1.9	1.1	1.5	1.4	0.9
	49	0.0	0.0	0.2	0.1	0.3	0.7	0.0	0.3	0.4	0.9	0.1	0.4	1.0	2.0	1.0	0.6	1.3	1.9	1.1	1.5	1.4	1.1
	3	0.3	0.2	0.4	0.1	0.4	0.8	0.1	0.6	0.4	0.9	0.3	0.4	1.0	2.0	1.0	0.9	1.4	1.9	1.1	1.5	1.4	1.2
Mar	100	0.0	0.0	0.2	0.0	0.0	0.8	0.0	1.4	3.0	8.5	1.5	4.1	9.6	6.6	8.5	4.1	7.0	8.0	7.3	6.3	5.8	4.9
	77	0.0	0.0	1.4	1.3	3.0	1.4	0.0	1.4	3.0	8.5	1.5	4.1	9.6	6.6	8.5	5.2	7.0	8.0	7.3	6.3	5.8	4.9
	75	0.0	0.1	2.9	1.5	3.0	4.8	0.0	1.4	3.1	8.5	1.5	4.1	9.6	7.3	8.5	5.2	7.4	8.0	7.3	6.3	5.9	4.9
	49	0.0	0.1	2.9	1.5	3.4	4.8	0.3	3.1	5.2	8.5	1.5	4.1	9.6	7.3	8.5	5.2	7.4	8.0	7.3	6.3	5.9	5.3
	3	2.3	1.4	3.9	1.5	4.6	5.1	1.2	4.8	5.3	8.5	2.7	4.1	9.6	7.3	8.5	6.2	7.6	8.0	7.3	6.3	5.9	5.5

Average monthly runoff (mm) for the Wadi Hanifah under five different probabilities of LULC 2030 scenarios for the Wadi Hanifah catchment. (Continued)

Month	Probabilities %	1	2	3	4	5	6	7	8	9	10	11	12	13	14	15	16	17	18	19	20	21	22
Apr	100	0.0	0.0	0.1	0.0	0.0	0.4	0.0	0.8	1.5	5.5	0.9	2.5	6.1	6.0	6.0	2.6	5.4	7.2	5.6	5.6	5.1	4.0
	77	0.0	0.0	0.7	0.7	1.6	0.7	0.0	0.8	1.5	5.5	0.9	2.6	6.1	6.0	6.0	3.6	5.4	7.2	5.6	5.6	5.1	4.0
	75	0.0	0.1	1.5	0.8	1.6	3.6	0.0	0.8	1.5	5.5	0.9	2.6	6.1	7.1	6.0	3.6	5.9	7.2	5.6	5.6	5.2	4.0
	49	0.0	0.1	1.5	0.8	1.9	3.6	0.2	2.0	2.7	5.5	0.9	2.6	6.1	7.1	6.0	3.6	5.9	7.2	5.6	5.6	5.2	4.5
	3	1.0	0.5	2.3	0.8	2.7	3.8	0.6	3.2	2.8	5.5	1.7	2.6	6.1	7.1	6.0	4.6	6.2	7.2	5.6	5.6	5.2	4.7
May	100	0.0	0.0	0.0	0.0	0.0	0.0	0.0	0.2	0.2	1.8	0.2	0.7	1.9	4.9	2.2	0.8	2.4	5.9	2.6	3.2	2.9	2.0
	77	0.0	0.0	0.1	0.1	0.3	0.1	0.0	0.2	0.2	1.8	0.2	0.7	1.9	4.9	2.2	1.3	2.4	5.9	2.6	3.2	2.9	2.0
	75	0.0	0.0	0.3	0.1	0.3	1.1	0.0	0.2	0.2	1.8	0.2	0.7	1.9	5.9	2.2	1.3	2.8	5.9	2.6	3.2	3.0	2.0
	49	0.0	0.0	0.3	0.1	0.4	1.1	0.0	0.6	0.4	1.8	0.2	0.7	1.9	5.9	2.2	1.3	2.8	5.9	2.6	3.2	3.0	2.4
	3	0.2	0.1	0.5	0.1	0.6	1.2	0.1	1.2	0.5	1.8	0.5	0.7	1.9	5.9	2.2	2.0	3.0	5.9	2.6	3.2	3.0	2.6
Jun	100	0.0	0.0	0.0	0.0	0.0	0.0	0.0	0.0	0.0	0.0	0.0	0.0	0.0	0.7	0.0	0.0	0.1	0.9	0.1	0.3	0.3	0.1
	77	0.0	0.0	0.0	0.0	0.0	0.0	0.0	0.0	0.0	0.0	0.0	0.0	0.0	0.7	0.0	0.0	0.1	0.9	0.1	0.3	0.3	0.1
	75	0.0	0.0	0.0	0.0	0.0	0.1	0.0	0.0	0.0	0.0	0.0	0.0	0.0	1.2	0.0	0.0	0.2	0.9	0.1	0.3	0.3	0.1
	49	0.0	0.0	0.0	0.0	0.0	0.1	0.0	0.0	0.0	0.0	0.0	0.0	0.0	1.2	0.0	0.0	0.2	0.9	0.1	0.3	0.3	0.2
	3	0.0	0.0	0.0	0.0	0.0	0.1	0.0	0.0	0.0	0.0	0.0	0.0	0.0	1.2	0.0	0.1	0.2	0.9	0.1	0.3	0.3	0.2
Jul	100	0.0	0.0	0.0	0.0	0.0	0.0	0.0	0.0	0.0	0.0	0.0	0.0	0.0	0.1	0.0	0.0	0.0	0.2	0.0	0.1	0.0	0.0
	77	0.0	0.0	0.0	0.0	0.0	0.0	0.0	0.0	0.0	0.0	0.0	0.0	0.0	0.1	0.0	0.0	0.0	0.2	0.0	0.1	0.0	0.0
	75	0.0	0.0	0.0	0.0	0.0	0.0	0.0	0.0	0.0	0.0	0.0	0.0	0.0	0.3	0.0	0.0	0.0	0.2	0.0	0.1	0.0	0.0
	49	0.0	0.0	0.0	0.0	0.0	0.0	0.0	0.0	0.0	0.0	0.0	0.0	0.0	0.3	0.0	0.0	0.0	0.2	0.0	0.1	0.0	0.0
	3	0.0	0.0	0.0	0.0	0.0	0.0	0.0	0.0	0.0	0.0	0.0	0.0	0.0	0.3	0.0	0.0	0.0	0.2	0.0	0.1	0.0	0.0

Average monthly runoff (mm) for the Wadi Hanifah under five different probabilities of LULC 2030 scenarios for the Wadi Hanifah catchment. (Continued)

Month	Probabilities %	1	2	3	4	5	6	7	8	9	10	11	12	13	14	15	16	17	18	19	20	21	22	
Aug	100	0.0	0.0	0.0	0.0	0.0	0.0	0.0	0.0	0.0	0.0	0.0	0.0	0.0	0.1	0.0	0.0	0.0	0.1	0.0	0.0	0.0	0.0	0.0
	77	0.0	0.0	0.0	0.0	0.0	0.0	0.0	0.0	0.0	0.0	0.0	0.0	0.0	0.1	0.0	0.0	0.0	0.1	0.0	0.0	0.0	0.0	0.0
	75	0.0	0.0	0.0	0.0	0.0	0.0	0.0	0.0	0.0	0.0	0.0	0.0	0.0	0.1	0.0	0.0	0.0	0.1	0.0	0.0	0.0	0.0	0.0
	49	0.0	0.0	0.0	0.0	0.0	0.0	0.0	0.0	0.0	0.0	0.0	0.0	0.0	0.1	0.0	0.0	0.0	0.1	0.0	0.0	0.0	0.0	0.0
	3	0.0	0.0	0.0	0.0	0.0	0.0	0.0	0.0	0.0	0.0	0.0	0.0	0.0	0.1	0.0	0.0	0.0	0.1	0.0	0.0	0.0	0.0	0.0
Sep	100	0.0	0.0	0.0	0.0	0.0	0.0	0.0	0.0	0.0	0.0	0.0	0.0	0.0	0.1	0.0	0.0	0.0	0.1	0.0	0.0	0.0	0.0	0.0
	77	0.0	0.0	0.0	0.0	0.0	0.0	0.0	0.0	0.0	0.0	0.0	0.0	0.0	0.1	0.0	0.0	0.0	0.1	0.0	0.0	0.0	0.0	0.0
	75	0.0	0.0	0.0	0.0	0.0	0.0	0.0	0.0	0.0	0.0	0.0	0.0	0.0	0.1	0.0	0.0	0.0	0.1	0.0	0.0	0.0	0.0	0.0
	49	0.0	0.0	0.0	0.0	0.0	0.0	0.0	0.0	0.0	0.0	0.0	0.0	0.0	0.1	0.0	0.0	0.0	0.1	0.0	0.0	0.0	0.0	0.0
	3	0.0	0.0	0.0	0.0	0.0	0.0	0.0	0.0	0.0	0.0	0.0	0.0	0.0	0.1	0.0	0.0	0.0	0.1	0.0	0.0	0.0	0.0	0.0
Oct	100	0.0	0.0	0.0	0.0	0.0	0.2	0.0	0.1	0.6	0.5	0.1	0.3	0.6	0.1	0.8	0.3	0.4	0.1	0.6	0.5	0.4	0.4	0.4
	77	0.0	0.0	0.3	0.2	0.5	0.3	0.0	0.1	0.6	0.5	0.1	0.3	0.6	0.1	0.8	0.3	0.4	0.1	0.6	0.5	0.4	0.4	0.4
	75	0.0	0.0	0.5	0.3	0.5	0.6	0.0	0.1	0.6	0.5	0.1	0.3	0.6	0.1	0.8	0.3	0.4	0.1	0.6	0.5	0.4	0.4	0.4
	49	0.0	0.0	0.5	0.3	0.5	0.6	0.1	0.2	0.9	0.5	0.1	0.3	0.6	0.1	0.8	0.3	0.4	0.1	0.6	0.5	0.4	0.4	0.4
	3	0.0	0.0	0.6	0.3	0.7	0.7	0.2	0.3	0.9	0.5	0.2	0.3	0.6	0.1	0.8	0.4	0.4	0.1	0.6	0.5	0.4	0.4	0.4
Nov	100	0.0	0.0	0.2	0.0	0.0	0.7	0.0	0.4	2.9	2.7	0.4	1.2	3.0	3.1	3.5	1.3	2.5	3.7	3.3	3.1	2.8	2.3	2.3
	77	0.0	0.0	1.3	1.3	3.1	1.4	0.0	0.4	2.9	2.7	0.4	1.2	3.0	3.1	3.5	1.7	2.5	3.7	3.3	3.1	2.8	2.3	2.3
	75	0.0	0.1	2.9	1.5	3.1	5.7	0.0	0.4	3.0	2.7	0.4	1.2	3.0	3.4	3.5	1.7	2.7	3.7	3.3	3.1	2.9	2.3	2.3
	49	0.0	0.1	2.9	1.5	3.6	5.7	0.3	1.0	5.3	2.7	0.4	1.2	3.0	3.4	3.5	1.7	2.7	3.7	3.3	3.1	2.9	2.5	2.5
	3	1.4	0.9	4.2	1.5	5.0	6.1	1.2	1.6	5.4	2.7	0.8	1.2	3.0	3.4	3.5	2.2	2.8	3.7	3.3	3.1	2.9	2.6	2.6

Average monthly runoff (mm) for the Wadi Hanifah under five different probabilities of LULC 2030 scenarios for the Wadi Hanifah catchment. (Continued)

Month	Probabilities %	1	2	3	4	5	6	7	8	9	10	11	12	13	14	15	16	17	18	19	20	21	22
Dec	100	0.0	0.0	0.0	0.0	0.0	0.1	0.0	0.4	0.6	2.5	0.4	1.2	2.9	2.2	2.9	1.2	2.2	2.6	2.6	2.5	2.3	1.8
	77	0.0	0.0	0.3	0.3	0.6	0.3	0.0	0.4	0.6	2.5	0.4	1.2	2.9	2.2	2.9	1.6	2.2	2.6	2.6	2.5	2.3	1.8
	75	0.0	0.0	0.6	0.3	0.6	1.6	0.0	0.4	0.6	2.5	0.4	1.2	2.9	2.5	2.9	1.6	2.4	2.6	2.6	2.5	2.3	1.8
	49	0.0	0.0	0.6	0.3	0.8	1.6	0.1	0.9	1.1	2.5	0.4	1.2	2.9	2.5	2.9	1.6	2.4	2.6	2.6	2.5	2.3	2.0
	3	0.7	0.4	0.9	0.3	1.1	1.7	0.2	1.5	1.1	2.5	0.8	1.2	2.9	2.5	2.9	1.9	2.5	2.6	2.6	2.5	2.3	2.1

Average monthly discharge (m³/s) for the Wadi Hanifah under five different probabilities of LULC 2030 scenarios for the Wadi Hanifah catchment.

Month	Probabilities %	1	2	3	4	5	6	7	8	9	10	11	12	13	14	15	16	17	18	19	20	21	22
		Jan	100	0.03	0.03	0.12	0.01	0.12	0.02	0.17	0.03	0.36	0.50	0.04	0.07	0.65	0.29	1.30	0.28	0.34	0.40	2.11	0.31
77	0.03		0.03	0.20	0.03	0.25	0.03	0.17	0.03	0.50	0.64	0.04	0.07	0.79	0.29	1.50	0.34	0.34	0.40	2.31	0.31	0.19	2.94
75	0.03		0.03	0.28	0.03	0.34	0.09	0.17	0.03	0.66	0.79	0.04	0.07	0.94	0.32	1.69	0.34	0.37	0.40	2.52	0.31	0.19	3.15
49	0.03		0.03	0.28	0.03	0.34	0.09	0.21	0.05	0.74	0.90	0.04	0.07	1.05	0.32	1.80	0.34	0.37	0.40	2.63	0.31	0.19	3.28
3	0.07		0.05	0.40	0.03	0.47	0.10	0.31	0.08	0.99	1.17	0.06	0.07	1.34	0.32	2.16	0.42	0.38	0.40	3.01	0.31	0.19	3.66
Feb	100	0.02	0.03	0.09	0.01	0.09	0.01	0.18	0.02	0.26	0.27	0.02	0.02	0.31	0.09	0.51	0.11	0.09	0.14	0.72	0.11	0.07	0.89
	77	0.02	0.03	0.12	0.01	0.12	0.01	0.18	0.02	0.29	0.31	0.02	0.02	0.35	0.09	0.55	0.12	0.09	0.14	0.76	0.11	0.07	0.93
	75	0.02	0.03	0.13	0.01	0.13	0.03	0.18	0.02	0.31	0.33	0.02	0.02	0.37	0.12	0.60	0.12	0.10	0.14	0.82	0.11	0.07	1.00
	49	0.02	0.03	0.13	0.01	0.13	0.03	0.18	0.02	0.33	0.35	0.02	0.02	0.39	0.12	0.62	0.12	0.10	0.14	0.84	0.11	0.07	1.02
	3	0.06	0.05	0.19	0.01	0.19	0.02	0.22	0.02	0.42	0.45	0.02	0.02	0.49	0.12	0.75	0.15	0.10	0.14	0.98	0.11	0.07	1.17
Mar	100	0.01	0.03	0.09	0.01	0.08	0.03	0.16	0.04	0.34	0.54	0.06	0.10	0.78	0.38	1.67	0.40	0.49	0.53	2.77	0.39	0.24	3.52
	77	0.01	0.03	0.21	0.04	0.28	0.04	0.16	0.04	0.56	0.76	0.06	0.11	1.00	0.38	1.97	0.49	0.49	0.53	3.07	0.39	0.24	3.83
	75	0.01	0.04	0.35	0.05	0.43	0.13	0.16	0.04	0.79	0.99	0.06	0.11	1.23	0.41	2.24	0.49	0.51	0.53	3.35	0.39	0.25	4.11
	49	0.01	0.04	0.35	0.05	0.44	0.13	0.22	0.08	0.93	1.16	0.06	0.11	1.40	0.41	2.41	0.49	0.51	0.53	3.53	0.39	0.25	4.30
	3	0.22	0.13	0.73	0.05	0.83	0.13	0.39	0.12	1.49	1.76	0.09	0.11	2.03	0.41	3.12	0.57	0.53	0.53	4.25	0.39	0.25	5.03

Average monthly discharge (m³/s) for the Wadi Hanifah under five different probabilities of LULC 2030 scenarios for the Wadi Hanifah catchment. (Continued)

Month	Probabilities %	1	2	3	4	5	6	7	8	9	10	11	12	13	14	15	16	17	18	19	20	21	22
		Apr	100	0.01	0.03	0.08	0.01	0.07	0.02	0.17	0.03	0.26	0.39	0.04	0.07	0.55	0.36	1.26	0.29	0.39	0.50	2.20	0.35
77	0.01		0.03	0.16	0.03	0.19	0.03	0.17	0.03	0.39	0.52	0.04	0.07	0.68	0.36	1.47	0.37	0.39	0.50	2.42	0.35	0.22	3.09
75	0.01		0.03	0.23	0.03	0.26	0.10	0.17	0.03	0.54	0.67	0.04	0.07	0.83	0.42	1.69	0.37	0.42	0.50	2.66	0.35	0.22	3.34
49	0.01		0.03	0.23	0.03	0.27	0.10	0.20	0.06	0.63	0.78	0.04	0.07	0.94	0.42	1.80	0.37	0.42	0.50	2.77	0.35	0.22	3.47
3	0.11		0.07	0.43	0.03	0.48	0.10	0.32	0.09	0.96	1.15	0.07	0.07	1.32	0.42	2.27	0.46	0.45	0.50	3.26	0.35	0.22	3.98
May	100	0.01	0.03	0.06	0.01	0.05	0.01	0.17	0.02	0.18	0.21	0.02	0.03	0.25	0.28	0.66	0.13	0.17	0.40	1.23	0.20	0.12	1.59
	77	0.01	0.03	0.09	0.01	0.08	0.01	0.17	0.02	0.21	0.24	0.02	0.03	0.29	0.28	0.75	0.18	0.17	0.40	1.31	0.20	0.12	1.68
	75	0.01	0.03	0.10	0.01	0.09	0.03	0.17	0.02	0.25	0.28	0.02	0.03	0.32	0.33	0.84	0.18	0.19	0.40	1.43	0.20	0.13	1.79
	49	0.01	0.03	0.10	0.01	0.09	0.03	0.18	0.03	0.27	0.31	0.02	0.03	0.36	0.33	0.87	0.18	0.19	0.40	1.46	0.20	0.13	1.84
	3	0.03	0.04	0.15	0.01	0.14	0.03	0.22	0.04	0.37	0.42	0.03	0.03	0.47	0.33	1.04	0.23	0.20	0.40	1.64	0.20	0.13	2.04
Jun	100	0.01	0.03	0.05	0.01	0.04	0.01	0.15	0.01	0.15	0.12	0.01	0.01	0.12	0.03	0.16	0.05	0.01	0.05	0.17	0.02	0.01	0.15
	77	0.01	0.03	0.07	0.01	0.05	0.01	0.15	0.01	0.16	0.14	0.01	0.01	0.14	0.03	0.18	0.05	0.01	0.05	0.19	0.02	0.01	0.17
	75	0.01	0.03	0.06	0.01	0.05	0.00	0.15	0.01	0.16	0.13	0.01	0.01	0.13	0.05	0.19	0.05	0.01	0.05	0.20	0.02	0.01	0.18
	49	0.01	0.03	0.06	0.01	0.05	0.00	0.16	0.01	0.16	0.14	0.01	0.01	0.14	0.05	0.19	0.05	0.01	0.05	0.20	0.02	0.01	0.18
	3	0.02	0.03	0.07	0.01	0.05	0.00	0.18	0.01	0.18	0.16	0.01	0.01	0.15	0.05	0.21	0.05	0.01	0.05	0.21	0.02	0.01	0.20

Average monthly discharge (m³/s) for the Wadi Hanifah under five different probabilities of LULC 2030 scenarios for the Wadi Hanifah catchment. (Continued)

Month	Probabilities %	1	2	3	4	5	6	7	8	9	10	11	12	13	14	15	16	17	18	19	20	21	22
		Jul	100	0.01	0.03	0.05	0.01	0.04	0.01	0.14	0.01	0.13	0.11	0.01	0.01	0.11	0.00	0.12	0.04	0.00	0.00	0.08	0.00
77	0.01		0.03	0.07	0.01	0.05	0.01	0.14	0.01	0.15	0.13	0.01	0.01	0.13	0.00	0.13	0.04	0.00	0.00	0.09	0.00	0.00	0.05
75	0.01		0.03	0.06	0.01	0.05	0.00	0.14	0.01	0.14	0.12	0.01	0.01	0.12	0.00	0.13	0.04	0.00	0.00	0.09	0.00	0.00	0.04
49	0.01		0.03	0.06	0.01	0.05	0.00	0.15	0.01	0.15	0.12	0.01	0.01	0.12	0.00	0.12	0.04	0.00	0.00	0.08	0.00	0.00	0.04
3	0.01		0.03	0.06	0.01	0.05	0.00	0.17	0.01	0.16	0.13	0.01	0.01	0.13	0.00	0.13	0.04	0.00	0.00	0.09	0.00	0.00	0.05
Aug	100	0.01	0.02	0.04	0.01	0.03	0.00	0.14	0.01	0.12	0.11	0.01	0.01	0.11	0.00	0.12	0.04	0.00	0.00	0.08	0.00	0.00	0.03
	77	0.01	0.02	0.06	0.01	0.05	0.01	0.14	0.01	0.14	0.12	0.01	0.01	0.12	0.00	0.13	0.04	0.00	0.00	0.09	0.00	0.00	0.05
	75	0.01	0.02	0.05	0.01	0.04	0.00	0.14	0.01	0.13	0.11	0.01	0.01	0.11	0.00	0.12	0.04	0.00	0.00	0.09	0.00	0.00	0.04
	49	0.01	0.02	0.05	0.01	0.04	0.00	0.15	0.01	0.14	0.11	0.01	0.01	0.11	0.00	0.12	0.04	0.00	0.00	0.09	0.00	0.00	0.04
	3	0.01	0.03	0.06	0.01	0.04	0.00	0.16	0.01	0.15	0.12	0.01	0.01	0.12	0.00	0.13	0.04	0.00	0.00	0.09	0.00	0.00	0.04
Sep	100	0.01	0.03	0.05	0.01	0.04	0.00	0.13	0.01	0.13	0.12	0.01	0.01	0.12	0.00	0.13	0.04	0.00	0.00	0.10	0.00	0.00	0.06
	77	0.01	0.03	0.06	0.01	0.05	0.01	0.13	0.01	0.14	0.13	0.01	0.01	0.13	0.00	0.14	0.04	0.00	0.00	0.11	0.00	0.00	0.07
	75	0.01	0.03	0.06	0.01	0.05	0.00	0.13	0.01	0.14	0.12	0.01	0.01	0.12	0.00	0.13	0.04	0.00	0.00	0.10	0.00	0.00	0.06
	49	0.01	0.03	0.06	0.01	0.05	0.00	0.14	0.01	0.15	0.13	0.01	0.01	0.13	0.00	0.13	0.04	0.00	0.00	0.10	0.00	0.00	0.06
	3	0.01	0.03	0.06	0.01	0.05	0.00	0.16	0.01	0.16	0.14	0.01	0.01	0.13	0.00	0.14	0.04	0.00	0.00	0.10	0.00	0.00	0.07

Average monthly discharge (m³/s) for the Wadi Hanifah under five different probabilities of LULC 2030 scenarios for the Wadi Hanifah catchment. (Continued)

Month	Probabilities %	1	2	3	4	5	6	7	8	9	10	11	12	13	14	15	16	17	18	19	20	21	22
		Oct	100	0.01	0.03	0.06	0.01	0.06	0.01	0.13	0.01	0.18	0.19	0.02	0.02	0.21	0.00	0.26	0.07	0.03	0.01	0.26	0.03
77	0.01		0.03	0.09	0.01	0.10	0.01	0.13	0.01	0.22	0.23	0.02	0.02	0.25	0.00	0.30	0.07	0.03	0.01	0.30	0.03	0.02	0.32
75	0.01		0.03	0.11	0.01	0.11	0.02	0.13	0.01	0.25	0.25	0.02	0.02	0.27	0.00	0.32	0.07	0.03	0.01	0.32	0.03	0.02	0.34
49	0.01		0.03	0.11	0.01	0.11	0.02	0.15	0.02	0.28	0.28	0.02	0.02	0.30	0.00	0.35	0.07	0.03	0.01	0.35	0.03	0.02	0.36
3	0.02		0.03	0.13	0.01	0.13	0.02	0.18	0.02	0.33	0.33	0.02	0.02	0.35	0.00	0.40	0.07	0.03	0.01	0.40	0.03	0.02	0.41
Nov	100	0.02	0.03	0.10	0.01	0.10	0.03	0.15	0.02	0.36	0.43	0.03	0.04	0.52	0.19	0.92	0.17	0.19	0.26	1.41	0.20	0.12	1.81
	77	0.02	0.03	0.23	0.05	0.32	0.04	0.15	0.02	0.60	0.67	0.03	0.04	0.75	0.19	1.19	0.20	0.19	0.26	1.68	0.20	0.12	2.08
	75	0.02	0.04	0.39	0.05	0.48	0.16	0.15	0.02	0.88	0.95	0.03	0.04	1.04	0.21	1.50	0.20	0.20	0.26	1.99	0.20	0.13	2.40
	49	0.02	0.04	0.39	0.05	0.49	0.16	0.22	0.03	1.04	1.12	0.03	0.04	1.21	0.21	1.67	0.20	0.20	0.26	2.17	0.20	0.13	2.58
	3	0.16	0.10	0.70	0.05	0.82	0.16	0.38	0.05	1.55	1.65	0.04	0.04	1.75	0.21	2.25	0.24	0.21	0.26	2.75	0.20	0.13	3.17
Dec	100	0.02	0.03	0.10	0.01	0.11	0.01	0.16	0.02	0.28	0.35	0.03	0.04	0.43	0.13	0.75	0.16	0.16	0.18	1.11	0.16	0.10	1.40
	77	0.02	0.03	0.14	0.02	0.16	0.01	0.16	0.02	0.34	0.41	0.03	0.04	0.49	0.13	0.84	0.19	0.16	0.18	1.20	0.16	0.10	1.49
	75	0.02	0.04	0.18	0.02	0.20	0.04	0.16	0.02	0.41	0.48	0.03	0.04	0.56	0.14	0.93	0.19	0.17	0.18	1.29	0.16	0.10	1.59
	49	0.02	0.04	0.18	0.02	0.20	0.04	0.18	0.03	0.45	0.53	0.03	0.04	0.61	0.14	0.98	0.19	0.17	0.18	1.34	0.16	0.10	1.65
	3	0.10	0.07	0.30	0.02	0.33	0.05	0.23	0.04	0.63	0.72	0.04	0.04	0.82	0.14	1.21	0.22	0.17	0.18	1.58	0.16	0.10	1.89

Average monthly runoff (mm) for the Wadi As Silayy under five different probabilities of LULC 2030 scenarios for the Wadi As Silayy catchment.

Month	Probabilities %	1	2	3	4	5	6	7	8	9	10	11
Jan	100	0.5	0.2	1.8	1.6	7.1	3.2	2.1	5.8	4.8	5.1	3.2
	77	1.8	1.4	6.0	2.2	8.9	3.9	2.2	5.8	4.9	5.1	3.2
	75	2.4	1.5	7.2	7.9	9.9	6.6	4.8	6.3	5.8	5.1	3.2
	49	2.5	2.3	7.6	7.9	9.9	6.7	4.9	6.3	5.8	5.2	3.9
	3	4.2	4.5	7.8	7.9	9.9	8.0	4.9	6.3	5.8	5.2	3.9
Feb	100	0.1	0.0	0.5	0.5	1.9	1.0	0.4	1.2	0.7	1.6	0.7
	77	0.5	0.4	1.9	0.6	2.4	1.1	0.4	1.2	0.7	1.6	0.8
	75	0.7	0.4	2.5	2.4	2.8	2.0	1.2	1.4	0.9	1.6	0.8
	49	0.7	0.7	2.8	2.4	2.8	2.0	1.2	1.4	0.9	1.6	1.0
	3	1.3	1.5	2.9	2.4	2.8	2.5	1.2	1.4	0.9	1.6	1.0
Mar	100	0.6	0.2	2.3	2.1	8.7	3.8	3.6	9.1	8.5	7.2	4.4
	77	2.2	1.7	6.7	2.9	10.6	4.6	3.7	9.1	8.5	7.2	4.4
	75	2.9	1.8	7.7	8.9	11.7	7.6	7.2	9.6	10.0	7.2	4.4
	49	3.1	2.8	8.1	8.9	11.7	7.7	7.2	9.6	10.0	7.3	5.2
	3	4.8	4.9	8.2	8.9	11.7	8.8	7.2	9.6	10.0	7.3	5.2
Apr	100	0.5	0.1	1.7	1.5	6.7	3.1	2.4	6.7	5.4	6.4	3.5
	77	1.7	1.3	5.9	2.1	8.3	3.7	2.5	6.7	5.5	6.4	3.5
	75	2.2	1.4	7.2	7.6	9.3	6.4	5.8	7.3	6.6	6.4	3.5
	49	2.3	2.2	7.7	7.7	9.3	6.5	5.9	7.3	6.6	6.5	4.3
	3	4.0	4.5	7.9	7.7	9.3	7.8	5.9	7.3	6.6	6.5	4.3
May	100	0.1	0.0	0.6	0.5	2.6	1.3	1.5	4.9	3.1	5.0	1.6
	77	0.6	0.5	2.7	0.6	3.4	1.6	1.6	4.9	3.2	5.0	1.7
	75	0.8	0.5	3.6	3.5	3.9	2.9	4.3	5.5	4.0	5.0	1.7
	49	0.9	0.9	4.0	3.5	3.9	2.9	4.4	5.5	4.0	5.1	2.3
	3	1.8	2.1	4.1	3.5	3.9	3.7	4.4	5.5	4.0	5.1	2.3
Jun	100	0.0	0.0	0.0	0.0	0.0	0.1	0.1	0.3	0.1	0.8	0.1
	77	0.0	0.0	0.2	0.0	0.1	0.1	0.1	0.3	0.1	0.8	0.1
	75	0.0	0.0	0.4	0.2	0.1	0.2	0.4	0.4	0.2	0.8	0.1
	49	0.0	0.0	0.5	0.2	0.1	0.2	0.4	0.4	0.2	0.8	0.2
	3	0.1	0.2	0.5	0.2	0.1	0.2	0.4	0.4	0.2	0.8	0.2
Jul	100	0.0	0.0	0.0	0.0	0.0	0.0	0.0	0.0	0.0	0.2	0.0
	77	0.0	0.0	0.0	0.0	0.0	0.0	0.0	0.0	0.0	0.2	0.0
	75	0.0	0.0	0.1	0.0	0.0	0.0	0.0	0.0	0.0	0.2	0.0
	49	0.0	0.0	0.1	0.0	0.0	0.0	0.0	0.0	0.0	0.2	0.0
	3	0.0	0.0	0.1	0.0	0.0	0.0	0.0	0.0	0.0	0.2	0.0
Aug	100	0.0	0.0	0.0	0.0	0.0	0.0	0.0	0.1	0.1	0.1	0.0
	77	0.0	0.0	0.0	0.0	0.0	0.0	0.0	0.1	0.1	0.1	0.0
	75	0.0	0.0	0.0	0.0	0.0	0.0	0.0	0.1	0.1	0.1	0.0
	49	0.0	0.0	0.0	0.0	0.0	0.0	0.0	0.1	0.1	0.1	0.0
	3	0.0	0.0	0.0	0.0	0.0	0.0	0.0	0.1	0.1	0.1	0.0

Average monthly runoff (mm) for the Wadi As Silayy under five different probabilities of LULC 2030 scenarios for the Wadi As Silayy catchment. (Continued)

Month	Probabilities %	1	2	3	4	5	6	7	8	9	10	11
Sep	100	0.0	0.0	0.0	0.0	0.0	0.0	0.0	0.1	0.0	0.1	0.0
	77	0.0	0.0	0.0	0.0	0.0	0.0	0.0	0.1	0.0	0.1	0.0
	75	0.0	0.0	0.0	0.0	0.0	0.0	0.0	0.1	0.0	0.1	0.0
	49	0.0	0.0	0.0	0.0	0.0	0.0	0.0	0.1	0.0	0.1	0.0
	3	0.0	0.0	0.0	0.0	0.0	0.0	0.0	0.1	0.0	0.1	0.0
Oct	100	0.0	0.0	0.1	0.1	0.4	0.2	0.1	0.2	0.2	0.1	0.4
	77	0.1	0.1	0.3	0.1	0.4	0.2	0.1	0.2	0.2	0.1	0.4
	75	0.1	0.1	0.3	0.4	0.5	0.3	0.1	0.2	0.2	0.1	0.4
	49	0.1	0.1	0.3	0.4	0.5	0.3	0.1	0.2	0.2	0.1	0.4
	3	0.2	0.2	0.3	0.4	0.5	0.3	0.1	0.2	0.2	0.1	0.4
Nov	100	0.5	0.1	1.7	1.6	6.8	3.0	1.4	3.9	3.2	3.3	2.0
	77	1.7	1.3	5.4	2.2	8.4	3.7	1.5	3.9	3.3	3.3	2.0
	75	2.3	1.4	6.3	7.2	9.3	6.1	3.2	4.1	3.9	3.3	2.0
	49	2.4	2.2	6.6	7.2	9.3	6.2	3.2	4.1	3.9	3.3	2.4
	3	3.8	4.0	6.7	7.2	9.3	7.2	3.2	4.1	3.9	3.3	2.4
Dec	100	0.3	0.1	1.0	0.9	3.8	1.7	1.0	2.6	2.3	2.3	1.6
	77	0.9	0.7	3.2	1.2	4.6	2.1	1.0	2.6	2.3	2.3	1.6
	75	1.3	0.8	3.9	4.1	5.2	3.5	2.2	2.8	2.7	2.3	1.6
	49	1.3	1.2	4.1	4.2	5.2	3.5	2.2	2.8	2.7	2.4	1.9
	3	2.2	2.4	4.2	4.2	5.2	4.2	2.2	2.8	2.7	2.4	1.9

Average monthly discharge (m³/s) for the Wadi As Silayy under five different probabilities of LULC 2030 scenarios for the Wadi As Silayy catchment.

Month	Probabilities %	1	2	3	4	5	6	7	8	9	10	11
		100	0.44	0.40	0.26	0.04	1.19	0.22	0.05	0.19	1.53	2.66
Jan	77	0.58	0.57	0.67	0.05	1.93	0.25	0.05	0.19	2.30	3.43	0.13
	75	0.68	0.58	0.77	0.13	2.24	0.38	0.10	0.21	2.80	3.95	0.13
	49	0.70	0.71	0.80	0.13	2.41	0.38	0.11	0.21	2.99	4.16	0.16
	3	0.96	1.01	0.81	0.13	2.98	0.43	0.11	0.21	3.61	4.78	0.16
	100	0.38	0.39	0.14	0.02	0.92	0.10	0.01	0.04	1.03	1.42	0.03
Feb	77	0.38	0.42	0.29	0.02	1.11	0.11	0.01	0.04	1.22	1.61	0.03
	75	0.41	0.43	0.33	0.05	1.21	0.14	0.03	0.05	1.38	1.78	0.03
	49	0.41	0.46	0.35	0.05	1.27	0.14	0.03	0.05	1.44	1.85	0.05
	3	0.50	0.56	0.35	0.05	1.47	0.16	0.03	0.05	1.65	2.06	0.05
	100	0.43	0.40	0.31	0.05	1.22	0.24	0.08	0.30	1.66	3.25	0.16
Mar	77	0.61	0.61	0.73	0.06	2.06	0.27	0.08	0.30	2.53	4.12	0.17
	75	0.73	0.63	0.82	0.14	2.39	0.42	0.15	0.31	3.09	4.70	0.17
	49	0.75	0.77	0.84	0.14	2.56	0.42	0.15	0.31	3.27	4.92	0.19
	3	1.00	1.07	0.85	0.14	3.12	0.47	0.15	0.31	3.88	5.52	0.19
	100	0.41	0.41	0.25	0.04	1.13	0.21	0.06	0.23	1.46	2.85	0.13
Apr	77	0.54	0.56	0.67	0.05	1.84	0.23	0.06	0.23	2.20	3.59	0.13
	75	0.63	0.58	0.79	0.13	2.17	0.36	0.13	0.25	2.75	4.16	0.13
	49	0.65	0.71	0.83	0.13	2.36	0.37	0.13	0.25	2.94	4.39	0.16
	3	0.91	1.03	0.84	0.13	2.95	0.42	0.13	0.25	3.59	5.04	0.16
	100	0.33	0.38	0.13	0.02	0.84	0.11	0.03	0.16	1.00	2.03	0.06
May	77	0.34	0.41	0.33	0.02	1.09	0.11	0.04	0.16	1.27	2.29	0.06
	75	0.38	0.41	0.40	0.06	1.24	0.17	0.09	0.18	1.54	2.58	0.06
	49	0.39	0.47	0.43	0.06	1.34	0.17	0.09	0.18	1.65	2.72	0.08
	3	0.52	0.61	0.44	0.06	1.62	0.20	0.09	0.18	1.95	3.02	0.08
	100	0.29	0.35	0.07	0.01	0.67	0.04	0.00	0.01	0.68	0.85	0.00
Jun	77	0.22	0.31	0.08	0.01	0.57	0.03	0.00	0.01	0.57	0.74	0.00
	75	0.22	0.31	0.08	0.01	0.56	0.02	0.01	0.01	0.56	0.73	0.00
	49	0.23	0.31	0.08	0.01	0.57	0.02	0.01	0.01	0.56	0.74	0.00
	3	0.22	0.27	0.08	0.01	0.52	0.02	0.01	0.01	0.52	0.69	0.00
	100	0.26	0.33	0.06	0.01	0.60	0.03	0.00	0.00	0.60	0.66	0.00
Jul	77	0.20	0.29	0.05	0.01	0.49	0.02	0.00	0.00	0.48	0.54	0.00
	75	0.20	0.28	0.04	0.01	0.47	0.01	0.00	0.00	0.44	0.50	0.00
	49	0.20	0.28	0.03	0.01	0.46	0.01	0.00	0.00	0.44	0.49	0.00
	3	0.18	0.22	0.03	0.01	0.38	0.00	0.00	0.00	0.36	0.41	0.00

Average monthly discharge (m³/s) for the Wadi As Silayy under five different probabilities of LULC 2030 scenarios for the Wadi As Silayy catchment. (Continued)

Month	Probabilities %	1	2	3	4	5	6	7	8	9	10	11
		Aug	100	0.24	0.31	0.06	0.01	0.57	0.03	0.00	0.00	0.57
77	0.19		0.27	0.05	0.01	0.46	0.02	0.00	0.00	0.45	0.49	0.00
75	0.18		0.27	0.03	0.01	0.43	0.01	0.00	0.00	0.41	0.46	0.00
49	0.18		0.26	0.02	0.01	0.42	0.01	0.00	0.00	0.40	0.44	0.00
3	0.17		0.21	0.02	0.01	0.35	0.00	0.00	0.00	0.32	0.37	0.00
Sep	100	0.24	0.30	0.06	0.01	0.56	0.03	0.00	0.00	0.56	0.61	0.00
	77	0.19	0.26	0.04	0.01	0.45	0.02	0.00	0.00	0.45	0.50	0.00
	75	0.18	0.26	0.03	0.01	0.43	0.01	0.00	0.00	0.41	0.46	0.00
	49	0.18	0.25	0.02	0.01	0.41	0.01	0.00	0.00	0.40	0.44	0.00
	3	0.17	0.20	0.02	0.01	0.35	0.00	0.00	0.00	0.33	0.37	0.00
Oct	100	0.24	0.28	0.07	0.01	0.58	0.04	0.00	0.00	0.60	0.67	0.01
	77	0.20	0.26	0.07	0.01	0.51	0.04	0.00	0.00	0.53	0.60	0.01
	75	0.21	0.26	0.06	0.01	0.50	0.03	0.00	0.01	0.51	0.58	0.01
	49	0.21	0.26	0.05	0.01	0.49	0.03	0.00	0.01	0.50	0.57	0.01
	3	0.20	0.22	0.05	0.01	0.45	0.02	0.00	0.01	0.46	0.52	0.01
Nov	100	0.37	0.35	0.24	0.04	1.05	0.21	0.04	0.13	1.33	2.09	0.09
	77	0.52	0.51	0.61	0.05	1.74	0.23	0.04	0.13	2.05	2.81	0.09
	75	0.61	0.53	0.69	0.12	2.02	0.35	0.07	0.14	2.49	3.26	0.09
	49	0.63	0.65	0.71	0.12	2.17	0.36	0.07	0.14	2.65	3.44	0.10
	3	0.86	0.91	0.72	0.12	2.67	0.40	0.07	0.14	3.19	3.98	0.10
Dec	100	0.37	0.36	0.17	0.03	0.94	0.14	0.02	0.09	1.13	1.66	0.06
	77	0.42	0.43	0.38	0.03	1.29	0.15	0.03	0.09	1.49	2.02	0.06
	75	0.47	0.44	0.43	0.07	1.44	0.21	0.05	0.09	1.73	2.27	0.06
	49	0.48	0.50	0.45	0.07	1.53	0.21	0.05	0.09	1.82	2.38	0.08
	3	0.61	0.65	0.45	0.07	1.81	0.23	0.05	0.09	2.12	2.68	0.08